copy A

LIBRARY
ROYAL AIRCRAFT ESTABLISHMENT
BEDFORD.

BELGIQUE
CANADA
DANMARK
DEUTSCHLAND
ELLÁS
FRANCE
ISLAND
ITALIA
LUXEMBOURG
NEDERLAND
NORGE
PORTUGAL
TURKIYE
UNITED KINGDOM
UNITED STATES

AGARDograph

THE USE OF ANALOGUE COMPUTERS IN SOLVING PROBLEMS OF FLIGHT MECHANICS

by

F. C. HAUS
Professor at the Universities of Ghent and Liège

J. CZINCZENHEIM
Chief Engineer, Louis Bréguet Aircraft Works

L. MOULIN
Civil, Electrical and Mechanical Engineer,
Training Centre for Experimental Aerodynamics

JUNE 1960

AGARDograph 44

NORTH ATLANTIC TREATY ORGANIZATION

ADVISORY GROUP FOR AERONAUTICAL RESEARCH AND DEVELOPMENT

(ORGANISATION DU TRAITE DE L'ATLANTIQUE NORD)

THE USE OF ANALOGUE COMPUTERS IN SOLVING PROBLEMS OF FLIGHT MECHANICS

F.C. Haus
Professor at the Universities of Ghent and Liège

J. Czinczenheim
Chief Engineer, Louis Bréguet Aircraft Works

L. Moulin
Civil, Electrical and Mechanical Engineer,
Training Centre for Experimental Aerodynamics

June 1960

SUMMARY

Part I of this AGARDograph establishes the equations of motion for an aircraft which has a rigid structure, taking into account additional relationships introduced into the standard equations as a result of operational conditions. It also discusses the bases for calculating the general equations of motion for an aircraft with a non-rigid structure.

The characteristics of the motion defined by these equations are easily studied by means of analogue calculations.

Part II deals with the principles of analogue calculation, while Part III is concerned with the application of such calculations to the solution of certain problems relating to the mechanics of an aircraft.

A number of questions concerned with the following are discussed in turn: the motion of aircraft with a rigid structure; the behaviour of aircraft with a non-rigid structure; the response of aircraft fitted with an automatic pilot; the calculation of landing trajectories.

Part IV illustrates a particular problem: the automatic holding of an approach trajectory. The author shows how analogue calculations make it possible to study in detail the action of numerous parameters, and to choose, from among possible solutions, those which are worth adopting.

629.13.014.57:518.5

3f2b1

SOMMAIRE

La première partie de l'Agardographie établit les équations du mouvement de l'avion à structure indéformable, en tenant compte de relations supplémentaires que les conditions d'utilisation ajoutent aux équations classiques; elle indique aussi les bases sur lesquelles les équations générales du mouvement de l'avion à structure déformable, peuvent être établies.

Les propriétés du mouvement défine par ces équations peuvent être étudiées facilement par le calcul analogique.

La seconde partie expose les principes du calcul analogique, tandis que la troisième partie est consacrée à l'application de ce calcul à la solution d'un certain nombre de problèmes de mécanique de l'avion.

De nombreux problèmes relatifs au mouvement d'avions à structure rigide, au comportement d'avions à structure non rigide, à la réponse de l'avion muni d'un pilote automatique, à la réalisation de trajectoires d'atterrissage, sont étudiés successivement.

La quatrième partie traite, à titre d'exemple, d'un problème particulier: la tenue automatique d'une trajectoire d'approche. Il est montré comment le calcul analogique permet d'étudier en détail l'action de nombreux paramètres et permet de choisir, parmi les solutions possibles, celles qui méritent d'être retenues.

629.13.014.57:518.5

3f2b1

C O N T E N T S

PART I

THE PROBLEMS OF AIRCRAFT MOTION

		Page
CHAPTER 1 -	KINEMATICS OF THE AEROPLANE by F.C. Haus	
	1.1 Reference Trihedrals	1
	1.2 Relative Position of Two Trihedrals	3
	1.3 Position and Motion of the Aeroplane in Space	6
	1.4 Trihedrals Depending on Velocity	7
	1.5 Motions of the Atmosphere Itself	9
	1.6 Angles of Attack and Side-Slip	10
CHAPTER 2 -	DYNAMICS OF THE AEROPLANE WITH A RIGID STRUCTURE by F.C. Haus	
	2.1 Structural Deformation and Configuration of the Aeroplane	11
	2.2 External Actions	12
	2.2.1 Gravity Force	12
	2.2.2 Aerodynamic Forces	13
	2.2.3 Gyroscopic Effects	17
	2.3 General Equations of Motion of an Aeroplane	18
	2.4 Control Surfaces	20
	2.5 Velocity and Load Disturbances	21
	2.6 Equations of Motion Following a Steady State	23
CHAPTER 3 -	TRANSFORMATION AND SOLUTION OF THE EQUATIONS OF MOTION OF A RIGID AEROPLANE by F.C. Haus	
	3.1 Non-Dimensional Expression of the Disturbance Velocities	25
	3.1.1 Linear and Angular Velocities	25
	3.1.2 Angles of Attack and Side-Slip	25
	3.1.3 Linear Velocities Expressed as a Function of Angles	25
	3.1.4 Motion of the Surrounding Air	27
	3.2 Determination of Increments $\Delta X, \Delta Y \ldots\ldots \Delta N$ in the Linear Case	27
	3.3 System of Equations Written in a Non-Dimensional Form	31
	3.4 Integration of Linear Systems	36
	3.5 Transformation Formulae	39

Page

3.6 Further Relations 40
3.7 Block-Diagrams 42
3.8 Laplace Transformation and Transfer Functions 43
3.8.1 Definition of the Transformation 43
3.8.2 Transformation Properties 43
3.8.3 Definition of the Transfer Function 45
3.8.4 Properties of the Transfer Functions 46
3.8.5 Block Splitting 47
3.9 Non-Stationary Effects 47
3.10 Non-Linearity of Aerodynamic Forces, in Relation to Variables 49
3.11 Usefulness of Analogue Computers 50
3.12 The Establishing of Transformation Formulae 51

CHAPTER 4 - DYNAMICS OF THE NON-RIGID AEROPLANE
by J. Czinczenheim

4.1 Generalized Coordinates 56
4.2 Equations of Motion 57
4.2.1 Determination of Forces and Moments 58
4.2.1.1 Inertia Forces 58
4.2.1.2 Gravity Forces 61
4.2.1.3 Elastic Forces 62
4.2.1.4 Damping Forces 62
4.2.1.5 Aerodynamic Forces 62
4.2.2 General Form of the Equations of Motion 65
4.3 Study of Some Particular Cases 67
4.3.1 Motion of a Rigid Aeroplane with a Movable Control (Free or Attached by Springs or Servo-Controlled) 67
4.3.2 Motion of a Rigid Aeroplane Controlled by an Accelerometer 70
4.3.3 Stability of an Aeroplane with a Flexible Fuselage 72
4.3.4 Study of the Influence of Deformations in Arbitrary Modes 73
4.4 Functional Diagram Corresponding to a Non-Rigid Aeroplane 74

List of Figures for Part I 75

PART II

THE ANALOGUE COMPUTER

CHAPTER 5 - PRINCIPLES OF ANALOGUE COMPUTATION
by L. Moulin

5.1 Introduction 85

Page

5.2 High-Gain Amplifier Capabilities 86
5.3 Elementary Operation 88
5.3.1 Sign Inversion 88
5.3.2 Multiplication by a Constant Factor 88
5.3.3 Integration 91
5.3.4 Summation 92
5.4 Operational Limitations 93

CHAPTER 6 - SOLUTION OF LINEAR SYSTEMS OF EQUATIONS
by L. Moulin

6.1 Homogeneous Systems Without Second Member 94
6.2 Modifications of the Set-Up 96
6.3 Initial Conditions 97
6.4 Non-Homogeneous Equations 98
6.5 Choice of the Set-Up 98

CHAPTER 7 - NON-LINEAR FUNCTION GENERATION
by L. Moulin

7.1 Multipliers 100
7.1.1 Servo-Multipliers 100
7.1.2 Division 101
7.1.3 Electronic Multiplier 102
7.1.4 Note 104
7.2 Generation of Non-Linear Functions 104
7.2.1 Non-Linear Potentiometers 104
7.2.2 Cathode Ray Tube 105
7,2.3 Servo-Potentiometers 105
7.2.4 Conducting Ink 106
7.2.5 Taped Potentiometer 106
7.2.6 Diode Generators 106
7.2.7 Non-Linear Functions of Two Variables 109

CHAPTER 8 - SPECIAL FEATURES OF ANALOGUE COMPUTATION
by L. Moulin

8.1 Set-Up of Transfer Functions 110
8.2 Operational Restrictions 111

List of Figures for Part II 113

PART III

THE USE OF ANALOGUE COMPUTERS

Page

CHAPTER 9 - PROBLEMS OF KINEMATICS
by F.C. Haus and L. Moulin

9.1 Introduction 121
9.2 Solution of the Main Problems Using the Euler Angles 121
9.2.1 First Problem 121
9.3 Solution of the Problems Using Direction Cosines 125
9.3.1 First Problem 125
9.3.2 Second Problem 126

CHAPTER 10 - MOTION OF AN AEROPLANE WITH RIGID STRUCTURE
by J. Czinczenheim and F.C. Haus

10.1 Linear Problems 127
10.1.1 Longitudinal Motion 128
10.1.1.1 Linearized Equations of the Longitudinal Motion 128
10.1.1.2 Wiring Diagram 130
10.1.1.3 Examples 130
10.1.2 Lateral Motion 134
10.1.2.1 Linearized Equations of Lateral Motion 134
10.1.2.2 Setting-Up Scheme 135
10.1.2.3 Examples 135
10.1.3 The Permanent Motion Considered as a Helical Motion (Linear Equations) 136
10.2 Non-Linear Problems 138
10.2.1 Inertia Coupling 138
10.2.1.1 History 138
10.2.1.2 Equation of Problems Involving Inertia Coupling Terms 139
10.2.1.3 Application of Analogue Computers 141
10.2.2 Aerodynamic Non-Linearities 144
10.2.2.1 Approximation by a Polynomial 144
10.2.2.2 Use of Function Generators 144
10.2.2.3 Non-Linearity Combinations 146
10.2.3 Non-Stationary Aerodynamic Actions 151
10.2.3.1 Constant Delay in the Appearance of an Aerodynamic Effect 151
10.2.3.2 Non-Stationary Aerodynamic Effects 153

Page

CHAPTER 11 - MOTION OF A NON-RIGID AIRCRAFT
by J. Czinczenheim

11.1 Supplementary Degrees of Freedom Their Representation on the Computer 156
11.2 Some Particular Cases 156
11.2.1 Combination of a Gust with the First Mode of Wing Bending 156
11.2.1.1 Equations of Motion 157
11.2.1.2 Passing to the Transforms 159
11.2.1.3 Results 160
11.2.2 Influence of Wing Torsional Rigidity on Aileron Effectiveness 160
11.2.2.1 Equations of Motion 160
11.2.2.2 Set-Up 162
11.2.2.3 Discussion of the Results 162
11.2.2.4 Other Problems 163

CHAPTER 12 - THE ACTION OF THE CONTROLS
by F.C. Haus

12.1 Effort Applied by the Pilot 164
12.2 Different Types of Controls 164
12.2.1 Reversible Manual Control 164
12.2.2 Reversible Controls Using Tabs 166
12.2.3 Irreversible Control by Hydraulic Jack Without Direct Connection Between Stick and Control Surface 167
12.2.4 Manual Control Assisted by Hydraulic Jacks 167
12.2.5 Electrical Servo-Controls 168
12.3 Generators of 'Artificial Feel' 168
12.4 Imperfections of the Controls 170
12.5 Response of the Aircraft to a Force Exerted by the Pilot. Case of Reversible Controls 170
12.6 Use of Analogue Computer. Study of the Longitudinal Motion of an Aircraft Flying Stick-Free 172
12.7 Transfer Functions of Positioning Servo-Mechanisms 176
12.7.1 Existence of a Transfer Function 176
12.7.2 Control by Means of a Jack 177
12.7.3 Control by an Electric Motor 178
12.7.4 Miscellaneous Cases 181
12.8 Response of the Aircraft to Pilot Action in the Case of Servo-Controls 181
12.9 Use of the Analogue Computer 183
12.9.1 Different Ways of Investigation 183

Page

12.9.2 Use of the Computer Alone 184
12.9.3 Determination of an Optimum Artificial-Feel Generator 185

CHAPTER 13 - AUTOMATIC CONTROL
by F.C. Haus

13.1 Artificial Stability 188
13.2 Analogue Study for the Schematic Case 191
13.3 The Physical Action of Various Elementary Control Equations 192
13.3.1 Longitudinal Motion 193
13.3.2 Lateral Motion 194
13.4 Actual Realization 196
13.4.1 Positioning Servo-Controls 197
13.4.2 Control Involving an Integration 199
13.5 Analogue Study of Real Cases 200
13.5.1 Phase Advance 200
13.5.2 Filtration 202
13.5.3 Progressive Attenuation of the Signals 202
13.5.4 Progressive Attenuation of the Feed-Back 202
13.6 Application 203
13.6.1 Longitudinal Motion 203
13.6.1.1 Aircraft with Dynamic Characteristics Defined by Linear Equations (Linear Control Equations) 203
13.6.1.2 Aircraft with Non-Linear Aerodynamic Characteristics 205
13.6.2 Lateral Motion 206
13.6.3 Non-Linear Automatic Pilotage 207
13.7 Partial Simulation 207
13.8 The Use of the Manual Control when an Automatic Pilot is in Action 208
13.8.1 Classification 208
13.8.2 Controls in Parallel 210
13.8.3 Differential Control 212
13.8.4 Control Without Direct Connection Between the Pilot and the Control Surface 213
13.8.5 The Practical Consequences of the Large Number of Alternative Arrangements 214
13.9 Response of the Aircraft to the Action of the Human Pilot 215
13.9.1 The Influence of the Type of Automatic Pilot Used 215

Page

13.9.2 Block Diagrams 216
13.9.3 Study by the Analogue Computer 216
13.9.3.1 High-Speed Aircraft 216
13.9.3.2 Low-Speed Aircraft 219
13.10 Guidance Following an Alignment 219
13.10.1 Principle 219
13.10.2 Properties of the Trajectories 220
13.10.3 Guidance Along an Approach Trajectory 221
13.10.4 Applications 221
13.11 Automatic Control of Flare-Out 224
13.11.1 Statement of the Problem 224
13.11.2 Effect of Error Signal 226
13.11.3 Tests on the Computer 228
13.11.4 Other Problems 231
13.12 Aeroplane Equipped with a Gust Damper 232

List of Figures for Part III 236

PART IV

A CASE OF AEROPLANE GUIDANCE, AS AN EXAMPLE OF ANALOGUE COMPUTER UTILIZATION

CHAPTER 14 - GENERAL DISCUSSION
by F.C. Haus

14.1 The Purpose of this Investigation 325
14.2 Problem of the Approach Path 325
14.3 Basic Considerations of the Investigation 326
14.4 Methods Used in the Investigation 327

CHAPTER 15 - EQUATIONS OF MOTION OF THE AEROPLANE
by F.C. Haus

15.1 Notation System 328
15.2 Equations of Motion 329
15.3 Input and Output Signals 330
15.3.1 Longitudinal Motion 330
15.3.2 Lateral Motion 331
15.4 Mechanical and Aerodynamic Characteristics of the Aeroplane under Consideration 332

Page

CHAPTER 16 - AUTOMATIC GUIDANCE
by F.C. Haus

16.1 The Control Equations 335
16.1.1 Longitudinal Motion 335
16.1.2 Lateral Motion 335
16.2 Criticism of these Equations 336
16.3 Irregularities in the Signals 338
16.4 General Remarks on the Motion 339

CHAPTER 17 - LATERAL BEHAVIOUR OF THE AEROPLANE
by F.C. Haus

17.1 Stability with Controls Fixed 342
17.2 Response to a Step Function 343
17.3 Frequency Response 343
17.4 Different Degrees of Stability 343
17.5 First Degree Stability 344
17.6 Second Degree Stability 345
17.7 Combination of Two Error Signals 346
17.8 Third Degree Stability 347
17.9 More Complex Conditions for Obtaining Third Degree Stability 348
17.10 Continuous Variation of A_4 349

CHAPTER 18 - GUIDANCE IN THE LOCALIZER PLANE
by F.C. Haus

18.1 Contents of this Chapter 351
18.2 Control Subject to Three Error Signals 351
18.3 Detailed Discussion of Certain Combinations 353
18.4 Initial Displacement of ψ 355
18.5 Effect of a Side Gust 356
18.6 Comparison with American Research 357

CHAPTER 19 - REMARKS ON THE LATERAL MOTION
by F.C. Haus

19.1 Effect of Time in Control Movement 360
19.2 Motion with Variable Gain of y 360
19.3 Distortion Effects 361
19.4 Effect of B_4 362
19.5 Semi-Automatic Control 363
19.6 Final Remarks 364

Page

CHAPTER 20 - LONGITUDINAL BEHAVIOUR OF THE AEROPLANE
by F.C. Haus

20.1 Stability with Controls Fixed 365
20.2 Response to a Step Function 365
20.3 Frequency Response 366
20.4 Different Degrees of Stability 366
20.5 Stability with no Account Taken of Altitude 366
20.6 Second Degree of Stability 368
20.7 The Long-Period Oscillation 369
20.8 Damping by a Term $\delta_e = A_1\theta$ 369
20.9 Other Possibilities of Damping 370

CHAPTER 21 - MAINTENANCE OF THE GLIDE PATH
by F.C. Haus

21.1 Contents of this Chapter 372
21.2 Basic Conditions 373
21.3 More Complex Conditions 373
21.4 Power Control 374
21.5 Superposition of the Effects of B_3 and B_4 376
21.6 Combinations Investigated for Other Initial Deflections 379
21.7 Initial Condition ζ_0 (or Entering the Glide Path) 380
21.8 The Gust u_a 382
21.9 The Gust w_a 383

CHAPTER 22 - REMARKS ON THE LONGITUDINAL MOTION
F.C. Haus

22.1 Progressive Variation of the Gain in A_4 or B_4 385
22.2 Integral Control 385
22.3 Improving the Damping 386
22.4 The Use of an Accelerometer 388
22.5 Use of the Air-Speed Indicator 388
22.6 More Elaborate Cases 391
22.7 Comparison with Caroll and Tyler Tests 392
22.8 Final Remarks 393

List of Figures for Part IV 394

REFERENCES 549

DISTRIBUTION

NOTATION

a	speed of sound
a	acceleration minus acceleration of gravity (= j-g)
a	time constant
b	span
b_0, b_1, b_2	coefficients forming part of C_H
c	wing chord
d	distance or length
d_i	aeroelastic distortion of mode i (4.1)
g	acceleration of gravity
h	height
h_v	height of centre of vertical tail surface
h_A, h_s	heights defined in 13.11.1
h	a generalized coordinate - in particular, the generalized coordinate characterizing fuselage bending (4.3.3)
h	as a subscript, a particular value of k (4)
$i(i_x, i_y, i_z)$	symbolic expression for radius of inertia (3.3)
$i(i_x, i_y, i_z)$	moments of inertia of a control surface (4.3.1)
i	number of degrees of freedom or modes of deformation (4.1)
j	true acceleration of centre of gravity
k	number of points considered (4)
l, m, n	direction cosines
$l(l_H, l_v)$	distance between tail surfaces and centre of gravity
l	half chord (= ½ c) (4.2.1.5)
l	condensed symbol, used in 11.2.1.1
l'	elevator chord

m	total mass of aircraft
m_k	mass of point P_k (4.2.1.1)
m	flow of oil (12.7.2)
m_f	mass of a control surface
n	load factor
$\vec{n}_k$	normal at point P_k (4.2.1.5)
p, q, r	increments of components of angular velocity
$\hat{p}, \hat{q}, \hat{r}$	increments of components of angular velocity (non-dimensional)
p	local pressure (4.2.1.5)
q	generalized coordinate (4.1)
$r(r_x, r_y, r_z)$	radius of inertia
s	Laplace variable
s	general expression of a displacement (4.2.1.5)
t	time
$\hat{t}$	aerodynamic time (non-dimensional)
u, v, w	components of velocity increments
$\hat{u}, \hat{v}, \hat{w}$	components of velocity increments (non-dimensional)
u_a, v_a, w_a	components of velocity of the atmosphere
x, y, z	projections of a distance on to the three axes
x, y, z	aerodynamic axes (1.4)
x_v, y_v, z_v	velocity axes (1.4)
x_f, y_f, z_f	axes fixed to the hinge of a control surface (4.3.1)
x_c, y_c, z_c	coordinates of C with respect to G (4.3.1)
x	general expression for an input signal
y	general expression for an output signal

A B	proportionality factors in a control equation
$C \begin{cases} C_x, C_y, C_z \\ C_l, C_m, C_n \end{cases}$	coefficients of aerodynamic reactions with respect to body axes
$\begin{cases} C_{x*}, C_{y*}, C_{z*} \\ C_{l*}, C_{m*}, C_{n*} \end{cases}$	coefficients of aerodynamic reactions with respect to aerodynamic axes
C_D	drag coefficients
C_L	lift coefficients
C_H	hinge moment coefficient
$C_I \begin{cases} C_{I_x}, C_{I_y} \\ C_{I_z}, C_{I_{zx}} \end{cases}$	inertia coefficients (3.3)
C	aerodynamical resultant moment
C	capacity (Part II)
D	drag
D	distance between origin of axes and transmitter (Part V)
$\|D\|$	modulus of an amplitude (3.1.2.d)
E	modulus of elasticity
F	resultant aerodynamic force
F	force applied to stick by pilot
F_0	dry friction
$F(t)$	response to a step input
$F(s)$	Laplace transform of response $F(t)$
G	centre of gravity of aeroplane
G	weight of plane (Part IV)
G	modulus of elasticity (4.3.4)
$G(s)$	general expression of a transfer function

H	hinge moment
H_e	elevator hinge moment
$H(t)$	response to a pulse input
$H(s)$	Laplace transform of response $H(t)$
$I \begin{cases} I_x, I_y \\ I_z, I_{zx} \end{cases}$	moments and products of inertia
J	moment of inertia of a control surface
L, M, N	components of aerodynamic moment
L_r, M_r, N_r	moments of a rigid surface (4.2.1.1)
L_d, M_d, N_d	moments produced by the distortion (4.2.1.1)
$L_u, \ldots . N_r$	derivatives of the moments with respect to a velocity
L	lift
L_H	lift of horizontal tailplane
L	distance between origin of axes and transmitter
L	self induction (12.7.3)
$\mathcal{L}$	Laplace transform
$\mathcal{L}^{-1}$	inverse Laplace transform
M	Mach number
M	generalized mass (4.2.1.3)
M_h	generalized mass for deformation mode h
M	mass of the aircraft (4.2 and 11.2.1)
$\mathfrak{m}$	kinetic momentum
$\mathfrak{m}$	moment about control column articulation
$\mathfrak{m}_p$	moment exerted by pilot about the articulation
$\mathfrak{m}_f, \mathfrak{m}_r$	moments exerted by artificial feel generator about the articulation
N	normal force

N_v	normal force on vertical tail surface
O	origin of earth axes
P, Q, R	angular velocities about three axes
P_k	point k (4.2)
$P_{0,k}$	point k of the rigid aeroplane (4.2)
Q	moment exerted by propulsion system
Q_c	coefficient of moment Q
Q_h	generalized force corresponding to the generalized coordinate h (4.2.1.1)
Q	wing bending moment (11.2.1)
R	electrical resistance (Part II)
R_e	input resistance (Part II)
R_c	feedback resistance (Part II)
R(w)	general expression of a frequency response (Part IV)
S	wing area
S_H	horizontal tail-plane area
S_v	vertical tail-plane area
S′	elevator area
$\mathring{s}$	conventional surface defining screw
T	thrust
T_c	thrust coefficient
T	kinetic energy (4.2.1.1)
T	period
$T_{1/2}$	time necessary to obtain an amplitude reduced to one-half
V	velocity
V_0	velocity at time t = 0

V_a	velocity of surrounding atmosphere
V_r	relative velocity
V_s	projection of velocity on plane of symmetry
$\mathfrak{U}, \mathfrak{V}, \mathfrak{W}$	projections of the velocity
V	voltage (Part II)
V_e	input voltage (Part II)
V_s	output voltage (Part II)
W	virtual work (4.2.1.1)
W	power (Part V)
X, Y, Z	aircraft axes
X, Y, Z	projections of a vector
X, Y, Z	projections of a force F on the axes
X_r, Y_r, Z_r	projections of force F for a rigid aeroplane
X_d, Y_d, Z_d	projections of force due to frame distortion
Z	impedance (Part II)
Z_e	input impedance (Part II)
Z_c	feedback impedance (Part II)
1(t)	unit function
$\Upsilon(t)$	Dirac function or pulse
α	angle of attack
α	increment in angle of attack
α_r	angle of attack with respect to relative wind
α_p	real angle of attack of wing profile } 10.2.3.1 and 13.12
α_e	angle of attack of tail plane } 10.2.3.1 and 13.12
α_h	angle of attack of horizontal tail (12.2)
α_g	variation of angle of attack due to a gust ($= w_a/V_0$) (13.12)

β	angle of side-slip
β	increase in angle of side-slip
β_r	angle of side-slip with respect to relative wind
γ	angle of path
δ	symbol of a variation (4.2.1.1)
δ	displacement or deflection
δ_a	aileron deflection
δ_e	elevator deflection
δ_r	rudder deflection
δ_f	flap deflection
δ_t	tab deflection
δ_s	control column displacement
δ_m	engine control displacement
ϵ	error signal or error
ϵ	airflow deflection
λ	accelerometer deflection (4.3.2)
λ	root of the characteristic equation
λ	condensed symbol, used in 11.2.1.1
μ	aircraft density
μ	symbolic representation of a variable (4.2.2)
ρ	specific mass of air
σ	strength of a signal (Ch.12 and 13)
σ_k	elementary area around point P_k (4.2.1.5)
τ	aerodynamic or dimensionless time unit
ξ_i, η_i, ζ_i	components of a distortion d_i (4.2.1.1)
ζ	damping coefficient

ξ	angle between chord and principal axis of inertia
ξ	angle of tail-setting relative to wing chord
ζ	slope of glide path
χ	dihedral angle between two planes
φ, θ, ψ	rotation angles (called Euler angles)
ω	general expression of an angular frequency
ω	frequency using the aerodynamic time as time unit (Part IV)
ω_n	frequency of undamped oscillation
Γ	servo-motor torque (12.7.3)
Γ	acceleration at a point (4.2.1)
Γ_1, Γ_2	condensed symbols used in 11.2.1
Φ, Θ, ψ	rotation angles (called Euler angles)
Φ	airscrew pitch angle (11.2.2.3)
$\Phi(t), \psi(t)$	Wagner and Küssner time functions
$\Phi(s), \psi(s)$	Laplace transforms of the preceding functions
Ω	resultant angular velocity
Ω_h	angular frequency of deformation mode h (4.2.1.3)

PART I - THE PROBLEMS OF AIRCRAFT MOTION

CHAPTER 1

KINEMATICS OF THE AEROPLANE

F. C. Haus*

1.1 REFERENCE TRIHEDRALS

Several different trihedrals are necessary to study the motion of an aeroplane. These trihedrals can be:

(A) Completely attached to the aeroplane (dynamic)

(B) Attached to the ground (geodetic)

(C) Partially attached to the aeroplane

(D) Attached to the trajectory and to the aeroplane.

(A) *Dynamic Trihedrals*

We define a dynamic trihedral as any system of axes invariably attached to the aeroplane, and represent it, in a general way, by GXYZ .

Let G be the centre of gravity of the aeroplane. This point is the origin of the axes drawn along by the combined translational and rotational motions of the aeroplane.

All aeroplanes have a plane of symmetry. We shall find it convenient to position the axes GX and GZ in the plane of symmetry, placing axis GX along a particular direction of the aeroplane.

The trihedral will be clockwise, and the directions of the axes positive, as follows:

GX forwards

GY to the right (see Fig. 2)

GZ downwards.

We must find a suitable direction along which to place the axis GX . We may choose among the following:

---

*Professor, Universities of Gand and Liège, Belgium

(1) Direction of a principal axis of inertia;

(2) Direction of the wing chord. (This chord can be, at choice, the geometrical chord of the wing or the chord of no-lift);

(3) Projection V_s on the plane of symmetry, of the velocity attained at a predetermined instant $t = 0$, the axis so defined remaining attached to the aeroplane, whatever may be the future evolutions of the latter;

We thus obtain three different trihedrals; all, however, having the same axis OY.

The first trihedral depends on the mass distribution of the aeroplane. This is the inertia trihedral; it results in the greatest simplification in the writing of the equations of motion of the aeroplane, which contain no product of inertia.

The second trihedral is determined by the external configuration of the aeroplane (we call it the chord trihedral). Its use generally entails the introduction into the equations of the product of inertia. This trihedral is determined once and for all; the moments and product of inertia are invariable.

The third trihedral is determined by the intial conditions of flight. Its location on the aeroplane, and consequently the values of the moments and products of inertia, will depend on these initial flight conditions and may thus vary from one problem to another. This trihedral will be referred to by the expression: trihedral of initial conditions.

The angles included between the axes GX corresponding to the three definitions given above are as follows (see Fig.1):

α_0 - angle between direction V_{s0} and the chord;

ξ - angle between the chord and the axis of inertia.

We shall begin by using the chord trihedral, but from Section 3.1 onwards we shall refer the motion of the aeroplane to the trihedral of initial conditions, because of simplifications which will be introduced at that time.

The axes of the dynamic trihedral, whichever definition of the latter is used, are called 'body axes'.

(B) *Trihedral Attached to the Ground, or Geodetic Trihedral*

Let O be the position of an observer on the ground.

This point is the origin of a system of axes $OX'Y'Z'$ attached to the ground. Axis OZ' will be positive when directed vertically downwards. Axes OX' and OY' may be chosen arbitrarily, provided they are attached to the ground and the trihedral is clockwise. The trihedral so defined is the geodetic trihedral (see Fig.2).

(C) *Trihedrals Partially Attached to the Aeroplane*

It will be useful, for a better understanding of the problem, to define trihedrals whose origins are attached to the aeroplane but for which the directions of the axes are invariable. We shall use two trihedrals of this type. Both have the centre of gravity as origin.

(a) *Geoparallel trihedral $GX'Y'Z'$*

This trihedral is defined by the axes GX', GY', GZ', which remain always parallel to the axes fixed to the ground.

(b) *Trihedral of initial position $GX_0Y_0Z_0$*

This trihedral is defined by axes GX_0, GY_0, GZ_0, which remain always parallel to the directions which the body axes had at the instant $t = 0$.

The trihedrals so described, attached to the centre of gravity, are drawn along by the translational motions of the aeroplane, but not by its rotational motions.

(D) *Trihedrals Dependent on the Aeroplane's Trajectory*

These trihedrals will be defined in Section 1.4.

1.2 RELATIVE POSITION OF TWO TRIHEDRALS

Consider any two trihedrals $OX_0Y_0Z_0$, $OX_1Y_1Z_1$ having the same origin.

The relative orientation of two trihedrals may be defined in two different ways:

(a) By the direction cosines of the three axes of one trihedral in relation to the other;

(b) By a series of rotations bringing one trihedral into coincidence with the other.

We will now examine these two methods of approach.

(a) *Direction cosines*

Consider a unit vector along each of the axes OX_0, OY_0, OZ_0 and let:

l_1, m_1, n_1 be the projections on OX_1, OY_1, OZ_1 of unit vector along OX_0

l_2, m_2, n_2 be the projections of unit vector along OY_0

l_3, m_3, n_3 be the projections of unit vector along OZ_0 .

These 9 quantities constitute the direction cosines of the trihedral $OX_0Y_0Z_0$ in relation to the trihedral $OX_1Y_1Z_1$.

Let:

X_0, Y_0, Z_0 be the projections of a vector on the first trihedral

X_1, Y_1, Z_1 be the projections of the same vector on the second trihedral.

The direction cosines enable us to write the following matrix equations which constitute the transformation formulae:

$$\begin{bmatrix} X_1 \\ Y_1 \\ Z_1 \end{bmatrix} = \begin{bmatrix} l_1 & l_2 & l_3 \\ m_1 & m_2 & m_3 \\ n_1 & n_2 & n_3 \end{bmatrix} \begin{bmatrix} X_0 \\ Y_0 \\ Z_0 \end{bmatrix} \tag{1.1}$$

and conversely:

$$\begin{bmatrix} X_0 \\ Y_0 \\ Z_0 \end{bmatrix} = \begin{bmatrix} l_1 & m_1 & n_1 \\ l_2 & m_2 & n_2 \\ l_3 & m_3 & n_3 \end{bmatrix} \begin{bmatrix} X_1 \\ Y_1 \\ Z_1 \end{bmatrix} \tag{1.2}$$

(a-i) *Derivatives of direction cosines*

When trihedral 0 is fixed and trihedral 1 is in motion with angular velocity Ω, the direction cosines l_1 ..... n_3 will vary.

If for instance P, Q, R are the projections of Ω on axes OX_1, OY_1, OZ_1, the derivatives with respect to time of the direction cosines will be given by 9 relations, the first 3 of which are as follows:

$$\left.\begin{aligned} \dot{l}_1 &= m_1R - n_1Q \\ \dot{m}_1 &= n_1P - l_1R \\ \dot{n}_1 &= l_1Q - m_1P \end{aligned}\right\} \tag{1.3}$$

(b) *Rotations*

Let us first examine the case of two trihedrals $OX_0Y_0Z_0$, $OX_1Y_1Z_1$, motionless and independent, but with the same origin O. We can bring the trihedral $OX_0Y_0Z_0$ into coincidence with trihedral $OX_1Y_1Z_1$ by 3 successive rotations (Fig.3).

Several systems of rotation may be used. The most convenient one for the study of the motion of an aeroplane is as follows:

A rotation ψ about OZ_0, bringing OX_0 on to OX_i and OY_0 on to OY_i

A rotation θ about OY_i, bringing OX_i on to OX_1 and OZ_0 on to OZ_i

A rotation φ about OX_1, bringing OY_i on to OY_1 and OZ_i on to OZ_1.

Correlation between rotations and direction cosines can easily be established. Direction cosines are expressed in terms of the angles ψ, θ, φ in the following table (Table I):

TABLE I

Direction Cosines

Projection of unit vector along			*on*
OX_0	OY_0	OZ_0	
$l_1 = \cos\psi \cos\theta$	$l_2 = \sin\psi \cos\theta$	$l_3 = -\sin\theta$	OX_1
$m_1 = \cos\psi \sin\theta \sin\varphi - \sin\psi \cos\varphi$	$m_2 = \sin\psi \sin\theta \sin\varphi + \cos\psi \cos\varphi$	$m_3 = \cos\theta \sin\varphi$	OY_1
$n_1 = \cos\psi \sin\theta \cos\varphi + \sin\psi \cos\varphi$	$n_2 = \sin\psi \sin\theta \cos\varphi - \cos\psi \sin\varphi$	$n_3 = \cos\theta \cos\varphi$	OZ_1

(b-i) *Continuous rotation*

If trihedral 1 is subjected to a rotation of angular velocity Ω we may stop this trihedral in a series of instants t_n, t_{n+1}, ... and determine, for each of its positions, the rotations ψ, θ, φ which bring trihedral 0 on to the particular position of trihedral 1, without paying any attention to intermediate positions of the latter.

The angles ψ, θ, φ are functions of the instantaneous position of trihedral 1; they are thus functions of time.

One can establish the kinematic relations between the components P, Q, R of the angular velocity Ω of the rotation which brings the trihedral from position 0 to position 1, and the derivatives of the angles ψ, θ, φ with respect to time.

Thus we have:

$$\left.\begin{aligned} P &= \frac{d\varphi}{dt} - \frac{d\psi}{dt}\sin\theta \\ Q &= \frac{d\theta}{dt}\cos\varphi + \frac{d\psi}{dt}\cos\theta \sin\varphi \\ R &= \frac{d\psi}{dt}\cos\theta \cos\varphi - \frac{d\theta}{dt}\sin\varphi \end{aligned}\right\} \qquad (1.4)$$

or the inverse relations:

$$\left.\begin{aligned} \frac{d\varphi}{dt} &= P + \frac{\sin\theta}{\cos\theta}(Q\sin\varphi + R\cos\varphi) \\ \frac{d\theta}{dt} &= Q\cos\varphi - R\sin\varphi \\ \frac{d\psi}{dt} &= \frac{1}{\cos\theta}(Q\sin\varphi + R\cos\varphi) \end{aligned}\right\} \qquad (1.5)$$

A rotation $\theta = \pm \pi/2$ brings the axis OX into coincidence with OZ_0 and introduces $\cos\theta = 0$ into the previous formulae. This constitutes a singularity.

If the description of a motion actually performed is represented by the rotation described previously and leads to $\theta = \pm \pi/2$, the rotation system chosen must be discarded and another system chosen.

1.3 POSITION AND MOTION OF THE AEROPLANE IN SPACE

The position of the aeroplane in space is determined at any instant t by six elements which are functions of time:

(a) The three coordinates x_g, y_g, z_g of its centre of gravity, with respect to the geodetic trihedral $OX'Y'Z'$;

(b) The three angles Ψ, Θ, Φ defining the magnitude of the rotations one must carry out in the order indicated above to bring the geoparallel trihedral to the position occupied *at the instant* t by the dynamic trihedral attached to the aeroplane. These angles, therefore, determine the position of the aeroplane at any moment with respect to the geoparallel trihedral.

The position of the dynamic trihedral at instant $t = 0$ defines the initial trihedral $OX_0Y_0Z_0$. Let Ψ_0, Θ_0, Φ_0 be the angles defining the position of that trihedral with respect to the geoparallel trihedral.

If we want to determine the successive positions of the aeroplane with respect to the initial trihedral, we shall use angles ψ, θ, φ. These angles are *not* at all equal to the differences $\Psi - \Psi_0$, $\Theta - \Theta_0$, $\Phi - \Phi_0$. This is easy to see when we consider the particular case of an aeroplane the initial position $GX_0Y_0Z_0$ of which is any position, and the angular motion a rotational velocity Ω about the vertical (Fig.4).

The angles defining the position of the dynamic trihedral with respect to the geoparallel trihedral are:

at instant $t = 0$: Ψ_0, Θ_0, Φ_0

at instant $t = dt$: Ψ, Θ, Φ.

We have, therefore:

$$\Psi - \Psi_0 = \int \Omega dt$$

$$\Theta - \Theta_0 = 0$$

$$\Phi - \Phi_0 = 0$$

The rotations ψ, θ, φ, which express the same displacement, are the projections of the vector Ωdt on the axes GZ_0, GY_1, GZ; these three projections are generally different from zero.

The *motion* of the aeroplane at any instant is determined by two vectorial quantities:

(a) The velocity V of its centre of gravity

(b) The angular velocity Ω about the instantaneous axis of rotation.

An observer placed on the aeroplane will define the motion by the projections of V and Ω on the dynamic axes.

Let $\mathfrak{U}$, $\mathfrak{V}$, $\mathfrak{W}$ be the projections of V

P, Q, R be the projections of Ω.

The quantities

$$\frac{\mathfrak{U}}{V}, \frac{\mathfrak{V}}{V}, \frac{\mathfrak{W}}{V}$$

$$\frac{Pb}{2V}, \frac{Qc}{2V}, \frac{Pb}{2V}$$

are non-dimensional expressions of these components.

A motionless observer, that is to say an observer on the ground, will define the motion by the projections of V and Ω on the geodetic (or geoparallel) axes.

Let $\mathfrak{U}'$, $\mathfrak{V}'$, $\mathfrak{W}'$ be the projections of V on axes OX', OY', OZ'

P', Q', R' be the projections of Ω.

The table of direction cosines (Table I) enables us to proceed from the projections on the dynamic trihedral to the projections on the geodetic trihedral, knowing the instantaneous values of Ψ, Θ, Φ.

1.4 TRIHEDRALS DEPENDING ON VELOCITY

The two following trihedrals depend both on the velocity vector and on certain elements of the aeroplane (see Fig. 5):

(A) *Velocity Trihedral, Represented by* $Gx_v y_v z_v$

Axis Gx_v is directed along velocity vector.

Axis Gz_v will be the perpendicular to Gx_v, contained in the plane of symmetry and directed downwards. It will thus be the intersection of the plane of symmetry with the plane perpendicular to Gx_v at G .

Axis Gy_v will be perpendicular to the above two axes and will be directed towards the right.

(B) *Aerodynamic Trihedral, Represented by* Gxyz

Let V_s be the projection of the velocity on the plane of symmetry.

Axis Gx will be directed along this projection.

Axis Gz will be the axis perpendicular to the above axis, contained in the plane of symmetry and directed downwards.

Axis Gy will be normal to the plane of symmetry and directed towards the right.

This trihedral will here be called the aerodynamic trihedral.

Trihedrals $Gx_v y_v z_v$ and Gxyz have the common axis Gz. Therefore a simple rotation about axis Gz is sufficient to go from one to the other. Let us call β the rotation in a positive direction necessary to bring trihedral Gxyz into coincidence with trihedral $Gx_v y_v z_v$. The angle β is the angle of side-slip.

The aerodynamic trihedral Gxyz and the dynamic trihedral also have a common axis Oy, whichever definition is chosen for the trihedral.

We can always bring the trihedral Gxyz into coincidence with trihedral GXYZ by a rotation about axis Oy. Let α be this rotation when the dynamic trihedral GXYZ is the chord trihedral. The angle α is the angle of attack.

Combining rotations β and α it is possible to bring the velocity trihedral $Gx_v y_v z_v$ into coincidence with the dynamic chord trihedral GXYZ. A rotation $-\beta$ brings $Gx_v y_v z_v$ on to Gxyz; a rotation α brings Gxyz on to GXYZ.

Two rotations are sufficient to obtain this result because the velocity trihedral and the dynamic trihedral are not completely independent. Direction cosines for the axes Gx_v, Gy_v, Gz_v with respect to the chord trihedral are given in Table II.

The projections of the velocity on the dynamic axes are:

$$\left.\begin{aligned} U &= V \cos\alpha \cos\beta \\ V &= V \sin\beta \\ W &= V \sin\alpha \cos\beta \end{aligned}\right\} \qquad (1.6)$$

TABLE II

Direction Cosines

Gx_V	Gy_V	Gz_V	*in relation to*
$\cos\alpha \cos\beta$	$-\cos\alpha \sin\beta$	$\sin\alpha$	Gx
$\sin\beta$	$\cos\beta$	0	Gy
$\sin\alpha \sin\beta$	$-\sin\alpha \sin\beta$	$\cos\alpha$	Gz

Knowing V, α and β is equivalent to knowing the three projections U, V, W.

Note

The angle α_0, defined in Section 1.1, is nothing but the angle of attack at the instant $t = 0$.

Let α be the angle defined by axes Gx and GX of the trihedral of initial conditions. Then

$$\alpha = \alpha - \alpha_0$$

α represents the increase in angle of attack during a manoeuvre.

The position of the velocity trihedral will be defined with respect to the trihedral of initial position by means of a table similar to Table II, with α replaced by α.

1.5 MOTIONS OF THE ATMOSPHERE ITSELF

The velocity V considered up to now is the aeroplane's absolute velocity. The atmosphere in which the aeroplane manoeuvres, however, may have its own motions.

Let the vector V_a represent the air velocity at a point in the atmosphere.

In the most simple case, the vectors V_a acting at all points of a space large enough to contain the entire aeroplane are supposed to be equipollent.

The aeroplane will then be surrounded by a mass of air having the same true air velocity. The relative velocity of the aeroplane with respect to the ambient air will be $V_r = V - V_a$. The projections of V_r and V_a will be respectively:

U_r, V_r, W_r and U_a, V_a, W_a on the dynamic axes

U'_r, V'_r, W'_r and U'_a, V'_a, W'_a on the geoparallel axes.

A less regular distribution of air velocities can be imagined. If the true air velocity varies from one point to another close to the aeroplane, the derivatives $\partial U_a/\partial x$ ..... $\partial W_a/\partial z$ will no longer be zero (x, y, z here being the distances to the centre of gravity, measured in a direction parallel to the body axes). An unequal distribution of W_a along the span or the length corresponding to $\partial W_a/\partial y \neq 0$ or $\partial W_a/\partial x \neq 0$ subjects the aeroplane to rolling or pitching moments. The following analysis does not anticipate the advent of such components and is limited to the case of equipollent vectors V_a.

Note

A more general survey which supposes the derivatives $\partial W_a/\partial y$, $\partial W_a/\partial x$, ... not to be zero but of constant value in the whole space occupied by the aeroplane, is possible. Such a distribution of atmospheric motions is equivalent to the appearance of a rotational component P_a or Q_a of that motion. An uneven distribution of U_a along the span, giving $\partial U/\partial y \neq 0$, would be equivalent to a rotational component R_a of that motion. The introduction of such components in our study does not seem necessary.

1.6 ANGLES OF ATTACK AND SIDE-SLIP

If we tie a trihedral $Gx_{vr}y_{vr}z_{vr}$ to the relative velocity V_r as we did when we defined the trihedral Gxyz with respect to the absolute velocity, and if we carry out the same reasoning as in Section 1.4, we shall be able to define the body axes with respect to the trihedral $Gx_{vr}y_{vr}z_{vr}$ by means of two angles which we shall now call β_r and α_r (see Fig. 6).

These angles are the real angles of side-slip and attack, whereas the angles β and α defined previously are only apparent angles of side-slip and attack.

The aerodynamic reactions exerted on an aeroplane depend on real angles of side-slip and attack, and not on the apparent angles. Real angles and apparent angles coincide when the atmosphere does not have motion of its own; no distinction is to be made in this case.

On the other hand, when the atmosphere has its own motions (especially if these are variable) one must make the distinction between the two series of angles.

Note. Stability axes are frequently referred to in the literature, but the definition of these axes varies with different authors. Most define stability axes as the kind of body axes determined by the trihedral of initial conditions. Others call stability axes those which are defined by the aerodynamic trihedral. For this reason, we do not use the expression 'stability axes' here.

CHAPTER 2

DYNAMICS OF THE AEROPLANE WITH A RIGID STRUCTURE

F.C.Haus

We make a distinction between the non-rigid aeroplane that can be deformed under the action of exterior forces, and the aeroplane with a rigid structure which cannot be deformed by such forces. Chapter 4 is concerned with non-rigid structures. Chapters 2 and 3 deal with the rigid aeroplane.

2.1 STRUCTURAL DEFORMATION AND CONFIGURATION OF THE AEROPLANE

Two preliminary remarks must be made:

(a) *Control surfaces*

The aeroplane with a rigid structure has movable control surfaces. The displacement of these surfaces will not be considered here as a deformation of the structure of the aeroplane, but as a change in its configuration.

The position of the 3 main controls will be defined by the following deflection angles:

δ_e position of the elevator

δ_a position of the ailerons

δ_r position of the rudder.

As a particular case of the deformation δ_e, we have the displacement of the horizontal part of the tail unit when it is entirely movable.

Positive directions are:

For δ_e rotation causing increase of the angle of attack

δ_a displacement of the right aileron downwards

δ_r rotation in the direction of positive R .

Displacements δ_e, δ_a, δ_r of the control surfaces are produced by pilot action, human or automatic.

Besides these principal deformations, there are several others, corresponding to the displacement of various auxiliary surfaces: flaps, spoilers, etc. These displacements will be defined, as we proceed, by appropriate symbols.

(b) *Masses in rotational motion*

We shall write in Section 2.3 the equations of motion of the aeroplane considering it as made up of an assemblage of fixed masses. But the aeroplane is a system possessing moving interior masses, namely the rotors of the turbo-reactors and the propellers. Under the action of the velocities and accelerations of the centre of gravity, these moving masses will exert reaction forces on the structure of the aeroplane.

These reactions have been studied theoretically a number of times by Duncan and others[1]. They can be converted to gyrostatic actions as long as the propellers have at least three blades.

The equations of motion of the aeroplane, written for a system of fixed masses, may be used, provided that the gyrostatic actions be considered as external forces transmitted through the engine or turbo-prop mounting.

2.2 EXTERNAL ACTIONS

External forces and moments acting on the aeroplane are essentially:

gravity

aerodynamic forces exerted by the ambient medium.

We must, in accordance with the above remarks, add the gyroscopic effects.

2.2.1 Gravity Force

Let m be the mass of the aeroplane.

Gravity exerts a force mg, always applied at the centre of gravity and directed vertically. Its components along geoparallel axes are thus: 0, 0, mg (Fig.7).

Its components along the dynamic axes,

$$(mg)_x, \qquad (mg)_y, \qquad (mg)_z$$

can be obtained from the following general expressions:

$$\left.\begin{aligned} (mg)_x &= -\, mg \sin\Theta \\ (mg)_y &= +\, mg \cos\Theta \sin\Phi \\ (mg)_z &= +\, mg \cos\Theta \cos\Phi \end{aligned}\right\} \qquad (2.1)$$

in which angles Θ and Φ determine, at any instant, the position of the body axes with respect to the geoparallel axes. These expressions are useful only if quantities Θ and Φ are given explicitly, which is not always the case. The position of the dynamic trihedral may be defined by rotations ψ, θ, φ from an initial trihedral $GX_0Y_0Z_0$ different from the geoparallel trihedral, and itself defined by 3 angles Ψ_0,

Θ_0, Φ_0. We must then perform a double transformation to find the projections of the gravity force on the dynamic axes.

A first projection of vector 0, 0, mg on trihedral $GX_0Y_0Z_0$ gives:

$$\left.\begin{aligned} mg_{x0} &= -\, mg \sin\Theta_0 \\ mg_{y0} &= +\, mg \cos\Theta_0 \sin\Phi_0 \\ mg_{z0} &= +\, mg \cos\Theta_0 \cos\Phi_0 \end{aligned}\right\} \qquad (2.2)$$

Applying the direction cosines table, each of these quantities supplies 3 components on trihedral GXYZ.

Thus we have the following:

$$\left.\begin{aligned} mg_x &= -\, mg \sin\Theta_0 \cos\theta \cos\psi \\ &\quad + mg \sin\Phi_0 \cos\Theta_0 \cos\theta \sin\psi \\ &\quad - mg \cos\Phi_0 \cos\Theta_0 \sin\theta \\ mg_y &= -\, mg \sin\Theta_0 (-\cos\varphi \sin\psi + \sin\varphi \sin\theta \cos\psi) \\ &\quad + mg \sin\Phi_0 \cos\Theta_0 (\cos\varphi \cos\psi + \sin\varphi \sin\theta \sin\psi) \\ &\quad + mg \cos\Phi_0 \cos\Theta_0 (\sin\varphi \cos\theta) \\ mg_z &= -\, mg \sin\Theta_0 (\sin\varphi \sin\psi + \cos\varphi \sin\theta \cos\psi) \\ &\quad + mg \sin\Phi_0 \cos\Theta_0 (-\sin\varphi \cos\psi + \cos\varphi \sin\theta \sin\psi) \\ &\quad + mg \cos\Phi_0 \cos\Theta_0 (\cos\theta \cos\varphi) \end{aligned}\right\} \qquad (2.3)$$

When the angles ψ, θ, φ are small, these expressions can be linearized.

Assuming sines of ψ, θ, φ equal to the angles ψ, θ, φ, and cosines equal to unity, and neglecting sine products, the projections become:

$$\left.\begin{aligned} mg_x &= mg[-\sin\Theta_0 + (\sin\Phi_0 \cos\Theta_0)\,\psi - (\cos\Phi_0 \cos\Theta_0)\theta] \\ mg_y &= mg[\sin\Phi_0 \cos\Theta_0 + (\sin\Theta_0)\,\psi + (\cos\Phi_0 \cos\Theta_0)\varphi] \\ mg_z &= mg[\cos\Phi_0 \cos\Theta_0 - (\sin\Phi_0 \cos\Theta_0)\,\psi - (\sin\Theta_0)\theta] \end{aligned}\right\} \qquad (2.4)$$

2.2.2 Aerodynamic Forces

Forces exerted by the ambient medium may be divided as follows:

(A) Aerodynamic forces and moments exerted by the ambient medium on the outer surfaces of the aeroplane;

(B) Forces and moments exerted by the ambient medium or by fluids acting upon the propulsive parts of the aeroplane.

Forces (A), which act upon the *outer surface* of the aeroplane, can always be reduced to a resultant force F and a moment C.

Forces (B) are exerted by the propellers, the fixed or moving turbine blades, and the inside walls of the nozzles; they are finally transmitted to the structure of the aeroplane.

These forces comprise a thrust T and a moment Q. In the case of a jet-propelled aeroplane, we may consider these two categories of efforts as being produced by:

the outside flow

the inside flow.

The projections of the sum (F + T) on the dynamic axes are represented by X, Y, Z.

The projections of the sum (C + Q) will be represented by L, M, N.

These components are expressed as functions of the relative velocity by non-dimensional factors C_x ..... C_n (incorrectly called coefficients):

$$\left.\begin{aligned} X &= C_x \, S \, \tfrac{1}{2}\rho V^2 & L &= C_l \, b \, S \, \tfrac{1}{2}\rho V^2 \\ Y &= C_y \, S \, \tfrac{1}{2}\rho V^2 & M &= C_m \, c \, S \, \tfrac{1}{2}\rho V^2 \\ Z &= C_z \, S \, \tfrac{1}{2}\rho V^2 & N &= C_n \, b \, S \, \tfrac{1}{2}\rho V^2 \end{aligned}\right\} \qquad (2.5)$$

in which S is the wing area

b is the wing span

c is the wing chord

ρ is the specific density of the air.

A distinction must be made between steady motion, quasi-stationary motion, and variable motion.

Aerodynamic forces depend, in the case of steady motion, on values (supposed constant) of a certain number of variables. These are listed below.

In quasi-stationary motion, it can be assumed that the aerodynamic forces are, at any moment, completely defined by the values of the same variables and their derivatives at the instant under consideration.

Variable motion is that in which we cannot determine the aerodynamic forces at a chosen instant, without allowing for previous history.

The following is concerned with steady flow. Quasi-stationary and variable flows will be studied in Sections 3.2 and 3.9. The analysis of forces and moments leads us to study separately the different aerodynamic forces:

(A) *Outside Flow*

Let us represent by C_{xa} ..... C_{na} that part of the coefficients C_x ..... C_n due to outside flow.

The factors C_{xa} ..... C_{na} depend on:

(a) The real incidence and side-slip angles α_r and β_r, themselves functions of the components U, V, W, U_a, V_a, W_a

(b) The angular velocities, generally expressed by non-dimensional factors

(c) The Mach number M

(d) The outside configuration of the aeroplane, defined by various deformations δ

(e) The action exerted by the propulsive unit on the external flow.

(B) *Inside Flow*

The reaction forces of the engine unit comprise:

(1) The alteration of factors C_{xa} ..... C_{na} due to the action of the propulsion system on the outside flow, referred to in (e) above;

(2) The effects produced directly by the propulsive units, which can be reduced to a force T and a couple Q.

The direct and indirect effects of the motor-propulsion unit depend on the variables which define the functioning of the motor-propulsion system.

In the case of a motor-propulsion unit equipped with a variable-pitch propeller (constant speed propeller), the pilot has two controls by which he can alter:

the admission pressure of the gas

the revolutions per minute.

In the case of a jet-propulsion system, the pilot controls the fuel flow by regulating the pump output. When large variations in fuel flow are foreseen (afterburning) the nozzle outlet section of the diffuser must be variable. Finally, variations in velocity sometimes need modifications of the inlet section of the jet.

In most of the problems relative to the dynamics of the aeroplane, we can characterize the reactions of a motor-propulsion unit by a single variable which defines the power symbolically. We shall call this variable δ_m. It constitutes a degree of freedom for the pilot.

Physically, δ_m will represent the manifold pressure in the case of a piston engine, or the output of the injection pump in the case of a jet engine.

In order to take into account the reactions produced by the outside flow, in the general expressions given above, the force T and moment Q will have to be defined by factors T_c and Q_c so that:

$$\begin{aligned} T &= T_c \, \mathcal{S} \, \tfrac{1}{2}\rho V^2 \\ Q &= Q_c \, \mathcal{S} \, l \, \tfrac{1}{2}\rho V^2 \end{aligned} \tag{2.6}$$

in which $\mathcal{S}$ and l represent a surface and length conventionally defined.

The projections

$$(T_c)_x, \qquad (T_c)_y, \qquad (T_c)_z$$

$$(Q_c)_x, \qquad (Q_c)_y, \qquad (Q_c)_z$$

of previous factors will have to be added to the factors representing the effect of outside flow in order to obtain the factors defining the total aerodynamic reaction:

$$\begin{aligned} C_x &= C_{x,a} + (T_c)_x \frac{\mathcal{S}}{S} & \qquad C_l &= C_{l,a} + (Q_c)_x \frac{\mathcal{S}}{S}\frac{b}{l} \\ C_y &= C_{y,a} + (T_c)_y \frac{\mathcal{S}}{S} & \qquad C_m &= C_{m,a} + (Q_c)_y \frac{\mathcal{S}}{S}\frac{c}{l} \\ C_z &= C_{z,a} + (T_c)_z \frac{\mathcal{S}}{S} & \qquad C_n &= C_{n,a} + (Q_c)_z \frac{\mathcal{S}}{S}\frac{b}{l} \end{aligned} \tag{2.7}$$

The use of coefficients T_c and Q_c leads to certain difficulties in practice. Quantities T and Q vary little with velocity. Their representation, as a function of the square of the velocity, introduces factors T_c and Q_c which will vary greatly with speed.

In the theoretical study, we shall nevertheless still make use of the overall aerodynamic forces X, Y, Z, L, M, N and of corresponding coefficients, in order to reduce the number of terms appearing in the formulae. This does not mean that we shall not, in the examples considered, deal separately with forces due to inside and outside flow.

Note

When no confusion is possible between total forces and forces due to outside flow, we shall discontinue using the subscript a for the latter.

Particular Cases

It is possible to design controls producing moments about the 3 axes by using compressed jets, acting on a lever arm in such a way that the reactions produced by

these jets exert moments. The fluid used is taken from the interior flow. The moments exerted will depend on the nozzle output and will vary little with the speed of the aeroplane. These jet controls are interesting for vertical take-off aeroplanes.

The case of jet controls is not foreseen, either in this study or in the examples considered. It could easily be considered, however.

2.2.3 Gyroscopic Effects

Gyroscopic couples, considered, by virtue of what has already been said, as exterior actions, will be expressed as follows:

Let I be the moment of inertia of the gyroscope

ω its angular velocity of rotation

ω_x, ω_y, ω_z, its projections on the dynamic axes.

Under the action of the rotation Ω, with components P, Q, R applied to the whole aeroplane, the gyroscope exerts a reaction couple Q which can be written in vectorial notation as follows:

$$\vec{Q}_g = I\,\vec{\omega} \wedge \vec{\Omega} \tag{2.8}$$

The components of this reaction couple are:

$$\left.\begin{aligned} L_g &= I\,(\omega_y R - \omega_z Q) \\ M_g &= I\,(\omega_z P - \omega_x R) \\ N_g &= I\,(\omega_x Q - \omega_y P) \end{aligned}\right\} \tag{2.9}$$

These expressions become simpler when the axis of rotation of the gyroscope is parallel to the plane of symmetry of the aeroplane.

In that case, if λ is the angle between the axis of the gyroscope and the axis OX, we have:

$$\left.\begin{aligned} \omega_x &= \omega \cos\lambda \\ \omega_y &= 0 \\ \omega_z &= -\omega \sin\lambda \end{aligned}\right\} \tag{2.10}$$

and the components of the gyroscopic couple become:

$$\left.\begin{aligned} L_g &= I\,\omega\,Q \sin\lambda \\ M_g &= I\,\omega\,(-P \sin\lambda - R \cos\lambda) \\ N_g &= I\,\omega\,Q \cos\lambda \end{aligned}\right\} \tag{2.11}$$

2.3 GENERAL EQUATIONS OF MOTION OF AN AEROPLANE

Let us now proceed to the equations of motion with reference to the body axes.

The mass m and the moments of inertia are assumed constant. Let I_x, I_y, I_z be the moments of inertia about the dynamic axes, and I_{xz} the product of inertia about the axes GX and GZ. The products of inertia I_{xy} and I_{yz} are zero, the plane XGZ being a plane of symmetry.

The equations of motion of the aeroplane can be written in vectorial form as follows, $\vec{m}$ being the kinetic momentum:

$$\left.\begin{aligned} m\frac{d\vec{V}}{dt} + m\,\vec{\Omega} \wedge \vec{V} &= \vec{F} + \vec{T} + m\vec{g} \\ \frac{d\vec{m}}{dt} + \vec{\Omega} \wedge \vec{m} &= \vec{C} + \vec{Q} + \vec{Q}_g \end{aligned}\right\} \qquad (2.12)$$

For the dynamic axes, the equations of motion may be written in the algebraic form:

$$\left.\begin{aligned} m\left(\frac{du}{dt} + qw - rv\right) &= X + (mg)_x \\ m\left(\frac{dv}{dt} + ru - pw\right) &= Y + (mg)_y \\ m\left(\frac{dw}{dt} + pv - qu\right) &= Z + (mg)_z \\ I_x\frac{dp}{dt} - I_{zx}\frac{dr}{dt} + (I_z - I_y)\,qr - I_{zx}\,pq &= L + L_g \\ I_y\frac{dq}{dt} + (I_x - I_z)\,pr + I_{zx}\,(p^2 - r^2) &= M + M_g \\ I_z\frac{dr}{dt} - I_{zx}\frac{dp}{dt} + (I_y - I_x)\,pq + I_{zx}\,qr &= N + N_g \end{aligned}\right\} \qquad (2.13)$$

The product of inertia I_{zx} becomes zero if we choose the inertia trihedral as the system of dynamic axes. The projections of the gravity force are given by Equation (2.4) as a function of the variables ψ, θ, φ and initial conditions Ψ_0, Θ_0, Φ_0.

The gyroscopic couples are given by Equation (2.11) as a function of P, Q, R. The forces and aerodynamic moments are functions (considered as known) of the variables u, v, w, P, Q, R and their derivatives, and, also, of the other above-mentioned parameters. These parameters, which we consider as excitations or inputs, are:

The positions of the control surfaces: δ_e, δ_a, δ_r

The working characteristics of the motor-propulsion units determined by the engine controls, δ_m

The dragging velocities $\mathcal{U}_a$, $\mathcal{V}_a$, $\mathcal{W}_a$ of the ambient medium.

The kinematic relations (Eqn.(1.5)) give rise to 3 more equations, relating derivatives of the angles φ, θ, ψ to the angular velocities. We thus obtain a system of 9 equations with 9 variables, the integration of which is possible when the excitations are known as functions of time.

Note

(1) *Permanent movements*

The expression for gravity projections as a function of angles Ψ, Θ, Φ shows that the only displacement for which these projections remain constant is a helical displacement about a vertical axis (Ψ variable, Θ and Φ constant). This displacement constitutes therefore the only possible permanent movement.

Circular flying at constant altitudes, straight and level or inclined flying, constitute degenerated cases of this movement.

(2) *Accelerations and loading factors*

Let us call j_x, j_y, j_z the acceleration components of the centre of gravity. Then

$$\left.\begin{aligned} j_x &= \frac{d\mathcal{U}}{dt} + Q\mathcal{W} - R\mathcal{V} \\ j_y &= \frac{d\mathcal{V}}{dt} + R\mathcal{U} - P\mathcal{W} \\ j_z &= \frac{d\mathcal{W}}{dt} + P\mathcal{V} - Q\mathcal{U} \end{aligned}\right\} \qquad (2.14)$$

The following quantities, viz.

$$\left.\begin{aligned} a_x &= j_x - g_x \\ a_y &= j_y - g_y \\ a_z &= j_z - g_z \end{aligned}\right\} \qquad (2.15a)$$

equal to the acceleration minus the gravity force, may be considered as generalized accelerations; they may be measured by accelerometers. Taken with opposite sign, they represent an apparent gravity force in the direction of the axes.

The quantity

$$n = -\frac{a_z}{g} = \cos\Theta\cos\Phi - \frac{1}{g}\left(\frac{dW}{dt} + QU - PV\right) \qquad (2.15b)$$

constitutes the loading factor of the wings. It is equal to 1 in straight and level flight.

Any quantity $\Delta n = n-1 > 0$ indicates an overload. It is useful to recall here the acceleration components at a point distinct from the centre of gravity.

Let x, y, z be the coordinates of point P, measured from the centre of gravity. Components j_{Px}, j_{Py}, j_{Pz} of the acceleration at point P will be given by 3 formulae of which only the third is given here:

$$j_{Pz} = j_z + \frac{dp}{dt}y - \frac{dq}{dt}x + p(rx - pz) - q(qz - ry)$$

The acceleration components, minus the apparent gravity, will be, at point P :

$$a_{Px} = j_{Px} - g_x$$

$$a_{Py} = j_{Py} - g_y$$

$$a_{Pz} = j_{Pz} - g_z$$

2.4 CONTROL SURFACES

The deflections of the control surfaces come into the previous equations by their influence on the aerodynamic forces and moments X ..... N. In the most general case, the aerodynamic forces and moments depend on the angles of deflection and their successive derivatives.

A rigorous theory should take into account the effect of the displacement of the control surfaces on the terms of inertia.

The theory explained by M. Czinczenheim, in Section 4.3.1, takes this effect into account; terms in $\ddot{\delta}$ are added to Equations (2.13), but this effect is of little importance and is always neglected.

If positions δ_e, δ_a, δ_r of the 3 control surfaces actually constitute excitations of the aeroplane's motion, these parameters are, nevertheless, not variables of which the magnitude is given explicitly at each moment.

Even in the simplest case of a control corresponding to the scheme in Figure 113, where the position δ_e of the control surface is connected with the position δ_s of the control column, the pilot takes little notice of the position of the stick and is interested in nothing but the force F he must exert on it.

The position of the control surface is a result of an equilibrium between the different moments applied around the hinge. This is expressed in the last group of terms in Equation 4.45, where we have represented:

the moment H_r transmitted by the control gear

the aerodynamic hinge moment H equal to $H_\delta \delta + H_{\dot\delta} \dot\delta + H_{\ddot\delta} \ddot\delta$

and, depending consequently on the position of the control surface,

the inertia reactions of the control surface.

Free control flying appears as a particular case, in which the moment H_r transmitted by the control gear is zero.

These remarks are made here to show that the system will have to be completed by equations defining the deflections δ_e, δ_a, δ_r in relation to the variables which determine them.

These equations will take particular forms depending on the practical means adopted: e.g., direct controls, servo-controls, having or not an artificial feel device.

2.5 VELOCITY AND LOAD DISTURBANCES

It is best to change variables every time the evolution studied has a permanent motion as starting point at instant $t = 0$, and to adopt new variables called perturbation variables.

(A) *Disturbance Velocities*

Consider a steady motion determined by:

Constant values of linear and angular velocities, which we shall call u_0, v_0, w_0, p_0, q_0, r_0;

Fixed positions of control surfaces, which we shall conventionally take as origin of displacements δ_e, δ_a, δ_r;

Constant values of Θ and Φ, which we shall write as Θ_0 and Φ_0.

We have:

$$V_0 = \sqrt{u_0^2 + v_0^2 + w_0^2}$$

This steady motion takes place at instant $t = 0$.

Any action of the pilot on the controls, any atmospheric disturbance, any irregularity of the propulsive unit occurring at $t > 0$, will modify the motion. The aeroplane will describe a trajectory defined by velocities

$$\left.\begin{aligned} U &= u_0 + u & P &= p_0 + p \\ V &= v_0 + v & Q &= q_0 + q \\ W &= w_0 + w & R &= r_0 + r \end{aligned}\right\} \qquad (2.16)$$

The increments

$$u, \quad v, \quad w$$

$$p, \quad q, \quad r$$

are called perturbation velocities.

(B) *Aerodynamic Forces*

Any aerodynamic action X ..... N will be considered as made up of the sum of the action at instant $t = 0$ and of an increment. We write:

$$X = X_0 + \Delta X$$

.....

$$N = N_0 + \Delta N$$

Forces at instant $t = 0$ and increments will be expressed in terms of velocity V_0 by:

$$\left.\begin{aligned} X = X_0 + \Delta X &= (C_{X0} + \Delta C_X)\ S\ \tfrac{1}{2}\rho V_0^2 \\ &\cdots\cdots\cdots\cdots\cdots\cdots\cdots\cdots\cdots \\ N = N_0 + \Delta N &= (C_{N0} + \Delta C_N)\ S\ b\ \tfrac{1}{2}\rho V_0^2 \end{aligned}\right\} \qquad (2.17)$$

Factors ΔC_X, ΔC_Y, ... ΔC_N are functions of:

(a) the characteristics of the initial steady motion

(b) the instantaneous values of:

$$\left.\begin{aligned} \hat{u} = \frac{u}{V_0}, \quad \hat{v} = \frac{v}{V_0}, \quad \hat{w} = \frac{w}{V_0}, \\ \hat{p} = \frac{pb}{2V}, \quad \hat{q} = \frac{qc}{2V}, \quad \hat{r} = \frac{rb}{2V} \end{aligned}\right\} \qquad (2.18)$$

(c) the derivatives of the preceding quantities

(d) the excitations communicated to the aeroplane, including the control movements and atmospheric disturbances.

(C) *Orientation of the Aeroplane*

The position of the dynamic trihedral is determined, in the initial conditions, by the angles Θ_0 and Φ_0, and in every one of the successive positions by 3 rotations ψ, θ, φ to be operated from $GX_0Y_0Z_0$.

The projections of gravity will be subjected to increments which are functions of ψ, θ, φ.

2.6 EQUATIONS OF MOTION FOLLOWING A STEADY STATE

The steady state defined above is realized at instant $t = 0$, and satisfies the following equations:

$$\left.\begin{aligned}
m(q_0 w_0 - r_0 v_0) &= X_0 + (mg_{x0}) \\
m(r_0 u_0 - p_0 w_0) &= Y_0 + (mg_{y0}) \\
m(p_0 v_0 - q_0 u_0) &= Z_0 + (mg_{z0}) \\
(I_z - I_y)\, q_0 r_0 - I_{zx}\, q_0 p_0 &= L_0 - I\omega\, q_0 \sin\lambda \\
(I_x - I_z)\, r_0 p_0 + I_{zx}(p_0^2 - r_0^2) &= M_0 + I\omega(p_0 \sin\lambda - r_0 \cos\lambda) \\
(I_y - I_x)\, p_0 q_0 + I_{zx}\, q_0 r_0 &= N_0 + I\omega\, q_0 \cos\lambda
\end{aligned}\right\} \qquad (2.19)$$

The ensuing motion produced by a known excitation or input (pilot's order, atmospheric disturbance) satisfies the general Equations (2.13) in which we replace:

each variable, such as u, by $u_0 + u$

aerodynamic forces, such as X, by $X_0 + \Delta X$

and in which we introduce the projections of the gravity forces, defined by Equations (2.4), in their linearized form.

Let us subtract Equation (2.19) for the steady state from the modified Equations (2. In expressions such as:

$$\begin{aligned}
(QW - q_0 w_0) &= [(q_0 + q)(w_0 + w) - q_0 w_0] \\
&= q_0 w + w_0 q + qw
\end{aligned}$$

we neglect the product qw of the perturbation velocities.

We are left with the following system:

$$\left.\begin{aligned}
m\left[\frac{du}{dt} + (q_0 w + w_0 q) - (r_0 v + v_0 r)\right] &= \Delta X + mg[(\sin\Phi_0 \cos\Theta_0)\psi - (\cos\Phi_0 \cos\Theta_0)\theta] \\
m\left[\frac{dv}{dt} + (r_0 u + u_0 r) - (p_0 w + w_0 p)\right] &= \Delta Y + mg[(\sin\Theta_0)\psi + (\cos\Phi_0 \cos\Theta_0)\varphi] \\
m\left[\frac{dw}{dt} + (p_0 v + v_0 p) - (q_0 u + u_0 q)\right] &= \Delta Z + mg[-(\sin\Phi_0 \cos\Theta_0)\varphi - (\sin\Theta_0)\theta]
\end{aligned}\right\} \qquad (2.20)$$

$$
\left.
\begin{aligned}
I_x \frac{dp}{dt} - I_{zx} \frac{dr}{dt} + (I_z - I_y)(q_0 r + q r_0) - I_{zx}(q_0 p + p_0 q) &= \Delta L - I\omega\, q \sin\lambda \\
I_y \frac{dq}{dt} + (I_x - I_z)(r_0 p + p_0 r) + I_{zx}(2p_0 p - 2r_0 r) &= \Delta M + I\omega(-p \sin\lambda - r \cos\lambda) \\
I_z \frac{dr}{dt} - I_{zx} \frac{dp}{dt} + (I_y - I_x)(p_0 q + q_0 p) + I_{zx}(q_0 r + r_0 q) &= \Delta N + I\omega\, q \cos\lambda
\end{aligned}
\right\} \qquad (2.20)
$$

in which the exterior actions represented by their increments Δ must still be written in relation to the perturbation velocities and the excitations.

The system of equations is linear inasmuch as the expression of the exterior forces in relation to disturbances is itself linear.

The kinematic equations will be written by replacing, in the set of Equations (1.5), quantities P, Q, R by $(p_0 + p)$, $(q_0 + q)$, $(r_0 + r)$.

Assuming sines and tangents of φ and θ equal to the angles themselves, and cosines equal to unity, we get:

$$
\left.
\begin{aligned}
\frac{d\varphi}{dt} &= (p_0 + p) + (r_0 + r)\,\theta \\
\frac{d\theta}{dt} &= (q_0 + q) - (r_0 + r)\,\varphi \\
\frac{d\psi}{dt} &= (r_0 + r) - (q_0 + q)\,\varphi
\end{aligned}
\right\} \qquad (2.21)
$$

Linearization will lead finally to the neglecting of terms in $r\theta$, $r\varphi$, and $q\varphi$.

The motion of the aeroplane is thus defined by a system of 9 equations relating the variables:

$$u, \quad v, \quad w$$

$$p, \quad q, \quad r$$

$$\psi, \quad \theta, \quad \varphi$$

CHAPTER 3

TRANSFORMATION AND SOLUTION OF THE EQUATIONS OF MOTION OF A RIGID AEROPLANE

F.C.Haus

The object of this chapter is:

(1) To transform the system of equations developed in Chapter 2, in order to introduce non-dimensional quantities;

(2) To find out the extent to which the linearization is compatible with fact.

3.1 NON-DIMENSIONAL EXPRESSION OF THE PERTURBATION VELOCITIES

3.1.1 Linear and Angular Velocities

The quantities $\hat{u}$, $\hat{v}$, $\hat{w}$, $\hat{p}$, $\hat{q}$, $\hat{r}$, defined by formulae (2.18), are the non-dimensional perturbation velocities.

3.1.2 Angles of Attack and Side-Slip

The angles of attack and side-slip will be the sum of their values at instant $t = 0$, plus increments α and β:

$$\left.\begin{aligned} \boldsymbol{\alpha} &= \alpha_0 + \alpha \\ \boldsymbol{\beta} &= \beta_0 + \beta \end{aligned}\right\} \tag{3.1}$$

We intend to consider the increments α and β as fundamental variables.

3.1.3 Linear Velocities Expressed as a Function of Angles

Let us write

$$V = V_0\left(1 + \frac{\Delta V}{V_0}\right) \tag{3.2}$$

and introduce (3.1) and (3.2) in expressions (1.6). We find the projections U, V, W to be:

$$\left.\begin{aligned} U = u_0 + u = V_0\left(1 + \frac{\Delta V}{V_0}\right)\cos(\alpha_0 + \alpha)\,\cos(\beta_0 + \beta) \end{aligned}\right\}$$

$$\left.\begin{aligned} \mathcal{V} &= v_0 + v = V_0\left(1 + \frac{\Delta V}{V_0}\right)\sin(\beta_0 + \beta) \\ \mathcal{W} &= w_0 + w = V_0\left(1 + \frac{\Delta V}{V_0}\right)\sin(\alpha_0 + \alpha)\cos(\beta_0 + \beta) \end{aligned}\right\}$$

Let us develop these expressions assuming that the perturbations of angles α and β remain small ($\sin\alpha = \alpha$, $\cos\alpha = 1$) and that the products of the perturbations may be neglected.

We get:

$$\left.\begin{aligned} u_0 &= V_0 \cos\alpha_0 \cos\beta_0 \\ v_0 &= V_0 \sin\beta_0 \\ w_0 &= V_0 \sin\alpha_0 \cos\beta_0 \end{aligned}\right\} \qquad (3.3)$$

$$\left.\begin{aligned} u &= V_0\left[\frac{\Delta V}{V_0}\cos\alpha_0 \cos\beta_0 - \alpha \sin\alpha_0 - \beta \sin\beta_0 \cos\alpha_0\right] \\ v &= V_0\left[\frac{\Delta V}{V_0}\sin\beta_0 + \beta \cos\beta_0\right] \\ w &= V_0\left[\frac{\Delta V}{V_0}\cos\beta_0 \sin\alpha_0 + \alpha \cos\alpha_0 \cos\beta_0 - \beta \sin\beta_0 \sin\alpha_0\right] \end{aligned}\right\} \qquad (3.4)$$

The most general initial conditions will be represented by angles α_0 and β_0 different from zero.

Angle α_0 depends on the choice of axis OX. α_0 will always be reduced to zero if the third rather than the second dynamic trihedral is chosen.

Angle β_0 , on the contrary, cannot be reduced to zero if there is initial sideslip, but it is unusual to study an evolution with such an initial condition.

When $\alpha_0 = \beta_0 = 0$, we have:

$$\left.\begin{aligned} \hat{u} &\equiv \frac{u}{V_0} = \frac{\Delta V}{V_0} \\ \hat{v} &\equiv \frac{v}{V_0} = \beta \\ \hat{w} &\equiv \frac{w}{V_0} = \alpha \end{aligned}\right\} \qquad (3.5)$$

3.1.4 Motion of the Surrounding Air

We always assume the surrounding air to be motionless at instant $t = 0$. Dragging velocities are then disturbances, and we can represent their projections on the dynamic axes by u_a, v_a, w_a.

When such air velocities appear, aerodynamic forces are determined by the relative velocity

$$V_r = V_0\left(1 + \frac{\Delta V_r}{V_0}\right) \tag{3.6}$$

and by the real angles of attack and side-slip α_r and β_r.

The perturbations of relative velocity, of real angle of attack and of real angle of side-slip may, when the chord axes are used and infinitesimals of higher order can be neglected, be written as follows:

$$\left.\begin{aligned} \hat{u}_r &= \hat{u} - \frac{u_a}{V_0} \\ \alpha_r &= \alpha_r - \alpha_0 = \alpha - \frac{w_0}{V_0} + \alpha_0 \frac{u_a}{V_0} \\ \beta_r &= \beta_r - \beta_0 = \beta - \frac{v_a}{V_0} \end{aligned}\right\} \tag{3.7}$$

If we use the third dynamic trihedral, the term $\alpha_0(u_a/V_0)$ disappears in the second equation.

3.2 DETERMINATION OF INCREMENTS ΔX, ΔY, ... ΔN IN THE LINEAR CASE

We must know the expression for increments ΔC_x, ΔC_y, ΔC_z, ΔC_l, ΔC_m, ΔC_n as a function of the variables $\hat{u}$, α, β, $\hat{p}$, $\hat{q}$, $\hat{r}$, of their derivatives and of Mach number.

Linearization consists in assuming that the variables act independently, their results being simply added together, and that any action is proportional to the variable concerned. We shall use linearization whenever possible

(a) *Effect of perturbations* $\hat{u} = u_0/V_0$

The general relation:

$$\Delta X = X - X_0 = \left(C_{x_0} + \frac{\partial C_x}{\partial \hat{u}}\,\hat{u}\right) S\,\tfrac{1}{2}\rho V_0^2\,(1+\hat{u})^2 - C_x\,S\,\tfrac{1}{2}\rho V_0^2$$

enables us to write, neglecting the square of the disturbance:

$$\left.\begin{aligned} \Delta X &= \left(2\,C_{x_0} + \frac{\partial C_x}{\partial \hat{u}}\right) \hat{u}\, S\, \tfrac{1}{2}\rho V_0^2 \\ \Delta C_x &= \left(2\,C_{x_0} + \frac{\partial C_x}{\partial \hat{u}}\right) \hat{u} \end{aligned}\right\} \qquad (3.8)$$

The derivative $\partial C_x/\partial \hat{u}$ is representative of the Mach number.

If we consider the velocity of sound, a, as constant, we have:

$$\left.\begin{aligned} \Delta M &= \frac{V_0}{a}\,\hat{u} \\ \frac{\partial C_x}{\partial \hat{u}} &= \frac{\partial C_x}{\partial M}\,\frac{V_0}{a} \end{aligned}\right\} \qquad (3.9)$$

(b) *Effect of perturbations* α, β, $\hat{p}$, $\hat{q}$, $\hat{r}$

We shall have partial increments ΔC_x :

$$\left.\begin{aligned} \Delta C_x &= \frac{\partial C_x}{\partial \alpha}\,\alpha \\ &\cdots\cdots\cdots\cdots\cdots \\ &\cdots\cdots\cdots\cdots\cdots \\ \Delta C_x &= \frac{\partial C_x}{\partial \hat{r}}\,\hat{r} \end{aligned}\right\} \qquad (3.10)$$

(c) *Notation*

Derivatives of coefficients are represented by a condensed notation:

$$\frac{\partial C_x}{\partial \hat{u}} = C_{x_u} \qquad \frac{\partial C_x}{\partial \hat{p}} = C_{x_p}$$

$$\frac{\partial C_x}{\partial \beta} = C_{x_\beta} \quad \text{also } C_{x_v} \qquad \frac{\partial C_x}{\partial \hat{q}} = C_{x_q}$$

$$\frac{\partial C_x}{\partial \alpha} = C_{x_\alpha} \quad \text{also } C_{x_w} \qquad \frac{\partial C_x}{\partial \hat{r}} = C_{x_r}$$

Sometimes the C is omitted and one writes merely: x_u , x_p , etc.

(d) *Quasi-stationary flow*

When the assumption of the linearity of the phenomena is acceptable, harmonic (or sinusoidal) flows are well amenable to calculation. Let us study the consequences of a harmonic variation of the variable α on a coefficient such as C_m.

Let:

α_0 be the value about which α varies

A the amplitude of the variation of α

C_{m_0} the magnitude of C_m for $\alpha = \alpha_0$

ω the frequency.

The excitation is:

$$\alpha = \alpha_0 + A \sin\omega t \tag{3.11}$$

Any harmonic excitation enables us to define two components of the aerodynamic reaction considered:

an in-phase component

an out-of-phase component.

If the physical phenomenon producing the moment M can be represented by linear differential equations, the increment ΔC_m will be a function of time:

$$\begin{aligned} \Delta C_m(t) &= C_m(t) - C_{m_0} \\ &= A|D| \sin(\omega t + \varphi) \\ &= A|D| (\cos\varphi \sin\omega t + \sin\varphi \cos\omega t) \end{aligned} \tag{3.12}$$

in which $|D|$ is a modulus

$A|D|\cos\varphi$ defines the in-phase component

$A|D|\sin\varphi$ defines the out-of-phase component.

Components in phase and out of phase of the various aerodynamic factors may be calculated by theoretical methods. Certain results have been obtained experimentally.

Figures 8 and 9, taken from an NACA T.N.[3], give an example of modulus $|D|$ and of the phase angle φ corresponding to the moment and lift coefficients, as a function ω.

A quasi-stationary motion is a sufficiently slow motion to allow the instantaneous magnitude of an aerodynamic force to be expressed as a function of the instantaneous values and of the derivatives of the variables.

In this case, we shall write:

$$\Delta C_m = C_{m_\alpha}\,\alpha + \frac{c}{2V}\,C_{m_{\dot\alpha}}\,\dot\alpha \tag{3.13}$$

in which $$\frac{c}{2V}\,C_{m_{\dot\alpha}} = \frac{\partial C_m}{\partial \dot\alpha}$$

The factor $c/2V$ is used to make the quantity $C_{m_{\dot\alpha}}$ non-dimensional.

Identifying expressions (3.12) and (3.13) for a slow phenomenon, that is to say writing $\omega = 0$ explicitly and taking values of C_{m_α} and $C_{m_{\dot\alpha}}$ corresponding to zero frequency, we have:

$$\left.\begin{aligned} C_{m_\alpha} &= |D|\ \lim(\cos\varphi)_{\omega=0} \\ C_{m_{\dot\alpha}} &= \frac{2V_0}{c}\ |D|\ \lim\left(\frac{\sin\varphi}{\omega}\right)_{\omega=0} \end{aligned}\right\} \tag{3.14}$$

The expression for the aerodynamic actions in a quasi-stationary flow is thus related to the properties of the frequency response of these actions when the system is subjected to a harmonic input.

(e) *Superposition of effects*

The linearization of the increment ΔC_m, in relation to variables $\hat u$, α, β, $\hat p$, $\hat q$, $\hat r$ and their derivatives, leads to:

$$\Delta C_m = \left[\left(2\,C_{m_0} + C_{m_u}\right)\hat u + C_{m_\alpha}\,\alpha + C_{m_\beta}\,\beta + C_{m_p}\,\hat p + C_{m_q}\,\hat q + C_{m_r}\,\hat r\right] \tag{3.15a}$$

for the action of variables,

and $$\Delta C_m = \frac{c}{2V_0}\left[C_{m_{\dot u}}\,\frac{\dot u}{V_0} + C_{m_{\dot\alpha}}\,\dot\alpha + C_{m_{\dot\beta}}\,\dot\beta + C_{m_{\dot p}}\,\frac{d\hat p}{dt} + C_{m_{\dot q}}\,\frac{d\hat q}{dt} + C_{m_{\dot r}}\,\frac{d\hat r}{dt}\right] \tag{3.15b}$$

for the action of derivatives.

The terms C_{m_u} and $C_{m_{\dot u}}$ include the effect of Mach number variation.

Note

Factors $c/2V_0$ introduced to maintain the coefficients $C_{x_{\dot u}}$, $C_{y_{\dot u}}$, ... $C_{z_{\dot u}}$ ... $C_{m_{\dot u}}$ in their non-dimensional form must be replaced by $b/2V_0$ in the case of coefficients of lateral forces or moments Y, L, N.

(f) *Action of control surfaces*

The action of the control surfaces will also be calculated independently of other disturbances. It may be represented by coefficients such as:

$$C_{x_{\delta_e}} = \frac{\partial C_x}{\partial \delta_e} ; \quad C_{z_{\delta_e}} = \frac{\partial C_z}{\partial \delta_e} ; \quad C_{m_{\delta_e}} = \frac{\partial C_m}{\partial \delta_e}$$

or

$$\Delta C_x = C_{x_{\delta_e}} \delta_e$$

$$\Delta C_m = C_{m_{\delta_e}} \delta_e$$

We can make allowance for the effect of speed of deflection by using appropriate coefficients.

(g) *Action of atmospheric disturbances*

When the atmosphere is subjected to variable dragging motion, the increments ΔC_x , ... ΔC_n do not depend on the variables $\hat{u}$, α , β defining the increments of absolute velocity, but on the quantities $\hat{u}_r$, α_r , β_r defined in Section 3.1.4.

The use of $\hat{u}_r$, α_r , β_r in the expressions defining the applied forces and moments introduces explicitly, in the equations, excitations (or inputs) consisting of ambient velocity disturbances.

Note (i)

When we consider the action of the variables β , $\hat{p}$, $\hat{r}$, to be introduced in moments acting in the plane of symmetry, the sign of the reactions must be independent of the sign of β , $\hat{p}$, $\hat{r}$. If, for instance, a side-slip to the right produces a nose-down motion, a side-slip to the left will have the same effect; it will not cause a nose-up movement of the aeroplane.

We must therefore admit that the disturbances β , $\hat{p}$, $\hat{r}$, to be introduced in the expressions of actions ΔX , ΔZ , ΔM , will be the absolute values of the disturbances, the sign of the derivatives $\partial C_x / \partial \beta$, ... being defined in consequence.

We could also use the squares of the disturbances: β^2 , p^2 , r^2 , and the derivatives with respect to the squares, but the equations would then lose their linear character.

Note (ii)

In fact, theoretical calculations and wind tunnel experiments generally lead to a definition of exterior forces and moments in the aerodynamic axes or in the wind axes. The determination of the coefficients with respect to the body axes will require the use of transformation formulae.

3.3 SYSTEM OF EQUATIONS WRITTEN IN A NON-DIMENSIONAL FORM

The first 3 equations of system (2.20) had the dimensions of a force (ΔX, ΔY, ΔZ); the last 3 had the dimensions of a moment (ΔL, ΔM, ΔN).

We shall write these equations in such a way that they will all be non-dimensional, the terms representing aerodynamic forces and moments being reduced to coefficients $\Delta C_x \ldots \Delta C_n$, the development of which has been defined above. Simultaneously, we shall replace variables u, v, w by variables $\hat{u}$, α, β.

The writing of dimensionless equations requires a certain number of conventions:

(a) *Definition of aeroplane density* μ *and aerodynamic time unit* τ

Put:

$$\mu = \frac{m}{\rho S c} \tag{3.16}$$

$$\tau = \frac{\mu c}{V_0} \tag{3.17}$$

The density of the aeroplane, μ , is non-dimensional. The aerodynamic time unit τ has the dimensions of time.

(b) *Representation of moments and products of inertia*

The moments and products of inertia are represented, either by coefficients, or by ratios.

The use of inertia coefficients having dimensions of time squared is convenient.

We can take:

$$\left.\begin{aligned} C_{I_x} &= \frac{I_x}{\tfrac{1}{2}\rho S b V_0^2} \\ C_{I_z} &= \frac{I_z}{\tfrac{1}{2}\rho S b V_0^2} \\ C_{I_{zx}} &= \frac{I_{zx}}{\tfrac{1}{2}\rho S b V_0^2} \\ C_{I_y} &= \frac{I_y}{\tfrac{1}{2}\rho S c V_0^2} \end{aligned}\right\} \tag{3.18}$$

We can also use non-dimensional ratios of lengths.

Given:

$$I_x = m r_x^2$$

$$I_y = m r_y^2$$

$$I_z = m r_z^2$$

Then:

$$\left.\begin{aligned} i_x &= \frac{4I_x}{mb^2} = \frac{4r_x^2}{b^2} \\ i_y &= \frac{4I_y}{mc^2} = \frac{4r_y^2}{c^2} \\ i_z &= \frac{4I_z}{mb^2} = \frac{4r_z^2}{b^2} \end{aligned}\right\} \qquad (3.19)$$

and in the same way:

$$i_{zx} = \frac{4I_{zx}}{mb^2}$$

(c) *Gyroscopic couples*

Gyroscopic couples may be written in a non-dimensional form:

$$\left.\begin{aligned} C'_{l_q} &= + \frac{2\ I\omega\ \sin\lambda}{\tfrac{1}{2}\rho\, Sbc\, V_0} \\ C'_{m_p} &= - \frac{2\ I\omega\ \sin\lambda}{\tfrac{1}{2}\rho\, Sbc\, V_0} \\ C'_{m_r} &= - \frac{2\ I\omega\ \cos\lambda}{\tfrac{1}{2}\rho\, Sbc\, V_0} \\ C'_{n_q} &= + \frac{2\ I\omega\ \cos\lambda}{\tfrac{1}{2}\rho\, Sbc\, V_0} \end{aligned}\right\} \qquad (3.20)$$

These ratios can be compared to aerodynamic coefficients of coupling. The effect of gyroscopic couples will be represented, in the equations, by these factors.

The principal aim of dimensionless equations is to introduce the variables $\hat{u}$, α , β . We must thus replace u_0 , v_0 , w_0 , u , v , w in system (2.20) by their values expressed in (3.3) and (3.4) as functions of the initial values V_0 , α_0 , β_0 and the variables $\hat{u}$, α , β.

We give below the 6 equations written for the particular case where $\alpha_0 = 0$ and $\beta_0 = 0$. It is easy to re-establish the terms in α_0 and β_0 , if necessary by reworking the calculation.

Let us mention finally that the systems indicated below are written in *linear form,* by cancelling the products of the disturbances. This simplification is not valid in all cases. In Section 10.2 we shall come upon problems where it is necessary to introduce these products.

If we take the non-dimensional quantities $\hat{u}$, α , β , and the dimensional quantities p , q , r , as variables, the equations of motion may be written in the following form:

$$
\left.
\begin{aligned}
2\tau \frac{d\hat{u}}{dt} + 2\tau(q_0\alpha - r_0\beta) &= \Delta C_x + \frac{2\tau g}{V_0}[(\sin\Phi_0 \cos\Theta_0)\,\psi - (\cos\Phi_0 \cos\Theta_0)\theta] \\
2\tau \frac{d\beta}{dt} + 2\tau(r_0\hat{u} + r - p_0\alpha) &= \Delta C_y + \frac{2\tau g}{V_0}[(\sin\Theta_0)\,\psi + (\cos\Phi_0 \cos\Theta_0)\varphi] \\
2\tau \frac{d\alpha}{dt} + 2\tau(p_0\beta - q_0\hat{u} - q) &= \Delta C_z + \frac{2\tau g}{V_0}[-(\sin\Phi_0 \cos\Theta_0)\,\varphi - (\sin\Theta_0)\theta] \\
C_{I_x} \frac{dp}{dt} - C_{I_{xz}} \frac{dr}{dt} + \left(C_{I_z} - \frac{c}{b} C_{I_y}\right)(q_0 r + r_0 q) - C_{I_{xz}}(q_0 p + p_0 q) &= \\
&= \Delta C_L + C'_{l_q} \frac{c}{2V} q \\
C_{I_y} \frac{dq}{dt} + \frac{b}{c}\left[C_{I_x} - C_{I_z}\right](r_0 p + p_0 r) + C_{I_{xz}} \frac{b}{c}(2p_0 p - 2r_0 r) &= \\
&= \Delta C_m + C'_{m_p} \frac{b}{2V} p + C'_{m_r} \frac{b}{2V} r \\
C_{I_z} \frac{dr}{dt} - C_{I_{xz}} \frac{dp}{dt} + \left[\frac{c}{b} C_{I_y} - C_{I_x}\right](p_0 q + q_0 p) + C_{I_{xz}}(q_0 r + r_0 q) &= \\
&= \Delta C_n + C'_{n_q} \frac{c}{2V} q
\end{aligned}
\right\} \quad (3.21)
$$

To these 6 equations are added the 3 kinematic equations 2.21. If we use the 6 non-dimensional variables $\hat{u}$, α , β , $\hat{p}$, $\hat{q}$, $\hat{r}$, the equations of motion take the following form:

$$
\left.
\begin{aligned}
2\tau \frac{d\hat{u}}{dt} + 4\tau \frac{V_0}{c}\left[\hat{q}_0\alpha - \frac{c}{b}\hat{r}_0\beta\right] &= \Delta C_x + \frac{2\tau g}{V_0}[(\sin\Phi_0 \cos\Theta_0)\,\psi - (\cos\Phi_0 \cos\Theta_0)\theta \\
2\tau \frac{d\beta}{dt} + 4\tau \frac{V_0}{c}\frac{c}{b}[\hat{r}_0\hat{u} + \hat{r} - \hat{p}_0\alpha] &= \Delta C_y + \frac{2\tau g}{V_0}[(\sin\Theta_0)\,\psi + (\cos\Phi_0 \cos\Theta_0)\varphi]
\end{aligned}
\right\} \quad (3.22)
$$

$$2\tau \frac{d\alpha}{dt} + 4\tau \frac{V_0}{c}\left[\frac{c}{b}\hat{p}_0\beta - \hat{q}_0\hat{u} - \hat{q}\right] = \Delta C_z + \frac{2\tau g}{V_0}[-(\sin\Phi_0 \cos\Theta_0)\varphi - (\sin\Theta_0)\theta] \quad (3.22)$$

$$i_x\tau \frac{d\hat{p}}{dt} - i_{zx}\tau \frac{d\hat{r}}{dt} + 2\tau \frac{V_0}{c}\left[i_z - i_y \frac{c^2}{b^2}\right](\hat{q}_0\hat{r} + \hat{r}_0\hat{q}) - 2\tau \frac{V_0}{c} i_{zx}(\hat{q}_0\hat{p} + \hat{p}_0\hat{q}) =$$

$$= \Delta C_l + C'_{l_q}\hat{q}$$

$$i_y\tau \frac{d\hat{q}}{dt} + 2\tau \frac{V_0}{c}[i_x - i_z](\hat{r}_0\hat{p} + \hat{p}_0\hat{r}) + 2\tau \frac{V_0}{c} i_{xz}(2\hat{p}_0\hat{p} - 2\hat{r}_0\hat{r}) =$$

$$= \Delta C_m + C'_{m_p}\hat{p} + C'_{m_r}\hat{r}$$

$$i_z\tau \frac{d\hat{r}}{dt} - i_{xz}\tau \frac{d\hat{p}}{dt} + 2\tau \frac{V_0}{c}\left[i_y \frac{c^2}{b^2} - i_x\right](\hat{p}_0\hat{q} + \hat{q}_0\hat{p}) + 2\tau \frac{V_0}{c} i_{zx}(\hat{q}_0\hat{r} + \hat{r}_0\hat{q}) =$$

$$= \Delta C_n + C'_{n_q}\hat{q}$$

but the reduced angular velocities must be introduced in the kinematic expressions:

$$\left.\begin{aligned} \frac{d\varphi}{dt} &= (\hat{p}_0 + \hat{p})\frac{2V_0}{b} + r_0 \frac{2V_0}{b}\theta \\ \frac{d\theta}{dt} &= (\hat{q}_0 + \hat{q})\frac{2V_0}{c} - r_0 \frac{2V_0}{b}\varphi \\ \frac{d\psi}{dt} &= (\hat{r}_0 + \hat{r})\frac{2V_0}{c} + q_0 \frac{2V_0}{c}\varphi \end{aligned}\right\} \quad (3.23)$$

The following substitutions can still be made:

(1) Making allowance for the equality approached:

$$mg + C_{z_0} \tfrac{1}{2}\rho S V_0^2 = 0$$

we obtain easily:

$$\frac{2\tau g}{V_0} = -C_{z_0}$$

The group of factors $2\tau g/V_0$ appears in front of all terms representing a gravity effect. It may be replaced by the lift coefficient C_{L_0} equal in other respects to $-C_{z_0}$.

(2) The group of factors $2\tau V_0/c$ can be replaced by 2μ, in front of terms representing centrifugal forces, in the completely non-dimensional system.

(3) Writing $\hat{t} = t/\tau$, we define a non-dimensional time $\hat{t}$, the unit of which is τ seconds.

The time derivative becomes

$$\tau \frac{d}{dt} = \frac{d}{d(t/\tau)} = \frac{d}{d\hat{t}}$$

The factor τ , by which every derivative is multiplied, vanishes if we use non-dimensional time as the variable of integration.

If we change the time variable in this way, we must also change it in the kinematic equations, after multiplying both sides by τ .

Substitution of real time for aerodynamic time is not convenient for problems dealt with by an analogue computer, when certain real elements are introduced into the system (for example: the human pilot).

Note

Aeroplane density is sometimes defined by the ratio $m/\frac{1}{2}\rho Sc$. The corresponding aerodynamic time is then $\mu c/V_0$ and will also be called τ .

3.4 INTEGRATION OF LINEAR SYSTEMS

The aerodynamic coefficients and other characteristics of the aeroplane, assumed to be rigid, being known, the previous equations enable us to predict the motion of the aeroplane as a result of:

An initial disturbance affecting one or more of the variables u , v , w , p , q , r , φ , θ , ψ ;

An input or excitation produced by a modification in the dragging velocities of the ambient air;

An excitation produced by the controls;

An excitation produced by a modification, ordered or not, of the power output of the motor-propulsion unit.

Well-known methods exist for the integration of a linear differential system. It is not our purpose to study these methods here. They generally lead to tedious calculations, in spite of the simplicity of the theory on which their determination is based. Nevertheless we should like to mention a few fundamental concepts.

(1) *Equations without a second member*

When the variables we consider as excitations or inputs, viz.

$$u_a \ , \quad v_a \ , \quad w_a$$

$$\delta_e \, , \quad \delta_a \, , \quad \delta_r$$

$$\delta_m$$

remain zero, the system of equations is said to be homogeneous or without second member.

Values of output variables remaining zero:

$$u \, , \quad v \, , \quad w$$

$$p \, , \quad q \, , \quad r$$

$$\varphi \, , \quad \theta \, , \quad \psi$$

satisfy the system.

If one or more of these variables undergo an initial perturbation the cause of which may remain unknown, then at a given instant which we shall take as time origin, all variables start to vary.

This variation is described by the integral of the differential system without second member, from initial conditions represented by foreseen perturbations.

(2) *Equations with second member*

Equations are said to be with a second member when the input variables do not remain constantly zero, and are known functions of time.

We may consider the case of only one non-zero input variable, because we are able to add together solutions corresponding to several excitations.

An input or excitation variable can be:

(a) a particular function of time, called a step unit

(b) a particular function of time, called an impulse unit

(c) any function of time

(d) a harmonic function of time.

(a) *Step unit*

The input variable x is the product $x.1(t)$ in which the function $1(t)$ has the property of possessing a numerical value equal to:

0 for any value of $t < 0$

1 for any value of $t > 0$.

The function 1(t) is said to be a step unit function.

The system's response to the function 1(t) is the indicial response.

(b) *Impulse unit*

Let $\mathcal{U}(t)$ be a function which can be derived, and whose value increases from 0 to 1 during an interval of time Δt decreasing gradually.

Its derivative $\mathcal{d}(t)$, initially zero, reaches during this interval of time a maximum value of $1/\Delta t$; this maximum increases gradually.

By definition we have:

$$\int_{-\infty}^{+\infty} \mathcal{d}(t)\, dt = \mathcal{U}_{+\infty} - \mathcal{U}_{-\infty} = 1 \qquad (3.24)$$

In the limit, $\mathcal{U}(t)$ tends to the discontinuous function 1(t) and function $\mathcal{d}(t)$ becomes infinity for $t = 0$ and zero for any other value.

The improper function defined by this property and that of having an integral equal to unity, is known by the name of unit impulse or Dirac function. We shall call it $\mathcal{d}(t)$.

The response to the impulse function is called impulse response.

(c) *Any function of* (t)

Consider an excitation $x = f(t)$, in which $f(t)$ is any function.

The response to any input can be determined as a function of the indicial response or of the impulse response, by Duhamel's integral.

Let $F(t)$ be the indicial response

$H(t)$ be the impulse response

$y(t)$ the response asked for.

Duhamel's formulae, as is easy to prove by expressing the excitation as a series of steps or impulses (see Figs.10(a) and (b)), can be written:

$$y(t) = f(o)\, F(t) + \int_0^t f'(\tau)\, F(t-\tau)\, d\tau \qquad (3.25)$$

$$y(t) = \int_0^t f(\tau)\, H(t-\tau)\, d\tau \qquad (3.26)$$

or:

$$y(t) = f(o)\ F(t) + \int_0^t f'(t-\tau)\ F(\tau)\ d\tau \qquad (3.27)$$

$$y(t) = \int_0^t f(t-\tau)\ H(\tau)\ d\tau \qquad (3.28)$$

(d) *Harmonic function*

An excitation $x = a \sin \omega t$ produces firstly a transient motion. Then, when the transient motion has vanished, a harmonic motion takes place, where all the variables of the system are sinusoidal functions of time, with angular frequency equal to that of the excitation.

The amplitude of each response, and its phase angle in relation to the excitation, are functions of the frequency of the excitation.

The stationary response so defined is the frequency response. Its calculation is always very simple.

3.5 TRANSFORMATION FORMULAE

Theoretical or experimental data available often define the aerodynamic reactions produced by the exterior flow by means of their projections on the aerodynamic axes Gxyz or even in the wind axes.

The positive projections of forces and moments along the aerodynamic axes should logically be defined by appropriate symbols. We could, for instance, use the following notations:

$$C_{x^*} \qquad C_{y^*} \qquad C_{z^*}$$

$$C_{l^*} \qquad C_{m^*} \qquad C_{n^*}$$

with the restriction that $C_{m^*} = C_m$ and $C_{y^*} = C_y$.

Angular velocities in the aerodynamic system being expressed by components p^* , q^* , r^* in the aerodynamic axes, derivatives of coefficients with respect to angular velocities will be expressed by derivatives such as $C_{l^*}{}_{r^*}$, $C_{n^*}{}_{p^*}$, etc. A derivative such as $C_{l^*}{}_{r^*}$ expresses the derivation of the moment about the axis Gx with respect to r^* angular velocities about axis Gz ; whereas the derivative C_{l_r} expresses the same quantities in relation to the dynamic axes GX and GZ .

The use of transformation formulae is necessary when it is desired to introduce known quantities, defined in aerodynamic axes, in the equations written for the body axes. A general layout of these formulae is given in Section 3.12. The use of wind axes would involve more elaborate formulae.

We should point out here a difficulty resulting from a universally adopted convention:

The projections of aerodynamic forces exerted by the exterior flow in the directions Gx and Gz are considered positive when they point in the *negative* direction of the axes. These projections are the drag and lift; in British notation, these are defined by the symbols C_D and C_L .

Transformation formulae, which enable us to find the components of the forces in relation to the dynamic axes, are expressed as a function of the angle $\alpha = \alpha_0 + \alpha$.

In the light of the foregoing remark, the transformation formulae for the forces become:

$$\left.\begin{aligned} C_x &= C_{x_0} + \Delta C_x = (C_{L_0} + \Delta C_L)\sin(\alpha_0 + \alpha) - (C_{D_0} + \Delta C_D)\cos(\alpha_0 + \alpha) \\ C_z &= C_{z_0} + \Delta C_z = -(C_{L_0} + \Delta C_L)\cos(\alpha_0 + \alpha) - (C_{D_0} + \Delta C_D)\sin(\alpha_0 + \alpha) \end{aligned}\right\} \quad (3.29)$$

When the dynamic axes considered are the axes corresponding to $\alpha_0 = 0$, we get:

$$\left.\begin{aligned} C_{X_0} &= -C_{D_0} & \Delta C_x &= C_L\,\alpha - \Delta C_D \\ C_{Z_0} &= -C_{L_0} & \Delta C_z &= -\Delta C_L - C_D\,\alpha \end{aligned}\right\} \quad (3.30)$$

In French notation, drag and lift are represented by C_x and C_z . These coefficients thus indicate forces acting in the negative direction of the corresponding dynamic axes; the use of such notations may lead to some confusion.

Moments C_{l*} and C_{n*} are, on the contrary, considered positive along the positive direction of axes G_x and G_y .

Transformation formulae are thus written with the following signs:

$$\left.\begin{aligned} C_l &= -C_{n*}\sin\alpha + C_{l*}\cos\alpha \\ C_n &= +C_{n*}\cos\alpha + C_{l*}\sin\alpha \end{aligned}\right\} \quad (3.31)$$

These expressions may be developed for the purpose of obtaining equilibrium values and increments.

3.6 FURTHER RELATIONS

In the general case, the system of:

6 equations of motion

and 3 kinematic equations

must be completed by further relations.

Besides the transformation formulae defined in the preceding section, necessary because the expressions for aerodynamic reactions we must introduce in the calculations are not defined in the body axes, the use of further relations may be necessary when one studies:

(a) the effect of known atmospheric perturbations

(b) the action of controls

(c) the effect of changes in altitude.

(a) *Influence of known atmospheric perturbations*

Atmospheric perturbations, when known, are expressed in terms of the components u'_a , v'_a , w'_a of the atmospheric motions, in the geoparallel axes.

The projection of these excitations on the dynamic axes depends on the aeroplane's motion, in other words on the result looked for. We must therefore add to the system of equations the transformation formulae which enable us to calculate u_a , v_a , w_a in terms of the given quantities u'_a , v'_a , w'_a .

In the most general case, this leads to finding the projections u'_a , v'_a , w'_a on the initial axes by means of constant angles ψ_0 , Θ_0 , Φ_0 , then to determining the variation of each of these projections on the dynamic axes by means of angles ψ , θ , φ , functions of the aeroplane's response.

(b) *Influence of controls*

The study of the aeroplane's motion produced by the deflection angles δ_e , δ_a , δ_r can be made when these angles are defined as functions of time.

For an aeroplane flown by a pilot, any relation $\delta = f(t)$ expresses the fact that the aeroplane is subjected to an input applied by the pilot in accordance with a known law and constitutes an equation describing the pilot's action.

The integration of the system to which we have added the preceding relation is possible and will describe the trajectory followed. But the pilot's decision does not necessarily define, straight away, a deflection.

The decision is presented in the form of a control displacement δ_s or a force F applied to the control.

It is well known that the pilot has a better feel for force than for displacement. The independent variable, subjected to the pilot's will, is, in fact, the force he exerts.

If it is desired to calculate the response of the aeroplane to a given force exerted by the pilot, the complete relationship between the displacements of the controls and this force must be known.

Servo-mechanisms and artificial-feel devices can produce control deflections which are not related in a simple way to the force F. An equation defining the deflections in relation to the force F applied by the pilot, will have to be written.

Any equation relating the control deflections to the excitations acting upon the control system, may be called a control equation.

For an aeroplane having reversible controls, the control equation in the control-free case is nothing other than the hinge balance condition.

For an aeroplane equipped with an automatic pilot, these equations will describe the general behaviour of the error detectors and of the servo-mechanisms.

(c) *Altitude effect*

If the evolution comprises changes in altitude, these changes are determined by the following relation:

$$-z_t - z_0 = \int_{t_0}^{t} (-V \sin\Theta + V \sin\Phi \cos\Theta + W \cos\Phi \sin\Theta)\, dt \qquad (3.32)$$

The specific mass and temperature of the air will vary according to the laws defining the atmosphere.

Variations in specific mass will modify the factor τ.

Variations in temperature will modify the velocity of sound, a, that is to say the Mach number M corresponding to the speed V.

Neumark has shown[6] that this effect is negligible if differences in altitude result from the oscillations of the aeroplane about a horizontal trajectory. The effect may become considerable, however, if the trajectory is not horizontal.

3.7 BLOCK-DIAGRAMS

The relationship between the different variables entering into a problem and the part that these variables play in the whole of a phenomenon, are clarified by the lay-out of a block-diagram.

A block-diagram is built up of a succession of rectangles joined by lines. The rectangles represent the elements of the chain; the lines represent the variables which command the action or are a result of the action of each element. They are the input or output variables.

Figure 136 is the block-diagram for a system which will be studied in detail in Section 12.9.

3.8 LAPLACE TRANSFORMATION AND TRANSFER FUNCTIONS

3.8.1 Definition of the Transformation

The Laplace transformation is an operation which makes a function $\varphi(s)$ of a complex variable s correspond to any function $f(t)$ of a real variable t.

The function $\varphi(s)$ is related to the function $f(t)$ by the following relation, called a Laplace transformation:

$$\varphi(s) = \int_0^{\infty} e^{-st} f(t)\, dt \tag{3.33}$$

which exists only if the integral is convergent.

Also, the function $f(t)$ is related to the function $\varphi(s)$ by the inverse relation

$$f(t) = \frac{1}{2\pi i} \oint_{-\infty i}^{+\infty i} e^{-st} \varphi(s)\, ds \tag{3.34}$$

called Cauchy's relation.

In the latter, the symbol $\oint_{-\infty i}^{+\infty i} e^{-st} \varphi(s)\, ds$ indicates an integral extended to a line of the complex plane, varying from $-\infty i$ to $+\infty i$ The connection between the functions $f(t)$ and $\varphi(s)$ may be written in several ways. The following expressions are often used:

$$\varphi(s) = \mathcal{L} f(t) \tag{3.35}$$

$$f(t) = \mathcal{L}^{-1} \varphi(s) \tag{3.36}$$

which mean $\varphi(s)$ is the Laplace transform or 'image' of $f(t)$

$f(t)$ is the 'original' of $\varphi(s)$.

3.8.2 Transformation Properties

By application of the fundamental expression (3.33) transforms of many functions can be worked out. We will mention only the results of interest to the unit step $1(t)$ and the impulse function $\delta(t)$:

$$\mathcal{L}\, 1(t) = \frac{1}{s} \tag{3.37}$$

$$\mathcal{L}\, \delta(t) = 1 \tag{3.38}$$

Additive properties can be applied to Laplace transforms:

$$\mathcal{L}[f_1(t) + f_2(t)] = \mathcal{L}f_1(t) + \mathcal{L}f_2(t) = \varphi_1(s) + \varphi_2(s) \tag{3.39}$$

whence results the possibility of multiplying a function $f(t)$ by a numerical factor:

$$\mathcal{L}[n\ f(t)] = n\ \mathcal{L}f(t) = n\ \varphi(s) \tag{3.40}$$

Derivative and integral transforms of function $f(t)$ are respectively:

$$\mathcal{L}\left[\frac{df(t)}{dt}\right] = s\ \varphi(s) - f(o) \tag{3.41}$$

$$\mathcal{L}\left[\int_0^t f(t)\ dt\right] = \frac{1}{s}\varphi(s) \tag{3.42}$$

Changing the origin of variable t leads to:

$$\mathcal{L}\ f(t - t_1)\ dt = e^{-st_1}\ \varphi(s) \tag{3.43}$$

The compound (or convolution) product transform appears in a simple form.

Let

$f_1(t)$ and $f_2(t)$ be two functions of variable t

$\varphi_1(s)$ and $\varphi_2(s)$ their transforms.

The integral

$$\int_0^t f_1(\tau)\ f_2(t - \tau)\ d\tau \tag{3.44}$$

from which τ disappears and which is a function only of t, is the compound product of the functions f_1 and f_2. The transform of this product is:

$$\mathcal{L} \int_0^t f_1(\tau)\ f_2(t - \tau)\ d\tau = \varphi_1(s)\ \varphi_2(s) \tag{3.45}$$

Applying the Laplace transformation to the linear differential equation systems is the basis of the modern integration methods of these systems (Heaviside's Method). It also leads to a very important concept, viz. that of transfer functions.

Subsequently, when we wish to express the Laplace transform of a time function such as $u(t)$, $v(t)$, ... or $x(t)$, $y(t)$, we shall use the notation $u(s)$, $v(s)$ .... $x(s)$, $y(s)$ without looking for the corresponding Greek letter. In fact, simply expressing the fact that the variable u, v being dealt with is a function of s is sufficient to indicate we are concerned with a Laplace transform.

3.8.3 Definition of the Transfer Function

Let us consider a mechanical or electrical system, subjected to an input variable x, which is magnified to an output variable y.

The two variables are functions of time, $x(t)$ and $y(t)$. When these two variables have Laplace transforms $x(s)$ and $y(s)$, the transfer function of the system is, by definition, the ratio $y(s)/x(s)$.

The transfer function will be represented by $G(s)$ in what follows.

An aeroplane is a system subjected to several independent input variables (δ_e, w_a for example). It produces several output variables ($\hat{u}$, α, θ for example) which can be considered independently of each other.

Let m = number of inputs

n = number of outputs.

When linearization is acceptable, the n outputs are related to the m inputs by a set of n differential equations.

The action of each of the input variables (the $m-1$ others being zero) can be calculated separately. The input being considered, which will be denoted by x, will activate the n outputs, but we can eliminate $n-1$ outputs by successive derivations of these equations and isolate the nth output, called y. We obtain a differential equation

$$B_n \frac{d^n y}{dt^n} + \ldots + B_1 \frac{dy}{dt} + B_0 y = A_m \frac{d^m x}{dt^m} + \ldots + A_1 \frac{dx}{dt} + A_0 x \qquad (3.46)$$

in which we replace the time independent variables $y(t)$ and $x(t)$ and all their successive derivatives by their images $y(s)$ and $x(s)$.

Successive application of the following formulae:

$$\mathcal{L} \frac{dy}{dt} = s\, y(s) - y_0 \qquad (3.47)$$

$$\mathcal{L} \frac{d^2 y}{dt^2} = s[s\, y(s) - y_0] - \left(\frac{dy}{dt}\right)_0 \qquad (3.48)$$

shows that when initial values of y and its derivatives are zero, the Laplace transform of the equation becomes:

$$(B_n s^n + \ldots + B_1 s + B_0)\, y(s) = (A_m s^m + \ldots + A_1 s + A_0)\, x(s) \qquad (3.49)$$

and the aeroplane's transfer function:

$$G(s) = \frac{y(s)}{x(s)} = \frac{A_m s^m + \ldots + A_1 s + A_0}{B_n s^n + \ldots + B_1 s + B_0} \qquad (3.50)$$

The transfer function of a mechanical system represented by linear equation is always an expression of the type given above.

The transfer function concept is not exclusive to linear systems. Non-linear equations will lead to transfer functions inasmuch as they possess a Laplace transform, that is to say as far as the integral defined by (3.33) converges.

The transfer function concept, however, does not cover all the cases and may not be unduly extended.

Let us consider an electrical system, called quadripole in a general way. When subjected to an input signal comprising a voltage V_1, and an intensity I_1, it magnifies this signal to a voltage V_2 and an intensity I_2. The two elements, voltage and intensity, forming either the input or the output signal, are not independent of each other. The behaviour of such a system is characterized by a transfer matrix relating the two elements of the output to the two elements of the input.

It is not our aim here to study the properties of the transfer matrices.

Electrical systems may be represented by transfer functions when it is not necessary to consider the two components, voltage and intensity, of the input or output signals. The behaviour of the filter, referred to in Section 13.5.2, is represented by a transfer function on the supposition that the filter is followed by an infinite resistance.

A system transforming an electrical signal into a mechanical displacement may be represented by a transfer function in certain simple cases.

3.8.4 Properties of the Transfer Functions

(a) When a mechanical or electrical system possesses only one input and one output, it is characterized by a single transfer function.

When such a system has m independent inputs and n independent outputs, each output/input ratio defines a transfer function. The number of these is thus equal to the product of the inputs by the outputs.

(b) Transfer functions of first and second order systems, such as, for instance,

$$B_1 \frac{dy}{dt} + B_0 y = A_0 x \qquad (3.51)$$

$$B_2 \frac{d^2y}{dt^2} + B_1 \frac{dy}{dt} + B_0 = A_1 \frac{dx}{dt} + A_0 x \qquad (3.52)$$

depend on a reduced number of parameters and their properties are well known.

(c) The transfer function of a linear system possesses a particular physical meaning when the variable s is merely imaginary. In that case, we have:

$$s = i\omega$$

Replacing s by $i\omega$ in $G(s)$, we get an expression $G(i\omega)$ which defines the response of the system in terms of frequency, for instance the response of the system to a harmonic excitation $x = \sin\omega t$.

(d) The splitting of a system in block-diagrams combines itself, fortunately, with the representation of the effect of each elementary block-diagram by the transfer functions.

The transfer function of a number of blocks, placed in series, and commanding each other directly, is equal to the product of the elementary transfer functions if the downward blocks do not react on those preceding them. It must however be understood that the transfer functions do not multiply mutually, in a general way.

(e) Let us mention lastly that the inverse of a system's transfer function is sometimes called the impedance of the system, by analogy with electrical phenomena. By the same analogy, the transfer function is called admittance.

3.8.5 Block Splitting

It is sometimes possible to replace a block having a transfer function of a high order by a series of interlinked blocks each having a first or second order transfer function.

Vedrov, Romanov and Surina[5] have shown that this was the case for total transfer functions, defining respectively the longitudinal and the transverse motions of the aeroplane.

The block characteristic of the aeroplane's longitudinal motion (Fig. 11), comprising an input δ_e and a series of outputs, gives rise, for each output, to a transfer function which is of 4th order in α, V, θ, and of 5th order in z. This block is equivalent to a series of elementary blocks, each characterized by a transfer of 1st or 2nd order, articulated as indicated in Figure 12. It is important, nevertheless, to notice that the set-up supposes that the input δ_e influences the moment C_m but does not influence the lift C_L, which is a great simplification.

A separation of the same kind is presented by the same authors for the transfer function defining the lateral movement.

3.9 NON-STATIONARY EFFECTS

The variation of the lift or any other aerodynamic action constitutes a non-stationary effect if, having a linear relation in steady flow

$$C_L = C_{L_\alpha}\,\alpha + C_{L_0} \tag{3.53}$$

a sudden increase $\Delta\alpha$ does not immediately produce the increment ΔC_L corresponding to the linear relation, but produces a lift which varies with time, thus:

$$\Delta C_L(t) = C_{L_\alpha} \Phi(t) \Delta\alpha \tag{3.54}$$

$\Phi(t)$ being a function which tends more or less rapidly towards unity as time increases.

The product $C_{L_\alpha} \Phi(t)$ is the indicial response. If the incidence α, instead of varying in steps, varies continuously as a function of time, as $\alpha(t)$, the lift at instant t will be given by Duhamel's integral:

$$C_L(t) = C_{L_\alpha}\left[\int_0^t \dot{\alpha}(\tau)\ \Phi(t-\tau)\ d\tau\right] \tag{3.55}$$

an expression to which should be added:

$$\Delta C_L(t) = C_{L_\alpha} \Phi(t) \Delta\alpha_0$$

if the incidence underwent, also, a sudden and finite increase $\Delta\alpha_0$ at time zero.

It is clear that in these conditions the lift is not defined at a given instant, subsequent to $t = 0$, by the angle of attack α and its derivative $\dot{\alpha}$ realized at the instant t under consideration, but that it depends on the complete variation history of the angle of attack.

Time histories of α, different when $t < t_1$ but becoming identical after t_1, will not produce equal lifts for $t > t_1$ (Fig. 13).

The variation of C_L with α can be defined as follows by using Laplace transforms.

Let $C_L(s)$ and $\alpha(s)$ be the transforms of $C_L(t)$ and $\alpha(t)$.

In the same manner, let $\Phi(s)$ be the transform of $\Phi(t)$.

Relation (3.55) will be written:

$$C_L(s) = C_{L_\alpha}\ s\ \alpha(s)\ \Phi(s) \tag{3.56}$$

Wing action, transforming the angle of attack α to a lift force represented by the coefficient C_L, can be characterized by a transfer function which will be:

$$\frac{C_L(s)}{\alpha(s)} = C_{L_\alpha}\ s\ \Phi(s) = G(s) \tag{3.57}$$

The corresponding indicial output will be:

$$C_L(s)_1 = G(s)\frac{1}{s} = C_{L_\alpha}\ \Phi(s) \tag{3.58}$$

3.10 NON-LINEARITY OF AERODYNAMIC FORCES, IN RELATION TO VARIABLES

The linearity hypothesis existing in the steady state between the forces and aerodynamic moments, and the variables by which they are produced, nearly always ceases to be valid when aerodynamic phenomena do not conform to a simple theoretical scheme. The advent of flow separation, the formation of shock waves, the interference of shock waves with the boundary layer, always destroy linearity. The advent of such phenomena is, also, always marked by a behaviour of the aeroplane very different from that suggested by calculations from linear expressions of the reactions.

The complete study of the aeroplane motion includes the resolution of two successive problems:

(a) Knowing the fluid flow, to determine the reactions exerted on the aeroplane;

(b) Given these reactions, to compute the motion of the aeroplane.

The present treatment is limited to the study of the second problem. In this limited treatment, we assume that the expression for the reactions is known for steady and quasi-steady flows, but that it may deviate from the linearity laws, making the approximations given in Sections 3.1 and 3.2 invalid.

In fact, we may introduce non-linearities in the formulae giving the increase in force ΔX , ... ΔN by using 2nd degree terms of series expansion.

This gives, for an aerodynamic factor such as C_m varying non-linearly with the variable $\boldsymbol{\alpha} = \alpha_0 + \alpha$.

$$\Delta C_m = C_m(\boldsymbol{\alpha}) - C_m(\alpha_0) = \frac{dC_m}{d\alpha}\alpha + \frac{1}{2}\frac{d^2C_m}{d\alpha^2}\alpha^2 + \ldots \qquad (3.59)$$

It often happens that an aerodynamic factor is a non-linear function of 2 variables. Figures 14a and 14b represent a factor C_m , a non-linear function of variables α and M . One can express the increment ΔC_m corresponding to increments

$$\alpha = \boldsymbol{\alpha} - \alpha_0$$

$$\Delta M = M - M_0$$

by:

$$\Delta C_m = C_m(\boldsymbol{\alpha}, M) - C_m(\alpha_0, M_0)$$

$$= \frac{\partial C_m}{\partial \alpha}\alpha + \frac{\partial C_m}{\partial M}\Delta M + \frac{1}{2}\frac{\partial^2 C_m}{\partial \alpha^2}\alpha^2 + \frac{\partial^2 C_m}{\partial \alpha \partial M}\alpha\,\Delta M + \frac{1}{2}\frac{\partial^2 C_m}{\partial M^2}(\Delta M)^2 \qquad (3.60)$$

Some factors may depend on 3 variables. This is the case for C_n which, in fact, depends on α , β , M .

Such a case would be difficult to study as a whole. We obtain convenient expressions when limiting the possible combinations by admitting that C_n varies always linearly with β. It is then sufficient to write that derivative $C_{n\beta}$ is a non-linear function of variables α and M. This simplification leads necessarily to $C_n = 0$ when $\beta = 0$, which, in fact, is always true.

The introduction of squares and products of disturbances no longer allows the resolution of systems by the classical integration methods of linear systems.

3.11 USEFULNESS OF ANALOGUE COMPUTERS

Bearing in mind all the foregoing, we say that the system of equations of motion for the aeroplane:

(a) Must frequently be accompanied by supplementary equations

(b) Offers terms difficult to handle when we wish to take into account non-stationary effects

(c) Does not always present itself in a linear form.

Systems so formed become almost unmanageable; their integration cannot be undertaken by usual mathematical means unless they are completely linearized, and calculations become tedious when the order of the system exceeds the 4th.

An arbitrary uncoupling in longitudinal and lateral motions enables us to reduce the order of the system.

The uncoupled motion theory, using 4th order linear systems, is absolutely classical.

This theory will not be presented here again. It is a useful method, but does not permit easy determination of the motion of the aeroplane when this motion comprises both longitudinal and lateral movements. It is not applicable in cases (b) and (c) mentioned above.

It is far from impossible that purely mathematical research will lead to new methods allowing the integration of the equations in the previous cases.

It seems nevertheless certain that the use of analogue computers is a practical way of resolving all problems connected with aeroplane motion.

The integration of high-order linear equations is straightforward and the solution of problems depending on equations not entirely linear is possible in many cases.

Function generators permit the introduction into the calculation of non-linear variation of aerodynamic factors without having to call upon series expansions. Systems to be resolved may comprise a higher and higher number of non-linearities, as the equipment used becomes more important.

Due to a property that will be discussed later, it is possible to introduce the equations into the computer in the form of Laplace transforms. This is a valuable property for the study of non-stationary phenomena, because of the simple structure of equations when written as transforms.

When equations are written as transforms, transfer functions appear immediately. Simple set-ups often enable us to simulate the transfer functions corresponding to different blocks. This justifies the idea of splitting the scheme into elementary blocks.

Lastly, the part played by the analogue computer is not necessarily limited to the resolution of the equations written previously. We can imagine that part of the aeroplane's behaviour is directly simulated and that the result of this simulation, appearing as a voltage, is used by the computer to determine the final result.

3.12 THE ESTABLISHING OF TRANSFORMATION FORMULAE

Consider, in a general way, a system $GX_1Y_1Z_1$ and a system $GX_2Y_2Z_2$ having a common axis GY.

Let η be the angle necessary in order to bring the first system into coincidence with the second (Fig.15).

The aerodynamic coefficients in the two systems are related as follows:

$$C_{x_2} = C_{x_1} \cos\eta - C_{z_1} \sin\eta$$

$$C_{y_2} = C_{y_1}$$

$$C_{z_2} = C_{z_1} \cos\eta + C_{x_1} \sin\eta$$

$$C_{l_2} = C_{l_1} \cos\eta - C_{n_1} \sin\eta$$

$$C_{m_2} = C_{m_1}$$

$$C_{n_2} = C_{n_1} \cos\eta + C_{l_1} \sin\eta$$

Angular velocities are related thus:

$$p_2 = p_1 \cos\eta - r_1 \sin\eta$$

$$q_2 = q_1$$

$$r_2 = p_1 \sin\eta + r_1 \cos\eta$$

Derivatives with respect to α , $\dot{\alpha}$ and q of the coefficients involved in the longitudinal motion are obtained immediately:

$$C_{x_2,\alpha} = C_{x_1,\alpha} \cos\eta - C_{z_1,\alpha} \sin\eta$$

$$C_{x_2,\dot{\alpha}} = C_{x_1,\dot{\alpha}} \cos\eta - C_{z_1,\dot{\alpha}} \sin\eta$$

$$C_{x_2,q} = C_{z_1,q} \cos\eta - C_{z_1,q} \sin\eta$$

$$C_{z_2,\alpha} = C_{z_1,\alpha} \cos\eta + C_{x_1,\alpha} \sin\eta$$

$$C_{z_2,\dot{\alpha}} = C_{z_1,\dot{\alpha}} \cos\eta + C_{x_1,\dot{\alpha}} \sin\eta$$

$$C_{z_2,q} = C_{z_1,q} \cos\eta + C_{x_1,q} \sin\eta$$

$$C_{m_2,\alpha} = C_{m_1,\alpha}$$

$$C_{m_2,\dot{\alpha}} = C_{m_1,\dot{\alpha}}$$

$$C_{m_2,q} = C_{m_1,q}$$

Amongst the derivatives involved in the lateral motion, those with respect to β and $\dot{\beta}$ are obtained in a similar way:

$$C_{y_2,\beta} = C_{y_1,\beta}$$

$$C_{y_2,\dot{\beta}} = C_{y_1,\dot{\beta}}$$

$$C_{l_2,\beta} = C_{l_1,\beta} \cos\eta - C_{n_1,\beta} \sin\eta$$

$$C_{l_2,\dot{\beta}} = C_{l_1,\dot{\beta}} \cos\eta - C_{n_1,\dot{\beta}} \sin\eta$$

$$C_{n_2,\beta} = C_{n_1,\beta} \cos\eta + C_{l_1,\beta} \sin\eta$$

$$C_{n_2,\dot{\beta}} = C_{n_1,\dot{\beta}} \cos\eta + C_{l_1,\dot{\beta}} \sin\eta$$

but derivatives with respect to p_2 and r_2 are more complex:

$$C_{y_2,p_2} = C_{y_1,p_1}\cos\eta - C_{y_1,r_1}\sin\eta$$

$$C_{y_2,r_2} = C_{y_1,p_1}\sin\eta + C_{y_1,r_1}\cos\eta$$

$$C_{l_2,p_2} = C_{l_1,p_1}\cos^2\eta - \left(C_{l_1,r_1} + C_{n_1,p_1}\right)\sin\eta\cos\eta + C_{n_1,r_1}\sin^2\eta$$

$$C_{l_2,r_2} = C_{l_1,r_1}\cos^2\eta + \left(C_{l_1,r_1} - C_{n_1,p_1}\right)\sin\eta\cos\eta - C_{n_1,p_1}\sin^2\eta$$

$$C_{n_2,p_2} = C_{n_1,p_1}\cos^2\eta + \left(C_{l_1,r_1} - C_{n_1,p_1}\right)\sin\eta\cos\eta - C_{l_1,r_1}\sin^2\eta$$

$$C_{n_2,r_2} = C_{n_1,r_1}\cos^2\eta + \left(C_{l_1,r_1} + C_{n_1,p_1}\right)\sin\eta\cos\eta + C_{l_1,p_1}\sin^2\eta$$

In the problem studied here, we suppose that system (1) is the aerodynamic system, and that system (2) is the system attached to the aeroplane. We shall also define here the system attached to the aeroplane as being that where axis OX coincides with the projection of the velocity at time $t = 0$. At this instant coefficients and derivatives in both systems are necessarily equal.

After a time dt, axis OX makes an angle α with Oxv. The preceding formulae are applicable, the angle η being nothing other than α, but we must take into account the fact that aerodynamic derivatives expressed in system (1) may vary themselves due to the increase α of the angle of attack.

The aerodynamic coefficients and their derivatives at an angle of attack $(\alpha_0 + \alpha)$, in the aerodynamic system, are supposed known. They are expressed as functions of their values at angle α_0 by expressions such as:

$$\left(C_{z^*}\right)_{\alpha_0+\alpha} = \left(C_{z^*}\right)_{\alpha_0} + \alpha\left(C_{z^*_\alpha}\right)_{\alpha_0} + \tfrac{1}{2}\alpha^2\left(C_{z^*_{\alpha^2}}\right)_{\alpha_0}$$

$$\left(C_{l^*p^*}\right)_{\alpha_0+\alpha} = \left(C_{l^*p^*}\right)_{\alpha_0} + \alpha\left(C_{l^*p^*_\alpha}\right)_{\alpha_0}$$

The derivatives of the coefficients in relation to dynamic axes GXYZ, at variable incidence α, may be written in terms of successive derivatives of coefficients at constant incidence α_0 in the axes Gxyz, in the following way:

$$C_{x_\alpha} = \left(C_{x^*_\alpha} - C_{z^*}\right)_{\alpha_0} + \alpha\left(\tfrac{1}{2}C_{x^*_{\alpha^2}} - \tfrac{1}{2}C_{z^*} - C_{z^*_\alpha}\right)_{\alpha_0}$$

$$C_{x_{\dot\alpha}} = \left(C_{x^*_{\dot\alpha}}\right)_{\alpha_0} + \alpha\left(C_{x^*_{\dot\alpha_\alpha}} - C_{z^*_{\dot\alpha}}\right)_{\alpha_0}$$

$$C_{x_q} = \left(C_{x^*_q}\right)_{\alpha_0} + \alpha\left(C_{x^*_{q_\alpha}} - C_{z^*_q}\right)_{\alpha_0}$$

$$C_{z_\alpha} = \left(C_{z^*_\alpha} + C_{x^*}\right)_{\alpha_0} + \alpha\left(\tfrac{1}{2} C_{z^*_{\alpha^2}} - \tfrac{1}{2} C_{z^*} + C_{x^*_\alpha}\right)_{\alpha_0}$$

$$C_{z_{\dot\alpha}} = \left(C_{z^*_\alpha}\right)_{\alpha_0} + \alpha\left(C_{z^*_{\dot\alpha_\alpha}} + C_{x^*_{\dot\alpha}}\right)_{\alpha_0}$$

$$C_{z_q} = \left(C_{z^*_q}\right)_{\alpha_0} + \alpha\left(C_{z^*_{q_\alpha}} + C_{x^*_q}\right)_{\alpha_0}$$

$$C_{m_\alpha} = \left(C_{m_\alpha}\right)_{\alpha_0} + \alpha\left(\tfrac{1}{2} C_{m_{\alpha_\alpha}}\right)_{\alpha_0}$$

$$C_{m_{\dot\alpha}} = \left(C_{m_{\dot\alpha}}\right)_{\alpha_0} + \alpha\left(C_{m_{\dot\alpha_\alpha}}\right)_{\alpha_0}$$

$$C_{m_q} = \left(C_{m_q}\right)_{\alpha_0} + \alpha\left(C_{m_{q_\alpha}}\right)_{\alpha_0}$$

$$C_{y_\beta} = \left(C_{y_\beta}\right)_{\alpha_0} + \alpha\left(C_{y_{\beta_\alpha}}\right)_{\alpha_0}$$

$$C_{y_{\dot\beta}} = \left(C_{y_{\dot\beta}}\right)_{\alpha_0} + \alpha\left(C_{y_{\dot\beta_\alpha}}\right)_{\alpha_0}$$

$$C_{y_p} = \left(C_{y_{p^*}}\right)_{\alpha_0} + \alpha\left(C_{y_{p^*_\alpha}} - C_{y_{r^*}}\right)_{\alpha_0}$$

$$C_{y_r} = \left(C_{y_{r^*}}\right)_{\alpha_0} + \alpha\left(C_{y_{r^*_\alpha}} - C_{y_{p^*}}\right)_{\alpha_0}$$

$$C_{l_\beta} = \left(C_{l^*_\beta}\right)_{\alpha_0} + \alpha\left(C_{l^*_{\beta_\alpha}} - C_{n^*_\beta}\right)_{\alpha_0}$$

$$C_{l_{\dot\beta}} = \left(C_{l^*_{\dot\beta}}\right)_{\alpha_0} + \alpha\left(C_{l^*_{\dot\beta_\alpha}} - C_{n^*_{\dot\beta}}\right)_{\alpha_0}$$

$$C_{l_p} = \left(C_{l^*_{p^*}}\right)_{\alpha_0} + \alpha\left(C_{l^*_{p^*_\alpha}} - C_{l^*_{r^*}} - C_{n^*_{p^*}}\right)_{\alpha_0}$$

$$C_{l_r} = \left(C_{l^*_{r^*}}\right)_{\alpha_0} + \alpha\left(C_{l^*_{r^*_\alpha}} - C_{l^*_{p^*}} - C_{n^*_{r^*}}\right)_{\alpha_0}$$

$$C_{n_\beta} = \left(C_{n^*_\beta}\right)_{\alpha_0} + \alpha\left(C_{n^*_{\beta_\alpha}} + C_{l^*_\beta}\right)_{\alpha_0}$$

$$C_{n_{\dot\beta}} = \left(C_{n^*_{\dot\beta}}\right)_{\alpha_0} + \alpha\left(C_{n^*_{\dot\beta_\alpha}} + C_{l^*_{\dot\beta}}\right)_{\alpha_0}$$

$$C_{n_p} = \left(C_{n^*_{p^*}}\right)_{\alpha_0} + \alpha\left(C_{n^*_{p^*_\alpha}} - C_{l^*_{p^*}} - C_{n^*_{r^*}}\right)_{\alpha_0}$$

$$C_{n_r} = \left(C_{n^*_{r^*}}\right)_{\alpha_0} + \alpha\left(C_{n^*_{r^*_\alpha}} - C_{l^*_{r^*}} - C_{n^*_{r^*}}\right)_{\alpha_0}$$

Finally, the derivatives, with respect to a control deflection, will be:

$$C_{x_\delta} = \left(C_{x^*_\delta}\right)_{\alpha_0} + \alpha\left(C_{x^*_{\delta_\alpha}} - C_{z^*_\delta}\right)_{\alpha_0}$$

$$C_{y_\delta} = \left(C_{y_\delta}\right)_{\alpha_0} + \alpha\left(C_{y_{\delta_\alpha}}\right)_{\alpha_0}$$

$$C_{z_\delta} = \left(C_{z^*_\delta}\right)_{\alpha_0} + \alpha\left(C_{z^*_{\delta_\alpha}} + C_{x^*_\delta}\right)_{\alpha_0}$$

$$C_{l_\delta} = \left(C_{l^*_\delta}\right)_{\alpha_0} + \alpha\left(C_{l^*_{\delta_\alpha}} - C_{n^*_\delta}\right)_{\alpha_0}$$

$$C_{m_\delta} = \left(C_{m_\delta}\right)_{\alpha_0} + \alpha\left(C_{m_{\delta_\alpha}}\right)_{\alpha_0}$$

$$C_{n_\delta} = \left(C_{n^*_\delta}\right)_{\alpha_0} + \alpha\left(C_{n^*_{\delta_\alpha}} - C_{l^*_\delta}\right)_{\alpha_0}$$

Note

We will calculate, as an example, the derivative C_{z_α}. The definition of C_{z_α} gives

$$C_{z_\alpha} = \frac{1}{\alpha}\left[\left(C_z\right)_{\alpha_0+\alpha} - \left(C_z\right)_{\alpha_0}\right]$$

$$\left(C_z\right)_{\alpha_0+\alpha} - \left(C_z\right)_{\alpha_0} = \left(C_{z^*}\right)_{\alpha_0+\alpha}\cos\alpha + \left(C_{x^*}\right)_{\alpha_0+\alpha}\sin\alpha - \left(C_{z^*}\right)_{\alpha_0}$$

$$\left(C_{z^*}\right)_{\alpha_0+\alpha} = \left(C_{z^*}\right)_{\alpha_0} + \alpha\left(C_{z^*_\alpha}\right)_{\alpha_0} + \tfrac{1}{2}\alpha^2\left(C_{z_{\alpha^2}}\right)_{\alpha_0} + \ldots.$$

$$\left(C_{x^*}\right)_{\alpha_0+\alpha} = \left(C_{x^*}\right)_{\alpha_0} + \alpha\left(C_{x^*_\alpha}\right)_{\alpha_0} + \ldots.$$

Since

$$\cos\alpha = 1 - \tfrac{1}{2}\alpha^2$$

$$\sin\alpha = \alpha$$

Then

$$C_{z_\alpha} = \frac{1}{\alpha}\left[\left(C_{z^*}\right)_{\alpha_0} + \alpha\left(C_{z^*_\alpha}\right)_{\alpha_0} + \tfrac{1}{2}\alpha^2\left(C_{z^*_{\alpha^2}}\right)_{\alpha_0}\right]\left[1 - \tfrac{1}{2}\alpha^2\right]$$

$$+ \left[\left(C_{x^*}\right)_{\alpha_0} + \alpha\left(C_{x^*_\alpha}\right)_{\alpha_0}\right] - \frac{1}{\alpha}\left(C_{z^*}\right)_{\alpha_0}$$

$$= \left(C_{z^*_\alpha}\right)_{\alpha_0} + \left(C_{x^*}\right)_{\alpha_0} + \alpha\left[\tfrac{1}{2}C_{z^*_{\alpha^2}} - \tfrac{1}{2}C_{z^*} + C_{x^*_\alpha}\right]_{\alpha_0}$$

CHAPTER 4

DYNAMICS OF THE NON-RIGID AEROPLANE

J.Czinczenheim*

The aim in previous chapters was the study of the motion of the aeroplane considered as rigid. With the increase in size and speeds of aeroplanes, and also with the paring down of their structure, deformations under the action of aerodynamic and inertia loads can no longer be always neglected. These deformations, by altering the loads, also alter the aeroplane's motion and create thus a coupling between the elastic deformations and the dynamics of the aeroplane.

In order to study the motion of such a system resulting from the aerodynamic and inertia forces considered previously, it is necessary to add elastic forces (and eventually structural or artificial damping forces). Local profile deformations and plastic deformations will, however, not be dealt with here.

The whole of these forces condition not only the flight dynamics of the aeroplane, but also its vibration qualities (free vibrations, forced vibrations and flutter) and its structural stability (divergence). These various phenomena may be studied either simultaneously, accepting the resulting complexity, or individually, their separation being somewhat difficult.

4.1 GENERALIZED COORDINATES

An aeroplane that can be deformed possesses an infinite number of degrees of freedom, a rigorous study of which would lead to partial differential equations. The solution of such systems of equations would meet with great difficulties. It is preferable to look for approximate solutions by means of simplifications reducing the problem to one having a finite number of degrees of freedom. The method to be described here is the one most frequently used. Other methods exist, but their field of application is more limited.

The motion of the deformable aeroplane can be defined by superimposing, on the motion of a rigid aeroplane, as reference, the displacements corresponding to the deformations. If, at instant t, P_0 is any point of the rigid reference aeroplane and P the corresponding point of the non-rigid aeroplane, the deformation will be defined by the vector

$$\vec{d}(P_0,t) = \overrightarrow{P_0P} \tag{4.1}$$

To reduce the problem to a finite number of degrees of freedom, we make the approximate hypothesis that the deformation vector may be represented by an expression such as

$$\vec{d}(P_0,t) = \sum_{1}^{n} \vec{d_i}(P_0)\, q_i(t) \tag{4.2}$$

---

* *Ingénieur en Chef à la Société des Ateliers d'Aviation Louis Bréguet*

$\vec{d}_i(P_0)$ being vectors independent of time, and called modes of deformation, dependent only on the point considered, and $q_i(t)$ functions of time, called generalized coordinates.

In fact, if we take a sufficiently large number of arbitrary modes (checking, nevertheless, the conditions at the limits of actual deformation), the deformation of the structure will be obtained with as great an accuracy as we wish. In order to define the motion of the aeroplane, we need only determine the generalized coordinates.

In the most general case, the problem thus leads to n degrees of freedom in addition to those of the rigid aeroplane.

Expression (4.2) for the deformation of the aeroplane constitutes the basis of the semi-rigid representation. We could determine the connecting forces to be introduced in order that the actual structure should really be deformed according to relation (4.2). If the connecting forces so determined are small in relation to exterior loads, the approximation for the deformation of the structure can be considered satisfactory.

In practice, arbitrary modes are not chosen, but modes approaching the actual deformations.

In order to limit ourselves to deformations which can exert an influence on the dynamics of flight of the aeroplane (and at the same time exclude phenomena such as flutter, which can be dealt with in a similar way), we may note that the motions met with in the dynamics of flight have frequencies of the order of 1 or 2 cycles/sec maximum (except for the engines) whereas the normal modes of vibration of the aeroplane generally have higher frequencies. Deformation modes having an influence on the general motion of the aeroplane will thus be the normal modes of low frequency, mostly the fundamental modes of the wings, fuselage, tail unit, and sometimes the next mode. These modes and the parameters which follow are generally available for computation, having been previously determined from vibration calculations.

Except where otherwise stated, degrees of freedom chosen to represent the deformations will thus be the normal modes of vibration.

4.2 EQUATIONS OF MOTION

The semi-rigid representation would enable us to obtain the equations of motion by Lagrange's equations. However, to define the motion of the aeroplane by this method we should have to use position parameters instead of the usual velocity parameters. To overcome this difficulty, Lagrange's equations will only be used to determine the equations relative to the generalized coordinates of deformation, whereas the equations of the motion of the centre of gravity and about the centre of gravity will be obtained by writing down that the resultant of the exterior forces is in equilibrium with the inertia forces and that the resultant moment of the exterior forces balances the inertia forces.

4.2.1 Determination of Forces and Moments

4.2.1.1 Inertia Forces

Let x_{0k}, y_{0k}, z_{0k} be the coordinates of any point P_{0k} of the reference aeroplane, $\xi_i(x_{0k},y_{0k},z_{0k})$, $\eta_i(x_{0k},y_{0k},z_{0k})$, $\zeta_i(x_{0k},y_{0k},z_{0k})$ the components of the mode $\vec{d}_i(P_{0k})$. The expression of the absolute velocity of point P_k, homologue of P_{0k} , will be given by:

$$\vec{V}_{P_k} = V_{e_{P_k}} + \sum_i \vec{d}(P_{0,k})\ \dot{q}_i(t) \tag{4.3}$$

$\vec{V}_{e_{P_k}}$ being the dragging velocity of P_k .

Components of $\vec{V}_{P_k}$ will be

$$\left.\begin{aligned} &u_{G_0} + qz_{0k} - ry_{0k} + \sum_i (q\zeta_i - r\eta_i)q_i + \sum_i \xi_i \dot{q}_i \\ &v_{G_0} + rx_{0k} - pz_{0k} + \sum_i (r\xi_i - p\zeta_i)q_i + \sum_i \eta_i \dot{q}_i \\ &w_{G_0} + py_{0k} - qx_{0k} + \sum_i (p\eta_i - q\xi_i)q_i + \sum_i \zeta_i \dot{q}_i \end{aligned}\right\} \tag{4.4}$$

The expression of absolute acceleration $\vec{\Gamma}_{P_k}$ approximated to the second order is:

$$\vec{\Gamma}_{P_k} = \vec{\Gamma}_{P_{0k}} + \sum_i \vec{d}_i(x_{0k},y_{0k},z_{0k})\ \ddot{q}_i(t) \tag{4.5}$$

the components of which are:

$$\left.\begin{aligned} &\dot{u}_{G_0} + \dot{q}z_{0k} - \dot{r}y_{0k} + \sum_i \xi_i(x_{0k},y_{0k},z_{0k})\ \ddot{q}_i(t) \\ &\dot{v}_{G_0} + \dot{r}x_{0k} - \dot{p}z_{0k} + \sum_i \eta_i(x_{0k},y_{0k},z_{0k})\ \ddot{q}_i(t) \\ &\dot{w}_{G_0} + \dot{p}y_{0k} - \dot{q}x_{0k} + \sum_i \zeta_i(x_{0k},y_{0k},z_{0k})\ \ddot{q}_i(t) \end{aligned}\right\} \tag{4.6}$$

Let us recall that coordinates x_{0k},y_{0k},z_{0k} are those of a point P_{0k} of the rigid aeroplane of reference, in a system of axes attached to the reference aeroplane of which the centre of gravity is G_0 .

The equilibrium of the resultant of the exterior forces and the forces of inertia will thus be written

$$\sum_k m_k \vec{\Gamma}_k = \vec{F} \tag{4.7}$$

and the equilibrium of the resultant moment of the exterior forces and the inertia forces is expressed by

$$\sum_k m_k \overrightarrow{G_0 P_k} \wedge \vec{\Gamma}_{P_k} = \vec{\mathfrak{M}} \tag{4.8}$$

Vectorial equations lead to the six following equations:

$$\left.\begin{aligned}
&M\dot{u}_{G_0} + \sum_i \left[\sum_k m_k \xi_i(x_{0k}, y_{0k}, z_{0k})\right] \ddot{q}_i = X_r + \Delta X_d \\
&M(\dot{v}_{G_0} + V_0 r) + \sum_i \left[\sum_k m_k \eta_i(x_{0k}, y_{0k}, z_{0k})\right] \ddot{q}_i = Y_r + \Delta Y_d \\
&M(\dot{w}_{G_0} - V_0 q) + \sum_i \left[\sum_k m_k \zeta_i(x_{0k}, y_{0k}, z_{0k})\right] \ddot{q}_i = Z_r + \Delta Z_d
\end{aligned}\right\} \tag{4.9}$$

$$\left.\begin{aligned}
&I_{x_0}\dot{p} - I_{x_0 z_0}\dot{r} + \sum_i \left[\sum_k m_k(\xi_i y_{0k} - \eta_i z_{0k})\right] \ddot{q}_i = L_r + \Delta L_d \\
&I_{y_0}\dot{q} + \sum_i \left[\sum_k m_k(\eta_i z_{0k} - \zeta_i x_{0k})\right] \ddot{q}_i = M_r + \Delta M_d \\
&I_{z_0}\dot{r} - I_{x_0 z_0}\dot{p} + \sum_i \left[\sum_k m_k(\zeta_i x_{0k} - \xi_i y_{0k})\right] \ddot{q}_i = N_r + \Delta N_d
\end{aligned}\right\} \tag{4.10}$$

These equations, laid down in the frame of linearization, are different from those of the rigid aeroplane in the following ways:

(a) in the first members, to the forces and moment of inertia forces of the rigid aeroplane must be added terms of inertia couplings due to the deformations;

(b) in the second members, to the forces and moments X_r, Y_r, Z_r, L_r, M_r, N_r of the rigid aeroplane, must be added forces and moments ΔX_d, ΔY_d, ΔZ_d, ΔL_d, ΔM_d, ΔN_d due to the deformations.

To these equations must be added equations relative to generalized coordinates q_k which will be obtained by Lagrange's method.

The kinetic energy of the system is

$$\left.\begin{aligned}
2T &= \sum_k m_k V_k^2 \\
&= \sum_k m_k \left\{\left[\alpha + \sum_i (q\zeta_i - r\eta_i)\, q_i + \sum_i \xi_i \dot{q}_i\right]^2 + \right. \\
&\qquad + \left[\beta + \sum_i (r\xi_i - p\zeta_i)\, q_i + \sum_i \eta_i \dot{q}_i\right]^2 + \\
&\qquad \left. + \left[\gamma + \sum_i (p\eta_i - q\xi_i)\, q_i + \sum_i \zeta_i \dot{q}_i\right]^2 \right\}
\end{aligned}\right\} \tag{4.11}$$

with:

$$\left.\begin{aligned} \alpha &= u_{G_0} + qz_{0k} - ry_{0k} \\ \beta &= v_{G_0} + rx_{0k} - pz_{0k} \\ \gamma &= w_{G_0} + py_{0k} - qx_{0k} \end{aligned}\right\} \tag{4.12}$$

Approximating to the second order we get

$$\frac{\partial T}{\partial q_h} = \sum_k m_k V_0 \, (q\zeta_h - r\eta_h) \tag{4.13}$$

$$\left.\begin{aligned} \frac{d}{dt}\left(\frac{\partial T}{\partial \dot{q}_h}\right) = \sum_k m_k \Bigg\{ &\left[\dot{u}_{G_0} + \dot{q}z_{0k} - \dot{r}y_{0k} + \sum_i \xi_i \ddot{q}_i\right]\xi_h + \\ &+ \left[\dot{v}_{G_0} + \dot{r}x_{0k} - \dot{p}z_{0k} + \sum_i \eta_i \ddot{q}_i\right]\eta_h + \\ &+ \left[\dot{w}_{G_0} + \dot{p}y_{0k} - \dot{q}x_{0k} + \sum_i \zeta_i \ddot{q}_i\right]\zeta_h \Bigg\} \end{aligned}\right\} \tag{4.14}$$

$$\left.\begin{aligned} \frac{d}{dt}\left(\frac{\partial T}{\partial \dot{q}_h}\right) - \frac{\partial T}{\partial q_h} = \sum_k m_k \Bigg\{ &\left[\dot{u}_{G_0} + \dot{q}z_{0k} - \dot{r}y_{0k} + \sum_i \xi_i \ddot{q}_i\right]\xi_h + \\ &+ \left[\dot{v}_{G_0} + \dot{r}x_{0k} - \dot{p}z_{0k} + rV_0 + \sum_i \eta_i \ddot{q}_i\right]\eta_h + \\ &+ \left[\dot{w}_{G_0} + \dot{p}y_{0k} - \dot{q}x_{0k} + qV_0 + \sum_i \zeta_i \ddot{q}_i\right]\zeta_h \Bigg\} \end{aligned}\right\} \tag{4.15}$$

If the virtual work of the forces acting is written in the form $\delta W = \sum_h Q_h \, \delta_{q_h} +$ terms independent of δ_{q_h}, the equation of motion relative to the coordinate q_h will be

$$\sum_k m_k \left\{\left[\dot{u}_{G_0} + \dot{q}z_{0k} - ry_{0k} + \sum_i \xi_i \ddot{q}_i\right]\xi_h + \left[\dot{v}_{G_0} + rV_0 + \dot{r}x_{0k} + \dot{p}z_{0k} + \sum_i \eta_i \ddot{q}_i\right]\eta_h + \right.$$

$$\left. + \left[\dot{w}_{G_0} - qV_0 + py_{0k} - qx_{0k} + \sum_i \zeta_i \ddot{q}_i\right]\zeta_h \right\} = Q_h \tag{4.16}$$

The quantity Q_h appearing in the second member is the generalized force to be calculated for every generalized coordinate.

Equations (4.9), (4.10) and (4.16), with initial conditions, determine the motion entirely. It remains to explain the right hand side of these equations.

It is important to notice that up to now we have not made use of the hypothesis that modes $\overrightarrow{d_i}$ are normal modes. Equations (4.9), (4.10) and (4.16) thus remain valid for any modes, but can be simplified in the case of normal modes.

4.2.1.2 Gravity Forces

(a) The resultant of gravity forces is given by the same expressions as for the rigid aeroplane. The gravity components in axes attached to the aeroplane of reference will therefore be:

$$\left.\begin{array}{l} -Mg\ \sin\Theta_0 \quad - Mg\ \cos\Theta_0\ \theta \\ Mg\ \sin\Theta_0\ \psi + Mg\ \cos\Theta_0\ \varphi \\ Mg\ \cos\Theta_0 \quad - Mg\ \sin\Theta_0\ \theta \end{array}\right\} \qquad (4.17)$$

This is the same as given by Equation (2.4) when $\Phi_0 = 0$.

(b) The resultant moment of the gravity forces about the centre of gravity is zero. If we neglect the movement of the centre of gravity with respect to that of the rigid aeroplane, gravity forces do not come into the moment equations.

The motion of the aeroplane not being referred to its own centre of gravity, but to the point G_0 , which is the centre of gravity of the rigid aeroplane, we may account for the corrective terms, generally small, by means of the expressions

$$\left.\begin{array}{l} g\ \cos\Theta_0\ \sum_i \left(\sum_k m_k\ \eta_i\right) q_i \\ -g\ \sin\Theta_0\ \sum_i \left(\sum_k m_k\ \eta_i\right) q_i \ - g\ \cos\Theta_0\ \sum_i \left(\sum_k m_k\ \xi_i\right) q_i \\ g\ \sin\Theta_0\ \sum_i \left(\sum_k m_k\ \eta_i\right) q_i \end{array}\right\} \qquad (4.18)$$

(c) The contribution of the gravity force to the generalized forces is obtained by calculating the virtual work:

$$\delta W = g \sum_k m_k\ \delta z_k \qquad (4.19)$$

δz_k being the projection of the virtual displacement of P_k along the vertical. If α_1, β_1, γ_1 are the direction cosines of the vertical line related to G_0XYZ

$$\delta W = \sum_k m_k\ g \left[\alpha_1 \sum_i \xi_i\ \delta q_i + \beta_1 \sum_i \eta_i\ \delta q_i + \gamma_1 \sum_i \zeta_i\ \delta q_i\right] +$$

$$+ \text{terms independent of } \delta q_i \qquad (4.20)$$

and the component relative to q_k will be

$$Q_h = g \sum_k m_k\ (\alpha_1 \xi_h + \beta_1 \eta_h + \gamma_1 \zeta_h) \qquad (4.21)$$

with

$$\left.\begin{aligned} \alpha_1 &= -\sin\Theta_0 - \cos\Theta_0\ \theta \\ \beta_1 &= \sin\Theta_0\ \psi + \cos\Theta_0\ \varphi \\ \gamma_1 &= \cos\Theta_0 - \sin\Theta_0\ \theta \end{aligned}\right\} \qquad (4.22)$$

4.2.1.3 Elastic Forces

The contribution of the elastic forces can be calculated in several ways. The main advantage of using normal modes of vibration is the simplicity of the expression for the work of the elastic forces, due to the absence of elastic couplings (and also of inertia coupling). The resultant and resultant moment of these forces are zero. If the normal modes used have an impulse Ω_h and a generalized mass M_h defined by $M_h = \sum_k m_k(\xi^2{}_k + \eta^2{}_k + \zeta^2{}_k)$, the contribution of elastic forces to the relative generalized force of coordinate q_k will be

$$-M_k\ \Omega^2{}_k\ q_k^* \qquad (q_k^* = q_{k_0} + q_k)$$

where q_{k_0} is the value of the generalized coordinate at equilibrium

q_k the variation with respect to equilibrium.

Vibration calculations as well as ground measurements give at one and the same time Ω_k and M_k .

4.2.1.4 Damping Forces

In some problems it is necessary to take into account damping forces of several types (other than the aerodynamic forces). We might be led to introduce a damper in a command circuit, or to make allowance for the damping of the structure or of a servo-command, or of several types of friction, etc. The corresponding terms must always be evaluated in each case in an appropriate way.

4.2.1.5 Aerodynamic Forces

The aerodynamic forces to be used in the study of a non-rigid aeroplane may be quasi-stationary forces or non-stationary forces more or less complete. Frequencies appearing with structure deformations are generally higher than those corresponding to the motion of a rigid aeroplane. For equal speeds, the reduced frequency $\omega l/V$ (l = half-chord of mean profile) is thus higher in the case of the deformable aeroplane. As long as the value of this reduced frequency is sufficiently small (less than 0.05 for instance) we may limit ourselves to the use of quasi-stationary forces (but even then difficulties may arise).

On the other hand, when the reduced frequency is higher, or in the presence of rapid movements due to gusts for instance, the use of quasi-stationary forces is not always justified and must be thoroughly discussed. In such cases, non-stationary forces may be used, which at the expense of some difficulties lead to valid results.

Thus, in the calculation of aerodynamic forces, depending on the circumstances considered, we may use one of the following approximate methods:

(1) Quasi-stationary forces, taking into account spring forces and damping forces. The influence of elongation is evaluated as in steady motion.

(2) To the previous forces, we may add terms due to accelerations, which may be calculated by means of the non-steady two-dimensional flow theory, neglecting the effect of wake due to the variations of the circulation.

(3) Non-stationary two-dimensional harmonic forces, their expression being assumed valid in slightly damped or amplified movements. Aspect ratio corrections may be applied to the results for two-dimensional flows.

(4) Non-stationary harmonic forces for finite aspect ratios.

(5) Non-stationary forces for any type of motion, two-dimensional or otherwise. Their expressions contain integrals representative of the influence of past motion (due to wake).

In classical flight dynamics, approximation (1) or (2) is used; nevertheless, more severe approximations have been made in some cases.

In order to illustrate the complexity of the calculations met with in the case of non-steady forces, an example will be considered later (see Section 11.2.1). Propulsive forces may usually be treated like pressures, or may be considered separately; this is also true for tangential forces.

In cases (1), (2), (3) and (4), the pressure at any point of a supporting surface can be expressed as a difference $\Delta p = p_{\text{lower side}} - p_{\text{upper side}}$, thus:

$$\begin{aligned}\Delta p = {} & p_0 + p_u u + p_v v + p_w w + p_p p + p_q q + p_r r + \\ & + p_{\dot{u}}\dot{u} + p_{\dot{v}}\dot{v} + p_{\dot{w}}\dot{w} + p_{\dot{p}}\dot{p} + p_{\dot{q}}\dot{q} + p_{\dot{r}}\dot{r} + \\ & + \sum_i \left(p_{q_i} q_i^* + p_{\dot{q}_i}\dot{q}_i + p_{\ddot{q}_i}\ddot{q}_i \right)\end{aligned} \tag{4.23}$$

where p_0 is the difference in pressure at equilibrium
while p_λ is the derivative $\partial \Delta p / \partial \lambda$ arising in Equation (4.29).

p_0, p_u, p_v, etc. are functions of the point considered (and eventually of the reduced frequency).

From expression (4.23) we infer the resultant, the resultant moment and the generalized force.

Let α_{n_k}, β_{n_k}, γ_{n_k}, be the direction cosines of the normal $\overrightarrow{n_k}$ directed from the lower side towards the upper side, $\Delta\sigma_k$ an element of surface enclosing P_k, and $\vec{\delta}_{s_k}$ the virtual displacement of P_k. The components of this displacement are

$$\left.\begin{aligned} \delta_{x_k} &= \sum_j \xi_j \, \delta q_j + \text{terms independent of } \delta q_j \\ \delta_{y_k} &= \sum_j \eta_j \, \delta q_j + \quad " \qquad " \qquad " \quad \delta q_j \\ \delta_{z_k} &= \sum_j \zeta_j \, \delta q_j + \quad " \qquad " \qquad " \quad \delta q_j \end{aligned}\right\} \tag{4.24}$$

The resultant of the aerodynamic forces will be:

$$\vec{F} = \sum_k \Delta p \, \vec{n}_k \Delta\sigma_k \tag{4.25}$$

The resultant moment will be:

$$\vec{\mathcal{M}} = \sum_k \overrightarrow{G_0 P_k} \wedge \Delta p \, \vec{n}_k \Delta\sigma_k \tag{4.26}$$

The virtual work of the aerodynamic forces can be written:

$$\delta W = \sum_k \Delta p \, \vec{n}_k \, \vec{\delta}_{s_k} \Delta\sigma_k \tag{4.27}$$

The analytic expressions of previous quantities are:

$$\begin{aligned} X = X_0 &+ X_u u + X_v v + X_w w + X_p p + X_q q + X_r r + \\ &+ X_{\dot{u}} \dot{u} + X_{\dot{v}} \dot{v} + X_{\dot{w}} \dot{w} + X_{\dot{p}} \dot{p} + X_{\dot{q}} \dot{q} + X_{\dot{r}} \dot{r} + \\ &+ \sum_i \left(X_{q_i} q_i^* + X_{\dot{q}_i} \dot{q}_i + X_{\ddot{q}_i} \ddot{q}_i \right) \end{aligned} \tag{4.28}$$

Y, Z, L, M, N will be defined in the same way, by substitution of the symbol concerned.

In each of the equations, the derivatives X_u, X_v, ... N_q will be given by:

$$\left.\begin{aligned} X_\lambda &= \sum_k p_\lambda \, \alpha_{nk} \Delta\sigma_k \quad (\lambda = o, u, v, w, \dot{u}, \dot{v}, \dot{w}, p, q, r, \dot{p}, \dot{q}, \dot{r}, q_i^*, \dot{q}_i, \ddot{q}_i) \\ Y_\lambda &= \sum_k p_\lambda \, \beta_{nk} \Delta\sigma_k \\ Z_\lambda &= \sum_k p_\lambda \, \gamma_{nk} \Delta\sigma_k \\ L_\lambda &= \sum_k p_\lambda \, (y_{ok}\gamma_{nk} - z_{ok}\beta_{nk}) \Delta\sigma_k \\ M_\lambda &= \sum_k p_\lambda \, (z_{ok}\alpha_{nk} - x_{ok}\gamma_{nk}) \Delta\sigma_k \\ N_\lambda &= \sum_k p_\lambda \, (x_{ok}\beta_{nk} - y_{ok}\alpha_{nk}) \Delta\sigma_k \end{aligned}\right\} \tag{4.29}$$

The virtual work will be

$$\delta W = \sum_h Q_h \, \delta q_h \tag{4.30}$$

with

$$Q_h = Q_{h_0} + Q_{h_u} u + Q_{h_v} v + Q_{h_w} w + \ldots\ldots \qquad (4.28\text{ bis})$$

and, in a general way

$$Q_\lambda = \sum_k p_\lambda (\alpha_{nk}\, \xi_h + \beta_{nk}\, \eta_h + \gamma_{nk}\, \zeta_h)\, \Delta\sigma_k \qquad (4.29\text{ bis})$$

The equilibrium of the aeroplane is determined by the equations obtained by cancelling the perturbation terms in the different equations. We thus obtain:

$$\left.\begin{aligned} -Mg\,\sin\Theta_0 + X_0 + \sum_i X_{q_i} q_{i_0} &= 0 \\ Y_0 + \sum_i Y_{q_i} q_{i_0} &= 0 \\ Mg\,\cos\Theta_0 + Z_0 + \sum_i Z_{q_i} q_{i_0} &= 0 \\ L_0 + \sum_i L_{q_i} q_{i_0} &= 0 \\ M_0 + \sum_i M_{q_i} q_{i_0} &= 0 \\ N_0 + \sum_i N_{q_i} q_{i_0} &= 0 \end{aligned}\right\} \qquad (4.31)$$

$$g \sum_k m_k (-\xi_h\, \sin\Theta_0 + \zeta_h\, \cos\Theta_0) - M_h \Omega^2{}_h q_{h_0} + Q_{h_0} + \sum_i Q_{h_{q_i}} q_{i_0} = 0 \qquad (4.32)$$

These equations are the fundamentals of static aeroelasticity.

In the dynamic equations of motion, constant terms cancel out and there remain only the perturbation terms.

4.2.2 General Form of the Equations of Motion

It is now possible to write the equations of motion explicitly by combining the previous results. In order to obtain them in a condensed form, let us put:

$$\left.\begin{aligned} \sum_k m_k\, \xi_i &= \int \xi_i\, dm = M\, \xi_i^0 \\ \sum_k m_k\, \eta_i &= \int \eta_i\, dm = M\, \eta_i^0 \\ \sum_k m_k\, \zeta_i &= \int \zeta_i\, dm = M\, \zeta_i^0 \\ \sum_k m_k (y_{0k}\zeta_i - z_{0k}\eta_i) &= \int (y_0\zeta_i - z_0\eta_i)\, dm = k_{x_i} \\ \sum_k m_k (z_{0k}\xi_i - x_{0k}\zeta_i) &= \int (z_0\xi_i - x_0\zeta_i)\, dm = k_{y_i} \end{aligned}\right\} \qquad (4.33a)$$

$$\sum_k m_k(x_{0k}\eta_i - y_{0k}\xi_i) = \int(x_0\eta_i - y_0\xi_i)\,dm = k_{z_i} \qquad (4.33a)$$

$$\left.\begin{aligned} M_h &= \int(\xi_h^2 + \eta_h^2 + \zeta_h^2)\,dm \\ M_{ij} &= \int(\xi_i\xi_j + \eta_i\eta_j + \zeta_i\zeta_j)\,dm = 0 \end{aligned}\right\} \qquad (4.33b)$$

(This is the orthognal relation of normal modes).

$$\left.\begin{aligned} X_\lambda &= \int p_\lambda \alpha_n\,d\sigma \\ Y_\lambda &= \int p_\lambda \beta_n\,d\sigma \\ Z_\lambda &= \int p_\lambda \gamma_n\,d\sigma \\ L_\lambda &= \int p_\lambda(y_0\gamma_n - z_0\beta_n)\,d\sigma \\ M_\lambda &= \int p_\lambda(z_0\alpha_n - x_0\gamma_n)\,d\sigma \\ N_\lambda &= \int p_\lambda(x_0\beta_n - y_0\alpha_n)\,d\sigma \end{aligned}\right\} \qquad (4.34a)$$

$$Q_{h_\lambda} = \int p_\lambda(\xi_h\alpha_n + \eta_h\beta_n + \zeta_h\gamma_n)\,d\sigma \qquad (4.34b)$$

and making use of the symbolic notation

$$\begin{aligned} X_\mu = {} & X_u u + X_v v + X_w w + X_p p + X_q q + X_r r + \\ & + \sum_k (X_{q_i} q_i + X_{\dot{q}_i}\dot{q}_i + X_{\ddot{q}_i}\ddot{q}_i) + \\ & + X_{\dot{u}}\dot{u} + X_{\dot{v}}\dot{v} + X_{\dot{w}}\dot{w} + X_{\dot{p}}\dot{p} + X_{\dot{q}}\dot{q} + X_{\dot{r}}\dot{r} \end{aligned} \qquad (4.35)$$

with $Y_\mu\mu$, $Z_\mu\mu$, $L_\mu\mu$, $M_\mu\mu$, $N_\mu\mu$, $Q_{h_\mu}\mu$ having a similar meaning.

Under these conditions, the equations of motion become:

$$\left.\begin{aligned} M(\dot{u}_{G_0} + \sum_i \overset{0}{\xi_i}\ddot{q}_i + g\cos\Theta_0.\theta) &= X_\mu\mu \\ M(\dot{v}_{G_0} + V_0 r + \sum_i \overset{0}{\eta_i}\ddot{q}_i - g\sin\Theta_0.\varphi - g\cos\Theta_0.\varphi) &= Y_\mu\mu \end{aligned}\right\} \qquad (4.36)$$

$$\left.\begin{aligned}
M(\dot{w}_{G_0} - V_0 q + \sum_i \zeta_i^0 \ddot{q}_i + g \sin\Theta_0 . \theta) &= Z_\mu \mu \\
I_{x_0} \dot{p} - I_{x_0 z_0} \dot{r} + \sum_i k_{x_i} \ddot{q}_i &= L_\mu \mu \\
I_{y_0} \dot{q} + \sum_i k_{y_i} \ddot{q}_i &= M_\mu \mu \\
I_{z_0} \dot{r} - I_{x_0 z_0} \dot{p} + \sum_i k_{z_i} \ddot{q}_i &= N_\mu \mu
\end{aligned}\right\} \qquad (4.36)$$

$$M\left[\xi_h \dot{u}_{G_0} + \eta_h^0 \left(\dot{v}_{G_0} + r V_0\right) + \zeta_h^0 \left(\dot{w}_{G_0} - q V_0\right)\right] + k_{x_h} \dot{p} + k_{x_h} \dot{q} + k_{z_h} \dot{r} + M_h \ddot{q}_h$$

$$= Mg\left[-\xi_h^0 \cos\Theta_0 . \theta + \eta_h^0 (\sin\Theta_0 . \psi + \cos\Theta_0 . \varphi) - \zeta_h^0 \sin\Theta_0 . \theta\right] -$$

$$- M_h \Omega_h^2 q_h + Q_{h_\mu} \mu \qquad (4.37)$$

These equations are the fundamentals of dynamic aeroelasticity.

If modes $\overrightarrow{d_i}$ should happen not to be normal modes, terms $\sum_i' M_{i_h} \ddot{q}_i$ must be added in the last equation, and the expression of the work of the elastic forces eventually modified. For further details see Section 4.3.4.

4.3 STUDY OF SOME PARTICULAR CASES

From the general equations (4.36) and (4.37) we may infer the equations of motion corresponding to particular cases which appear frequently in practice. Let us consider as an example the following cases.

4.3.1 Motion of a Rigid Aeroplane with a Movable Control (Free or Attached by Springs or Servo-Controlled)

In order to study the general case where the control hinge may have any direction, let us consider the trihedral of origin C attached to the control Cx_f, y_f, z_f, axis Cz_f coinciding with the hinge, the coordinates of C being x_c, y_c, z_c, those of the centre of gravity of the control with respect to Cx_f, y_f, z_f being x_f, y_f, z_f and the direction cosines of the axes of the trihedral Cx_f, y_f, z_f with respect to the reference trihedral being

$$\left.\begin{array}{ccc}
\alpha_x & \beta_x & \gamma_x \\
\alpha_y & \beta_y & \gamma_y \\
\alpha_z & \beta_z & \gamma_z
\end{array}\right\} \qquad (4.38)$$

We may apply the general theory of Section 4.2.

We must still introduce the quantities m_f = mass of the control surface, and i_z, i_{xz}, i_{yz} - inertia moments and products of the surface:

$$\left.\begin{aligned} i_z &= \int (x_f^2 + y_f^2)\, dm \\ i_{xz} &= \int x_f z_f\, dm \\ i_{yz} &= \int y_f z_f\, dm \end{aligned}\right\} \qquad (4.39)$$

In these conditions the coupling terms of the equations of motion will be given by:

$$\left.\begin{aligned} M\xi^0 &= m_f(\alpha_y X_f - \alpha_x Y_f) \\ M\eta^0 &= m_f(\beta_y X_f - \beta_x Y_f) \\ M\zeta^0 &= m_f(\gamma_y X_f - \gamma_x Y_f) \end{aligned}\right\} \qquad (4.40)$$

$$\left.\begin{aligned} k_x &= m_f[y_c(\gamma_y X_f - \gamma_x Y_f) - z_c(\beta_y X_f - \beta_x Y_f) + \alpha_z i_z - \alpha_x i_{xz} - \alpha_y i_{yz} \\ k_y &= m_f[z_c(\alpha_y X_f - \alpha_x Y_f) - x_c(\gamma_y X_f - \gamma_x Y_f) + \beta_z i_z - \beta_x i_{xz} - \beta_y i_{yz} \\ k_z &= m_f[x_c(\beta_y X_f - \beta_x Y_f) - y_c(\alpha_y X_f - \alpha_x Y_f) + \gamma_z i_z - \gamma_x i_{xz} - \alpha_y i_{yz} \end{aligned}\right\} \qquad (4.41)$$

$$M_h = i_z \qquad (4.42)$$

We thus have all the inertia terms.

The aerodynamic forces can be obtained from those which act upon the rigid aeroplane by adding to them the components of the resultant and the resultant moment due to the deflection of the control surfaces.

The generalized force is given by:

$$Q_{h_\lambda} = \int p_\lambda[(\alpha_y x_f - \alpha_x y_f)\alpha_n + (\beta_y x_f - \beta_x y_f)\beta_n + (\gamma_y x_f - \gamma_x y_f)\gamma_n]\, d\sigma \qquad (4.43)$$

To give a simple interpretation of these results, let us suppose that axis x_f is situated in the chord plane of the control surface. The perpendicular will then be directed along axis y_f and we shall have:

$$\alpha_n = \alpha_y \qquad \beta_n = \beta_y \qquad \gamma_n = \gamma_y$$

$$Q_{h_\lambda} = \int p_\lambda[(\alpha_y x_f - \alpha_x y_f)\alpha_y + (\beta_y y_f - \beta_x y_f)\beta_y + (\gamma_y x_f - \gamma_x y_f)\gamma_y]\, d\sigma \qquad (4.43bis)$$

$$Q_{h_\lambda} = \int p_\lambda x_j\, d\sigma$$

which is the hinge moment of the aerodynamic forces referred to the control surface.

The equations of motion of the aeroplane with movable control surface will therefore be:

$$\left.\begin{aligned}
&M(\dot{u}_{G_0} + g\cos\Theta_0\,\theta) && + M\,\xi^0\ddot{\delta} &&= X_r + X_\delta\delta + X_{\dot\delta}\dot\delta + X_{\ddot\delta}\ddot\delta\\
&M(\dot{v}_{G_0} + V_0 r - g\sin\Theta_0\,\psi - g\cos\Theta_0\,\varphi) && + M\,\eta^0\ddot{\delta} &&= Y_r + Y_\delta\delta + Y_{\dot\delta}\dot\delta + Y_{\ddot\delta}\ddot\delta\\
&M(\dot{w}_{G_0} - V_0 q + g\sin\Theta_0\,\theta) && + M\,\zeta^0\ddot{\delta} &&= Z_r + Z_\delta\delta + Z_{\dot\delta}\dot\delta + Z_{\ddot\delta}\ddot\delta\\
&I_{x_0}\dot{p} - I_{x_0z_0}\dot{r} + k_x\ddot{\delta} && && = L_r + L_\delta\delta + L_{\dot\delta}\dot\delta + L_{\ddot\delta}\ddot\delta\\
&I_{y_0}\dot{q} + k_y\ddot{\delta} && && = M_r + M_\delta\delta + M_{\dot\delta}\dot\delta + M_{\ddot\delta}\ddot\delta\\
&I_z\dot{r} - I_{x_0z_0}\dot{p} + k_z\ddot{\delta} && && = N_r + N_\delta\delta + N_{\dot\delta}\dot\delta + N_{\ddot\delta}\ddot\delta
\end{aligned}\right\} \quad (4.44)$$

$$M\left[\xi^0\dot{u}_{G_0} + \dot\eta^0\left(\dot{v}_{G_0} + V_0 r\right) + \zeta^0\left(\dot{w}_{G_0} - V_0 q\right)\right] + k_x\dot{p} + k_y\dot{q} + k_z\dot{r} + i_z\ddot{\delta}$$

$$= Mg\left[-\xi^0\cos\Theta_0\,\theta + \eta^0(\sin\Theta_0\,\psi + \cos\Theta_0\,\varphi) - \zeta^0\sin\Theta_0\,\theta\right] - i_z\Omega^2\delta +$$

$$+ H_r + H_\delta\delta + H_{\dot\delta}\dot\delta + H_{\ddot\delta}\ddot\delta \qquad (4.45)$$

These general equations, once particularized, can be applied to the treatment of several problems such as:

(a) Snaking (the movable control surface is the rudder or eventually the aileron);

(b) Porpoising (when the movable control surface is the elevator);

(c) The study of the stability of a servo-controlled aeroplane with artificial feel in the control circuit (mass balance, spring tab, damper, etc.). In this case there is no aerodynamic force in the last equation, which is useful then to determine the motion of the rod system;

(d) The stabilization of manually controlled aeroplanes by means of mass balances and spring tabs in the control circuit.

Note

(c) The equation of motion of the control surface contains, as particular cases, equations given by B.Etkin in his excellent book 'Dynamics of Flight' (Equations 4.8.13 for the elevator, 4.9.4 for the rudder and 4.10.8 for the aileron)[2].

As an example, we shall give particulars for the control equation in the case of an elevator with no sweep-back (Fig.4.5.6 of the book mentioned).

Since the z_f axis must constitute the hinge, following adopted conventions, we have the following table:

$$\alpha_x = -1 \qquad \beta_x = 0 \qquad \gamma_x = 0$$

$$\alpha_y = 0 \qquad \beta_y = 0 \qquad \gamma_y = 1$$

$$\alpha_z = 0 \qquad \beta_z = 1 \qquad \gamma_z = 0$$

$$X_f = l \qquad Y_f = 0 \qquad Z_f = 0$$

$$x_c = -l \qquad y_c = 0 \qquad z_c = 0$$

Making use of the definitions of the different quantities entering into the equation we find successively:

$$M\xi^0 = 0 \qquad M\eta^0 = 0 \qquad M\zeta^0 = m_f e$$

$$k_x = i_{xz} = 0 \qquad k_y = m_f l_e + i_z \qquad k_z = 0$$

by symmetry.

Under these conditions the equation of motion becomes:

$$m_f e\left(\dot{w}_{G_0} - V_0 q\right) + (m_f l_e + i_z)\dot{q} + i_z\ddot{\delta} = H$$

an equation identical to Equation 4.8.13 of the book mentioned previously, with the following relations between the symbols:

$$i_z = I_e$$

$$m_f e = m_e l_e$$

$$\dot{w}_{G_0} - V_0 q = ac_z$$

$$m_f l_e + i_z = -P_{ex}$$

The hinge moment of the aerodynamic forces due to pilot action and elasticity is

$$H = H_e + F_e$$

The term in PR of Equation 4.8.13, being of second order, does not appear in the general equation.

4.3.2 Motion of a Rigid Aeroplane Controlled by an Accelerometer

When an aeroplane is equipped with an accelerometer giving steering orders proportional to detected accelerations, we may consider that the equations of motion of the centre of gravity and of the motion about the centre of gravity are altered only by aerodynamic forces and moments due to control deflections. The study of the motion shows, in fact, that the accelerometer does not give orders proportional to the accelerations but that there remain parasitic terms which it is important to know. The general theory of Section 4.2 can be applied very simply.

Let x_a, y_a, z_a be the coordinates of the mass of the accelerometer in its equilibrium position referred to the centre of gravity of the aeroplane; α , β , γ the direction cosines of the direction of its motion; λ its linear displacement from its equilibrium position, relative to the aeroplane.

The deformation may be defined by:

$$\overrightarrow{d_h q_h} \quad \left.\begin{matrix} \lambda\alpha_1 \\ \lambda\beta_1 \\ \lambda\gamma_1 \end{matrix}\right\} \text{ for the accelerometer's mass} \qquad \left.\begin{matrix} 0 \\ 0 \\ 0 \end{matrix}\right\} \text{ for other points of the aeroplane}$$

We have thus:

$$\xi = \alpha_1$$

$$\eta = \beta_1$$

$$\zeta = \gamma_1$$

and

$$q_h = \lambda$$

$$\left.\begin{aligned} M\,\xi^0 &= m_a\alpha_1 \\ M\,\eta^0 &= m_a\beta_1 \\ M\,\zeta^0 &= m_a\gamma_1 \end{aligned}\right\} \qquad (4.46a)$$

$$\left.\begin{aligned} k_x &= (y_a\gamma_1 - z_a\beta_1)m_a \\ k_y &= (z_a\alpha_1 - x_a\gamma_1)m_a \\ k_z &= (x_a\beta_1 - y_a\alpha_1)m_a \end{aligned}\right\} \qquad (4.46b)$$

$$M_h = m_a \qquad (4.47)$$

The equation of motion of the accelerometer will be:

$$m_a\left[\alpha_1\dot{u}_{G_0} + \beta_1\left(\dot{v}_{G_0} + V_0 r\right) + \gamma_1\left(\dot{w}_{G_0} - V_0 q\right) + (y_a\gamma_1 - z_a\beta_1)\dot{p} + \right.$$

$$\left. + (z_a\alpha_1 - x_a\gamma_1)\dot{q} + (x_a\beta_1 - y_a\alpha_1)\dot{r}\right] + m_a\ddot{\lambda}$$

$$= m_a g[-\alpha_1 \cos\Theta_0\,\theta + \beta_1(\sin\Theta_0\,\psi + \cos\Theta_0\,\varphi) - \gamma_1 \sin\Theta_0\,\theta] - m_a\Omega^2\lambda \qquad (4.48)$$

It is obvious that the reading of the accelerometer, λ , is only correct for rectilinear motion, under the condition that accelerations should be slow. In other cases, the accelerometer readings will be altered by gravity terms, by the

error in position as well as by the inertia effect of the mass of the accelerometer.

The previous equation, together with the equations of motion of the aeroplane, enable us to study the stability of the aeroplane when subjected to accelerations (tangential, normal or a combination). Simpler cases will be studied later.

4.3.3 Stability of an Aeroplane with a Flexible Fuselage

The flexibility of the fuselage may have considerable influence on the dynamic stability, and even on the static stability. (For example, in the case of bombers with very long fuselages).

Because of symmetry, vertical flexibility influences only the longitudinal motion.

If we call $\zeta(x)$ the component, along G_0z, of the deformation mode of the fuselage, h the corresponding generalized coordinate, other components being zero, it follows, from symmetry, by the general method given in Section 4.2 that

$$\left.\begin{aligned} M\,\xi^0 &= 0 \\ M\,\eta^0 &= 0 \\ M\,\zeta^0 &= \int \zeta\,dm \end{aligned}\right\} \qquad (4.49a)$$

$$\left.\begin{aligned} k_x &= \int y_0\,\zeta\,dm = 0 \\ k_y &= \int -x_0\,\zeta\,dm \\ k_z &= 0 \end{aligned}\right\} \qquad (4.49b)$$

$$M = \int \zeta^2\,dm \qquad (4.50)$$

As far as the aerodynamic forces are concerned we find:

$$\alpha_n \neq 0 \qquad \beta_n \neq 0 \qquad \gamma_n \neq 1$$

$X_\lambda \neq 0$ but can be written $X_\lambda \lambda$

$Y_\lambda = 0$

$Z_\lambda = \int p_\lambda\,d\sigma$ = resultant of pressure forces

$$L_\lambda = 0$$

$$M_\lambda = -\int p_\lambda x_0\,d\sigma$$

$$N_\lambda = 0$$

$$Q_\lambda = \int p_\lambda \zeta\,d\sigma$$

The four equations of longitudinal motion will be (neglecting aerodynamic forces due to accelerations):

$$\left.\begin{aligned} M\left(\dot{u}_{G_0} + g\cos\Theta_0\,\theta\right) &= X_r + X_h h + X_{\dot{h}}\dot{h} \\ M\left(\dot{w}_{G_0} + g\sin\Theta_0\,\theta - V_0 q\right) + \left(\int \zeta\, dm\right)\ddot{h} &= Z_r + Z_h h + Z_{\dot{h}}\dot{h} \\ I_y\dot{q} - \left(\int x_0 \zeta\, dm\right)\ddot{h} &= M_r + M_h h + M_{\dot{h}}\dot{h} \end{aligned}\right\} \qquad (4.51)$$

$$M\,\zeta^0\left(\dot{w}_{G_0} - qV_0\right) - \left(\int x_0\zeta\, dm\right)\dot{q} + M_{\ddot{h}}\ddot{h}$$

$$= Mg(-\zeta^0 \sin\Theta_0\,\theta) - M_h\Omega_h^2\, h + Q_r + Q_h h + Q_{\dot{h}}\dot{h} \qquad (4.52)$$

The expression for aerodynamic forces due to fuselage bending can be obtained from the characteristics of the tail unit.

The discussion relative to the influence of fuselage flexibility follows from the previous equations. The characteristic equation is one of 6th degree. It is easier to study the problem on an analogue computer, which gives the answer directly. In particular it is possible to determine the stiffness required for the dynamic stability to be acceptable.

4.3.4 Study of the Influence of Deformations in Arbitrary Modes

The use of normal modes is not always essential and in some cases it may be interesting to use arbitrary modes. The equations of forces and moments remain then unchanged and only the equation of the generalized force is modified.

The orthogonality relation

$$M_{ih} = \int(\xi_i\xi_h + \eta_i\eta_h + \zeta_i\zeta_h)\, dm = 0 \qquad (4.53)$$

being no longer satisfied, coupling terms appear under the form

$$\sum_i M_{h_i}\ddot{q}_i \quad \text{instead of } M_h\,\ddot{q}_h$$

In the same way, elastic terms will take the form

$$-\sum_i a_{h_i}\, q_i \text{ instead of } M_h\Omega_h^2 q_h$$

If, for instance, the deformation of the structure results from the combination of bending with torsion, the work done by the elastic forces will be

$$W = -\frac{1}{2}\int\left[EI\left(\frac{\partial^2 y}{\partial s^2}\right)^2 + GJ\left(\frac{\partial\theta}{\partial s}\right)^2\right] ds \qquad (4.54)$$

If we put:

$$y = c_1(x)q_1 + c_2(x)q_2 + \ldots\ldots + c_n(x)q_n$$

$$\theta = d_1(x)q_{n+1} + d_2(x)q_{n+2} + \ldots\ldots + d_n(x)q_{n+2}$$

we deduce

$$Q_h = \sum_i a_{h_i} q_i$$

with

$$a_{h_i} = \int EI\ c_h''\ c_i''\ dx \qquad \text{for } 0 < i \leqslant n$$

$$a_{h_i} = \int GJ\ d_h''\ d_h''\ dx \qquad \text{for } n < i \leqslant 2n$$

$$c_h'' = \frac{\partial^2 c_h}{\partial s^2}$$

The resolution of the problem in arbitrary modes is quite straightforward, except that the number of terms is increased in the last equation. Nevertheless, the choice of adequate modes is more delicate, and the number of elastic degrees of freedom is more important than the strict minimum. This might have the result of complicating the calculations which the adoption of normal modes can generally avoid.

4.4 FUNCTIONAL DIAGRAM CORRESPONDING TO A NON-RIGID AEROPLANE

Comparison between the equations of motion with those of the rigid aeroplane shows that from the point of view of the block diagram of the rigid aeroplane we can take the rigid aeroplane as a basis, but this must be completed by:

(a) As many extra equations as there are generalized coordinates;

(b) In each equation aerodynamic and inertia coupling terms are added and in the equation of generalized forces extra elastic terms and eventually damping terms are added.

Examples will be dealt with in Chapter 11 showing practical applications of the above theory.

LIST OF FIGURES

		Page
Fig.1	Location of axis OX	76
Fig.2	Earth and aeroplane axes	76
Fig.3	Rotations ψ, θ, φ	77
Fig.4	Action of a rotation Ω about the vertical	77
Fig.5	Angles of attack and sideslip in steady air	78
Fig.6	Angles of attack and sideslip in non-steady air	78
Fig.7	Projection of gravity on axes GX_0, Y_0, Z_0	79
Fig.8	Amplitude and phase of C_m for sinusoidal variation of α	80
Fig.9	Amplitude and phase of C_L for sinusoidal variation of α	80
Fig.10	(a) Dividing an input into steps	81
	(b) Dividing an input into pulses	81
Fig.11	Overall transfer function of an aircraft	81
Fig.12	Division into partial transfer functions of the 2nd order	82
Fig.13	Variation of angle of attack with time	82
Fig.14	Presentation of C_m as a function of α and M	83
Fig.15	Rotation η	84
Fig.16	Characteristic elements of an elevator	84

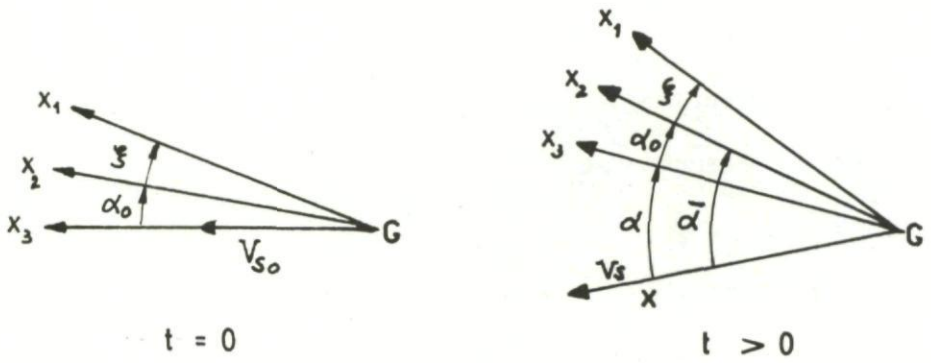

Fig.1 Location of axis OX

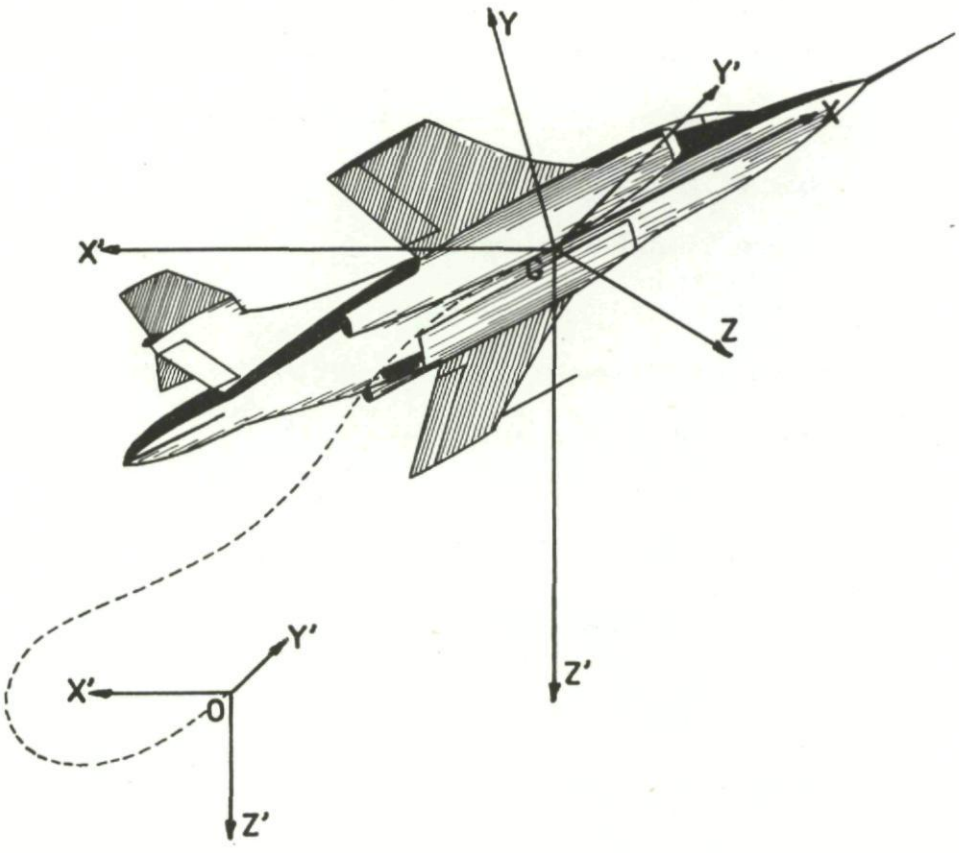

Fig.2 Earth and aeroplane axes

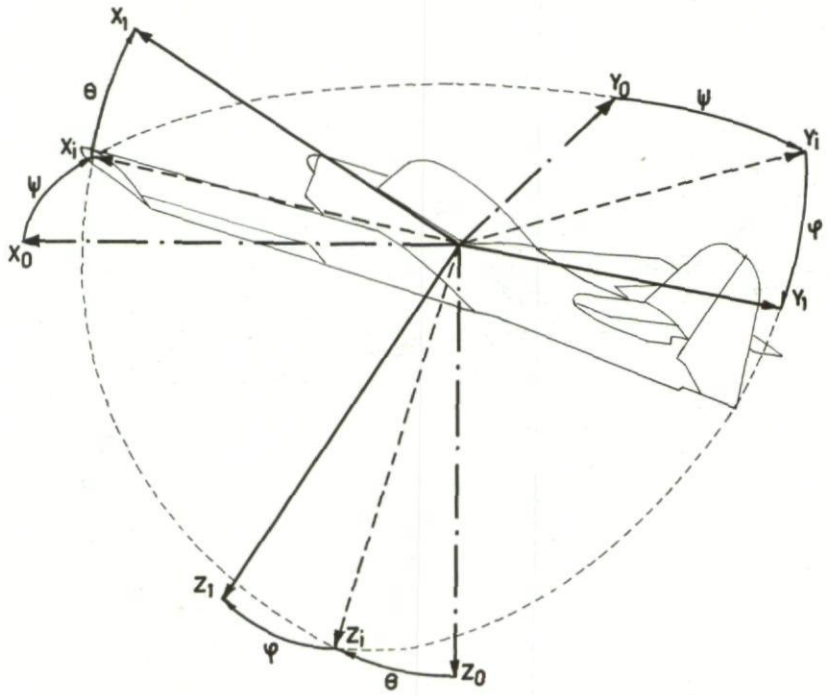

Fig.3 Rotations ψ, θ, φ

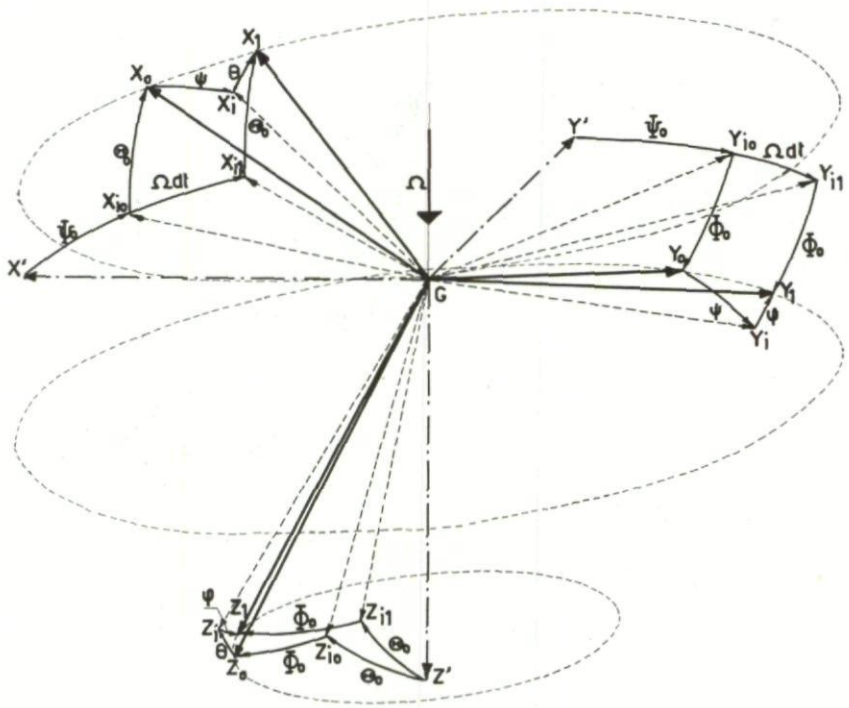

Fig.4 Action of a rotation Ω about the vertical

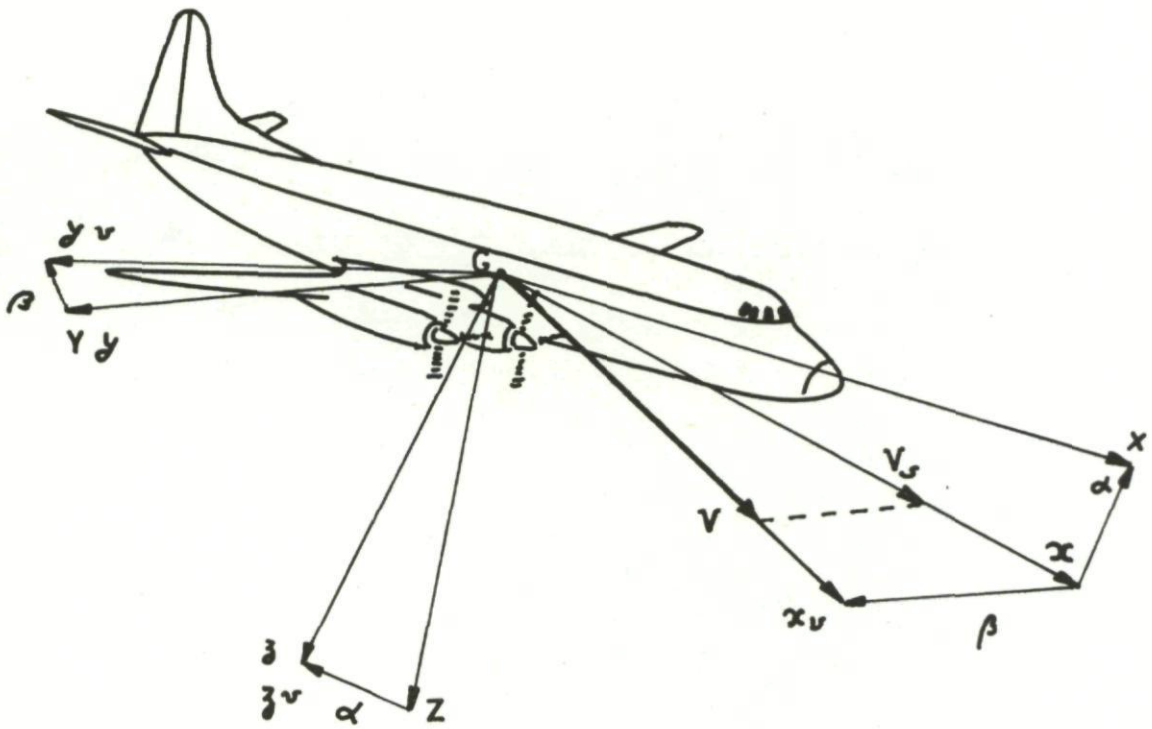

Fig.5 Angles of attack and sideslip in steady air

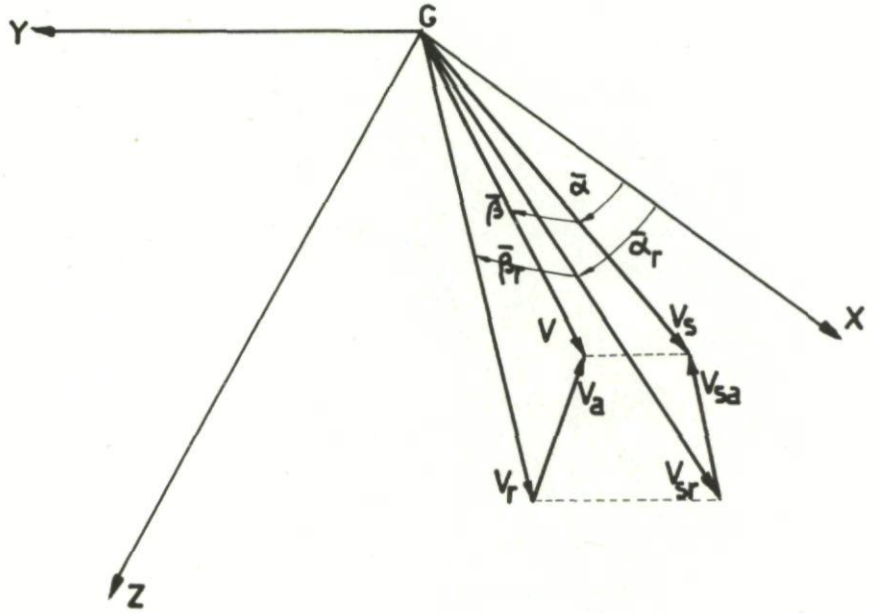

Fig.6 Angles of attack and sideslip in non-steady air

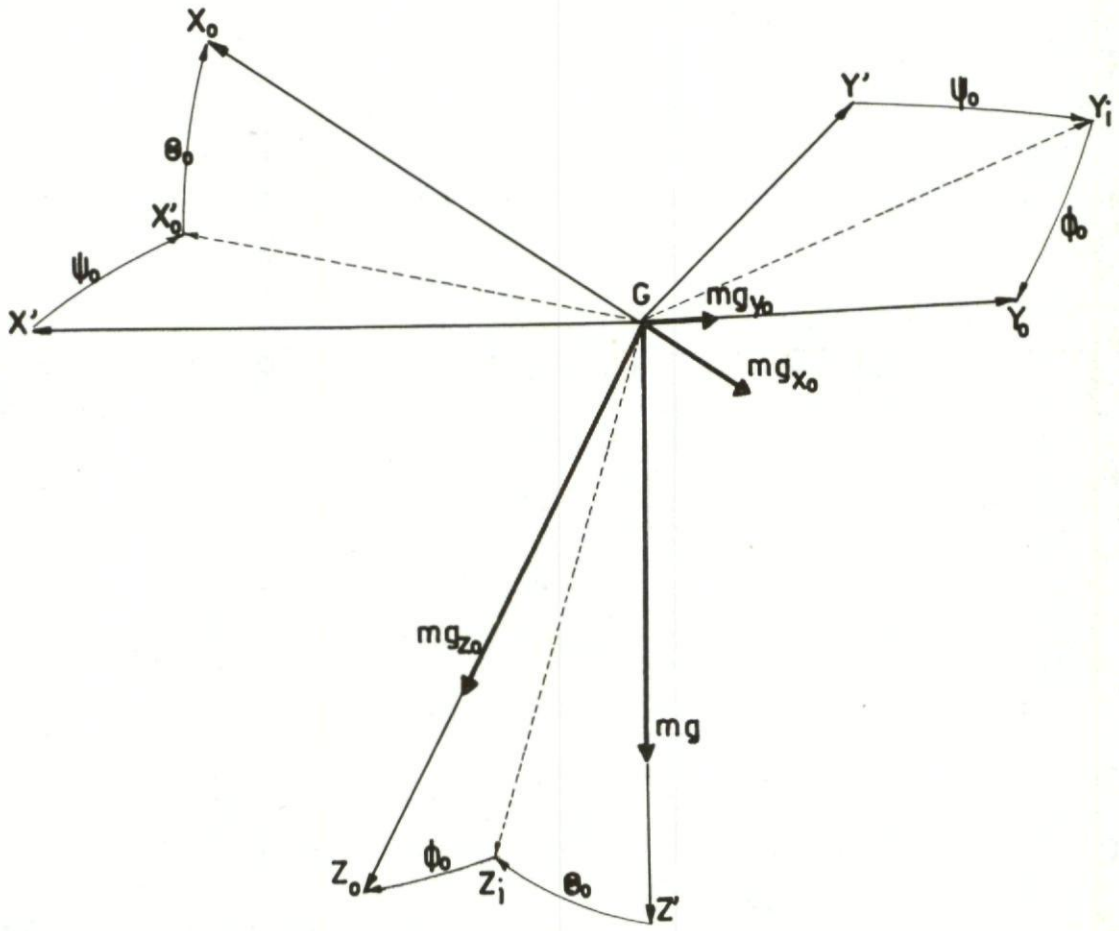

Fig.7 Projection of gravity on axes GX_0, Y_0, Z_0

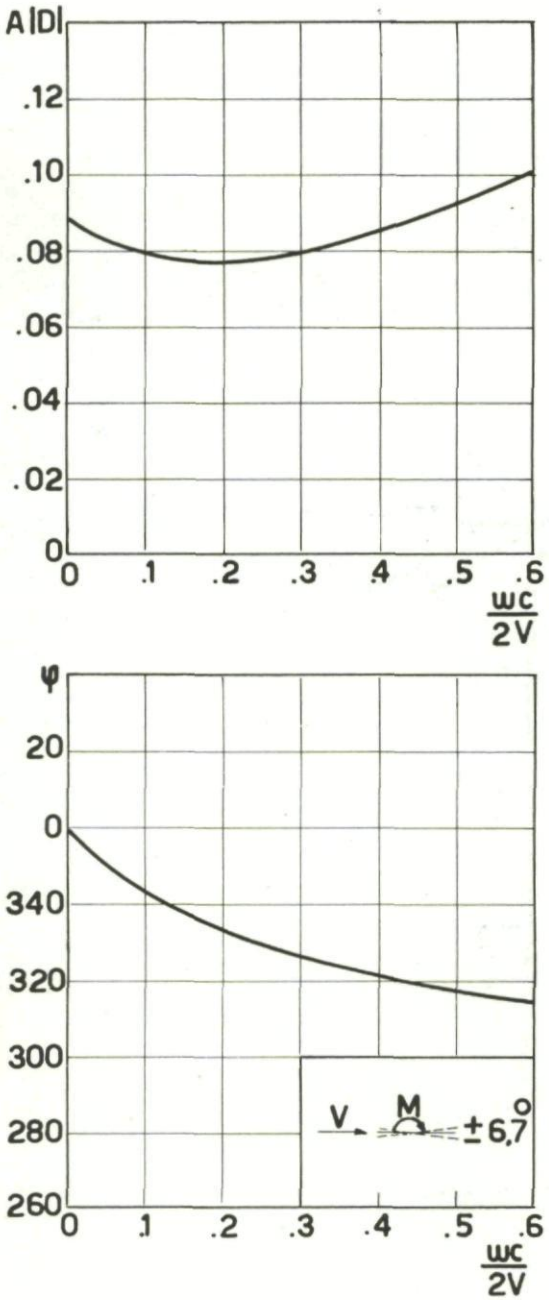

Fig.8 Amplitude and phase of C_m for sinusoidal variation of α

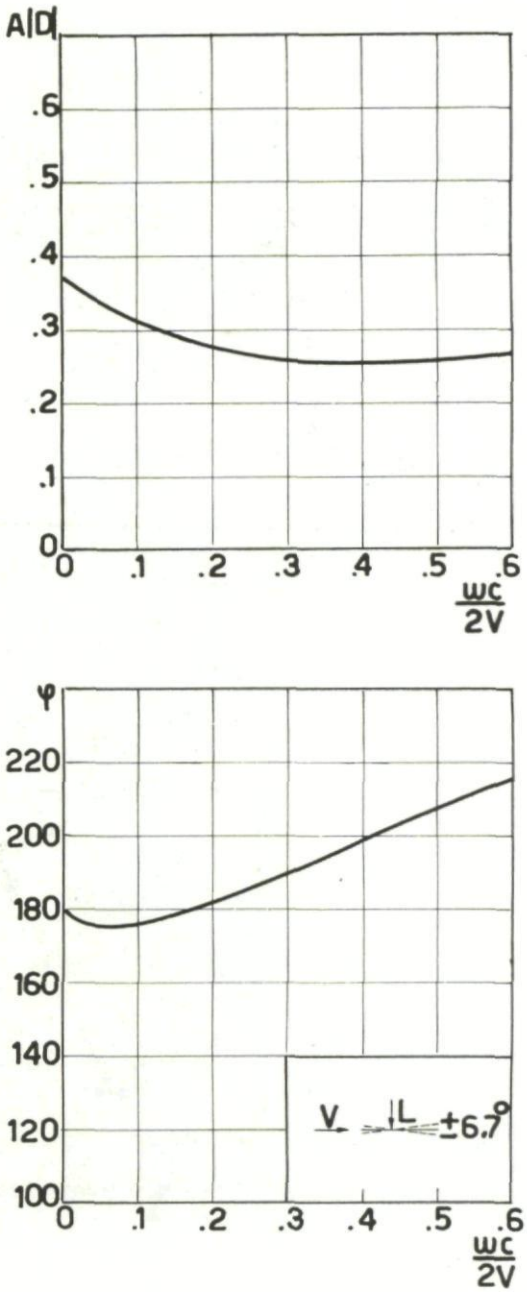

Fig.9 Amplitude and phase of C_L for sinusoidal variation of α

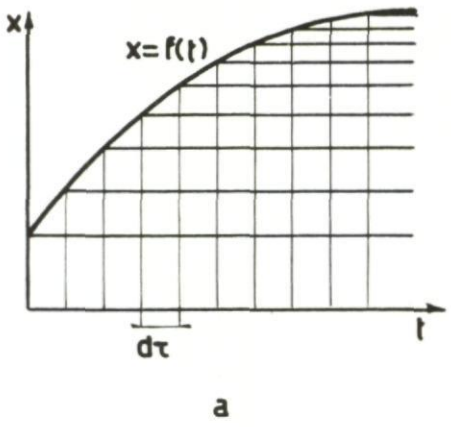

Fig.10(a) Dividing an input into steps

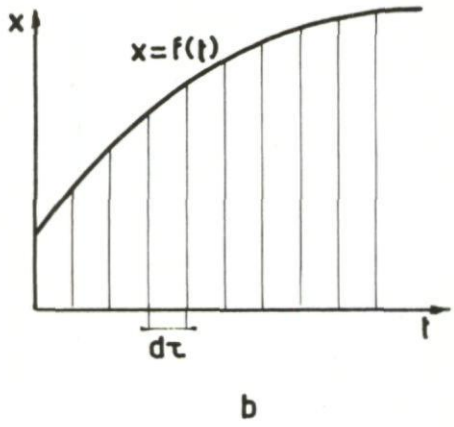

Fig.10(b) Dividing an input into pulses

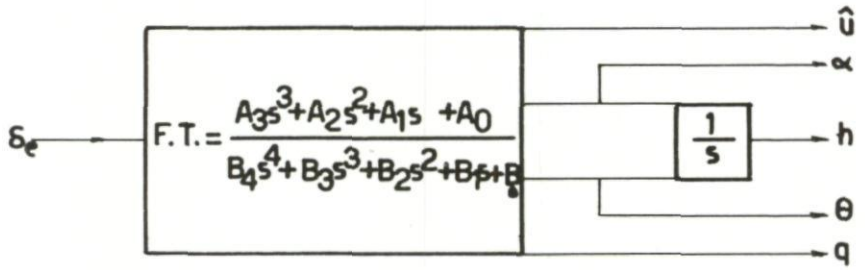

Fig.11 Overall transfer function of an aircraft

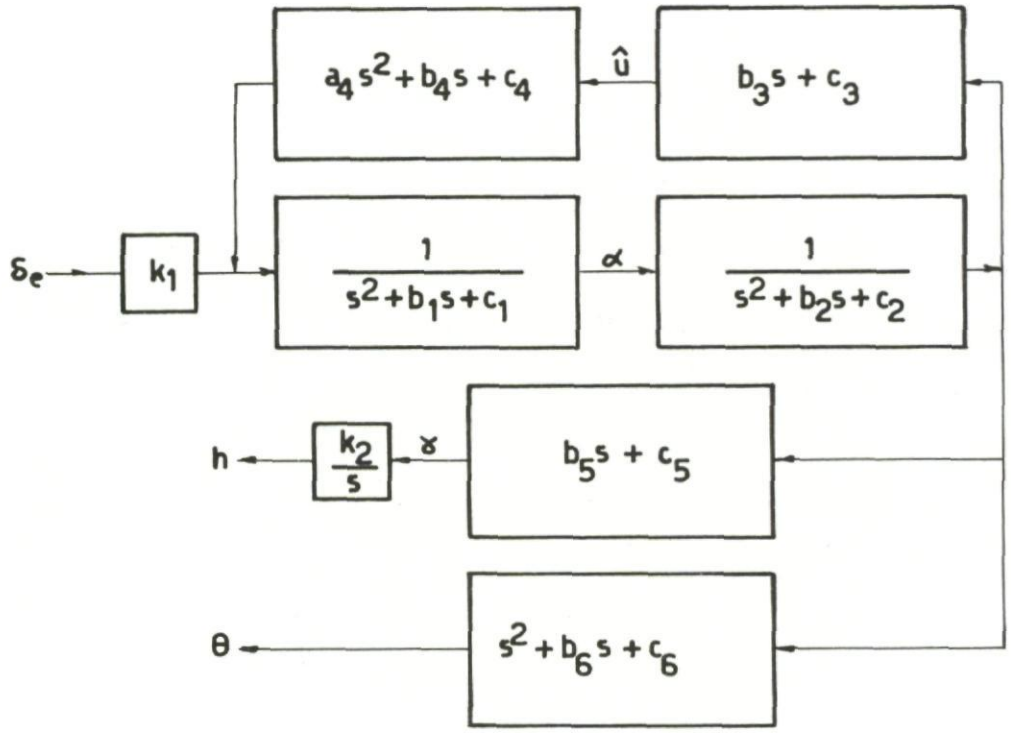

Fig.12 Division into partial transfer functions of the 2nd order

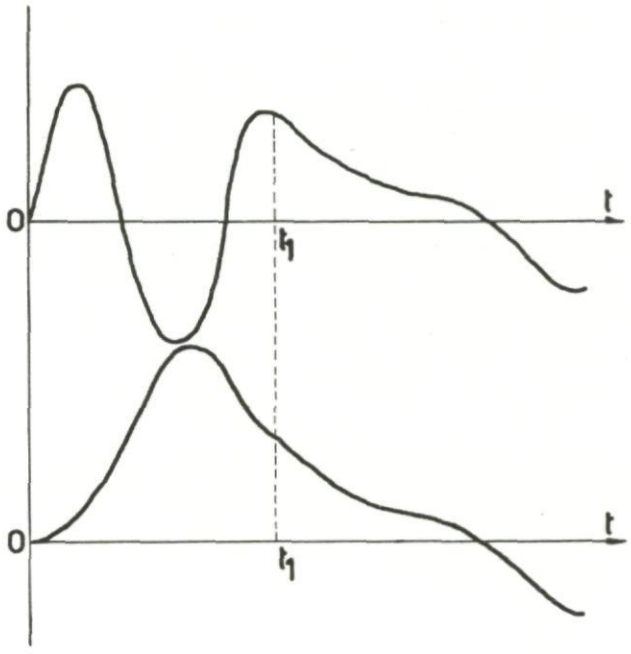

Fig.13 Variation of angle of attack with time

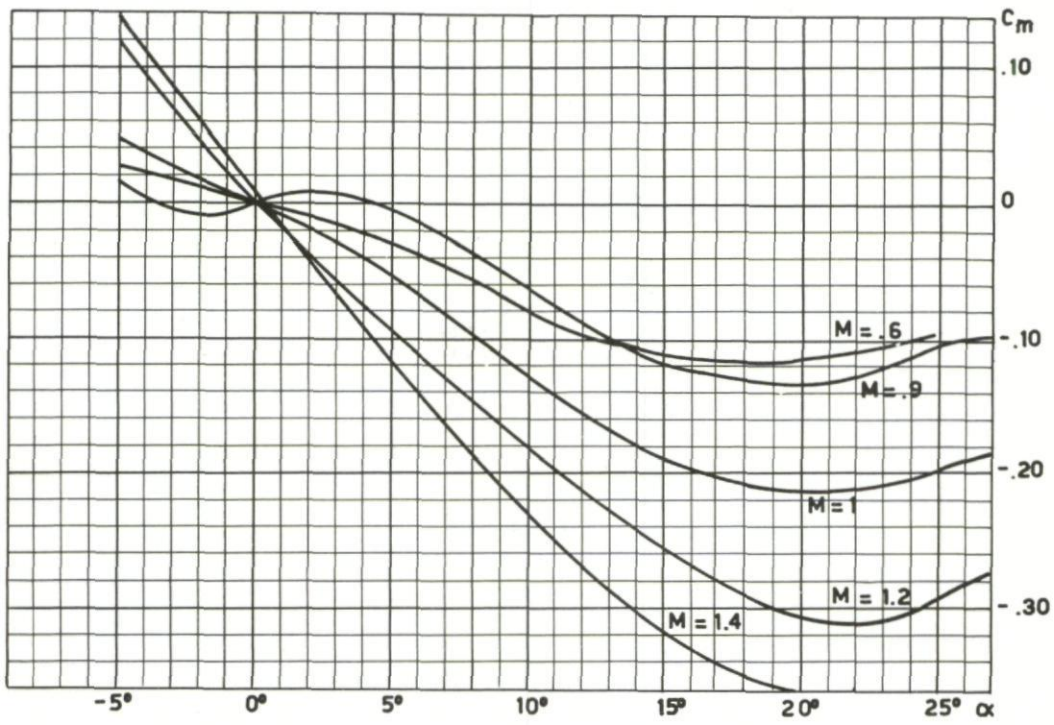

(a)

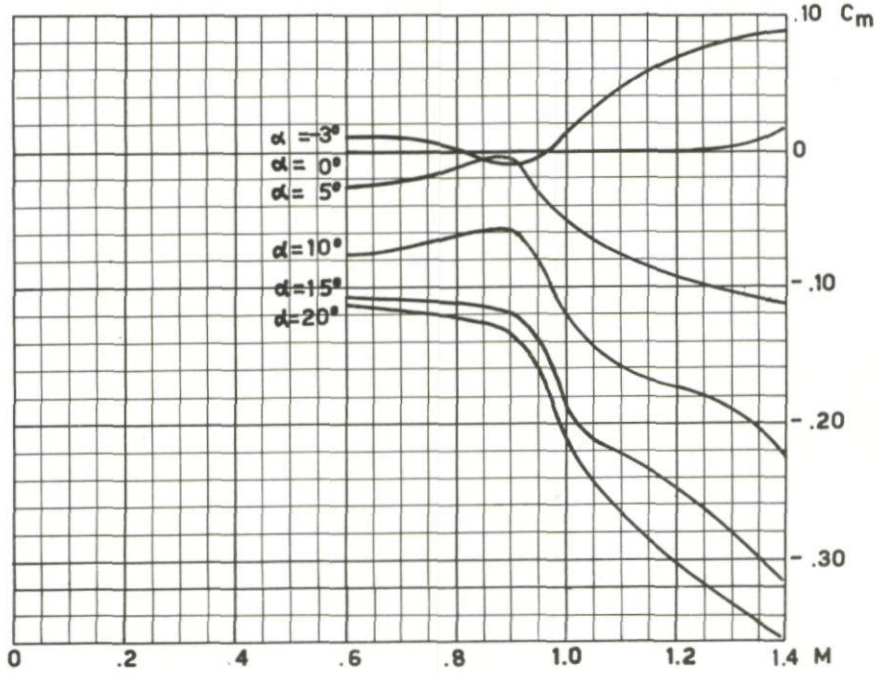

(b)

Fig.14 Presentation of C_m as a function of α and M

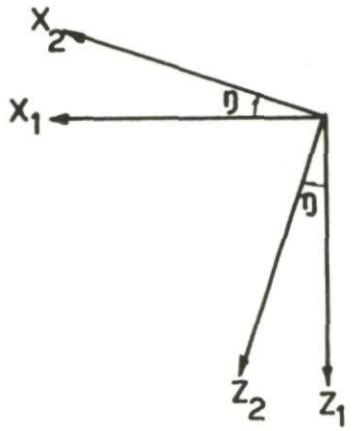

Fig.15 Rotation η

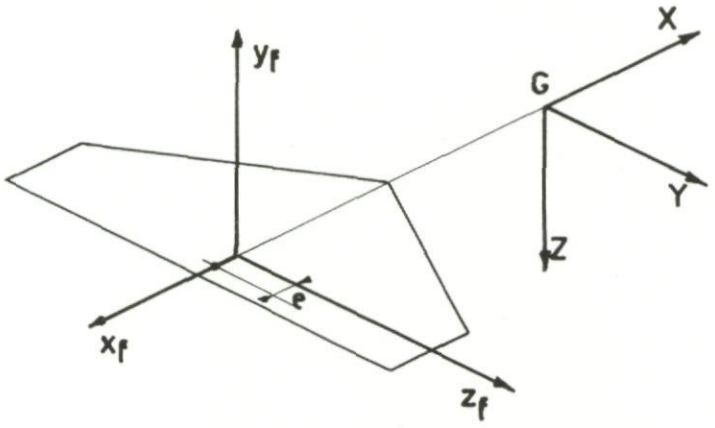

Fig.16 Characteristic elements of an elevator

PART II - THE ANALOGUE COMPUTER

L. Moulin*

CHAPTER 5

PRINCIPLES OF ANALOGUE COMPUTATION

5.1 INTRODUCTION

The fundamental principle of analogue computation is to substitute for the study of a given physical phenomenon, the study of another phenomenon called the support of the analogy, the analysis of which is easier than that of the former.

It is necessary that, at any time, a well defined agreement shall exist between the parameters and the variables of both phenomena, in such a way that the results deduced from the analysis of the second phenomenon may be applied to the first one; the support of this analogy will therefore be such as to be governed by equations similar to those describing the phenomenon which is under consideration.

Many problems of dynamics have been solved using electrical analogue networks, both phenomena being then connected by the well-known electro-mechanical analogy. The electrical analogue network can be set up from the mechanical sketch, a mass corresponding either to a capacitance or to an inductance, a mechanical resistance to an electrical one, and a mechanical stiffness either to an inductance or to a capacitance, according to the type of analogy which is used. In the first case, the current represents a force and the voltage a velocity, while in the second one the voltage is related to a force and the current to a velocity.

The application of such a principle leads to the design of an electrical network as an analogue to a given mechanical system, by physical rather than mathematical reasoning; the design of such a circuit can thus be quite difficult.

On the other hand, the analogy principle can be applied, starting directly from the equations of the problem, forgetting the detailed correspondence between the elements of the systems. In order to do so, the equations of the phenomenon are written down, displaying all the elementary mathematical operations to be performed, or connecting the different variables by suitable transfer functions; the analogue set-up can then be obtained by the use of calculation blocks which are able to perform the required elementary operations or to provide between output and input the transfer functions which are needed for the solution of the problem.

Such blocks are made of electrical elements and are connected in such a way that they constitute a general electrical circuit, the equations of which are similar to those of the system to be analyzed.

This method is particularly useful when the problem is to find out the history of any amount of variables, in terms of the time.

*Ingénieur Civil Electricien Mécanicien, T.C.E.A.

Any variable is then represented by an electrical voltage, and for each of them the value of the analogue voltage will be in agreement.

The time history of the solution is thus immediately obtained by direct recording of the electrical voltages.

The only objection to the use of an analogue computer lies in its somewhat limited accuracy.

Sometimes it is useful, when dealing with the mathematics of a problem having time as the independent variable, to work with the Laplace transforms of the functions instead of the real functions themselves. The equations which are then obtained connect the images of the functions through transfer functions. Calculation blocks having the same transfer functions can be built up and connected together according to the information obtained from the transformed equations.

One of the interesting properties of the analogue computer is that it is not necessary to carry out the inverse transformation, for the direct calculation gives the solution of the original system of equations as a function of time.

The construction of independent calculation blocks, performing a given elementary operation or having a given transfer function, has only been made possible because of the availability of high-gain d.c. amplifiers. Such amplifiers are the fundamental components of an analogue computer.

The main objection to the use of analogue computers is their limited accuracy. The accuracy does not depend only on the quality of the components, but also on the care of the operator in presenting the system of equations to be solved in a form which will result in least error. Under normal conditions, the accuracy of an analogue computer may be expected to be of the order of 1 or 2%.

5.2 HIGH-GAIN AMPLIFIER CAPABILITIES

The elementary operations to be performed in order to solve a system of differential equations are:

inversion of sign

multiplication of a variable by a constant factor

addition of two or more variables

integration of a variable.

These operations are sufficient for the solution of a linear system. If the system is not linear, it must also be possible to compute the products of variables. Furthermore, if one of the equations of the problem is given as an experimental curve, it must be possible to introduce this curve into the computer by means of a generator of non-linear functions of one or more variables.

The d.c. amplifier, fitted with suitable input and feedback impedances, is able to perform the four elementary operations just listed which are necessary to the solution of a system of linear differential equations. For non-linear operations, it is necessary to turn to the use of photoelectric, electro-mechanical or electronic devices.

The calculation blocks using the high-gain d.c. amplifiers for the solution of linear problems will be analyzed first; then several non-linear set-ups will be described.

Consider a d.c. amplifier, the gain of which is equal to $-A$ (Fig.17), connected to an input impedance Z_e and a feedback impedance Z_c. The input and output voltages are respectively V_e and V_s with respect to a zero level which is the same for all the computing elements. In the following sections it is to be understood that all voltages are given with respect to this reference.

Assuming that the amplifier grid current is zero, Kirchhoff's law applied to the nodal point N gives

$$I_e = I_c \tag{5.1}$$

or

$$\frac{V_e - V}{Z_e} = \frac{V - V_s}{Z_c} \tag{5.2}$$

together with

$$V_s = -A\,V \tag{5.3}$$

From these equations, the relation between the input and output voltages can be computed. Eliminating V, we obtain the following steps:

$$\frac{V_e + \frac{V_s}{A}}{Z_e} = \frac{-\frac{V_s}{A} + V_s}{Z_c} \tag{5.4}$$

and

$$\frac{V_s}{V_e} = -\frac{Z_c}{Z_e}\,\frac{1}{1 + \frac{1}{A}\left(1 + \frac{Z_c}{Z_e}\right)} \tag{5.5}$$

In the particular case where the assumption is made that the gain of the amplifier is infinitely high, the last equation reduces to

$$\frac{V_s}{V_e} = -\frac{Z_c}{Z_e} \tag{5.6}$$

In practice, the amplifier gain should be high enough to insure the validity of Equation (5.6) with sufficient accuracy; the values of the gain generally used in analogue computing technique vary between 50,000 and 500,000.

The error between the approximate value of the ratio V_s/V_e (Eq.5.6) and the actual value given by Eq.(5.5), expressed as a relative error with respect to the actual value, is given in terms of the values of the input and feedback impedances and of the actual gain, by

$$\epsilon = \frac{\frac{1}{A}\left(1 + \frac{Z_c}{Z_e}\right)}{1 + \frac{1}{A}\left(1 + \frac{Z_c}{Z_e}\right)} \tag{5.7}$$

It is seen that if $Z_c = Z_e$, the gain has to be higher than 2×10^3 in order to have an error smaller than 10^{-3}. On the other hand, the error due to the finite value of the gain of the amplifier is more important, for a given value of the gain, if the ratio Z_c/Z_e is greater, that is if the amplification factor of the output voltage is greater. Equation (5.6) shows that, using a high-gain amplifier, wired as in Figure 17, it is possible to achieve between output and input voltages a transfer function Z_c/Z_e, which can be reduced to a constant coefficient, and also that the sign of the output voltage is inverted.

5.3 ELEMENTARY OPERATION

The use of various types of input impedances and counter-reactions will make it possible to perform the different elementary operations mentioned in 5.2.

5.3.1 Sign Inversion

According to Equation (5.6), it is obvious that if

$$\frac{Z_c}{Z_e} = 1 \tag{5.8}$$

a single sign inversion is obtained, for Equation (5.6) reduces to

$$V_s = - V_e \tag{5.9}$$

In order to satisfy Equation (5.8), the input and feedback impedances must be similar and have the same values. Since the accuracy of the computation depends directly on the accuracy with which Equation (5.8) is satisfied, it is obvious that the nature of the impedances will be chosen so as to provide the best possible calibration; therefore resistances are used. The sketch of the wiring for the operational amplifier used as a sign inverter is given in Figure 18 while its conventional or symbolic representation, used to draw the general sketch of interconnections, or block diagram, is given in Figure 19.

5.3.2 Multiplication by a Constant Factor

The multiplication of a variable by a constant factor c is obtained with a set-up similar to that shown in Figure 18; to insure the accuracy, the impedances are again resistances, but with different values, so as to satisfy, from Equation (5.6), the relation

$$\frac{V_s}{V_e} = -\frac{Z_c}{Z_e} = -\frac{R_c}{R_e} = -c \qquad (5.10)$$

The corresponding circuit is given in Figure 20 with the symbolic representation in Figure 21; usually, the value of the coefficient is reproduced inside the symbolic triangle.

However, the use of single resistances is of little practical value, because in order to multiply by a factor which is not a whole number, both resistances have to be adjusted by combination with other accurate resistances, in series or in parallel. This considerably complicates the preparatory work necessary for the solution of a given problem.

A more flexible device uses variable resistors instead of fixed ones; but here also the work of preparation is transferred partly into the previous calculations of the setting of the resistances, partly in the setting itself, which is usually made with a Wheatstone bridge, by comparison with a calibrated reference resistance. A variant of this process is illustrated in Figure 22; the two resistances R_e and R_c form part of a potentiometer, having a connection from the wiper to the input of the d.c. amplifier. The accurate setting of the ratio R_c/R_e is, however, critical.

The most widely used method, particularly in the large computing units, involves a potentiometer, the extreme points of which are respectively connected to the variable which has to be multiplied and to the zero reference of the computer; the sliding contact is wired to the input impedance of the d.c. amplifier (Fig.23).

If R is the total resistance of the potentiometer and c the value of the resistance between the zero reference and the slider, we have the relation

$$V_e = cV \qquad (5.11)$$

and from Equation (5.6)

$$V_s = -\frac{R_c}{R_e} V_e = -c\,\frac{R_c}{R_e} V \qquad (5.12)$$

Equation (5.12) shows that the values of the input and feedback resistances may be definitely fixed in order to give a multiplication factor like 1, 5 or 10. Any value of c between 0 and 1 can then be obtained from the potentiometer. The value of the ratio R_c/R_e may generally not exceed 10, for the reasons given in Section 5.2; such a set-up thus gives the possibility of multiplying a variable by a constant factor extending from 0 to 10, or of dividing by a number which is included, theoretically, between 0.1 and infinity, and practically between 0.1 and 10^3 or 10^4 according to the position of the last significant number which can be read on the potentiometer dial.

The setting of the coefficient is often achieved by connecting the potentiometer between a stabilized reference voltage, usually 100 volts, and the zero reference of the computer. The voltage read between the wiper and the same zero reference is equal to $100\,c$ when the adequate setting is completed.

The symbolic representation of the potentiometer is given in Figure 25.

It is also reliable to achieve the setting by comparison with a calibrated potentiometer as illustrated in Figure 25. Both potentiometers are fed with a reference voltage, the absolute value of which is no longer of importance. The reference potentiometer B is previously set at a convenient value and then the potentiometer A is adjusted till the indicator connected between the wipers gives a zero reading.

The use of potentiometers as described above introduces a further source of error in the calculations; assuming indeed that the gain of the d.c. amplifier is infinite or at least very high, Equation (5.3) shows that we may write as a good approximation

$$V = -\frac{V_s}{A} \approx 0$$

It follows that to connect the potentiometer to the input impedance of the amplifier is equivalent to adding a resistance in parallel on its lower part (Fig.27); such a combination gives

$$\frac{V_e - V}{(1 - c)R} + \frac{V_e}{cR} + \frac{V_e}{R_e} = 0 \qquad (5.13)$$

or

$$V_e\left[\frac{1}{cR} + \frac{1}{R_e} + \frac{1}{(1 - c)R}\right] = \frac{V}{(1 - c)R}$$

and finally

$$\frac{V_e}{V} = \frac{c}{1 + c(1 - c)R/R_e} \qquad (5.14)$$

whereas the following

$$\frac{V_e}{V} = c \qquad (5.15)$$

would have been expected.

In such a situation, the voltage which is picked up by the sliding contact is no longer representative of the reading on the dial of the potentiometer; the error introduced by the input impedance of the amplifier, which is usually called the loading error, can be evaluated by subtracting Equation (5.15) from Equation (5.14):

$$\epsilon = \frac{c - \dfrac{c}{1 + c(1 - c)R/R_e}}{\dfrac{c}{1 + c(1 - c)R/R_e}}$$

$$= c(1 - c)\frac{R}{R_e} \qquad (5.16)$$

The relative error will be smaller if the ratio R/R_e is smaller. Since the value of the input impedance is generally equal to 1 megohm, the maximum value of the total resistance of the potentiometer may not exceed 100,000 ohms; the most widely used values vary between 10,000 and 100,000 ohms.

The error to the loading of the potentiometers can be eliminated in two different ways, either by calculation or by suitable setting technique. The error can be computed beforehand from Equation (5.16) and the reading which corresponds to the correct setting altered accordingly, but this requires prior calculations and reduces the simplicity of the operation.

The most elegant way to eliminate the loading error is to set the potentiometer when it is already connected to the load. Such a condition is illustrated in Figures 28 and 29, which correspond respectively to Figures 24 and 26. This method is thus used when the general interconnection is wired, provided it is possible to avoid the computation to run when this is achieved. The operational amplifiers are fitted, therefore, with a suitable restraining device which will be described later on.

5.3.3 Integration

In order to obtain an output voltage equal to the time integral of the input voltage, using an operational amplifier circuit similar to that of Figure 17, we must have

$$V_s = -\int V_e \, dt$$

or

$$V_s = -\frac{1}{s} V_e \qquad (5.17)$$

Referring to Figure 17, if the input impedance is a resistance R, and if the feedback impedance Z_c is a capacitance C, we obtain, substituting in Equation (5.6),

$$\frac{V_s}{V_e} = -\frac{\frac{1}{s}C}{R} = -\frac{1}{s\,R\,C} \qquad (5.18)$$

which is equivalent to Equation (5.17). The amplification factor is now equal to $1/RC$. As for the operational amplifiers used to multiply by a constant factor, the capacitance located in the feedback loop will be given a fixed value, while the input resistance will be such as to provide an amplification factor of 1.5 or 10.

The multiplication by any coefficient will again be obtained with a potentiometer in front of the input impedance of the operational amplifier. This can be slightly simplified by using an input resistance having a value in accordance with the integrating capacitance; in order to save the accuracy of the integration, it is better to avoid any modification of the value of the feedback capacitance.

The circuitry of an integrator is sketched in Figure 30 and its corresponding symbol in Figure 31; the value of the constant factor a multiplying the input voltage is usually reproduced in front of the input connection.

From a theoretical point of view, the differentiation can also be performed with an operational amplifier. We have only to change over the impedances used for the integration to obtain the sketch of Figure 32 with the equation

$$\frac{V_s}{V_e} = -\frac{R}{1/sC}$$

or

$$V_s = RCsV_e \tag{5.19}$$

The amplification factor is then equal to RC. But the differentiation is always hard to perform accurately by physical means, using for instance pneumatic or mechanical techniques, and troubles are also encountered with the operational amplifier. Such a device, as shown in Figure 32, is never used in analogue computation, since the amplification of the noise produced by the operation is such that sufficient accuracy cannot be obtained. It is necessary, in order to overcome the difficulty, either to re-write the formulation of the problem in order to avoid any differentiation, or to perform an approximate differentiation, introducing a time lag in the differentiating circuit.

5.3.4 Summation

All the elementary operations can be performed, not only on one single variable, but also on the sum of several variables.

Consider (Fig.33) the enlargement of the basic circuit of the operational amplifier, still involving a feedback impedance Z_c and n input voltages $V_{e,1} \cdots V_{e,n}$ connected to a common input of the d.c. amplifier through n input impedances $Z_{e,1} \cdots Z_{e,n}$. From Equation (5.3)

$$V = -\frac{V_s}{A} \approx 0$$

and then, from Kirchhoff's law,

$$\sum_{i=1}^{m} \frac{V_{e,i}}{Z_{e,i}} = -\frac{V_s}{Z_c} \tag{5.20}$$

we find

$$V_s = -Z_c \Sigma \frac{V_{e,i}}{Z_{e,i}} \tag{5.21}$$

The input impedances are always resistances of integer values, eventually preceded by potentiometers which give a multiplication factor a_i. If the feedback impedance

is a resistance, the circuit will give the sum of n variables, each of them being multiplied by its own coefficient, and if the feedback impedance is a capacitance, the time integral of that sum will be obtained. The number of input terminals of the operational amplifiers used in analogue computing technique vary, according to the importance of the facility, from 1 to 10. Usually, the gain of each input channel is a fixed quantity, and either all the channels have the same gain or a given amount of them have a gain of unity, other ones a gain of 5 or 10. In Figures 34 and 35 respectively are drawn the symbols representing a summator-integrator and a single summator.

5.4 OPERATIONAL LIMITATIONS

Most of the analogue computers are fed with a 100 volt stabilized d.c. voltage. The d.c. amplifiers are designed to behave linearly in a voltage range extending in absolute value from 0 to 100 volts. If this upper limit is exceeded the response of the amplifier is no longer linear, and saturation appears. Thus, none of the voltages used for the computation may be, at any time, greater than 100 volts.

On the other hand, it is possible that, in the inner circuitry of a d.c. amplifier, changes of voltages occur with time, producing an additional and undesirable output voltage. Such a trouble inherent in d.c. amplifiers is called drift.

The additional output voltages due to the drift introduce a source of errors in the computation, and these can become very large, especially if the outputs have to be integrated later.

The largest analogue computers use d.c. amplifiers with automatic balance of the drift; anyway, it is important to know what are the limitations introduced by the computing equipment itself, and to keep them in mind when preparing the equations of the problem for analogue solution.

CHAPTER 6

SOLUTION OF LINEAR SYSTEMS OF EQUATIONS

6.1 HOMOGENEOUS SYSTEMS WITHOUT SECOND MEMBER

Consider the simple system of equations

$$\left.\begin{aligned} a_1\frac{d^2x}{dt^2} + a_2\frac{dx}{dt} + a_3x + a_4y &= 0 \\ b_1\frac{d^2y}{dt^2} + b_2\frac{dy}{dt} + b_3y + b_4y &= 0 \end{aligned}\right\} \qquad (6.1)$$

The variables x and y have to be replaced by voltages X and Y which are related to the variables by the equations

$$\left.\begin{aligned} X &= \alpha x \\ Y &= \beta y \end{aligned}\right\} \qquad (6.2)$$

where α and β are the scale factors.

The real time t and the time τ of the computer are connected by the relation

$$t = k\tau \qquad (6.3)$$

where k is the time scale factor.

The physical nature of the problem to be solved gives rough indications about the choice of the scale factors. They have to be such that the voltages do not exceed 100 volts when the variables reach their maximum reasonably expected value. On the other hand, to insure accuracy, it is not desirable to perform the calculations on voltages which lie in the vicinity of zero.

The choice of the time scale provides an opportunity to slow down or speed up the resolution. If k is less than unity, the solution will be slowed down; if k is greater than unity, the behaviour of the system is accelerated. We have

$$\left.\begin{aligned} \frac{d}{dt} &= \frac{d}{dk\tau} = \frac{1}{k}\frac{d}{d\tau} \\ \text{and} \quad \frac{d^n}{dt^n} &= \frac{d^n}{d(k\tau)^n} = \frac{1}{k^n}\frac{d^n}{d\tau^n} \end{aligned}\right\} \qquad (6.4)$$

It is generally desirable to speed up the resolution of a problem.

Since the gain of a d.c. amplifier is finite, this introduces a slight error in each operational element; since the complete set-up involves integrators, most of these errors are integrated and the final accuracy obtained will be improved by shorter duration of the computation. Furthermore, if the drift of the amplifiers is not automatically balanced during the time they work, a second source of error develops with time. Both considerations thus lead to the conclusion that a result will be more accurate if it is obtained in a shorter run of the computer.

But the speeding-up process has, on the other hand, its own drawback. Since the time scale is then greater than unity, the coefficients of the time derivatives could be considerably reduced by the scaling, leading to the setting of the potentiometers at such low values that the systematic error of the potentiometer reading may no longer be considered as negligible; even for larger time factors it might be impossible to set up the coefficients. On one hand, it is thus desirable to speed up the solution but, on the other hand, the process is limited by ability and accuracy requirements, such that conditions of compromise have to be selected.

When choosing the time scale, it is also necessary to take into account the frequencies of variation of the different quantities, and they are not always easily evaluated *a priori*, except in very simple cases. It is indeed important that the highest frequency of the solution be less than the maximum frequency of the recording equipment and also - this is a more severe limitation - of the electro-mechanical devices used to deal with the non-linear operations.

Transforming the equations of the problem into X, Y, τ relations, we have:

$$\frac{a_1}{\alpha}\frac{1}{k^2}\frac{d^2X}{d\tau^2} + \frac{a_2}{\alpha}\frac{1}{k}\frac{dX}{dt} + \frac{a_3}{\alpha}X + \frac{a_4}{\beta}Y = 0$$

$$\frac{b_1}{\beta}\frac{1}{k^2}\frac{d^2X}{d\tau^2} + \frac{b_2}{\beta}\frac{1}{k}\frac{dY}{dt} + \frac{b_3}{\alpha}Y + \frac{b_4}{\alpha}X = 0$$

or, simplifying,

$$\left.\begin{aligned} A_1\frac{d^2X}{d\tau^2} + A_2\frac{dX}{d\tau} + A_3X + A_4Y &= 0 \\ B_1\frac{d^2Y}{d\tau^2} + B_2\frac{dY}{d\tau} + B_3Y + B_4X &= 0 \end{aligned}\right\} \qquad (6.5)$$

Using the principles stated in Chapter 5, the block diagram actually obtained is drawn in Figure 36.

If the physical system, which is described by Equation (6.5), is stable, the analogue electrical system will stay at rest if $X = Y = 0$, but will give the solutions $X = f_1(\tau)$ and $Y = f_2(\tau)$ if one or more initial conditions X_0, Y_0; $(dX/d\tau)_0$, $(dY/d\tau)_0$ are applied and are different from zero.

The proper way to introduce the initial conditions in the computer is discussed in Section 6.3.

6.2 MODIFICATIONS OF THE SET-UP

It is obvious that the set-up shown in Figure 36 may only be used when all the channels of the computer have a gain equal to unity, if the following conditions are satisfied:

$$A_1 \quad \text{and} \quad B_1 \qquad > 1$$

$$A_2, A_3, A_4, \; B_2, B_3, B_4 \; < 1$$

If amplification factors of 10 are available, these conditions become

$$A_1 \quad \text{and} \quad B_1 \; > 0.1$$

$$A_2 \ldots\ldots B_4 \; < 10$$

When these conditions are not satisfied, the difficulty can be overcome by using other configurations.

(a) Equation (6.5) can be respectively divided by the coefficient of the time derivative of highest order. The potentiometers $1/A_1$ and $1/B_1$ are suppressed in doing so. The conditions to be satisfied are then:

$$\frac{A_2}{A_1}, \; \frac{A_3}{A_1}, \; \frac{A_4}{A_1} \; < 1 \text{ or } 10$$

$$\frac{B_2}{B_1}, \; \frac{B_3}{B_1}, \; \frac{B_4}{B_1} \; < 1 \text{ or } 10$$

according to the available gains. However, if a set of solutions is expected for different values of the coefficients A_1 and B_1, the block diagram of Figure 36 proves to be the most useful since the modification of the value of A_1, for instance, requires only one potentiometer to be reset, whereas in the other cases all the potentiometers representing A_4, A_3, A_2 have also to be reset.

(b) Another way of wiring the problem is to insert a potentiometer in the feedback loop of a summator. When the coefficient A_1 is less than unity, it is impossible to obtain, from $A_1(d^2X/d\tau^2)$, the value $d^2X/d\tau^2$ through a potentiometer, since the coefficient $1/A_1$ is greater than unity. On the other hand, when dividing the coefficients $A_2, A_3 \ldots$ by A_1 as was done in the previous section, one might obtain a result which is also greater than unity. The value $d^2X/d\tau^2$ can however be obtained by wiring a potentiometer, which is set at the value A_1, in the feedback loop of the operational amplifier. This means that one terminal of the feedback resistance R_c is connected to the zero reference through the potentiometer, and that a voltage equal to the A_1 fraction of the voltage existing at that terminal of the resistance is fed to the nodal point N (Fig.37). The theory of the summator shows indeed that,

when the electric current flowing to N is reduced by a given ratio due to the presence of the resistance R_c, the output voltage V_s is multiplied by the same ratio.

Introducing now a potentiometer in the loop is not favourable to the accuracy, since this is equivalent to multiplying the gain by a factor A_1, and in fact this reduces the gain since $A_1 < 1$. The use of such a process should, therefore, be avoided when the coefficients A_1 are too small.

(c) When the values of the coefficients A_1 ..... B_4 are such that it is impossible to use satisfactorily one of the processes just mentioned, we should then have to change the first scaling in such a way that the maximum or minimum coefficients are corrected to values which are more convenient.

Note

The block diagrams shown as examples in various chapters of Part III will be simplified and consist only of the outputs and inputs of each integration loop. The connections between the output of a loop and the inputs of the summators will generally be omitted.

The summator will be symbolized by a triangle; the feedback loop which is located inside the triangle is thus omitted.

The diagrams will be established as in condition (a), all the coefficients being divided by the coefficient of the time derivative of highest order (coefficients A_1 and B_1 in the example considered above).

It will always be possible to substitute for the block diagram represented, another one using separate potentiometers to introduce the coefficients, which have to be located either in the inner feedback loop or at the input, according to whether those coefficients are less or greater than unity.

6.3 INITIAL CONDITIONS

In order to solve a system of differential equations, the initial values of the different variables must be introduced into the integrators, before running the computation, in such a way that the integrations start from the appropriate level when the computer is switched on. Two different processes are used:

1st Method

The capacitances of the integrators are previously loaded with a voltage corresponding to the initial condition, so that when the integration is started the output voltage of the integrator is equal to that condition, but it is then necessary to be able to restrain the computation during the previous loading operation.

2nd Method

A constant voltage representing the initial value is introduced, at the initiation of the computation, in a summator where it is added to the output voltage of

the integrator. This method involves an additional operational amplifier for each initial condition.

The first method is generally to be preferred, and each integrator is fitted with a system of relay switches energized from a master switch at the control panel.

When setting the initial conditions, the input impedance is grounded (Fig.38) and the capacitance is loaded through a variable resistance from a reference voltage E. In computing the configuration, the input impedance is again connected to the d.c. amplifier (Fig.39) and the loading connection is grounded.

The system is designed so that the computation can be stopped at any time, holding the instantaneous values of the voltages, which can thus be measured more accurately if desired. In order to hold the instantaneous values when the run is stopped, the input impedance is grounded again while the loading loop is kept in the same position (Fig.40).

6.4 NON-HOMOGENEOUS EQUATIONS

Non-homogeneous equations involve a second member which represents one or several excitation functions of the time. These excitations are also represented by electrical variables for which scaling factors have also to be defined. The system (6.5) has been re-written, with the assumption that an excitation function Z is present:

$$\left.\begin{aligned} A_1 \frac{d^2X}{d\tau^2} + A_2 \frac{dX}{d\tau} + A_3X + A_4Y &= A_5Z \\ B_1 \frac{d^2Y}{d\tau^2} + B_2 \frac{dY}{d\tau} + B_3Y + B_4X &= B_5Z \end{aligned}\right\} \qquad (6.6)$$

The analogue set-up differs from the preceding one; voltages $-A_5Z$ and $-B_5Z$ have now to be introduced respectively as input of the first summator of each integration loop. The Z voltages may have any possible shape in terms of time, the unit function being only a particular case. The generation of voltages representing excitations varying with time may be obtained from external devices. It is pointed out that, in principle, any variable excitation could be generated from the appropriate displacement of the sliding contact of a potentiometer.

6.5 CHOICE OF THE SET-UP

Several different set-ups can often be used for the solution of a given problem. They generally differ both from the point of view of accuracy of the final result and of probability of saturation of the amplifiers. It might be useful to compare, for the different possible configurations, the risk of saturation and the accuracy of the solution. This can be illustrated as follows:

(a) If one integrator and one phase inverter have to be connected in cascade, it is more convenient to locate the integrator upstream, in order to avoid the

errors introduced by the phase inverter being magnified by the integration process;

(b) If the number of terms to be added is larger than the number of input channels of a summator, it is necessary to use at least two summators in parallel. Then care has to be taken to avoid sending all positive voltages to the one summator and all negative voltages to the other one, otherwise the risk of saturating both summators is largely increased; in order to decrease it, negative and positive voltages should be equally distributed to the two summators.

Although these remarks follow from simple straightforward reasoning, a more careful study is necessary if it is desired to compare the merits and drawbacks of several alternative set-ups.

CHAPTER 7

NON-LINEAR FUNCTION GENERATION

A system of non-linear differential equations can be solved with an analogue computer, provided a calculation block is available delivering an output voltage which varies according to the shape of the non-linear functions which are involved in the equations.

Such blocks are actually available, which enable the following operations to be performed:

(a) the product of two variables

(b) the division of one variable by another

(c) the generation of any relation between two variables (or more) which is given by a curve (without algebraic expression).

7.1 MULTIPLIERS

7.1.1 Servo-Multipliers

One of the first elaborate devices to be used to multiply two variables was composed of an electro-mechanical system, involving servo-driven potentiometers. The servo-motor itself (Fig.41) is actuated by the output voltage of a differential amplifier, and moves the wiper of a potentiometer which is fed by the reference voltages of the computer. The voltage picked up by the wiper is sent to the differential amplifier together with the variable voltage V, in such a way that the motor shifts the wiper until it reaches a geometrical position of equilibrium which is directly related to the input voltage V. For any positive value of V, this position is the $V/100$th part of the distance between the neutral point of the potentiometer and the $+100$ terminal. If the wiper of a second similar potentiometer is fixed on the shaft of the servo-motor (Fig.42), this one will also be geometrically located at a distance equivalent to $V/100$. If, now, the terminals of the second potentiometer are connected to the variable voltages $\pm X$, the voltage at the wiper will be equal to the $V/100$th part of the voltage X, that is $VX/100$.

Several potentiometers (very often five) are usually fixed on the servo-multiplier shaft. Such a device is then able to deliver the product of four different variables by a fifth one.

The use of the servo-multiplier is limited mainly by the fact that an accurate positioning of the sliding contacts can only be achieved when the servo-motor is actuated by slowly varying voltages, the maximum frequency being usually less than a few cycles per second. This is the reason why, in analogue multiplication technique, the variable having the slowest variations must be chosen to drive the servo-multiplier.

The error due to the loading of the multiplying potentiometers must be faced, as well as in the case when using the potentiometers to multiply a variable by a constant coefficient. If the wiper of a potentiometer is wired to the input impedance of an operational amplifier, this is equivalent (Fig.43) to connecting an additional resistance in parallel in the potentiometer. In such conditions, the geometrical distance between the neutral point and the feeding terminal is no longer representative of the 'electrical' distance between these two points, the value of the latter being sensitive to the amount of additional resistance in parallel; the voltage Y at the sliding contact of the potentiometer is then no longer equal to the product of the two variables.

This error can be eliminated if the control potentiometer itself is loaded by the same amount. The actual location of the wipers will then differ from the V/100th part of the geometrical distance between the neutral point and the terminal, but will be equal to the V/100th part of the 'electrical' distance between these points. The wiper of the multiplying potentiometer will then pick up a voltage which is again proportional to the product of the variables (Fig.44).

When several multiplying potentiometers however, fixed on the same shaft, are used simultaneously, there is the implication, in order to compensate the loading error in the same way, that all of them are connected to equal input impedances. If not, the compensating load applied to the control potentiometer will only be able to eliminate the loading error of certain multiplying potentiometers; if the number of operational amplifiers of the computer is not sufficient, then reluctantly we must resort to the less satisfactory technique of loading the control potentiometer to the same amount as is most widely used in the multiplying potentiometers.

If sufficient amplifiers are used, it is then possible to eliminate completely the loading error by inserting an insulating amplifier between the wipers of the multiplying potentiometers and the input impedances to which they are connected; the insulating amplifier used is a single-phase inverter. The control potentiometer may then be loaded with the value of the input impedance of the insulating amplifiers.

7.1.2 Division

The operation of division looks to be easily capable of being performed with the same set-up, by now feeding the control potentiometer with the variables ±X and the multiplying potentiometers with reference voltages ±A. The voltage at the wiper of the latter should then be equal to VA/X .

However, the variations of the variable X have an effect upon the gain of the control loop of the servo-motor, spoiling its accuracy. To cope with this difficulty, the gain of the loop must be automatically controlled and kept nearly constant whatever may be the value of the voltage feeding the control potentiometer.

Such a device is not very often used, and the division is usually performed as a solution of an implicit equation. Several configurations can be used to satisfy such an equation, and the one which is the most often described in the specialized literature has been reproduced here.

If the variable x has to be divided by the variable y, within a constant factor C, the solution will be a voltage such as

$$w = -C\frac{x}{y}$$

This leads to the solution of the implicit equation

$$x + \frac{wy}{C} = 0 \qquad (7.1)$$

The corresponding block diagram is illustrated in Figure 45.

The dividing variables have to be positive and have variations slow enough not to exceed the frequency capabilities of the servo-motor. Furthermore, the values of y must be significantly larger than zero in order to avoid the saturation of the amplifier.

There is no universal agreement on the symbols to be used for representing servo-multipliers, or, in fact, other non-linear devices.

7.1.3 Electronic Multiplier

The principle of the electronic multiplier is based on amplitude and frequency modulation of a rectangular wave in such a way that the mean value is made proportional to the required product of two variables.

Consider (Fig.46) a given variable x, the value of which is equal to X during the time T_1 and zero during the time T_2, defining a rectangular wave having an amplitude X and a period $T_1 + T_2$, with a mean value computed during one period equal to

$$\frac{XT_1}{T_1 + T_2}$$

If the wave amplitude is proportional to the variable x, and if the time intervals T_1 and T_2 are such that the ratio $T_1/(T_1 + T_2)$ is made proportional to a second variable y, the mean value obtained by suitable filtering of the rectangular wave will be proportional to the product of the variables x and y.

The electronic set-up used to generate the time intervals T_1 and T_2 is illustrated in Figure 47. A multivibrator with two stable positions is the basic component; when the input voltage is equal to E_1, the multivibrator switches to the first stable position and the output voltage is equal to a given constant; when the input voltage becomes equal to another given value E_s, the output voltage, which then corresponds to the second stable position, is continuously equal to zero. The multivibrator controls an electronic switch, which conducts only when it is energized by any output of the multivibrator different from zero. The multivibrator is fed from the output of a summation integrator having as inputs the product of a varying voltage X by a constant coefficient β, and a reference voltage V which is multiplied by a coefficient α when flowing through the electronic switch.

If at the starting point the input voltage of the multivibrator is considered to be equal to E_1, the output voltage has then a constant level different from zero, and the electronic switch closes. The input of the integrator is then

$$\beta X - \alpha V$$

This voltage is integrated until it reaches the value E_s; since the analogue integration inverts the signs, E_s will be reached only if the following conditions are satisfied:

$$\beta X - \alpha V < 0$$

or

$$\beta X < \alpha V$$

The values of α and β must thus be chosen accordingly. The level E_s is reached within a time T_1 such that

$$K\int_0^{T_1} (\beta X - \alpha V)\,dt = E_1 - E_s \tag{7.2}$$

Since it is assumed that the waves have ideal rectangular shapes, which means that the commutations are carried out so quickly that one may consider that the voltages keep a constant level during a period, the variables X and Y are then handled as constants in Equation 7.2 and we obtain:

$$T_1 = \frac{E_s - E_1}{K(\alpha V - \beta X)} \tag{7.3}$$

When this time interval has elapsed, the voltage level E_s is reached, the output of the multivibrator falls down to zero, and the electronic switch opens. The remaining input of the integrator is then equal to βX, and by virtue of integration will decrease until the value E_1 is reached again. The actual period of integration T_2 is given by

$$K\int_0^{T_2} \beta X\,dt = E_s - E_1 \tag{7.4}$$

and, by similar reasoning, the following result is obtained:

$$T_2 = \frac{E_s - E_1}{K\beta X} \tag{7.5}$$

Combining Equations 7.3 and 7.5, we have

$$\frac{T_1}{T_1 + T_2} = \frac{\beta X}{\alpha V} \tag{7.6}$$

We conclude from this that a rectangular wave can be obtained from the modulation of a voltage y by means of an electronic switch controlled by a bistable multivibrator, provided the variation of y is such that the voltage may be assumed constant during the period T_1 .

When the rectangular wave is filtered (Fig.48), the output voltage of the filter is equal to the mean value

$$-\gamma Y \frac{T_1}{T_1 + T_2}$$

or, by virtue of Equation 7.6,

$$-\frac{\gamma\beta}{\alpha}\frac{XY}{V}$$

The coefficients involved in this formula, as well as the reference voltage V , are usually arranged so that the output of the filter is equal to $-XY/100$.

7.1.4 Note

The devices which are used to multiply two variables, among which the most widely used have just been described, have been designed with the object of enlarging the capabilities of the analogue computer, but they do not have a great deal to do with the fundamental analogue principle itself. Furthermore, such devices do not give the same accuracy as can be obtained with digital computers, and the benefits of the analogue computation are not altered if the multiplications are performed outside the computer, provided the solution can be obtained sufficiently fast, so that it can be immediately fed back into the analogue computer. The actual trend, leading to the improvement of the accuracy of such non-linear computations, is to perform them on fast digital computers; the voltages are first coded into digits, and the digital results of the multiplication or division are translated again in continuous voltages, suitable for the continuation of the analogue process.

7.2 GENERATION OF NON-LINEAR FUNCTIONS

Numerous systems are actually available for feeding into an analogue computer any non-linear function of one or several variables. The most important among them are described in the following sections.

7.2.1 Non-Linear Potentiometers

These potentiometers are fed by reference voltages, and their wiring is arranged so that the wiper, forced into correct position by a control variable, picks up a voltage which is proportional to the value of the non-linear function required.

The non-linearity can be produced by several configurations: by using resistance wires, wound on a card of constant width, the distance between two consecutive windings being varied in accordance with the non-linear function; or by winding a resistance wire of constant cross-sectional area on to a card of variable width, the interval

between consecutive windings being now kept constant; or by using wires of variable cross-sectional area, the other characteristics remaining at a constant value. Such potentiometers are mainly used to generate trigonometric functions, and are involved in calculation blocks capable of transforming rectangular coordinates into polar coordinates and vice versa.

When dealing with any type of non-linear function, greater flexibility is generally sought, because one should not contemplate having to construct a special potentiometer for each particular function.

7.2.2 Cathode Ray Tube

This device (Fig.49) consists mainly of a cathode ray tube, coupled with a photocell. An opaque mask having the shape of the function $f(x)$ of the variable x, in rectangular coordinates, is cemented on to the screen of the cathode ray tube. The voltage representative of the variable x controls the horizontal deflection plates of the tube. The vertical deflection is controlled by an external voltage V, flowing first through a d.c. amplifier; the voltage V is conditioned to give an upward deflection to the electron beam. When this upward deflected electron beam overshoots the top of the mask, it acts on the photocell which sends, through the d.c. amplifier, a correcting voltage to the vertical deflection plates; this voltage tends to deflect the electron beam back into a downward direction.

A feedback system is made up in doing so, forcing the electron beam to follow the opaque border of the mask. The voltage acting on the vertical deflection plates of this closed loop system is then proportional to the value $f(x)$ of the non-linear function. Several drawbacks are inherent in such a generator; first, the accuracy is not very satisfactory; furthermore, the machining of the masks represents a rather lengthy preliminary work; finally, the function to be generated must have a simple and smooth shape, because it is not easy to take many details into account, due to the small area which is required for the mask.

7.2.3 Servo-Potentiometers

The principle of these generators is taken from the design of electro-mechanical servo-multipliers. The control system itself is similar: an electric motor, now driving a drum, is forced to take a geometrical position directly related to a control variable (Fig.50). A conducting curve, made of a folded copper bar, representing the function $f(x)$ to be introduced into the computer is cemented on to the drum. The conducting curve has a point of contact with a linear potentiometer which is connected at the terminals to reference voltages; the contact acts just as a wiper. The voltage, proportional to the value of $f(x)$, which corresponds to a given angular position of the drum, is then picked up by the conducting curve. The capability of the device is in fact a little larger, since a product of the form $yf(x)$ can be directly obtained if the positive and negative values of the voltage y are substituted for the reference voltages, in a similar fashion as was done for the multiplying type of potentiometer.

The frequency limitation of such generators is the same as that of the servo-multipliers. A loading compensation has also to be added to the control potentiometer, so that the *geometrical* rotation of the drum shall be in agreement with the *electrical* one.

The preliminary work of machining the conducting curve is rather lengthy, and the proper fastening is a delicate job; furthermore, if the same curve is frequently used, its mechanical properties are found to be rapidly spoiled.

7.2.4 Conducting Ink

In order to avoid this latter drawback, due to the mechanical contact between the conducting curve and the linear potentiometer, the use of a conducting ink, which is energized by a high frequency current, has been developed. A stylus, which is made sensitive to the magnetic field expanding from the energized line, is forced to follow the curve, mechanically driving the wiper of a linear potentiometer connected to reference voltages; the voltage at the wiper is again proportional to the value of the actual function.

7.2.5 Taped Potentiometer

The preceding set-ups are expected to reproduce the true shape of the function which is generated. Both generators which are now being described are, on the other hand, based on an approximate representation of the function; the plot is divided into a given number of intervals, within which the curve must be accurately compared to straight lines. Feeding a linear potentiometer at intermediate points with voltages which are proportional to the value of the function at that point (Fig.51), it is possible to pick up anywhere the approximate value of the function, by means of a sliding contact which is controlled by the variable itself. The intermediate feeders are made of auxiliary potentiometers, connected to reference voltages.

It is necessary that the curvature of the curve be everywhere so small that the comparison to straight portions shall be accurately valid at any point. It must indeed be pointed out that the locations of the intermediate break points are usually definitely fixed at equal distances from one another.

When setting the problem, the auxiliary potentiometers are adjusted in cascade; but, for instance, when the value $f(x_0)$ has been calibrated, the setting of the next value $f(x_1)$ reacts on the first one, and so on; so that, in fact, the setting of a taped potentiometer is an iterative process. Some analogue computers, however, are provided with auxiliary components which make it possible to carry out a straightforward setting.

7.2.6 Diode Generators

The diode generator has the advantage that it provides a simple way of varying the length of the intervals inside which the curve is compared to a straight line. This generator is basically built with diodes, the ideal characteristic line of which is reproduced in Figure 52.

When the applied voltage is less than E_s, the diode does not conduct; it switches to conducting properties when the voltage reaches the level E_s. The voltage E_s may be either positive or negative, and the slope of the characteristic depends on the value of the resistance inserted in the diode circuit. The generator involves a set of diodes which is organized in such a way that, at the end of a straight portion of the curve, a further diode starts to conduct; the slope of its characteristic is

determined so that, adding its effect to those of the other conducting diodes, the actual slope of the following straight portion is accurately achieved; the location of the break points may be adjusted as desired.

However, the curves which can be generated must match the requirement that the slopes of the successive straight portions increase continuously, since it is impossible to obtain a negative slope from a diode circuit. If this condition is not fulfilled, two different curves must be generated separately and afterwards subtracted, in order to give finally the suitable shape.

Diodes are very often used in more simple circuits than those used for the generation of arbitrary functions, in order to simulate elementary discontinuous functions, which are usually encountered in the study of the details of control mechanisms. Among these functions, the simulation of absolute values, thresholds, stops, dry friction and hysteresis will be briefly described.

Consider first a potentiometer of total resistance R (Fig.53) with terminals respectively connected to voltages V and E having opposite signs; the position of the wiper divides the resistance into two parts, (1 - a) and (a) respectively, and the voltage at the wiper becomes equal to zero when the setting coefficient a satisfies the equation

$$a = \frac{|V|}{|E| + |V|}$$

(1) *Absolute value*

The curve showing the output voltage V_s in terms of the input voltage V_e is drawn in Figure 54a and its simulation is obtained from the circuit which is sketched in Figure 54b. The two portions of the curve can be defined by:

$$V_s = -KV_e \qquad -\infty < V_e \leqslant 0$$

$$V_s = +KV_e \qquad 0 \leqslant V_e \leqslant \infty$$

In the first case, the diode which is directly connected to the output amplifier conducts, while in the second one the circuit including the intermediate amplifier is operating. The value of the coefficient K may be varied as desired by setting the gain of the amplifiers accordingly.

(2) *Threshold*

The basic relationships for such a system can be written, if the slopes of the characteristics are both equal to K (Fig.55a), as:

$$V_s = K(V_1 - V_e) \qquad -\infty < V_e \leqslant V_1$$

$$V_s = 0 \qquad V_1 \leqslant V_e \leqslant V_2$$

$$V_s = K(V_e - V_2) \qquad V_2 \leqslant V_e < +\infty$$

The simulation is obtained from the circuit shown in Figure 55b.

If $V_e < V_1$, the voltage at station A is positive and the upper diode does not conduct while, since the voltage at station B is also positive, the lower diode does conduct. When $V_1 < V_e < V$, the voltages at A and B are respectively positive and negative, and not one of the diodes conducts; the input of the amplifier is thus equal to zero, as well as the output. If $V_e > V_2$, the situation is inverted with respect to the first case.

(3) *Stops*

The simulation of a stop corresponds to the function which is illustrated in Figure 56a, and is described by the following relations:

$$V_s = V_1 \qquad -\infty < V_e \leqslant V_1/K$$

$$V_s = KV_e \qquad V_1/K \leqslant V_e \leqslant V_2/K$$

$$V_s = V_2 \qquad V_2/K \leqslant V_e < \infty$$

The corresponding circuit is shown in Figure 56b.

The input and feedback resistances of the d.c. amplifiers are such as to provide a gain K . When $V_1 \leqslant V_s \leqslant V_2$, the voltage at A is positive, and negative at B , so that no diode is active and the amplifier works as a single multiplier. But as soon as V_s reaches the level V_2 , the voltage at B becomes positive and the lower diode starts conducting; its action is equivalent to the addition of an impedance, which is practically equal to zero, in parallel on the d.c. amplifier, the gain of which drops down to zero. From thereon, the output voltage V_s remains constant. It must be noted that in such conditions the feedback impedance is, in fact, equal to a portion of the resistance of the potentiometer, plus the internal resistance of the diode. A residual gain will thus continue to exist and the slopes of the characteristics will be slightly different from zero.

The same result can be obtained with a similar circuit, which does not involve the d.c. amplifier (Fig.56c).

(4) *Dry friction*

In the most general case where the tilting does not occur at the origin but for a given value E of the input voltage (dotted line in Figure 57a), the corresponding equations are

$$V_s = V_2 \qquad -\infty < V \leqslant E$$

$$V_s = V_1 \qquad E \leqslant V < \infty$$

where V is again the unrestricted value of the output voltage. When E = 0 , the solution is directly derived, as a particular case, from the last section, where the coefficient K is made infinitely large. The circuitry is accordingly modified by suppressing the feedback resistance of the d.c. amplifier; the way of reasoning is

identical. The shift of the origin is achieved by the addition of a constant voltage at the input of the amplifier (Fig.57b).

(5) *Hysteresis*

A hysteresis cycle as illustrated in Figure 58a, having an amplitude E, is simulated with the circuit of Figure 58b. If we assume that the initial value of V_e is zero, none of the diodes acts as a conductor and the output voltage V_s is equal to zero. The segment OA is thus followed until V_e reaches the value $\frac{1}{2}E$. The lower diode then starts conducting and the behaviour of the circuit is similar to that of a simple time lag generator; the time constant is small, in accordance with the low values of the resistances involved, and also because the value of the capacitance used can be made small; this time constant may thus be usually neglected, so that the straight portion AB is obtained. When point B is reached, that is when the voltage V_e starts decreasing, the difference between V_e and V_s becomes smaller than $\frac{1}{2}E$ and the diode does not conduct any more; the output V_s remains constant until the difference takes the value $-\frac{1}{2}E$ at point C; the other diode starts conducting at that time; and the process goes on.

7.2.7 Non-Linear Functions of Two Variables

Several types of generators have been designed, but since they are still somewhat in the prototype stage, by which is meant that they are not yet extensively included as the basic equipment of an analogue computer, they will not be described here.

Their use will increase the accuracy of the solution of those problems which involve non-linear functions of two variables, since, without them, approximate representations have to be used.

CHAPTER 8

SPECIAL FEATURES OF ANALOGUE COMPUTATION

8.1 SET-UP OF TRANSFER FUNCTIONS

The previous sections have shown how an analogue computer is able to solve systems of differential equations which are written in an explicit form in terms of time.

When the analysis of a physical system is carried out using Laplace's transformation, the equations are obtained in terms of the variable s, and a direct representation of these equations on an analogue computer is sought. It is easy to see that, when talking about differential equations, both the original equations and the transformed equations lead to the same analogue diagram. A differential equation of nth order transforms into a polynomial of nth degree in s; if the polynomial is then solved for the term of highest power in s, the second member has to be integrated in succession until the function of s itself is obtained. The analogue set-up which is obtained is entirely similar to that which one would derive from the original equations.

In fact, when a differential equation is simulated on an analogue computer, the electric circuit resulting from the interconnection of elementary calculation blocks, which is achieved by simple reasoning on a mathematical formulation, forms by itself a physical system having a general transfer function equal to that which is described by the equation.

Therefore, a differential equation can be solved by first finding out what is the corresponding transfer function, and then wiring a circuit having the same general transfer function.

The design of a circuit having a given transfer function is a simple problem of electrical engineering consisting of suitable combinations of impedances, which can be worked out without any reference to a differential equation. When considering this aspect of the question, it happens that the circuit which is found by this method is different from that which is obtained from the analogue representation of a differential equation corresponding to the same transfer function. Two different methods are thus available for constructing an electrical circuit to represent a given transfer function.

Consider as an example the transfer function corresponding to the introduction of a time constant T, which can be defined as

$$\frac{V_s}{V_e} = -\frac{K}{1 + Ts} \tag{8.1}$$

This formula can be re-written as a differential equation:

$$V_s = -\frac{1}{s}\left(V_s + \frac{K}{T} V_e\right) \tag{8.2}$$

from which the circuit illustrated in Figure 59 is immediately derived.

The same transfer function can also be achieved by a suitable arrangement of input and feedback impedances of a d.c. amplifier. The transfer function of the circuit which is shown in Figure 60a can be easily computed as

$$\frac{V_s}{V_e} = -\frac{R_c}{R_e}\frac{1}{1 + Ts} \tag{8.3}$$

The symbolic representation of this circuit is given in Figure 60b.

The first method shows an easy way to represent very rapidly any given transfer function, while the second one requires impedance calculations; this drawback can be somewhat alleviated, since tables giving the drawings of several circuits with their transfer function have been published.

In the very simple case just described, both diagrams are similar, but usually the method starting from the differential equation requires a larger number of operational amplifiers. This can be very easily checked, since a second order transfer function such as

$$G(s) = \frac{1}{s^2 + as + b}$$

corresponds to a circuit involving only one amplifier, while the circuit derived from the differential equation requires two.

8.2 OPERATIONAL RESTRICTIONS

The purpose of the preceding argument was to explain the basic principles of the analogue computer, and to show that such a method of calculation is useful for handling differential systems which are too complicated to be solved by usual analytical methods.

The third part of this Agardograph is devoted to its applications to the main problems which are encountered in the study of the flight of an aeroplane.

However, all the practical details necessary for the correct performance of the calculations have not so far been mentioned. There are certain operational restrictions on the computer as well; amongst these the most important are:

To check the block diagram and the connections before starting the computation;

To check from time to time the accuracy of the results;

To avoid any saturation;

To keep the drift of the amplifiers at a low level.

These checks are almost a matter of practice, so these points will not be detailed here; it will however be pointed out that we have to distinguish between ordinary and stabilized amplifiers, as far as the last point is concerned.

The d.c. amplifiers are subject to drift, an error voltage due to the unbalance of the amplifier perturbing the normal output voltage. The origins of the drift are: small changes of the supply voltage with time, variations of the filament voltages, modifications of internal resistances or tube characteristics. The value of the drift can be reduced if the constancy of the characteristics of those elements is improved, but it cannot be entirely eliminated. The presence of the drift decreases the accuracy of the computation and requires frequent balancing of the amplifiers.

The drift is considerably reduced with stabilized amplifiers; such amplifiers involve an auxiliary circuit which provides a continuous balance according to the following principle. The grid voltage of the input of the amplifier must be equal to zero; if an error voltage appears at that point, it is sent to an auxiliary circuit where it is modulated by a synchronous vibrator. The alternative signal which is produced in this way is then amplified by an a.c. amplifier, and demodulated by the same synchronous vibrator; this sends a d.c. signal back. This voltage is then reintroduced at the input of the d.c. amplifier in such a way that it brings the grid voltage back to zero (Fig.61). The demodulation is worked out in phase with the modulation so that, if the error voltage is inverted, the output voltage of the demodulator is also inverted. Such a device, which has been designed to give automatic balance of the drift of a d.c. amplifier, results in a further advantage: for low frequencies, it increases the overall gain of the amplifier since the gain of the a.c. amplifier used in the balancing circuit is added to the gain of the d.c. amplifier itself; the accuracy of low-frequency computations is thus considerably increased.

However, when a stabilized amplifier is saturated, the capacitances of the balancing circuit are loaded and a certain time elapses before they are discharged; after saturation has occurred, a given recovery time interval is necessary before the computation can be started again.

LIST OF FIGURES

		Page
Fig.17	Elementary calculation block	115
Fig.18	Sign inverter	115
Fig.19	Symbolic representation of an inverter	115
Fig.20	Inversion and multiplication	115
Fig.21	Symbolic representation	115
Fig.22	Use of a potentiometer instead of 2 resistances	115
Fig.23	Use of the potentiometer	115
Fig.24	Calibration of a potentiometer	115
Fig.25	Symbolic representation of a potentiometer	115
Fig.26	Comparison with a calibrated potentiometer	115
Fig.27	Loading error of a potentiometer	115
Fig.28	Elimination of the loading error	116
Fig.29	Elimination of the loading error	116
Fig.30	Integrator set-up	116
Fig.31	Symbolic representation of an integrator	116
Fig.32	Theoretical set-up of a differentiating device	116
Fig.33	Summator set-up	116
Fig.34	Symbolic representation of a summator integrator	116
Fig.35	Symbolic representation of a summator	116
Fig.36	Resolution of a set of linear differential equations	116
Fig.37	Inserting a resistance in the feedback loop of a summator	117
Fig.38	Introduction of initial conditions	117
Fig.39	Computing configuration	117

Fig.40	Hold configuration	117
Fig.41	Servo-driven potentiometer	117
Fig.42	Mechanical servo multiplier	117
Fig.43	Loading error of a multiplier	117
Fig.44	Correction of the loading error	117
Fig.45	Set-up performing a division	117
Fig.46	Modulation of a rectangular wave	118
Fig.47	Principle of the electronic multiplier	118
Fig.48	Principle of the electronic multiplier	118
Fig.49	Cathode ray tube used as a function generator	118
Fig.50	Servo potentiometer used as a function generator	118
Fig.51	Taped potentiometer used as a function generator	118
Fig.52	Ideal characteristic of a diode	119
Fig.53	Point of zero voltage	119
Fig.54	(a) Absolute value of a variable	119
	(b) Set-up simulating the absolute value of a variable	119
Fig.55	(a) Threshold	119
	(b) Set-up simulating a threshold	119
Fig.56	(a) Stop or maximum of a variable	119
	(b) Set-up producing a stop	119
	(c) Other set-up producing a stop	119
Fig.57	(a) Dry friction	119
	(b) Set-up simulating dry friction	119
Fig.58	(a) Hysteresis	120
	(b) Set-up simulating hysteresis	120
Fig.59	Elaboration of a time constant	120
Fig.60	(a) Other set-up elaborating a time constant	120
	(b) Symbolic representation	120
Fig.61	Scheme of a stabilized amplifier	120

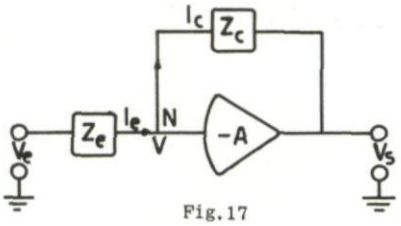

Fig.17

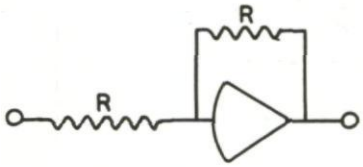

Fig.18

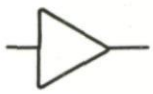

Fig.19

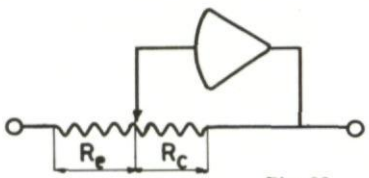

Fig.22

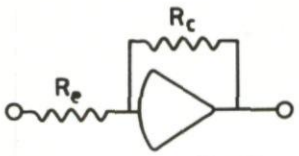

Fig.20

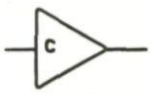

Fig.21

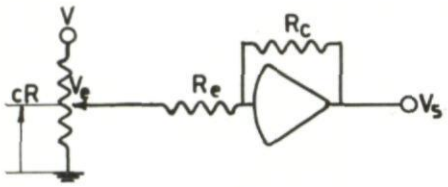

Fig.23

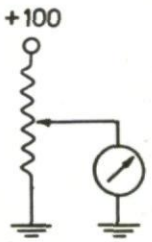

Fig.24

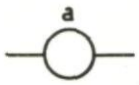

Fig.25

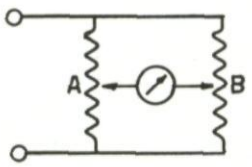

Fig.26

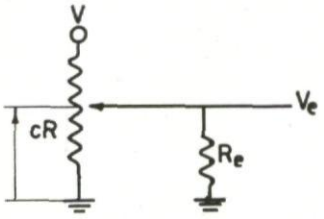

Fig.27

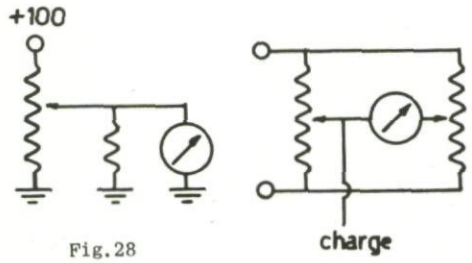

Fig.28

Fig.29

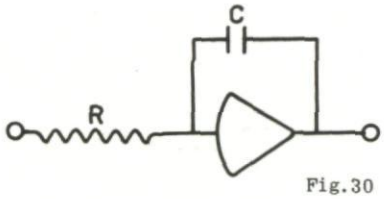

Fig.30

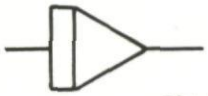

Fig.31

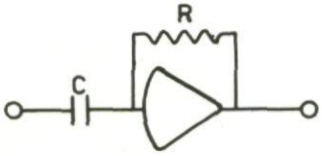

Fig.32

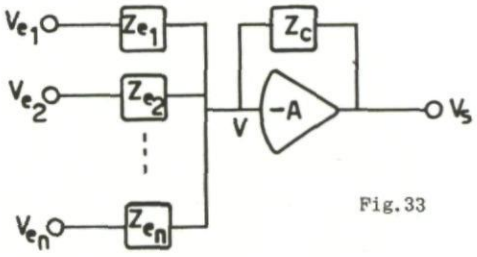

Fig.33

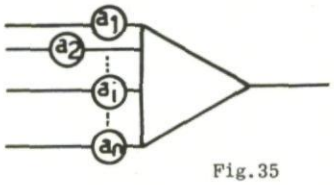

Fig.35

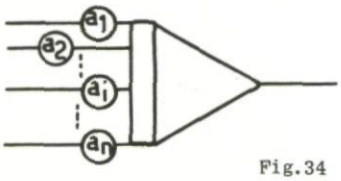

Fig.34

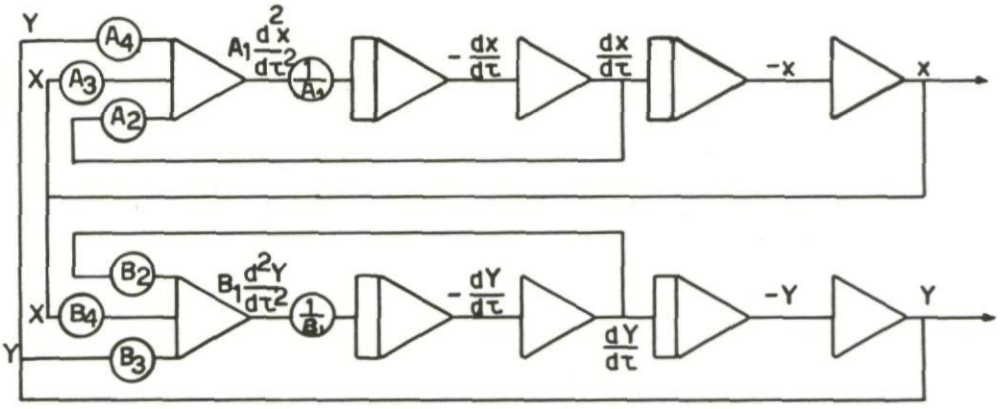

Fig.36

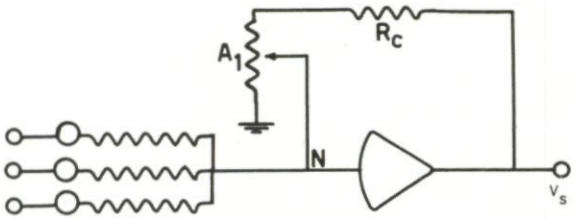

Fig.37

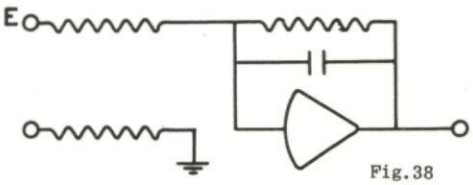

Fig.38

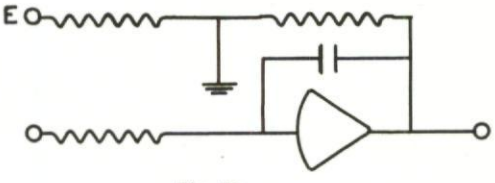

Fig.39

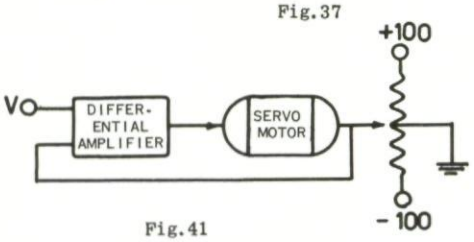

Fig.41

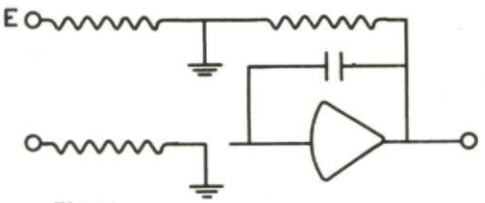

Fig.40

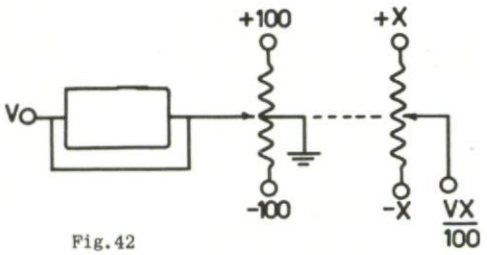

Fig.42

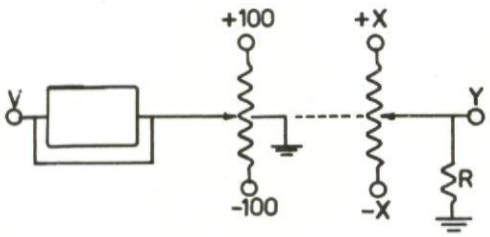

Fig.43

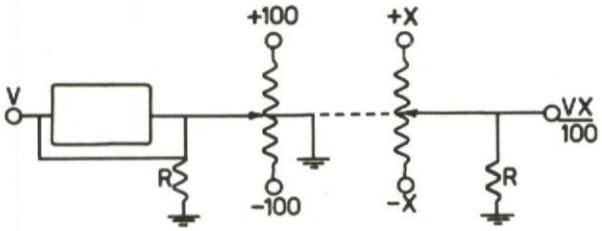

Fig.44

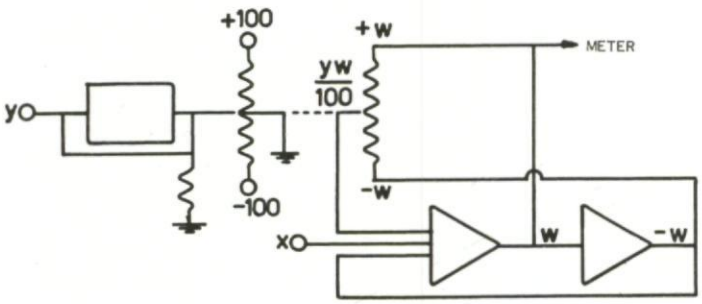

Fig.45

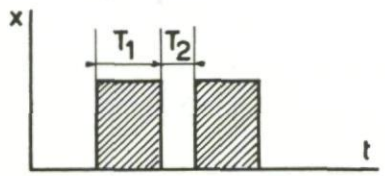

Fig.46

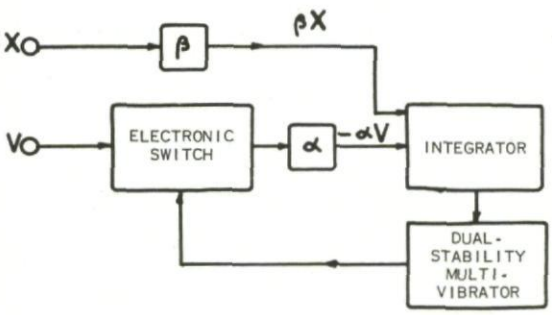

Fig.47

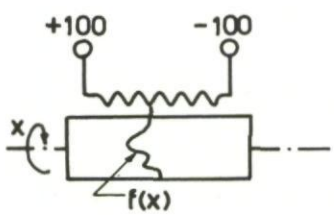

Fig.50

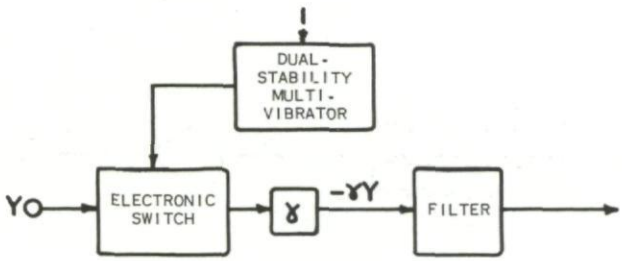

Fig.48

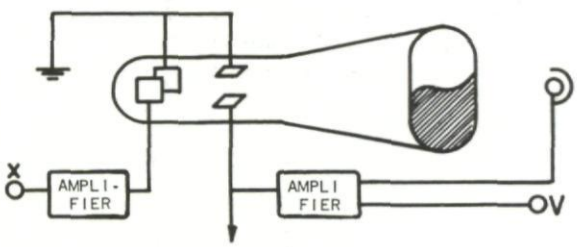

Fig.49

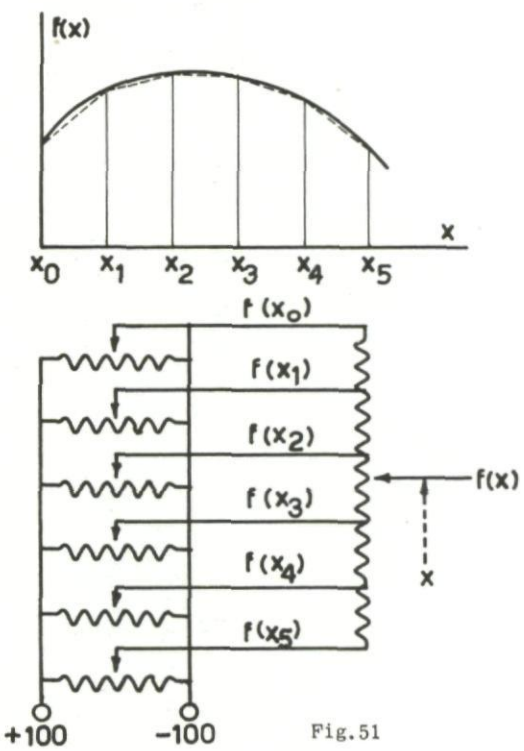

Fig.51

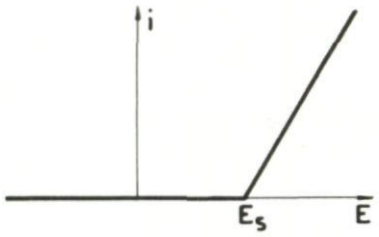

Fig.52

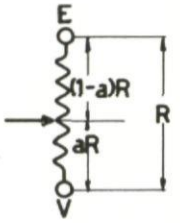

Fig.53

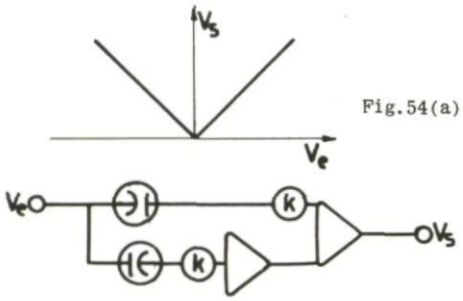

Fig.54(a)

Fig.54(b)

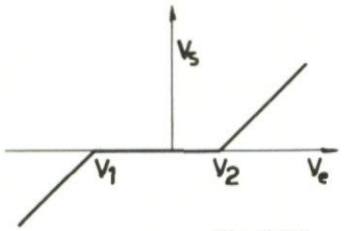

Fig.55(a)

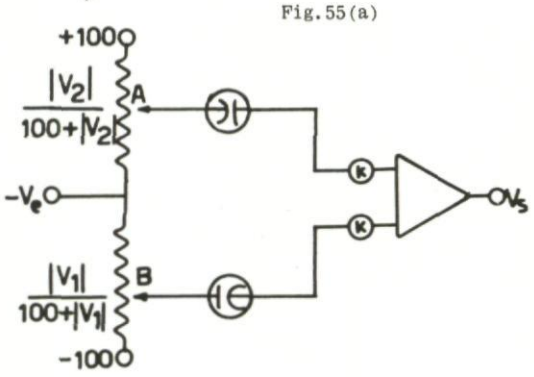

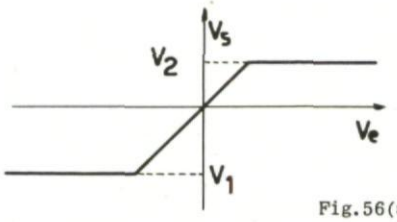

Fig.56(a)

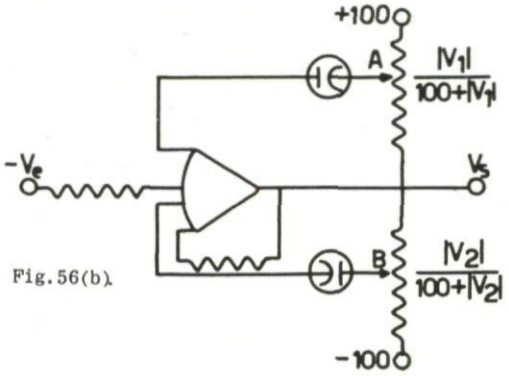

Fig.56(b)

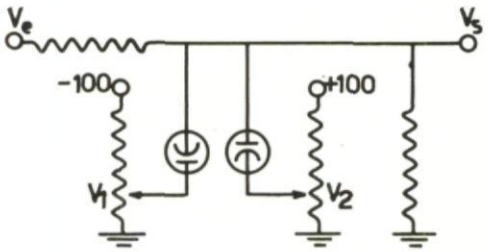

Fig.56(c)

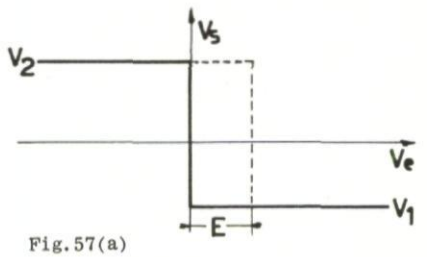

Fig.57(a)

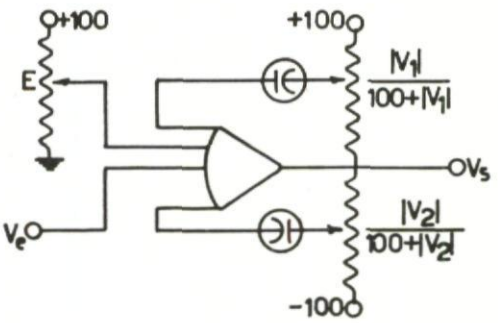

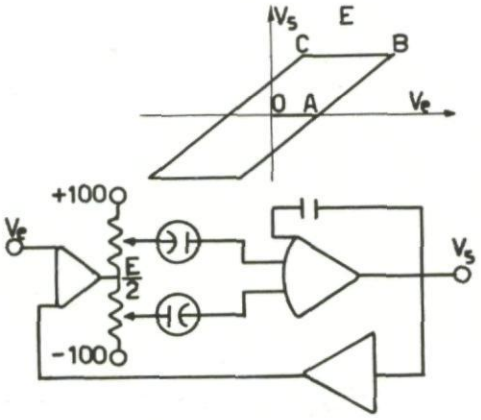

Fig.58(a)

Fig.58(b)

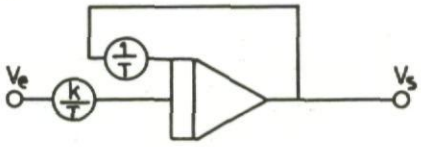

Fig.59

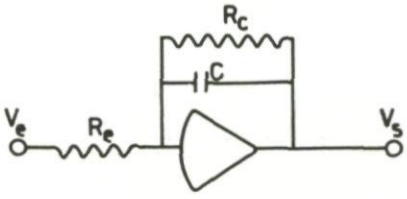

Fig.60(a)

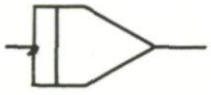

Fig.60(b)

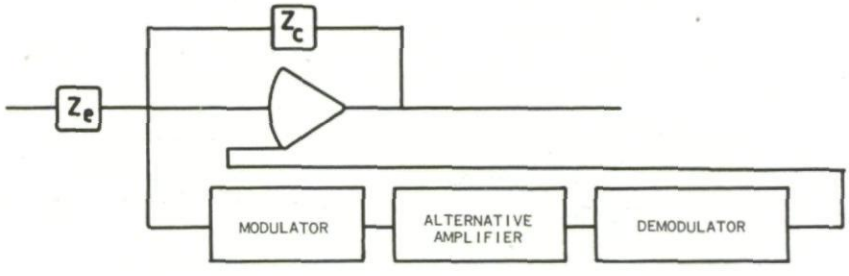

Fig.61

PART III - THE USE OF ANALOGUE COMPUTERS

CHAPTER 9

PROBLEMS OF KINEMATICS

F.C.Haus and L.Moulin

9.1 INTRODUCTION

The application of the analogue computer to the solution of the main problems related to the kinematics of aircraft motion will be studied in this chapter. These problems are as follows:

(a) Knowing the three angular velocity components P,Q,R of the aircraft, related to the body axes, to calculate the coordinates defining the orientation of the aeroplane in relation to the ground, or geoparallel, axes.

(b) Knowing the three components of a moving vector related to the ground axes, and also the motion of the aeroplane, to calculate the projections of this vector on the aircraft body axes.

The position of the moving axes in relation to the ground axes can be determined by two sets of coordinates; either by the angles ψ, θ, φ, called the Euler angles, or by the direction cosines of the system of moving axes relative to the ground axes. These give two different solutions to each problem.

9.2 SOLUTION OF THE MAIN PROBLEMS USING THE EULER ANGLES

9.2.1 First Problem

The rotations φ, θ, ψ are related to the aeroplane angular velocities P,Q,R by Equations (1.5), which are repeated here for convenience:

$$\left.\begin{aligned} \dot{\varphi} &= P + \dot{\psi}\sin\theta \\ \dot{\theta} &= Q\cos\varphi - R\sin\varphi \\ \dot{\psi} &= Q\frac{\sin\varphi}{\cos\theta} + R\frac{\cos\varphi}{\cos\theta} \end{aligned}\right\} \qquad (9.1)$$

The problem consists of the integration of this set of equations. We have to make use of resolvers, or devices generating the trigonometric functions of a known angle.

Such a device, whose principle has been explained in Section 7.2.1, is similar to a servo-multiplier: a servo-motor will produce an angular displacement proportional to the applied voltage. The shaft carries two brushes placed at exactly 90 degrees,

and containing a potentiometer like that shown in Figure 62. The resistance in each 90° sector varies sinusoidally, so that the brush A making an angle θ with the neutral line collects a voltage proportional to the sine of this angle.

This device permits multiplication by a constant factor K. The upper and lowest points of the potentiometer must be of opposite sign. As the voltage K may vary within very large limits, the control mechanism must be fitted with an automatic gain stabilizer in order to limit the errors of the result.

The resolvers are symbolically represented as indicated in Figure 63, the inverter being included in the symbolic representation. The variable that commands the angular displacement of the shaft is, in this case, the angle θ.

The components P, Q, R are functions of time obtained by the integration of the flight equations; the Euler angles will be other functions of time, resulting from the integration of the set of Equations (9.1). They are obtained with the set-up represented in Figure 64. The dotted lines represent connections that would ordinarily be included in the symbolical representation but they have been reproduced here for clearness.

The last of Equations (9.1) presents a singularity when $\theta = \pm 90^{o}$. The proposed method of calculation is only applicable when the aircraft motion involves values of $\theta = \pm 90^{o}$. The singularity produced by $\theta = \pm 90^{o}$ can be avoided by the choice of a different sequence of rotations, but will always affect the rotation to be applied in the second place.

If we use three rotations occurring in the order ψ', φ', θ', Equations (1.4) and (1.5) will be replaced by:

$$\left.\begin{aligned} P &= \frac{d\varphi'}{dt}\cos\theta' - \frac{d\psi'}{dt}\cos\varphi'\sin\varphi' \\ Q &= \frac{d\theta'}{dt} + \frac{d\psi'}{dt}\sin\varphi' \\ R &= \frac{d\varphi'}{dt}\sin\theta' + \frac{d\psi'}{dt}\cos\varphi'\cos\theta' \end{aligned}\right\} \qquad (9.2)$$

$$\left.\begin{aligned} \frac{d\varphi'}{dt} &= P\cos\theta' + R\sin\theta' \\ \frac{d\theta'}{dt} &= Q - \frac{d\psi'}{dt}\sin\varphi' \\ \frac{d\psi'}{dt} &= -R\frac{\sin\theta'}{\cos\varphi'} + R\frac{\cos\theta'}{\cos\varphi'} \end{aligned}\right\} \qquad (9.3)$$

The values of the rotations ψ', φ', θ' differ slightly from the values of the angles ψ, φ, θ just defined.

If we use three rotations occurring in the order θ'', ψ'', φ'', we will get the equations:

$$\left.\begin{aligned} P &= \frac{d\varphi''}{dt} + \frac{d\theta''}{dt}\sin\psi'' \\ Q &= \frac{d\theta''}{dt}\cos\psi''\cos\varphi'' + \frac{d\psi''}{dt}\sin\varphi'' \\ R &= \frac{d\psi''}{dt}\cos\varphi'' - \frac{d\theta''}{dt}\cos\psi''\sin\varphi'' \end{aligned}\right\} \qquad (9.4)$$

$$\left.\begin{aligned} \frac{d\varphi''}{dt} &= P - \sin\psi''\frac{d\theta''}{dt} \\ \frac{d\theta''}{dt} &= \frac{1}{\cos\psi''}(Q\cos\varphi'' - R\sin\varphi'') \\ \frac{d\psi''}{dt} &= Q\sin\varphi'' + R\cos\varphi'' \end{aligned}\right\} \qquad (9.5)$$

Here again, the numerical values of θ'', ψ'', φ'' will differ from the sets θ', ψ', φ' or θ, ψ, φ.

The singularity occurs every time the second rotation reaches the values $\pm 90^{o}$. If it is certain that the amplitude of one of the three angles will never reach $\pm 90^{o}$, we may always apply the method just indicated, choosing the order of rotations in such a way that this particular angle will be the second. This requires rewriting all the equations in terms of the Euler angles.

If we are not certain that we can avoid an angle of 90° in the second rotation, we may use the process incorporated in the Tridac computer and described by S.J.Gait[6]. This process consists of dividing the second rotation into two parts, i.e. in utilizing four rotations instead of three.

In the case of the sequence θ'', ψ'', φ'', the rotations will take place respectively around:

an initial axis OY_0

an intermediate axis OZ_i

a final axis OX_1

The rotation ψ'' will be prevented from becoming equal to 90° by adding a preliminary rotation ψ_s'' around OZ_0. This supplementary and redundant rotation will occur at an angular velocity $d\psi_s''/dt$ which may have a constant value and must be chosen in order to prevent ψ'' from becoming equal to 90°. Figure 65 shows the correspond-

ing displacements. As a consequence of the supplementary rotation, the rotations θ'' and ψ'' will be executed around the intermediate axes $OY_{0,i}$ and OZ_i. The equations which relate the angular velocities P, Q, R to the derivatives of the angles become:

$$\left.\begin{aligned} \frac{d\varphi''}{dt} &= P - \sin\psi'' \frac{d\theta''}{dt} + \cos\psi \sin\theta \frac{d\psi_s''}{dt} \\ \frac{d\theta''}{dt} &= \frac{1}{\cos\psi''} (Q \cos\varphi'' - R \sin\varphi'') + \frac{d\psi_s''}{dt} \sin\theta'' \sin\psi'' \\ \frac{d\psi''}{dt} &= Q \sin\varphi + R \cos\varphi - \frac{d\psi_s''}{dt} \cos\theta \end{aligned}\right\} \qquad (9.6)$$

By an appropriate choice of the rotation ψ_s'' and the angular velocity $d\psi_s''/dt$ it will always be possible to avoid the appearance of a singularity in the equations.

9.2.2 Second Problem

The Euler angles being known, we wish to find the components, on the moving axes, of a vector whose components on the ground axes are known.

Theoretically, the response is given by the matrix Equation (1.1), where the terms of the transformation matrix are written as a function of the Euler angles, as given in Table I.

It is, nevertheless, preferable to proceed by progressive steps in the development of the set-up, considering each rotation successively.

Let

X_0, Y_0, Z_0 be the projections of vector $\vec{V}$ on the axis $OX_0Y_0Z_0$

X_1, Y_1, Z_1 be the projections of vector $\vec{V}$ on the axis $OX_1Y_1Z_1$

X , Y , Z be the projections of vector $\vec{V}$ on the intermediate axes.

The three successive rotations described in Section 1.2.b will correspond to the following three matrix equations:

$$\begin{vmatrix} X \\ Y \\ Z_0 \end{vmatrix} = \begin{vmatrix} \cos\psi & \sin\psi & 0 \\ -\sin\psi & \cos\psi & 0 \\ 0 & 0 & 1 \end{vmatrix} \begin{vmatrix} X_0 \\ Y_0 \\ Z_0 \end{vmatrix}$$

$$\begin{vmatrix} X_1 \\ Y \\ Z \end{vmatrix} = \begin{vmatrix} \cos\theta & 0 & -\sin\theta \\ 0 & 1 & 0 \\ \sin\theta & 0 & \cos\theta \end{vmatrix} \begin{vmatrix} X \\ Y \\ Z_0 \end{vmatrix}$$

$$\begin{vmatrix} X_1 \\ Y_1 \\ Z_1 \end{vmatrix} = \begin{vmatrix} 1 & 0 & 0 \\ 0 & \cos\varphi & \sin\varphi \\ 0 & -\sin\varphi & \cos\varphi \end{vmatrix} \begin{vmatrix} X_1 \\ Y \\ Z \end{vmatrix}$$

Each of these equations corresponds to a set

$$X = X_0 \cos\psi + Y_0 \sin\psi$$

$$Y = -X_0 \sin\psi + Y_0 \cos\psi$$

$$Z_0 = Z_0$$

$$X_1 = X \cos\theta - Z_0 \sin\theta$$

$$Y = Y$$

$$Z = X \sin\theta + Z_0 \cos\theta$$

$$X_1 = X_1$$

$$Y_1 = Y \cos\varphi + Z \sin\varphi$$

$$Z_1 = -Y \sin\varphi + Z \cos\varphi$$

The three sections indicated a, b, c in Figure 66 describe the set-up that will produce the solution on an analogue computer.

9.3 SOLUTION OF THE PROBLEMS USING DIRECTION COSINES

9.3.1 First Problem

The equations (1.3), rewritten here:

$$\dot{l}_i = m_i R - n_i Q$$

$$\dot{m}_i = n_i P - l_i R$$

$$\dot{n}_i = l_i Q - m_i P$$

with $i = 1, 2, 3,$ must be integrated, using the angular velocities as inputs, and the initial values $(\dot{l}_i)_0$, $(\dot{m}_i)_0$, $(\dot{n}_i)_0$ as integration constants.

This operation requires the use of multipliers. We will represent the servo-multiplier schematically by the symbol given in Figure 67.

The set-up which produces the integration of the equations will be utilized three times, in order to obtain the nine direction cosines.

When the multipliers produce the product of one variable, such as P, with several others, such as n_1, n_2, n_3, the six multipliers corresponding to the scheme of Figure 68, combined with nine integrators, will permit the calculation of the nine direction cosines.

9.3.2 Second Problem

When the direction cosines are known, the projections of a vector on the body axes $OX_1Y_1Z_1$ will be obtained as functions of the projections of the same vector on the axes $OX_0Y_0Z_0$, by Formula 1.1, rewritten here:

$$X_1 = l_1X_0 + l_2Y_0 + l_3Z_0$$

$$Y_1 = m_1X_0 + m_2Y_0 + m_3Z_0$$

$$Z_1 = n_1X_0 + n_2Y_0 + n_3Z_0$$

The set-up for the calculation is represented in Figure 69.

Remark

The direction cosine method does not present the inconvenience associated with a possible discontinuity as is the case with the Euler angle method. On the other hand, when one considers the results of a calculation, the Euler angles have a clear physical significance, which is not the case with the direction cosines.

The two methods require different analogue computer equipment and the complete solution of any problem requires a different number of operational amplifiers according to the method chosen. The choice between the two methods will, in practical cases, nearly always be influenced by the equipment available.

CHAPTER 10

MOTION OF AN AEROPLANE WITH RIGID STRUCTURE

J. Czinczenheim and F. C. Haus

10.1 LINEAR PROBLEMS

(A) *Introduction*

In spite of the earlier works of Joukovsky and Lanchester, the first analytical study of the linear equations representing the motion of an aeroplane is credited to G. H. Bryan (1911).

Since then the dynamic stability equations of rectilinear steady motion, applied to both longitudinal and lateral disturbances, have been analysed systematically.

The analytical theory has brought out the nature of the unsteady motions:

(a) Long-and short-period oscillations in longitudinal motion;

(b) Oscillatory Dutch roll and aperiodic phenomenon in lateral motion.

However, difficulties in measuring certain aerodynamic derivatives and the dynamic behaviour of aeroplanes generally satisfactory when their static stability was ensured, have for a long time relegated the dynamic studies to the background, and one has been restricted to a qualitative check of dynamic stability using Routh's criterion; no one has ever gone beyond the determination of the roots of the system's characteristic equation.

The situation has changed in the last fifteen years. Increases in speed and altitude, the development of automatic pilots, the great variety in shape of modern aircraft and their tendency to instability, and finally the appearance of special vehicles such as VTOL, STOL, and space vehicles, have brought with them a need for elabor dynamic studies, while improvements in measuring techniques and in the calculati aerodynamic derivatives have provided the necessary input data.

Research in these directions has been readily promoted, firstly by the introduction of operational methods, then by the-use of analogue computing machines.

The tasks accomplished with the help of these computers does not present a very general character and constitute studies of particular cases.

The speed with which the equations of motion can be resolved by computing machines enables us, nevertheless, by progressively varying the data, to discover how the solutions vary.

The accumulation of results, coupled with a careful examination of the wiring diagram, may to a certain extent replace an analytical discussion of the equations.

(B) *Field of Application*

In what follows, the equations of motion will be written in their usual form, as a function of the time variable t, and will be fed into the computer in this form.

The computer enables a study to be made of the resulting motion, starting from a steady motion regime:

(1) By an initial disturbance of one or more of the variables of the motion, the controls remaining locked;

(2) By an input due to control displacement, of which the evolutions are known;

(3) By an input due to surrounding air movements, the controls being locked;

(4) By any combination of the above inputs.

(C) *Study of Disturbances Produced in a Rectilinear Motion*

The steady motion considered is a rectilinear one, during which the inclination $\Phi_0 = 0$.

The attitude $\Theta_0 \neq 0$, but is sufficiently small for us to assume that $\cos\Theta_0 = 1$ and $\sin\Theta_0 = \Theta_0$.

10.1.1 Longitudinal Motion

10.1.1.1 Linearized Equations of the Longitudinal Motion

The system is reduced to:

$$\left.\begin{aligned} 2\tau \frac{d\hat{u}}{dt} &= \Delta C_x + C_{z_0}\theta \\ 2\tau \frac{d\alpha}{dt} + 2\tau q &= \Delta C_z + C_{z_0}\Theta_0\theta \\ C_{IY} \frac{dq}{dt} &= \Delta M \\ \frac{d\theta}{dt} &= q \end{aligned}\right\} \qquad (10.1)$$

In order to bring forward the lift and drag coefficients, let us replace C_{z_0}, ΔC_z and ΔC_x by the quantities C_{L_0}, ΔC_L and ΔC_D. The part of the increments ΔC_L, ΔC_D, ΔC_m depending on the variables $\hat{u}$, α, q, $\dot{\alpha}$ will be developed as indicated previously. We shall only retain the important terms of this development. The part

of the increments depending on input will be represented by $(\Delta C_L)_i$, $(\Delta C_D)_i$, $(\Delta C_m)_i$.

Under these conditions, the system becomes:

$$\left.\begin{aligned}
&2\tau \frac{d\hat{u}}{dt} + \left(2C_{D_0} + C_{D_u}\right)\hat{u} + \left(C_{D_\alpha} - C_{L_0}\right)\alpha + C_{D_q}\frac{c}{2V}q + C_{L_0}\theta = -(\Delta C_D)_i \\
&2\tau \frac{d\alpha}{dt} + \left(2C_{L_0} + C_{L_u}\right)\hat{u} + \left(C_{L_\alpha} + C_{D_0}\right)\alpha + \left(C_{L_q}\frac{c}{2V} - 2\tau\right)q - C_{D_0}\theta = -(\Delta C_L)_i \\
&C_{I_y}\frac{dq}{dt} - C_{m_u}\hat{u} - C_{m_\alpha}\alpha - C_{m_q}\frac{c}{2V}q - C_{m_{\dot{\alpha}}}\frac{c}{2V}\dot{\alpha} = (\Delta C_m)_i \\
&\frac{d\theta}{dt} = q
\end{aligned}\right\} \quad (10.2)$$

Let us recall that the quantities C_D , C_L and C_m include the influence of the propellers (see Fig. 70):

$$\left.\begin{aligned}
C_D &= C_{D_\alpha} - C_{T,x^*} \\
C_L &= C_{L_\alpha} - C_{T,z^*} \\
C_m &= C_{m_\alpha} + C_T\frac{d}{C}
\end{aligned}\right\} \quad (10.3)$$

and that in steady flow

$$\left.\begin{aligned}
C_{D_0} &= -\frac{mg\sin\gamma_0}{\frac{1}{2}\rho S V_0^2} \\
C_{L_0} &= +\frac{mg\cos\gamma_0}{\frac{1}{2}\rho S V_0^2} \\
C_m &= 0
\end{aligned}\right\} \quad (10.4)$$

The angle of the initial slope, γ_0 , is identical to Θ_0 when the choice of axes is such that $\alpha_0 = 0$.

10.1.1.2 Wiring Diagram

The solution of the 4th order linear differential system written above, is obtained by following a classical set-up, represented by Figure 71. Initial disturbances of variables $\Delta\hat{u}$, $\Delta\alpha$, $\Delta\theta$ will be introduced by charging the integrator condensers.

Inputs will be introduced by altering voltages representing $(\Delta C_D)_i$, $(\Delta C_L)_i$, $(\Delta C_m)_i$. These tensions may vary with respect to time in an arbitrary way (step, ramp function).

10.1.1.3 Examples

(a) *Solution of a system of equations without second member for an initial condition*

The system of equations has been set up with numerical values corresponding to an aeroplane of the DC-6 type. Inputs $(\Delta C_D)_i$, $(\Delta C_L)_i$, $(\Delta C_m)_i$ are zero. Initial conditions θ_0 and α_0 have been introduced by charging the corresponding integrator condenser. These conditions were first introduced separately, then simultaneously.

Outputs are given in Figures 72, 73 and 74. The output for the initial condition θ_0 belongs entirely to the slow or phugoid oscillation.

The output to initial condition α_0 enables us to find, at the beginning of the curves α , θ and q , the short-period oscillation. After this has vanished, the long-period oscillation remains.

The output to equal initial conditions θ_0 and α_0 is exactly the sum of the output to these two initial conditions acting separately.

(b) *Response of the aeroplane to a step deflection of the elevator*

In this case,

$$\left.\begin{aligned} (\Delta C_D)_i &= 0 \\ (\Delta C_L)_i &= \frac{S_h}{S}\,\frac{\partial C_{L_h}}{\partial \delta_e}\,\delta_e \\ (\Delta C_m)_i &= \frac{\partial C_m}{\partial \delta_e}\,\delta_e \end{aligned}\right\} \qquad (10.5)$$

where S_h represents the area of the tailplane

C_{L_h} represents its lift coefficient.

Figure 75 represents the output of the same aeroplane to a positive step-deflection δ_e (nose-down motion).

In the diagram of α and q the part belonging to the rapid oscillation is easily found.

The aeroplane tends to a nose-down position in flight, corresponding to final values of:

$$\frac{\theta}{\delta_e} = -3.22 \qquad \frac{\alpha}{\delta_e} = -2.865 \qquad \frac{\hat{u}}{\delta_e} = +12.62$$

The lay-out of this diagram is absolutely classical. Another example is shown in Part IV. Figure 280 represents the indicial response to a deflection in the nose-up direction. On this diagram, time is represented in aerodynamic time, the unit of which is equal to 7.05 seconds. One of the curves indicates the changes in level z.

(c) *Effect of the slope of the trajectory on stability*

An aeroplane may fly at the same speed, that is to say at the same lift coefficient C_{L_0}, on trajectories of different slope γ_0, by the use of different powers. The stability of such motions is not the same.

The term $-C_{D_0}\theta$ in the second equation can be written $+(C_{L_0}\sin\gamma)\theta$. This term always destabilizes the long-period oscillation.

The stability of the aeroplane dealt with in previous examples has been studied for a slope angle $\gamma_0 = 30^o$. The diagrams refer respectively to the initial conditions:

$$\theta_0 = 0.10 \text{ radian (Fig. 76)}$$

$$\alpha_0 = 0.10 \text{ radian (Fig. 77)}$$

and to the step-deflection $\delta_e = 0.10$ radian (Fig. 78)

The phugoid oscillation is unstable.

The angle $\gamma_0 = 30^o$, quite large, has been chosen in order to obtain a striking example, but decrease in stability already appears for much smaller angles γ_0.

To bring an aeroplane on to a climbing trajectory requires the use of extra power. Because of this, the aerodynamic derivatives can be altered. The derivative C_{m_α} has a less negative value at high power than at low power. This is another reason for the destabilization of the motion.

The unfavourable effect due to the inclination of the trajectory may be important in STOL aircraft.

(d) *Gust influence*

An elementary method enabling us to study the effect of gusts consists in introducing the effect of atmospheric velocity disturbances u_a and w_a by writing:

$$-(\Delta C_D)_i = \left(2C_{D_0} + C_{D_u}\right)\frac{u_a}{V} + \left(C_{D_\alpha} - C_{L_0}\right)\frac{w_a}{V} \qquad (10.6)$$

$$-(\Delta C_L)_i = \left(2C_{L_0} + C_{L_u}\right)\frac{u_a}{V} + \left(C_{L_\alpha} + C_{D_0}\right)\frac{w_a}{V} \qquad (10.6)$$

$$(\Delta C_m)_i = -\left(C_{m_u}\right)\frac{u_a}{V} - \left(C_{m_\alpha}\right)\frac{w_a}{V}$$

The analogue set-up is immediate. Voltages representing inputs u_a/V and w_a/V, multiplied by the adequate factor, are introduced by means of supplementary inputs on the adding units (see Fig. 79).

The input is a time function, determined in the problem that we are prepared to solve. We may, in particular, take a step function. In that case, the effect is the same as if we took initial conditions

$$\hat{u} = -\frac{u_a}{V} \qquad \text{and} \qquad \alpha = -\frac{w_a}{V}$$

In Part IV, Figures 325 and 330 represent the result of positive gusts u_a and w_a (i.e. rear gusts and downward gusts) studied in this way. Here again unit τ on the time scale is equal to 7.05 seconds. This way of computing is very crude and does not take into account:

(a) Transient effects;

(b) The fact that the gust w_a is not exerted at the same time on the wings and the tail unit.

Transitory actions are due to Küssner and Wagner effects. We shall see, in Section 11.2.1, how to take them into account.

The fact that the wings and tail unit are not subjected to the action of the gust w_a simultaneously leads us:

(1) To express the aerodynamic action exerted on the wings and that exerted on the tail unit separately;

(2) To introduce a delay equal to l/V_0 seconds in the action of the gust on the tail unit.

An analogue computer output of the action of the gust w_a on an aeroplane, taking this delay into account, is indicated in Section 13.12.

(e) *Response of a fast aeroplane to a step-deflection of the elevator (supersensitivity of elevator)*

Previous examples have emphasised the long-period oscillation. In fact, the rapid oscillation is generally the more important one. It is easy to demonstrate certain consequences of the rapid oscillation by the use of the analogue computer.

In the transonic region, with increasing Mach number, a given manoeuvre of the elevator results in greater and greater transient overshoots of the load factor. This overshooting renders piloting unpleasant and reduces precision.

This phenomenon can be studied quantitatively on the analogue computer by varying the parameters of the problem, such as Mach number, altitude, and position of the centre of gravity.

The increase in Mach number reduces the static margin and the damping. These effects alter the coefficients C_{m_α} and C_{m_q}, and bring with it, at a given altitude, a reduction of the period and of the damping of rapid longitudinal oscillations. The load factor to which the aeroplane is subjected in the manoeuvre receives an increment

$$\Delta_n = \frac{1}{g} V_0 (q - \dot{\alpha}) \tag{10.7}$$

and will be given by another adding unit (see Fig. 80).

Figure 81 represents the load factor at different Mach numbers for a step deflection of the elevator. It appears that the period decreases and the overshoot increases.

Figure 82 shows the variation of dynamic overshoot as a function of Mach number.

(f) *Direct determination of the manoeuvring load on the tail plane*

The manoeuvring load constitutes an important factor in the design calculations of the fuselage and tail structure. It may be calculated directly by adding to the scheme set-up for the equations of motion, the scheme (Fig. 83) corresponding to the following formula:

$$\Delta N_H = \tfrac{1}{2}\rho V^2 S_H \left\{ C_{L_{\alpha,H}} \left[1 - \frac{d\epsilon}{d\alpha} \right] \alpha + \frac{l_H}{V_H} \frac{d\theta}{dt} + \frac{d\epsilon}{d\alpha} \frac{l_H}{V_0} \frac{d\alpha}{dt} + C_{L_{H,\delta_e}} \delta_e \right\} \tag{10.8}$$

We have studied a manoeuvre during which we have applied a rapid triangular deflection with the maximum speed that the control allows, during increments of time Δt.

Figure 84 represents the load on the tailplane for a deflection time of 0.135 second.

Figure 85 represents the loading factor of the whole aeroplane for increasing deflection times. A time equal to 0.135 second brings the wing loading factor to $\Delta n = 8$.

Critical conditions of the manoeuvring load are obtained by scanning in altitude and Mach number.

(g) *The outgoing of airbrake*

The airbrake introduces an additional drag ΔC_D accompanied by a moment ΔC_m. The results are represented in Figure 86 for an aeroplane flying at $M = 0.95$.

We have assumed that:

$$\Delta C_D = 0.05$$

$$\Delta C_z = 0$$

$$\Delta C_m = -0.03,\ 0,\ +0.03$$

We can appreciate the aeroplane's sensibility to the moment induced by the airbrake. Outputs in load factors are rapid and would be difficult to cancel out with the elevator. In this calculation, the output of the simulated airbrake was not instantaneous but lasted for one second.

Airbrakes causing a nose-up pitch are more effective than those causing no moment at all.

10.1.2 Lateral Motion

10.1.2.1 Linearized Equations of Lateral Motion

Equations 1.3.3.b, describing the lateral motion from an initial rectilinear motion of slope $\gamma_0 = \Theta_0$ and lateral inclination Φ_0 zero, simplify to:

$$\left.\begin{aligned} 2\tau \frac{d\beta}{dt} + 2\tau r &= \Delta C_y + \frac{2\tau g}{V_0}\left[\sin\Theta_0\ \psi + \varphi\right] \\ C_{I_x} \frac{dp}{dt} - C_{I_{zx}} \frac{dr}{dt} &= \Delta C_l \\ C_{I_z} \frac{dr}{dt} - C_{I_{zx}} \frac{dp}{dt} &= \Delta C_n \end{aligned}\right\} \qquad (10.9)$$

Let us develop ΔC_y, ΔC_L, ΔC_n in relation to the disturbances of p, r, and β and represent by $(\Delta C_y)_i$, $(\Delta C_l)_i$, $(\Delta C_n)_i$ the actions due to the input being considered; we get:

$$\left.\begin{aligned} &2\tau \frac{d\beta}{dt} - C_{y_\beta}\beta - C_{y_p}\frac{bp}{2V_0} - \left(C_{y_r}\frac{b}{2V_0} - 2\tau\right)r - C_{y_{\dot\beta}}\frac{b}{2V_0}\dot\beta - C_{L_0}\varphi - \\ &\qquad - C_{L_0}\Theta_0\ \psi = (\Delta C_y)_L \\ &C_{I_x}\frac{dp}{dt} - C_{I_{xz}}\frac{dr}{dt} - C_{l_\beta}\beta - C_{l_p}\frac{bp}{2V_0} - C_{l_r}\frac{br}{2V_0} - C_{l_{\dot\beta}}\frac{b}{2V_0}\dot\beta = (\Delta C_l)_i \\ &C_{I_z}\frac{dr}{dt} - C_{I_{xz}}\frac{dp}{dt} - C_{n_\beta}\beta - C_{n_p}\frac{bp}{2V_0} - C_{n_r}\frac{br}{2V_0} - C_{n_{\dot\beta}}\frac{b}{2V_0}\dot\beta = (\Delta C_n)_i \end{aligned}\right\} \qquad (10.10.a)$$

and, with φ, ψ, θ small,

$$\left.\begin{aligned} p = \frac{d\varphi}{dt} \end{aligned}\right\} \qquad (10.10.b)$$

$$r = \frac{d\psi}{dt} \qquad \left.\begin{matrix} \\ \\ \end{matrix}\right\} \qquad (10.10.b)$$

The equations in this form are convenient for studying the stability of small motions but become incorrect when it is desired to study the response to a control displacement of an aeroplane flying under a slope $\gamma \neq 0$. The difficulty arises from the approximation introduced for the component of the gravity force along the Y-axis. In the general case, the exact value of this component is the value mg_y given by formula (2.4). If the angles θ and φ remain small, without ψ necessarily being small, the relations

$$p = \dot{\varphi}, \qquad q = \dot{\theta}, \qquad r = \dot{\psi}$$

remain valid to the second order, but the gravity term must be corrected by replacing the quantity

$$C_{L_0}(\Theta_0\psi + \varphi)$$

by

$$C_{L_0}(\Theta_0 \sin\psi + \varphi)$$

under the hypothesis of an initial motion with zero bank.

10.1.2.2 Setting-Up Scheme

The system is of 5th order when the initial slope $\gamma_0 = \Theta_0$ is different from zero. It is reduced to 4th order when $\Theta_0 = 0$.

Figure 87 represents the set-up for the lateral problem. Orders are introduced in $(\Delta C_y)_i$, $(\Delta C_l)_i$, $(\Delta C_n)_i$ either in step form, or slope function, etc.

Initial conditions are introduced by charging the integrator condensers giving β, p, r, φ, ψ.

10.1.2.3 Examples

(a) *Response to a step input of the ailerons or the rudder*

Inputs $(\Delta C_y)_i$, $(\Delta C_l)_i$, $(\Delta C_n)_i$ are written as functions of the control displacement, as in the case of longitudinal motion.

Figures 209 and 210 represent the indicial response of an aeroplane in a landing configuration.

(b) *Influence of Mach number and altitude on the dynamic stability (frequency and damping)*

Checking of the damping qualities of a prototype in all its flight conditions plays an important part in the study of the aeroplane. Several damping criteria have been established in order to assess flight handling. One of these criteria utilized these

past years required a damping time function of the period. To assess the aeroplane according to this criterion, it was sufficient to solve the characteristic equation without seeking for the aeroplane's response. Nevertheless, application of the previous criterion to several aeroplanes has shown that the simple consideration of the damping as a function of the period is not sufficient. Actually, the necessary damping is expressed in relation to the parameter $(\varphi/\beta \times 1/V)$. The verification of this condition requires the knowledge of the amplitude of the variables φ, β , which involves the determination of the aeroplane's response to external disturbance.

Figure 88 shows this condition applied to a transonic aeroplane.

(c) *Study of the effectiveness of lateral control at low speed*

With many aeroplanes, difficulties of lateral control have arisen near the stall. In some cases the loss of efficiency was a result of wing tip stall and decrease in aileron efficiency at high incidence.

In other cases, in particular on aeroplanes with swept back wings, a considerable loss, if not the total loss, of efficiency has been recorded even when no flow separation occurred. This difficulty can be explained by the modification of the nature of the aeroplane's response to aileron action as the speed decreases progressively.

Aerodynamic derivatives of highly swept back wing and short span aeroplanes undergo important variations with the lift coefficient. Figure 89 is a typical example of the variation of the principal aerodynamic derivatives with lift coefficient. The increase in the derivative C_{l_β} with lift, together with a possible decrease in C_{n_β} in the same conditions, leads to a slightly damped dutch roll. Although at low lifts these oscillations disturb the roll velocity due to aileron action little, they appear at high lifts with great intensity (Fig.90). This phenomenon may lead to an inversion of lateral inclination when associated with inverse yaw.

10.1.3 The Permanent Motion Considered as a Helical Motion (Linear Equations)

The most general trajectory that can be followed in steady motion consists of a helix with vertical axis along which the aeroplane flies at constant speed.

The slope of the trajectory, γ_0 , is equal to the attitude Θ_0 of the aeroplane when the body axes are chosen corresponding to $\alpha_0 = 0$. The components of the vector rotation $\vec{\Omega}$ are:

$$\left.\begin{aligned} P_0 &= -\Omega_0 \sin\Theta_0 \\ Q_0 &= \Omega_0 \cos\Theta_0 \sin\Phi_0 \\ R_0 &= \Omega_0 \cos\Theta_0 \cos\Phi_0 \end{aligned}\right\} \qquad (10.11)$$

Let us re-write the equations with the following substitutions:

Replacing the ΔC_z's and the ΔC_x's by ΔC_L and ΔC_D;

Representing inputs by $(\Delta C_D)_i$ ..... $(\Delta C_n)_i$;

Taking into account gyroscopic effects (terms in C′);

Expanding the aerodynamic coefficients in relation to the variables.

We must, as far as the knowledge of the numerical values permits it, introduce the derivatives of:

$$C_x,\ C_z,\ C_m \qquad (\text{or } C_D,\ C_L,\ \text{and } C_m)$$

with respect to β, p, r; and the derivatives of C_y, C_l, C_n with respect to $\hat{u}$, α, q .

These derivatives, generally not well known, do not appear in the equations written below, but they should be added if known and if it were discovered that they presented noteworthy values:

$$\left.\begin{aligned}
&2\tau\left[\frac{d\hat{u}}{dt} + q_0\alpha - r_0\beta + \frac{q}{V_0}\left(\sin\Phi_0\cos\Theta_0\,\psi - \cos\Phi_0\cos\Theta_0\,\theta\right)\right] + \left(2C_{D_0} + C_{D_{\hat{u}}}\right)\hat{u} + \\
&\qquad + \left(C_{D_\alpha} - C_{L_0}\right)\alpha + C_{D_q}\frac{c}{2V_0}\,q = -(\Delta C_D)_i \\
&2\tau\left[\frac{d\beta}{dt} + r - p_0\alpha + r_0\hat{u} - \frac{q}{V_0}\left(\sin\Theta_0\,\psi + \cos\Phi_0\cos\Theta_0\,\varphi\right)\right] - C_{y_\beta}\beta - C_{y_p}\frac{b}{2V_0}\,p - \\
&\qquad - C_{y_r}\frac{b}{2V_0}\,r - C_{y_{\dot\beta}}\frac{b}{2V_0}\,\dot\beta = (\Delta C_y)_i \\
&2\tau\left[\frac{d\alpha}{dt} - q + p_0\beta - q_0\hat{u} + \frac{q}{V_0}\left(\sin\Theta_0\,\theta + \sin\Phi_0\cos\Theta_0\,\varphi\right)\right] + \left(2C_{L_0} - C_{L_{\hat{u}}}\right)\hat{u} + \\
&\qquad + \left(C_{L_\alpha} + C_{D_0}\right)\alpha + C_{L_q}\frac{c}{2V_0}\,q = -(\Delta C_L)_i \\
&C_{I_x}\frac{dp}{dt} - C_{I_{zx}}\frac{dr}{dt} + \left(C_{I_z} - \frac{c}{b}C_{I_y}\right)(q_0r + r_0q) - C_{I_{xz}}(q_0p + p_0q) - C_{l_\beta}\beta - \\
&\qquad - C_{l_p}\frac{b}{2V_0}\,p - C_{l_r}\frac{b}{2V_0}\,r - C_{l_{\dot\beta}}\frac{b}{2V_0}\,\dot\beta - C_{l_q}q = (\Delta C_l)_i
\end{aligned}\right\} \quad (10.12)$$

$$C_{I_y}\frac{dq}{dt} - \frac{b}{c}\left(C_{I_x} - C_{I_z}\right)(p_0 r + r_0 p) + C_{I_{xz}}\frac{b}{c}(2p_0 p - 2r_0 r) - C_{m_{\hat{u}}}\hat{u} -$$

$$- C_{m_\alpha}\alpha - C_{m_q}\frac{c}{2V_0}q - C_{m_{\dot{\alpha}}}\frac{c}{2V_0}\dot{\alpha} - C'_{m_p}p - C'_{n_r}r = (\Delta C_m)_i \qquad (10.12)$$

$$C_{I_z}\frac{dr}{dt} - C_{I_{zx}}\frac{dp}{dt} + \left(\frac{c}{b}C_{I_y} - C_{I_x}\right)(p_0 q + q_0 p) + C_{I_{xz}}(q_0 r + r_0 q) -$$

$$- C_{n_\beta}\beta - C_{n_p}\frac{bp}{2V_0} - C_{n_r}\frac{b}{2V_0}r - C_{n_{\dot{\beta}}}\frac{b}{2V_0}\dot{\beta} - C'_{n_q}q = (\Delta C_n)_i$$

If we study separately the disturbances of the variables $\hat{u}$, α, q and those of the variables β, p, q , we uncouple the movements: in this case, the evolution of the disturbances affecting the longitudinal motion is defined by equations 1, 3, 5, in which we assume that $\beta = p = r = 0$, whereas the evolution of the disturbances affecting the lateral motion is defined by equations 2, 4, 6, in which we have, furthermore, that $\hat{u} = \alpha = q = 0$.

We can thus study usefully the horizontal turn, in which we have $\Theta_0 = 0$.

A complete study of the real motion in a helical trajectory is not compatible with the hypothesis of the uncoupling of the motions. We must then study simultaneously the six equations of motion (plus the 3 kinematic equations) and note that:

(a) Terms such as the product $(C_{I_x} - C_{I_z})(p_0 r + r_0 p)$, appearing in the 5th equation, introduce an inertia coupling between the longitudinal and the lateral motions.

(b) Derivatives of the aerodynamic forces of one group, in relation to the velocities of the other, are no longer zero and produce an aerodynamic coupling.

10.2 NON-LINEAR PROBLEMS

The main non-linearities in problems dealing with the dynamics of the aeroplane are those due to inertia coupling, to variation of aerodynamic coefficients, and to non-stationary effects.

10.2.1 Inertia Coupling

10.2.1.1 History

For more than thirty years dynamics of flight has been studied by means of linearized equations.

So far as non-linear systems have been concerned, mathematical means as well as the possibilities of calculating machines were extremely restricted. Also, the few comparisons made between the results of linear calculation and of flight tests seemed to show that the study of the linear case was sufficient. But as early as 1945, a

re-examination of the validity of linearization was made, and in 1948 Phillips[27] introduced inertia coupling terms in what is now a classical study on the stability of an aeroplane in uniform rolling motion.

The taking into account of non-linear coupling terms was necessary as a result of the F-100 accidents, which demonstrated that the fin and rudder loads calculated by means of linear equations were incorrect. As a consequence of these accidents, the complete equations of flight dynamics were submitted to a careful study in order to determine which terms should be retained and which neglected. The numerous studies undertaken with this aim required the utilization of digital or analogue computers, the non-linearity of the problem making a quantitative analytical study impossible.

The principal reasons for the growing importance of the coupling terms are:

(a) *Mass distribution*

Ten years ago, the rolling moments of inertia were of the same order of magnitude as the pitching moments of inertia, whereas today the rolling moment of inertia has become smaller.

(b) *Weathercock stability*

On aeroplanes in which the fuselage tends to become larger and larger, weathercock stability is difficult to ensure. This is particularly true in supersonic flight. The instability of the fuselage being independent of Mach number as a first approximation, stabilization due to the fin, proportional to the gradient of the transverse force, decreases as the Mach number increases in supersonic flight. It follows that the coefficient C_{n_β} of weathercock stability decreases as M increases and finally becomes zero.

Furthermore, at high incidence, separation occurs on long fuselages and on low aspect ratio wings, leading generally to a decrease in C_{n_β} (creating also an aerodynamic non-linearity).

(c) *Controllability*

Due to servo-controls, the angular velocities about the three axes have notably increased. The same is true for the terms of coupling proportional to the product of two angular velocities.

(d) *Inclination of the principal axis of inertia*

The inclination of the rolling's principal axis of inertia introduces terms of coupling through the product of inertia.

10.2.1.2 Equation of Problems Involving Inertia Coupling Terms

(a) The linearized systems, written under different forms in (2.20), (3.21) and (3.32), are not precise enough. Terms comprising the products of variables must be kept and the analogue computer must have multipliers.

(b) Inertia coupling produces high angular velocities and significantly increases angles of incidence and side-slip.

The aircraft's security will be put in danger by the increase of load on the tail unit produced by the angular velocities and the angles α and β.

It is therefore better to determine the tail loads at once. These can be obtained by means of the following formulae:

$$\Delta L_M = \tfrac{1}{2}\rho V^2 S_H \left\{ \left(\frac{\partial C_L}{\partial \alpha} \right)_H \left[\left(1 - \frac{d\epsilon}{d\alpha} \right) \alpha + \frac{q l_H}{V} + \frac{d\epsilon}{d\alpha} \frac{l_H}{V} \dot{\alpha} \right] + \left(\frac{\partial l_L}{\partial \delta_e} \right)_H \delta_e \right\} \qquad (10.13)$$

$$\Delta Y_Y = \tfrac{1}{2}\rho V^2 S_V \left\{ \left(\frac{\partial C_Y}{\partial \beta} \right)_V \left[\left(1 - \frac{d\epsilon_v}{d\beta} \right) \beta - \frac{p h_v}{V} + \frac{r l_v}{V} - \frac{d\epsilon_v}{d\beta} \frac{l_v}{V} \dot{\beta} \right] + \left(\frac{\partial C_Y}{\partial \delta_r} \right)_v \delta_r \right\} \qquad (10.14)$$

which complete the system equations.

(c) In the expression for aerodynamic forces, derivatives of forces of one group in relation to the velocities of the other will be introduced every time these derivatives present an adequate numerical value.

Aerodynamic derivatives will be considered in this Section as constants. This is not always a sufficiently good approximation. We shall see later on how more complex aerodynamic factors are introduced.

(d) If calculations or experiments leading to the knowledge of derivatives have determined this in relation to the aerodynamic axes (attached to the relative wind), the derivatives with respect to the dynamic axes must be determined by using the formulae given in Section 3.12.

It is clear that simplifications must be adopted. The most usual are the following:

(i) One is limited to a study of the motion obtained from a rectilinear motion. We thus take $p_0 = q_0 = r_0 = 0$.

(ii) Coupling being due to rapid manoeuvres, we may assume (and verify *a posteriori*) that the critical phase occurs at the beginning of the motion during which the velocity cannot change to any significant extent. We may then neglect the equation obtained by the projection of forces on the X-axis and consider V = constant. (This is not justifiable when the aerodynamic derivatives undergo rapid variations with Mach number, in transonic flight for instance).

(iii) Terms due to gravity are neglected.

The previous simplification has already made the action of gravity disappear in the equilibrium of forces in the direction of GX. The new hypothesis consists in making them disappear also in the equilibrium of forces GY and GZ.

This simplification avoids the calculation of the angles ψ, θ, φ by the integration of kinematic equations, and the introduction of these terms in the equations of

motion. This last operation would require generators of trigonometric functions when the angles become large.

These conventions lead us and other experimenters to reduce the system to:

$$\left.\begin{aligned}
&2\tau\frac{d\beta}{dt} + 2\tau(r - p\alpha) = \Delta C_y \\
&2\tau\frac{d\alpha}{dt} + 2\tau(p\beta - q) = \Delta C_z \\
&C_{I_x}\frac{dp}{dt} - C_{I_{zx}}\frac{dr}{dt} + \left[C_{I_z} - \frac{c}{b}C_{I_x}\right]rq - C_{I_{zx}}pq = \Delta C_l \\
&C_{I_y}\frac{dq}{dt} + \frac{b}{c}\left[C_{I_x} - C_{I_z}\right]pr + \frac{b}{c}C_{I_{xz}}(p^2 - r^2) = \Delta C_m + C'_{m_r}\frac{b}{2V}r \\
&C_{I_z}\frac{dr}{dt} - C_{I_{zx}}\frac{dp}{dt} + \left[\frac{c}{b}C_{I_y} - C_{I_x}\right]pq + C_{I_{zx}}qr = \Delta C_n + C'_{n_q}\frac{c}{2V}q
\end{aligned}\right\} \qquad (10.15)$$

Expressions ΔC_y ..... ΔC_n have to be developed along the lines indicated above.

Terms corresponding to the deflection of the control surfaces can be introduced, either by step signals, ramp signals, etc., or by means of a potentiometer producing voltages varying as the experimenter wishes.

10.2.1.3 Application of Analogue Computers

(a) *Coupling in a rolling pull-out*

Figure 91 represents a wiring diagram for a relatively simple case, namely, one where the derivatives of a group of aerodynamic coefficients with respect to the linear and angular velocities of the other group are zero, and where the remaining derivatives are constant.

Figure 92 represents a wiring diagram for the manoeuvring load on the tail unit.

Let us determine the maximum load on the fin resulting from an aileron deflection during a rolling pull-out (flight with a load factor $n > 1$) .

The flight conditions during which this load is a maximum cannot be foreseen *a priori*. It is therefore necessary to vary the Mach number and altitude to find the critical conditions.

Furthermore, the problem not being a linear one, it is necessary to consider the load factors between the minimum and maximum for the aircraft. The maximum load depends on the type of manoeuvre, particularly on the order in which the roll-pitch or pitch-roll manoeuvre is carried out, on the speed of the manoeuvre and the time elapsed between the initiation of control deflections.

Figure 93 represents the results for a transonic aeroplane, obtained during the research of critical conditions for the fin load. The flight speed considered was 500 kts.

The aeroplane, flying under variable load factors n, has been submitted to an aileron deflection corresponding to the maximum of the force furnished by the servo-control. The diagrams show the side-slip angle β and the three components p, q, r, of the angular velocity.

(b) *Divergence*

As was pointed out in Section 10.2.1.1, coupling manifests itself with intensity in supersonic flight. The drawbacks to it appear either under the form of excessive fin loads, or under the form of incorrect flight qualities (divergence, oscillatory roll, self-roll). Figure 94 shows a case of slow divergence with heavy load factors becoming very rapid under the influence of the coupling.

(c) *Investigation into the influence of the different parameters*

The complexity of coupling phenomena and the non-linearities which produce them do not permit general rules to be deduced or the influence of such or such a parameter to be foreseen in a precise way. We are only trying here to enumerate a few conclusions enabling some order to be got out of the results, conclusions which can, as a whole, be considered as valid for current high-speed aeroplanes.

(c.i) *Influence of mass distribution*

The dominant inertia coupling factor is the term $[(c/b)C_{I_y} - C_{I_x}]pq$ and we have shown, in the introduction, the numerous reasons which tended to increase it: thin wings of short span, a long fuselage heavily loaded.

With a positive pitch velocity, that is to say, with a load factor greater than unity, this term induces a side-slip pulling the nose of the aeroplane towards the outside of the turn. This side-slip tends to restrain the aeroplane's rotation when the equivalent dihedral is positive. With a negative pitch velocity (load factor smaller than unity), this side-slip effect is reversed and the rolling velocity finds itself increased.

(c.ii) *Influence of weathercock stability* C_{n_β}

With a positive load factor, an increase in weathercock stability decreases the side-slip, thus reducing the coupling effects. This is not always so with a negative load factor.

(c.iii) *Influence of* C_{l_β}

If C_{l_β} decreases, it is generally stated that side-slip under a positive load factor increases at high speed, so that the importance of the coupling phenomenon tends to increase. On the other hand, with a negative load factor, the decrease of C_{l_β} tends to reduce the coupling.

(c.iv) *Influence of yawing moment due to aileron deflection*

The inverse yaw, corresponding generally to classical ailerons, is unfavourable to positive load factors, favourable to negative load factors. For a configuration with a spoiler - where the yaw induced is generally direct - the situation is reversed.

(c.v) *Influence of dampers*

The increase of the longitudinal damping coefficient tends to reduce side-slip, thus reducing the influence of coupling phenomena. The increase of lateral damping has little influence and depends on the incidence. There is little to be expected from the use of a yaw damper for the purpose of reducing coupling effects.

(c.vi) *Influence of inclination of principal roll axis of inertia*

The inclination in the dive direction of the principal roll axis of inertia is generally unfavourable, increasing the coupling phenomenon.

(c.vii) *Influence of flight parameters*

For a given aeroplane, there exist an average speed and altitude for which the load on the fin goes through a maximum.

The side-slip due to coupling tends to increase with altitude, since the importance of the aerodynamic terms is reduced in comparison with that of the inertia terms; but the decrease of indicated airspeed, or of dynamic pressure, with altitude, compensates this effect so far as the load on the fin is concerned.

Conversely, side-slip due to coupling tends to decrease when the indicated airspeed increases (effects of losses in directional stability, with Mach number having been put aside), but the load on the tail fin increases with dynamic pressure.

(c.viii) *Influence of the manoeuvre*

Coupling phenomena appear during a pitch-roll evolution, but because of the non-linearity of the phenomenon, the results depend on the type of manoeuvre carried out, on the way the controls are deflected, and on the whole history of the motion.

This is why generally a rough aileron displacement under a load factor does not lead to the same results as an elevator action during a roll. It may be noted also that a simple roll may lead to more important side-slip after a few turns than during the first one. Finally, some divergences may appear which depend on the roughness of the control surface movements.

10.2.2 Aerodynamic Non-Linearities

The problem consists in the calculation of the aeroplane's motion when aerodynamic actions cannot be represented by linear expressions.

10.2.2.1 Approximation by a Polynomial

A coefficient function of a single variable can often be approximated by a polynomial composed of the first two terms of its series (see Section 3.10). We may have:

$$\Delta C_m = C_{m_\alpha}\alpha + \tfrac{1}{2}C_{m_{\alpha^2}}\alpha^2 \qquad (3.58)$$

with $C_{m_{\alpha^2}}$ having a constant value. A multiplier is necessary to calculate the square of α.

A coefficient function of two variables, like C_l as a function of α and β, can be expressed easily in the analogue computer in some particular cases, for instance when the function C_l has the shape represented in Figure 95. In such a case, the two second derivatives $\partial^2 C_l/\partial\alpha^2$ and $\partial^2 C_l/\partial\beta^2$ are zero, and the second derivative $\partial^2 C_l/\partial\alpha\partial\beta$ is a constant.

The increase ΔC_l when passing from a point 1 (α_0, β_0) to a point 2 $(\alpha_0+\alpha, \beta_0+\beta)$ is given by:

$$\Delta C_l = \left(C_{l_\beta}\right)_{\alpha_0}\beta + \left(C_{l_\alpha}\right)_{\beta_0}\alpha + C_{l_{\beta_\alpha}}\alpha\beta \qquad (10.16)$$

In order to calculate the second term, we again need a multiplier.

A control action C_l for instance, depends sometimes in the same way on the incidence; the increase ΔC_l produced by the ailerons may be expressed by:

$$\Delta C_l = \left(C_{l_{\delta_a}}\right)_{\alpha_0}\delta_a + \left(C_{l_\alpha}\right)_{\delta_{a,0}}\alpha + \left(C_{l_{\delta_{a_\alpha}}}\right)^{\delta_a}\alpha \qquad (10.17)$$

When $\beta_0 = \delta_{a,0} = 0$, $(C_{l_\alpha})_{\beta_0} = (C_{l_\alpha})_{\delta_{a,0}} = 0$.

Such functions are often met in the representation of aerodynamic actions coming into problems of inertia couplings, where incidence changes are great.

When a coefficient function of two variables varies in a more complex way, we try to make use of the development indicated in Section 3.10. The carrying out of this development involves three multipliers.

10.2.2.2 Use of Function Generators

When a coefficient function of a simple variable cannot be approximated by a polynomial, the use of a function generator always enables us to calculate the function.

Continuous and non-continuous functions may be approximated as indicated in Section 7.3.6 by diode function generators, supplying non-continuous lines which differ slightly from the exact curve. Furthermore, it is possible to provide these function

generators with supplementary devices which create progressive links between the segments.

A great deal of work has been done in these conditions and we mention here two publications relative to the effect of aerodynamic non-linearities.

(a) *Discontinuous function*

In a theoretical work the N.A.C.A. has studied the rapid motion of an aeroplane about its centre of gravity, defined by the system

$$\left.\begin{aligned} -2\tau \frac{d\alpha}{dt} + 2\tau \frac{\partial\theta}{\partial t} - C_L(\alpha) &= C_{L_\delta}\delta \\ C_{I_y} \frac{d^2\theta}{dt^2} - C_{m_q} \frac{c}{2V_0} \frac{d\theta}{dt} - C_m(\alpha) - C_{m_{\dot\alpha}} \frac{c}{2V} \dot\alpha &= C_{m_\delta}\delta \end{aligned}\right\} \qquad (10.18)$$

in which the functions $C_m(\alpha)$ and $C_L(\alpha)$ are non-linear[8].

Theoretically calculated results have been compared with results obtained on an analogue computer where the functions $C_m(\alpha)$ and $C_L(\alpha)$, represented by a series of segments, were obtained by diodes.

In one of the cases studied, C_m varies with α as indicated in Figure 96.

For $\alpha < -2^\circ$ $\qquad C_{m_\alpha} = -3$

$-2^\circ < \alpha < +2^\circ$ $\qquad C_{m_\alpha} = +1.5$

$+2^\circ < \alpha$ $\qquad C_{m_\alpha} = -3$

and C_{L_α} is constant.

In the zone $-2^\circ < \alpha < +2^\circ$, the stability condition of the rapid oscillation,

$$\frac{\partial C_m}{\partial \alpha} < -\frac{\partial C_L}{\partial \alpha} \frac{\partial C_m}{\partial q} \frac{1}{2\mu} \qquad (10.19)$$

is not satisfied for values attained by the aerodynamic derivatives

$$\frac{\partial C_m}{\partial \alpha} = +3 \qquad \text{and} \qquad \frac{\partial C_m}{\partial q} = -20.43$$

The aeroplane possesses no stable equilibrium position in this zone. On the other hand, the manoeuvre controlled by an increase $\Delta\delta_e$ bringing the equilibrium position from $\alpha = +4^\circ$ to $\alpha = -4^\circ$, leads to stable curves presenting a minimum of anomalies (Fig.97), because the aeroplane remains only a limited time in the zone where the incidence is between -2° and $+2^\circ$.

The analogue computer has shown that this aeroplane can be put into sustained oscillations when it is equipped with an automatic pilot sensitive to attitude (see Section 13.6.7.2).

(b) *Continuous function*

M.Foody (Short Brothers) has studied the effect of a function $C_m(\alpha)$ having the shape represented in Figure 98, in a communication at an analogue computing meeting[9].

Complete equations (including those representing equilibrium along OX) have been set up, but the term $C_m(\alpha)$, that is to say part of ΔC_m due to variations of attack angles introduced in the adding unit calculating dq/dt, was given by a diode function generator, producing a non-continuous line slightly different from the original curve.

If the aeroplane is brought into balance at an incidence α_n for which the curve $C_m(\alpha)$ has a horizontal tangent, it is experienced that the applying of a positive deflection, thus bringing the aeroplane to smaller angles of incidence, gives a stable output, whereas a negative deflection causes the aeroplane to diverge (Fig.99).

If one examines the effect of a small deflection applied to an equilibrium position for an angle of incidence smaller than α_m, at a point on the curve where $C_m(\alpha)$ has not yet become rectilinear, we obtain the usual evolution of the aeroplane, but the diagrams are different inasmuch as the sign of δ_e is different, contrary to the linear case, where the diagrams are symmetrical (Fig.100).

The cases of non-linearities mentioned above are elementary ones. The analogue computer permits the repetition of real phenomena, such as the pitch-up corresponding to a $C_m(\alpha)$ function as in Figure 14.

10.2.2.3 Non-Linearity Combinations

10.2.2.3.1 Longitudinal motion of a short-take-off aeroplane. The stability and control of slow-speed aeroplanes give rise to particular problems due to the non-linearity of the equations of motion.

In the case of an aeroplane where the propeller slip stream influence on the wing plays an important part in the formation of lift, the aerodynamic reactions may no longer be expressed as linear functions of the variables α, u, q and the control deflection δ_e.

It is necessary to consider the propeller pitch Φ as a new variable. This pitch itself depends on the manifold pressure δ_m and the speed V ; it is determined by the 4th equation of the set given below.

The effect of the slip-stream will be expressed by terms including ϕ. On the other hand, non-linearities coming into the formation of the aerodynamic efforts must be taken into account.

In a particular case, the system was the following:

$$
\left.
\begin{aligned}
&\dot{u} + a_1 u - b_1 \alpha + d_1 \theta - l_1 \Phi + A_1 u^2 + B_1 \alpha^2 + H_1 \alpha_1 u = 0 \\
&\dot{\alpha} + a_2 u + b_2 \alpha - c_2 q + d_2 \theta + e_2 \Phi + H_2 \alpha u + A_2 u^2 = k_2 \delta_e \\
&\dot{q} - a_3 u + b_3 \alpha + c_3 q + e_3 \Phi + A_3 u^2 + H_3 \alpha u - L_3 \alpha \Phi - M_3 u \Phi + N_3 \Phi^2 = k_3 \delta_e \\
&\Phi - a_4 u = h_4 \delta_m \\
&\dot{\theta} = q
\end{aligned}
\right\} \qquad (10.20)
$$

(Note: the signs are chosen ± so as to keep the coefficients themselves positive). Besides this, there was a maximum in the term $b_2\alpha$, corresponding to a maximum value of the lift coefficient, and a sharp change in inclination of the C_m versus α curve, for a given value of α_c.

The term $B_1\alpha^2$ is due to the curvature of the polar; the terms A_1u^2, A_2u^2, A_3u^2 are due to the fact that we have not neglected the term u^2 compared with the term $2u_0u$, in view of the low value that u_0 may reach.

In evolutions at constant power:

$$\Phi = a_4 u$$

which enables the system to be simplified.

It is obvious that the resolution of the system requires the use of:

Multipliers giving six products or squares of variables;

A voltage limiting device on the term $b_2\alpha$;

An extra input $b_3(\alpha - \alpha_c)$ coming into action at incidence α_c, in order to produce at that moment an increase of C_{m_α}.

A wiring diagram is shown in Figure 101. As the load factor n is one of the quantities of which we wish to know the evolution, we must calculate first:

$$n = U_0(\dot{\theta} - \dot{\alpha}) \frac{1}{g}$$

The diagrams in Figures 102 and 103 represent the response to a step deflection δ_e of 2° in the nose-up direction, for a take-off and a cruising configuration respectively. It is well known that the phugoid period is related to the speed. In the case of flight study at take-off speed, a phugoid of a particularly small period appears (of the order of 5 or 6 seconds). The pilot could be embarrassed by this phugoid if he wished to carry out a steady flight at take-off speed but does not encounter this possible difficulty if he accelerates rapidly, which is normal after take-off. In cruising flight, the phugoid period is greater. The input considered, viz. 2° of deflection, is relatively much more effective at cruising speed than at take-off speed. This explains why the variation in amplitude of θ and u is greater.

Improvements have been brought about in these trajectories by the use of automatic controls (see Section 13.9.3.2). The set-up permits the study of the effect of engine power variations, δ_m ; no result of such experiment is indicated here.

10.2.2.3.2 Spin simulation. Motion in a spin comprises both the types of non-linearities which we have been considering:

Inertia coupling due to the importance of rotational velocities;

Non-linearity of aerodynamic coefficients due to high incidences and rates of rotation.

The source of the aerodynamic data to be used in these calculations is the roll balance which permits the measurement of the six coefficients C_x ..... C_n to be taken while the aeroplane is rolling about an axis parallel to the wind, at a rate of rotation

$$\omega = \frac{\Omega b}{2V}$$

with

$$\Omega^2 = P^2 + Q^2 + R^2$$

The motion of the aeroplane in a spin is necessarily defined by the equations of the set (2.13), which we rewrite here introducing gravity defined by the direction cosines of the vertical, and assuming that the products of inertia are zero:

$$\left.\begin{aligned}
m\left[\frac{dU}{dt} + QW - RV - gl_3\right] &= C_x \, S\tfrac{1}{2}\rho V^2 \\
m\left[\frac{dV}{dt} + RU - PW - gm_3\right] &= C_y \, S\tfrac{1}{2}\rho V^2 \\
m\left[\frac{dW}{dt} + PV - QU - gn_3\right] &= C_z \, S\tfrac{1}{2}\rho V^2 \\
I_x \frac{dP}{dt} + [I_z - I_y]QR &= C_l \, Sb\tfrac{1}{2}\rho V^2 \\
I_y \frac{dQ}{dt} + [I_x - I_z]RP &= C_m \, Sc\tfrac{1}{2}\rho V^2 \\
I_z \frac{dR}{dt} + [I_y - I_x]PQ &= C_n \, Sb\tfrac{1}{2}\rho V^2
\end{aligned}\right\} \qquad (10.21)$$

The N.A.C.A. tried to resolve these equations by means of an analogue computer in order to study the recovery of a completely established spin. With this aim, work was done with the above system of equations not transformed by linearization[10].

The method used included several simplifying hypotheses. It appears interesting or us to examine here the conditions in which the problem may be approached.

The spin studied, supposed right-handed, was a stationary motion for known values f the variables:

α = 46 degrees

β = - 3.4 degrees

u_0 = 149.5 ft/sec = 45.6 m/sec

v_0 = 12.97 ft/sec = 3.96 m/sec

w_0 = 155 ft/sec = 47.45 m/sec

V_0 = 216 ft/sec = 66 m/sec

P_0 = 1.508 rad/sec

Q_0 = 0.0152 rad/sec

R_0 = 1.5610 rad/sec

$\Omega = \sqrt{P^2 + Q^2 + R^2}$

Θ_0 = - 44 degrees

Φ_0 = + 0.56 degree

The following deflections secured equilibrium:

δ_e = - 20° (nose-up)

δ_a = + 14° (ailerons opposite to the spin)

δ_r = - 30° (ailerons with the spin)

Aerodynamic measurements, obtained on a roll balance whose velocity of rotation was $\omega_0 = \Omega_0 b/2V_0$ were available. For this velocity of rotation factors C_x , C_z , C_m were known in an interval of incidences extending from $\alpha = 0$ to $\alpha = 70°$. It was assumed that these factors were independent of side-slip.

On the other hand, C_y , C_l , C_n were measured in the same interval of incidence; it is stated that these results were dependent both on incidence and on side-slip.

Although the factors C_x ..... C_n depend on the three elementary rotations P , Q , R and necessarily vary with them, these variations have not been taken into account, and the path of spin recovery was calculated by introducing the C_x's ..... C_n's determined experimentally for only one rotational velocity.

On the other hand, the factor V^2 appearing in the expression for the forces and aerodynamic moments was supposed constant and equal to V_0^2 .

The integration of the equations was carried out taking account of the evolution of the gravity projections. For this purpose, direction cosines were determined by integration of the following equations:

$$\left.\begin{aligned} l_3 &= l_{3,0} + \int \dot{l}_3 \, dt \\ m_3 &= m_{3,0} + \int \dot{m}_3 \, dt \\ n_3 &= n_{3,0} + \int \dot{n}_4 \, dt \end{aligned}\right\} \qquad (10.22)$$

with

$$\left.\begin{aligned} l_{3,0} &= -\sin\Theta_0 \\ m_{3,0} &= +\sin\Phi_0 \cos\Theta_0 \\ n_{3,0} &= +\cos\Phi_0 \cos\Theta_0 \end{aligned}\right\} \qquad (10.23)$$

and

$$\left.\begin{aligned} \dot{l}_3 &= m_3 r - n_3 q \\ \dot{m}_3 &= n_3 p - l_3 r \\ \dot{n}_3 &= l_3 q - m_3 p \end{aligned}\right\} \qquad (10.24)$$

The angles of incidence α and β have been obtained from the following relations:

$$\mathrm{tn}\alpha = \frac{W}{U}$$

$$\mathrm{tn}\beta = \frac{V}{U}$$

The report published gives no indication of the apparatus used in order to express C_y , C_l , C_n in terms of α and β .

The wiring of the analogue computer being consistent with the set of equations indicated above, the computer was at rest for the initial values.

Voltages representing either:

Moments of roll or yaw, or

A force exerted along the thrust line,

have been applied and the response observed.

The motions obtained are indicated in the Reference. We shall limit ourselves here to considering the evolution due to the application of a yawing moment $\Delta C_n = -0.01$ opposed to the spin. This evolution describes recovery from a spin and is shown in Figure 104.

We must mention this work here because it very clearly defines the limits of analogue computing.

If measurements of C_x ..... C_n, by means of the roll balance, corresponding to angular velocities ω different from ω_0 had been available, one should have calculated the variable ω and expressed certain aerodynamic factors as functions of the quantities α, β and ω.

These calculations were discarded in the work mentioned above. The possibility of simulating a spin more accurately exists, but it depends on what means are available, and more precisely on the possibility of simulating functions of three or more variables.

10.2.3 Non-Stationary Aerodynamic Actions

When taking non-stationary actions into account, the aerodynamic coefficients multiplying α, $\dot{\alpha}$, etc., become also functions of the variable t. The most important cases to consider are:

A constant delay in the appearance of an aerodynamic effect;

A delay represented by the function of Küssner and Wagner.

10.2.3.1 Constant Delay in the Appearance of an Aerodynamic Effect

The example described below represents a problem different from those we have dealt with up to now. Having obtained, by flight tests, a given result, the analogue computer was set to work to try and discover the magnitude of a coefficient, or the slope of a function which, placed in the equations, reproduces in the computer the curve obtained experimentally.

Flight tests of an aeroplane flying at an incidence α_0 considerably greater than the angle of maximum lift had enabled the Cornell Aeronautical Laboratory to study, in 1949, the indicial response of an aeroplane for step displacements δ_e, in both directions[11,12].

Outputs in α, θ and acceleration $n = 1 + V\dot{\gamma}/g$ were measured during these tests. The corresponding curves are shown in Figures 106 and 107. Later, it was found impossible to reproduce, by calculation, the diagrams obtained during flight; the true curve $\dot{\gamma}$ was always delayed in relation to the calculated curve.

This suggested that the effects produced *on the wing* by a variable incidence $\alpha(t)$ were in fact produced by a fictitious incidence $\alpha_1(t)$ related to α by the relation

$$\alpha_1(t) = \alpha(t - a)$$

in which a defines a constant delay.

In order to prove this hypothesis on the analogue computer, the factor C_m had to be split up into two parts representing respectively the part due to the wing and that due to the tail, and the quantity $C_{m_{\dot{\alpha}}}\alpha$ replaced by $(C_{m_\alpha})_p\alpha_1 + (C_{m_\alpha})_e\alpha$. Furthermore the following terms were also replaced:

$$C_{L_\alpha}\alpha \quad \text{by} \quad C_{L_\alpha}\alpha_1$$

$$C_{m_{\dot{\alpha}}}\dot{\alpha} \quad \text{by} \quad C_{m_{\dot{\alpha}}}\dot{\alpha}_1$$

and the function $\alpha_1(t)$ simulated.

The equations of motion of the aeroplane about its centre of gravity were represented by the system:

$$\left.\begin{aligned} 2\tau\dot{\gamma} &= 2\tau(\dot{\alpha} - \dot{\theta}) = C_{L_\alpha}\alpha_1 + C_{L_{\delta_e}}\delta_e \\ C_{I_y}\ddot{\theta} &= (C_{m_\alpha})_p\alpha_1 + (C_{m_\alpha})_e\alpha + C_{m_q}\frac{c}{2V}q + C_{m_{\dot{\alpha}}}\frac{c}{2V}\dot{\alpha}_1 + C_{m_{\delta_e}}\delta_e \end{aligned}\right\} \qquad (10.25)$$

Amongst the different possible ways of defining a function α_1 delayed in relation to α the following relation was chosen:

$$\alpha_1 + \frac{a}{2}\dot{\alpha}_1 = \alpha - \frac{a}{2}\dot{\alpha} \qquad (10.26)$$

The set-up on the analogue computer representing the system is shown in Figure 105.

The results have led to closer agreement between the curve of γ calculated by taking this delay into account and the experimental curve (see Figures 106 and 107).

The reasons which gave rise to the use of the previous relation between α and α_1 result from the following:

The function $\alpha_1(t) = \alpha(t - a)$

can be developed:

$$\alpha_1(t) = \alpha(t) - a\dot{\alpha}(t) + \frac{a^2}{2}\ddot{\alpha}(t)$$

while the equivalent relation $\alpha_1(t + a) = \alpha(t)$

gives

$$\alpha_1(t) + a\dot{\alpha}_1(t) + \frac{a^2}{2}\ddot{\alpha}_1(t) = \alpha(t)$$

Approximating to the development to the first term gives respectively:

$$\alpha_1 = \alpha - a\dot{\alpha}$$

$$\alpha_1 + a\dot{\alpha}_1 = \alpha$$

Depending on the expression used, errors are either in one direction or the other, but they cancel out partially when the average is used:

$$\alpha_1 + \frac{a}{2}\dot{\alpha}_1 = \alpha - \frac{a}{2}\dot{\alpha} \tag{10.27}$$

A study of the error due to this approximation appears in the Reference.

10.2.3.2 Non-Stationary Aerodynamic Effects

Non-stationary effects which go together with the appearance of lift at incidences less than the incidence corresponding to maximum lift, are defined by Wagner and Küssner functions.

Wagner's function defines the variation of an aerofoil's lift in relation to time for a step unit variation α of angle of attack. Küssner's function defines the variation of an aerofoil's lift as a function of time for a step unit gust w_a.

Let: $\Phi(t)$ and $\Psi(t)$ be these functions.

The lift produced by a step unit input of α or w_a is therefore a function of time:

$$C_L(t) = \frac{\partial C_L}{\partial \alpha}\,\Phi(t)\,\alpha \tag{10.28}$$

$$C_L(t) = \frac{1}{V}\frac{\partial C_L}{\partial \alpha}\,\Psi(t)\,w_a \tag{10.29}$$

where factors $\Phi(t)$ and $\Psi(t)$ may be represented approximately.

$$\Phi(t) = 0.5 + 0.165(1 - e^{-at}) + 0.335(1 - e^{-bt}) \tag{10.30}$$

$$\Psi(t) = 0.5(1 - e^{-ct}) + 0.5(1 - e^{-dt}) \tag{10.31}$$

with

$$a = 0.0455 \times \frac{2V_0}{c}$$

$$b = 0.3 \times \frac{2V_0}{c}$$

$$c = 0.13 \times \frac{2V_0}{c}$$

$$d = \frac{2V_0}{c}$$

The lift produced at any instant by a variation of incidence $\alpha(t)$ or by a gust $w_a(t)$, varying with time, is given by Duhamel's integral:

$$C_L(t) = \frac{\partial C_L}{\partial \alpha}\left[\int_0^t \dot{\alpha}(\tau)\ \Phi(t - \tau)\ d\tau + \alpha(o)\ \Phi(t)\right] \tag{10.32}$$

$$C_L(t) = \frac{1}{V_0}\frac{\partial C_L}{\partial \alpha}\left[\int_0^t \dot{w}_a(\tau)\ \Psi(t - \tau)\ d\tau + w_a(o)\ \Psi(t)\right] \tag{10.33}$$

These expressions can be written in a more simple form when we change to Laplace transforms.

The transforms of the function Φ and Ψ are:

$$\Phi(s) = \frac{1}{s}\left[0.5 + 0.165\ \frac{a}{s + a} + 0.335\ \frac{b}{s + b}\right] \tag{10.34}$$

$$\Psi(s) = \frac{1}{s}\left[0.5\ \frac{c}{s + c} + 0.5\ \frac{d}{s + d}\right] \tag{10.35}$$

The transforms of Equations (10.32) and (10.33) become:

$$C_L(s) = \frac{\partial C_L}{\partial \alpha}\ s\ \alpha(s)\ \Phi(s) \tag{10.36}$$

$$C_L(s) = \frac{1}{V_0}\frac{\partial C_L}{\partial \alpha}\ s\ w_a(s)\ \Psi(s) \tag{10.37}$$

The corresponding transfer function will be:

$$G_1(s) = \frac{C_L(s)}{\alpha(s)} = \frac{\partial C_L}{\partial \alpha}\left[0.5 + 0.165\ \frac{a}{s + a} + 0.335\ \frac{b}{s + b}\right] \tag{10.38}$$

$$G_2(s) = \frac{C_L(s)}{w_a(s)} = \frac{1}{V_0}\frac{\partial C_L}{\partial \alpha}\left[0.5\ \frac{c}{s + c} + 0.5\ \frac{d}{s + d}\right] \tag{10.39}$$

Computer elements having these transfer functions will simulate Equations (10.32) and (10.33).

Transient effects which accompany the determination of lift are of very short duration. They are important only if their own periods of motion are very small.

This is not the case when the motion of the rigid aeroplane is studied, but it may occur if we take into account elastic deformations.

Wagner's and Küssner's functions come into the phenomena bringing structural deformations into the action; a problem making use of these functions is studied in Section 11.2.

CHAPTER 11

MOTION OF A NON-RIGID AIRCRAFT

J.Czinczenheim

11.1 SUPPLEMENTARY DEGREES OF FREEDOM. THEIR REPRESENTATION ON THE COMPUTER

As was established in Section 1.4.2, the motion of a non-rigid aircraft is determined by adding to the degrees of freedom for the rigid aeroplane, supplementary degrees of freedom, depending on the modes of deformation and the generalized coordinates. The choice of the supplementary degrees of freedom will be determined by the physical nature of the problem to be solved, and must be made carefully. It may happen that, after a first study, new degrees of freedom may have to be added in order to improve the precision.

The set-up of the computer for this problem will be made as in the case of a rigid aeroplane. Every equation defining a generalized coordinate involves the presence of a loop, whose entries are the generalized coordinates, their derivatives, and other variables that exert, by coupling, an action on the generalized coordinates.

11.2 SOME PARTICULAR CASES

11.2.1 Combination of a Gust with the First Mode of Wing Bending

It is desired to find the aircraft motion for gusts of different shape, and to predict the maximum load factor. In the example to be considered the aircraft is fitted with wing tip tanks, and it is required to study the influence of these tanks on the wing deformation, under the action of a gust.

The gust chosen is defined by the vertical velocity w_a of the ambient air; it is represented by an isosceles triangle, the base of which is proportional to the duration of the gust, and whose height is the maximum velocity of the gust.

Such a gust produces principally a vertical translation of the whole aircraft and a bending of the wing. It can be assumed that motion in pitch and higher order wing deformations are negligible.

The degrees of freedom used will be the vertical velocity w_{G_0} of the centre of gravity, and the fundamental mode of wing bending, characterized by a mode $\zeta_f(y)$ and a generalized coordinate $q_f(t)$.

It is assumed that the aircraft responses are so fast that it is necessary to take account of non-stationary effects.

11.2.1.1 Equations of Motion

The equations of motion are obtained by applying (4.34) and (4.36). They are:

$$M\left(\dot{w}_{G_0} + \zeta_f^0 \ddot{q}_f\right) = Z_{\mu}\mu \tag{11.1}$$

$$M\zeta^0 \dot{w}_{G_0} + m(\ddot{q}_f + \Omega^2 q_f) = Q_{\mu}\mu \tag{11.2}$$

M .being the mass of the aeroplane and m the generalized mass ($= \int \zeta^2 \, dm$) .

If the deformation mode used is the free symmetrical wing bending mode,

$$M\zeta^0 = \int \zeta \, dm = 0$$

and the two degrees of freedom are not inertially coupled.

The aerodynamic forces are defined by:

$$Z_{\mu}\mu = Z_{w_{G_0}} w_{G_0} + Z_{q_f} q_f + Z_a \tag{11.3}$$

$$Q_{\mu}\mu = Q_{w_{G_0}} w_{G_0} + Q_{q_f} q_f + Q_a \tag{11.4}$$

where:

Z_a = force produced by gust

$Z_{q_f} = \int p_{q_f} \, d\sigma$

$Z_w = \int p_w \, d\sigma$

$Z_a = \int p_a \, d\sigma$

Q_a = bending moment produced by gust

$Q_{q_f} = \int p_{q_f} \zeta \, d\sigma$

$Q_w = \int p_w \zeta \, d\sigma$

$Q_a = \int p_a \zeta \, d\sigma$

These quantities will be determined as functions of the angle of attack. The variation of angle of attack during the time interval τ , $\tau+d\tau$ on an element of wing span dy is

$$\frac{\dot{w}_{G_0} + \zeta \ddot{q}_f}{V_0} \, d\tau$$

The corresponding reaction dZ at time t will be:

$$dZ = \tfrac{1}{2}\rho V_0^2 c \, dy \, \frac{dC_z}{d\alpha}\left[\frac{\dot{w}_{G_0}(\tau) + \zeta \ddot{q}_f(\tau)}{V_0} \, d\tau \, \Phi(t - \tau)\right] \tag{11.5}$$

and, taking into account the angle of attack variations between times 0 and t ,

$$dZ = \tfrac{1}{2}\rho V_0 c\, dy \frac{dC_z}{d\alpha}\int_0^t \left[\dot{w}_{G_0}(\tau) + \zeta \ddot{q}_f(\tau)\right] \Phi(t - \tau)\, d\tau \tag{11.6}$$

Integrating over the whole wing, we have

$$Z_w w + Z_{q_f} q_f = \tfrac{1}{2}\rho V_0 S \frac{dC_z}{d\alpha} \int_0^t \left[\dot{w}_{G_0}(\tau) + \Gamma_1 \ddot{q}_f(\tau)\right] \Phi(t - \tau)\, d\tau \tag{11.7}$$

where

$$\Gamma_1 = \frac{\int \zeta c\, dy}{S} \tag{11.8}$$

By similar reasoning, we obtain

$$Q_w w + Q_{q_f} q_f = \tfrac{1}{2}\rho V_0 S \frac{dC_z}{d\alpha} \int_0^t \Gamma_1 \left[\dot{w}_{G_0}(\tau) + \Gamma_2 \ddot{q}_f(\tau)\right] \Phi(t - \tau)\, d\tau \tag{11.9}$$

where

$$\Gamma_2 = \frac{\int \zeta^2 c\, dy}{\Gamma_1} \tag{11.10}$$

The force Z_a and the bending moment Q_a produced by the gust are expressed as follows:

$$Z_a = \tfrac{1}{2}\rho V_0 S \frac{dC_z}{d\alpha} \int_0^t \dot{w}_a(\tau)\, \Psi(t - \tau)\, d\tau \tag{11.11}$$

$$Q_a = \tfrac{1}{2}\rho V_0 S \frac{dC_z}{d\alpha} \int_0^t \Gamma_1 \dot{w}_a(\tau)\, \Psi(t - \tau)\, d\tau \tag{11.12}$$

Combining the preceding results, we may write:

$$\lambda \dot{w}_{G_0} = \int_0^t \left[\dot{w}_G(\tau) + \Gamma_1 \ddot{q}_f(\tau)\right] \Phi(t - \tau)\, d\tau + \int_0^t \dot{w}_a(\tau)\, \Psi(t - \tau)\, d\tau \tag{11.13}$$

$$l(\ddot{q}_f + \Omega^2 q_f) = \int_0^t \left[\dot{w}_G(\tau) + \Gamma_2 \ddot{q}_f(\tau)\right] \Phi(t - \tau)\, d\tau + \int_0^t \dot{w}_a(\tau)\, \Psi(t - \tau) d\tau \tag{11.14}$$

where

$$\lambda = \frac{2M}{\rho V_0 S \dfrac{dC_z}{d\alpha}} \tag{11.15}$$

and

$$l = \frac{m}{\rho V_0 S \Gamma_1 \dfrac{dC_z}{d\alpha}} \tag{11.16}$$

11.2.1.2 Passing to the Transforms

Let us now write the same equations using the Laplace transformation. Let

$w_a(s)$	be	the	Laplace	transform	of	$w_a(t)$
$w_{G_0}(s)$	"	"	"	"	"	$w_{G_0}(t)$
$q_f(s)$	"	"	"	"	"	$q_f(t)$
$\Phi(s)$	"	"	"	"	"	$\Phi(t)$
$\Psi(s)$	"	"	"	"	"	$\Psi(t)$

Let us put

$$w_{G_0}(s) + \Gamma_1 s q_f(s) = A_1(s) \tag{11.17}$$

$$w_{G_0}(s) + \Gamma_2 s q_f(s) = A_2(s) \tag{11.18}$$

The preceding equations will be written:

$$\lambda s w_{G_0}(s) = sA_1(s)\,\Phi(s) + sw_a(s)\,\Psi(s) \tag{11.19}$$

$$l\left[s^2 q_f(s) + \Omega^2 q_f(s)\right] = sA_2(s)\,\Phi(s) + sw_a(s)\,\Psi(s) \tag{11.20}$$

The functions $\Phi(s)$ and $\Psi(s)$ are known (formulae 10.34 and 10.35) and one has to solve two equations relating the gust velocity input $w_a(s)$ and the two outputs: wing tip deflection $q_f(s)$, and centre of gravity displacement speed $w_{G_0}(s)$, both inputs and outputs being expressed as Laplace transforms:

$$s\lambda w_{G_0}(s) = A_1(s)\left[0.5 + 0.165\,\frac{a}{s+a} + 0.335\,\frac{b}{s+b}\right] + w_a(s)\left[0.5\,\frac{c}{s+c} + 0.5\,\frac{d}{s+d}\right] \tag{11.21}$$

$$l\left[s^2 q_f(s) + \Omega^2 q_f(s)\right] = A_2(s)\left[0.5 + 0.165\,\frac{a}{s+a} + 0.335\,\frac{b}{s+b}\right] + \\ + w_a(s)\left[0.5\,\frac{c}{s+c} + 0.5\,\frac{d}{s+d}\right] \qquad (11.22)$$

The given data (mass and wing flexibility) are included in the parameters λ , l , Ω .

The patching diagram (described in Fig.108) permits the resolution of these equations. It should be recalled that the computing element, represented in Figure 60a, gives the transfer function $a/(s + a)$ when $1/a = RC$.

As a result of the properties of analogue computer elements simulating a transfer function, any input simulating a time variation of the gust velocity will produce outputs corresponding to the time variation of the input.

11.2.1.3 Results

Figure 109 represents a record obtained in a particular case. During the study of the problem, the variables were the aeroplane mass, the weight of the tip tanks, and the duration of the gust. More than a hundred combinations were tested in order to find the critical cases.

For each aeroplane weight, a set of curves has been established giving the total deflection at the wing tip for different tank weights and gust durations. Figure 110 shows such a set.

11.2.2 Influence of Wing Torsional Rigidity on Aileron Effectiveness

The loss of aileron effectiveness due to torsional deformation of the wing is a well known phenomenon. Until now its study generally involved only the static aspect of the problem. With thin and relatively heavy wings, the dynamic phenomenon assumes some importance in rapid manoeuvres where inertia reactions may alter the initial response produced by a sudden aileron deflection.

11.2.2.1 Equations of Motion

The wing deflection will be represented by two generalized coordinates. The first describes the torsional fundamental mode and is a good approximation at the beginning of the manoeuvre when the inertia forces are predominant. The second describes the wing static deformation under the action of the aerodynamic forces produced by the aileron deflection, and gives a satisfactory approximation for a steady motion in roll. The combination of the two deformations gives satisfactory precision in the study of the whole manoeuvre.

The degrees of freedom considered will be:

(1) For the airframe motion, the angular velocity in roll, p ;

(2) For the wing deformation, the fundamental antisymmetric torsion mode

$$\zeta_t(x,y) = -\theta_t(y)\,(x - x_e)$$

with generalized coordinate q_t, and the static deformation produced by the action of the aerodynamic forces due to aileron deflection:

$$\zeta_s(x,y) = -\theta_s(y)\,(x - x_e)$$

with generalized coordinate q_s.

By application of the general method (described in Section 4.2) we obtain the equations:

$$\left.\begin{aligned}
&I_x\dot{p} + k_{x_t}\ddot{q}_t + k_{x_s}\ddot{q}_s \\
&\qquad = L_p p + L_{q_t} q_t + L_{q_s} q_s + L_{\dot{q}_t}\dot{q}_t + L_{\dot{q}_s}\dot{q}_s + L_{\delta_a}\delta_a \\
&k_{x_t}\dot{p} + m_{tt}\ddot{q}_t + m_{ts}\ddot{q}_s \\
&\qquad = Q_{t_p} p + \left(Q_{t_{q_t}} - a_{11}\right) q_t + \left(Q_{t_{q_s}} - a_{12}\right) q_s + \\
&\qquad\qquad + Q_{t_{\dot{q}_t}}\dot{q}_t + Q_{t_{\dot{q}_s}}\dot{q}_s + Q_{t_{\delta_a}}\delta_a \\
&k_{x_s}\dot{p} + m_{st}\ddot{q}_t + m_{ss}\ddot{q}_s \\
&\qquad = Q_{s_p} p + \left(Q_{s_{q_t}} - a_{21}\right) q_t + \left(Q_{s_{q_s}} - a_{22}\right) q_s + \\
&\qquad\qquad + Q_{s_{\dot{q}_t}}\dot{q}_t + Q_{s_{\dot{q}_s}}\dot{q}_s + Q_{s_{\delta_a}}\delta_a
\end{aligned}\right\} \qquad (11.23)$$

The coefficients of these equations have the following values:

$$\left.\begin{aligned}
k_{x_t} &= \int y_0 \zeta_t \, dm = -\int_y \theta_t y_0 (x - x_e) \frac{dm}{dy}\, dy \\
k_{x_s} &= \int y_0 \zeta_s \, dm = -\int_y y_0 (x - x_e) \frac{dm}{dy}\, dy \\
m_{tt} &= \int \zeta_t^2 \, dm = \int \theta_t^2 (x - x_e)^2 \, dm \\
m_{ts} &= m_{st} = \int \theta_{st}\theta_{ts} (x - x_e)^2 \, dm \\
m_{ss} &= \int \zeta_s^2 \, dm = \int \theta_s^2 (x - x_e)^2 \, dm
\end{aligned}\right\} \qquad (11.24)$$

The quantities a_{11}, $a_{12} = a_{21}$, a_{22} are the coefficients obtained from the virtual work of the elastic forces:

$$L_p = -\int p_p y_0 \, d\sigma$$

$$L_{q_t} = -\int p_{q_t} y_0 \, d\sigma$$

$$L_{\delta_a} = -\int p_{\delta_a} y_0 \, d\sigma$$

$$Q_{t_p} = -\int p_p \zeta_t \, d\sigma = \int p_p \theta_t (x-x_e) d\sigma = \int dy \theta_t \int p_p (x_g-x_e) dx$$

$$Q_{t_{q_t}} = -\int p_{q_t} \zeta_t \, d\sigma = \int p_{q_t} \theta_t (x-x_e) d\sigma = \int dy \theta_t \int p_{q_t} (x_g-x_e) dx$$

$$Q_{t_{q_s}} = -\int p_{q_s} \zeta_t \, d\sigma = \int p_{q_s} \theta_t (x-x_e) d\sigma = \int dy \theta_t \int p_{q_s} (x_g-x_e) dx$$

$$Q_{t_{\delta_a}} = -\int p_{\delta_a} \zeta_t \, d\sigma = \int p_{\delta_a} \theta_t (x-x_e) d\sigma = \int dy \theta_t \int p_{\delta_a} (x_g-x_e) dx$$

$$Q_{s_p} = -\int p_p \zeta_s \, d\sigma = \int p_p \theta_t (x-x_e) d\sigma = \int dy \theta_s \int p_p (x_g-x_e) dx$$

$$Q_{s_{q_t}} = -\int p_{q_t} \zeta_s \, d\sigma = \int p_{q_t} \theta_t (x-x_e) d\sigma = \int dy \theta_s \int p_{q_t} (x_g-x_e) dx$$

$$Q_{s_{q_s}} = -\int p_{q_s} \zeta_s \, d\sigma = \int p_{q_s} \theta_t (x-x_e) d\sigma = \int dy \theta_s \int p_{q_s} (x_g-x_e) dx$$

$$Q_{s_{\delta_a}} = -\int p_{\delta_a} \zeta_s \, d\sigma = \int p_{\delta_a} \theta_t (x-x_e) d\sigma = \int dy \theta_s \int p_{\delta_a} (x_g-x_e) dx$$

11.2.2.2 Set-Up

Figure 111 represents the set-up of an analogue computer for the preceding equations.

The calculations may be generalized and would permit the finding of the set-up representing the aeroelastic effects in the more general case, either for longitudinal or for lateral motion. The capacity of the computer may, nevertheless, limit theoretical possibilities.

11.2.2.3 Discussion of the Results

The results obtained with the analogue computer show the inertial effects during the non-steady phase of the motion, and the loss of aileron efficiency during the steady phase.

For an unswept wing, which is the only case covered by the preceding equations, it is found that the non-steady phase depends on the respective positions of the centre of torsion, the centre of gravity, and the secondary focus.

Figure 112 represents a recorded example of a response to aileron deflection.

11.2.2.4 Other Problems

The general method described in Section 4.2.2 is applicable in numerous cases. Only the most important ones are mentioned here:

(a) Influence of fuselage flexibility on the elevator or rudder control;

(b) Influence of torsional rigidity of the tail plane on the stability;

(c) Influence of the location of the servo-mechanism sensors on the stabilization of a non-rigid aeroplane;

(d) Alteration of the aerodynamic loads due to structural deformations.

CHAPTER 12

THE ACTION OF THE CONTROLS

F.C.Haus

12.1 EFFORT APPLIED BY THE PILOT

In Chapter 10 we carried out the calculation of the motion of an aircraft when the deflection δ_e is known as a function of time.

However, the control variable for the pilot is not the displacement of the control device, but the force F exerted on it and the problem of most practical interest in the case of manual control is the calculation of the motions of the aircraft, knowing the applied force.

To solve this latter problem, it is necessary to determine the displacement δ produced by a force F, for which we must know the mechanical behaviour of the control mechanism.

In many modern control systems, the command given by the pilot is applied by intermediate servo-mechanisms. Often, an automatic pilot acts on the controls at the same time as the human pilot.

Numerous different systems are possible. They behave very differently and an analogue computer can usefully be employed to predict the results given by the actual device.

12.2 DIFFERENT TYPES OF CONTROLS

A brief description of a certain number of control methods will be given here.

12.2.1 Reversible Manual Control

Let δ_s be the displacement of the stick, positive when the displacement is forward.

The control is replaced schematically by a lever for which

$$\delta_e = \delta_s \frac{d_2}{d_3} \tag{12.1}$$

The hinge moment H_e produced by the action of the aerodynamic forces on the elevator is positive when it tends to lower the trailing edge of the control surface.

This hinge-moment H_e (Fig.113) produces a moment $\mathcal{M}_e$ about the pivot of the stick:

$$\mathcal{M}_e = H_e \frac{d_2}{d_3} \tag{12.2}$$

positive when it tends to displace the stick forward.

Let $\mathcal{M}_p$ be the moment applied by the pilot:

$$\mathcal{M}_p = F\, d_1 \tag{12.3}$$

where F is the force exerted on the stick by the pilot. F is positive when the pilot pushes on the stick.

The condition of balance

$$\mathcal{M}_p + \mathcal{M}_e = 0 \tag{12.4}$$

shows that when H_e is positive the pilot must exert a negative force. He must pull the stick to balance a positive hinge-moment.

The moment H_e is described by a moment coefficient:

$$H_e = C_{H_e} S' l' \tfrac{1}{2} \rho V^2 \tag{12.5}$$

where S' is the area of the moving part of the control surface and l' is its chord length.

In the static condition, C_{H_e} is a function of the incidence α_h of the tailplane with deflection δ_e and of the tab setting δ_t. We can often linearize the function in the form:

$$C_{H_e} = b_0 + b_1\alpha_h + b_2\delta_e + b_3\delta_t \tag{12.6}$$

where α_h represents the true angle of attack of the tail. This angle is itself given by:

$$\alpha_h = \alpha - \epsilon + \xi + \frac{q l}{V_0} \tag{12.7}$$

where ϵ is the downwash angle due to the wings and ξ is the tail setting relative to the wing chordline.

We can write:

$$\epsilon = \epsilon_0 + \frac{d\epsilon}{d\alpha}\alpha \tag{12.8}$$

$$\alpha_h = \alpha\left(1 - \frac{d\epsilon}{dt}\right) + (\xi - \epsilon_0) + \frac{q l}{V_0} \tag{12.9}$$

and, as the sum $(\xi - \epsilon_0)$ is constant, we can incorporate the product $b_1(\xi - \epsilon_0)$ into b_0 .

The expression then becomes:

$$C_{H_e} = b_0 + b_1\left[\alpha\left(1 - \frac{d\epsilon}{dt}\right) + \frac{ql}{V_0}\right] + b_2\delta_e + b_3\delta_t \qquad (12.10)$$

In the dynamic condition, C_{H_e} depends on the derivatives of the variables. In the transonic region, C_{H_e} varies non-linearly with Mach number, and the simple relation given above ceases to be of use.

In the most simple control, the tab-setting δ_t remains constant during the course of a manoeuvre. The tab is used only to reduce the effort of the pilot in steady flight.

For a perfect control, the angular displacement of the stick, δ_s , is proportional to δ_e , but the force F is not proportional to δ_e ; it depends necessarily on the parameters α_h and V .

Classical methods of calculation exist for determining the forces F which it is necessary to apply in the steady state, to maintain the aircraft in level flight at different speeds, or along a curved flight path under various normal accelerations n .

However, secondary mechanical effects are superimposed on the aerodynamic effects. These are:

(a) The action of the accelerations on all the masses forming the control mechanism. The accelerations produce moments about the pivots of the system;

(b) Friction in the controls;

(c) Elasticity in the controls;

(d) The presence of backlash.

12.2.2 Reversible Controls Using Tabs

This control includes a device which adjusts the tab-setting δ_t relative to the position δ_ϵ of the elevator, in such a way that the quantity $b_3\delta_t$ would partially balance the effect of the term $b_2\delta_e$. In principle, such a control, shown in Figure 114, does not differ essentially from a simple reversible control.

There exist further types of control using tabs to reduce the stick force, such as:

(1) A free elevator, in which the adjustment of the tab setting by the pilot alone determines the position of the elevator;

(2) An elevator connected to the levers by springs, combining the above two cases.

The characteristics of these particular systems have often been analysed, and we would need to deviate from our programme to deal with them here.

12.2.3 Irreversible Control by Hydraulic Jack Without Direct Connection Between Stick and Control Surface

We wish to produce a deflection δ_e of the elevator, proportional to the displacement of the stick. This latter is connected only to the control valve of a hydraulic jack or servo-motor. Any displacement δ_s of the stick and of this control valve, above a certain value, admits the fluid in the jack on to the face of a piston.

A feed-back device sensitive to the displacement δ_e of the control returns the valve to the neutral position, when the displacement δ_e reaches a given value.

In the schematic diagram (Fig.115), the displacement of the stick advances the pivot A to A′. This movement brings B to B′ and opens the control valve. The piston is displaced, in its turn, producing the deflection δ_e, but causing, further, the displacement of point C. This point C, moving to C′, returns B′ to B, thus cutting off the supply of fluid and stopping the motion of the piston.

We can proportion the control such that the force on the piston is considerably greater than the hinge moment. In these conditions, the final position of the elevator becomes independent of the hinge moment.

The response will, nevertheless, lag behind the command. It will be defined by a transfer function:

$$G(s) = \frac{\delta_e(s)}{\delta_s(s)} \tag{12.11}$$

The control is irreversible. The pilot exerts only sufficient force to overcome the friction in the control valve. This force is constant and does not depend on the position taken up by the elevator. It disappears as soon as the movement is stopped, so that the stick force in steady flight is zero, no matter what the deflection of the elevator may be.

It is necessary to build in a device providing 'artificial feel' in order to simulate the handling characteristics of an aircraft using manual control.

12.2.4 Manual Control Assisted by Hydraulic Jacks

Types 1 and 3 just described constitute extreme cases. We can use an intermediate type of assisted control, where the effort producing the deflection of a control surface is supplied partly by the jack and partly by the direct action of the pilot.

We impose, as in the preceding two cases, the condition that the deflection δ_e be proportional to the stick displacement δ_s.

The schematic representation in Figure 116 shows that the displacement of the stick produces directly a deflection $\delta_{e,1}$ of the elevator equal to a fraction of

the required deflection, but produces at the same time a movement of the control valve of the servo-booster. This is put in motion, and increases the elevator deflection. When the required deflection δ_e is reached, the control valve is closed and the mechanism stops, but the force in the lever EF, balancing the hinge moment, is transmitted only in part to the rod AD and to the pilot's hand.

12.2.5 Electrical Servo-Controls

A control using an electric motor can produce a deflection δ proportional to a signal.

This signal may be related either to the stick displacement δ_s or to the stick force F. Well known transfer functions will relate the displacement to the signal.

12.3 GENERATORS OF 'ARTIFICIAL FEEL'

The controls often incorporate a device to provide artificial feel. Such apparatus is essential in cases 2 and 5, and is often used in cases 1 and 3. It is also necessary in the majority of manual pilot/auto-pilot combinations, which we shall study later.

Let us briefly describe the principle of artificial-feel devices. The forces can be functions of control deflection (cases a, b and c) or of the response of the aircraft (cases d and e).

The first cases give rise to the following possibilities:

(a) *Reaction proportional to the stick deflection* δ_s

The scheme in Figure 117 clearly shows the principle. An angular displacement δ_s of the stick in the positive sense (nose down) causes a displacement s of point N. The spring, in being stretched, exerts a tension $R = k_e s$ determined by the elastic modulus k_e, assumed positive. This tension R produces a moment about the pivot of the stick:

$$\mathcal{M}_{f_1} = -k_e\left(\frac{d_4 d_6}{d_5}\right)^2 \delta_s = K_1 \delta_s \qquad (12.12)$$

The condition of equilibrium:

$$\mathcal{M}_p + \mathcal{M}_f = 0 \qquad (12.13)$$

shows that F will be positive. The pilot must push on the stick to produce a displacement $\delta_s > 0$.

(b) *Reaction proportional to the displacement but a function also of* V^2

In moving the pivot P by a servo-mechanism sensitive to V^2, the ratio d_6/d_5 becomes a function of V^2.

(c) *Reaction proportional to rate of stick displacement*

The force is provided by a damping device (see Fig.118). We now have

$$\mathcal{M}_{f_2} = K_2 \frac{d\delta_s}{dt} \tag{12.14}$$

with $K_2 < 0$.

Note

The action of the simple device defined in (a) gives a response proportional to δ_s .

Arrangements giving a reaction which is a function of the displacement δ_s but not proportional to it, are possible (Fig.119).

Generators of an artificial-feel which is a function of the response of the aircraft work as indicated below.

The moment produced about the stick hinge will be designated by $\mathcal{M}_r$ when they depend on the aircraft responses. One encounters the following cases.

(d) *Reaction a function of the load factor*

The device shown in Figure 120 consists of a mass m , or bob weight, at point P , subject to a generalized acceleration. This mass produces a moment

$$\mathcal{M}_{r_1} = - ma_{P,z}d_7 \tag{12.15}$$

with d_7 considered positive when the bob weight is behind the stick.

The general expression for $a_{P,z}$ is given in Section 2.3. The quantity $a_{P,z}$ is equal to $\dot{\gamma}_z - g_z$ plus the complementary terms depending on the coordinates of point P , and functions of the angular velocities and accelerations. Among these terms, the term $-xq'$ is most important.

When point P is coincident with the centre of gravity, the moment $\mathcal{M}_{r,1}$ can be expressed as a function of the normal acceleration n :

$$\mathcal{M}_{r_1} = -mgd_7n = K_1'n \tag{12.16}$$

The sign of the moment changes with the sign of d_7 . The coefficient K_1' is negative when d_7 has the direction shown in Figure 120.

(e) *Artificial-feel proportional to the angular acceleration*

The apparatus represented by Figure 121 consists of bob weights disposed symmetrically about the centre of gravity, exerting a moment independent of the acceleration a_z of the centre of gravity, but depending on the angular acceleration $\dot{q}$:

$$\mathfrak{M}_{r,2} = \frac{d_4 d_6}{dq} d_m m\dot{q} = K_2' \dot{q} \qquad (12.17)$$

The coefficient K_2 is positive when the levers d_8 are orientated as shown in Figure 121 and negative when orientated in the opposite sense.

12.4 IMPERFECTIONS OF THE CONTROLS

The control mechanisms are affected by the following imperfections:

(a) *Inertia forces*

The physical components of the controls frequently introduce loads which exert a similar effect to that produced intentionally by balance weights. There is no justification for treating these moments separately. The concept of resisting moments can be generalized. In the following, the moments represent not only moments applied about the stick axis by balance weights introduced intentionally, but also those due to control imperfections.

(b) *Friction*

Often, the pilot does not produce any displacement until he exerts, in one direction or the other, a force F_0 (corresponding to a moment $\mathfrak{M}_0$ about the pivot of the stick). Dry friction is the cause of this phenomenon, and we can represent this schematically by a constant opposing force which arises as soon as the out-of-balance external forces produce a displacement.

(c) *Elasticity*

Elasticity combines with friction to interfere with the kinematic link which exists between δ_s and δ_e.

If a friction force F_0 exists in the neighbourhood of a control surface, the force F and the deflection δ_s will serve only to deform the linkage, without moving the control, so long as $F < F_0$ (see Figure 122).

(d) *Backlash*

Backlash is only mentioned here in passing.

12.5 RESPONSE OF THE AIRCRAFT TO A FORCE EXERTED BY THE PILOT. CASE OF REVERSIBLE CONTROLS

We suppose that in controlling the action which he exerts on the aircraft by a force F applied to the stick, the pilot is not influenced in that action by the position δ_s of the stick.

In the case considered, the elevator undergoes a deflection δ_e related to the displacement δ_s of the stick by linkage geometry. But the conditions are such that

there exists no unequivocal relation between δ_e and F. The displacement depends not only on the force, but on other factors also. The response of an aircraft to the excitations to which it is subjected is determined as a function of the deflection δ_e, by the system of equations already studied in Section 10.1. It is necessary now to add the equations determining the deflection δ_e as a function of the force F.

To this end, we must write the equation of equilibrium of the moments about the control hinge-line. This equation was given in Section 4.3.1 for the general case. We shall assume now that the elevator is statically balanced, thus simplifying the expression (Fig.123).

Let J be the moment of inertia of the elevator.

Referring the moments exerted by the balance weights to the elevator hinge, we have:

$$J \frac{d^2\delta_e}{dt^2} + J \frac{dq}{dt} = H_e + [(F - F_0)d_1 + \mathcal{M}_f + \mathcal{M}_r] \frac{d_3}{d_2} \tag{12.18}$$

where

$$\mathcal{M}_f = \mathcal{M}_{f_1} + \mathcal{M}_{f_2} = K_1\delta_s + K_2\dot{\delta}_s \tag{12.19}$$

$$\mathcal{M}_r = \mathcal{M}_{r_1} + \mathcal{M}_{r_2} = K_1'n + K_2'\dot{q} \tag{12.20}$$

$$H_e = \left\{ b_0 + b_1\left[\alpha\left(1 - \frac{d\epsilon}{d\alpha}\right) + \frac{ql}{V_0}\right] + b_2\delta_e + b_4\delta_e \right\} S'l'\tfrac{1}{2}\rho S(V_0 + \Delta V)^2 \tag{12.21}$$

The moments opposed to pilot action vary according to the design of the mechanism, and do not necessarily depend on all the variables considered. The hinge moment depends on the variables α, q, δ_e, $\dot{\delta}_e$, and $(V_0 + \Delta V)^2$. The dry friction force varies according to the sign of the rate of displacement as indicated above.

The calculation of the deflection cannot be made independently of the system of equations representing the motion of the aircraft, since it depends on certain output variables from that system.

We can calculate δ_e analytically as a function of F only if we neglect all the effects which render the equations non-linear. Thus we consider the following simplifications:

(1) In the expression H_e, we neglect ΔV^2 and the products of ΔV with the other variables;

(2) We write $\delta_e = \delta_s(d_2/d_3)$, that is to say, we neglect the deformations;

(3) We suppose that $\mathcal{M}_f$ is proportional to δ_s, that is we study only the case of artificial feel having linear characteristics;

(4) We must replace the friction force F_0 by a viscous resistance.

The equations for the aircraft together with that for the controls determine a 6th order system which presents a new natural frequency, corresponding to the displacement δ_e. This frequency is much higher than that of the oscillatory motions of the aircraft.

The problem contains a case of special importance, viz., the case where F is zero. This is the case of an aircraft flying 'stick free'.

The use of an analogue computer to solve the system of equations permits, on the contrary, the introduction of the non-linear effects. The most important is the friction force, which can easily be simulated by diode circuits.

Note

The moments $\mathfrak{M}_r$ produced by the feel device are functions of the response of the aircraft. They act about the stick pivot, in the same way as the moments applied by the pilot. They can help to improve the stability of an aircraft flying stick-free, if they act in the right sense.

12.6 USE OF ANALOGUE COMPUTER. STUDY OF THE LONGITUDINAL MOTION OF AN AIRCRAFT FLYING STICK-FREE

The equation

$$J\frac{d^2\delta_e}{dt^2} + J\frac{dq}{dt} = S'l'\tfrac{1}{2}\rho V_0^2\left\{b_1\left[\alpha\left(1 - \frac{d\epsilon}{dt}\right) + q\frac{l}{V}\right] + b_2\delta_e + b_4\frac{d\delta_e}{dt}\right\} +$$

$$+ (F - F_0)\frac{d_1 d_3}{d_2} + (\mathfrak{M}_f + \mathfrak{M}_r)\frac{d_3}{d_2} \qquad (12.22)$$

must be added to the system defining the motion of the aircraft. The moments $\mathfrak{M}_f$ and $\mathfrak{M}_r$ produced by the artificial feel generators will be expressed as functions of the variables concerned.

Figure 124 represents the wiring diagram for the case where the motion of the aircraft is represented by Equations (10.1), which become numerically*

$$\left.\begin{aligned} \frac{d\hat{u}}{dt} + 0.014\hat{u} - 0.039\alpha + 0.0885\theta &= 0 \\ \frac{d\alpha}{dt} + 0.175\hat{u} + 0.77\alpha - q &= -0.0708\delta_e \end{aligned}\right\} \qquad (12.23)$$

*This is the aircraft wherefrom the locked control behaviour has been calculated (Section 10.1.1.3). Its static margin is given by $C_{m_\alpha} = -0.74$.

$$\left.\begin{aligned} \frac{dq}{dt} + 0.0293\hat{u} + 2.21\alpha + 1.82q &= -6.04\delta_e \\ \frac{d\theta}{dt} - q &= 0 \end{aligned}\right\} \qquad (12.23)$$

where the control system corresponds to the following numerical values:

$$\frac{S' l' \tfrac{1}{2}\rho V_0^2}{J} = 2 \times 10^3$$

$$\left(1 - \frac{d\epsilon}{d\alpha}\right) = 0.60$$

$$\frac{l}{V_0} = 0.174 \quad \dagger$$

$$\frac{d_1 d_3}{d_2} = 0.175$$

$$b_2 = 0.15$$

$\mathfrak{M}_f = 0$ (no artificial feel depending on displacement of the stick)

$\mathfrak{M}_r = K(q - \dot{\alpha})$ (artificial feel depending on the acceleration sustained by the aircraft at its centre of gravity).

We have studied the case of viscous damping, without friction, corresponding to: $b_4 = -0.0025$, $F_0 = 0$, and, conversely, the case of friction without viscous damping, in which we have:

$$b_4 = 0 \qquad F_0 \neq 0 \qquad \text{(to be defined later).}$$

Different numerical values have been assigned to the coefficient b_1 . The scheme permits the solution of the following problems:

(1) *Investigation of the influence of the numerical value of* b_1 *on the stick-free stability*

This is the problem of stick-free flight, when $F = 0$. We consider the case of viscous damping. There is no artificial feel.

Equation (12.22) finally becomes:

$$\frac{d^2\delta_e}{dt} + \frac{dq}{dt} + 5\,\frac{d\delta_e}{dt} + 300\delta_e - 348b_1 q - 1200b_1\alpha = 0 \qquad (12.24)$$

$\dagger$The numerical value of l/V_0 has been raised to 0.174, in order to take account of the downwash time lag.

We know that when b_1 and b_2 are of the same sign, the static margin stick-fixed is greater than that stick-free.

On the contrary, if b_1 and b_2 are of opposite sign, the static margin stick-free is greater than that stick-fixed.

Figure 125 shows the time-variation of the variables α, θ, q, and δ_e subsequent to an initial perturbation $\Delta\alpha = \Delta\theta = 0.10$ radian, for b_1 respectively equal to:

$$+ 0.0833$$

$$+ 0.04165$$

$$0$$

$$- 0.04165$$

$$- 0.0833$$

(2) *Investigation of the response of an aircraft to the same initial conditions, but with a friction force*

The moment proportional to $d\delta_e/dt$ is replaced by a moment whose sign depends on $d\delta_e/dt$ but whose value remains constant. We have then fixed this value at that which the viscous damping would produce when $d\delta_e/dt = 0.1$ rad/sec. This consists of replacing the term $5d\delta_e/dt$ by a term

$$\frac{F_0}{J}\frac{d_1 d_3}{d_2} = \pm 0.5 \quad \text{sec}^{-2}$$

the $\pm$ sign being that of the derivative $d\delta_e/dt$. We have further studied the case of a friction force having twice this magnitude.

The circuit used for this analogue computation is shown in Figure 124.

The tests were made for the same initial perturbation $\Delta\alpha = \Delta\theta = 0.10$ rad. The result is shown in Figure 126 uniquely for the two values $b_1 = +0.0416$ and $b_1 = -0.0416$.

(3) *Investigation of the response of an aircraft fitted with a generator of artificial feel proportional to the load factor*

The case considered involves viscous damping and stick free $(F = F_0 = 0)$.

The moment produced about the stick pivot by the generator of artificial feel was:

$$\mathcal{M}_r = K(q - \dot{\alpha}) \qquad (12.25)$$

The corresponding moment about the elevator hinge-line was represented by:

$$\frac{d_3}{d_2}\frac{\mathfrak{M}_r}{J} = K(q - \dot{\alpha})$$

and the test was made with the value of K respectively equal to 0 and +50 sec^{-1}.

The original scheme was completed by the circuits having to introduce a term in $(q - \dot{\alpha})$ into the equation in $d^2\delta_e/dt^2$.

The initial condition is the same as in the preceding cases. The result is shown for the values of b_1 equal to +0.0416 and -0.0416 (Fig.127).

(4) *Investigation of the influence of a generator of artificial feel in the case of zero static margin*

The aircraft was supposed to present a zero static margin with stick fixed; we have then taken $C_{m_\alpha} = 0$ instead of $C_{m_\alpha} = -0.74$.

The coefficient of the term in α in the equation in dq/dt has become zero.

Stick free, the static margin falls further when b_1 is negative.

The analogue computer shows that the effect of the generator on artificial feel is clearly stabilizing.

Figure 128 shows the response of the aircraft to a perturbation $\Delta\alpha = \Delta\theta = 0.1$ rad for the case $b_1 = -0.0416$ with three values of K: 0, +50 and +100 sec^{-1}.

(5) *Response of the aircraft to a hinge moment applied suddenly*

The system defined by the equation characterizing the first problem was subject to an initial condition

$$F_0 \frac{d_1 d_2}{d_3}$$

The response is shown in Figure 129 for the cases

$$b_1 = 0.0416 \qquad b_1 = -0.0416$$

for a force F_0 characterized by a given value of

$$\frac{F_0 \dfrac{d_1 d_3}{d_2}}{J} = -5 \ sec^{-2}$$

The initial condition consisted in introducing into the integrator XI, an initial voltage of 50 volts through a resistance of 100 KΩ.

Note

(1) *Order of magnitude of the forces*

The presentation just made does not allow of an immediate realization of the magnitude of the forces brought into play.

In the kilogram-metre-second system, the moment of inertia of the elevator has dimensions FLT^{-2}.

If the dimensions of the aircraft are such that the numerical value of J in these units is 1 kg m sec^{-2}, the friction envisaged corresponds to a moment of 0.5 and 1 kgm about the hinge-line, that is to say, a frictional force measured at the stick of 0.5/0.415 and 1/0.715, or 0.7 and 1.4 kg.

The feel generator exerts about the hinge-line of the elevator, under the action of an incremental load factor $\Delta n = 1$, a moment:

$$\mathfrak{M}_r \frac{d_3}{d_2} = 4.4 \text{ kgm for } K = 50 \text{ sec}^{-1}$$

$$= 8.8 \text{ kgm for } K = 100 \text{ sec}^{-1}$$

The moment applied in problem 5 corresponded to a couple on the hinge of 5 kgm, that is a force on the stick of 7 kgs.

(2) *Note on the computer*

The calucations described in the present example have been effected with very small equipment, using equations which had not undergone any preliminary change of scale. This explains the use of occasionally unusual ratios between the input resistances and the feed-back resistances. We think, however, that they are effective in demonstrating the results that can be obtained at very low cost.

12.7 TRANSFER FUNCTIONS OF POSITIONING SERVO-MECHANISMS

12.7.1 Existence of a Transfer Function

The determination of an aircraft response, the controls of which are actuated by servo-mechanisms, can only be done if we know the transfer function of the servo-mechanism.

The scope of this study will be limited to positioning servo-mechanisms, which resolve the following problem: to produce a control surface deflection δ that is always proportional to an input x , i.e., $\delta = Ax$.

A servo-mechanism can only achieve this programme in an imperfect way. The servo-mechanism is characterized by a transfer function

$$G(s) = \frac{1}{A} \frac{\delta(s)}{x(s)} \qquad (12.26)$$

not equal to unity. This transfer function varies according to the characteristics of the servo-mechanism and must be reproduced by the analogue computer. We shall examine two main cases:

Case 1. The order or input x is the displacement δ_s of the control column, or of a mechanical part linked to the column. The servo-motor is a jack. The control deflection δ_e is proportional to the piston displacement.

Case 2. The input x is an electric voltage. The servo-motor is an electric motor. The control deflection δ_e is proportional to the angular displacement of the motor. The voltage, which acts as the input, may be proportional either to a stick displacement δ_s, or to the force F exerted by the pilot.

In both cases, the design of a positioning servo-mechanism involves the use of a feed-back device.

One must, at any time, subtract the control deflection angle, divided by A, from the input x. This gives a signal

$$\sigma = k\left(x - \frac{\delta}{A}\right) \tag{12.27}$$

where k is a simple proportionality factor. It is this signal σ which actuates the servo-motor.

12.7.2 Control by Means of a Jack

Let us look again at Figure 115. The input x is nothing but the displacement AA'; the signal σ is the displacement BB' of the slide valve; and the feed-back quantity δ/A is the displacement CC'. The lengths of the rods are such that the control valve comes again to its initial position ($\sigma = 0$) when the piston displacement has produced the required control deflection.

The analysis of the motion shows:

(1) That a minimum slide valve displacement is necessary before the admittance ports are uncovered - there is a threshold;

(2) The piston displacement will be proportional to the oil flow into the cylinder;

(3) The oil pressure action on the piston depends on the pressure loss through the cylinder ports; the pressure loss is a function of the port area and the oil flow m;

(4) The rotational equilibrium conditions of the control allow us to find the angular acceleration, resulting from the action of the pressure exerted on the piston and the opposite aerodynamic hinge moment.

The analysis is somewhat complicated. When it is possible to perform it, the behaviour of the servo-mechanism will be characterized by a relation

$$m = f(\sigma) \tag{12.28}$$

relating the oil flow to the valve position.

As the displacement speed of the piston and the control surface is proportional to m, we obtain finally:

$$\delta = k_1 \int m \, dt \tag{12.29}$$

and it becomes possible to simulate the transfer function

$$G(s) = \frac{\delta(s)}{x(s)}$$

with the set-up indicated in Figure 130, once the function $m = f(\sigma)$ is known. This set-up comprises a function generator simulating $m = f(\sigma)$ and an integrator.

In the particular case when

$$m = k_2 \sigma \tag{12.30}$$

we see immediately that

$$\delta = k_1 k_2 \int \sigma \, dt = k_1 k_2 \int \left(x - \frac{\delta}{A} \right) \tag{12.31}$$

or, in symbolical writing,

$$\delta(s) \left(1 + \frac{k_1 k_2}{A} \frac{1}{s} \right) = k_1 k_2 \frac{1}{s} x(s) \tag{12.32}$$

$$\delta(s) = A \frac{1}{1 + \frac{A}{k_1 k_2} s} x(s) \tag{12.33}$$

These relations define a first order transfer function which can be simulated by a block using only one amplifier.

12.7.3 Control by an Electric Motor

The input x gives a signal σ which appears to be an electrical voltage E. This signal can be amplified. Let us write:

$$E = k_1 \left(x - \frac{\delta}{A} \right) \tag{12.34}$$

The voltage E is applied to the armature of a d.c. motor with independent excitation, producing a constant induction field.

Let Γ be the torque exerted by the motor

Z the impedance of the armature ($= R + sL$)

Ω the angular velocity of the motor

$k_2\Omega$ the counter electromotive force.

The torque is proportional to the intensivity of the armature current

$$\Gamma = k_3 \frac{E - k_2\Omega}{Z}$$

Let k_4 be the reduction ratio of the transmission between the motor and the control surface:

$$\frac{d\delta}{dt} = k_4\Omega$$

and J_m be the inertia moment of the motor. Then the rotation equation of the control surface will be

$$J \frac{d^2\delta}{dt^2} + J\dot{q} + J_m \frac{1}{k_4} \frac{d^2\delta}{dt^2} = \frac{k_3}{Z}\left[k_1\left(x - \frac{1}{A}\delta\right) - \frac{k_2}{k_4}\frac{d\delta}{dt}\right] + H_e \qquad (12.35)$$

If we make the following simplifications:

(a) writing $H_e = k_5\delta_e$, with $k_5 < 0$, because it defines a resisting moment, and neglecting the effect of the outputs q and α on the hinge moment,

(b) neglecting $J\dot{q}$,

(c) neglecting the armature self induction, by writing $Z = R$, we obtain:

$$\left(J + \frac{1}{k_4} J_m\right)\frac{d^2\delta}{dt^2} + \frac{k_1k_3}{k_4R}\frac{d\delta}{dt} + \left(\frac{k_1k_3}{AR} - k_5\right)\delta = \frac{k_1k_3}{R} x \qquad (12.36)$$

The equation can be written in symbolic way:

$$(s^2 + 2\zeta\omega_n s + \omega_n^2)\delta(s) = \frac{\omega_n^2}{1 - AR\dfrac{k_5}{k_1k_3}} A\, x(s) \qquad (12.37)$$

or

$$\delta(s) = \frac{\omega_n^2}{s^2 + 2\zeta\omega_n s + \omega_n^2} \frac{1}{1 - AR\dfrac{k_5}{k_1k_3}} A\, x(s) \qquad (12.38)$$

with

$$\left.\begin{aligned} 2\zeta\omega_n &= \frac{\dfrac{k_1 k_3}{k_4 R}}{J + \dfrac{1}{k_4} J_m} \\ \omega_n^2 &= \frac{\dfrac{k_1 k_3}{AR} - k_5}{J + \dfrac{1}{k_4} J_m} \end{aligned}\right\} \qquad (12.39)$$

We know that ζ is the relative damping and ω_n the frequency of the undamped system. When a steady state $(s = 0)$ is reached, we will find:

$$\delta = K A x$$

with

$$K = \frac{1}{1 - AR \dfrac{k_5}{k_1 k_3}}$$

There will, therefore, be a static error

$$\Delta\delta = (1 - K)Ax$$

between the desired deflection

$$\delta = Ax$$

and the deflection actually obtained.

This static error can only be eliminated by one of the following processes:

(a) Suppression of the resisting moment, proportional to the control surface, which means $k_5 = 0$;

(b) Modification of the scheme by making use of a term depending on the integral of the error.

The theory of servo-mechanisms yields a complete theory on these solutions.

Note

(a) The case described is the most simple electric servo-control. If the motor is an a.c. two-phase one, the transfer function will always be of third order.

(b) The transfer function will also be of third order in the case of the d.c. motor, if the armature self-induction L is not neglected.

12.7.4 Miscellaneous Cases

Besides the two main cases just studied, we can find combinations where the input x is a voltage, or the servo-motor unit is a jack.

In this case, servo-valves, the scheme of which will be presented later (Section 13.4.1) will fulfill this function.

One could also use the electric signal to activate an electric motor of very low power, which should only displace the slide valve of the jack.

The determination of the transfer function for all possible arrangements would exceed the scope of this paper, in the same way as a survey of the cases where the representation of a servo-mechanism by a transfer function becomes inadequate and requires the use of a transfer matrix.

12.8 RESPONSE OF THE AIRCRAFT TO PILOT ACTION IN THE CASE OF SERVO-CONTROLS

The servo-motor transforms the signals given by the pilot into a control surface displacement. This introduces the alteration defined by the transfer function. The pilot signal may be either the force F exerted on the stick or the stick displacement.

When the input is so clearly indicated, it will be easy to find the aircraft response. But the input given by the pilot is not always transferred to the servo-mechanism in its original form. It may be altered by the action of the artificial-feel generator, when the latter is activated by the aircraft response.

In more intricate arrangements, the human pilot orders are combined with orders coming from the error detectors belonging to the automatic pilot. The behaviour of such devices will be considered in Sections 13.8 and 13.9.

The use of servo-controls not connected with an auto-pilot is becoming uncommon and we will only comment shortly on this case.

(a) *Control surface deflection proportional to pilot effort*

The effort exerted by the pilot on the stick is measured by a grip dynamometer. The electric signal produced by this device is the input acting on the servo-motor (Figs. 132 and 133). One has only to add the equation

$$\delta_e(s) = K\, G(s)\, F(s) \tag{12.40}$$

where $G(s)$ is the servo-control transfer function, to the equations of motion. This provides us with a system of equations relating the input F to the output variables u, α, q, θ in the case of the longitudinal motion. When one admits that the pilot is able to exert the required force on the stick, independently of the stick displacement δ_s, it seems useless to allow a stick displacement. The control column could be replaced by a fixed dynamometer.

Such an arrangement is, however, quite exceptional and has, to our knowledge, only been used for test purposes[13].

Pilots report that manual control with a fixed stick is possible but not so agreeable as control with a moving stick. This fact throws some doubt on the hypothesis that a pilot is able to control the force exerted when there is no displacement of the stick. The normal response of the pilot has its origin in training with controls where the control surface deflections are proportional to the stick displacements and, therefore, it seems that the normal response of the pilot is to exert an effort and to displace the stick simultaneously, the variable that the pilot can best appreciate being nevertheless the force rather than the displacement.

(b) *Control surface deflection as a function of the stick displacement*

In an elementary jack servo-control, as described in Section 12.2.3, the control deflection δ_e is related to the stick displacement δ_s by the transfer function G(s) defined in Section 12.7.2.

The response of the aircraft produced by a stick displacement will be obtained in a straightforward way by adding the relation

$$\delta_e(s) = G(s)\, \delta_s(s) \tag{12.41}$$

to the general equations of motion of the aeroplane.

But one may wish to determine the aircraft response when a given force is exerted on the stick. The phenomenon must then be analyzed in two phases:

(1) Determination of the input to the jack, which means the displacement of point A produced by a force acting on the stick;

(2) Knowing this displacement, we consider the transfer function of the jack as in the previous case.

The first point involves consideration of the equilibrium condition of the system comprising the stick, the artificial feel generators, and the slide valve (Figs. 134 and 135). The use of artificial feel generators is unavoidable in this case.

The displacement of the slide valve involves dry friction. The moment of this friction force around the pivot of the stick will be represented here by $\mathfrak{M}_d$.

Let I be the moment of inertia of the control column and of the mechanical parts linked to it. The equilibrium condition will be:

$$I \frac{d^2\delta_s}{dt^2} = Fd_1 + \mathfrak{M}_f + \mathfrak{M}_r + \mathfrak{M}_d \tag{12.42}$$

Due to the direct linkage between the stick and the valve, the valve displacement will be proportional to δ_s.

It seems at first sight that the moment of inertia I may be neglected in the preceding equation.

When

$$\mathcal{M}_f = K_1$$
$$\mathcal{M}_r = 0$$
$$\mathcal{M}_d \simeq 0$$

the stick displacement, and also the valve displacement, will be proportional to the force F, but when the artificial control forces depend on the aircraft response $\mathcal{M}_r \neq 0$, or on the speed of the displacements $\mathcal{M}_f = K_2\dot{\delta}_s$, there is no proportionality between the effort and the displacement.

As a first approximation, making $\ddot{\delta}_s = \dot{\delta}_s = 0$, we find that the variable δ_s is proportional to the sum of the moments exerted by the pilot and by the response of the aircraft.

The linkage between the valve and the control column will produce an elevator deflection δ_e proportional to $Fd_1 + \mathcal{M}_r$.

12.9 USE OF THE ANALOGUE COMPUTER

12.9.1 Different Ways of Investigation

The analogue computer can be of great use for determining the behaviour of an aircraft subjected to the control of a human pilot. Two different methods of investigation are possible:

Method 1

This method of investigation makes use of a flight simulator. The flight simulato is an aggregate where the aircraft behaviour is calculated by an analogue computer, while the control system behaviour is reproduced mechanically.

The stick and the pedals are like they are in an aircraft; they develop and oppose the same forces when they are displaced.

The two parts, computer and mechanical control system, are connected together. The displacement of the controls introduces into the computer voltages corresponding to the control displacements. The output voltages, produced by the computer and representing the response of the aircraft, must act on the control mechanism and develop control forces equal to those existing in the actual aircraft. These voltages act also on measuring intruments identical to ordinary flight instruments. In some cases they actuate a projector which can provide the experimenter with visual impressions similar to those that the actual pilot would experience.

The flight simulator permits the study of the aircraft motion by placing the experimenter in conditions similar to those which the pilot encounters in flight but, nevertheless, in an imperfect way due to the difficulty of reproducing the accelerations acting on the pilot.

The results obtained with a flight simulator depend to some extent on the behaviour of the experimenter himself.

Method 2

Only an analogue computer is used. There are no mechanical controls. The equations governing the controls are solved by the computer. The pilot's orders are simulated by voltages corresponding to the independent inputs F or δ_s. The experimenter does not feel the stick or pedal reactions and it is not necessary to perform the same movements as the actual pilot.

12.9.2 Use of the Computer Alone

As usual, the equations describing the operation of the controls and those defining the aircraft motions are represented on the computer.

The drawing of a block diagram makes the analysis of the system far easier. Figure 136 represents the block diagram of a servo-control using a jack, with the following forces exerted on the stick:

Pilot force F (the input);

Dry friction, corresponding to the valve friction;

Artificial control moment $\mathfrak{M}_f$ proportional to the stick deplacement;

Artificial control moment $\mathfrak{M}_r$ proportional to the normal acceleration at a point P different from the centre of gravity.

The first block represents the transformation of the force F into a displacement δ_s, which will be the input acting on the jack. The response of the jack will be governed by a transfer function which has to be simulated. It is shown in the most general case that this simulation involves the use of a function generator $m = f(\sigma)$ followed by an integrator.

The deflection δ_e is the output of the jack, and energizes the block representing the aircraft, the response of which was studied in Chapter 10.

As the equations defining the behaviour of the different parts of the system are resolved in separate loops on the analogue computer, it is possible to study easily the influence of the various factors which exert an influence on the transformation of the pilot force F into the displacement δ_s. In particular, we may investigate the effect of:

A change in the characteristics of the jack;

A change in the point P, where the bob weight producing the moment $\mathfrak{M}_r$ is located.

The first investigation involves alterations of the function $m = f(\sigma)$. The second investigation involves alteration of the factor multiplying the term in $\dot{q}$. This will occur in the block in which the acceleration a_n is calculated.

Monroe has shown[14] that the displacement of the bob weight location P will considerably affect the aircraft response.

12.9.3 Determination of an Optimum Artificial-Feel Generator

Let us consider a given aircraft. The behaviour of this aircraft is known and determined by its equations of motion. The aircraft includes a servo-control system whose transfer function is known, and should be fitted with an artificial control force generator. We wish to optimize the characteristics of this device.

The choice of the optimum feel generator may depend on the manoeuvre that will be performed, and the problem can only be solved when this manoeuvre is well defined. Moreover, the fulfilment of the manoeuvre involves the intervention of a human pilot whose behaviour may vary from one individual to another.

(a) *Use of the simulator*

The classical solution of such a problem requires the use of a flight simulator. The simulator must calculate the control force that would be produced by the artificial force generator under consideration and apply this force to the controls which are actuated by the experimenter.

The comparison of the responses (and of the pilot's reports) obtained with different artificial feels will allow us to grade the proposed devices. This method of study presents two difficulties:

(1) The responses of the flight simulator will depend on the experimenter's training as a pilot. For equal mechanical conditions they will vary from one pilot to another;

(2) The mechanical device that would exert at any time the force calculated by the computer is not an easy thing to build.

(b) *Using the computer only*

The problem can be studied using a computer alone. In this case the experimenter must be replaced by a computing element, reproducing the transfer function of a good (or medium) human pilot. This process has been followed by the N.A.S.A[15].

A well defined manoeuvre has been chosen - the pursuit of another aeroplane that is trying to escape. The pilot's aim will be to hold the pursued aeroplane in the centre of his gunsight, submitting his own aircraft to movements in θ and ψ according to the displacement observed in the sight.

We will deal only with the movement in the longitudinal plane. The error observed by the pilot is the difference

$$\epsilon' = \theta - \theta_i \tag{12.43}$$

between the attitude θ and the inclination with the horizon, θ_i, of the straight line joining the two aeroplanes.

The transfer function for the pilot is the function relating the force F to the error:

$$F(s) = G(s)\,\epsilon'(s) \tag{12.44}$$

The most simple response of a human being to a visual signal will include a constant delay time t_1 and a time constant t_2 producing the transfer function

$$G(s) = \frac{e^{-t_1 s}}{1 + t_2 s} \tag{12.45}$$

It seems, however, that the response of the human being will depend on the derivative of the error. Moreover, the force exerted by the pilot is probably not completely independent of the stick position δ_s. A better description of the pilot's behaviour will certainly be obtained when it is supposed that, for the same error signal, the force exerted, F, depends also on the error derivative and the stick position.

The Report referred to does not indicate all the details of the transfer function actually used.

The input acting on the servo-mechanisms is the sum $\mathcal{M}_p + \mathcal{M}_r + \mathcal{M}_f$.

The block diagram describing the system is represented in Figure 137; one of the elementary blocks represents the transfer function $G(s)$ of the pilot and it is clear that the moment $\mathcal{M}_p = Fd_1$ becomes a function of ϵ, $\dot{\epsilon}$, δ_s, while the moments $\mathcal{M}_f$ and $\mathcal{M}_r$ exerted by the artificial feel generators are functions of δ_s, $\dot{\delta}_s$, $\dot{q}$, n. The problem consists in finding, by trial and error, the best functions $\mathcal{M}_r$ and $\mathcal{M}_f$.

The tests were made by determining the indicial response of the whole system (pilot + aeroplane), to step variations of θ_i applied while the aeroplane was assumed to be flying in various conditions of:

static margin (or C_{m_α} derivative),

speed,

altitude.

In general, for every type of feel generator the response of the system varied according to the assumed flight conditions and were acceptable only in a small range of speed, altitude or static margin.

A feel generator producing:

$$\mathcal{M}_r = 0 \qquad \mathcal{M}_f = k_1 \delta_s$$

has given the results indicated in Figure 138 for a series of tests with the speed and altitude constant, and the static margin variable. The curves show that the results are strongly dependent on this parameter.

The use of an artificial-feel generator producing control moments $\mathfrak{M}_r$ dependent on a_n , q , $\dot{q}$ has produced responses which were nearly constant throughout a wide range of speeds, altitudes and static margins. These responses are reproduced in Figure 139 and the corresponding feel generator is considered the optimum.

As the classical feel generators produce control moments which are functions only of a_n and $\dot{q}$, the optimum generator should be activated by signals produced by a rate gyro.

CHAPTER 13

AUTOMATIC CONTROL

F. C. Haus

13.1 ARTIFICIAL STABILITY

The dynamic characteristics of an aircraft can be completely modified if the control surfaces are actuated as a function of the error in one or several variables with respect to the initial values.

The block diagram in Figure 140 represents an aircraft whose altitude is controlled as a function of the error in attitude.

When the attitude θ, measured by an appropriate device, differs from the imposed attitude θ_i, a comparator produces a signal

$$\epsilon = \theta_i - \theta \tag{13.1}$$

which is considered in servo-mechanism theory as the error. This error will produce an elevator deflection δ_e by the working of a servo-mechanism.

The relationship between the deflection δ_e and the error signal ϵ constitutes the control equation. This equation can be represented by the transfer function

$$\delta_e(s) = G(s)\,\epsilon(s) \tag{13.2}$$

The most simple conceivable relationship between δ_e and ϵ is a relationship of proportionality, viz.,

$$\delta_e = A\epsilon \tag{13.3}$$

where δ_e and ϵ are functions of the time variable t.

We generally take θ_i for the zero point of the scale in θ. The preceding equation then becomes

$$\delta_e = -A\theta \tag{13.4}$$

When the aeroplane undergoes a nose-up displacement, a nose-down moment must be applied. The control deflection δ_e will be positive and this entails a negative value for the constant A.

The negative sign may be considered as an inconvenience arising from the sign convention governing the control deflections. To avoid this inconvenience, we could consider an error ϵ' defined in the converse way, thus:

$$\epsilon' = \theta - \theta_i \tag{13.5}$$

allowing us to write

$$\delta_e = A(\theta - \theta_i) \tag{13.6}$$

becoming

$$\delta_e = A\theta \tag{13.7}$$

for $\theta_i = 0$, and leading directly to a positive coefficient A .

We can use variables other than θ to actuate the control surfaces.

In a general manner, the equations which relate the deflections δ_e, δ_a, δ_r or the throttle position δ_m to the changes in the variables

$$\begin{array}{lll} \alpha_r & \beta_r & \hat{u}_r \\ \theta & \varphi & \Psi \\ p & q & r \end{array}$$

to functions of these changes such as their derivatives, their integrals, or to the components of the generalized acceleration

$$\left.\begin{aligned} a_x &= \frac{du}{dt} + (qw - rv) + g \sin\theta \\ a_y &= \frac{dv}{dt} + (ru - pw) - g \sin\varphi \cos\theta \\ a_z &= \frac{dw}{dt} + (pv - qu) - g \cos\varphi \cos\theta \end{aligned}\right\} \tag{13.8}$$

are control equations.

The movements executed by the aircraft under the effect of the control equations will be obtained by writing into the equations of motion the aerodynamic control forces and moments $(\Delta C_x)_i$ ..... $(\Delta C_n)_i$ as a function of the errors in the variables. These excitations will depend on the aerodynamic effects of the control surfaces and the control equations.

These equations must take into account the real properties of the servo-mechanisms. Whenever possible the functioning of the servo-mechanism is defined by means of linear relationships.

When the chosen control equations exert a favourable effect, it can be said that the aircraft has been given artificial stability.

An extended choice can be made among the variables from which the errors are used. Certain variables can be utilized to actuate two different controls, and the number of possible combinations is very great.

It is useful to know the influence of the different control equations on the motion of the aircraft.

The hypothesis of proportionality permits the study of the physical action of the theoretical control equations, without the action being masked by the real behaviour of the servo-mechanism. It permits the establishment of an idealized theory on artificial stability which predicts the effect of the different control equations.

A theoretical study of artificial stability can be made by studying the following system of equations:

(a) By the classical analytical methods of solving linear systems;

(b) By the method of analysis used in the theory of servo-mechanisms (polar representation of the frequency responses, Nyquist's criterion);

(c) By the root locus method which constitutes a compromise between methods (a) and (b);

(d) In a limited fashion, by the method of rotating vectors;

(e) By analogue calculus.

The classical method of solving the differential equations has furnished (between 1925 and 1939) the first concepts on artificial stability. Its field of application is limited to the cases where the displacement of the control surfaces is proportional to the perturbations and the information gained from this method of approach results more from the solution of systems each corresponding to a particular case, than from the discussion of a general solution.

If the solution of the characteristic equation furnishes, without too much difficulty, the length of the periods and the damping of the modes proper of the artificially stabilized aircraft, the calculations become very long when one wants to determine the movements corresponding to given perturbations, and the accumulation of numerous results entails considerable work.

The methods used in the theory of servo-mechanisms permit a preview of the properties of the systems under control, without any previous resolution of the characteristic equation. They furnish numerous indications of aircraft behaviour when the control equations are relatively simple.

It is not our aim here to make comparisons between the different methods of approach to the problem; therefore we shall pass directly to the study, by the use of analogue computers, of an articicially stabilized aircraft.

The use of the analogue computer does not lend itself to a general theory, but it permits an increase in the amount of data by progressively modifying the parameters, and thus furnishes a group of solutions defining the phenomenon in an adequately practical manner. Moreover, the study with the analogue computer makes it possible to simulate the real action of the control mechanisms even when it is not linear. With the other methods, this is not possible.

13.2 ANALOGUE STUDY FOR THE SCHEMATIC CASE

We shall study longitudinal motion and lateral motion separately.

We will suppose that the control equations are proportionality relations between the deflection of the control surface and the divergence from the preset variable (e.g. θ_i).

The deflections, being supposed proportional to the divergence, will give expressions of the following type:

For the longitudinal motion:

$$\left.\begin{aligned} \delta_e &= A_1\theta + A_2\alpha_r + A_3\hat{u} + \ldots\ldots + A_m\dot{\theta} + \ldots + A_n\ddot{\theta} + \ldots \\ \delta_m &= B_1\theta + B_2\alpha_r + B_3\hat{u} + \ldots\ldots + B_m\dot{\theta} + \ldots + B_n\ddot{\theta} + \ldots \end{aligned}\right\} \qquad (13.9)$$

For the lateral motion:

$$\left.\begin{aligned} \delta_a &= A_1\Psi + A_2\beta_r + A_3\varphi + \ldots\ldots\ldots \\ \delta_r &= B_1\Psi + B_2\beta_r + B_3\varphi + \ldots\ldots\ldots \end{aligned}\right\} \qquad (13.10)$$

within each case the coefficients A_1, A_2 ...., B_1, B_2...., dependent on the sensitivity chosen for the control.

The principal aerodynamic actions produced by the deflections are defined by the following derivatives, for which it is necessary to know the value in each case:

$$\begin{array}{ccc} & \dfrac{\partial C_z}{\partial \delta_e} & \dfrac{\partial C_m}{\partial \delta_e} \\ \dfrac{\partial C_x}{\partial \delta_m} & \dfrac{\partial C_z}{\partial \delta_m} & \dfrac{\partial C_m}{\partial \delta_m} \end{array}$$

for longitudinal motion, and

$$\begin{array}{ccc} & \dfrac{\partial C_l}{\partial \delta_a} & \dfrac{\partial C_n}{\partial \delta_a} \\ \dfrac{\partial C_y}{\partial \delta_r} & \dfrac{\partial C_l}{\partial \delta_r} & \dfrac{\partial C_n}{\partial \delta_r} \end{array}$$

for lateral motion.

It may be noted that automatic control of the engines is rarely used.

The analogue representation will be very easy. Let us examine the longitudinal motion. The equation for moment equilibrium becomes:

$$C_{I_y} \frac{dq}{dt} - C_{m_u}\hat{u} - C_{m_\alpha}\alpha - C_{m_q} \frac{c}{2V_0} q - C_{m_{\dot{\alpha}}} \frac{c}{2V_0} \dot{\alpha}$$

$$= \frac{\partial C_m}{\partial \delta_e} (A_1\theta + A_2\alpha + A_3\hat{u} + \ldots A_m q + \ldots A_n \dot{q} \ldots) \qquad (13.11)$$

and is a linear equation with constant coefficients.

A supplementary entry into the computer is necessary because of the introduction of the term $(\partial C_m/\partial \delta_e)A_1\theta$ (Fig.141).

The other entries already exist, and it suffices to replace the coefficient C_{m_α} by $C_{m_\alpha} + (\partial C_m/\partial \delta_e)A_2$, etc.

The same modifications are carried out in the equations for lift and drag.

By introducing into the integrator some initial perturbations represented by the initial values of the variables α_0 , θ_0 , ... , the computer immediately gives the return movement so that it is possible to determine the best methods of control for improving the return and producing artificial stability.

An important remark

The preceding equations are only applicable to the study of motion in a steady atmosphere.

In a disturbed atmosphere, it is necessary to make the distinction between the real angle of attack or side-slip and the apparent angle.

If it is required to obtain the response to an atmospheric perturbation, it is necessary to introduce the excitation produced by this perturbation.

Finally, if we are studying a control equation containing the angles α and β , it will be necessary to specify whether the perturbation detectors are sensitive to the errors in the real angles α_r and β_r determined by the position of the relative velocity vector, or the apparent angles α and β determined by the position of the true velocity vector. Some comments on these points will be found in Part IV.

13.3 THE PHYSICAL ACTION OF VARIOUS ELEMENTARY CONTROL EQUATIONS

All control equations which make the angle of deflection depend on only one variable are known as 'elementary control laws'.

It is easy to verify from the analogue computer that the effect of different elementary laws is as follows:-

13.3.1 Longitudinal Motion

The action of the elevator is always defined by $\partial C_m/\partial \delta_e < 0$.

Variable θ

The positive coefficient A_1 makes the aircraft return to a constant attitude. It assures stability of position (or of attitude). The term in θ placed in the first member becomes $-(\partial C_m/\partial \delta_e)A_1\theta$ and is positive.

It was established by Klemin, Perrer and Wittner, before the analogue computer was ever used, that this term strongly increases the damping of a phugoid, but that it diminishes the damping of a rapid oscillation[16]. Tests with the analogue computer have always confirmed this.

Variable α

A positive factor A_2 has the effect of making, in an artificial manner, the C_{m_α} of the aircraft more negative.

Control as a function of α makes it possible to compensate for an instability due to a negative static margin (that is to say, $C_{m_\alpha} > 0$).

Applied to an aircraft having sufficient static margin, this type of control always diminishes the period of a rapid oscillation. It acts weakly on a slow oscillation in the sense that it diminishes the damping.

This type of automatic pilot, which was recommended many years ago, is no longer used, because of the difficulty in measuring the perturbations of the angle of attack.

Variable $u/V_0 = \hat{u}$

If it is desired to make the aircraft dive when the speed u decreases, it is necessary to make $A_3 < 0$. This intervention diminishes the period and the damping of the phugoid oscillation.

Variable $\dot{\theta} = q$

The control equation

$$\delta_e = A_5 q$$

increases the damping of the rapid oscillation for A_5 positive, but opposes the execution of commanded manoeuvres.

Variable $\dot{u}/V_0$

The control equation $\delta_e = A_7(\dot{u}/V_0)$, with $A_7 < 0$, strongly damps the slow oscillation.

Variable load factor n

The load factor n is related to the generalized acceleration, thus:

$$n = -\frac{a_z}{g} = -\frac{j_z - g_z}{g} \qquad (13.12)$$

It can also be expressed as a function of the variation in the trajectory angle γ (when Θ and Φ are zero):

$$n = 1 + \frac{V}{g}\frac{d\gamma}{dt} = 1 + \frac{V}{g}(q - \dot{\alpha})$$

The increase in the load factor is a consequence of an increase in lift, that is to say, an excessive angle of attack. From this we can expect that the control function including the load factor n, realizing a law $\delta_e = A_n(n - 1)$ with A_n positive, will improve the motion belonging to the rapid oscillation when the static margin is insufficient. It can be stated that this is true (see Section 13.6.1.1).

It is possible to consider the control function of $(n - 1)$ as a control consisting of two components proportional respectively to q and to $-\dot{\alpha}$. The first increases the damping of the rapid oscillation in a straightforward manner. The second also will influence the rapid oscillation, but it will act as a control in α with a phase lag of $\pi/2$.

Variable $\dot{q} = \ddot{\theta}$

The control equation $\delta_e = A_n\dot{q}$ acts as a modification in the moment of inertia of the aircraft. A factor $A_n < 0$ artificially produces a decrease in this moment, and in consequence diminishes the period of the rapid oscillation.

Variable $\delta_e = A_4 z$

With the sign convention adopted, an error in the altitude z is measured on an axis directed downwards. A control equation

$$\delta_e = A_4 z$$

will be favourable for the maintenance of the altitude when A_4 is negative. The use of such a control equation is disastrous on the damping of the slow oscillation (see Section 20.6).

13.3.2 Lateral Motion

Each control surface exercises two effects: a principal effect defined by

$$\frac{\partial C_l}{\partial \delta_a} \quad \text{and} \quad \frac{\partial C_n}{\partial \delta_r}$$

and a secondary effect defined by

$$\frac{\partial C_l}{\partial \delta_r} \quad \text{and} \quad \frac{\partial C_n}{\partial \delta_a}$$

The principal effect always corresponds to

$$\frac{\partial C_l}{\partial \delta_r} < 0 \quad \text{and} \quad \frac{\partial C_n}{\partial \delta_a} < 0$$

The sign of the secondary effects is not fixed in an invariable manner. However, we generally have $\partial C_l/\partial \delta_r > 0$ because the vertical tail unit is always situated above the axis OX.

Except for special precautions in the design of the ailerons we also have $\partial C_n/\partial \delta_a > 0$, which is an unfavourable characteristic and must be diminished.

Each of the interesting variables in lateral stability can be utilized to actuate either the ailerons or the rudder. Thus there are many possible combinations.

Again, the effect of certain elementary control laws may depend on the characteristics of the aircraft. Here we shall indicate only the effect of the most important combinations.

Variable φ

Actuating the ailerons with $A_3 > 0$ is a mode of control which allows the wings to be brought back quickly to the horizontal, but does not assure course stability.

Actuating the rudder with $B_3 > 0$, the response is favourable or unfavourable, in the same aircraft, according on the value of the coefficient B_3.

Variable ψ

Actuating the ailerons with $A_1 > 0$, this control renders the aircraft unstable in the case dealt with in Part IV, but the result may be different if the aircraft can be represented by another transfer function.

Actuating the rudder with $B_1 > 0$, the control equation $\delta_r = B_1\psi$ completely alters the behaviour of the aircraft and produces course stability. The motion of the aircraft allows two different oscillations of which an example is studied in Part IV.

Variable β

The action on the ailerons, $\delta_a = A_2\beta$, with $A_2 > 0$, is identical to making Cl_β more negative, that is to say, to an increase in the dihedral of the wing. It diminishes the tendancy to spiral instability, but can aggravate the oscillation known as Dutch roll.

The action of the rudder, $\delta_a = B_2\beta$, with $B_2 < 0$, is identical to making Cn_β more positive, that is to say, to an increase in weathercock stability. This mode of control would be able to cope with side-slip, but the rudder deflection proportional to β diminishes the damping of the Dutch roll and increases the tendency to snacking. Also it tends to favour spiral instability.

Variable $p = \dot{\varphi}$

The aileron deflection given by $\delta_a = A_7\dot{\varphi}$ with $A_7 > 0$ increases the damping. When flying at the angle of attack of normal flight, this damping is sufficient for an aircraft having classic configuration and must not be augmented.

The deflection of the rudder, $\delta_r = B_7\dot{\varphi}$ with $B_7 > 0$, will advance the wing which is dipping; the calculation shows that such an effect is not important.

Variable $r = \dot{\psi}$

The deflection of the rudder $\delta_r = B_5 r$ with B_5 positive, ameliorates the yaw damping coefficient and effectively contributes to the damping of the Dutch roll. In a turning manoeuvre the effect is nevertheless harmful, as the movement of the rudder then opposes the turn.

Variable $a_y = j_y - g_y$

The following balance of forces:

$$mj_y = Y + mg_y \tag{13.13}$$

shows us that the measured acceleration $a_y = j_y - g_y$ is proportional to the transverse aerodynamic force Y.

In the absence of a rudder deflection this force can be due only to a transverse slip, caused by

$$\Delta C_y = \frac{\partial C_y}{\partial \beta}\beta \tag{13.14}$$

The measurement of the transverse acceleration made at the centre of gravity can serve as a slip detecting device and the control as a function of the transverse acceleration will give results resembling those furnished by the control as a function of the side-slip.

Variables $\dot{r}$ *and* $\dot{p}$

As in the case of the longitudinal motion, the use of control signals consisting of second derivatives of the position angles has the same effect as the modifications on the moments of inertia.

13.4 ACTUAL REALIZATION

The controls may be:

(a) simple positioning controls

(b) controls requiring an integration.

13.4.1 Positioning Servo-Controls

In numerous cases, the device producing the artificial stability reduces to a positioning servo-mechanism whose object is to displace the control surface to a position δ determined by an error signal

$$\delta = A\epsilon'$$

This error signal may be a composite signal formed by the sum of several error signals, viz.

$$\epsilon' = \frac{1}{A}(A_1\theta + A_3\hat{u} + A_5\dot{q}) \tag{13.15}$$

In Section 12.7, we studied the operation of some systems permitting the determination of the position of a control surface as a function of an input of order x. The transfer functions so found remain valid when the input is an error signal ϵ'.

The arrangement utilized always consists of a feed-back signal δ/A which must be subtracted from the error signal ϵ' in order to produce the variable

$$\sigma = k\left(\epsilon' - \frac{\delta}{A}\right) \tag{13.16}$$

which characterizes either the position of the slide valve of the jack or the voltage fed to the armature of the electric motor.

This subtraction can be made in a more refined manner than that described by Figure 115. For example, if only one error signal is utilized, it is possible to perform the subtraction

$$\epsilon' - \frac{1}{A}\delta$$

by making the reaction act on the instrument which measures the error signal. The well known scheme of the Sperry A3, truly the ancestor of the attitude course holding automatic pilots, is a typical example of this mode of operation: the feed-back acts on the zero of the error detector (Fig. 142).

The theory of servo-mechanisms shows that one is often interested in using a compounded signal, formed by the error in the variable one wishes to stabilize plus its derivative. The feed-back signal must only interest the variable to be stabilized; the signal representing the derivative will be naturally annulled when an equilibrium state is established.

The use of a signal proportional to the integral of an error, frequently encountered in automation, is more rare in aircraft control problems.

The error signals furnished by the instruments detecting the perturbations possess very little energy and must be amplified. This amplification, as in the case of the eventual combination of several different signals, is made easier when the signals are presented in the form of electrical voltages.

Control by means of a hydraulic jack

When a jack is used as the motor, it is necessary to transform the electrical signal into a displacement of the distributor, and this can be done by using a servo-valve.

Two schemes for servo-valves are indicated. One (Fig. 143) is an on-or-off device; the other (Fig. 144) acts in a more progressive manner. They ensure the proportionality between the deflection and the error signal ϵ' with the same restrictions as those we have given for the mechanically controlled jack. Their transfer function can be simulated as indicated in Section 12.7.

By means of a preliminary evaluation of the effect of a given control equation, it is often found sufficient to use a transfer function of first order.

The control equation, incorporating the characteristics of the jack, contains a time constant a :

$$\delta_e + a \frac{d\delta_e}{dt} = A_1 \theta \tag{13.17}$$

It becomes, in symbolical writing,

$$\delta_e(s)[1 + as] = A_1 \theta(s) \tag{13.18}$$

and determines a transfer function

$$G(s) = \frac{1}{1 + as} \tag{13.19}$$

If we wish to introduce into the control equation the error in θ and its derivative, we get:

$$\delta_e + a \frac{d\delta_e}{dt} = A_1 \theta + A_5 \dot{\theta} = A_1(\theta + b\dot{\theta}) \tag{13.20}$$

This becomes:

$$\delta_e(s) = A_1 \left[\frac{1 + bs}{1 + as}\right] \theta(s) \tag{13.21}$$

Control by an electric motor

The transfer function defined in Section 12.7 is valid when the order x is any compound signal ϵ', provided that the assumptions made in 12.7 remain valid.

The deflection is related to the error signal by:

$$\delta(s) = G(s) \left[\frac{1}{1 + AR \dfrac{k_5}{k_1 k_3}}\right] Ax(s) \tag{13.22}$$

with $$G(s) = \frac{\omega_n^2}{s^2 + 2\zeta\omega_n s + \omega_n^2} \tag{13.23}$$

The simplest cases are those where the error signal is a function of a single variable, or of a variable and its derivative.

When we want to obtain

$$\delta_e = A_1\theta + A_5\dot{\theta} = A_1(\theta + b\dot{\theta}) \tag{13.24}$$

the servo-mechanism gives, in reality,

$$\delta_e(s) = G(s)\ (1 + bs)\left[\frac{1}{1 - A_1 R\,\frac{k_5}{k_1 k_3}}\right] A_1\,\theta(s) \tag{13.25}$$

13.4.2 Control Involving an Integration

Let us examine a completely different method. An electric motor, with independant excitations, is fed with a voltage proportional to this error signal ϵ', and actuates the distributor of a jack control by displacing the point A (Fig.145).

The jack includes a feed back device ensuring the proportionality between the displacement of the piston and that of point A.

If the resisting couple is zero, the speed of rotation of the motor is proportional to the voltage as soon as the steady régime is attained. This can be obtained if the moment of inertia J_m is small. Consequently, the speed of displacement of the piston is proportional to the error:

$$\frac{d\delta}{dt} = k\epsilon'$$

One gets, indirectly, a positioning servo-motor for the variable θ, if the signal ϵ' is proportional to the derivative $\dot{\theta}$, for we then have:

$$\frac{d\delta_e}{dt} = k\,A_5\dot{\theta} \tag{13.26}$$

$$\delta_e = k\,A_5\theta + C \tag{13.27}$$

The constant of integration is zero if there is no initial error.

In practice, the resisting couple is not zero, because of friction in the distributor. Moreover, the displacement of the piston is related to the displacement of the point A by the transfer function of the jack. The result indicated above is only valid to a first approximation.

The equations that determine more precisely the deflection of the control surface as a function of the signal may be established easily, taking account of the preceding discussion.

13.5 ANALOGUE STUDY OF REAL CASES

It has been assumed until now that the error of a variable was detected instantly, and that the control mechanism alone was responsible for the delay.

If the analysis is carried further, it is established that the sensor may also produce a delay. The measuring instrument used as an error detector necessarily has a time constant, but generally the delay introduced by the sensor is significantly less than the delay introduced by the servo-control and the transfer function of the sensor may be incorporated in that of the servo-mechanism. Nevertheless, two cases require deeper study:

(a) When one utilizes a composite signal, formed of the sum of several elementary signals furnished by measuring instruments having very different time constants;

(b) When one utilizes an error signal whose detection introduces, by its very principle, a time constant that is relatively important.

With these reservations, one establishes that the analogue computer permits the study of artificial stabilization in conditions that approach very nearly those of the real case. The composite signal of the type

$$\epsilon' = \frac{1}{A}(A_1\theta + A_2\alpha + A_3\hat{u} + ...) \qquad (13.28)$$

may be calculated from the output of the network representing the aeroplane; an analogue representation of the servo-mechanism's transfer function may be introduced between this composite error signal and the voltage representing the control deflections.

The transformation of the error signal into an electrical signal, normally achieved in all modern automatic pilots, opens the door to all the manipulations (one may say sophistications) of signals that it is possible to make, by means of correcting loops, on electrical signals. These manipulations are easy to simulate on the analogue computer. Some of them will be examined here.

13.5.1 Phase Advance

Application of the theory of servo-mechanisms to the aeroplane shows that the aeroplane returns more easily to the imposed trim θ_i when the command δ_e that is given to it possesses a phase advance over the error $\epsilon' = \theta - \theta_i$, to be corrected. The addition of a signal proportional to the derivative produces this phase advance.

The recourse to signals represented by electrical voltages permits one to obtain the composite signal

$$\epsilon' = A_1\theta + A_5\dot{\theta}$$

simply by the detection of the error θ by a position gyroscope, without it becoming necessary to measure the signal $\dot{\theta}$ by a rate gyro. In principle, it is sufficient to derive the signal θ, and to add to the original signal the derivative $\dot{\theta}$, multiplying θ and $\dot{\theta}$ by the coefficients A_1 and A_5, respectively. The resulting signal:

$$\epsilon' = A_1\theta + A_5\dot{\theta} = A_1\left(1 + \frac{A_5}{A_1}\,s\right)\theta \qquad (13.29)$$

has, with regard to θ, a phase advance that is a function of the frequency ω considered, and is equal to:

$$\mathrm{tn}^{-1}\,\frac{A_5}{A_1}\,\omega$$

The exact derivation of a variable may be made only by an active network, similar to that considered in Section 5.3.3. Such a network gives noise and the output must be filtered; this action alters the transfer function.

For an automatic pilot, one is generally satisfied to use passive networks whose purpose is not to achieve the exact derivation, but only to obtain a signal with a phase advance approaching the correct result.

For example, the network described in Figure 146 relates the input signal θ (voltage E_1) to the output signal (voltage E_2) by a transfer function

$$G(s) = \frac{1}{b}\left(\frac{1 + abs}{1 + as}\right) \qquad (13.30)$$

where $b = 1 + \dfrac{R_1}{R_2}$

$$a = \frac{R_1 \times R_2}{R_1 + R_2}\,C$$

Such a correction loop is often placed in the aeroplane between the error signal furnished by the detector and the input to the servo-motor.

The deflection δ and the error θ are then related by the products of the transfer functions of the loop and of the servo-mechanisms.

In the case of a servo-motor defined by a transfer function of the second order, the product of the transfer function will involve terms of the 3rd order in the denominator.

This would not be the case if the correction loop had only a derived signal added to the initial signal.

When one considers only low frequencies the 3rd order term in the denominator may be neglected in the calculation of the effect of such a device.

13.5.2 Filtration

It may be necessary to filter the signals in order to eliminate high-frequency oscillations caused, for example, by lack of precision of the detectors. A filter loop composed only of passive elements is represented in Figure 147.

The transfer function is

$$G(s) = \frac{E_2}{E_1} = \frac{1}{1 + as} \tag{13.31}$$

with $a = RC$.

This is the simplest filter one can imagine. Its action is based on the time constant it involves.

13.5.3 Progressive Attenuation of the Signals

The progressive attenuation, or the suppression of the signal ϵ with time, will require the subtraction from ϵ of a quantity $[1/(A + as)]\epsilon$. The transfer function is then:

$$G(s) = \left(1 - \frac{1}{1 + as}\right) = \frac{as}{1 + as} \tag{13.32}$$

Since the control equations

$$\delta_e = A_5\dot{\theta}$$

$$\delta_r = A_5\dot{\psi}$$

are favourable for the damping of transient perturbations, but have a harmful effect upon the execution of controlled manoeuvres, one sometimes introduces into the control equation a factor $as/(1+as)$ in order to produce the progressive decay of the response.

13.5.4 Progressive Attenuation of the Feed-Back

In some cases one reduces the feed-back signal with time. To understand the purpose of such an operation, one must remember that the effect of the feed-back signal is to make the response of the servo-mechanism proportional to the excitation, and that this purpose is effectively accomplished when the transfer function is unity.

The attenuation of the feed-back signal is the same as a progressive increase of the response to signals of long duration, but it has no effect when the excitation is of short duration. Such a solution has been used in the scheme referred to in Section 13.9.1.

13.6 APPLICATION

A considerable number of problems dealing with automatic control have been carried out on the analogue computer. Their results are rarely published, however, because they generally deal with specific cases. Nevertheless, we cite below some examples of response calculations by the resolution on an analogue computer, of systems formed by the combination of the equations of motion of the aircraft and the control equations.

13.6.1 Longitudinal Movement

13.6.1.1 Aircraft with Dynamic Characteristics Defined by Linear Equations (Linear Control Equations)

(A) *Control as a function of the error in the attitude condition* θ

In Figure 148 we indicate the control set-up for the automatic control of the aircraft whose behaviour with locked control has been studied in Section 10.1.1.3.

The consecutive movements for an initial error in the variable θ have been calculated for the following control equations:

(a) $\delta_e(s) = G(s)\, A_1\, \theta(s)$

with the transfer function of the mechanism $G(s)$ equal to unity and 4 different values of A_1 equal to 0.02, 0.05, 0.10, 0.20 (see Figs.149a and b).

(b) The same equation but with

$$G(s) = \frac{1}{1 + as}$$

The time constant introduced, a, had a considerable value: $a = 5$ seconds (see Figs. 50a and b).

(c) $(s) = G(s)[A_1\theta(s) + A_5 q(s)]$

with the transfer function equal to unity, the same values of A_1 but only one value of A_5, viz., $A_5 = 1$ (see Figs.151a and b).

(d) The same equation as in case (c), but again with

$$G(s) = \frac{1}{1 + as}$$

and $a = 5$ (see Figs.152a and b).

The evolution of the variables $\hat{u}$, α, θ, q, $(q\text{-}\dot{\alpha})$ and δ_e have been recorded and reproduced in the figures mentioned above. The variable $(q\text{-}\dot{\alpha})$ defines the load factor n:

$$n = 1 + \frac{V}{g}(q - \dot{\alpha}) = 1 + 11.3(q - \dot{\alpha}) \qquad (13.12)$$

In the 4 cases, the initial condition has been introduced by charging the condenser in the integrator: $\theta = \int q\, dt$. In cases (a) and (c), the switch $\mathfrak{I}_2$ was always closed.

The voltage corresponding to the initial condition, applied to θ at an instant $t < 0$ before the start of the calculation, was also applied to $\delta_e = A_1\theta_0$. The beginning of the calculation was commanded by the simultaneous opening of the 4 switches $\mathfrak{I}_1$ at $t = 0$.

The registration of δ_e gives the diagram represented by the continuous line, but the phenomenon corresponds physically to that which would be produced if the voltage θ_0 were applied suddenly at the instant $t = 0$. The voltage δ_e would have to pass instantaneously from 0 to δ_e following the interrupted line added to the recorded diagram.

In cases (b) and (d), the element producing the time constant a plays an important role when the calculation starts: the switch $\mathfrak{I}_2$ is synchronized with the switches $\mathfrak{I}_1$ but shuts when they open; the diagram represented by the continuous line then describes the real evolution of the voltage representing the deflection.

Comparison of the diagrams of case (a) with the response of the aircraft flying with blocked controls, for the same perturbation (Fig.72), brings into existence a progressive amelioration in the damping of the slow oscillation. A positive initial error θ instantaneously entails a positive deflection δ_e which increases the tail lift and produces a nose-down moment. This increase in tail lift manifests itself for all values of A_1 by the appearance of a positive load factor n and an initial decrease of the incidence. As might be expected, the effects are proportionately greater as A_1 is increased.

A part of the initial response belongs to the short-period oscillation; this movement is proportionately more marked as the coupling coefficient A_1 is increased.

The speed of recording has been chosen with a view to allowing a good registration of the long-period oscillations, but it harms the examination of the rapid oscillation.

Comparison of the diagrams for case (b) with those for case (a) shows the effect of the time constant a ; this has been chosen particularly high in order to emphasize the difference between the results.

The application of a slower deflection produces some visible effects in the curves.

Comparison of diagrams (c) with diagrams (a) shows the effect of adding into the control equation a component $\delta_e = A_5 q$ where A_5 is constant. The period of the slow oscillation is increased. The importance of movements depending on the short-period oscillation diminishes.

Finally, in the diagrams (d), the time constant cuts the peak of the curves representing the deflection; this again produces a decrease in the effects of the short-period oscillation.

(B) *Control as a function of acceleration*

The aircraft studied above represented a value of $C_{m_\alpha} = -0.72$. We have supposed the static margin to be lowered, the C_{m_α} derivative becoming respectively:

$$C_{m_\alpha} = 0 \quad \text{and} \quad C_{m_\alpha} = +0.167$$

We have analysed the action of an automatic pilot sensitive to the acceleration:

$$\delta_e = A_n \frac{V}{g} (q - \dot{\alpha}) = K(q - \dot{\alpha}) \tag{13.33}$$

The beginning of the response succeeding to a perturbation $\Delta\alpha = \Delta\theta = 0.1$ radian is indicated in Figure 153 for the aircraft with $C_{m_\alpha} = 0$ and in Figure 154 for the aircraft with $C_{m_\alpha} = +0.167$.

The registered variables are $\hat{u}$, α , θ and δ_e with a control equation consisting of a transfer function $G(s) = 1$ and the values of k indicated below:

$k = 0$ (blocked control)

$k = 0.10$ sec

$k = 0.25$ sec

$k = 0.50$ sec

$k = 1.00$ sec.

We notice that this kind of control clearly diminishes the instability of the motion.

13.6.1.2 Aircraft with Non-Linear Aerodynamic Characteristics

The NACA study for aircraft with non-linear characteristics[8] has been extended to the case of an aircraft for which C_m varies as indicated in Figure 96. The short-period oscillation was studied with an automatic pilot sensitive either to the angle-of-attack error and giving $\delta_e = A_2(\alpha - \alpha_i)$ or to the attitude error giving $\delta_e = A_1(\theta - \theta_i)$. In both cases, $A_1 = A_2 = +1$, and $\partial C_m/\partial\delta_e = -1.045$.

The artificial stability $(\partial C_m/\partial\delta_e)(d\delta_e/d\alpha)$ caused by the first control equation, produces a total $dC_m/d\delta_e$ equal to

$$\frac{\partial C_m}{\partial \alpha} + \frac{\partial C_m}{\partial \delta_e} \frac{d\delta_e}{d\alpha}$$

which, being equal to 0.465, remains in excess of the limit of instability in the range -2° to $+2^o$. Nevertheless, when the assigned value of α_i indicated at the automatic pilot, is carried suddenly from 0° to 1°, there is a sudden change in C_m , equal to

$$\Delta C_m = \frac{\partial C_m}{\partial \alpha} \alpha + \frac{\partial C_m}{\partial \delta_e} \frac{d\delta_e}{d\alpha} (\alpha - \alpha_i)$$

or $$\Delta C_m = \frac{1.045}{57.3} \quad \text{for} \quad \alpha_i = 1^\circ \text{ and } \alpha = 0^\circ$$

The curve giving C_m as a function of α is represented by the interrupted characteristic shown in Figure 96. It shows that the equilibrium position is displaced and is found at $\alpha = 2.5^\circ$, that is to say in a range where the stability is assured. Figure 155 indicates the evolution produced by $\Delta\alpha_i = 1^\circ$.

When the second control equation is used, the application of $\theta_i \neq 0$ does not modify C_{m_α} but introduces a disturbing moment

$$\Delta C_m = \frac{\partial C_m}{\partial \delta_e} \frac{d\delta_e}{d\alpha} (\theta - \theta_i)$$

The analogue computer makes a sustained oscillation appear. Figure 156 represents the oscillation produced by $\theta_i = 0.7^\circ$.

The appearance of this sustained oscillation due to the action of a position stabilizer on an aircraft which is unstable due to non-linear aerodynamics, constitutes a danger which, by using an analogue computer, we can examine in advance.

13.6.2 Lateral Motion

(1) *The effect of elementary control equations*

Results of calculation, for some elementary control equations utilizing error signals in ϕ and ψ , are given in Sections 17.5 and 17.6.

(2) *Amelioration of the characteristics of the aircraft F 86E*

Among the studies for which results have been published is a research report by Porter[17] relating to the artificial stabilization of the lateral movement of the F 86E.

The tests covered extended combinations in speed and altitude. The original report contains an indication of the values of the aerodynamic coefficients corresponding to the different cases studied.

Different control equations are proposed; their efficiency is estimated by the effect which they exert on an arbitrarily chosen input, in this case an input in the form of a pulse applied to the ailerons. We have extracted from the report the figures relating to the aircraft flying at a Mach number of 0.8 at 10,000 ft, and at a Mach number of 0.6 at 35,000 ft. The angle of attack in the second case exceeds the angle of attack corresponding to the first case by 10.2° (Fig.157).

The principal axis of inertia OX is directed between the velocity vectors corresponding to the two flight conditions. This means that it is directed beneath the

velocity vector in the first case and above it in the second case.

The aircraft has been excited by an aileron deflection δ_a and the response has been calculated for three different manoeuvres of the rudder corresponding to:

$$\delta_r = 0 \qquad \text{(locked rudder: Figs.158 and 161)}$$

$$\delta_r = G(s)[0.065a_y + 0.3\dot{\Psi}] \qquad \text{(Figs.159 and 162)}$$

$$\delta_r = G(s)\left[0.20a_y + \frac{s}{s+1}\dot{\Psi} - 0.25\dot{\Phi}\right] \qquad \text{(Figs.160 and 163).}$$

The transfer function $G(s)$, relating the combined error signal to the deflection δ_r, was a transfer function of 2nd order:

$$G(s) = \frac{\omega_n^2}{s^2 + 2\zeta\omega_n s + \omega_n^2} \tag{13.34}$$

for which the damping term ζ was 0.7 and the frequency without damping, ω_n, was 20 rad/sec.

The unpiloted aircraft presents, at the altitude indicated, a slightly damped oscillation which we want to eliminate.

By consequence of the position of the principal axis of inertia, the response in side-slip presents a first peak, in one sense or another, following the angle of attack of the aircraft. The two control equations proposed suppress the oscillation but the first does not lead to a sufficiently rapid disappearance of the side-slip. The second succeeds in doing this.

13.6.3 Non-Linear Automatic Pilotage

In principle, all pilots using a jack as prime mover are non-linear, but the approximation indicated in 12.7.2, which consists of utilizing a transfer function of first order, makes the equation defining the phenomenon linear.

The study of the control of the aircraft by linear relations suggests that in certain cases some essentially non-linear on-off elements could be used with success.

The simulation of such mechanisms is not studied here, but it is possible by utilizing the non-linear computing elements described in Chapter 2.

The use of elements using diodes permits the introduction of thresholds, the consideration of controls whose deflection is limited by a stop, and the use of on-off controls. Generally speaking, it permits the reproduction of the control equations corresponding to highly non-linear servo-mechanisms.

13.7 PARTIAL SIMULATION

The juxtaposition of an analogue computer integrating the equations of the aircraft, and a simulated cockpit containing a control column, pedals, etc., on which the human pilot acts, gives rise to some varied combinations which are known as flight simulators.

Similarly, the juxtaposition of an analogue computer representing the aircraft and of a mobile table subjected to movements reproducing the variables: p , q , r , Ψ , θ , Φ gives rise to some combinations permitting the study of an automatically piloted aircraft, by utilizing some elements of the real automatic control systems.

A mobile table, suspended by means of a universal joint, can be made to occupy at all instants the position Ψ , θ , Φ corresponding to that of the aircraft, if one realizes the necessary links between the motors controlling the 3 axes of the mobile table, and the output voltages p , q , r of the computer representing the aircraft.

By placing the position error detectors or the angular velocity sensors on such a table, it is possible to put into action all the apparatus of automatic control.

Again, it appears possible to make the servo-motors act on axes subjected to opposing moments, which should equal the values of the control hinge moments.

By measuring the angular displacements of the axes representing the control hinges, transforming the δ's thus measured to electrical voltages and re-injecting these voltages into the analogue computer, one can simulate the flight of an automatically piloted aircraft without having to simulate the components constituting the automatic pilot by their transfer function. The possibilities outlined here have been applied in some particularly well equipped laboratories.

It is important to note that the realization of such arrangements gives rise to some very delicate problems, the study of which goes beyond the scope of this paper. Note that it is necessary for the response of the table to be governed by transfer functions very little different from unity for fear of introducing experimental errors which can be greater than the errors eliminated by utilizing the components of the automatic pilot itself in place of computer elements.

The existence of a mobile table, created by makers of gyroscopes and used for the calibration of these instruments, has contributed to the realization of the equipment mentioned here.

13.8 THE USE OF THE MANUAL CONTROL WHEN AN AUTOMATIC PILOT IS IN ACTION

13.8.1 Classification

The human pilot must always be able to impose his will on the aircraft, even when the control surfaces are under the action of the automatic pilot. The human pilot must literally pilot through the automatic pilot.

Because of this it is necessary to combine the action of both the human and the automatic pilots. We will suppose here that the automatic pilot involves a jack, the valve of which is displaced as a function of the error signals received.

Following the relative disposition of the manual control and the automatic control, we are able to achieve three types of control:

(1) Controls in parallel

(2) Controls in series or differential

(3) Controls without direct connection between the pilot and the control surface.

These controls are characterized as follows.

(1) *Controls in parallel*

The control stick (or the pedals) are tied to the control surfaces by the usual linkages, but a hydraulic jack acting directly on the control surfaces is mounted in parallel with the control stick. This jack is commanded automatically as a function of the error signals (Fig.164). The pilot is aware of the action of the automatic mechanism because he sees the control stick and the pedals moving in front of him.

The pilot is not able to act directly on the control surfaces when the automatic pilot is functioning, because of the irreversibility of the jack; he must act indirectly in commanding the displacement of the jack, through the automatic pilot.

The pilot can, of course, take direct control by putting the jack out of service (disengage or connect together both sides of the piston).

We must always remember that if the control is made by a reversible element (an electric motor, for example), instead of by a jack, the pilot has the possibility of opposing the action of the automatic pilot by exerting a greater effort than the servo-motor.

Controls in parallel are the first which have been used. The different types are differentiated one from another by the manner in which the pilot is able to act on the servo-control.

(2) *Differential or series control*

The control surface is subjected to 2 commands: a deflection command δ_1 produced by the displacement δ_s of the manual control of the usual type, and a deflection command δ_2 produced by the jack actuated by the automatic pilot.

These two commands are combined by means of an adding device, and produce the real deflection

$$\delta_e = \delta_1 + \delta_2 \tag{13.35}$$

There exist several different methods of obtaining the algebraic sum of 2 displacements:

(a) Half the algebraic sum of two angular displacements can be obtained by a well known piece of apparatus: the differential. This is why the control described here may be called 'control by differential' or more simply, differential control.

(b) The same result can be obtained by inserting the jack in the control linkage, that is to say by placing the controls in series. A command is then transmitted by a variation in the length of the linkage (Fig.165).

In principle, the jack must displace the control surface and not the control stick. This result will be obtained only if the pilot opposes the displacement of the control stick by exerting a reaction. The pilot is then aware of the functioning of the servo-mechanism by the reaction he must apply in order to keep the control stick stationary. There is never a fixed relation between the position δ_s of the control stick and the displacement δ_e of the control surface.

(c) In a perfect differential control the displacement δ_2 would be added to δ_1, unknown to the pilot. In principle a simple means of adding the two actions δ_1 and δ_2 without interference would consist of splitting the control surface into two independent parts, and applying a command to each part. This procedure is hardly used, as a displacement of the control stick in the inverse sense cannot cancel a command δ_2. The command δ_2 leads to a deflection actually applied and the pilot can only cancel its effect by applying an opposing deflection δ_1 on the part of the control surface which he controls himself. It is clear that such a combination is unfavourable from the aerodynamic point of view.

We shall see later that the differential control can be completed by an action exerted by the pilot on the servo-control. In this case, the displacement δ_s of the stick produces not only the deflection δ_s imposed by the actual linkage but also actuates the jack in view of producing a deflection δ_2 to complete the action of δ_1.

(3) *Control without direct connection between the control stick and the control surfaces*

The pilot cannot directly control the displacement of the control surface. He can only control the valve of the jack concurrently with the automatic pilot.

Let us examine in more detail these three types of control, looking for, in particular, the methods by which the human pilot uses the automatic pilot to execute his orders.

13.8.2 Controls in Parallel

This method is the oldest and is only used with position automatic pilots. These autopilots fix the orientation of the aircraft in space by stabilizing the three angular coordinates Ψ, θ, Φ. The pilot imposes on the mechanism, by regulating the auto-pilot, the values of Ψ_i, Θ_i, Φ_i that must be maintained throughout the flight. These values are the inputs.

He then puts the aircraft in the required attitude by means of the normal manual controls and puts the automatic pilot in action when the error between the actual situation and the required situation is zero or insignificant. Once the automatic pilot is working the pilot no longer acts on the controls; he sees them moving in front of him. Such a procedure is known as 'autopilotage'.

The obligation of placing the aircraft in the exact orientation corresponding to the required values of Ψ_i , θ_i , Φ_i at the moment of switching to the automatic pilot is no longer required in modern equipment, if auxiliary units known as synchronizers are used. These devices act on the values of the reference variable, making them equal to those experienced by the aircraft during the time that the automatic pilot is not in service. One thus avoids the violent changes that would be produced by a difference between the actual values and the required values at the moment of the change in control.

The regulating devices are, in principle, cursor buttons, the displacements of which modify the input values of Ψ , Θ , Φ . Any change in the input values whilst in flight produces error signals and consequently control deflections, the effect of which is to produce transitory movements by which the aircraft passes from the old to the new, required value. With appropriate dispositions (for example, lag producing devices), it is possible to impose on the aircraft sufficiently progressive and damped movements for control by the manipulation of buttons to be realized in practice. Commands given in this manner are able to affect pitch, roll and yaw.

The two buttons controlling the pitch and the roll have been combined to form a control with two degrees of freedom, resembling the control stick. This control is sometimes called 'side stick'.

Artificial-feel moments, which produce a reaction in the pilot's hand, have even been applied on this auxiliary stick. This system, largely used around 1945, is tending to disappear, as it possesses certain drawbacks. One of these is the difference in action between the auxiliary stick and the main control stick.

The displacement $\delta_{s,a}$ of the auxiliary stick changes the input value θ_i and produces a deflection δ_e proportional to the difference $\theta - \theta_i$, while the displacement δ_s of the main stick produces a deflection proportional to δ_s .

The responses of the aircraft are different. The displacement of the auxiliary stick produces, after a brief delay, a response in attitude, while the displacement of the main stick produces in the first few seconds following its movement, a response in rate of pitch.

The commands given to the automatic pilot need not come from the cursor buttons or the auxiliary stick. It is possible to act on the automatic mechanism by an action exerted on the control stick itself. It is sufficient to measure, using an ad hoc dynamometer, the force exerted by the pilot on the control stick, and to send the signal thus produced to the automatic pilot.

The operation that consists of controlling the automatic pilot in an analogous manner to that of the pilot using direct control, is called the 'manoeuvre demand'.

In the schematic representation of Figure 166, the effort F applied by the pilot to the normal control is measured by a pick-up and transformed into a signal x proportional to F (x assumed positive when the pilot pushes the control stick forward). This signal is added algebraically to the error signals in attitude and rate of pitch produced by the attitude-holding automatic pilot.

The servo-motor produces, because of the classical feed-back coupling, a deflection

$$\delta_e = G(s)[kx + A_1\theta + A_5 q]$$

and all that happens is that the attitude input, instead of being $\theta_i = 0$, becomes $\theta_i = -(k/A_1)x$. As soon as the pilot ceases to apply the effort F on the control stick, the required value is $\theta_i = 0$ again and the aircraft returns to its original position.

Such a response from the aircraft is not generally considered satisfactory. It would be preferable if the aircraft, having been brought to the attitude θ_i by the effort F, would remain there without it being necessary to continue to apply the effort F. This can be made possible by employing a supplementary device; as soon as the pilot acts on the stick, an integrator of the angular speed q is put into action and this changes the input by adding a quantity equal to $\int q\,dt$ to the required value θ_i.

13.8.3 Differential Control

With the differential control arrangement, an attitude automatic pilot can be controlled by the action of the human pilot on the control stick, due to a signal x proportional to the displacement of the stick (Fig.167). The displacement δ_s of the control stick produces the direct displacement of the control.

$$\delta_1 = k_s\delta_s$$

and in addition, a signal $x = k_2\delta_s$, which is added to that produced by the error detectors actuating the servo-control. The sum of these signals actuates the servo-control and produces

$$\delta_2 = G(s)[A_1\theta + A_5 q + k_2\delta_s] \tag{13.36}$$

so that the total displacement of the control becomes

$$\delta_e = \delta_1 + \delta_2 = k\delta_s + G(s)[A_1\theta + A_5 q + k_2\delta_s] \tag{13.37}$$

Let us imagine that it is required to make the aircraft climb; we then apply $\delta_s < 0$. As long as the aircraft has not responded ($\theta = q = 0$), the deflection δ_e corresponds to an amplified displacement of the control stick. As soon as the aircraft responds, the signals θ and $q > 0$ annul the effect of the signal $k_2\delta_s$ and the deflection diminishes.

It is easy to show that when the stick undergoes a step displacement δ_s the final equilibrium condition of the aircraft will be a trajectory of constant slope if the automatic pilot contains an element sensitive to the attitude θ, but that it leads to a constant angular velocity q if the automatic pilot only contains an element sensitive to q, and does not possess an element sensitive to the attitude θ.

Although it is possible to use the differential control with an automatic position pilot, this type of arrangement is used principally with automatic pilots having a limited authority.

An automatic pilot with limited authority is not sensitive to the variables of position Ψ , Θ , Φ but only to their derivatives, or to the accelerations. It contributes to the artificial stabilization of the aircraft by improving the damping or the static margin, but always leaves to the human pilot the charge of choosing the flight conditions by the action of the usual controls.

13.8.4 Control Without Direct Connection Between the Pilot and the Control Surface

These devices are the most recent. The safety in functioning of servo-control is now improved in a manner such that the devices without direct connection tend to completely supplant the arrangements described previously.

A large number of different arrangements are possible. Let us examine, then, those which have a jack as the controlling motor. We will suppose that the jack involves an internal feed-back whereby the position of the attack point A determines the control deflection. We can classify the possible arrangements as follows:

(1) The human pilot acts directly on the distributor; the error detector of the automatic pilot doing the same by different means.

(2) The human pilot does not act directly on the distributor: he acts indirectly upon it by producing a signal which is added to the error signals produced by the automatic pilot.

As a typical arrangement of the first case let us look at that indicated in Figure 168.

The control stick is tied directly to the slide valve of the jack. Thus the pilot directly displaces the distributor, but the action of the automatic pilot is also added. This can be achieved if the automatic pilot varies the length of the linkage by which the pilot controls the slide valve.

Thus we again find the series control arrangement, but in this case the two piloting actions are additive and displace the distributor of the jack instead of the control surfaces directly.

Here also, the automatic pilot should displace the valve and not the control stick. The pilot must keep the stick stationary, unless we insert a greater friction force between the control stick and the variable-length linkage than that which is produced by the displacement of the distributor.

Figure 169 illustrates another arrangement also consisting of a direct connection between the control stick and the distributor, but utilizing an operating motor in parallel with the pilot. The action of the motor is represented schematically by a rack and a pinion.

The action exerted by the pilot is measured by a pick-up which produces a signal x . The electric motor is controlled by the sum of the error signals furnished by the automatic pilot, and some signal proportional to the effort exerted by the pilot. A device for disengaging the electric motor can be provided, so that the pilot can act directly on the distributor himself.

In the second type of control, there is no connection between the control stick and the valve of the jack (see Fig.170). The pilot acts on the valve only by altering the signals coming from the error detector. He produces this alteration by adding a signal δ_s proportional to the displacement of the control stick or proportional to the force F applied to it.

The resulting signal can actuate either a servo-valve or an electric motor giving a deflection proportional to the total signal, or a control producing a deflection speed proportional to the total signal, analogous to that described in Section 13.4.2.

The different arrangements indicated above can be completed by the addition of feel generators to the control stick.

13.8.5 The Practical Consequences of the Large Number of Alternative Arrangements

Automatic pilots can respond to different programmes. It is necessary to distinguish between:

Artificial stabilization or autostability

Autopilotage

Manoeuvre demand.

The realization of these different programmes entails a different choice of error signals, to which the automatic pilot will be sensitive.

The study of the resulting trajectories, after an initial disturbance of an aircraft controlled only by an automatic pilot, has been dealt with in Sections 13.3 and 13.4.

The study of the response of an aircraft to the action of a human pilot will be dealt with in Section 13.9.

The arrangements permitting the human pilot to pilot the aircraft concurrently with an automatic pilot, and often through the automatic control device, are very numerous. The solutions differ:

(a) By the relative arrangement of the manual control and the automatic control (Section 13.8.1);

(b) In the mechanical dispositions, which make it possible to build servo-controls producing displacements or speeds of displacement;

(c) In the devices producing artificial feel.

The response to any action of the pilot depends upon the choice of the variables whose divergence actuates the automatic pilot, and on the mechanical arrangement adopted to introduce his action in the control circuit.

Note

The descriptions given in this section deal with longitudinal control. The same means of coupling human action and autopilot response can be adopted for the control of the ailerons and the rudder.

13.9 RESPONSE OF THE AIRCRAFT TO THE ACTION OF THE HUMAN PILOT

13.9.1 The Influence of the Type of Automatic Pilot Used

Because of the large number of possible solutions, it has become normal, before constructing an aircraft prototype, to verify by means of a computer if the combination control system/automatic pilot/aircraft that it is proposed to use, will give correct responses.

We will examine here only the case of control without direct connection between the control link and the control surfaces.

In the case of piloting through an automatic pilot, the signal sent by the human pilot is added to the error signals.

A command in a step form will produce an alteration in the required value (input) of the reference variable to which the autopilot is sensitive, and the response of the aircraft will differ according to the choice of this reference. Flight tests show that such differences in behaviour, which can be easily predicted by the analogue computer, really exist.

Flight tests carried out by N.A.S A.[18,19] have shown that when a signal coming from the autopilot modifies

the value of the required attitude θ ,

the value of the required angular velocity q ,

the value of the normal acceleration (or load factor n),

the responses of the aircraft are different.

The three diagrams of Figure 171 correspond to a step displacement δ_s of the control stick. The order δ_s produces different displacements δ_e of the control surface. The evolution of the following variables:

attitude θ ,

angular velocity q ,

acceleration (or load factor n),

is entirely different in the first case than in either of the second or third cases.

Moreover, the production of a step displacement δ_s of the control column requires different stick forces F according to the type of artificial feel device.

Figure 172 shows the results obtained with a spring device producing:

$$\mathfrak{M}_f = k_1 \delta_s$$

or a damper producing

$$\mathfrak{M}_f = k_2 \delta_s$$

in the case of the automatic pilot controlling the attitude angle θ.

The report quoted above also contains the results concerning the control of the ailerons by the intermediary of an autopilot sensitive to either the angle of bank φ or the angular velocity in roll p.

13.9.2 Block Diagrams

The drawing of a block diagram always helps in the understanding of the aeroplane response, and its analysis by means of an analogue computer.

In the flight tests referred to above, the signal was the displacement δ_s of the control column, and not the force F. The block diagram is thus relatively simple (Fig.173). It must be noted, however, that the control used in the flight tests described involved an attenuation of the feed-back signal. This is a case where the set-up given in Section 3.5.5.4 has been used.

The block diagram in Figure 174 represents schematically a system in which the excitation is a force F applied to the control column. It differs from those studied in Chapter 12 by the presence of an automatic pilot.

13.9.3 Study by the Analogue Computer

When the block diagram of the system has been drawn, it is always possible to study the response of the system to an arbitrary excitation F or δ_e.

There are certainly a great number of test results which have not been published. We may refer to the following, obtained by Mr. Czinzenheim:

13.9.3.1 High-Speed Aircraft

The study of the manual control of an aircraft fitted with an autopilot according to the following arrangements was carried out. The control surface is actuated by a jack, of which the slide valve is displaced by the action of an electric motor. This motor runs at a speed proportional to a compounded signal x, of which the component parts are:

A signal $x_1 = KF$ proportional to the effort exerted by the pilot on the control stick and measured by a grip dynamometer;

A signal x_2 coming from the automatic pilot.

It is easy to see that the control involves an integration. In supposing that the transfer functions are equal to unity, we get:

$$\left.\begin{aligned} \frac{d\delta_e}{dt} &= x_1 + x_2 \\ \text{and} \qquad \delta_e &= \int (x_1 + x_2)\, dt \end{aligned}\right\} \tag{13.38}$$

There were two possible set-ups, according to whether or not the control stick is linked to the slide valve.

The first set-up (Fig.169) uses the control in parallel; the stick displacement δ_s is proportional to the displacement of the control surface, but the pilot cannot directly produce these displacements by an action exerted on the control stick, due to the irreversibility of the system. He produces these displacements only in an indirect manner, the system being activated by the electric motor which is put in action by the signal x_1 .

In the second set-up, there is no connection between the stick and the slide valve of the jack, but the stick, if not locked, must act against an artificial feel device in the absence of which the pilot would not be able to exert the force F (Fig.170).

Different hypotheses have been advanced on the type of automatic pilot.

1st case

The variables whose divergence actuate the automatic pilot are:

The angular velocity q , measured by a rate gyro;

The angular accleration $\dot{q}$, obtained by differentiating the preceding variable;

The velocity error $\hat{u}$.

In this case, we get:

$$\frac{d\delta_e}{dt} = K_1 F + K_2 \frac{d\theta}{dt} + K_3 \frac{d^2\theta}{dt^2} + K_4 \hat{u} \tag{13.39}$$

2nd case

The reference variables are:

The acceleration $\quad V \dfrac{d\theta}{dt} - \dfrac{1}{V_0} \dfrac{dw}{dt}$

Its derivative

The velocity error $\hat{u}$.

The control equation becomes

$$\frac{d\delta_e}{dt} = K_1 F + K_2 V_0 \left(\frac{d\theta}{dt} - \frac{1}{V_0} \frac{dw}{dt} \right) + K_3 V_0 \frac{d}{dt} \left(\frac{d\theta}{dt} - \frac{1}{V_0} \frac{dw}{dt} \right) + K_4 \hat{u} \qquad (13.40)$$

We may note that, when $k_4 = 0$, the two control equations immediately define the stick force per g .

In a steady state, we have:

$$\Delta ng = V_0 \frac{d\theta}{dt}$$

Writing $\frac{d\delta_e}{dt} = 0$, we have

$$\frac{F}{\Delta n} = - \frac{K_2}{K_1} \frac{g}{V_0} \qquad \text{in the first case}$$

$$\frac{F}{\Delta n} = - \frac{K_2}{K_1} g \qquad \text{in the second case}$$

The simulation has been made by representing the aircraft by a 4th order linear system, describing both the rapid oscillation and the phugoid. The aerodynamic derivatives are assumed to be independent of the Mach number.

The wiring diagram is independent of the variant adopted for the realization of the results, since the input F is assumed to be independent of the position of the control stick.

The coefficients K have been made to vary until a suitable response has been obtained. Flight tests have shown that the values considered as satisfactory were an excellent approximation to the flight values.

The response to a step effort F is given (Figs.175 and 176) for the first control equation, with the following coefficients:

$$K_1 = 0.00175 \text{ rad/sec/kg}$$

$$K_2 = 0.5$$

$$K_3 = 0.05 \text{ sec}$$

$$K_4 = 0 \text{ or } -0.000175 \text{ rad/m.}$$

The results of the flight tests have not only confirmed the analogue calculations qualitatively, but have shown that the pre-determination of the adjustments (that is to say, the values of the coefficients K_1, K_2, K_3) was possible. The values considered

as satisfactory from the point of view of the response of the computer constitute an excellent first approximation to the flight values.

13.9.3.2 Low-Speed Aircraft

The low-speed aircraft which is dealt with in Section 10.2.2.3.1 has been supposed provided with an automatic pilot using a control equation of the type

$$\delta_e = A_8\dot{z} + A_7\dot{u}$$

The response to the input excitation (displacement of the control stick in steps) is represented in Figures 177 and 178, and constitutes an improvement of the responses represented in Figures 102 and 103.

13.10 GUIDANCE FOLLOWING AN ALIGNMENT

13.10.1 Principle

The automatic guidance of an aeroplane following a given alignment is possible if we can produce error signals proportional to the projections of the shortest distance separating the aeroplane from the imposed alignment and utilize these signals for the command of the controls with the purpose of cancelling this distance.

Given a coordinate system $OX_gY_gZ_g$ fixed to the imposed alignment, such that:

OX_g is taken in the direction of the alignment

OY_g is taken horizontal and directed to the right

OZ_g is taken directed downward

the distance from the alignment to the aeroplane will be defined by:

y - projection on the axis OY_g

z - projection on the axis OZ_g (see Fig.179).

The flight conditions of the aeroplane on the imposed trajectory determine the constant motion, the departure from which is represented by linearized variables.

The origin of the angles ψ coincides with the imposed direction. The inclination with regard to the horizontal of the imposed alignment is γ_0 .

Separating the study of the longitudinal motions and the transverse motions, we may write:

$$\frac{dz}{dt} = -V_0(\gamma - \gamma_0) = V_0(\alpha - \theta) \qquad (13.41)$$

$$\frac{dy}{dt} = + V_0(\psi + \beta) \tag{13.42}$$

The errors z and y are therefore determined by integrals of the perturbations α, θ, ψ, β :

$$z = V_0\int(\alpha - \theta)dt + z_0 \tag{13.43}$$

$$y = V_0\int(\psi + \beta)dt + y_0 \tag{13.44}$$

The aeroplane will be linked to the desired trajectory if the longitudinal controls are activated as a function of the error z , and the lateral controls as a function of the error y . In certain cases, to avoid permanent errors, we also use the signals proportional to $\int z\,dt$ and $\int y\,dt$.

The control equations are written in the case of unit transfer functions:

$$\delta_e = A_1\theta + A_2\alpha + A_3\hat{u} + A_4 z + \ldots\ldots$$

$$\delta_t = B_1\theta + B_2\alpha + B_3\hat{u} + B_4 z + \ldots\ldots$$

$$\delta_a = A_1\psi + A_2\beta + A_3\varphi + A_4 y + \ldots\ldots$$

$$\delta_e = B_1\psi + B_2\beta + B_3\varphi + B_4 y + \ldots\ldots$$

The order of the system of equations of motion is increased by unity by these control equations. As a matter of fact, in the most simple linear case, the excitations $(\Delta C_x)_i$, ... $(\Delta C_n)_i$ are functions of the variables z or y . For this reason it is necessary to add Equation (13.41) to the differential system for the longitudinal motion and Equation (13.42) to the system for the lateral motion.

The longitudinal motion is defined by a system of differential equations of the 5th order, the lateral system by a system of equations of the 6th order.

13.10.2 Properties of the Trajectories

The properties of the trajectories determined by the control equations, including terms in y or in z can be predicted by the theory of servo-mechanisms. They can be studied in some fashion experimentally by resolving the system on the analogue computer. In both cases one may see that the terms of control in z or in y are clearly destabilizing.

One of the duties given to modern automatic pilots acting on the longitudinal motion often consists of maintaining a constant altitude. In this case, the error z will be furnished by a barometric reference: the difference between the ambient static pressure and an imposed static pressure.

The introduction of such an error signal into an automatic pilot tends to produce long-period oscillations, and must be compensated for by a sufficiently strong action of the error signals exerting a stabilizing influence. The user of the analogue computer is in a position to avoid considerable groping in the determination of the respective gains which will affect the different error signals.

13.10.3 Guidance Along an Approach Trajectory

The achieving of an automatic landing approach is a particular case of guidance on a given alignment. The error signals in z or in y can be obtained aboard the aeroplane or on the ground. There are therefore two systems differing essentially in principle. The ILS equipment is a receiver that permits obtaining the error signals aboard the aircraft. These signals are introduced into the automatic pilot by the approach coupler.

The AGCA is a radar that references, in relation to the ground, the position of the aeroplane, and determines its polar coordinates. These polar coordinates permit the calculation of the errors z and y whose values must be transmitted to the aeroplane. The AGCA is therefore a development of the GCA that constitutes a non-automatic system where the error signals consist of verbal indications given by radio-telephone.

The approach path is characterized by the following particulars:

(1) It is descending and makes an angle of 2.5° with the horizontal;

(2) The aeroplane is moving at constant speed;

(3) It is hoped to realize a speed of the order of 120 knots or 60 m/sec, as closely as the characteristics of the aeroplane permit.

This speed may correspond to a point of the polar defining the second flight régime*.

The ILS is characterized by the following particulars:

(1) The sensitivity of the system varies during the descent. Error signals of the same amplitude or intensity received by the aeroplane do not correspond to equal errors in z or y ;

(2) The height guidance furnished by ILS must be stopped at about 200 to 300 feet above the ground.

The AGCA is in an experimental state. The different operations to be effected each introduce a delay, and the total of these delays corresponds to a relatively important time constant.

13.10.4 Applications

(a) *Approach made in the first régime* of flight*

A complete study of approach guidance is reproduced in Part IV. This study makes apparent a large number of peculiarities of the motion, and is presented as an example of the possibilities of analogue calculation in the prediction of aircraft behaviour. It comprises the study of the longitudinal motion and those transverse motions of a motor engined aeroplane in the approach configuration.

---

*First régime is defined as a flight with normal attitude control. Second régime is defined as a flight with control reversal, the power required exceeding the available power.

The motion studied is a flight at a speed of 60 m/sec, corresponding to the value of the lift coefficient:

$$C_L = 1.145$$

for which C_D/C_L is a minimum.

The approach is thus made at an angle of attack smaller than that of minimum $C_D/(C_L^{3/2})$.

The aeroplane is equipped with constant-speed propellors. The effective power at constant throttle is assumed to be independent of the speed, so that the thrust T increases as the speed decreases. The operation of the elevator is normal and the aeroplane is in the first régime of flight.

The study of the motion performed immediately reveals the instability caused by the term $A_4 z$ and the corrective effect of the terms in $A_1\theta$, $A_8\dot{z}$ and $A_7\dot{u}$.

In practice, the same automatic pilot controls the aeroplane in cruise and during approach. In cruise, the control equation includes the terms $A_1\theta$ and $A_5\dot{\theta}$. It is normal that one tries to utilize the same terms in the control during the approach.

We have insisted throughout on the effectiveness of the term $A_7\dot{u}$ in the stabilization of the motion, and we have based our investigation on the use of this term.

If we consider solutions different from those that are used in practice, the result will not exclude the use of the terms $A_1\theta$ provided that ϵ' indicates clearly the error:

$$\epsilon' = \theta - \theta_a$$

with regard to the attitude θ_a corresponding to the approach flight and not to the attitude θ_c of cruise flight.

The study of the longitudinal motion has shown that it will be advantageous to make the engine power vary as a function of certain error signals.

The study of the lateral motion made us choose control equations which were similar to those in practical use.

The work described in another Chapter shows the ease with which the actual mechanism of the phenomenon is made understandable by the use of the analogue computer.

(b) *Approach made in the second régime of flight*

The jet aeroplane receives a constant thrust from its turbojet engines. If we examine the equilibrium condition

$$T - D = 0 \qquad (13.45)$$

for the trajectories covered at different incidences, we find that the effect of the elevator is reversed at all incidences greater than that corresponding to minimum thrust. The second régime begins earlier, and the imposed flight speed corresponding to a dangerous approach for a jet aircraft is strongly dependent on wing loading.

The equations of motion of the aeroplane may be linearized. The turbojet propulsion introduces

$$\frac{dT}{dV} = \frac{d}{dV}(T_c \tfrac{1}{2} \rho S V^2) = 0 \qquad (13.46)$$

That is to say:

$$\frac{\partial T_c}{\partial V} + \frac{2T_c}{V} = 0$$

and the response of the aeroplane may be determined in the same manner as in the case of the first régime.

Some response of the absolute speed V and the sinking velocity w' due to a step function input to the deflection δ_e and the thrust T have been obtained by Bismut and Bouttes for a modern fighter simulation and published in an AGARD Report[20].

These responses are indicated in Figures 180 and 181. At the speed of 130 m/sec the aeroplane is in the first régime, while at 65 m/sec it is in the second régime. In the latter case the tail-up motion of the elevator produces a descending flight path.

As a consequence of this inversion it is very difficult to maintain a fixed alignment.

During the work conducted at O.N.E.R.A., Bismut and Bouttes adopted the following scheme:

The landing is assumed to be made under manual control. A human pilot receives the error signals sent out from the computer, either in a visual form (ILS), or in the form of oral signals given by an assistant simulating the radio operator (GCA). The pilot also has available the visual signals giving the divergence of the speed, and introduces into the computer the electrical signals representing the deflection δ_e and the throttle setting δ_m by a stick and a throttle of the conventional types. The control equations

$$\delta_e(s) = A_4 \, G_1(s) \, z(s) \qquad (13.47)$$

$$\delta_m(s) = B_3 \, G_2(s) \, \frac{u(s)}{V_0} \qquad (13.48)$$

depend on the transfer function of the human operator and of the possibility of displacing the two controls simultaneously.

The simulation of a manoeuvre necessarily gives results which will depend on the experimenter's training as a pilot.

In one series of tests, the pilot was asked to follow a given alignment using only the elevator. The aeroplane was submitted to the action of a gust. Invariably, the pilot produced a divergent motion (Fig.182).

In another series of tests, the pilot was asked to maintain the speed of the imposed trajectory at all times, utilizing the two controls to this end.

For the same tests without external excitation to simulate gust loading, the trajectories shown in Figure 183 have been obtained.

For identical conditions, but supposing automatic control of the turbojets:

$$\delta_m = B_3 \frac{u}{V_0}$$

and limiting the pilot's task to control of the stick, the results indicated in Figure 184 were obtained. In this last test, the value of B_3 was chosen such that a speed reduction of 1 m/sec produced a thrust increase of 160 kgs.

It is, however, noteworthy that in the second test the pilot was able to give all his attention to the signal $z(s)$. It is possible, therefore, that his transfer function was better than in the preceding test.

The studies cited here bring to light:

(1) The difficulty of maintaining alignment when flying at high angle of attack;

(2) The favourable action produced by coupling the thrust to the speed.

A recent NASA publication[21] relating to some flight tests of the approach manoeuvre made with automatic control of the thrust has confirmed these conclusions.

13.11 AUTOMATIC CONTROL OF FLARE-OUT

13.11.1 Statement of the Problem

The problem of flare-out is the following: the aeroplane is following the approach trajectory and performs a straight descent at constant speed V_A corresponding to a rate of descent of 2.60 to 2.80 m/sec.

We represent the height above the ground by h (Fig.185). Having reached a point A , at height h_A , the pilot must effect the flare-out in an effort to reduce the rate of descent to a value between 0.30 and 0.50 m/sec at $h = 0$, when the aeroplane touches the ground. For a tricycle landing gear, the trim at this time must be such that the rear wheels touch the ground first.

During this manoeuvre the vertical acceleration must remain moderate. A strong acceleration would require a strong augmentation of the lift, which is not permissible because of the danger of stalling. The speed of the aeroplane diminishes equally. This is a favourable result, but the reduction of V does not constitute the principal object of the operation. X

Many studies have been effected with the aim of providing automatic control of flare-out. The analogue computer has played a large role in these studies.

The researchers working at Wright Field define the law of ideal descent, starting from a point A, by a differential equation relating h and t :

$$(h + h_s) + n \frac{dh}{dt} = 0 \qquad (13.49)$$

Possible numerical values for h_s and n are determined by the following examples:

(a) *Normal case at Wright Field*

The descent speed on the approach path is 2.60 m/sec. It is desired to commence flare-out at $h_0 = 9.20$ m , and to touch the ground with a vertical velocity of 0.30 m/sec. The equation of the trajectory may be verified for:

$$\frac{dh}{dt} = -2.60 \text{ m/sec} \qquad \text{with} \quad h = 9.20 \text{ m}$$

and for

$$\frac{dh}{dt} = 0.30 \text{ m/sec} \qquad \text{with} \quad h = 0$$

which gives:

$$n = 4 \text{ sec} \qquad \text{and} \qquad h_s = +1.20 \text{ m}$$

(b) *Another possible case*

The initial speed is 2.80 m/sec. The manoeuvre is begun at $h = 20$ m, and a vertical speed of 0.40 m/sec is desired at the ground. These requirements give:

$$n = 8.33 \text{ sec} \qquad \text{and} \qquad h_s = 1.66 \text{ m}$$

The curve $h(t)$ defined by the preceding differential equation is exponential. The quantity h_s is the distance between the asymptote to flight path and the ground. Transforming the time and the distance by:

$$x = \int V \, dt \qquad (13.50)$$

we obtain the trajectory:

$$h = f(x) \qquad (13.51)$$

which differs slightly from the curve $h = f(t)$ because of the relatively weak speed variations.

Achievement of automatic flare-out is possible only if the aeroplane receives the information of the height h over the ground. All the techniques of achieving an automatic flare-out are based on the existence of a precision altimeter, furnishing in a continuous fashion the aforementioned information. Such altimeters, utilizing ground reflection of electromagnetic waves, actually exist.

The derivation of the signal h, or the direct measure of the descent speed by any other means, permits one to obtain a compound signal

$$\epsilon_h = (h + h_s) + n \frac{dh}{dt} \tag{13.52}$$

where n has an arbitrarily imposed numerical value.

The problem of the automatic flare-out consists of finding some control equations defining the required elevator deflection δ_e and eventually the throttle setting δ_m that will cause the aeroplane to describe a trajectory with characteristics close to those of the ideal trajectory. These control equations will be functions of the signal ϵ_h and such additional signals as prove necessary.

The chosen control relations must be able to correct the effects of possible horizontal and vertical gusts. The essential point is that the aeroplane shall, at the moment of contact with the ground, possess a vertical speed differing only slightly from the imposed speed. It is desirable, besides, that the horizontal distance between the point of contact and the point A' undergoes only moderate variations.

The block diagram defining the behaviour of the aeroplane is represented in Figure 186.

The altitude h, resulting from the motion of the aeroplane, must be measured by an altimeter. The measurement is re-introduced in a computing machine that forms the signal:

Either by continuous derivation of the signal h (Case a)

Or by measurement of the velocity dh/dt by means of a special instrument (Case b).

The additional inputs to the block representing the automatic pilot indicate that this device may be aided by signals other than ϵ_h.

Several researchers: Porter[22], McCallum[23], Merriam[24], Markusen, McLane, and Pomeroy[25] have proposed control equations that are based on the theory of servomechanisms, and have utilized the analogue computer to determine the exact characteristics of the corresponding trajectories.

13.11.2 Effect of Error Signal

The signal ϵ_h is positive when the aeroplane is higher than it ought to be, taking account of the sinking speed it actually possesses. Considered in this aspect, it defines an error of altitude.

The signal may also be considered as defining an error of descent speed with regard to the speed corresponding to the true altitude. The vertical demanded speed $\dot{h}_c$ being equal to $-(h + h_s)/n$, we have:

$$\frac{1}{n}\epsilon_h = \frac{dh}{dt} - \dot{h}_c = \frac{dh}{dt} + \frac{1}{n}(h + h_s) \tag{13.53}$$

The signal ϵ_h is generally produced from the signal h by an instrument called the flare-out computer, which executes the derivation and calculation of the sum

$$(h + h_s) + n\frac{dh}{dt}$$

Introducing this signal into a servo-mechanism with a transfer function $KG(s)$, where K is a numerical coefficient > 0, we will have:

$$\delta_e(s) = K\,G(s)\,\epsilon_h(s) \tag{13.54}$$

In the particular case where $G(s) = 1$, we may pass to the time-dependent equation and will obtain:

$$\delta_e = K(h + h_s) + Kn\frac{dh}{dt} \tag{13.55}$$

Such an equation will direct the aeroplane towards the asymptote $h = -h_s$ if the final motion is a horizontal flight $dh/dt = 0$ realizable with the thrust used for the descent.

In Part IV (Section 21.2) we describe the behaviour of an aeroplane subject to a control relation:

$$\delta_e = A_4 z + A_8 \dot{z} \qquad \text{with} \quad z = -h$$

where the coefficients A_4 and A_8 are related by:

$$A_8 = \frac{0.946}{2.54} \times 7.05\, A_4 = 2.65\, A_4$$

The calculation is made for one initial condition in z, and one final trajectory having the same slope as the initial trajectory (Fig.299 and Fig.300). We have obtained an oscillatory trajectory.

In the problem studied here, it is clear that the trajectory determined by the integration of the equations of motion and the equations of control, for the initial conditions, viz.

$$\frac{dh}{dt} = 2.6 \text{ m/sec}$$

$$h = 9.20 \text{ m}$$

will be far from the trajectory defined by $\epsilon_h = 0$.

The trajectory, straight to begin with, can only be curved if an input ϵ_h activates δ_e , but this can only happen when ϵ_h is no longer zero.

A propeller-driven aeroplane descending at an angle of attack less than that corresponding to minimum power and controlled according to Equation (13.55) generally presents an oscillatory trajectory.

If the descending part of the oscillation occurs at the moment of contact with the ground, the instantaneous vertical speed may be absolutely prohibitive (Fig.187).

The trajectory of a jet aeroplane descending at an angle of attack equal to or greater than that corresponding to the maximum (L/D) ratio will be still worse.

13.11.3 Tests on the Computer

The block diagram corresponding to the simulation of the flare-out is presented in Figure 188.

The variables θ and α represent the deflections measured from the values corresponding to a constant descent prior to reaching point A.

All the following calculations are based on a transfer function for the mechanism between the signal and the deflection given by the expression

$$G(s) = \frac{0.0743\ s + 0.28}{0.00611\ s^2 + 0.0224\ s + 1}$$

The signal ϵ_h , obtained on the real aeroplane by direct measurement and derivation of the altitude, is calculated from the output signals of the circuits representing the aeroplane.

The true descent speed calculated by the above method is equal to $(dh/dt)_A + V(\theta - \alpha)$, and will be compared to the imposed descent speed: $\dot{h}_c = \frac{1}{n}(h + h_s) = \frac{1}{n}[h_A + \int h\ dt + h_s]$. The error ϵ_h will be

$$\frac{1}{n}\epsilon_h = \dot{h} - \dot{h}_c \qquad (13.53)$$

The trajectory obtained by a control equation of the form

$$\delta_e(s) = K\ G(s)\ \epsilon_h(s) \qquad (13.54)$$

will never be satisfactory. Thus, to obtain a stabilizing signal, it is important to send other stabilizing signals to the automatic pilot.

The authors of the various works have considered principally the signals θ and $\dot{\theta}$. They have studied the consequence of this additional information by the theory of servo-mechanisms, and have achieved the simulation of these methods of control. They have not utilized the control of the motors.

Porter has simulated the behaviour of a C-54 aircraft (military version of the DC-4),

MacCallum has considered the behaviour of the B-47,

Markusen has studied the DC-3,

Merriam has studied three different cases:

C-47 (military version of the DC-3, a two motored transport),

B-47 (turbojet bomber),

F-80 (turbojet fighter).

The most simple form of airborne equipment involves the utilization of the normal type of automatic pilot, sensitive to θ and $\dot{\theta}$. The error ϵ_h is added to the input θ or to the inputs θ and $\dot{\theta}$, following the scheme indicated in Figure 189.

This conception of the control of the flare-out presents the inconvenience that the term in θ (in reality the difference $\Theta - \Theta_A$) represents the difference with regard to the approach trajectory, and tends to return the aeroplane to this trajectory when it is actually desired to deviate from it.

Figure 190 (due to Porter) shows the trajectory for a gain such that an error ϵ_h/n of one foot/second produces the same effect as an error $\Delta\theta$ of 0.25 degree.

Figure 191 (due to MacCallum) shows the trajectory for a gain of 0.4 in ϵ_h/n. In the two cases, the action of the signal is insufficient to produce flare-out. Both authors have improved the trajectories by comparable processes.

Porter used the following procedure:

(a) Increasing the gain from 0.25 to 0.70 or even 1.0 but simultaneously increasing the component $A_5\dot{\theta}$. A supplementary circuit is used to render this increase more important than in the normal automatic pilot (Fig.192).

(b) Modification of the term in θ_A, increasing progressively the reference trim by a quantity:

$$\Delta\Theta_A = c\left[1 - \frac{h}{h_0}\right] \tag{13.56}$$

so that the term $A\theta$ becomes:

$$A[\Theta - (\Theta_A + \Delta\Theta_A)] \tag{13.57}$$

Figure 193 gives the trajectory obtained for $C = 3.75$.

MacCallum operated as follows:

(a) Either by suppressing the term $A_1\theta$ produced by the automatic pilot, and increasing the gain of the damping term $A_5\dot{\theta}$ (Fig.194);

(b) Or by maintaining the term $A_1\theta$ at the normal value produced by the automatic pilot, and increasing considerably (25 times) the damping term $A_5\dot{\theta}$, and the gain corresponding to the error signal ϵ_h (Fig.195);

(c) Or by applying a small gain to the signal ϵ_h, and adding a term proportional to the integral of the error such that this integral is always less than a given maximum value (Fig.196).

Generally speaking, the above modifications to the control equation improve the flare-out.

MacCallum completed his tests by studying the effect of a vertical gust. He chose a gust, either ascending or descending, of the order of 2.22 m/sec. The gust was applied 1.5 seconds after the flare-out was initiated, and had a duration of 1 second. Figures 194, 195 and 196 present the trajectories obtained by MacCallum for the three Cases (a), (b), (c) with and without the gust.

It is seen that the control laws chosen do not produce the desired flare-out when the gust described above is applied. The question is not considered as to whether or not the arbitrarily chosen gust corresponds to a perturbation to which an aeroplane in close proximity to the ground will actually be exposed.

The principle of the set-up used by Porter is shown in Figure 197.

The manner in which the given initial conditions must be introduced should be noted. The aeroplane is following a trajectory of slope

$$\gamma = (\theta_A + \theta) - (\alpha_A - \alpha) \tag{13.58}$$

corresponding to

$$\frac{dh}{dt} = V[(\theta_A - \alpha_A) + (\theta - \alpha)] \tag{13.59}$$

This descent speed will be formed by the computer by means of a term

$$V_A(\theta_A - \alpha_A) = \left(\frac{dh}{dt}\right)_A$$

which is introduced externally, and by a term

$$V_A(\theta - \alpha)$$

which will be provided by the set of equations for the aeroplane.

To obtain h,

$$h = h_A + \int \frac{dh}{dt}\, dt$$

it is necessary to introduce the altitude h_A .

There are, therefore, two items, $(dh/dt)_A$ and h_A , which must be introduced into the computer. These items are the initial conditions.

13.11.4 Other Problems

In a more recent work, Merriam considered the case of a flare-out initiated at high altitude. This permits one to increase n , and thus increases the stabilizing effect of the term dh/dt relative to the term in h .

Pursuing the analysis further, Merriam introduced the actual characteristics of the altimeter and computer.

In the first of the above schemes, the values of h and dh/dt resulting from the calculation of the trajectory are utilized in the formation of the signal.

In reality, the value of h is known only by measurement. The electronic altimeter furnishes the altitude, but with a noise level such that it must be lowered by filtration of the signal.

Moreover, the measured altitude is related to the true altitude by the transfer function

$$h_m(s) = \frac{1}{1 + \tau_1 s}\, h(s) \qquad (13.60)$$

As the derivation of the signal is imperfect, a second time constant is introduced, viz.

$$\frac{dh_m}{dt} = \frac{s}{1 + \tau_2 s}\, h_m(s) \qquad (13.61)$$

The signal ϵ_h furnished by the computer must be calculated taking account of the time constants produced by the measuring equipment.

Markusen has also considered the real properties of the equipment in the publication given above.

Both authors studied the effect of gusts. In addition, Markusen considered the transverse problem, which has not been considered here.

In the case of a transverse wind, the aeroplane flies with a crab angle, with respect to the ground. Shortly before touching the ground the pilot must produce a rotation about the axis OZ , in order to suppress this crab angle.

13.12 AEROPLANE EQUIPPED WITH A GUST DAMPER

The results of an interesting analogue study of a gust damper, made by R.W. Bouchert and C.C. Kraft, have been published by the N.A.C.A.[26].

The gust damper is formed by a servo-mechanism controlling the wing flaps, and following the indication of a wind vane located ahead of the wing. This wind vane, in following the direction of the local flow, will experience a rotation δ. This position will indicate the aerodynamic angle of incidence of the aeroplane (Fig. 198).

The equations of motion for a short-period oscillation of the aeroplane may be written by separating the aerodynamic forces exerted on the wing from those exerted on the tail surface.

Let:

α_p = the true or aerodynamic angle of attack of the wings

α_e = the true or aerodynamic angle of attack of the tail surface

α = the apparent angle of attack of the wing

α_g = the theoretical increase of the angle of attack due to a gust ($= -w_a/V_0$) (w_a is < 0 for an ascending gust)

δ_f = the deflection of the flaps

δ_e = the deflection of the elevator.

The aerodynamic coefficients corresponding to the wing or the tail surface are denoted by subscripts p or e, respectively.

The equations of motion are:

$$2\tau\left(\frac{d\alpha}{dt} - \frac{d\theta}{dt}\right) = \left(C_{z_\alpha}\right)_p \alpha_p + \left(C_{z_{\delta_f}}\right)_p \delta_f - \left(C_{z_\alpha}\right)_e \alpha_e + \left(C_{z_{\delta_e}}\right)_e \delta_e \qquad (13.62)$$

$$C_{I_y} \frac{d^2\theta}{dt^2} = \left(C_{m_\alpha}\right)_p \alpha_p + \left(C_{m_{\delta_f}}\right)_p \delta_f + \left(C_{m_\alpha}\right)_e \alpha_e + \left(C_{m_{\delta_e}}\right)_e \delta_e \qquad (13.63)$$

The study is limited to strong gusts, applied as a step function.

The gust produces an increase of angle of attack at the moment the specified element of the aeroplane enters the ascending gust. This increase is applied to the wind vane, the wing, and the tail surface, respectively, at times t_0, t_1 and t_2.

These increases will be designated by:

$$\alpha_{g,t_0} \qquad \alpha_{g,t_1} \qquad \alpha_{g,t_2}$$

The true angle of attack of the wings is given by:

$$\alpha_p = \alpha + \alpha_{g,t_1} \tag{13.64}$$

The true angle of attack of the tail surfaces is defined by:

$$\alpha_e = \alpha - \left(\frac{\partial \epsilon}{\partial \alpha}\alpha\right)^* + \alpha_{g,t_2} - \left(\frac{\partial \epsilon}{\partial \alpha}\alpha_{g,t_1}\right)^* - \left(\frac{\partial \epsilon}{\partial \delta_f}\delta_f\right)^* + l\dot{\theta} \tag{13.65}$$

The terms marked with an asterisk are affected by the delayed arrival of the deflection ϵ at the tail surface.

From the many possible methods of expressing the delay, N.A.C.A. chose the operator

$$\frac{1}{1 + l's}$$

The final expression for α_e is written:

$$\alpha_e = \alpha - \frac{\partial \epsilon}{\partial \alpha}\alpha\frac{1}{1 + l's} + \alpha_{g,t_2} - \frac{\partial \epsilon}{\partial \alpha}\alpha_{g,t_1}\frac{1}{1 + l's} + \frac{\partial \epsilon}{\partial \delta_f}\delta_f\frac{1}{1 + l's} + l\dot{\theta} \tag{13.66}$$

By eliminating α_p and α_e between Equations (13.62), (13.63), (13.64) and (13.66), we would obtain two differential equations between the usual variables (α , θ) and the excitations (α_{g,t_1}, α_{g,t_2}, δ_f and δ_e) . These equations are not written here, since the analogue resolution of the problem is simplified by the display of Equations (13.62), (13.63), (13.64) and (13.66) where the variables α_p and α_e are retained.

We may study the behaviour of an aeroplane not equipped with a gust alleviator. In this case $\delta_f = 0$.

It is simple to obtained the effect of a step deflection δ_e . The results given by the analogue computer are presented in Figure 199 for the case $\delta_e > 0$, where δ_e is made to excite the motion.

The acceleration is calculated by the formula:

$$j_z = V_0\left(\frac{d\theta}{dt} - \frac{d\alpha}{dt}\right) \tag{13.67}$$

and is positive when it is directed in the positive sense of the axis, i.e., downward.

The diagram gives the classical result if we study only the motion about the centre of gravity. If we want to determine the effects of a gust, the response to an excitation α_g must be calculated.

The effect of a step function excitation α_g is obtained by applying this excitation to the different terms at the corresponding times t_1 and t_2. The response is indicated in Figure 200.

We see that the aeroplane is undergoing an acceleration j_z in the top figure. The plot of $\dot{\theta}$ shows how the aeroplane tends to rise when only the wing is affected by the gust. The growth of $\dot{\theta}$ is terminated at time t_2, when the tail surface reaches the gust. When the non-steady motion is terminated, the acceleration of the aeroplane is again zero. The apparent angle of attack differs by the amount $-\alpha_g$, which gives a true variation of the angle of incidence α_p equal to zero.

When the aeroplane is equipped with a gust damper, the deflection δ_f of the flaps is controlled as a function of a signal E by a servo-mechanism having a transfer function of second order:

$$\delta_f(s) = \frac{\omega_n^2}{s^2 + 2\zeta\omega_n + \omega_n^2} E(s) \tag{13.68}$$

To begin with, the aeroplane is equipped with a wind vane that gives the relative alignment of the air stream in the form of a signal:

$$\delta_v = \alpha + \alpha_{g,t_0} - l_n\theta \tag{13.69}$$

where l_n is the distance from the wind vane to the centre of gravity.

The signal E is the sum of three terms:

The first is $K_1 \delta_v$

The second is a signal from the elevator control, and is required to permit the pilot to fly at different values of C_L. It is equal to $-K_1K_2\delta_e$.

The third signal (not present in all the cases studied) is proportional to the integral of the deflection δ_f. It decreases progressively to produce the progressive elimination of the deflection δ_f, and is equal to $-K_c\ 1/s\ \delta_f$.

Thus:
$$E = K_1\delta_v - K_1K_2\delta_e - K_c \frac{1}{s}\delta_f \tag{13.70}$$

Eliminating δ_v and E between Equations (13.68), (13.69) and (13.70), we obtain the equation for the behaviour of the flap in the form of a relation (13.71) between δ_f, θ, α, and the excitations δ_e and α_{g,t_0}:

$$\delta_f\left(s^2 + 2\zeta\omega_n s + \omega_n^2 + \omega_n^2 \frac{K_c}{s}\right) + s\theta(K_1 l_n \omega_n^2) - \alpha(K_1\omega_n^2)$$

$$= \alpha_{g,t_0}(K_1\omega_n^2) - \delta_e(K_1K_2\omega_n^2) \tag{13.71}$$

The response of the aeroplane to the excitations δ_e and α_g is thus determined. The step function excitation α_g must always be divided into three equal terms, applied at the times t_0, t_1 and t_2.

The original report studied these responses for a series of different cases.

The response to δ_e and α_g (step functions) are represented in Figures 201 and 202 for a simple case, characterized by a rapid response of the flap servo-motor, and $K_c = 0$.

The response to δ_e indicates that this is only an insensitive variation of the incidence. The flaps are raised, resulting in a reduction of lift and a downward acceleration n , which corresponds to an angular velocity of descent.

The response to a gust α_g shows that at t_0 the flaps begin to deflect upward. As a result, the aeroplane experiences a downward acceleration and dives slightly.

LIST OF FIGURES

		Page
Fig.62	Principle of the resolver	243
Fig.63	Schematic representation of the resolver	243
Fig.64	Variation of Euler angles produced by angular velocities p,q,r	243
Fig.65	Use of four rotations to displace the reference trihedral	244
Fig.66	Projections of a vector on two different sets of axes different by ψ, θ, φ	244
Fig.67	Schematic representation of a multiplier	245
Fig.68	Alteration of direction cosines due to angular velocities	245
Fig.69	Projections of a vector on two different sets of axes, the direction cosines being known	246
Fig.70	Definition of the coefficients	246
Fig.71	Longitudinal motion; computer set-up and table of coefficients	247
Fig.72	Longitudinal motion due to initial disturbance θ_0	248
Fig.73	Longitudinal motion due to initial disturbance α_0	248
Fig.74	Longitudinal motion due to initial disturbance $\theta_0 + \alpha_0$	249
Fig.75	Response to a step input δ_e	249
Fig.76	Longitudinal motion due to initial disturbance θ_0	250
Fig.77	Longitudinal motion due to initial disturbance α_0	250
Fig.78	Response to a step input δ_e	251
Fig.79	Atmospheric velocities as an input; set-up and table of coefficients	252
Fig.80	Calculation of the load factor; set-up and table of coefficients	252
Fig.81	Load factor response to an input δ_e	253
Fig.82	Overshoot of the load factor as a function of M	253
Fig.83	Calculation of the tailplane load; set-up and table of coefficients	254

		Page
Fig.84	Tailplane load due to a pulse in δ_e	254
Fig.85	Load factor acting on the aircraft	255
Fig.86	Action of air brakes	255
Fig.87	Lateral motion; computer set-up and table of coefficients	256
Fig.88	Verification of lateral motion stability criteria	257
Fig.89	Variation of lateral derivatives with C_L	257
Fig.90	Response in p to a step input δ_a	258
Fig.91	Combined motion of five variables; set-up and table of coefficients	259
Fig.92	Load on the tail surfaces; set-up and table of coefficients	260
Fig.93	Response to an action of δ_a and δ_e	260
Fig.94	Divergence during rolling pull-out	261
Fig.95	Particular case of C_l, function of α and β	261
Fig.96	C_{m_α} derivative with change of sign	262
Fig.97	Response to a control action δ_e	262
Fig.98	Actual curve C_m versus α	263
Fig.99	Response to $\delta_e > 0$ and $\delta_e < 0$	263
Fig.100	Response to $\delta_e > 0$ and $\delta_e < 0$	263
Fig.101	Longitudinal motion in a non-linear case. Set-up and table of coefficients	264
Fig.102	Longitudinal motion in a non-linear case	265
Fig.103	Longitudinal motion in a non-linear case	265
Fig.104	Recovery from a spin; simulation	266
Fig.105	Set-up of short oscillation with time lag in C_L	266
Fig.106	Flight test and computed motion	267
Fig.107	Flight test and computed motion	267

		Page
Fig.108	Coupling of aircraft trajectory and wing bending; set-up and table of coefficients	268
Fig.109	Response of generalized co-ordinate q to a pulse in w_a	268
Fig.110	Influence of wing tip weight and gust duration	269
Fig.111	Influence of torsional wing flexibility on response to ailerons; set-up and table	269
Fig.112	Influence of torsional wing flexibility; results	270
Fig.113	Most simple elevator control	270
Fig.114	Tab and control surface linked together	270
Fig.115	Servo control using a jack	271
Fig.116	Boosted control	271
Fig.117	Artificial feel produced by a spring	272
Fig.118	Artificial feel produced by a damper	272
Fig.119	Artificial feel non-proportional to stick displacement	272
Fig.120	Artificial feel produced by normal acceleration	272
Fig.121	Artificial feel produced by angular acceleration	273
Fig.122	Action of dry friction close to the control surface	273
Fig.123	Forces acting on a reversible control	273
Fig.124	Aircraft motion with free elevator control; computer set-up and table of coefficients	274
Fig.125	Action of coefficient b_1 on flight with free controls	275
Fig.126	Action of dry friction	277
Fig.127	Action of a bobweight, case $C_{m_\alpha} = 0$	279
Fig.128	Action of a bobweight, case $C_{m_\alpha} > 0$	281
Fig.129	Aircraft response when a couple is applied on the control system	282
Fig.130	Simulation of a servo control using a jack	283

		Page
Fig.131	Principle of the electric position servo control	283
Fig.132	Generation of a signal proportional to pilot effort	283
Fig.133	Control when pilot force is the input	284
Fig.134	Control when stick displacement is the input	284
Fig.135	Moments determining stick position	284
Fig.136	Block diagram; influence of pilot force on aircraft motion	285
Fig.137	Search for best artificial feel	285
Fig.138	Aircraft response; variable static margin at constant altitude and speed	286
Fig.139	Aircraft response; variable static margin, altitude and speed	286
Fig.140	Principle; control by error of θ	287
Fig.141	Alteration of computer set-up when automatic control is used	287
Fig.142	Feed-back acting on error sensor	287
Fig.143	Electric servo valve	288
Fig.144	Electric servo valve	288
Fig.145	Control involving an integration	288
Fig.146	Phase lead network	289
Fig.147	Filtering network	289
Fig.148	Automatic longitudinal stabilization; computer set-up and table of coefficients	289
Fig.149	Automatic control by error of θ	290
Fig.150	Automatic control by error of θ, plus time constant	291
Fig.151	Automatic control by error of θ and q	292
Fig.152	Automatic control by error of θ and α, plus time constant	293
Fig.153	Automatic control by the acceleration	294
Fig.154	Automatic control by the acceleration	295

		Page
Fig. 155	Automatic control by error of α	296
Fig. 156	Automatic control by error of θ	296
Fig. 157	Position of inertia axis versus velocity vector	297
Fig. 158	Aircraft response with locked rudder	297
Fig. 159	Aircraft response with automatic rudder control	298
Fig. 160	Aircraft response with automatic rudder control	298
Fig. 161	Aircraft response with locked rudder	299
Fig. 162	Aircraft response with automatic rudder control	299
Fig. 163	Aircraft response with automatic rudder control	300
Fig. 164	Principle of controls acting in parallel	300
Fig. 165	Principle of differential control	300
Fig. 166	Use of a signal representing pilot action	301
Fig. 167	Use of a signal representing stick displacement	301
Fig. 168	Human and automatic pilot acting differentially on slide valve of jack	302
Fig. 169	Human and automatic pilot acting in parallel on slide valve	302
Fig. 170	No direct linkage between control column and slide valve	303
Fig. 171	Flight test results with three different autopilots	303
Fig. 172	Flight test results with two different artificial-feel generators	304
Fig. 173	Use of a signal representing pilot's action; block diagram	304
Fig. 174	Use of a signal representing control column displacement; block diagram	305

		Page
Fig.175	Response to a step in the force exerted on the stick	306
Fig.176	Response to a step in the force exerted on the stick	307
Fig.177	Response to a step displacement of stick (slow aircraft)	308
Fig.178	Response to a step displacement of stick (slow aircraft)	308
Fig.179	Actual position of an aircraft with respect to a prescribed path	309
Fig.180	Simulation of aircraft motion following an elevator displacement	310
Fig.181	Simulation of aircraft motion following a thrust increase	311
Fig.182	Human pilot correcting effect of a gust	312
Fig.183	Aeroplane motion under control of a human pilot	313
Fig.184	Aeroplane motion under control of a human pilot, plus automatic thrust control	314
Fig.185	Flare-out at landing	315
Fig.186	Automatic flare-out control; block diagram	315
Fig.187	Disastrous effect of an oscillatory trajectory	316
Fig.188	Automatic flare-out control; block diagram	316
Fig.189	Automatic flare-out control; block diagram	316
Fig.190	Simulation of a flare-out	317
Fig.191	Simulation of a flare-out	317
Fig.192	Simulation of a flare-out	318
Fig.193	Simulation of a flare-out	318
Fig.194	Simulation of a flare-out; action of a gust	319

		Page
Fig.195	Simulation of a flare-out; action of a gust	320
Fig.196	Simulation of a flare-out; action of a gust	321
Fig.197	Simulation of an automatic flare-out and control; block diagram	322
Fig.198	Aircraft fitted with gust alleviating device	322
Fig.199	Response to a δ_e step without gust alleviation	323
Fig.200	Response to an α_g step without gust alleviation	323
Fig.201	Response to a δ_e step with gust alleviation	324
Fig.202	Response to an α_g step with gust alleviation	324

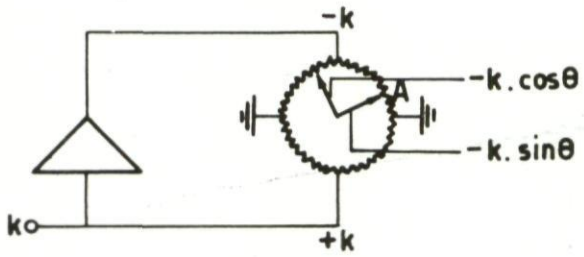

Fig.62 Principle of the resolver

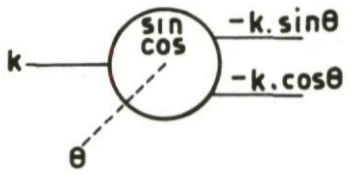

Fig.63 Schematic representation of the resolver

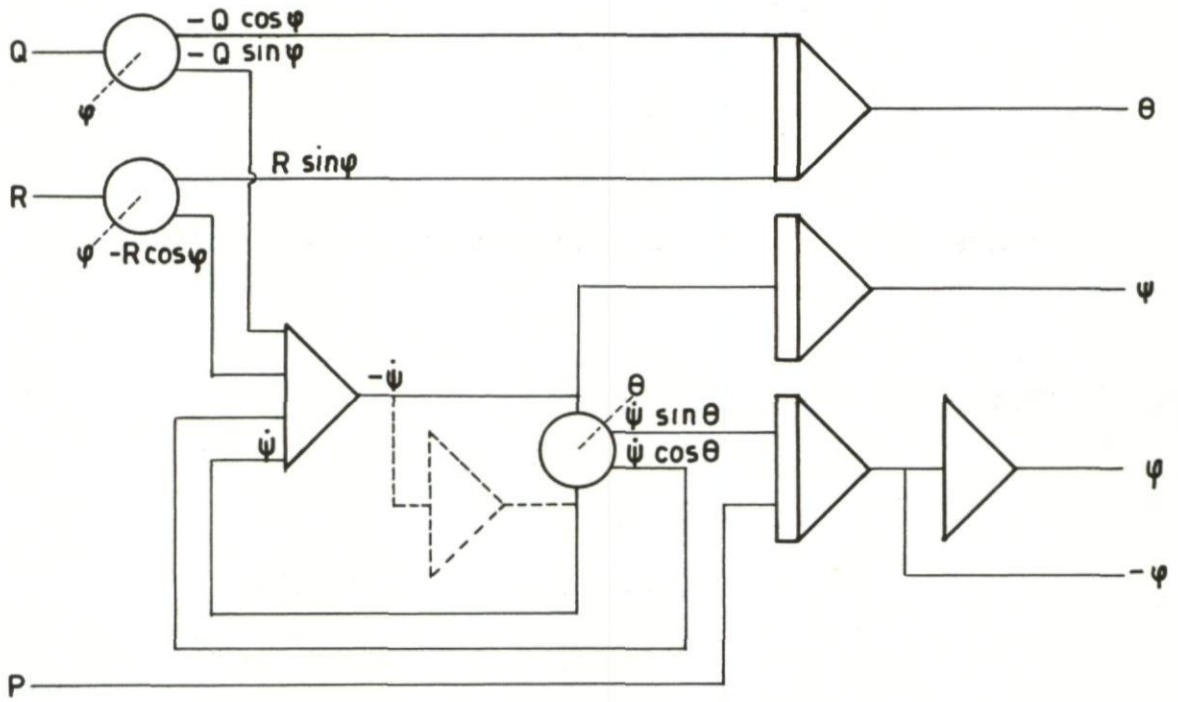

Fig.64 Variation of Euler angles produced by angular velocities p,q,r

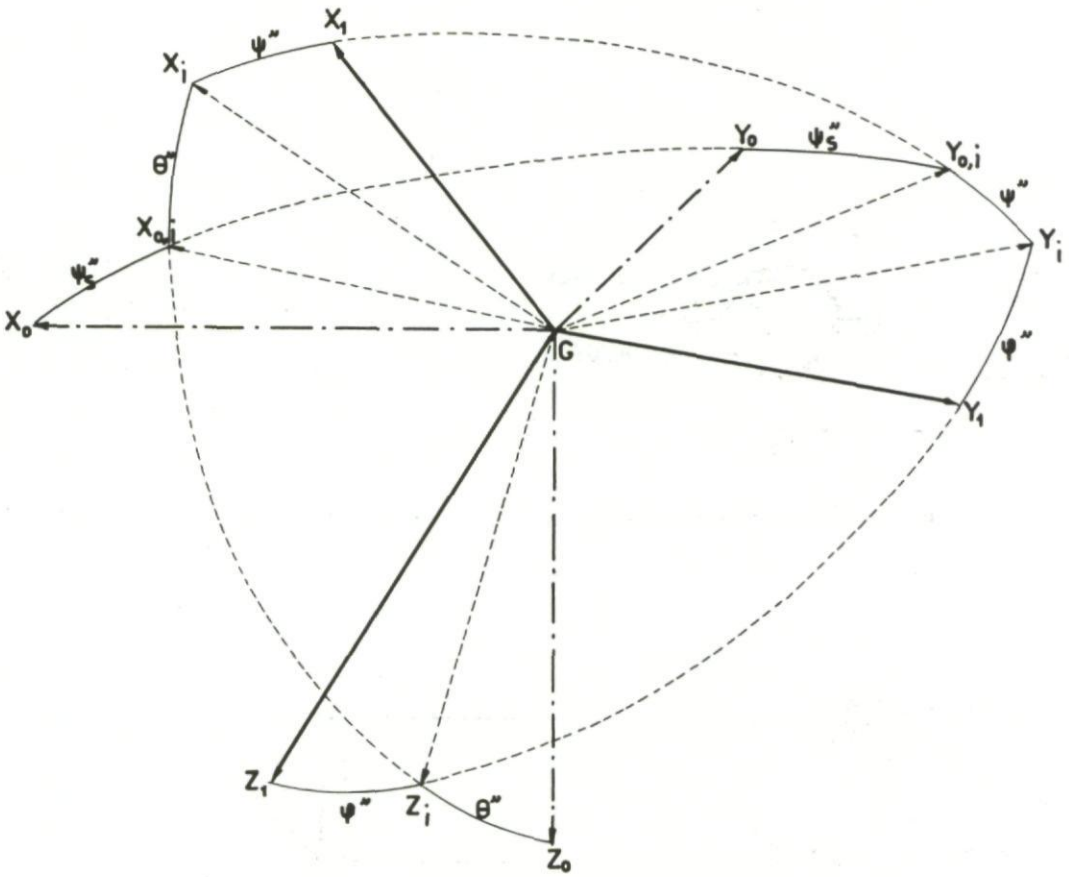

Fig.65 Use of four rotations to displace the reference trihedral

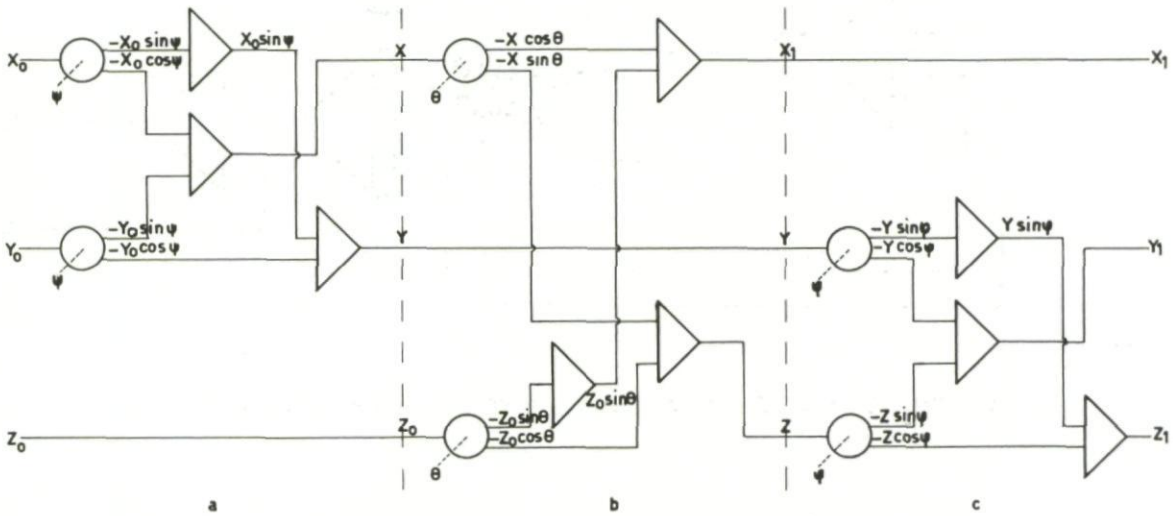

Fig.66 Projections of a vector on two different sets of axes different by ψ, θ, φ

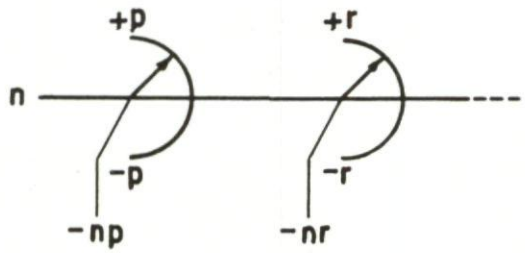

Fig.67 Schematic representation of a multiplier

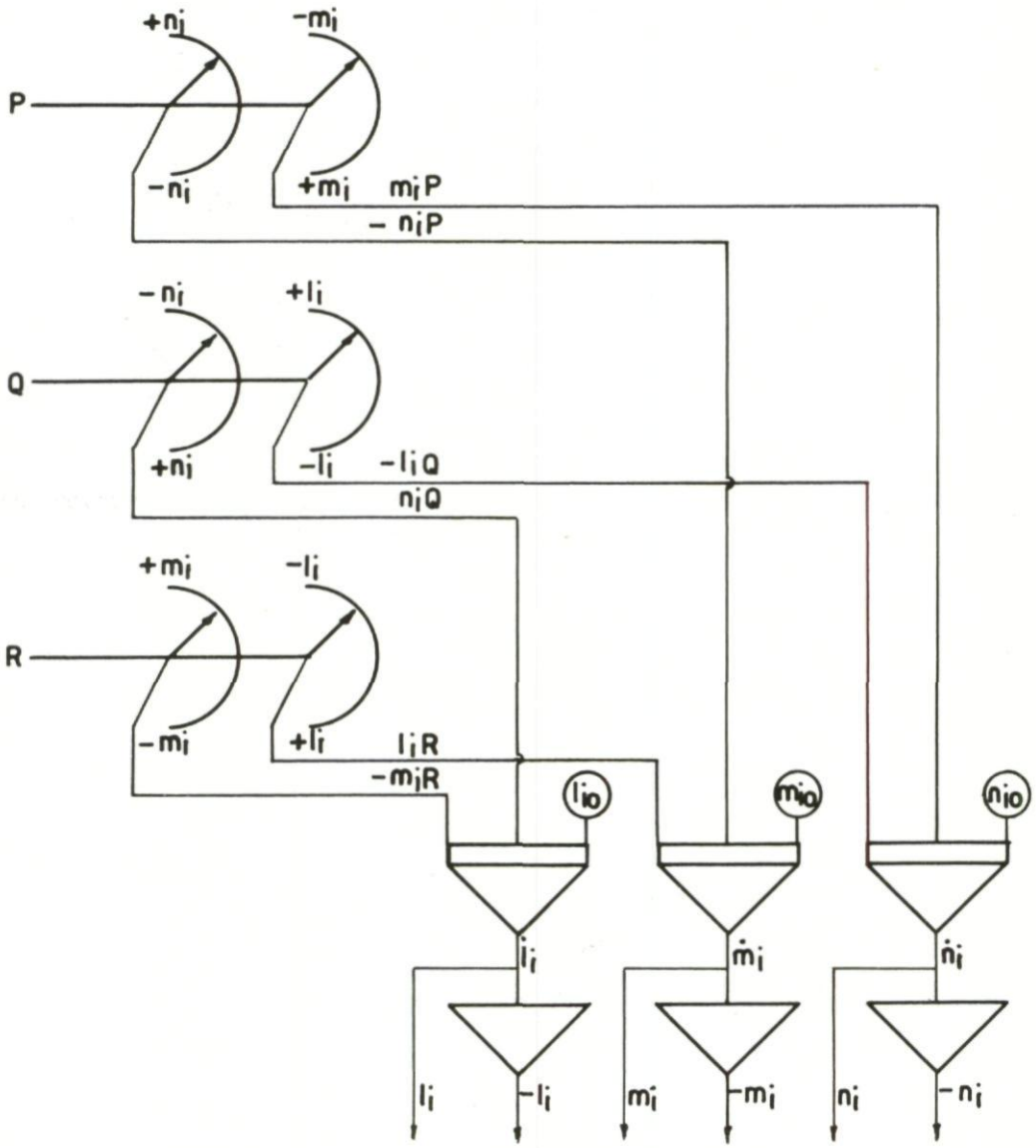

Fig.68 Alteration of direction cosines due to angular velocities

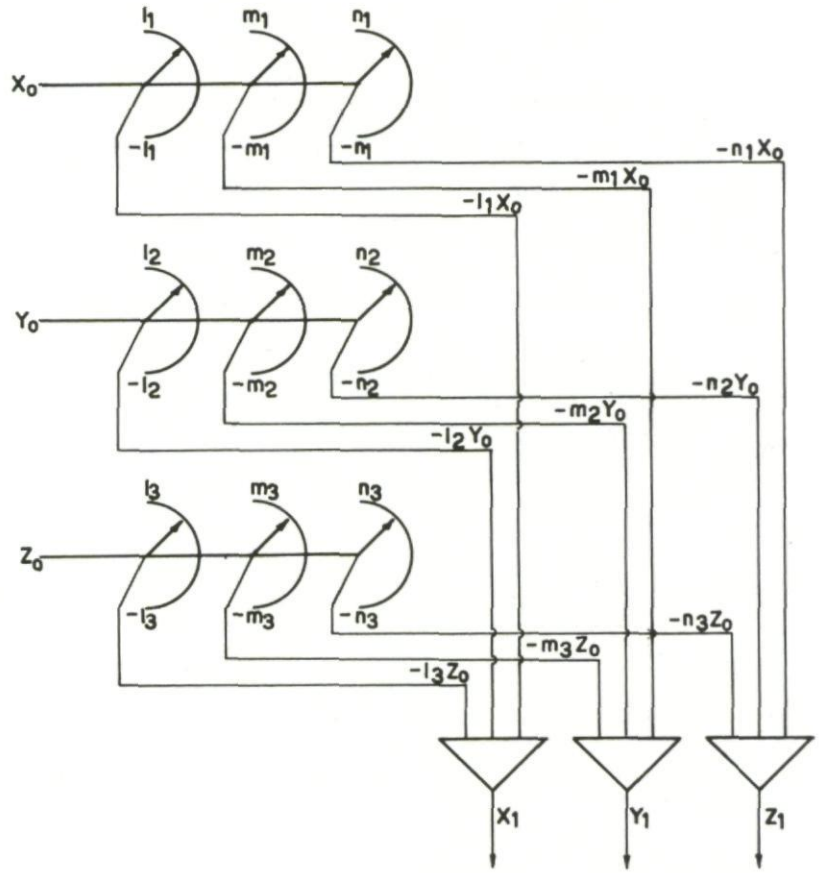

Fig.69 Projections of a vector on two different sets of axes, the direction cosines being known

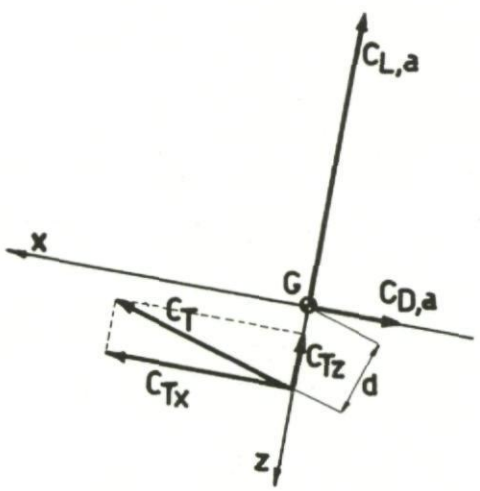

Fig.70 Definition of the coefficients

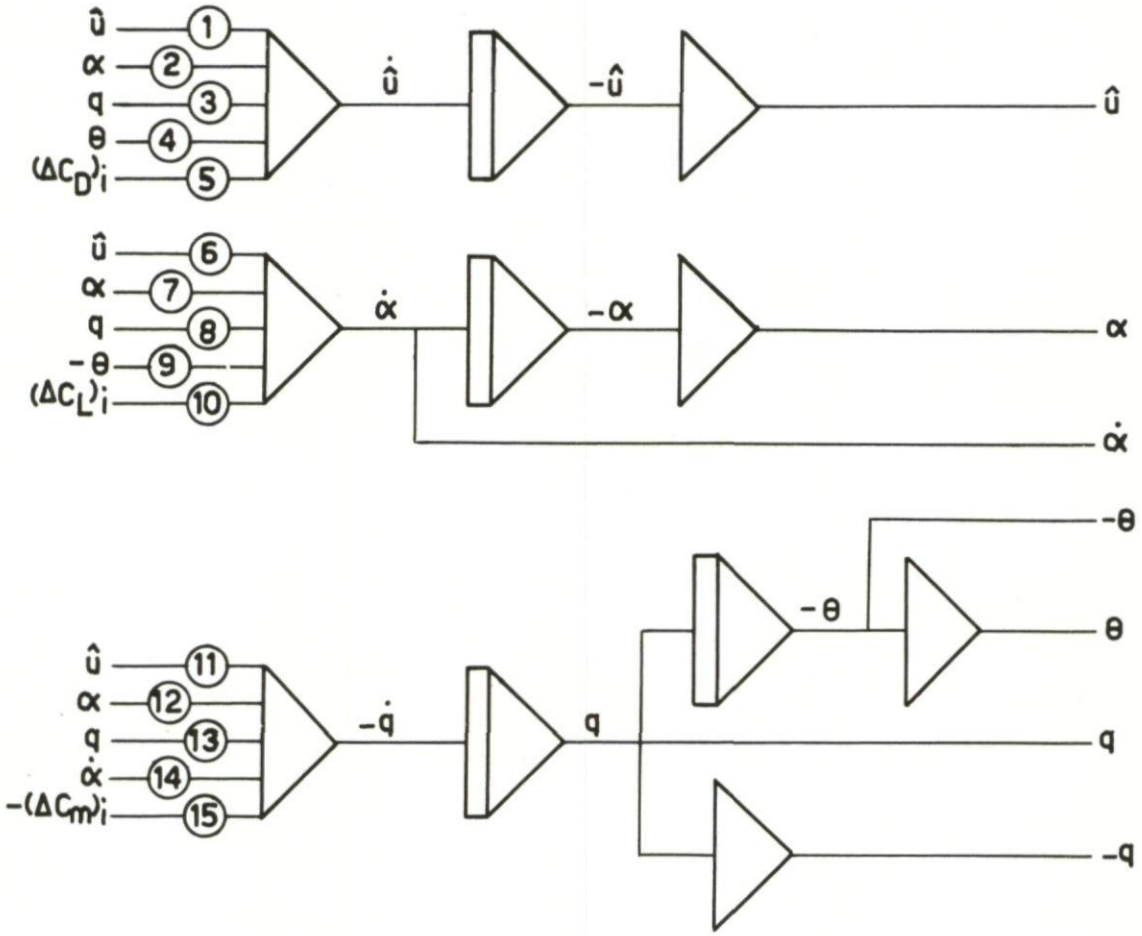

POTENTIOMETERS		
① $\frac{1}{2\tau}(2C_{D_o} + C_{D\hat{u}})$	⑥ $\frac{1}{2\tau}(2C_{L_o} + C_{L\hat{u}})$	⑪ $\frac{1}{C_{Iy}} C_{m\hat{u}}$
② $\frac{1}{2\tau}(C_{D\alpha} - C_{L_o})$	⑦ $\frac{1}{2\tau}(C_{L\alpha} + C_{D_o})$	⑫ $\frac{1}{C_{Iy}} C_{m\alpha}$
③ $\frac{1}{2\tau}\frac{c}{2V_o} C_{Dq}$	⑧ $\frac{1}{2\tau}(\frac{c}{2V_o} C_{Lq} - 2\tau)$	⑬ $\frac{1}{C_{Iy}}\frac{c}{2V_o} C_{mq}$
④ $\frac{1}{2\tau} C_{L_o}$	⑨ $\frac{1}{2\tau} C_{D_o}$	⑭ $\frac{1}{C_{Iy}}\frac{c}{2V_o} C_{m\dot{\alpha}}$
⑤ $\frac{1}{2\tau}$	⑩ $\frac{1}{2\tau}$	⑮ $\frac{1}{C_{Iy}}$

Fig.71 Longitudinal motion; computer set-up and table of coefficients

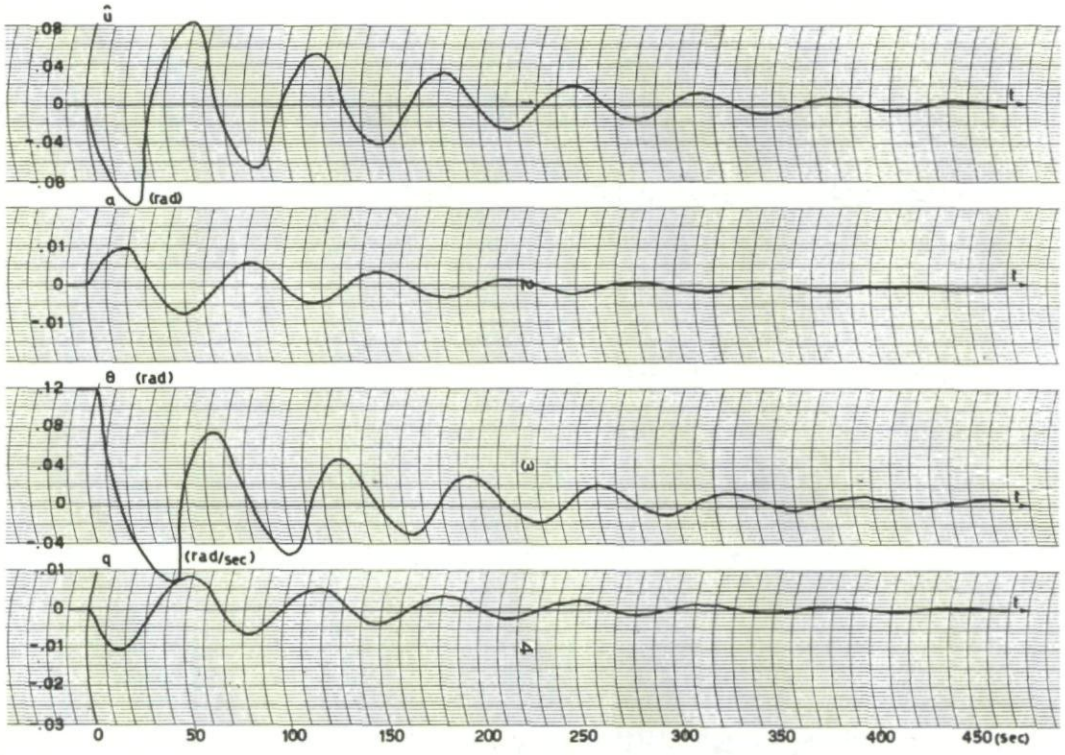

Fig. 72 Longitudinal motion due to initial disturbance θ_0

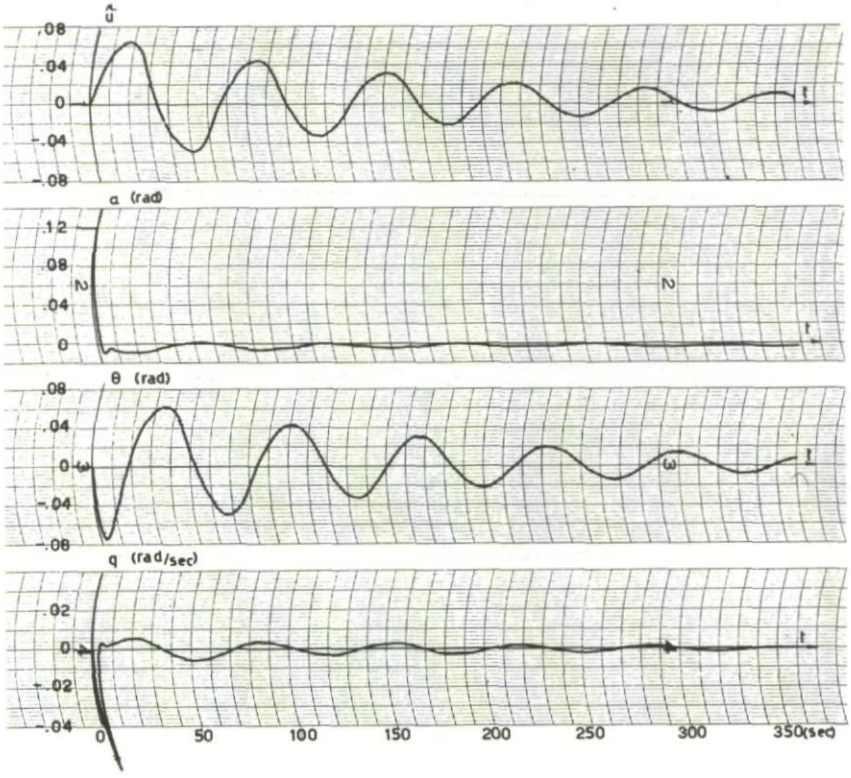

Fig. 73 Longitudinal motion due to initial disturbance α_0

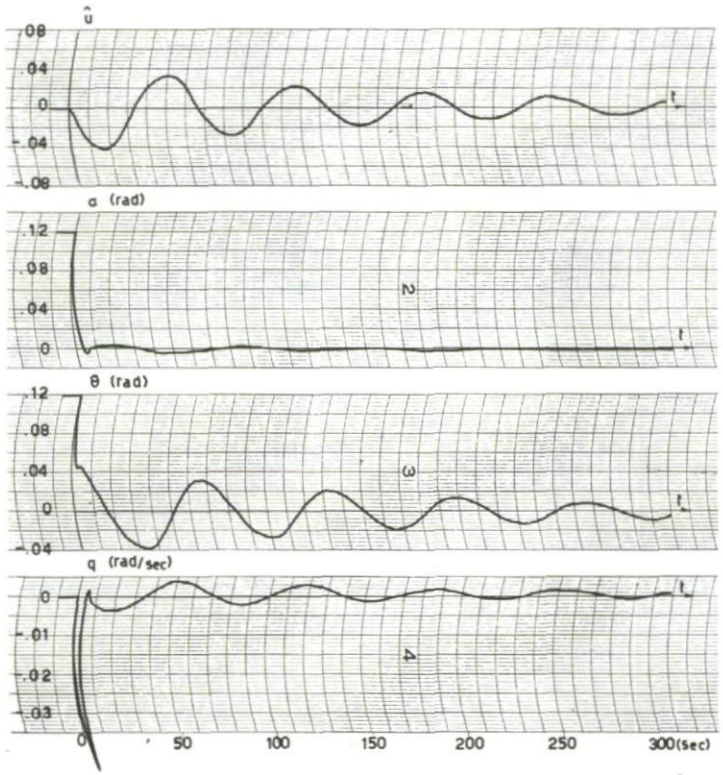

Fig.74 Longitudinal motion due to initial disturbance $\theta_0 + \alpha_0$

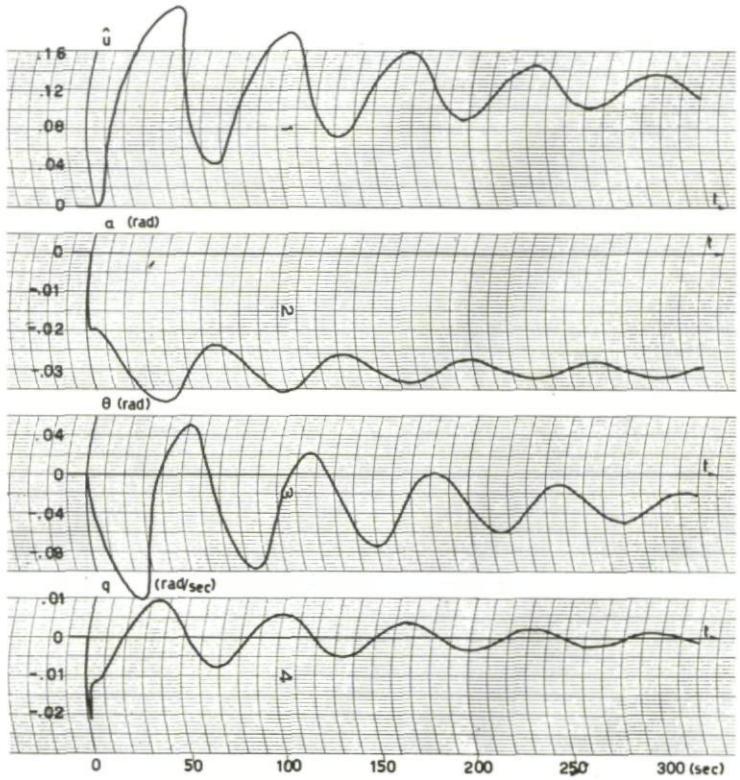

Fig.75 Response to a step input δ_e

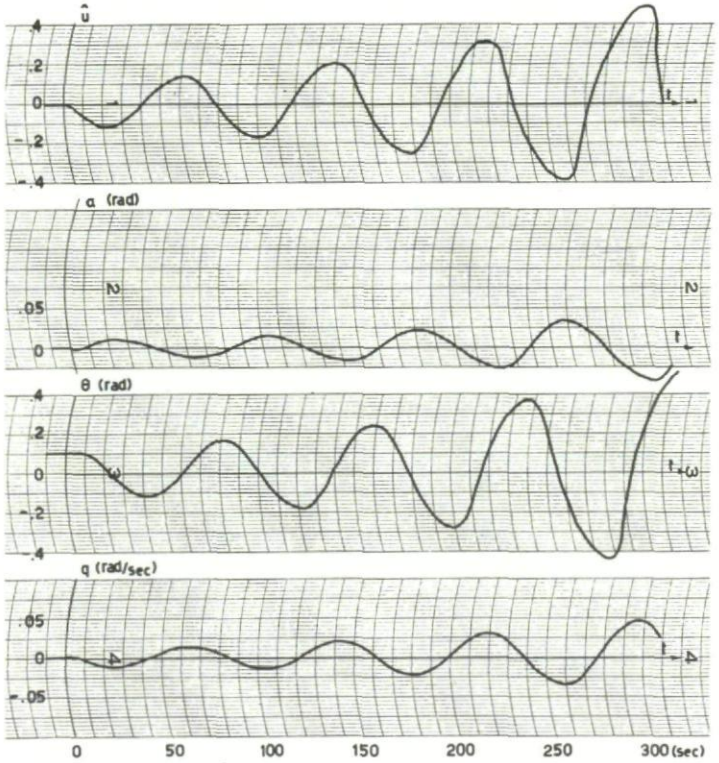

Fig.76 Longitudinal motion due to initial disturbance θ_0

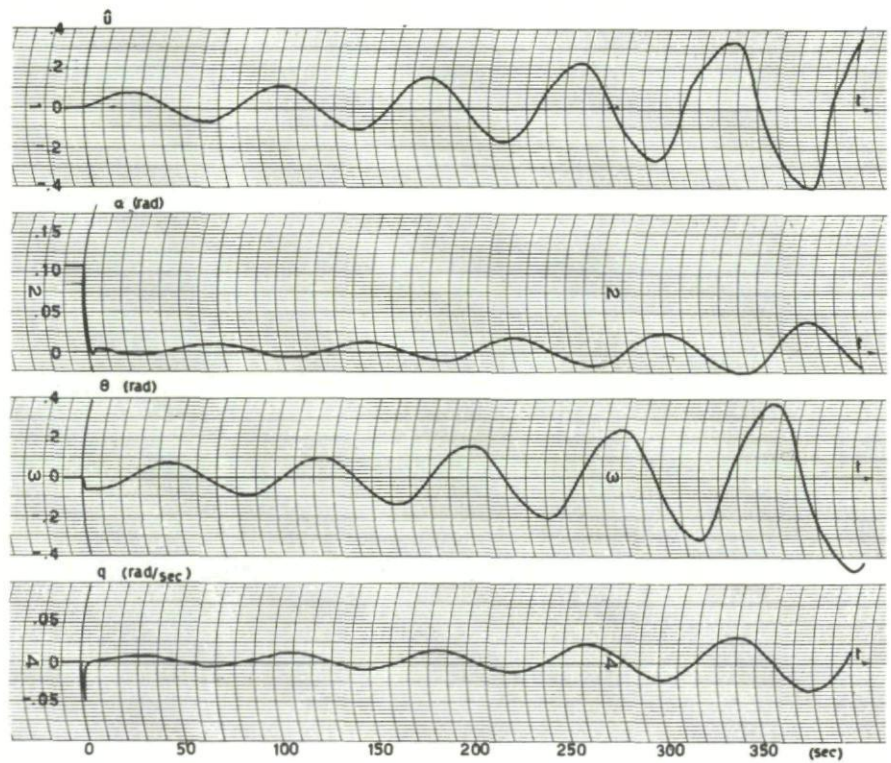

Fig.77 Longitudinal motion due to initial disturbance α_0

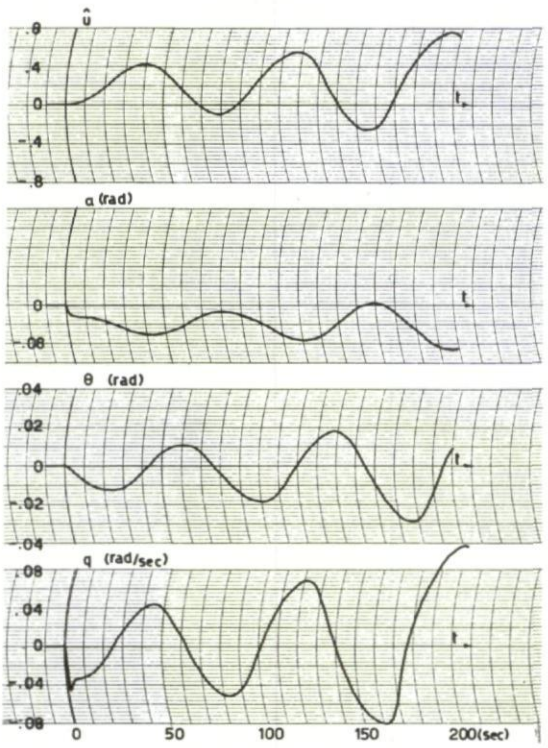

Fig. 78 Response to a step input δ_e

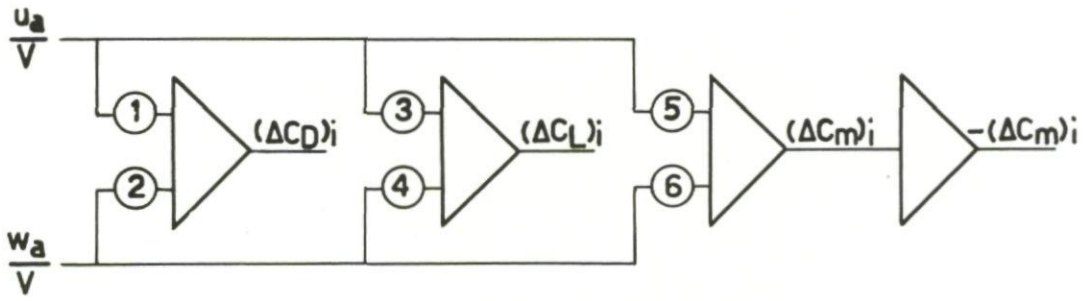

POTENTIOMETERS	
① $2C_{D_o} + C_{D\hat{u}}$	④ $C_{L_\alpha} + C_{D_o}$
② $C_{D_\alpha} - C_{L_o}$	⑤ $C_{m\hat{u}}$
③ $2C_{L_o} + C_{L\hat{u}}$	⑥ C_{m_α}

Fig. 79 Atmospheric velocities as an input; set-up and table of coefficients

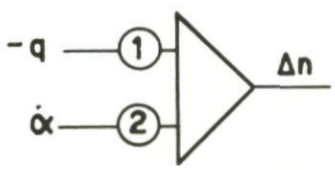

POTENTIOMETERS
① $\frac{V_o}{g}$
② $\frac{V_o}{g}$

Fig. 80 Calculation of the load factor; set-up and table of coefficients

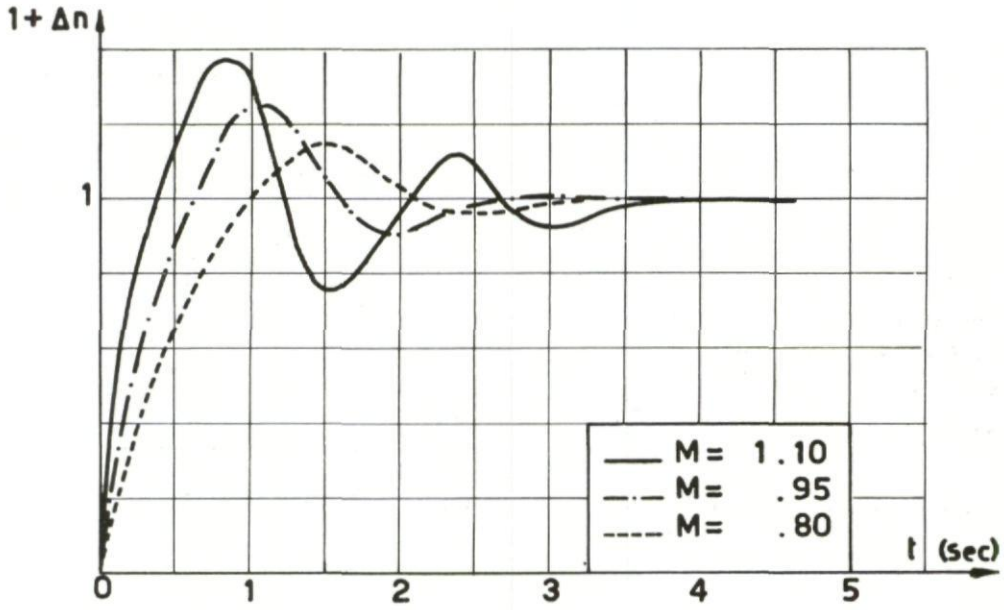

Fig.81 Load factor response to an input δ_e

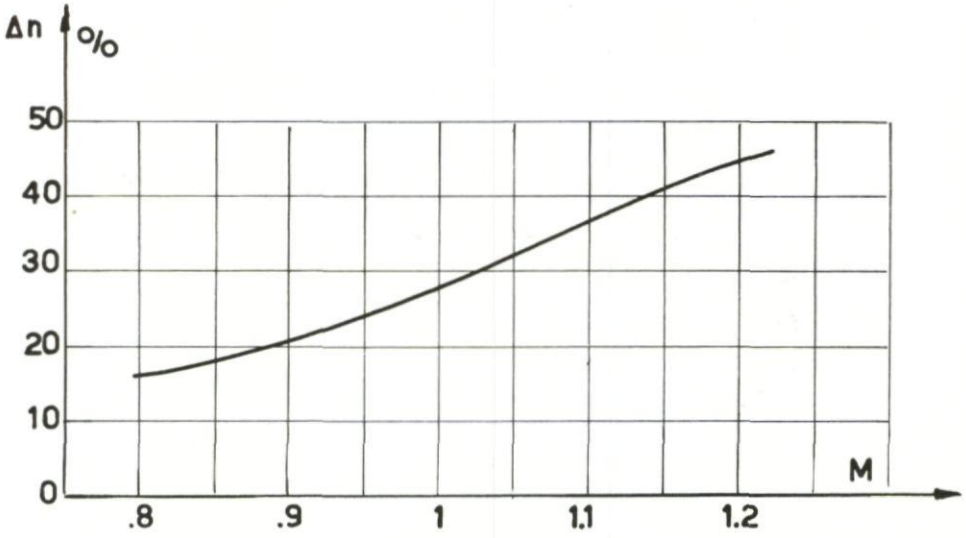

Fig.82 Overshoot of the load factor as a function of M

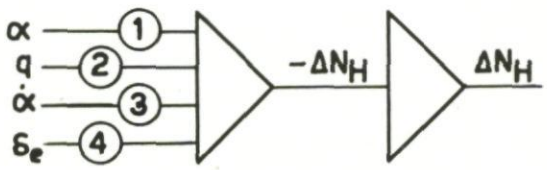

POTENTIOMETERS
① $\frac{\rho}{2} V^2 S_H (1 - \frac{d\varepsilon}{d\alpha}) C_{L_{\alpha,H}}$
② $\frac{\rho}{2} V^2 S_H \frac{L_H}{V_H}$
③ $\frac{\rho}{2} V^2 S_H \frac{L_H}{V_o} \frac{d\varepsilon}{d\alpha}$
④ $\frac{\rho}{2} V^2 S_H C_{L_H,\delta_e}$

Fig.83 Calculation of the tailplane load; set-up and table of coefficients

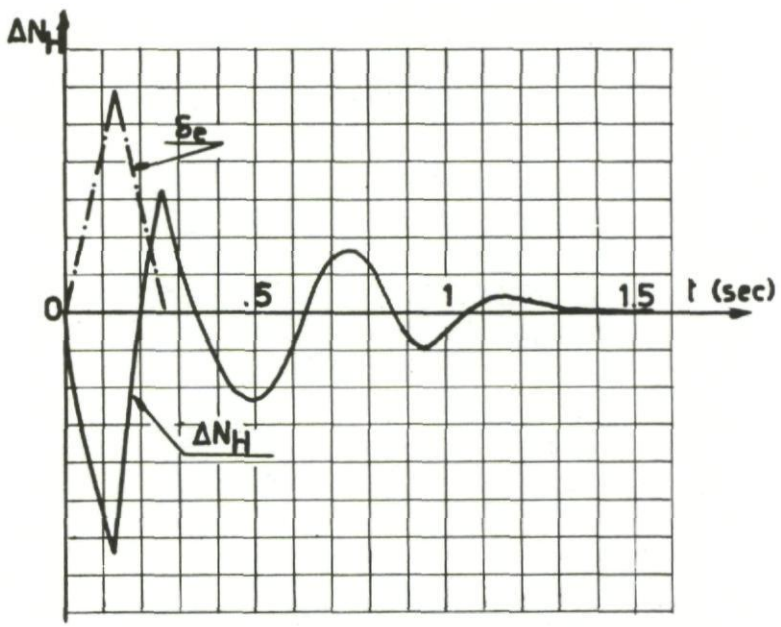

Fig.84 Tailplane load due to a pulse in δ_e

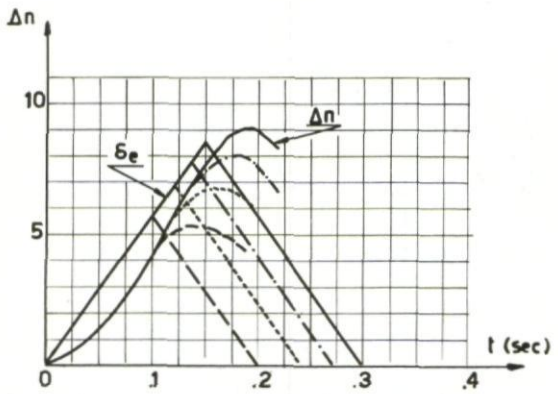

Fig.85 Load factor acting on the aircraft

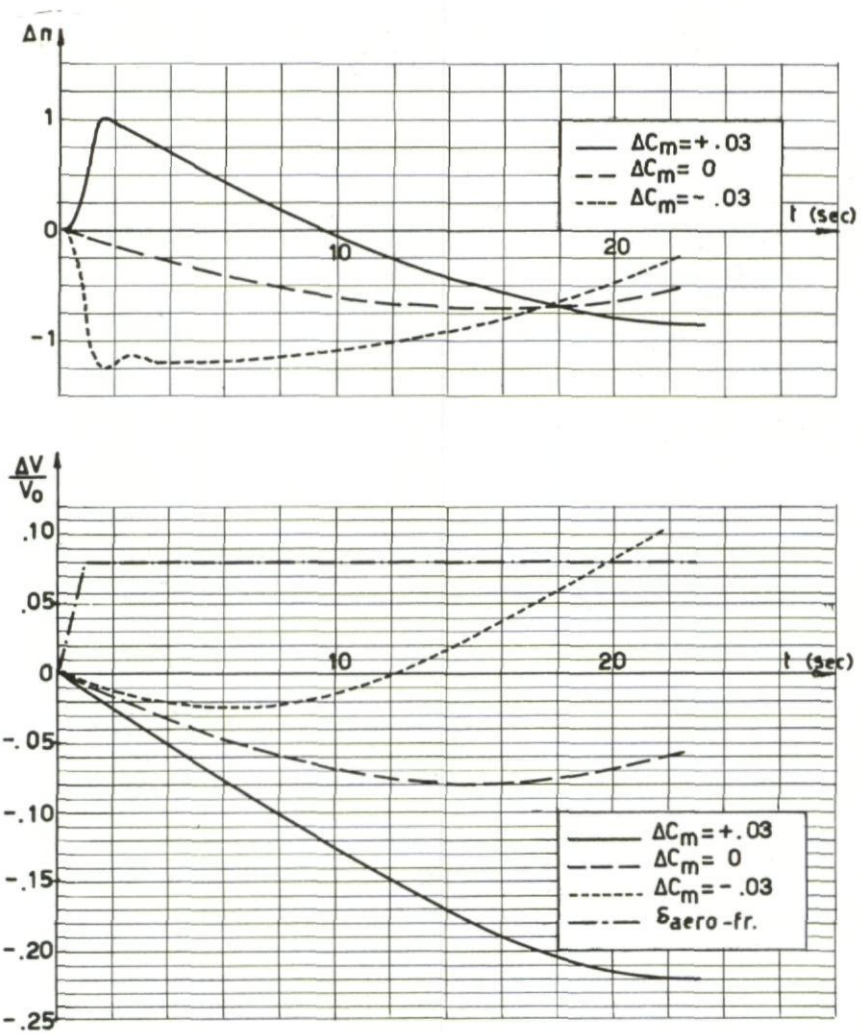

Fig.86 Action of air brakes

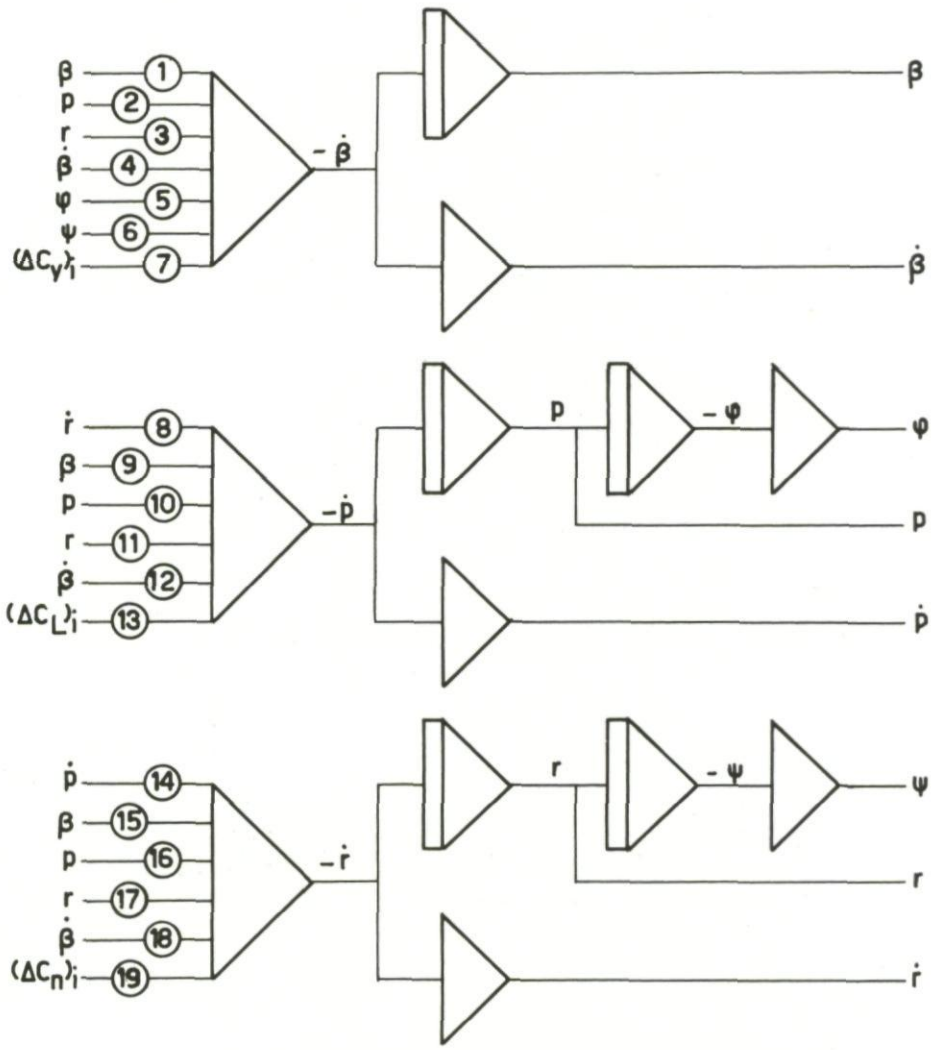

POTENTIOMETERS		
① $\frac{1}{2\tau} C_{y\beta}$	⑧ $\frac{1}{C_{IX}} C_{xz}$	⑭ $\frac{1}{C_{IZ}} C_{xz}$
② $\frac{1}{2\tau} \frac{b}{2V_0} C_{yp}$	⑨ $\frac{1}{C_{IX}} C_{L\beta}$	⑮ $\frac{1}{C_{IZ}} C_{n\beta}$
③ $\frac{1}{2\tau}(\frac{b}{2V_0} C_{yr} - 2\tau)$	⑩ $\frac{1}{C_{IX}} \frac{b}{2V_0} C_{Lp}$	⑯ $\frac{1}{C_{IZ}} \frac{b}{2V_0} C_{np}$
④ $\frac{1}{2\tau} \frac{b}{2V_0} C_{y\dot{\beta}}$	⑪ $\frac{1}{C_{IX}} \frac{b}{2V_0} C_{Lr}$	⑰ $\frac{1}{C_{IZ}} \frac{b}{2V_0} C_{nr}$
⑤ $\frac{1}{2\tau} C_{L_0}$	⑫ $\frac{1}{C_{IX}} \frac{b}{2V_0} C_{L\dot{\beta}}$	⑱ $\frac{1}{C_{IZ}} \frac{b}{2V_0} C_{n\dot{\beta}}$
⑥ $\frac{1}{2\tau} C_{L_0} \Theta_0$	⑬ $\frac{1}{C_{IX}}$	⑲ $\frac{1}{C_{IZ}}$
⑦ $\frac{1}{2\tau}$		

Fig. 87 Lateral motion; computer set-up and table of coefficients

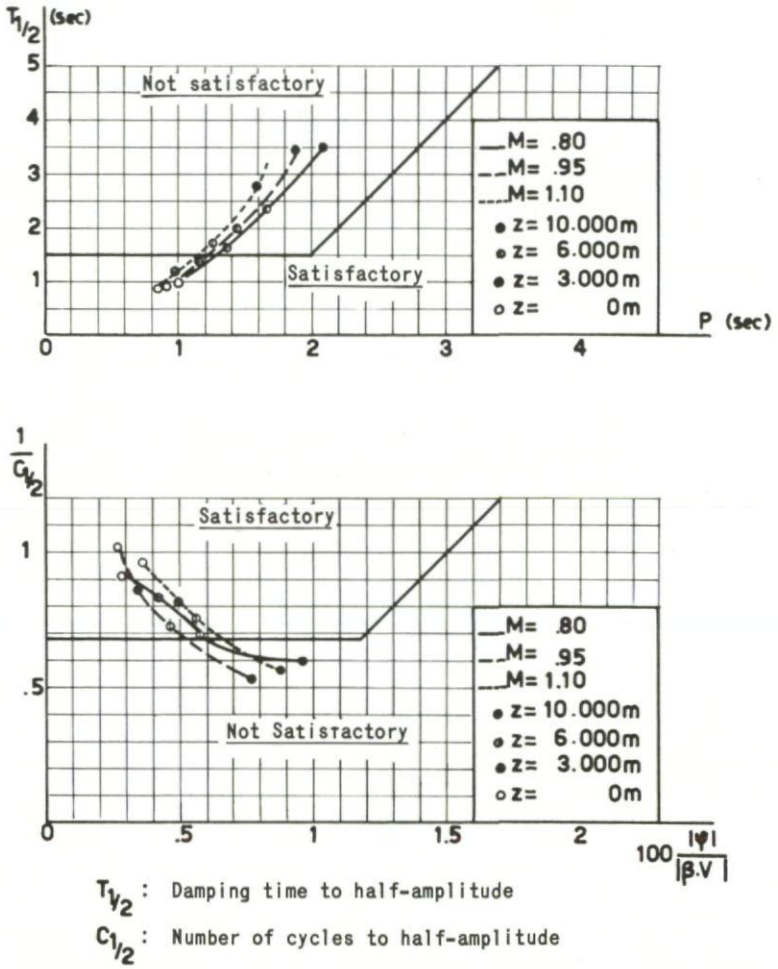

Fig.88 Verification of lateral motion stability criteria

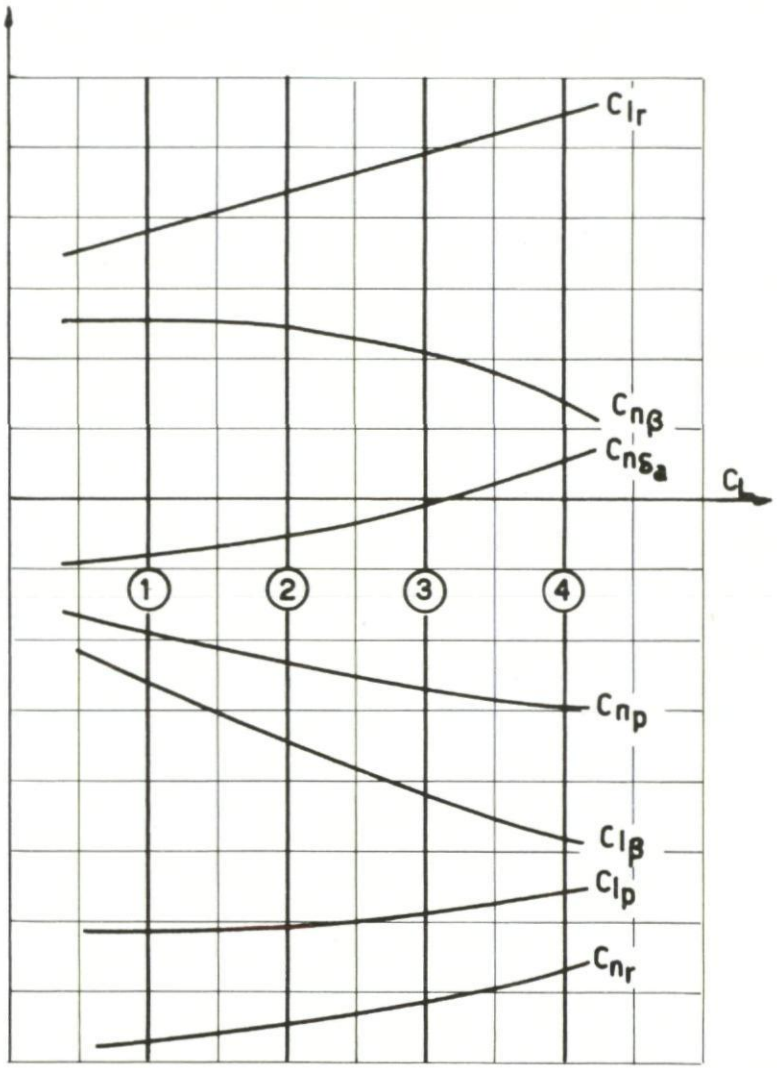

Fig.89 Variation of lateral derivatives with C_L

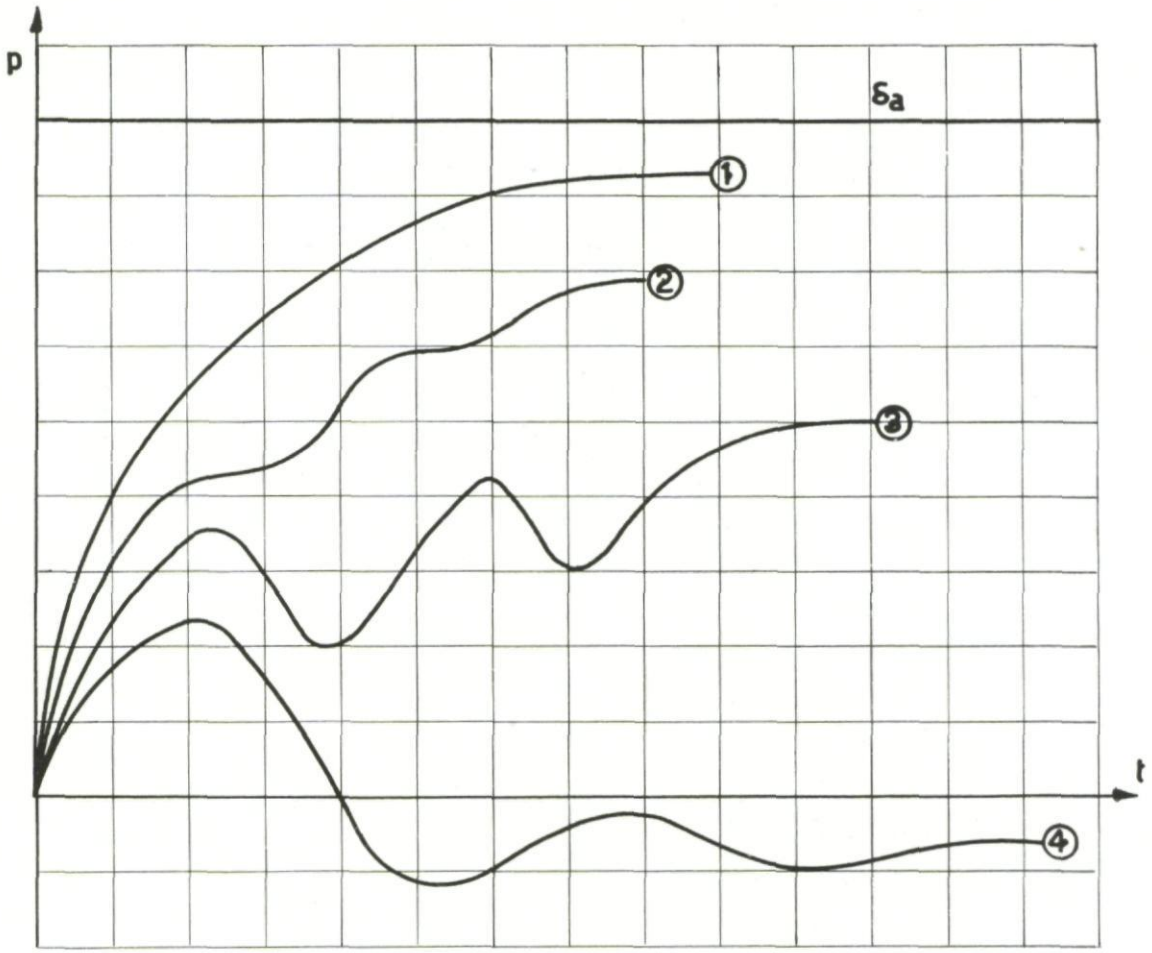

Fig. 90 Response in p to a step input δ_a

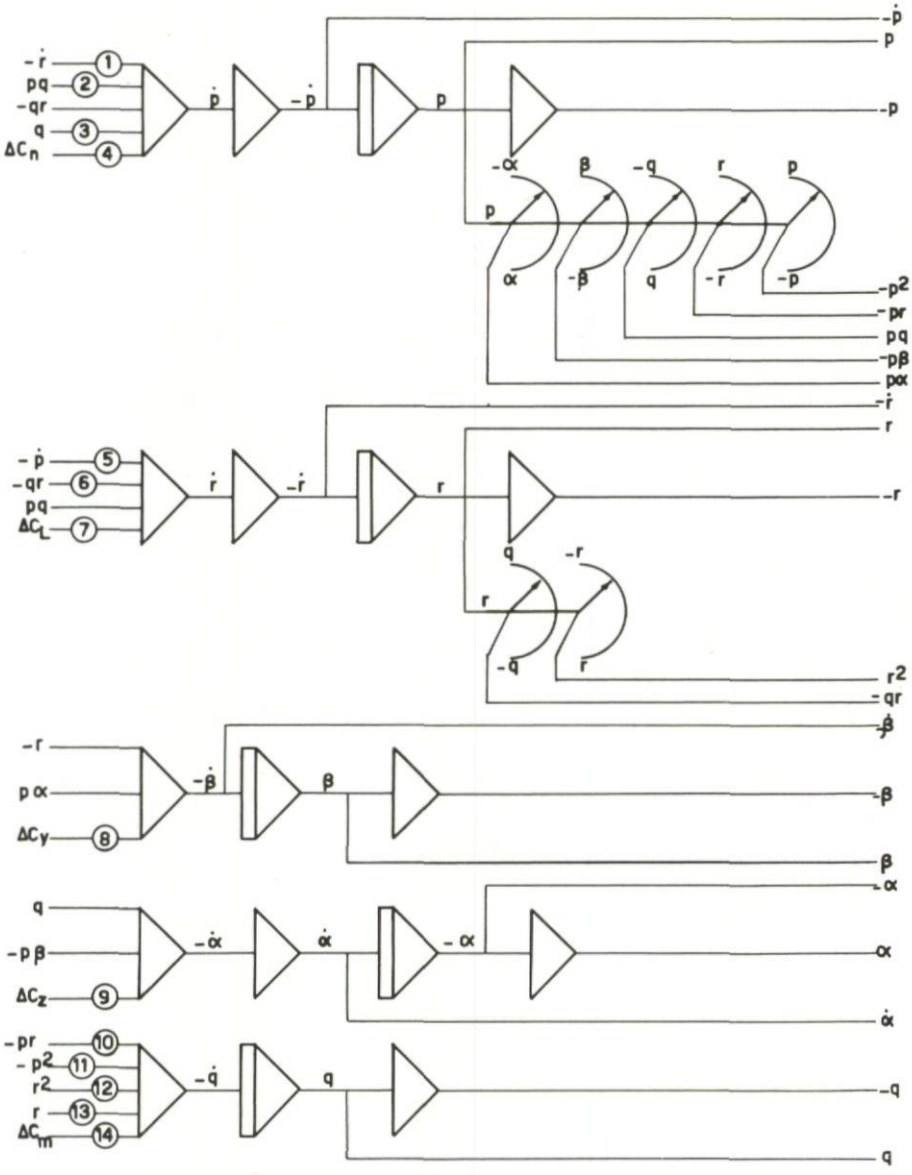

POTENTIOMETERS		
① $\frac{1}{C_{zx}} C_{Iz}$	⑥ $\frac{1}{C_{zx}}(C_{Iz} - \frac{c}{b} C_{Ix})$	⑪ $\frac{1}{C_{Iy}} \frac{b}{c} C_{zx}$
② $\frac{1}{C_{zx}}(C_{Iz} - \frac{c}{b} C_{Iy})$	⑦ $\frac{1}{C_{zx}}$	⑫ $\frac{1}{C_{Iy}} \frac{b}{c} C_{zx}$
③ $\frac{1}{C_{zx}} \frac{c}{2V_o} C'_{nq}$	⑧ $\frac{1}{2\tau}$	⑬ $\frac{1}{C_{Iy}} \frac{b}{2V_o} C'_{mr}$
④ $\frac{1}{C_{zx}}$	⑨ $\frac{1}{2\tau}$	⑭ $\frac{1}{C_{Iy}}$
⑤ $\frac{1}{C_{zx}} \cdot C_{Ix}$	⑩ $\frac{1}{2\tau} \frac{b}{c}(C_{Ix} - C_{Iz})$	

Fig. 91 Combined motion of five variables; set-up and table of coefficients

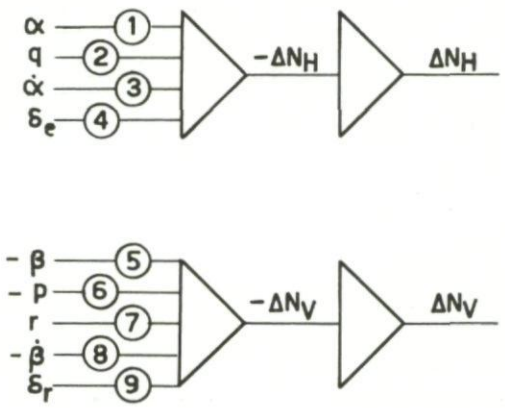

POTENTIOMETERS

① $\frac{\rho}{2} V_0^2 S_H \left(\frac{\partial C_L}{\partial \alpha}\right)_H \left(1 - \frac{d\varepsilon_H}{d\alpha}\right)$

② $\frac{\rho}{2} V_0^2 S_H \left(\frac{\partial C_L}{\partial \alpha}\right)_H \frac{L_H}{V_0}$

③ $\frac{\rho}{2} V_0^2 S_H \left(\frac{\partial C_L}{\partial \alpha}\right)_H \frac{L_H}{V_0} \cdot \frac{d\varepsilon_H}{d\alpha}$

④ $\frac{\rho}{2} V_0^2 S_H \left(\frac{\partial C_L}{\partial \delta_e}\right)_H$

⑤ $\frac{\rho}{2} V_0^2 S_V \left(\frac{\partial C_Y}{\partial \beta}\right)_V \left(1 - \frac{d\varepsilon_V}{d\beta}\right)$

⑥ $\frac{\rho}{2} V_0^2 S_V \left(\frac{\partial C_Y}{\partial \beta}\right)_V \frac{H}{V_V}$

⑦ $\frac{\rho}{2} V_0^2 S_V \left(\frac{\partial C_Y}{\partial \beta}\right)_V \frac{L_V}{V_V}$

⑧ $\frac{\rho}{2} V_0^2 S_V \left(\frac{\partial C_Y}{\partial \beta}\right)_V \frac{L_V}{V_0} \frac{d\varepsilon_V}{d\beta}$

⑨ $\frac{\rho}{2} V_0^2 S_V \left(\frac{\partial C_Y}{\partial \delta_r}\right)_V$

Fig. 92 Load on the tail surfaces; set-up and table of coefficients

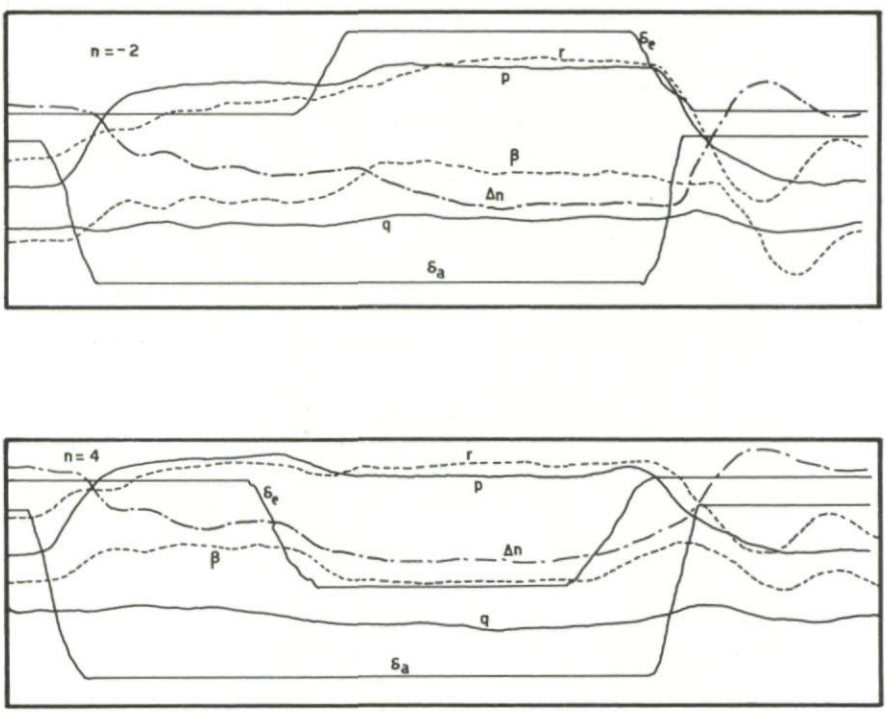

Fig. 93 Response to an action of δ_a and δ_e

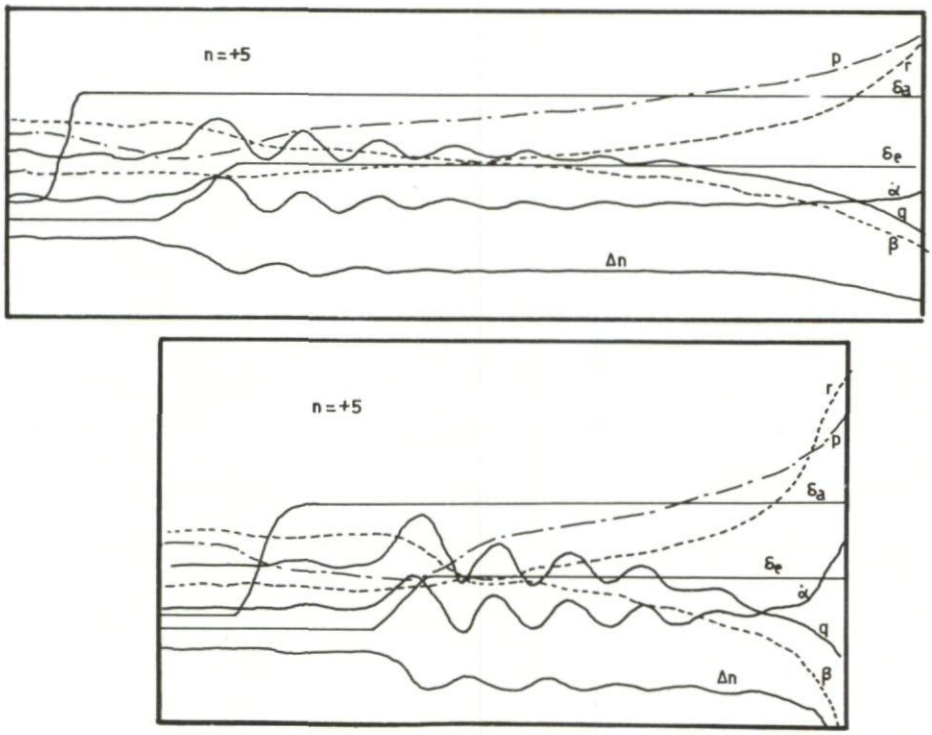

Fig. 94 Divergence during rolling pull-out

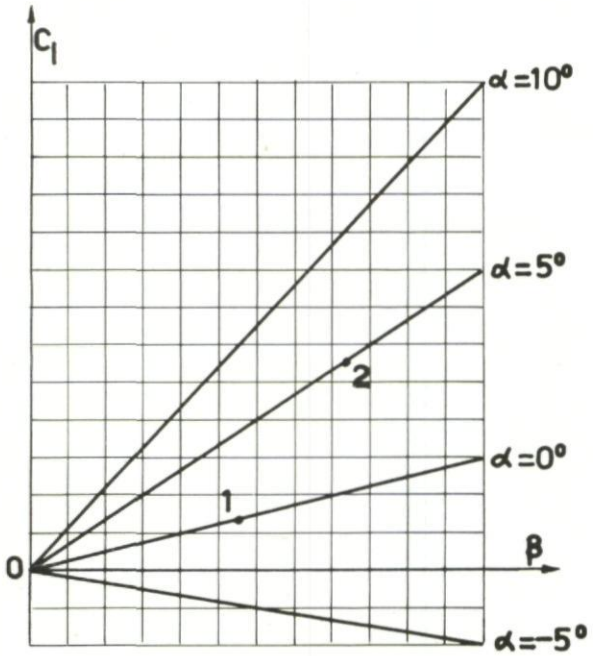

Fig. 95 Particular case of C_l, function of α and β

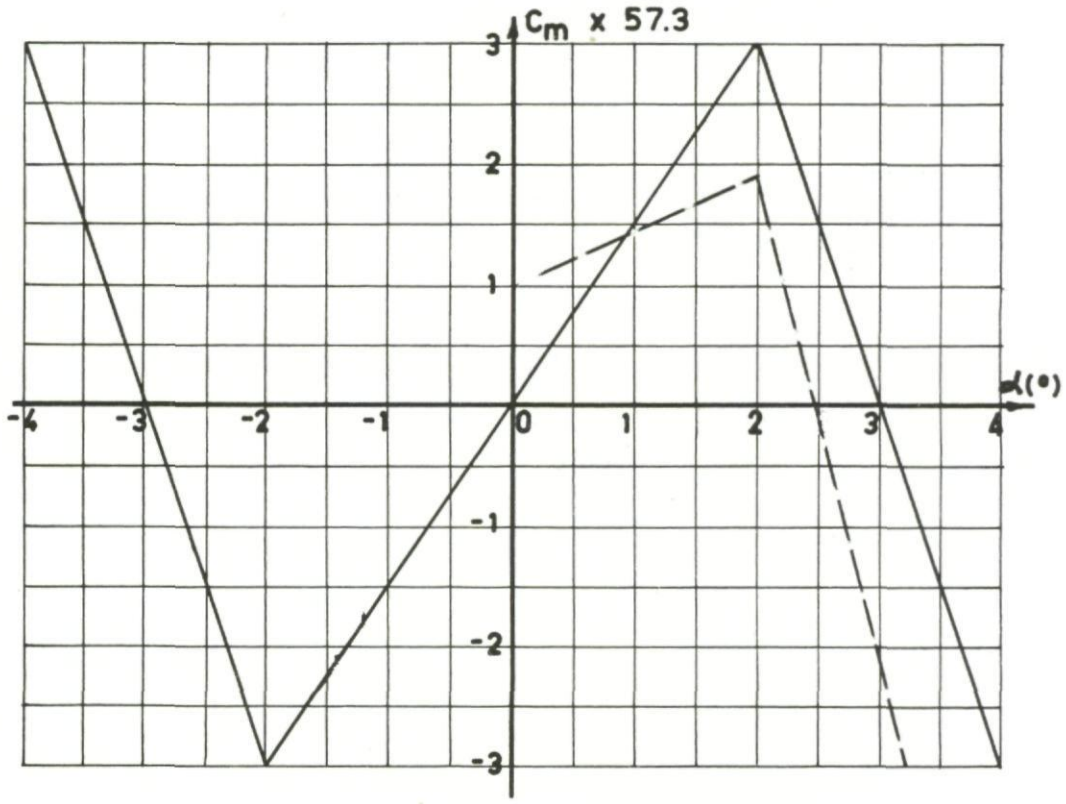

Fig.96 C_{m_α} derivative with change of sign

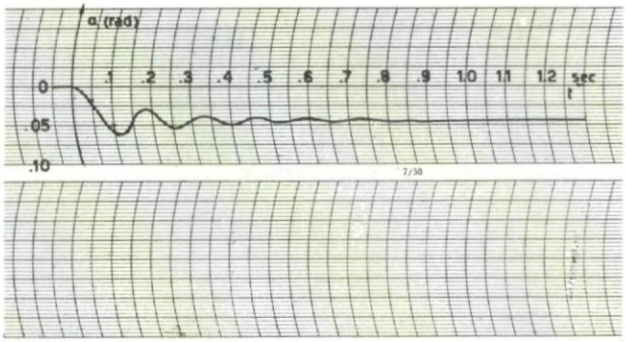

Fig.97 Response to a control action δ_e

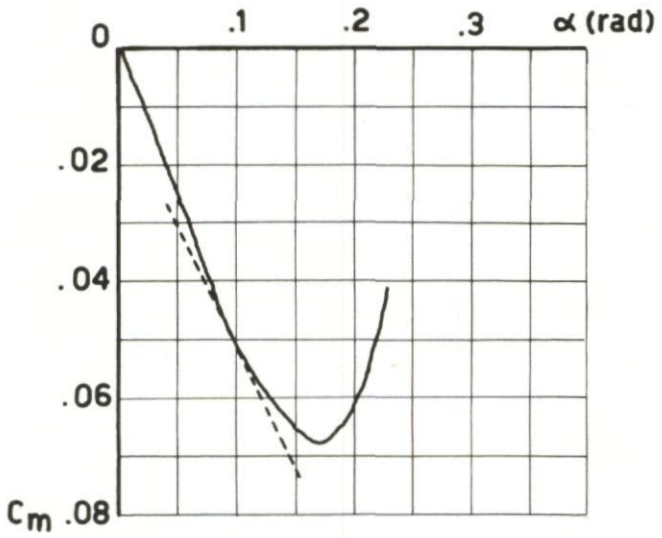

Fig.98 Actual curve C_m versus α

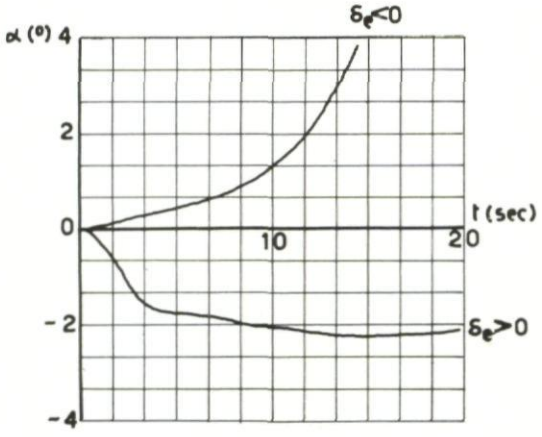

Fig.99 Response to $\delta_e > 0$ and $\delta_e < 0$

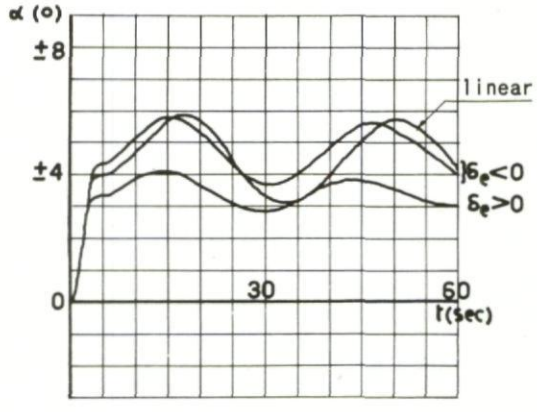

Fig.100 Response to $\delta_e > 0$ and $\delta_e < 0$

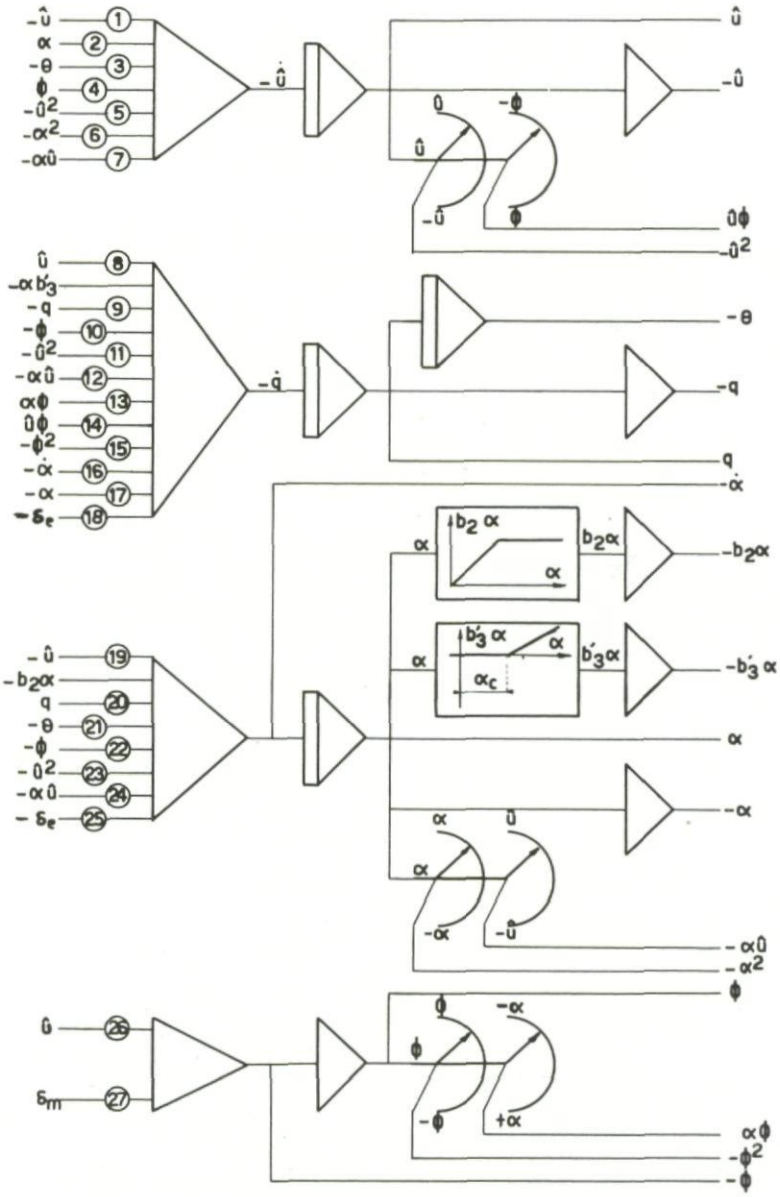

POTENTIOMETERS					
① a_1	⑥ B_1	⑪ A_3	⑯ m_3	㉑ d_2	㉖ a_4
② b_1	⑦ H_1	⑫ H_3	⑰ b_3	㉒ l_2	㉗ h_4
③ d_1	⑧ a_3	⑬ L_3	⑱ k_3	㉓ A_2	
④ l_1	⑨ c_3	⑭ M_3	⑲ a_2	㉔ H_2	
⑤ A_1	⑩ l_3	⑮ N_3	⑳ c_2	㉕ k_2	

Fig.101 Longitudinal motion in a non-linear case. Set-up and table of coefficients

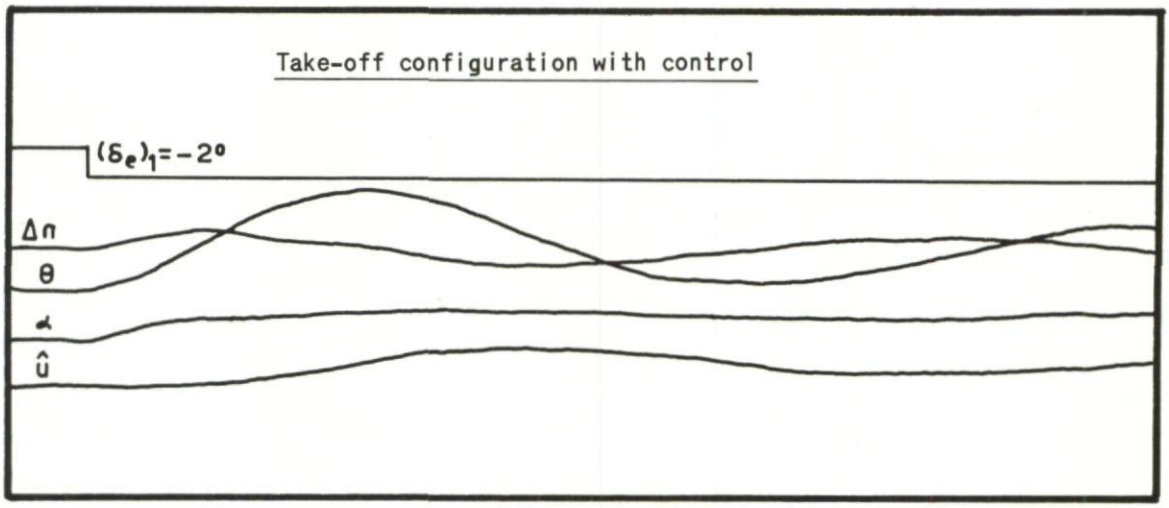

Fig.102 Longitudinal motion in a non-linear case

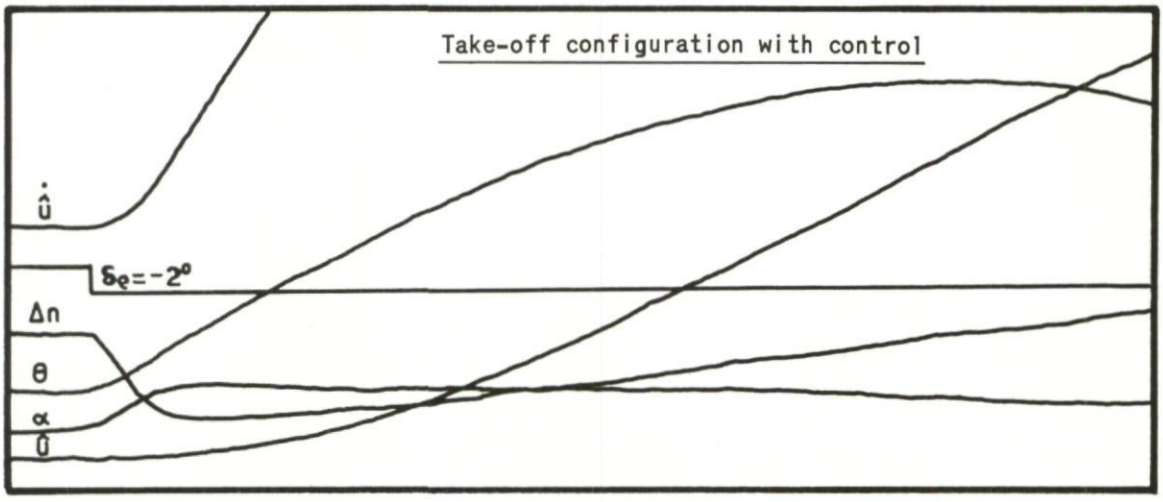

Fig.103 Longitudinal motion in a non-linear case

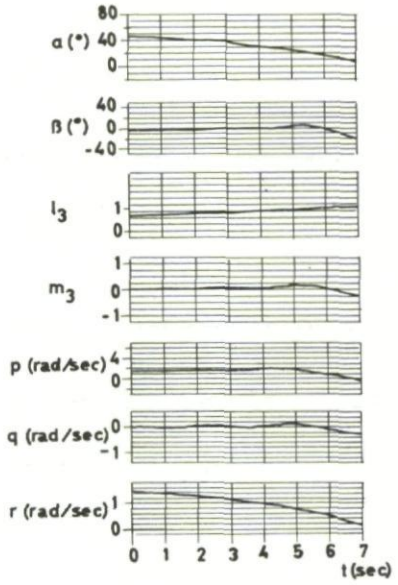

Fig.104 Recovery from a spin; simulation

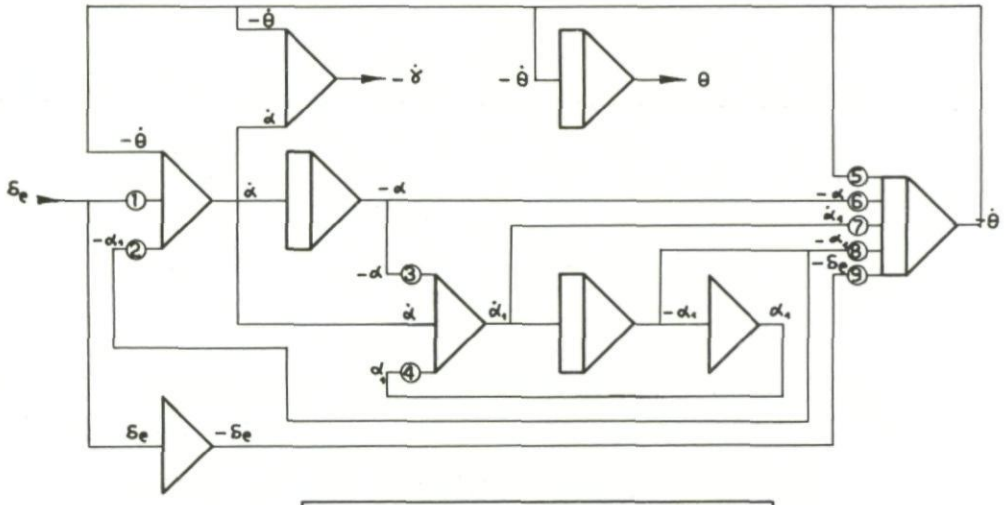

POTENTIOMETERS	
① $-C_{L_{\delta_e}} \frac{1}{2\tau}$	⑥ $-(C_{m_\alpha})_e \frac{1}{C_{Iy}}$
② $C_{L_\alpha} \frac{1}{2\tau}$	⑦ $C_{m_{\dot{\alpha}}} \frac{c}{2V_0} \cdot \frac{1}{C_{Iy}}$
③ $\frac{2}{a}$	⑧ $-(C_{m_\alpha})_p \frac{1}{C_{Iy}}$
④ $\frac{2}{a}$	⑨ $-C_{m_{\delta_e}} \frac{1}{C_{Iy}}$
⑤ $-C_{m_q} \frac{c}{2V_0} \cdot \frac{1}{C_{Iy}}$	

Fig.105 Set-up of short oscillation with time lag in C_L

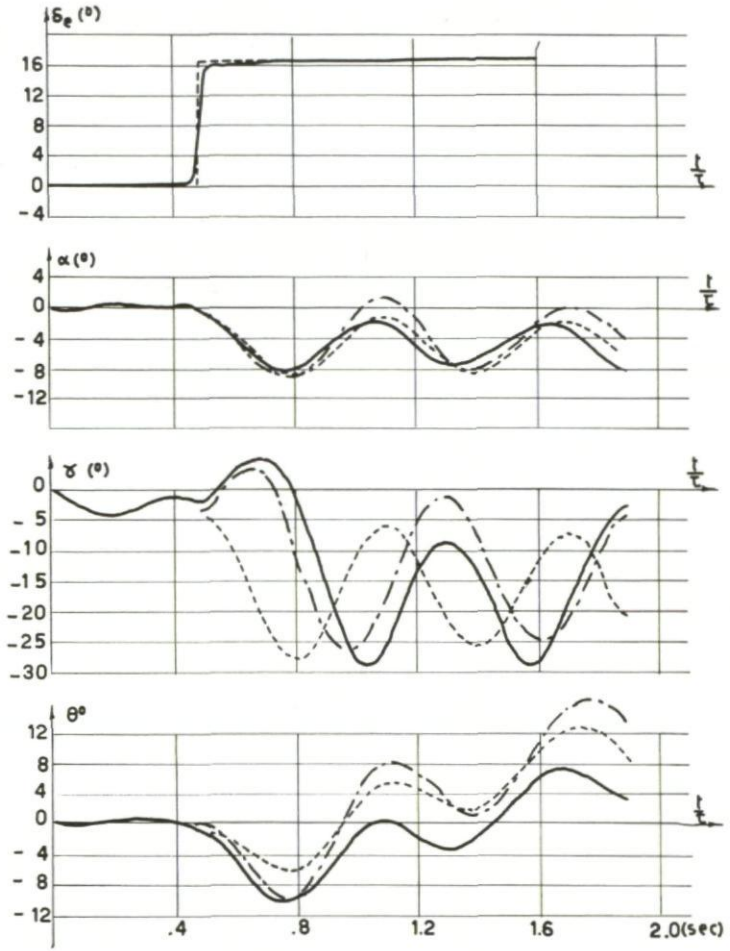

Fig.106 Flight test and computed motion

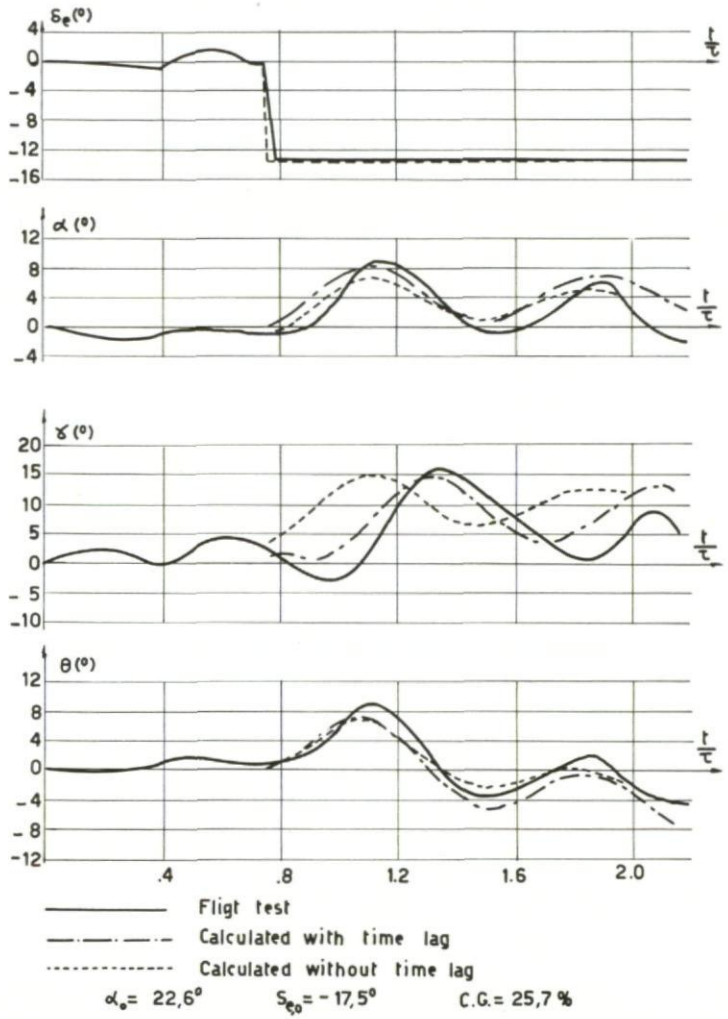

Fig.107 Flight test and computed motion

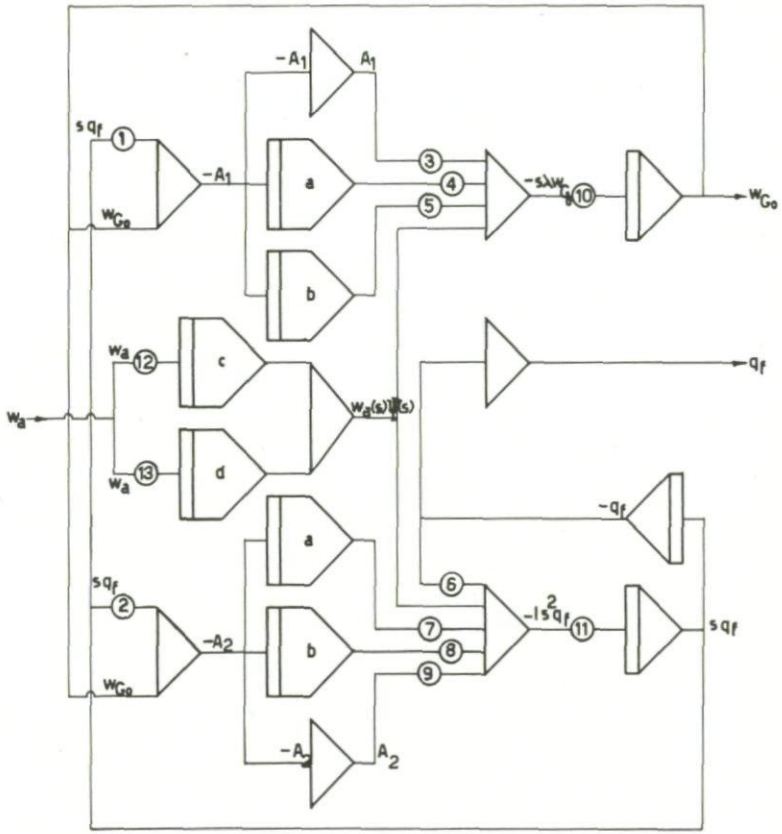

POTENTIOMETERS				
① Γ_1	④ 0,165	⑦ 0,165	⑩ $\frac{1}{\lambda}$	⑬ 0,5
② Γ_2	⑤ 0,335	⑧ 0,335	⑪ $\frac{1}{I}$	
③ 0,5	⑥ $\Omega^2 I$	⑨ 0,5	⑫ 0,5	

Fig. 108 Coupling of aircraft trajectory and wing bending; set-up and table of coefficients

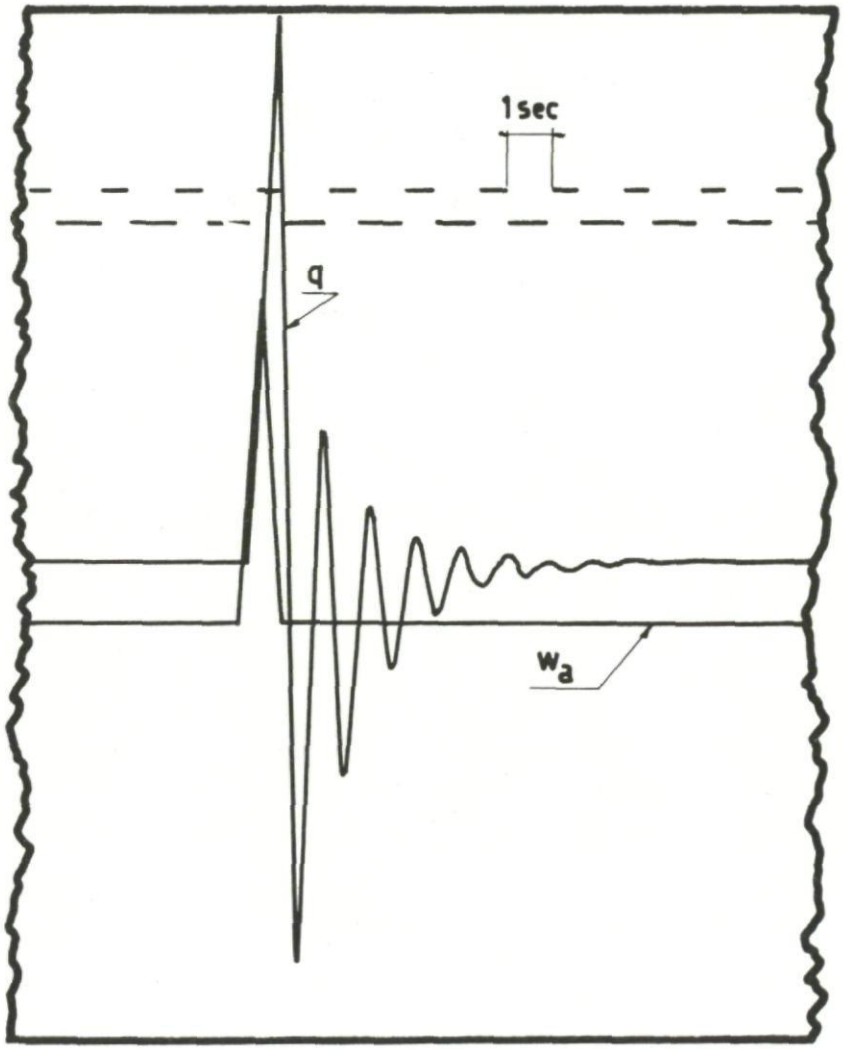

Fig. 109 Response of generalized co-ordinate q to a pulse in w_a

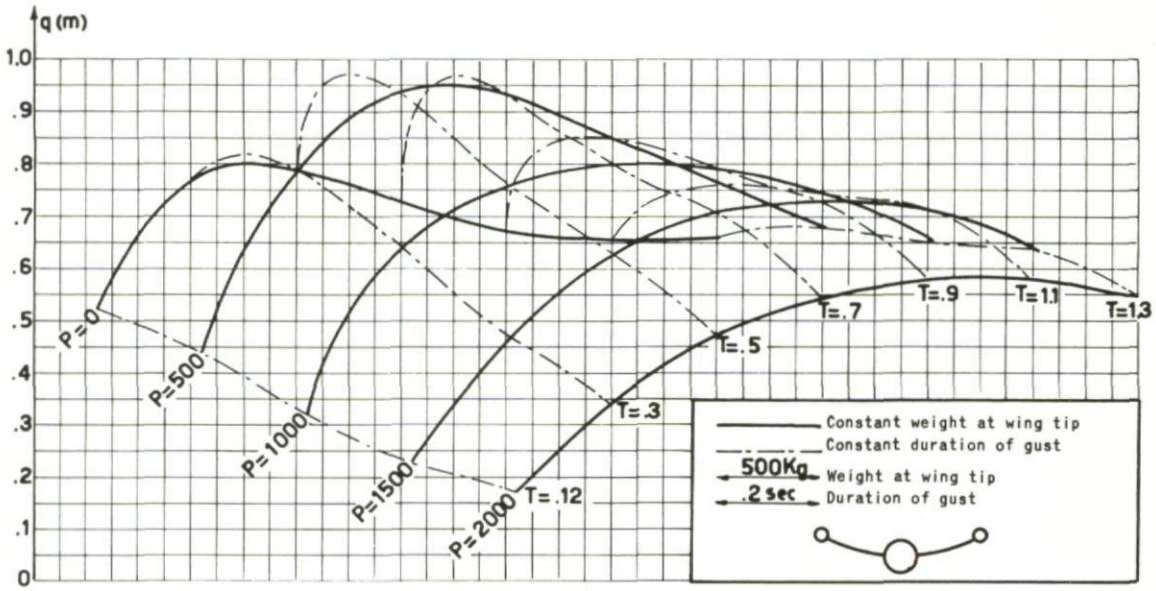

Fig.110 Influence of wing tip weight and gust duration

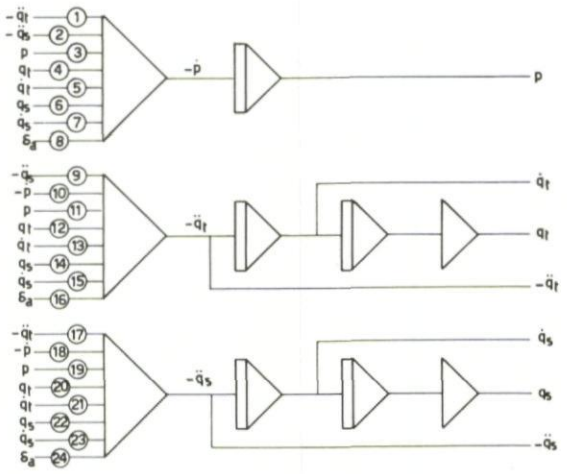

POTENTIOMETERS		
① $\frac{1}{I_x} k_{x_t}$	⑨ $\frac{1}{m_{tt}} m_{t_s}$	⑰ $\frac{1}{m_{ss}} m_{s_t}$
② $\frac{1}{I_x} k_{x_s}$	⑩ $\frac{1}{m_{tt}} k_{x_t}$	⑱ $\frac{1}{m_{ss}} k_{x_s}$
③ $\frac{1}{I_x} L_p$	⑪ $\frac{1}{m_{tt}} Q_{s_p}$	⑲ $\frac{1}{m_{ss}} Q_{s_p}$
④ $\frac{1}{I_x} L_{q_t}$	⑫ $\frac{1}{m_{tt}} (Q_{t_{q_t}} - a_{11})$	⑳ $\frac{1}{m_{ss}} (Q_{s_{q_t}} - a_{21})$
⑤ $\frac{1}{I_x} L_{\dot{q}_t}$	⑬ $\frac{1}{m_{tt}} Q_{t_{\dot{q}_t}}$	㉑ $\frac{1}{m_{ss}} Q_{s_{\dot{q}_t}}$
⑥ $\frac{1}{I_x} L_{q_s}$	⑭ $\frac{1}{m_{tt}} (Q_{t_{q_s}} - a_{12})$	㉒ $\frac{1}{m_{ss}} (Q_{s_{q_s}} - a_{22})$
⑦ $\frac{1}{I_x} L_{\dot{q}_s}$	⑮ $\frac{1}{m_{tt}} Q_{t_{\dot{q}_s}}$	㉓ $\frac{1}{m_{ss}} Q_{s_{\dot{q}_s}}$
⑧ $\frac{1}{I_x} L$	⑯ $\frac{1}{m_{tt}} Q_t$	㉔ $\frac{1}{m_{ss}} Q_s$

Fig.111 Influence of torsional wing flexibility on response to ailerons; set-up and table

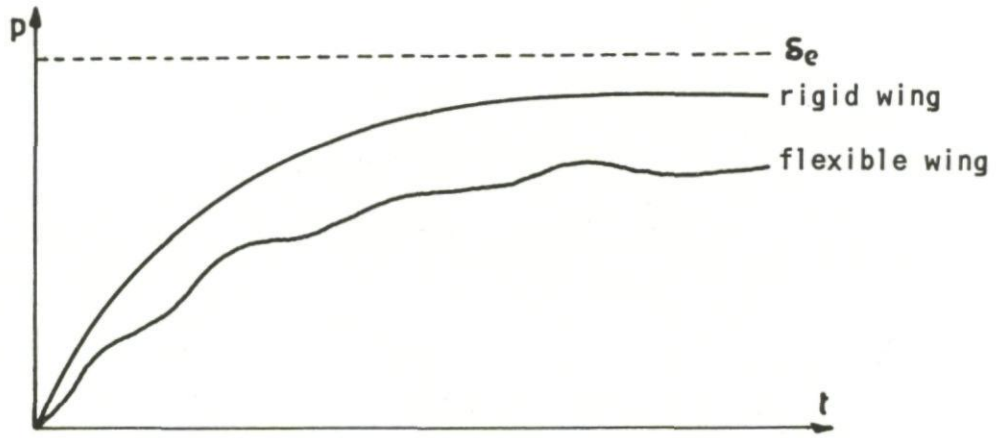

Fig.112 Influence of torsional wing flexibility; results

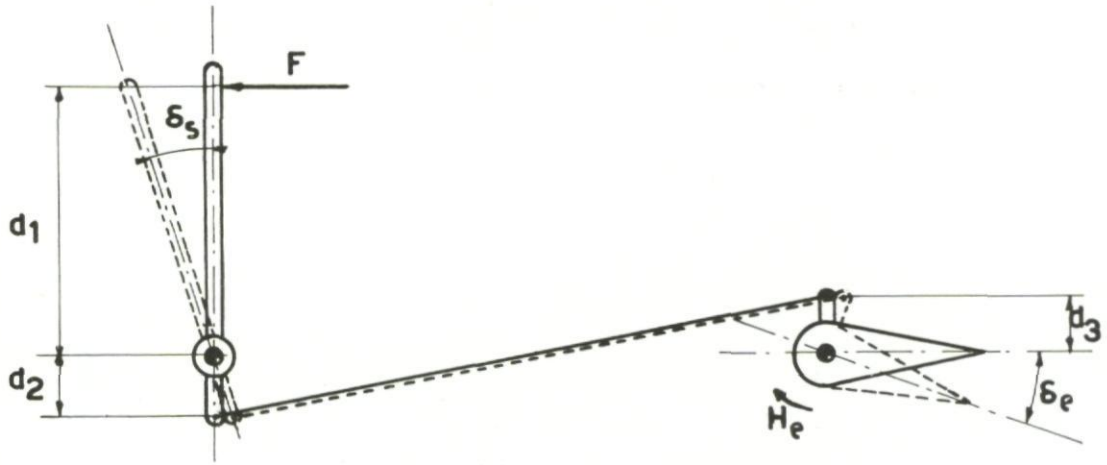

Fig.113 Most simple elevator control

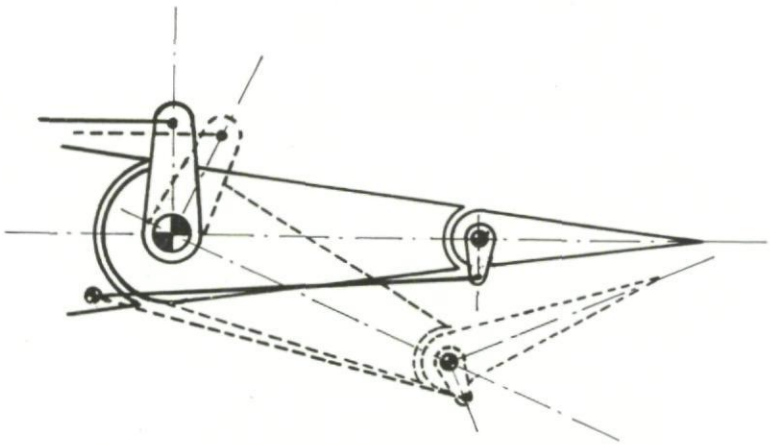

Fig.114 Tab and control surface linked together

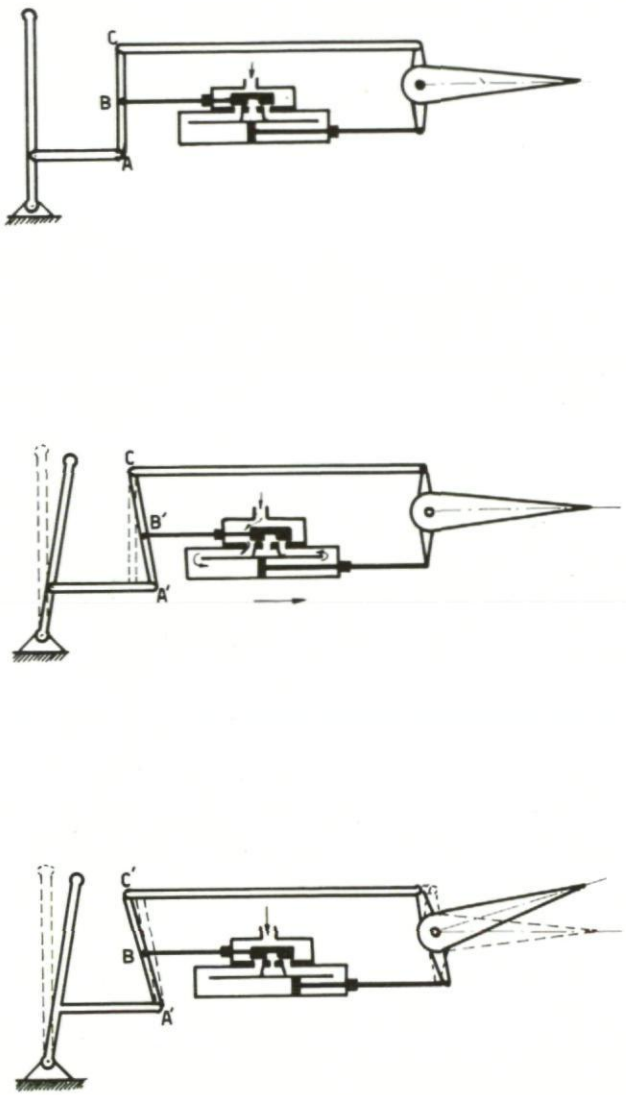

Fig.115 Servo control using a jack

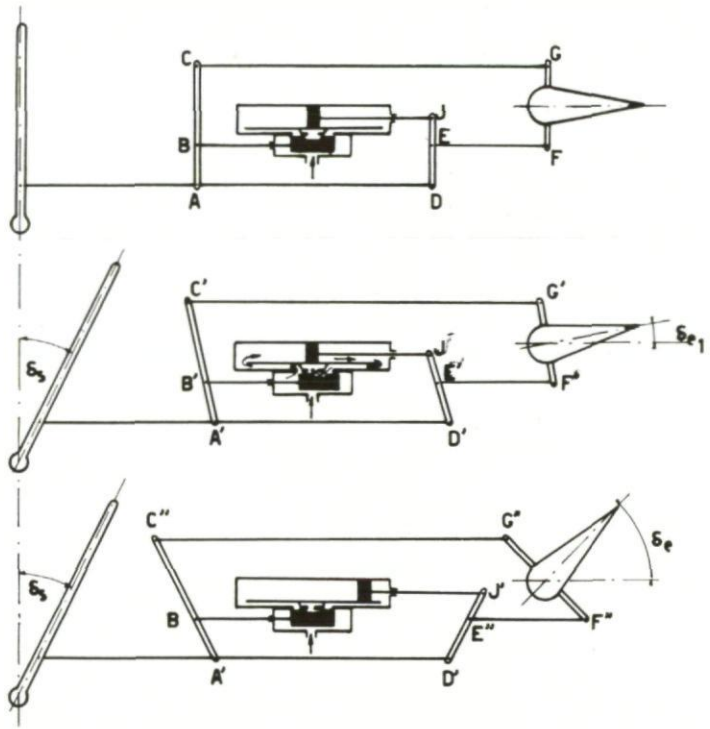

Fig.116 Boosted control

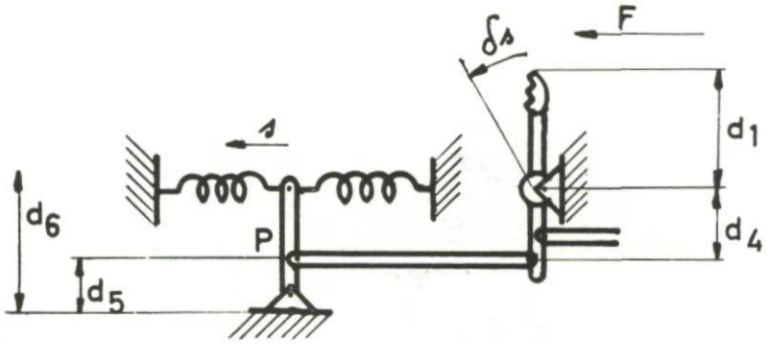

Fig.117 Artificial feel produced by a spring

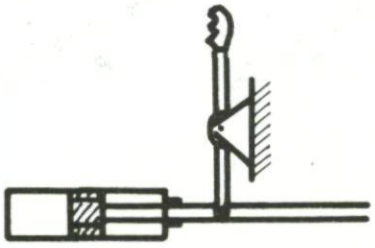

Fig.118 Artificial feel produced by a damper

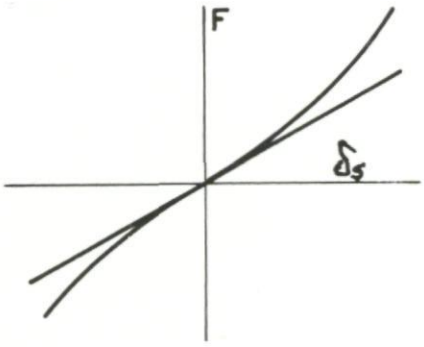

Fig.119 Artificial feel non-proportional to stick displacement

$$M = K.\delta_A$$

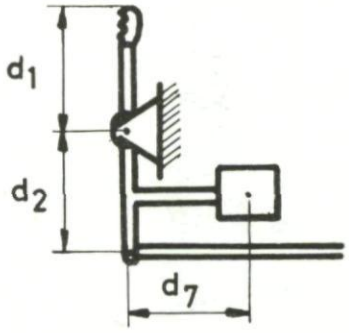

Fig.120 Artificial feel produced by normal acceleration

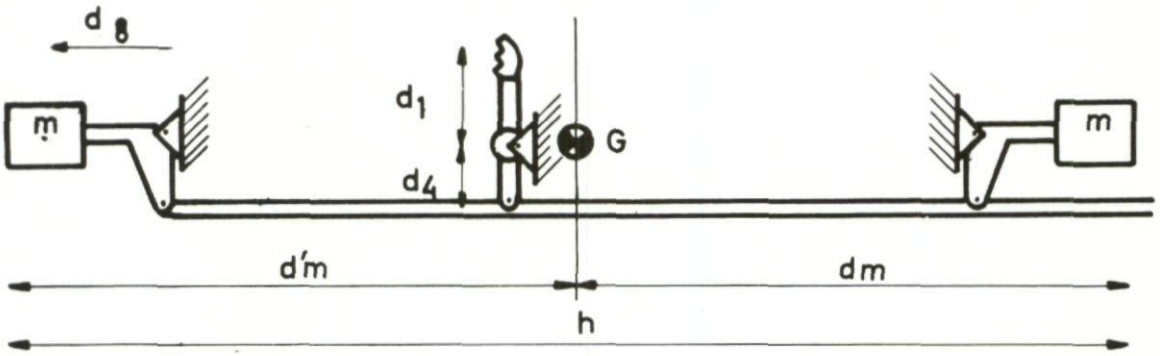

Fig. 121 Artificial feel produced by angular acceleration

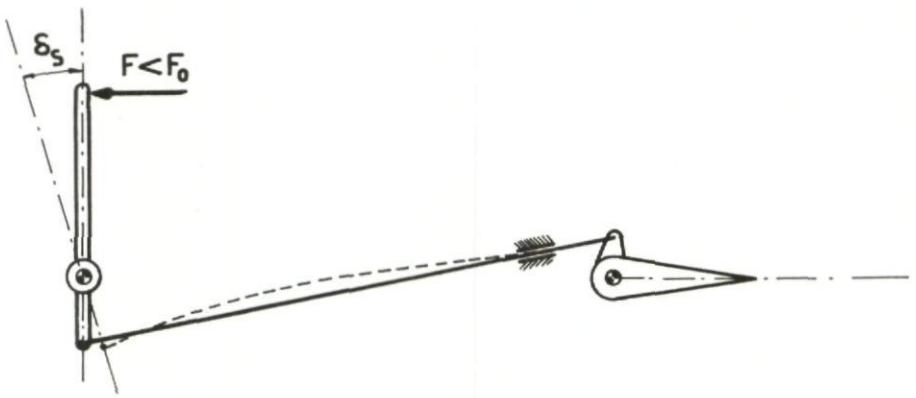

Fig. 122 Action of dry friction close to the control surface

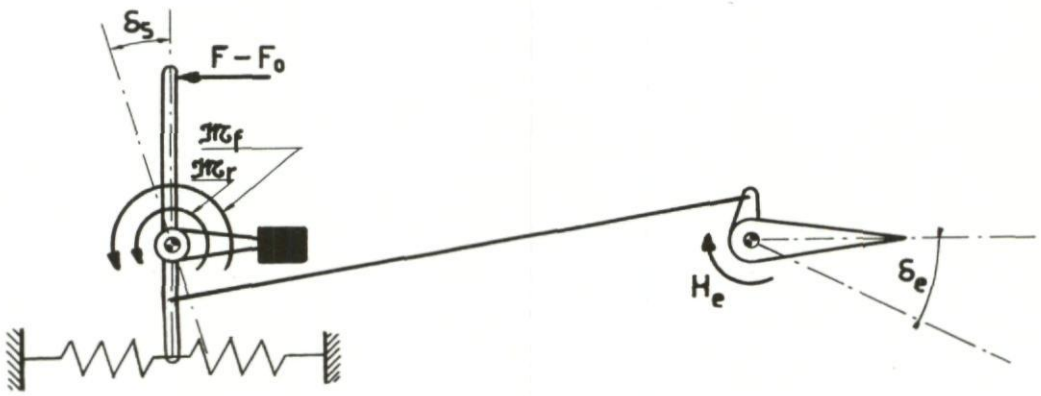

Fig. 123 Forces acting on a reversible control

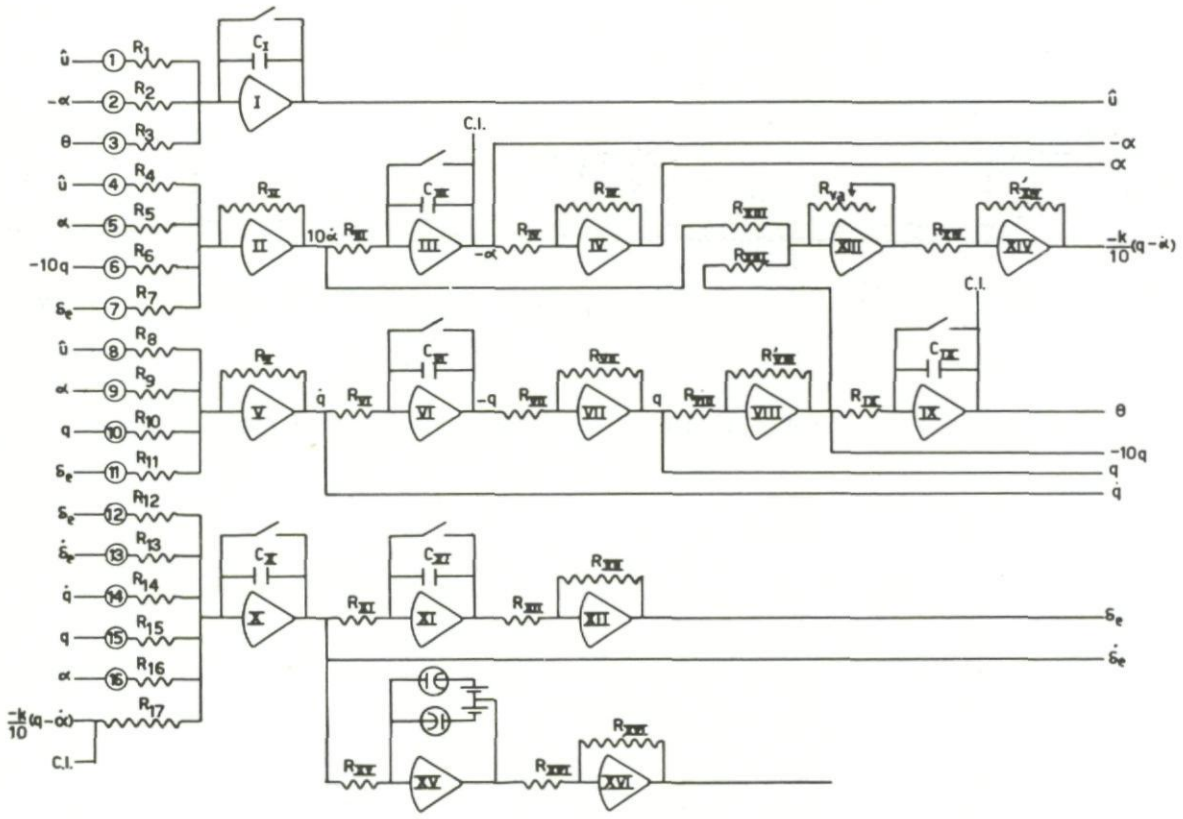

POTENTIOMETERS				
①	.140	R_1 = 1 MΩ	R_{II} = 1 MΩ	C_I = 10 μF
②	.390	R_2 = 1 MΩ	R_{III} = 1 MΩ	C_{III} = 10 μF
③	.885	R_3 = 1 MΩ	R_{IX} = 1 MΩ	C_{XI} = 10 μF
④	.875	R_4 = 500 KΩ	R_X = 100 KΩ	C_{IX} = 10 μF
⑤	.770	R_5 = 100 KΩ	R_{XI} = 100 KΩ	C_X = 1 μF
⑥	1	R_6 = 1 MΩ	R_{XII} = 1 MΩ	C_{XI} = 1 μF
⑦	.708	R_7 = 1 MΩ	R_{VIII} = 100 KΩ	
⑧	.293	R_8 = 1 MΩ	R'_{VIII} = 1 MΩ	
⑨	.443	R_9 = 20 KΩ	R_{IX} = 1 MΩ	
⑩	.910	R_{10} = 50 KΩ	R_{XI} = 1 MΩ	
⑪	.604	R_{11} = 10 KΩ	R_{XIII} = 1 MΩ	
⑫	1	R_{12} = 3333 Ω	R_{XIII} = 1 MΩ	
⑬	1	R_{13} = 200 KΩ	R_{XIV} = 100 KΩ	
⑭	1	R_{14} = 1 MΩ	R'_{XIV} = 1 MΩ	
⑮	.580 ou .290	R_{15} = 20 KΩ	R_{XV} = 1 MΩ	
⑯	1 ou .500	R_{16} = 10 KΩ	R_{XVI} = 1 MΩ	
		R_{17} = 100 KΩ	R_{va} = ou 50 KΩ 100 KΩ	

Fig.124 Aircraft motion with free elevator control; computer set-up and table of coefficients

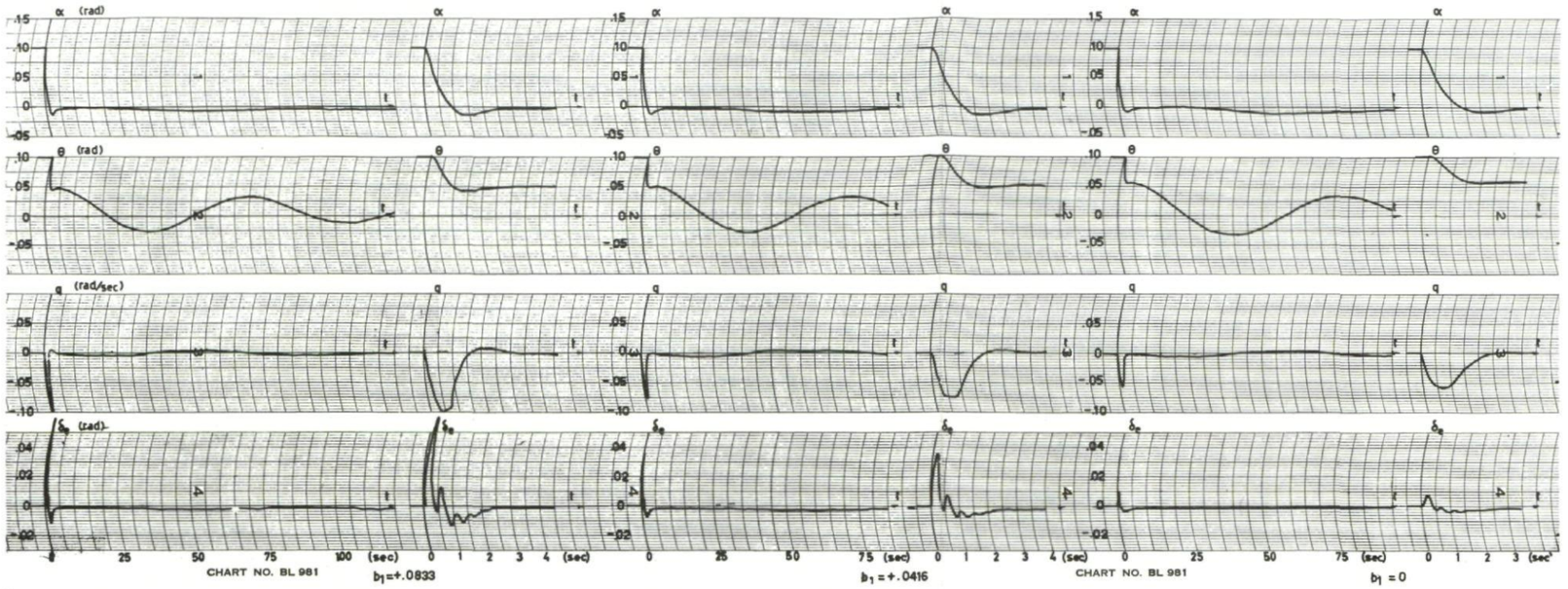

Fig. 125 Action of coefficient b_1 on flight with free controls

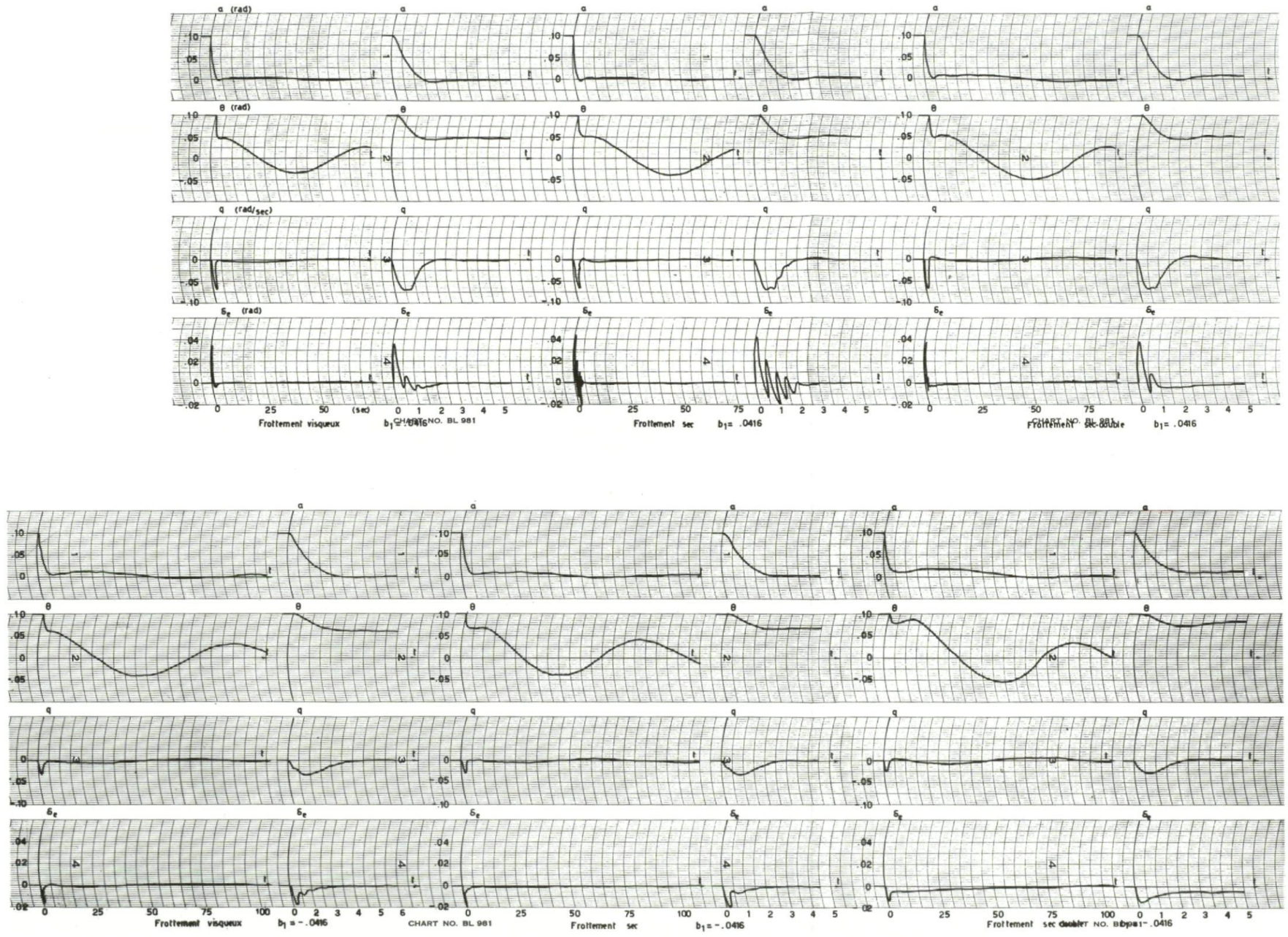

Fig.126 Action of dry friction

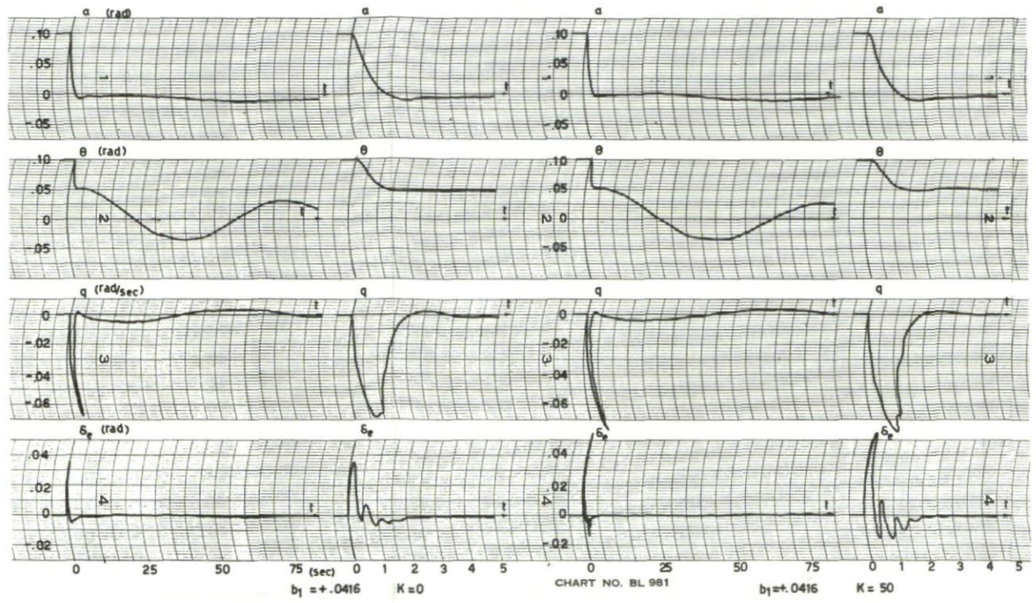

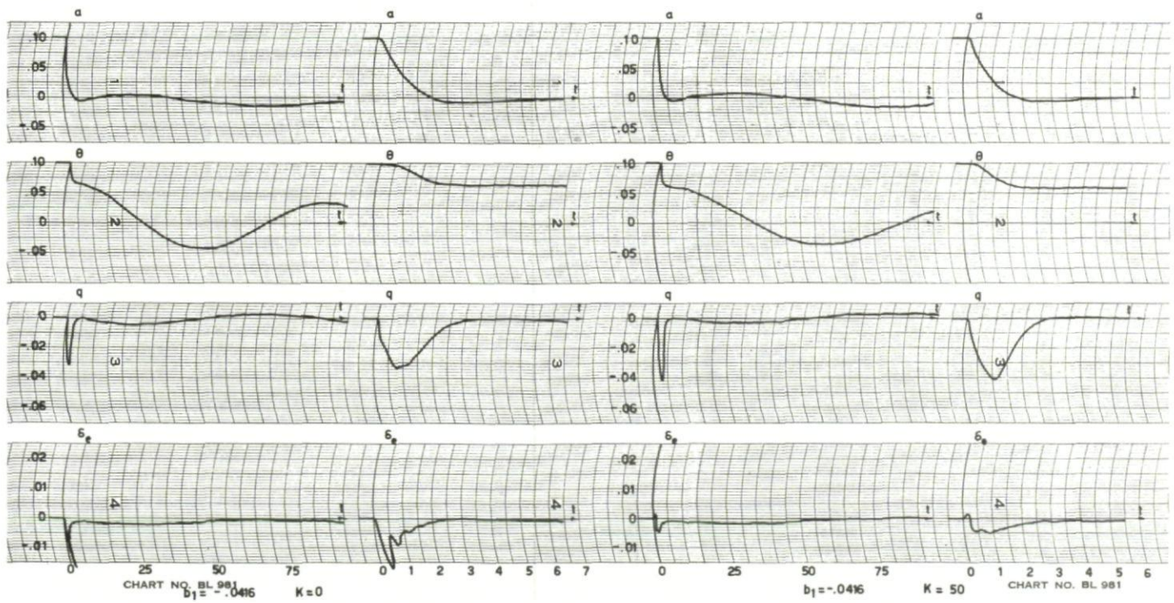

Fig. 127 Action of a bobweight, case $C_{m_\alpha} = 0$

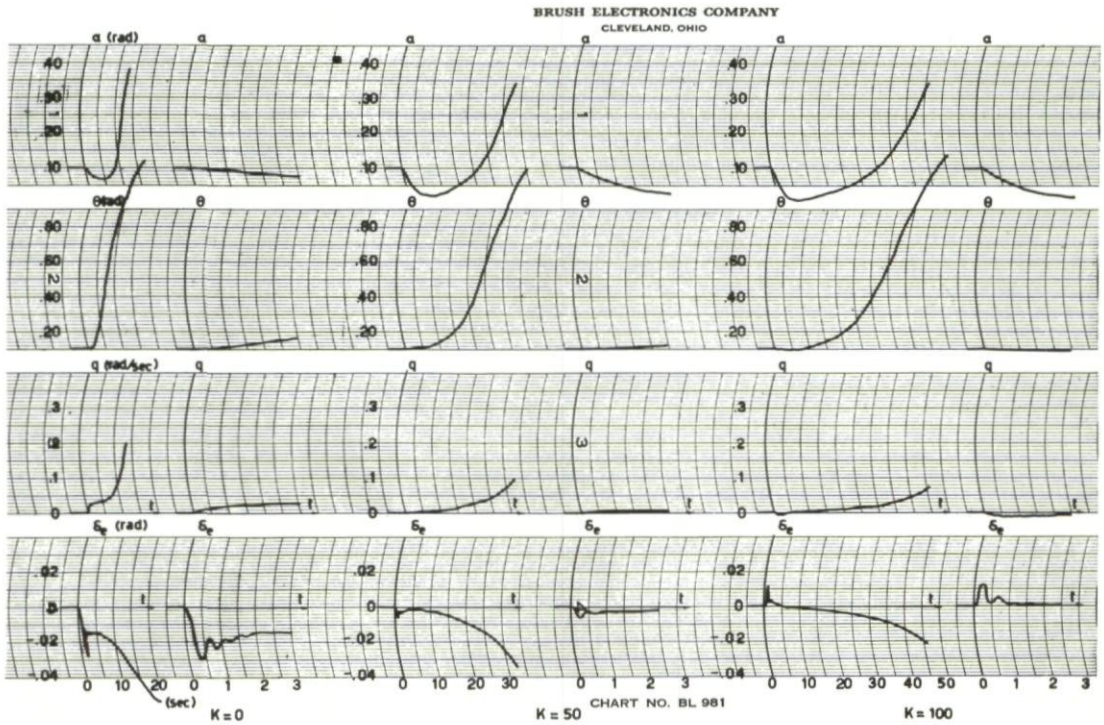

Fig. 128 Action of a bobweight, case $C_{m_\alpha} > 0$

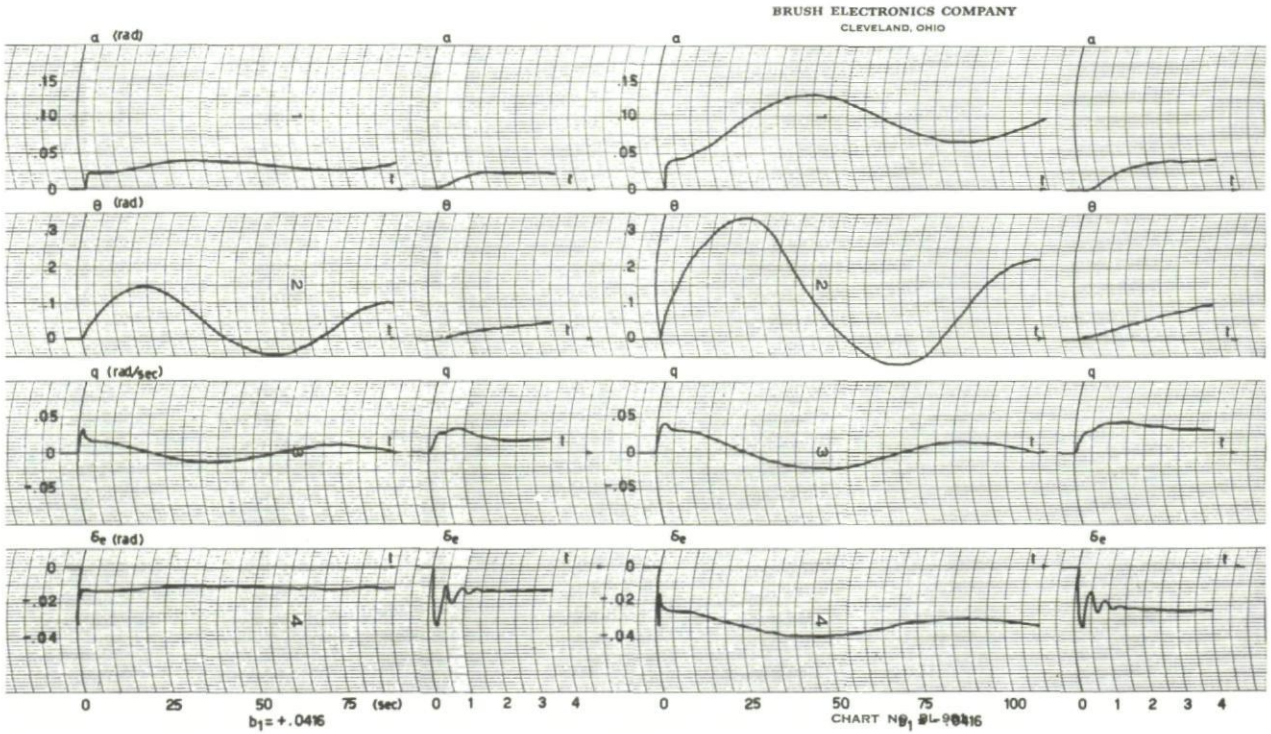

Fig.129 Aircraft response when a couple is applied on the control system

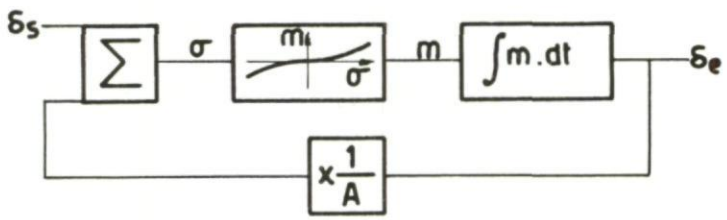

Fig.130 Simulation of a servo control using a jack

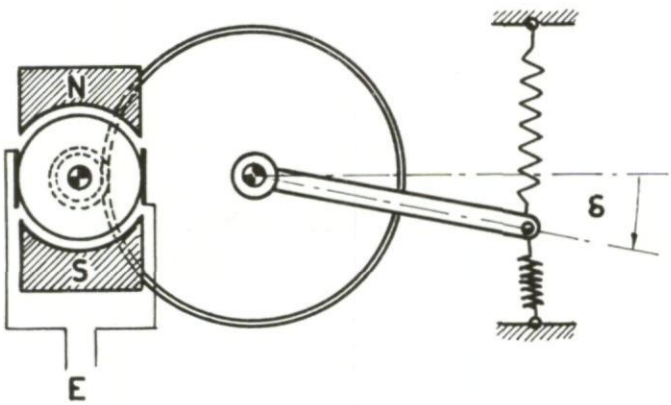

Fig.131 Principle of the electric position servo control

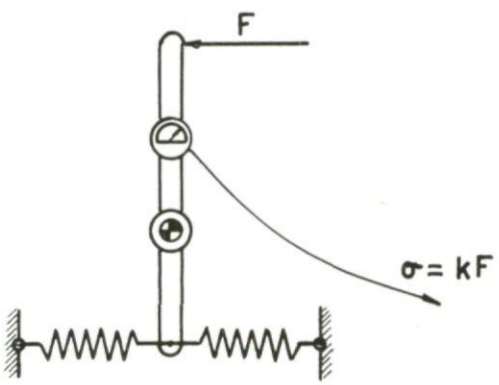

Fig.132 Generation of a signal proportional to pilot effort

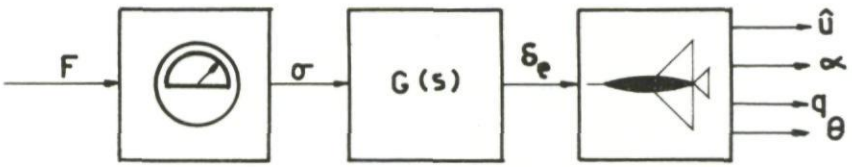

Fig.133 Control when pilot force is the input

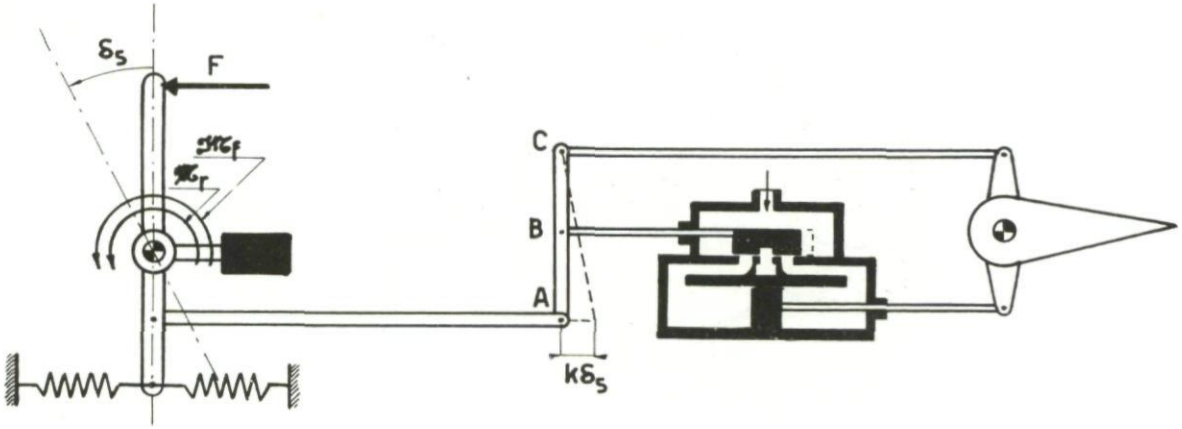

Fig.134 Control when stick displacement is the input

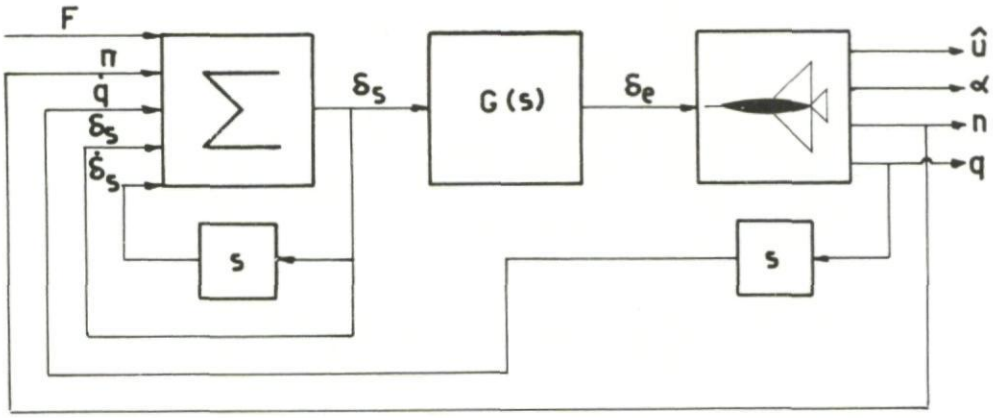

Fig.135 Moments determining stick position

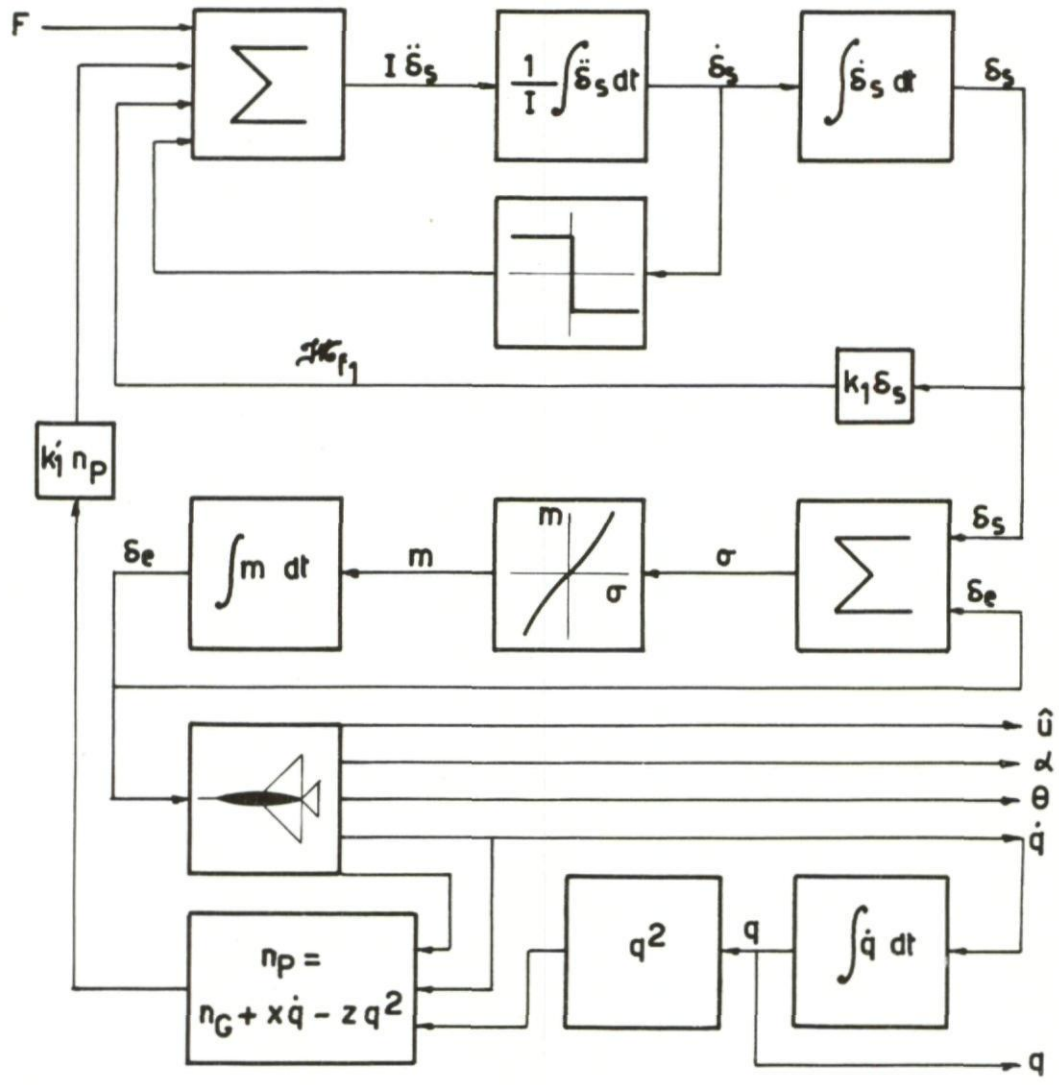

Fig. 136 Block diagram; influence of pilot force on aircraft motion

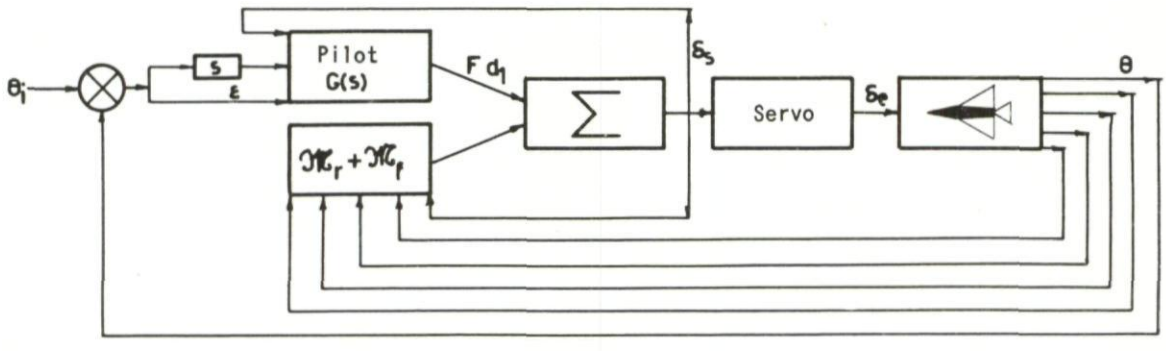

Fig. 137 Search for best artificial feel

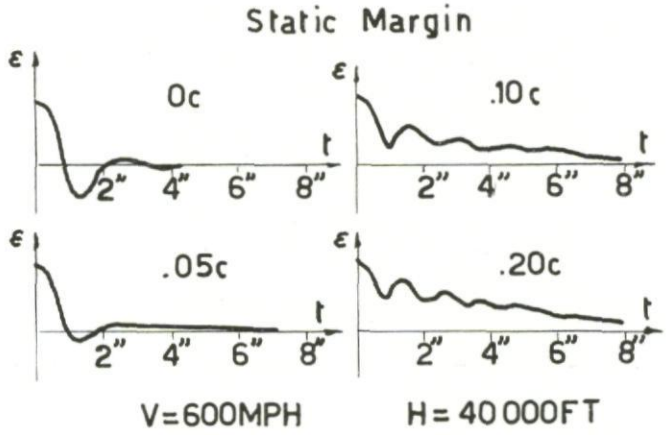

Fig.138 Aircraft response; variable static margin at constant altitude and speed

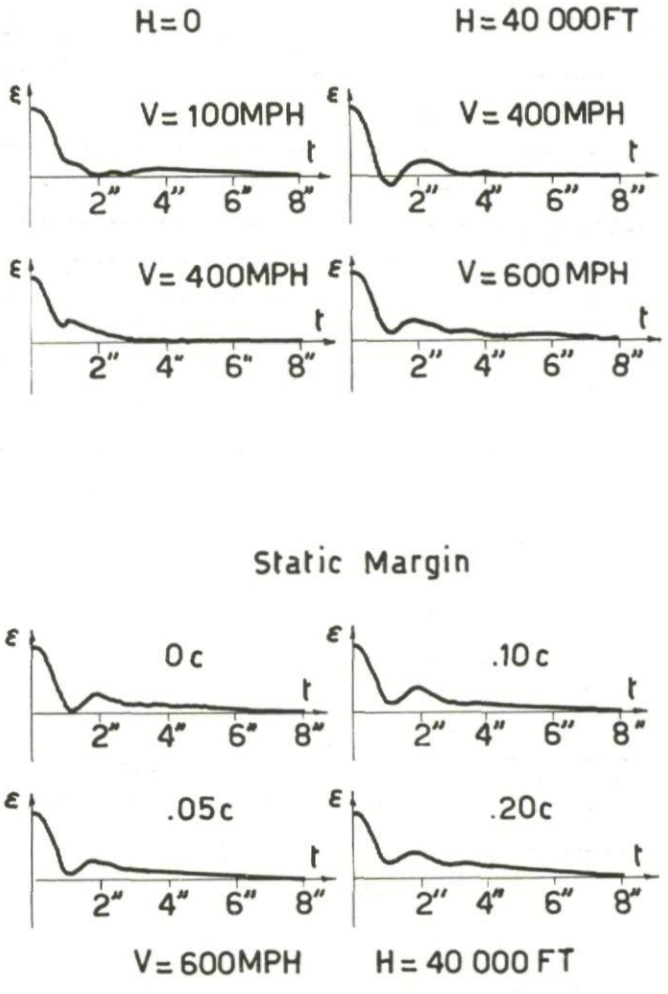

Fig.139 Aircraft response; variable static margin, altitude and speed

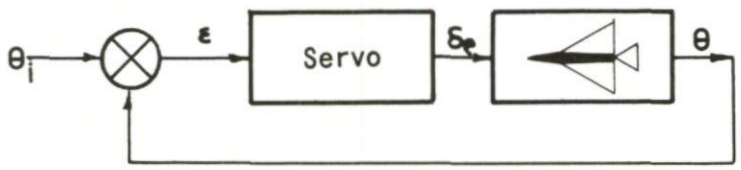

Fig.140 Principle; control by error of θ

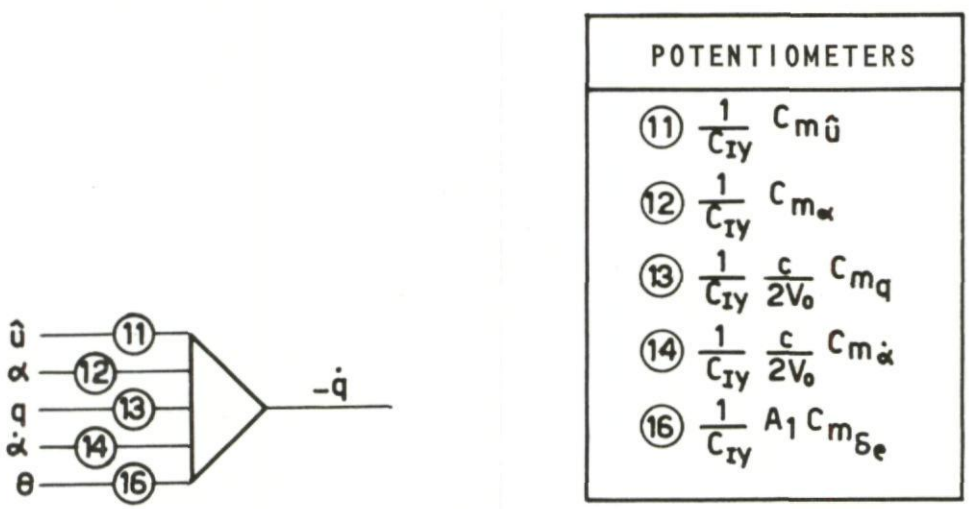

Fig.141 Alteration of computer set-up when automatic control is used

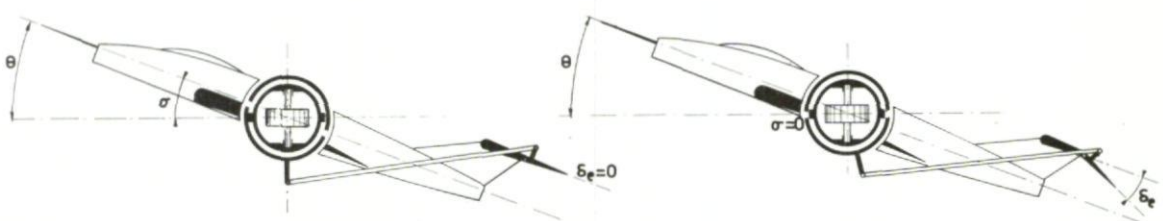

Fig.142 Feed-back acting on error sensor

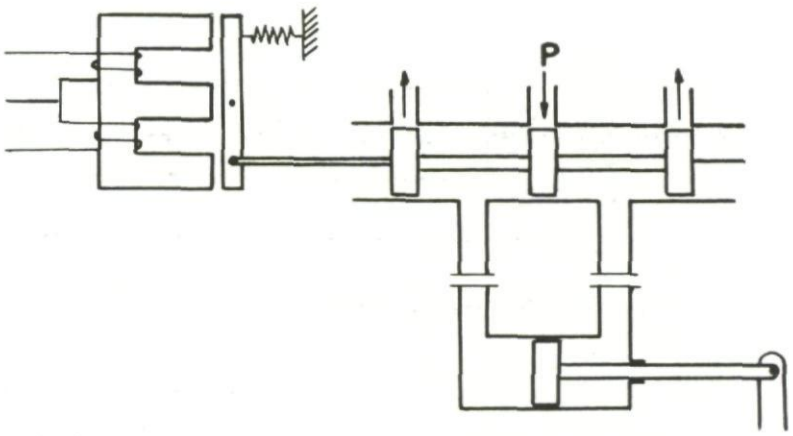

Fig. 143 Electric servo valve

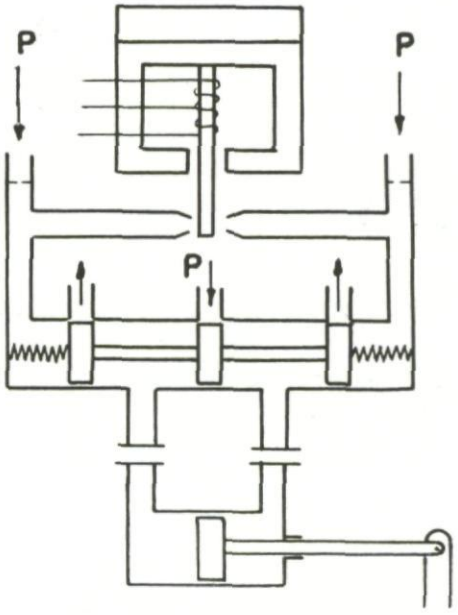

Fig. 144 Electric servo valve

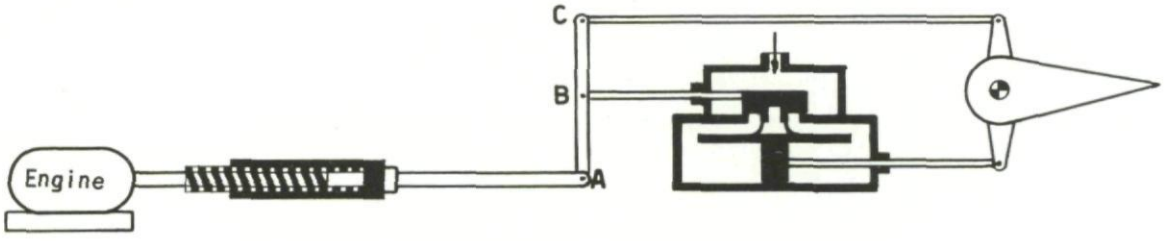

Fig. 145 Control involving an integration

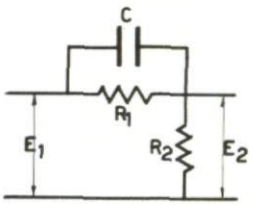

Fig. 146 Phase lead network

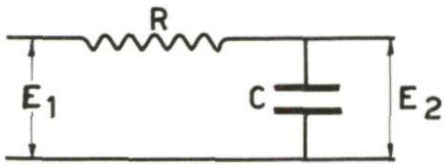

Fig. 147 Filtering network

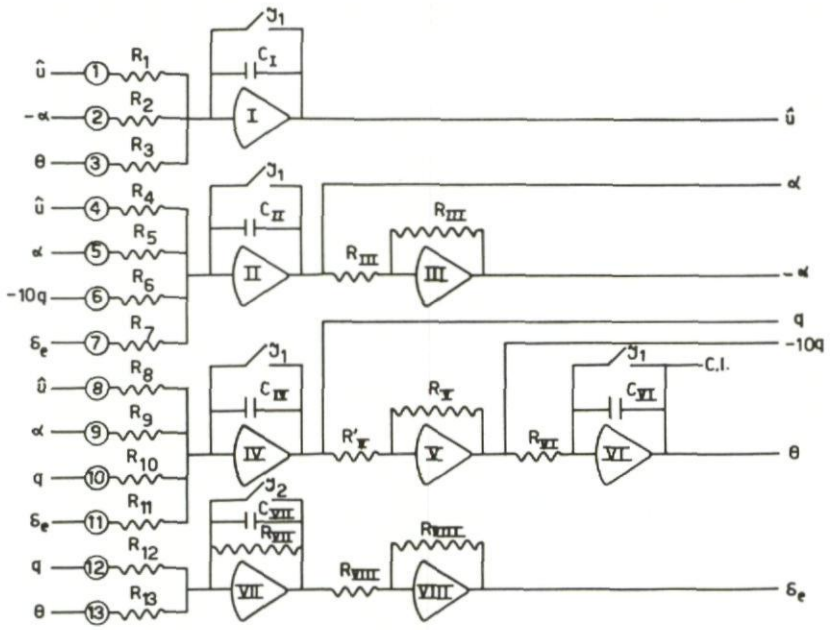

POTENTIOMETERS			
①	.140	R_1 = 1 MΩ	R_{III} = 1 MΩ
②	.390	R_2 = 1 MΩ	R_V = 100 KΩ
③	.885	R_3 = 1 MΩ	R'_V = 1 MΩ
④	.875	R_4 = 500 KΩ	R_{VI} = 1 MΩ
⑤	.770	R_5 = 100 KΩ	R_{VII} = 500 KΩ
⑥	1	R_6 = 1 MΩ	R_{VIII} = 1 MΩ
⑦	.708	R_7 = 1 MΩ	C_I = 10 μF
⑧	.293	R_8 = 1 MΩ	C_{II} = 10 μF
⑨	.443	R_9 = 20 KΩ	C_{IV} = 10 μF
⑩	.910	R_{10} = 50 KΩ	C_{VII} = 10 μF
⑪	.604	R_{11} = 10 KΩ	C_{III} = 10 μF
⑫	1	R_{12} = 500 KΩ	
⑬	Variable	R_{13} = 500 KΩ	

Fig. 148 Automatic longitudinal stabilization; computer set-up and table of coefficients

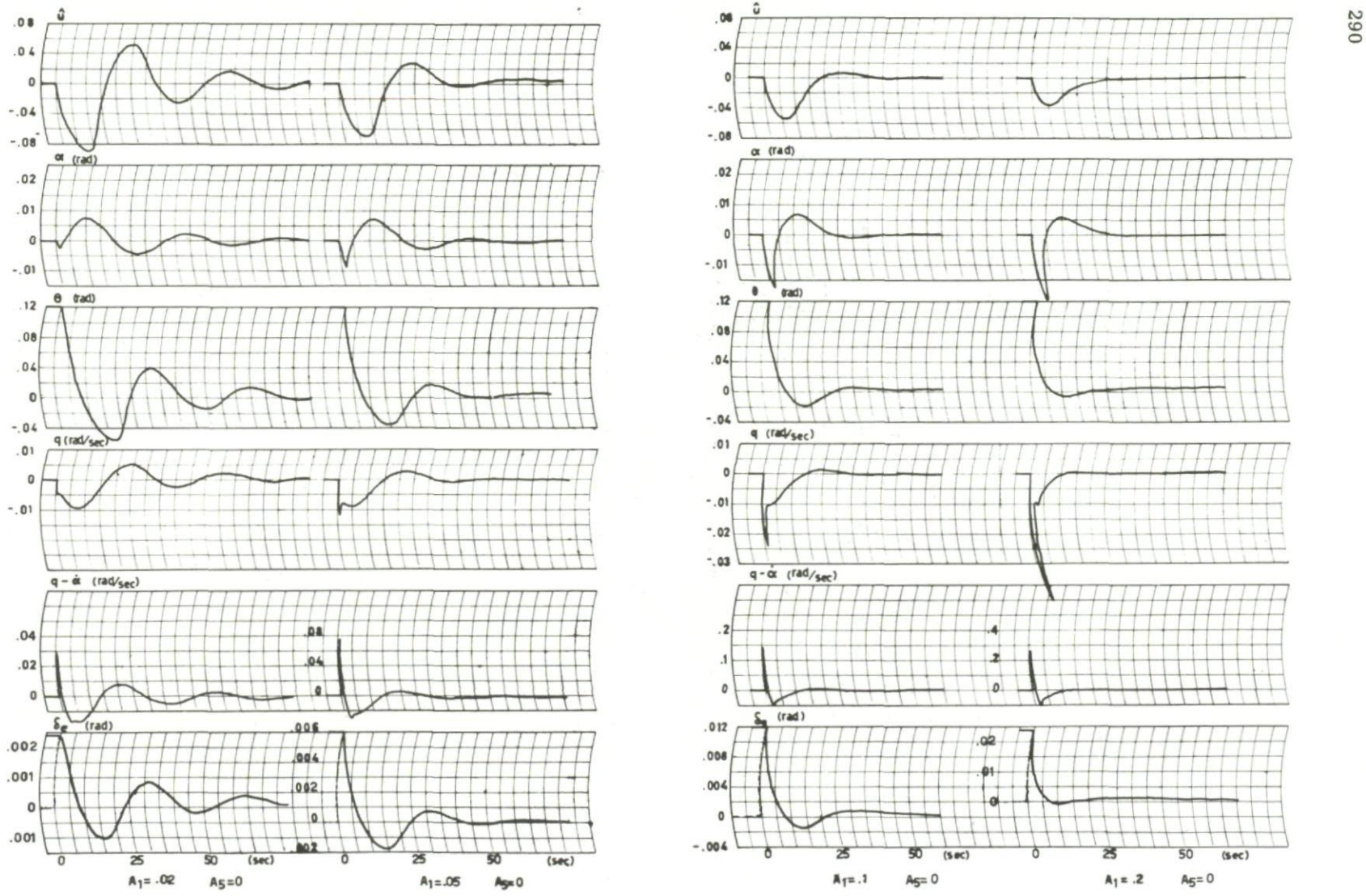

Fig.149 Automatic control by error of θ

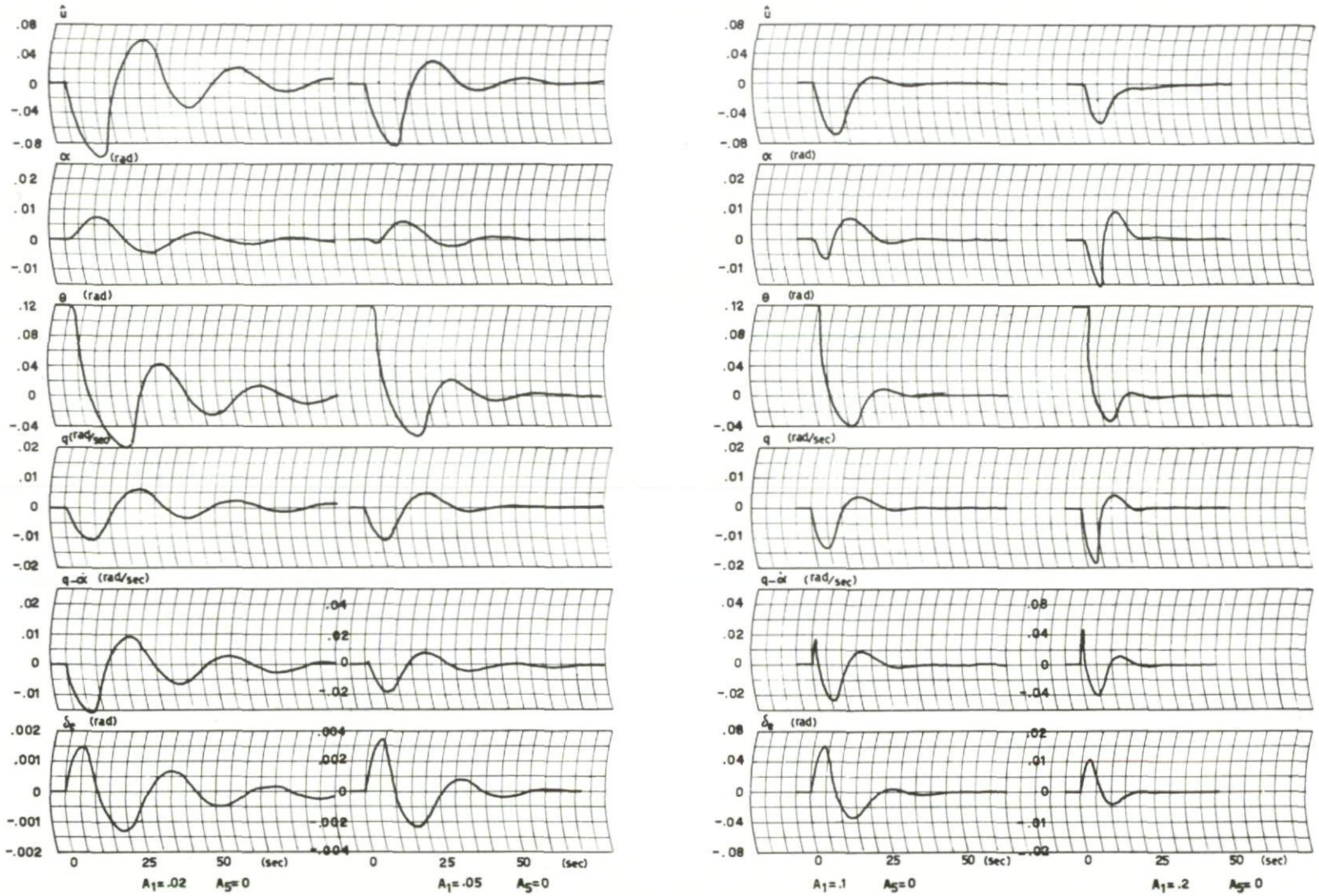

Fig.150 Automatic control by error of θ, plus time constant

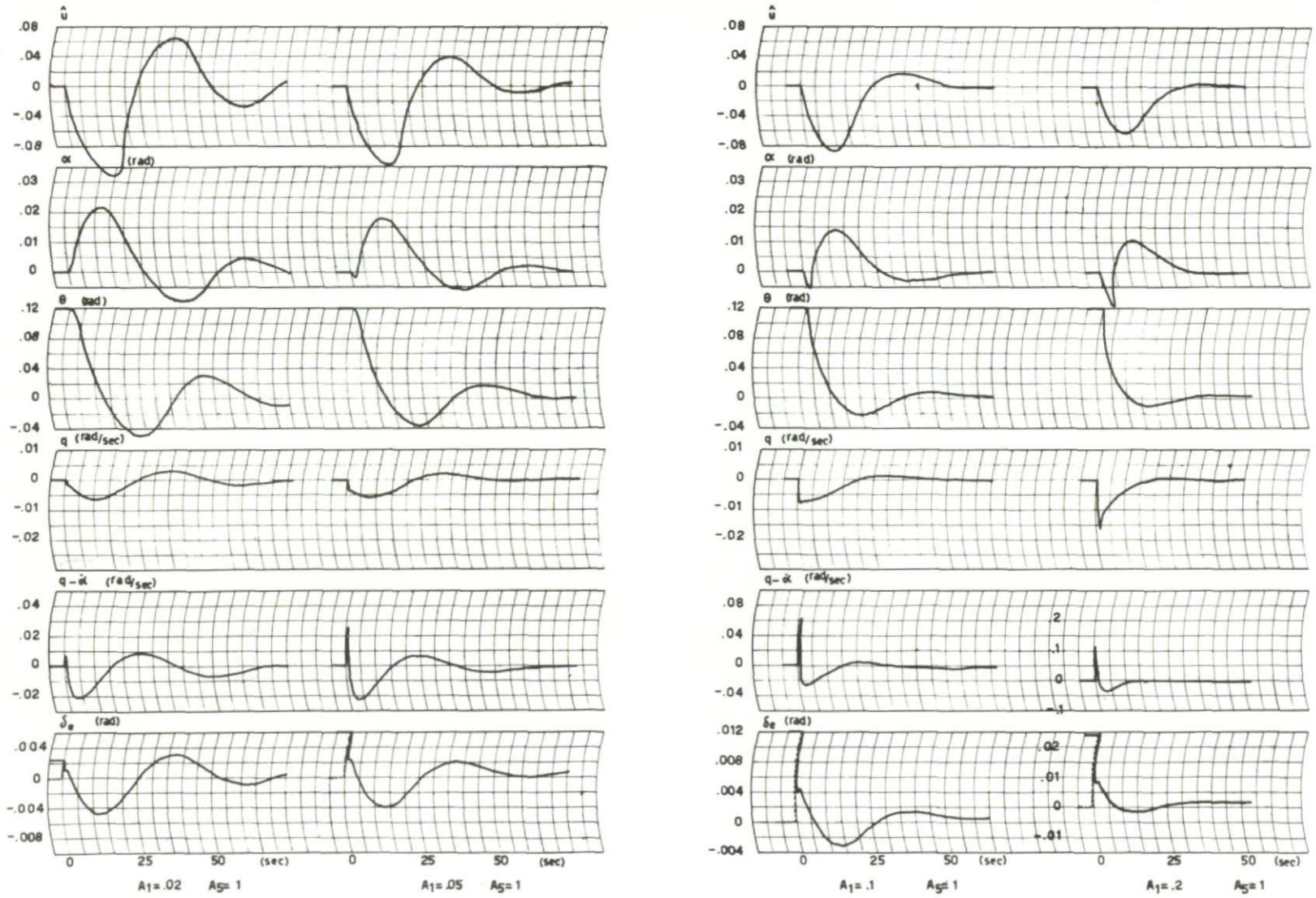

Fig.151 Automatic control by error of θ and q

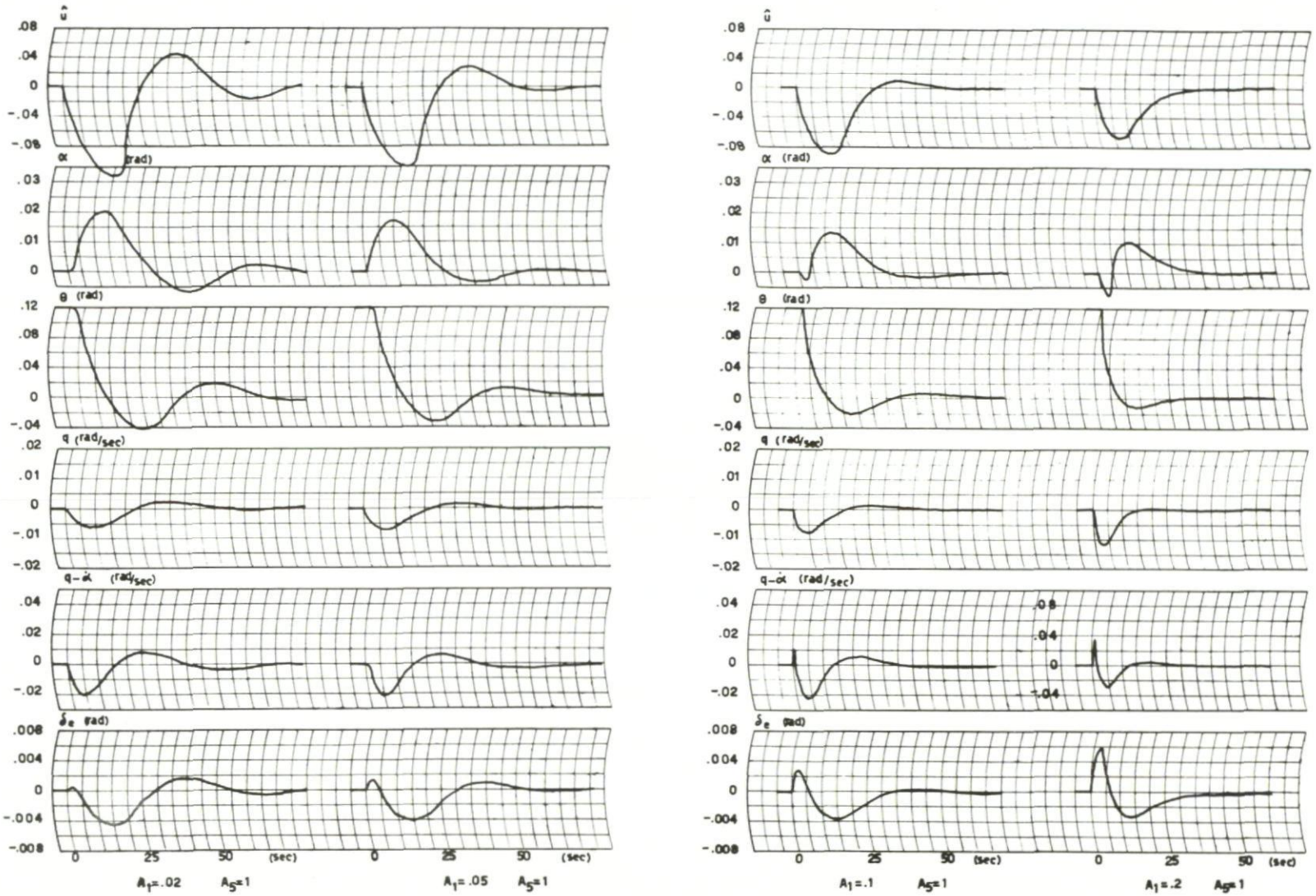

Fig.152 Automatic control by error of θ and α, plus time constant

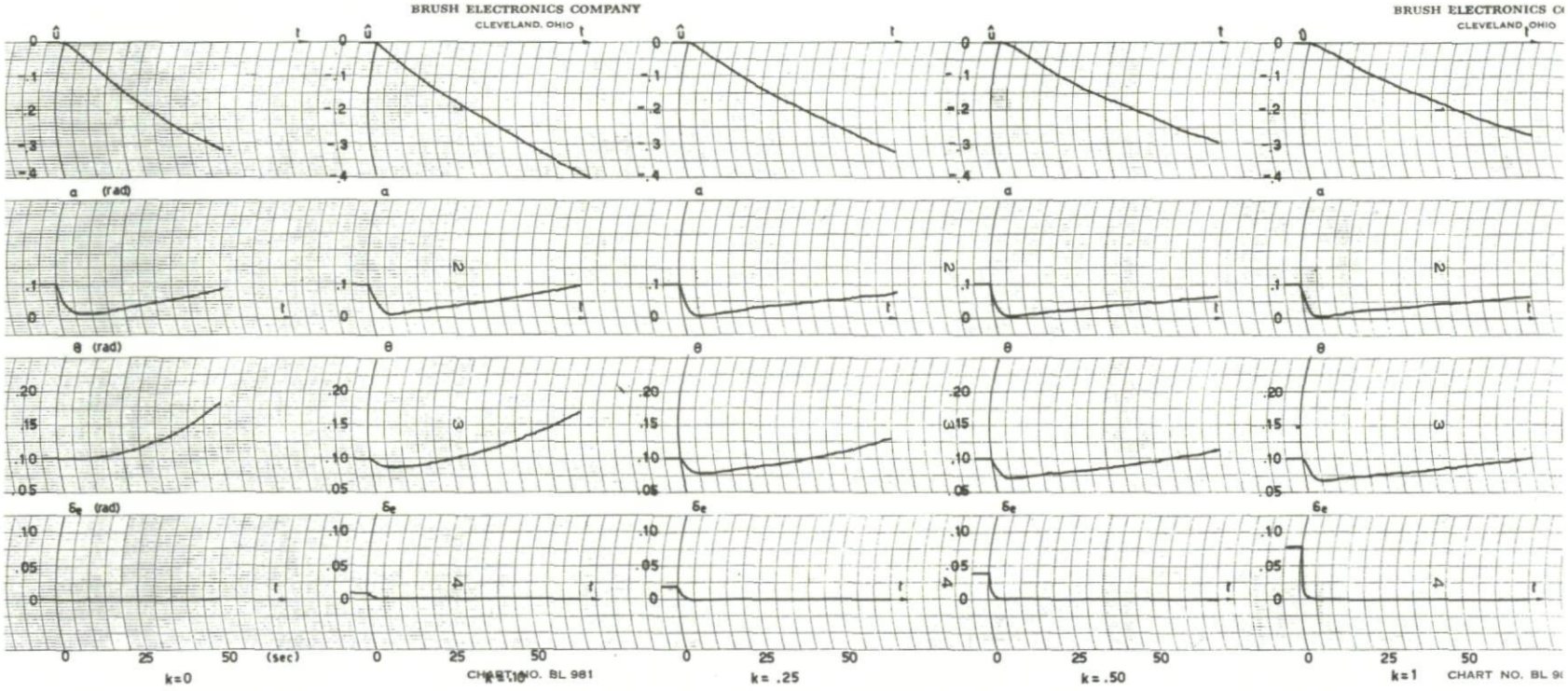

Fig.153 Automatic control by the acceleration

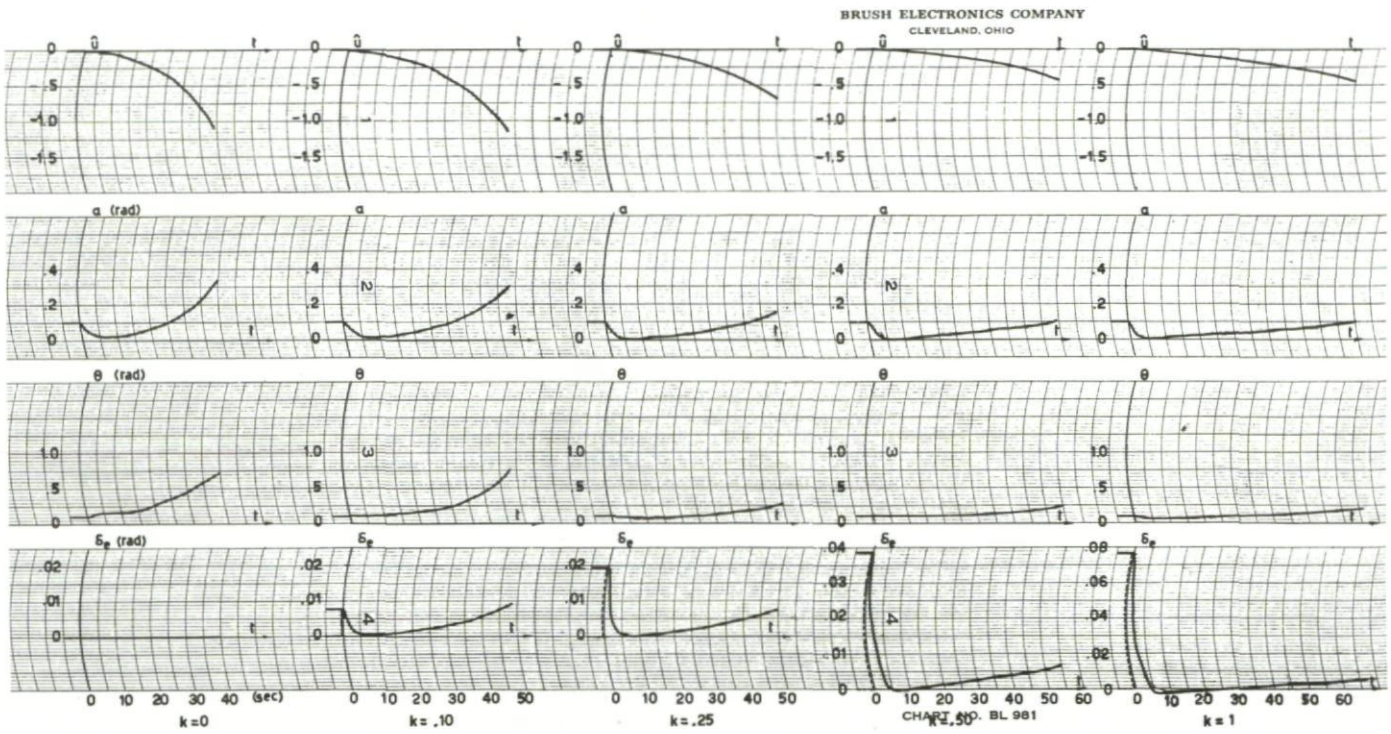

Fig.154 Automatic control by the acceleration

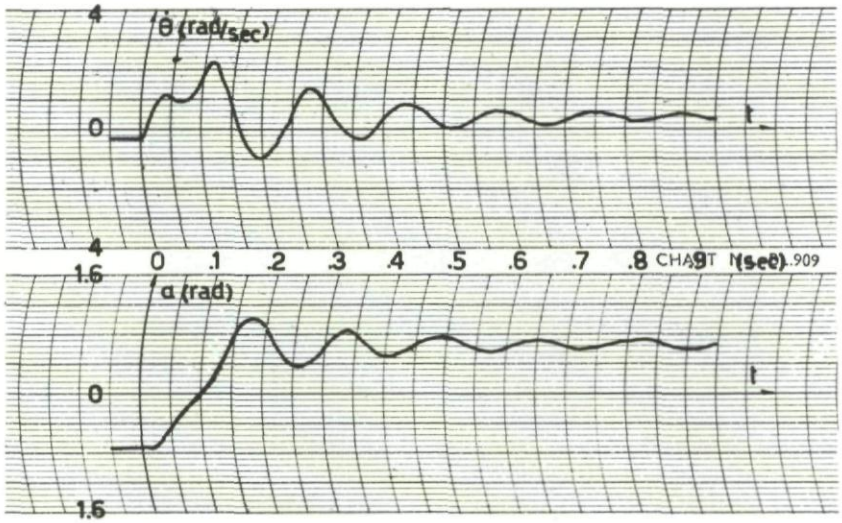

Fig.155 Automatic control by error of α

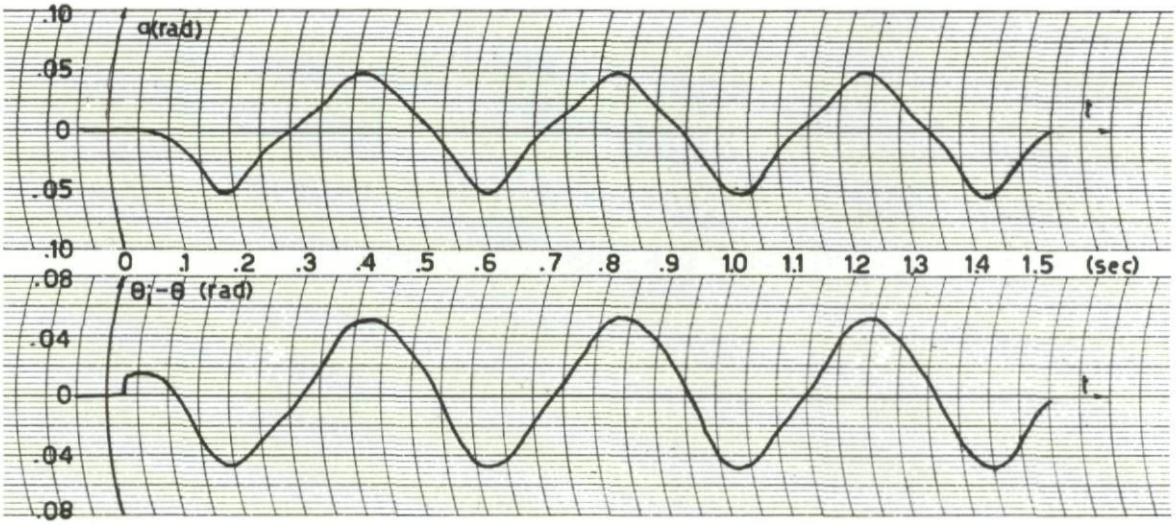

Fig.156 Automatic control by error of θ

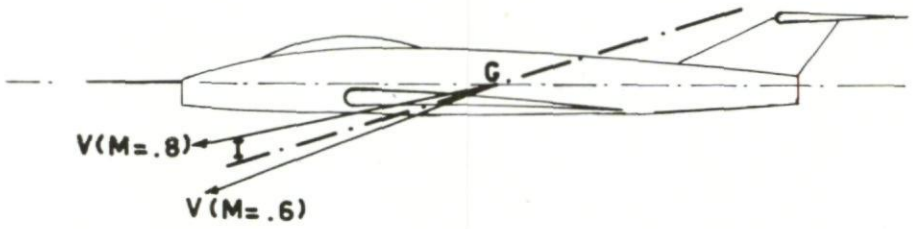

Fig.157 Position of inertia axis versus velocity vector

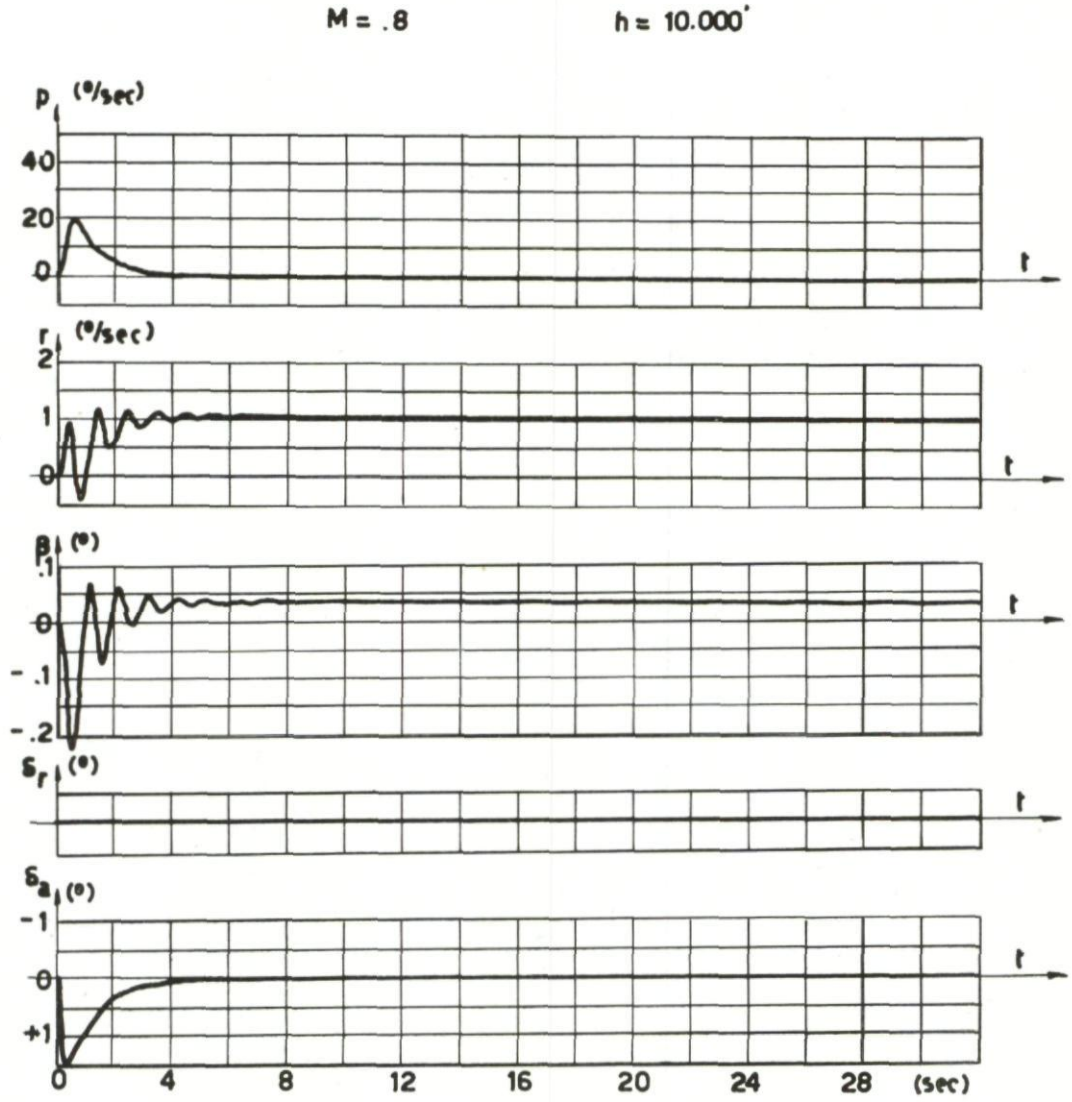

Fig.158 Aircraft response with locked rudder

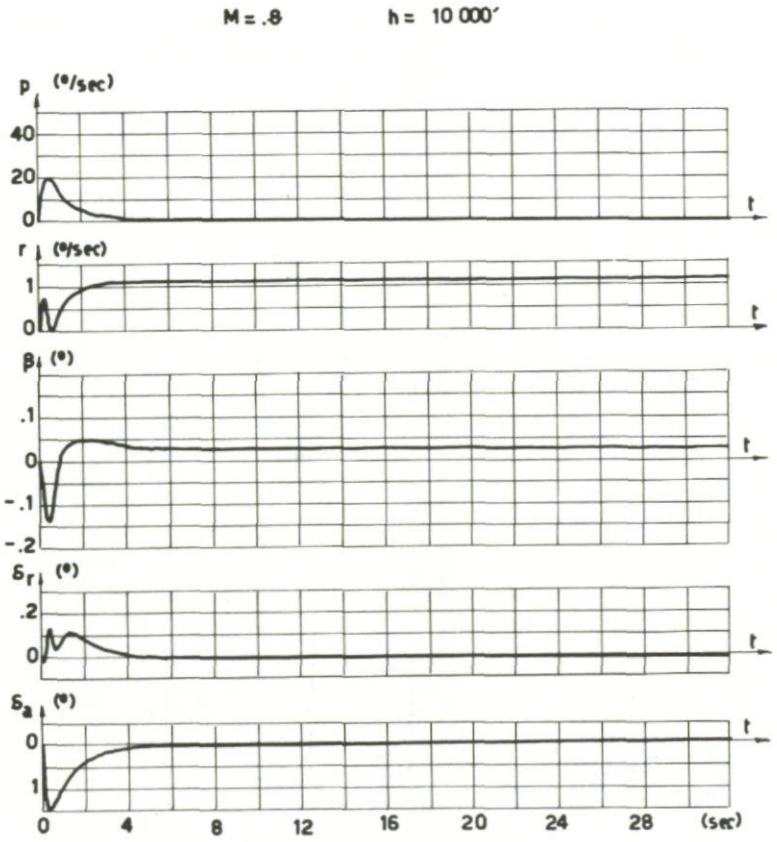

Fig. 159 Aircraft response with automatic rudder control

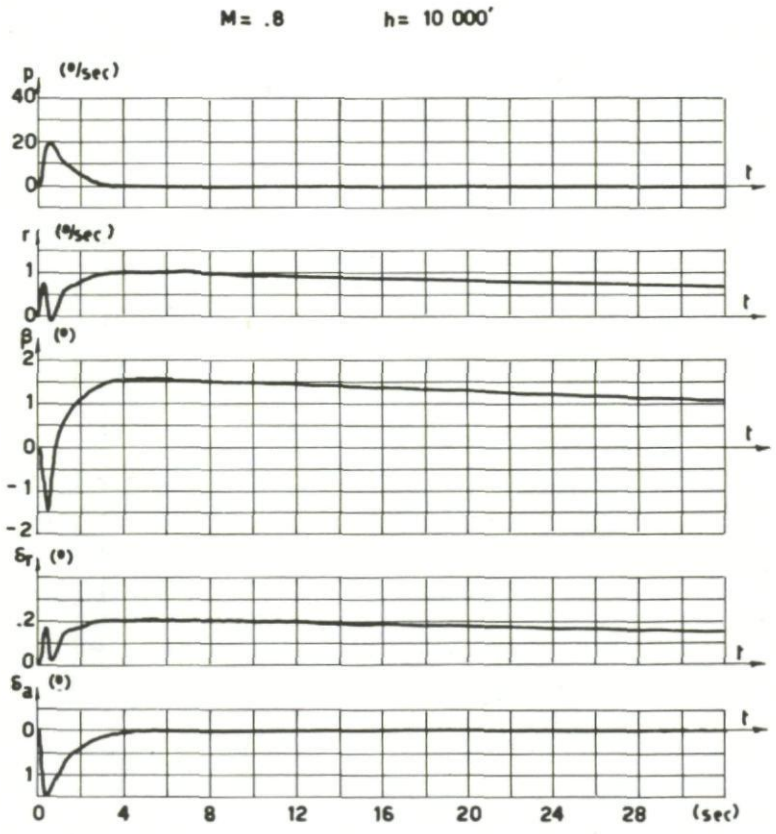

Fig. 160 Aircraft response with automatic rudder control

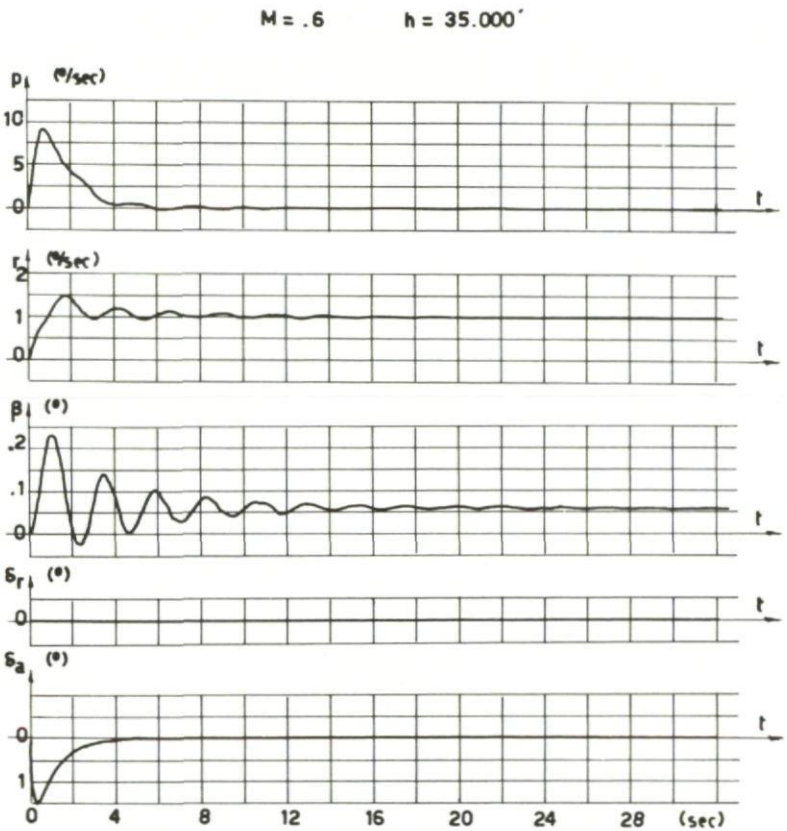

Fig.161 Aircraft response with locked rudder

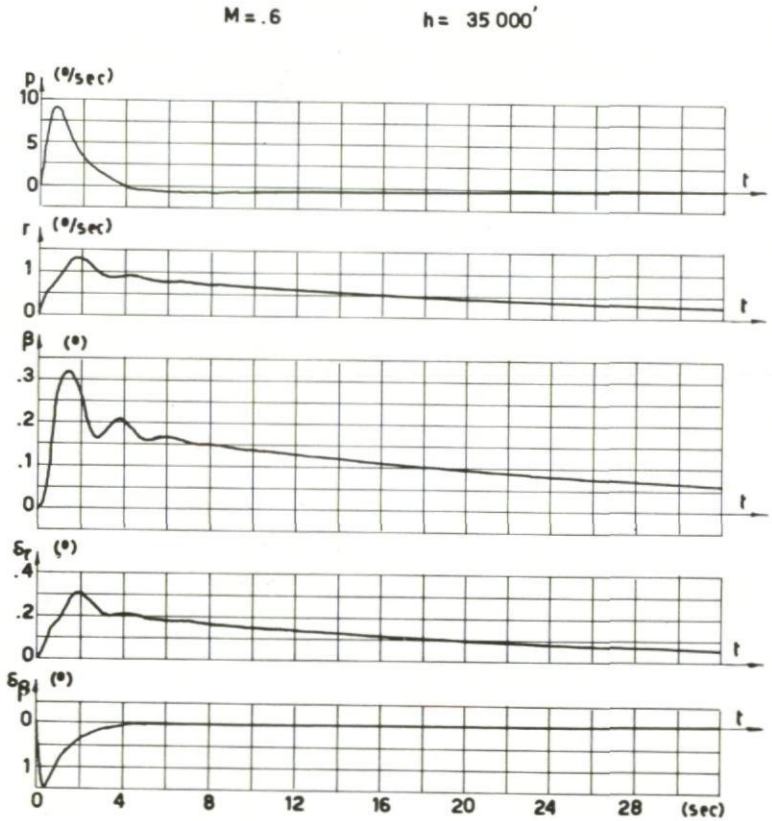

Fig.162 Aircraft response with automatic rudder control

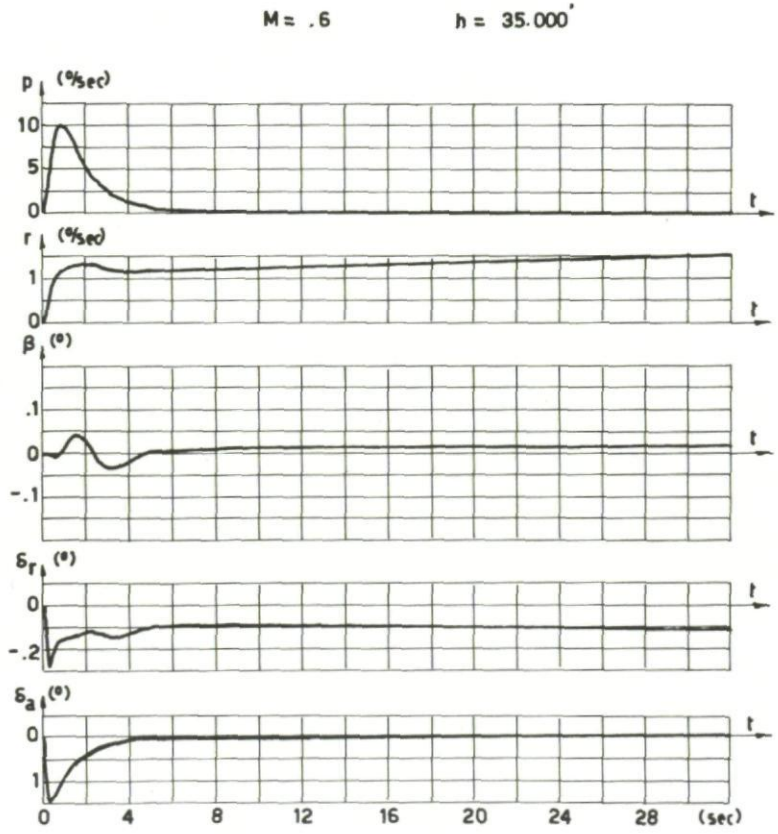

Fig.163 Aircraft response with automatic rudder control

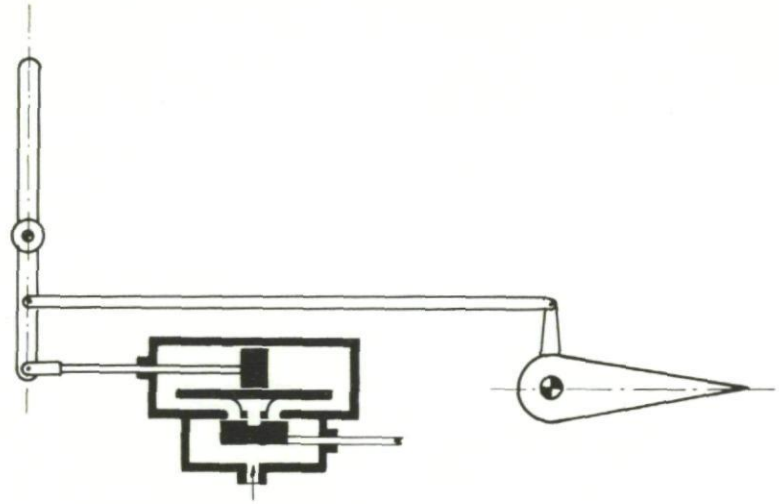

Fig.164 Principle of controls acting in parallel

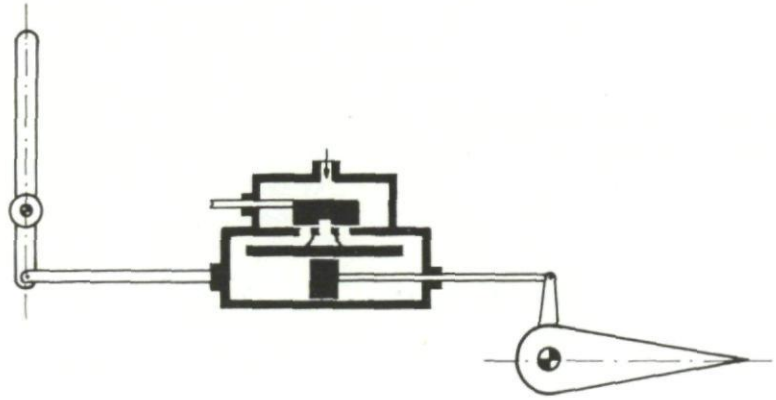

Fig.165 Principle of differential control

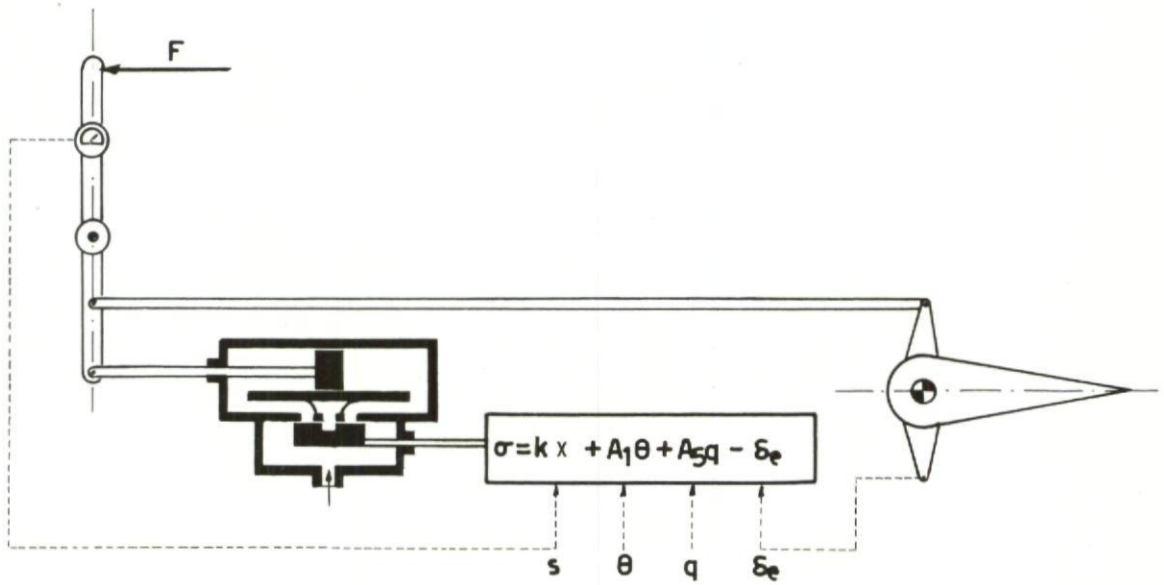

Fig.166 Use of a signal representing pilot action

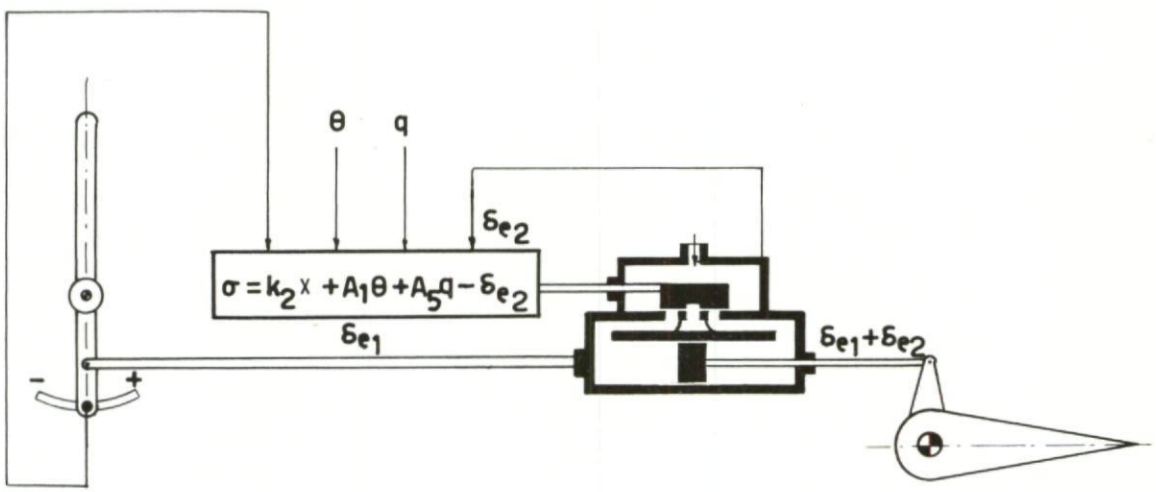

Fig.167 Use of a signal representing stick displacement

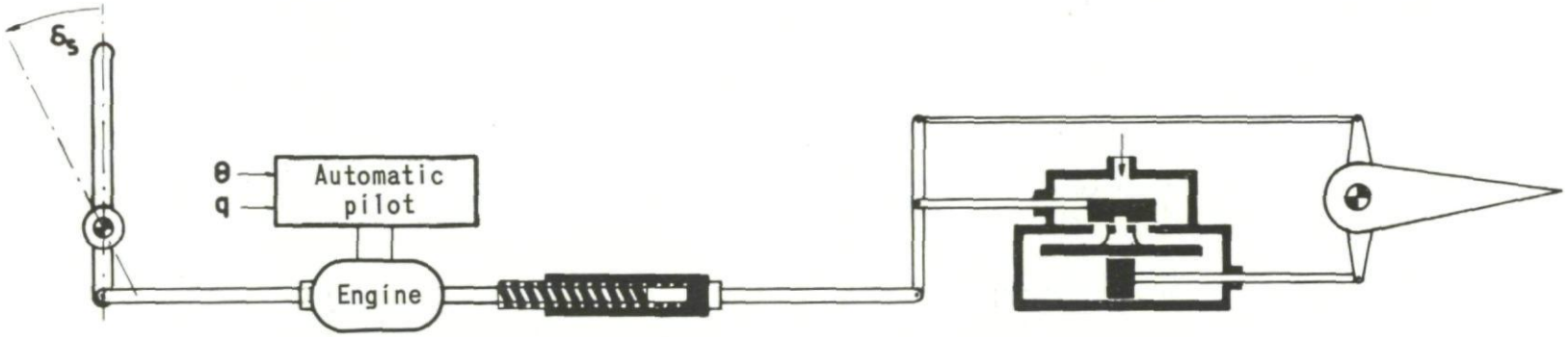

Fig.168 Human and automatic pilot acting differentially on slide valve of jack

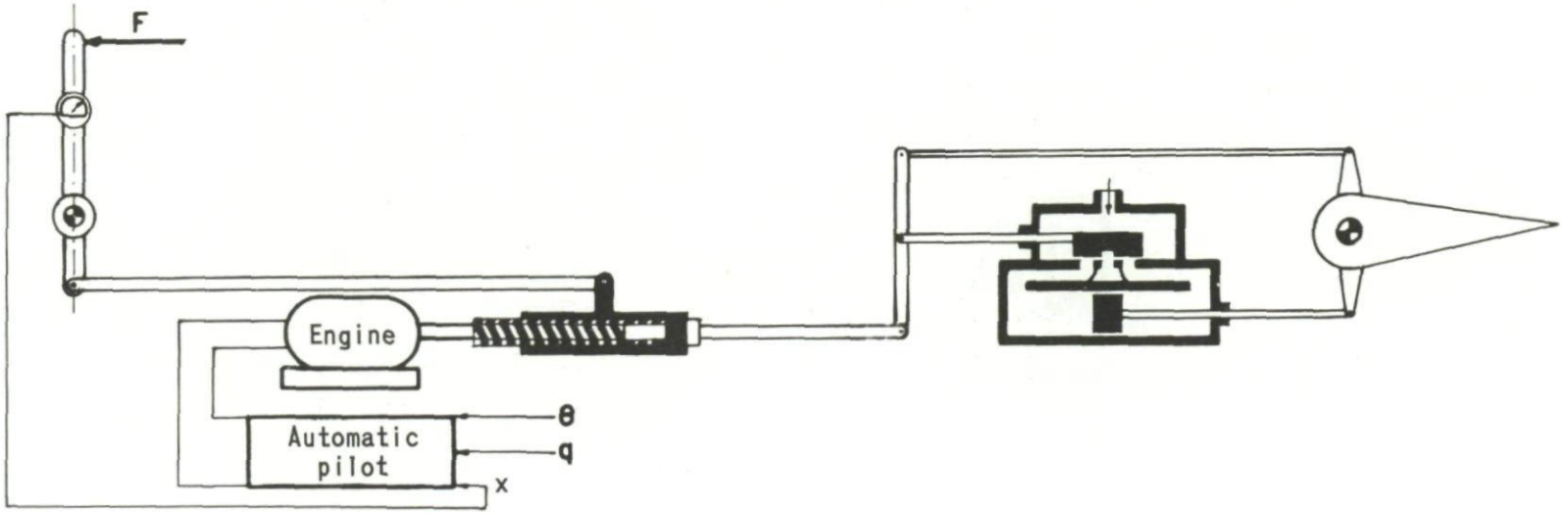

Fig.169 Human and automatic pilot acting in parallel on slide valve

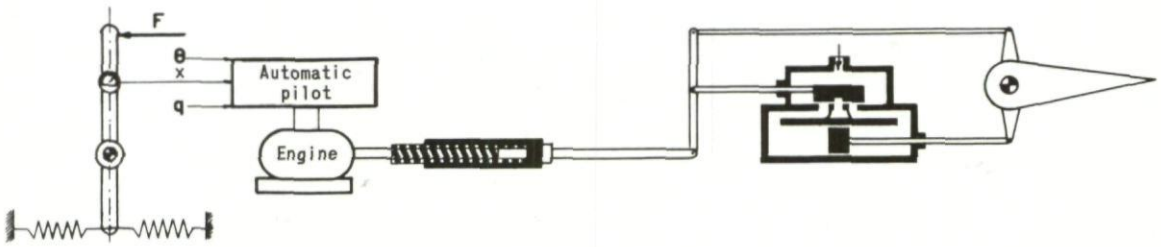

Fig.170 No direct linkage between control column and slide valve

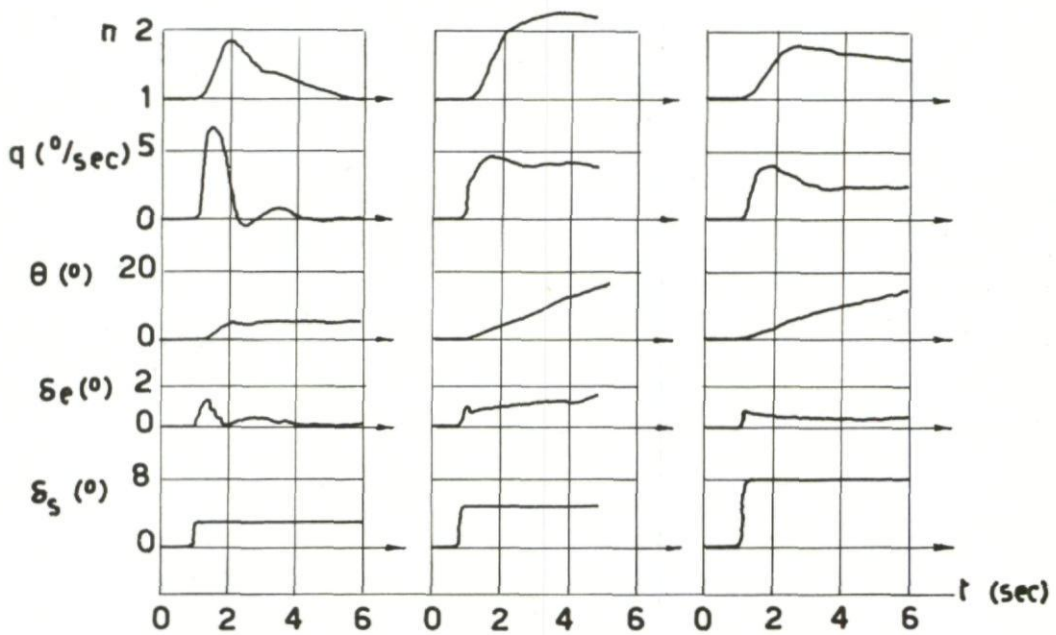

Fig.171 Flight test results with three different autopilots

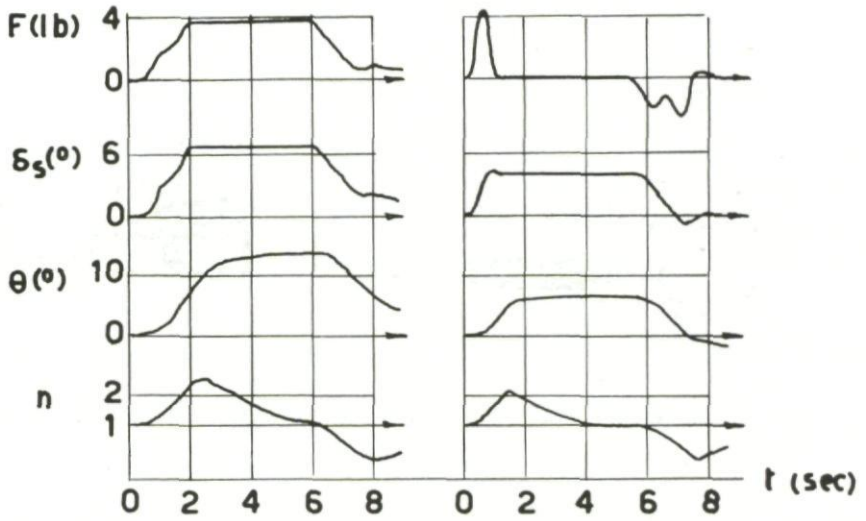

Fig.172 Flight test results with two different artificial-feel generators

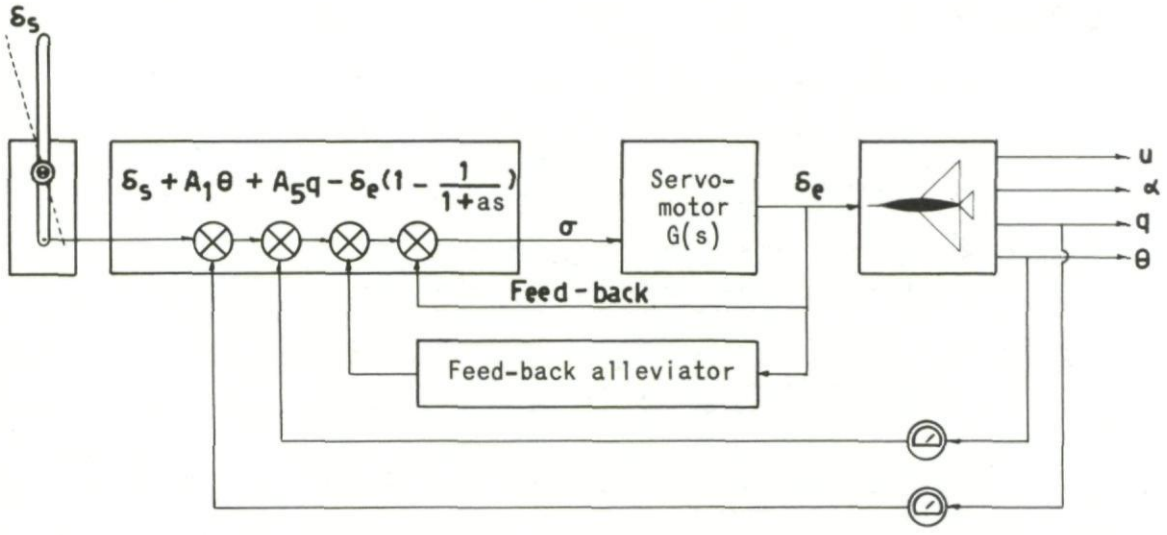

Fig.173 Use of a signal representing pilot's action; block diagram

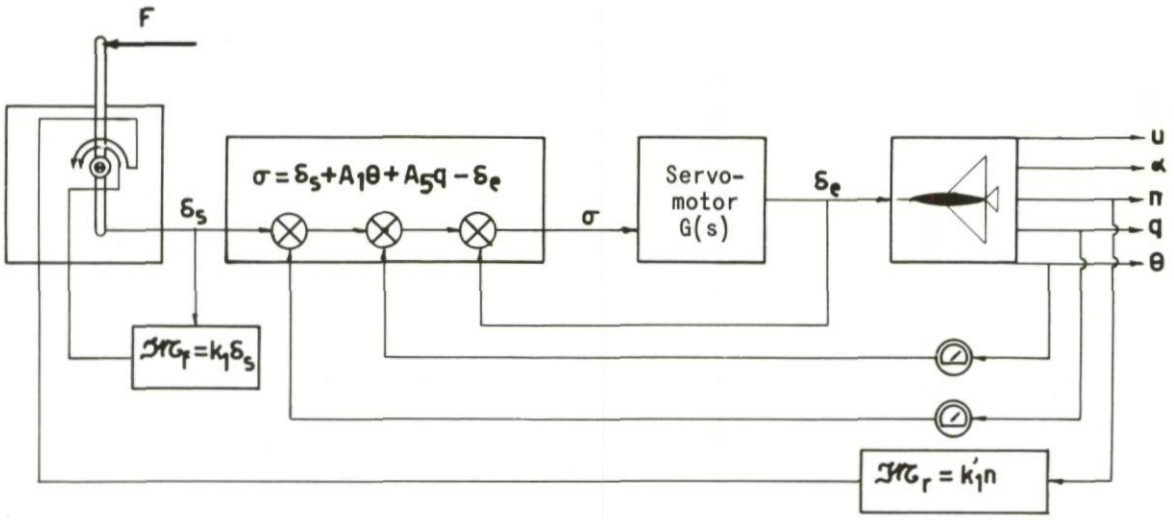

Fig. 174 Use of a signal representing control column displacement; block diagram

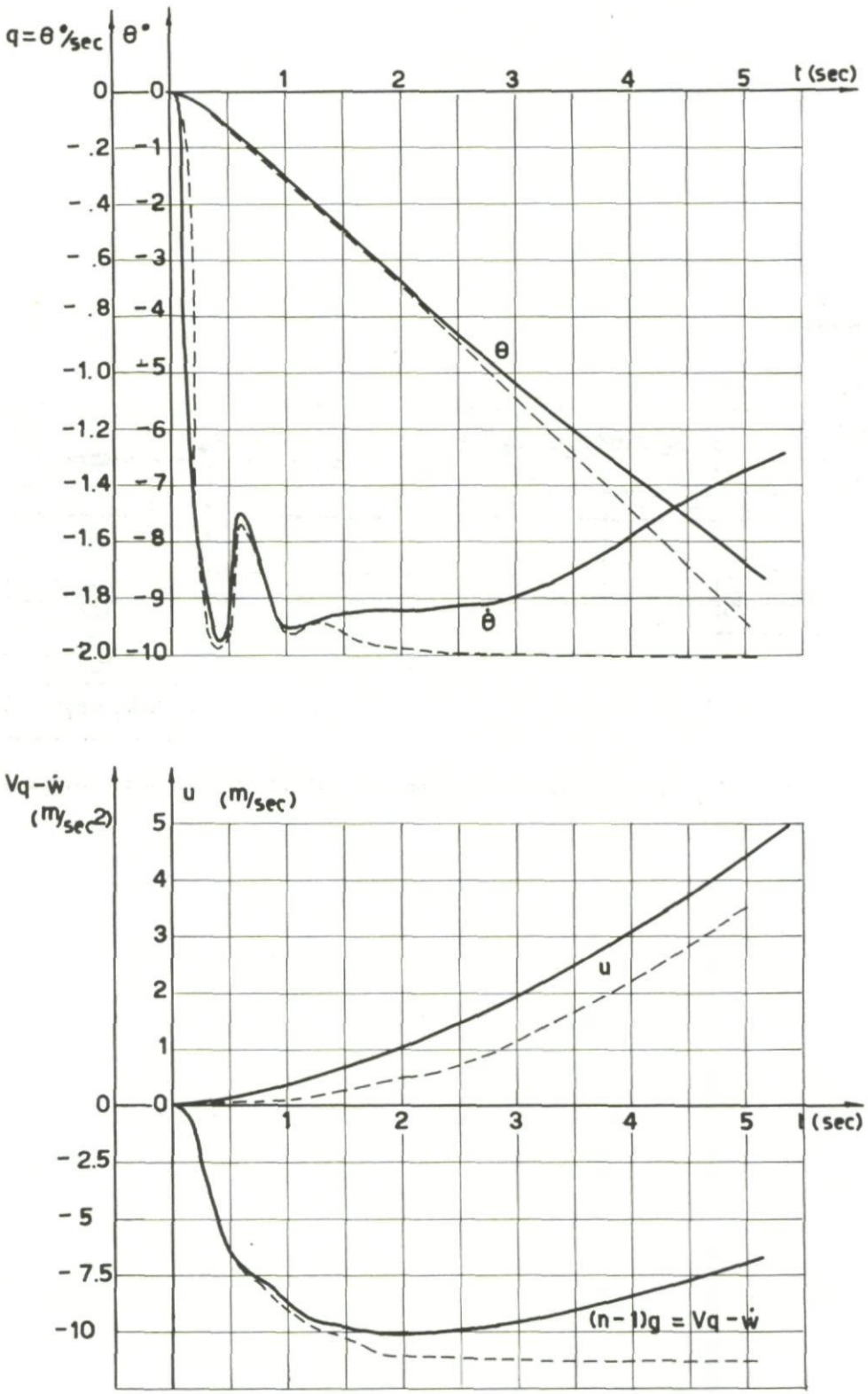

Fig.175 Response to a step in the force exerted on the stick

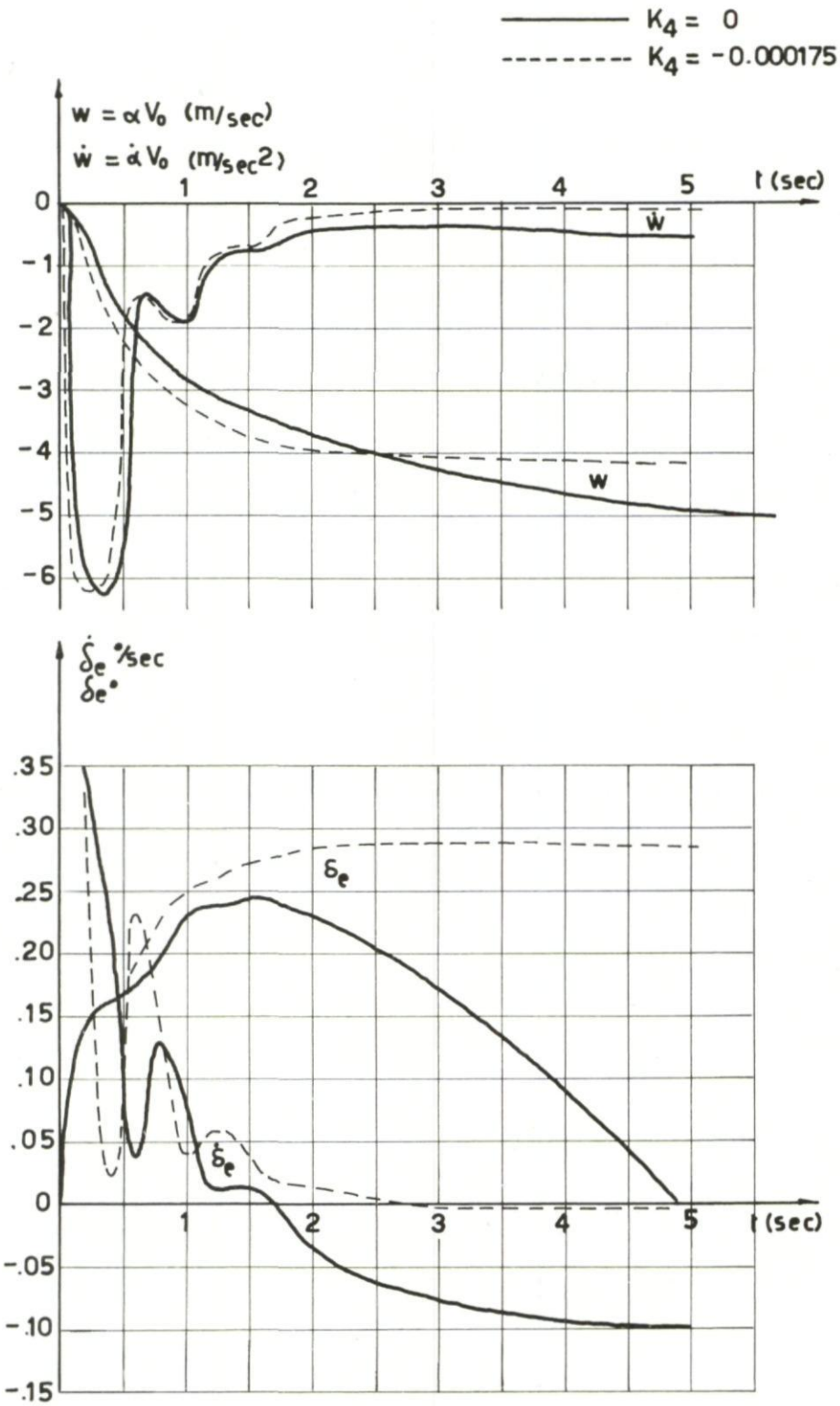

Fig. 176 Response to a step in the force exerted on the stick

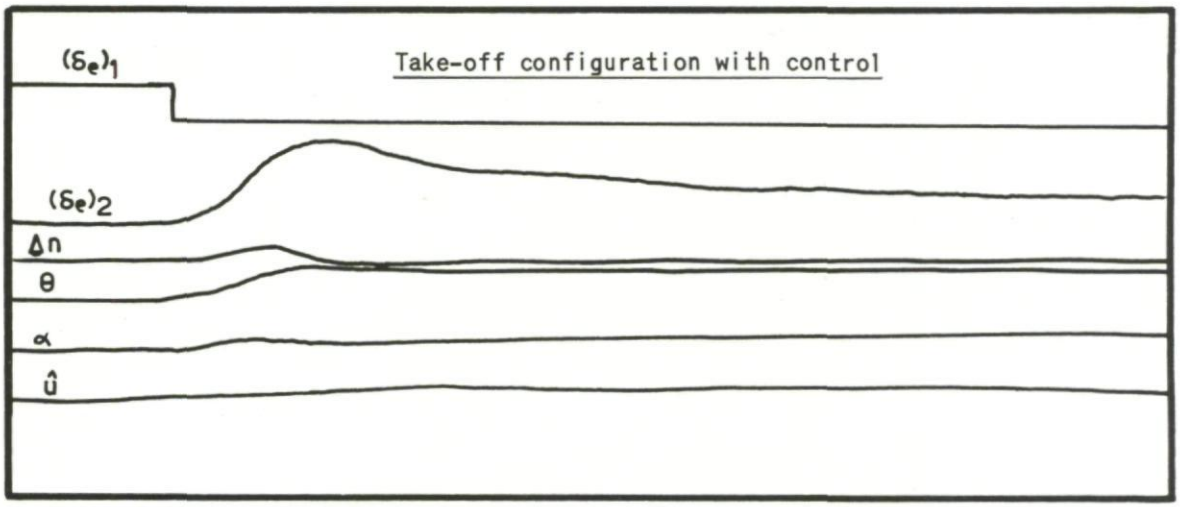

Fig.177 Response to a step displacement of stick (slow aircraft)

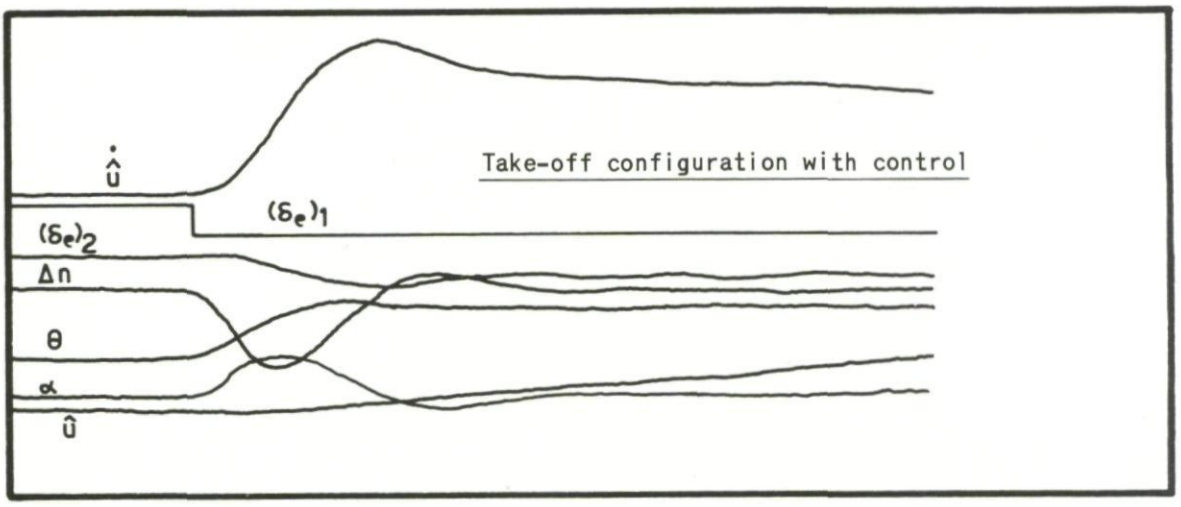

Fig.178 Response to a step displacement of stick (slow aircraft)

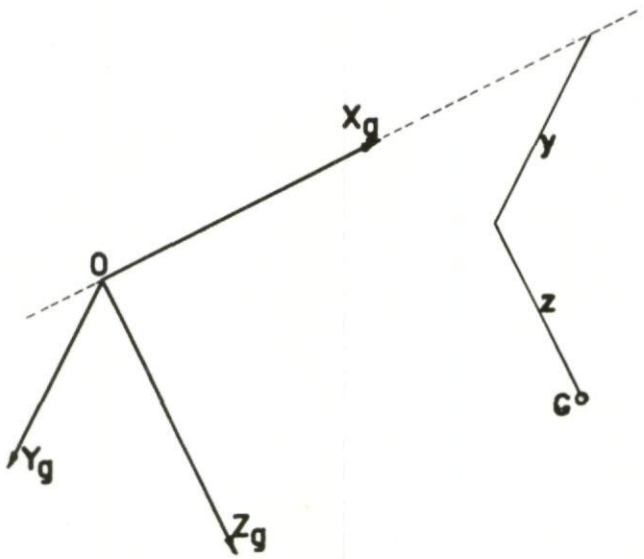

Fig.179 Actual position of an aircraft with respect to a prescribed path

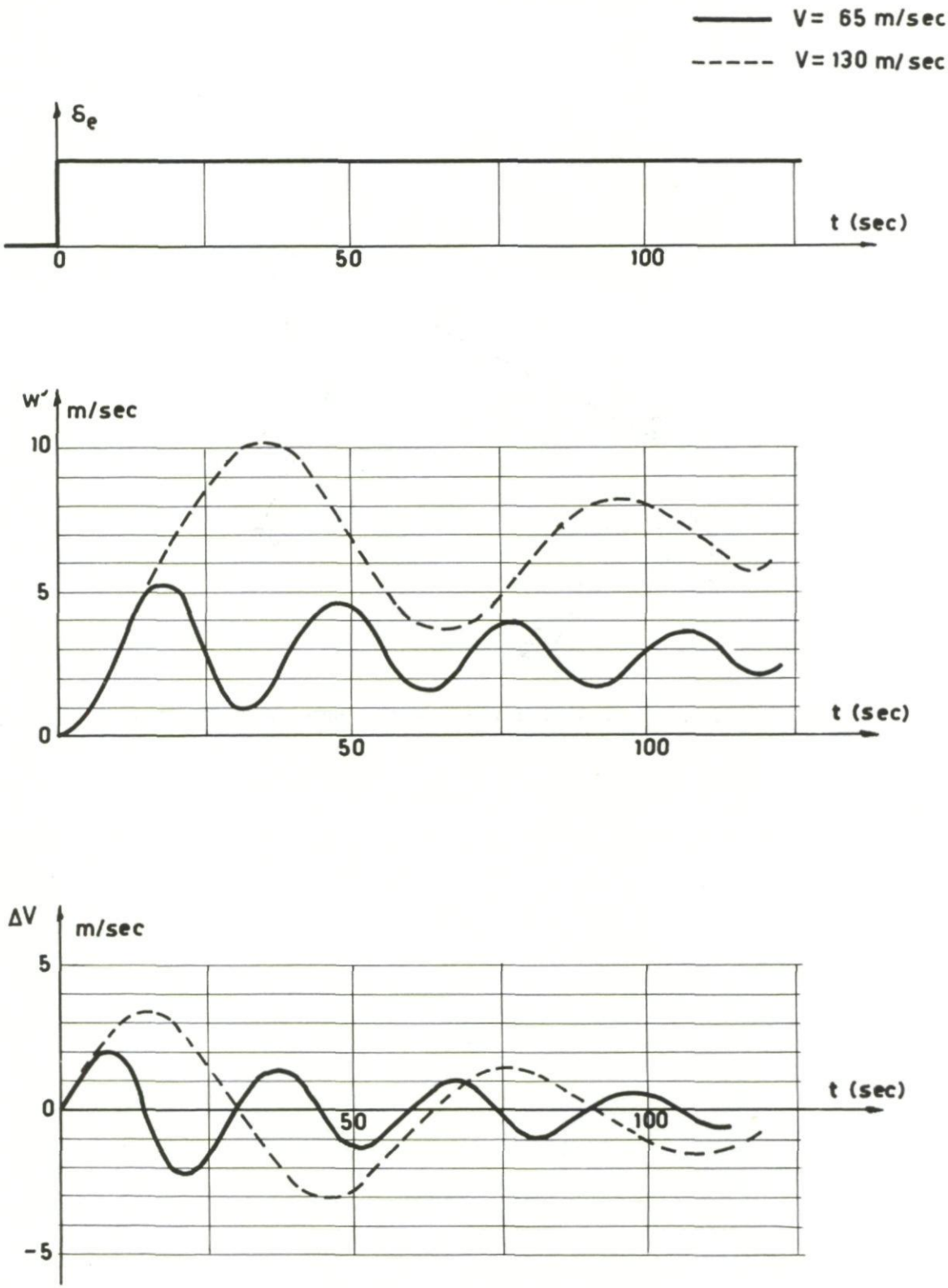

Fig.180 Simulation of aircraft motion following an elevator displacement

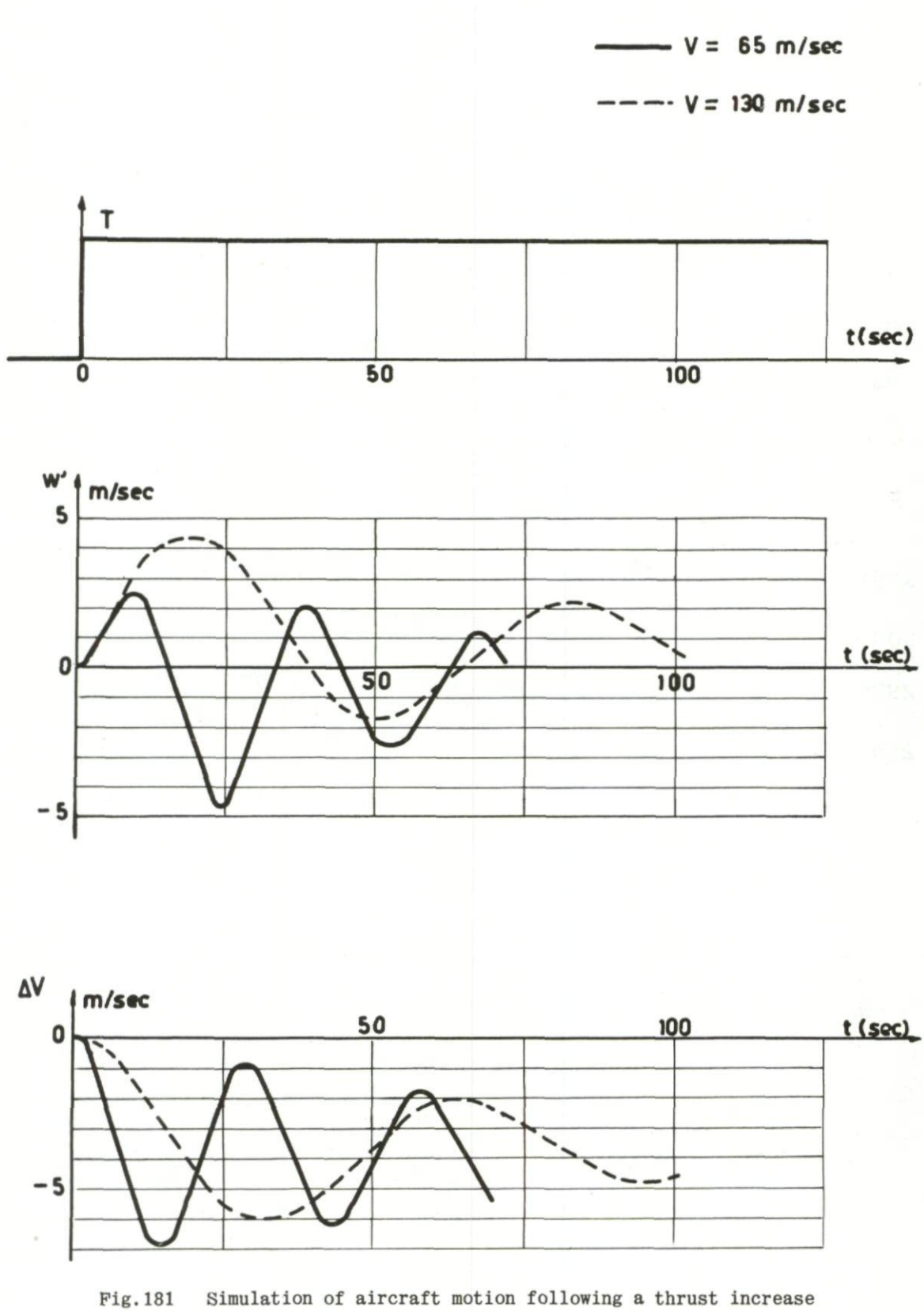

Fig.181 Simulation of aircraft motion following a thrust increase

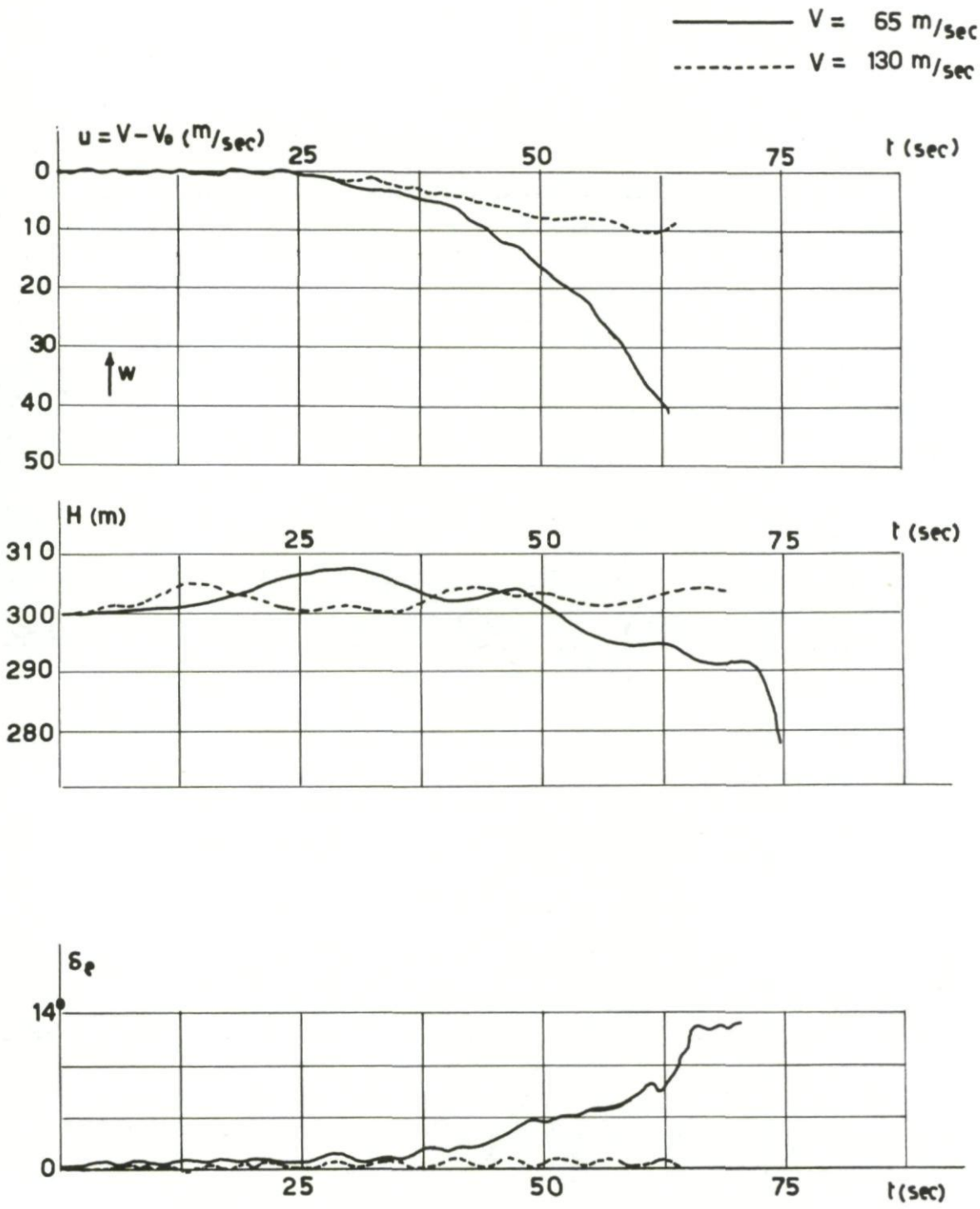

Fig.182 Human pilot correcting effect of a gust

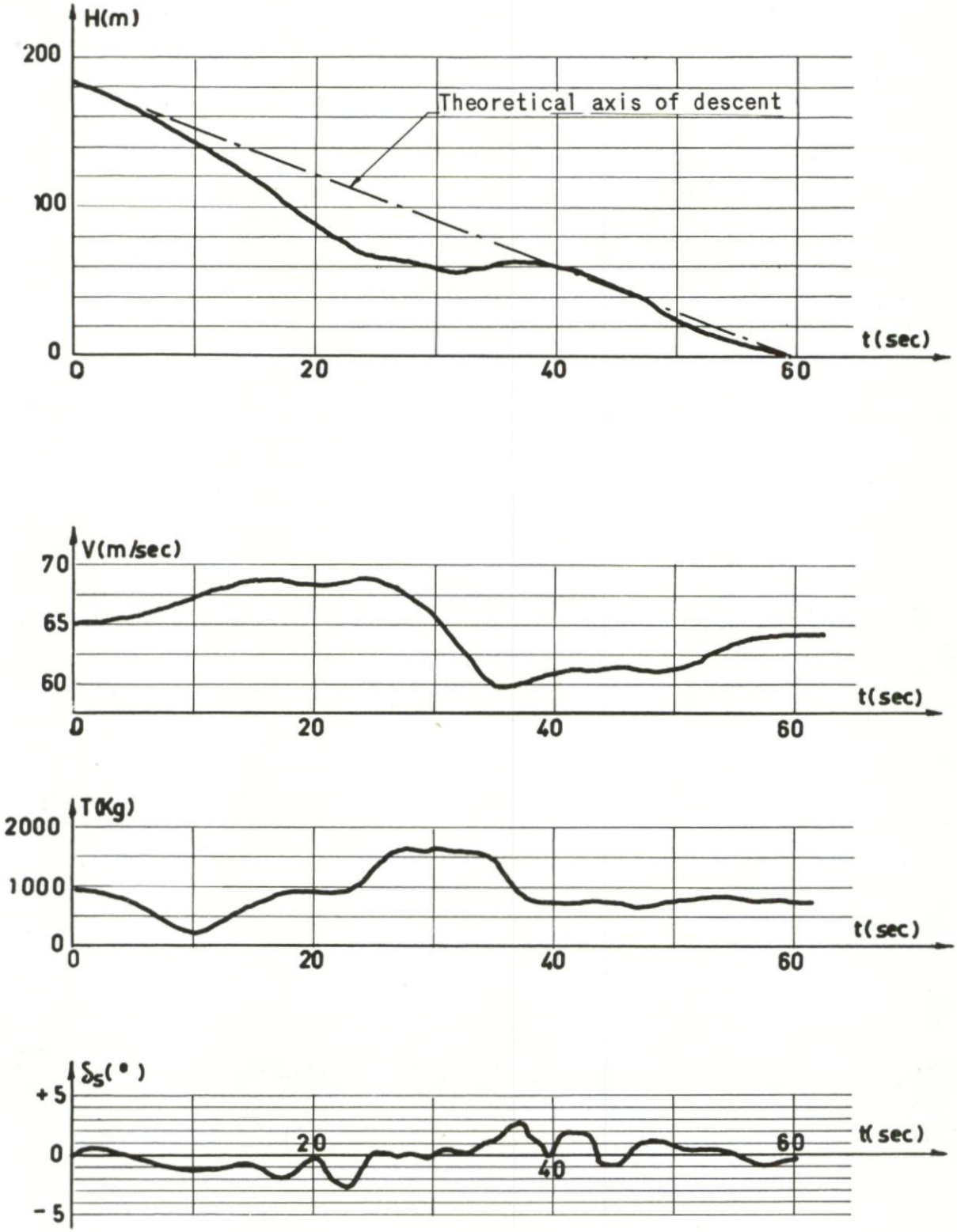

Fig. 183 Aeroplane motion under control of a human pilot

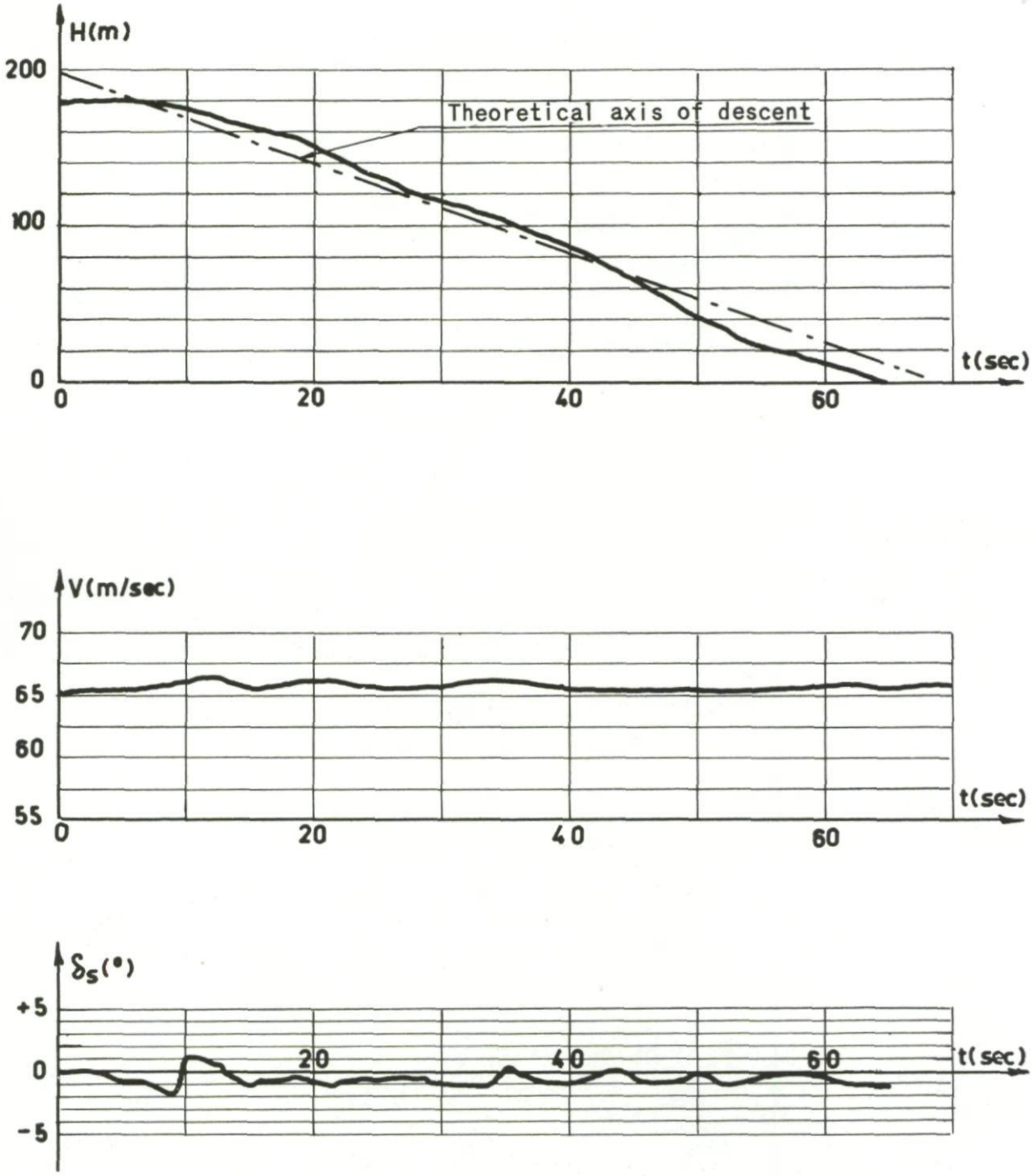

Fig.184 Aeroplane motion under control of a human pilot, plus automatic thrust control

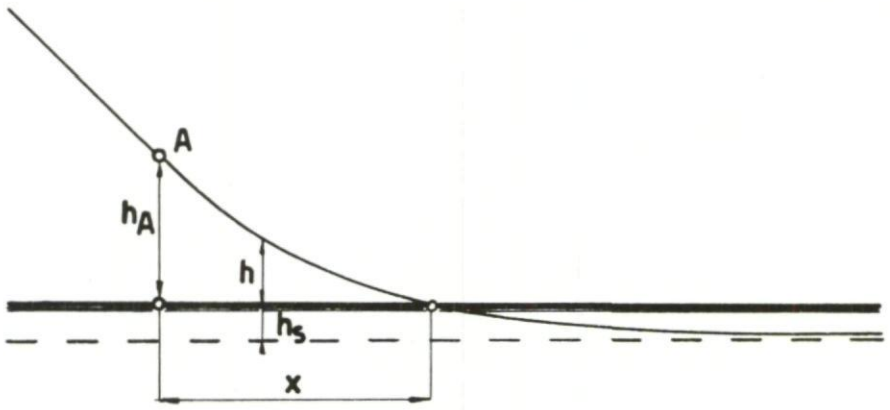

Fig. 185 Flare-out at landing

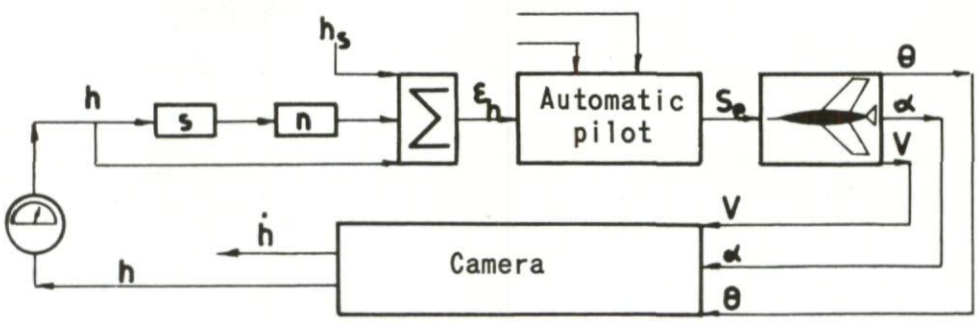

Case A

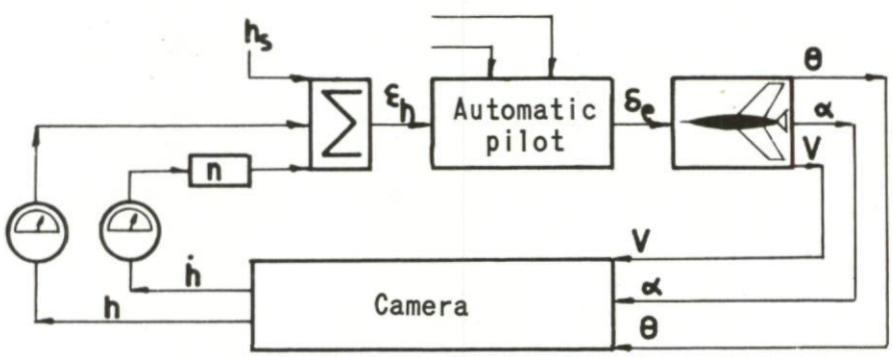

Case B

Fig. 186 Automatic flare-out control; block diagram

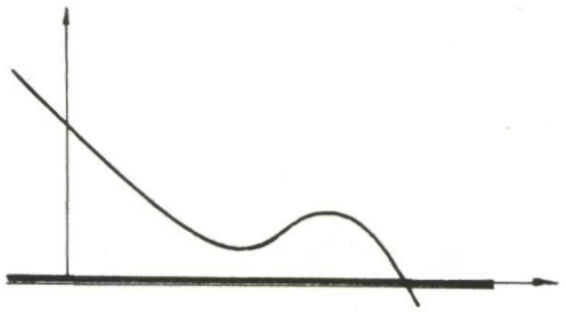

Fig.187 Disastrous effect of an oscillatory trajectory

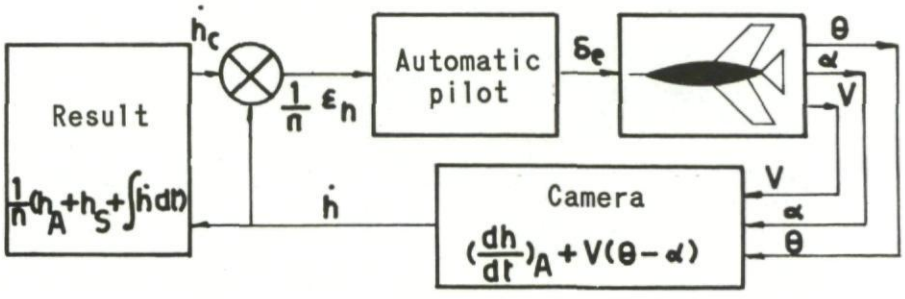

Fig.188 Automatic flare-out control; block diagram

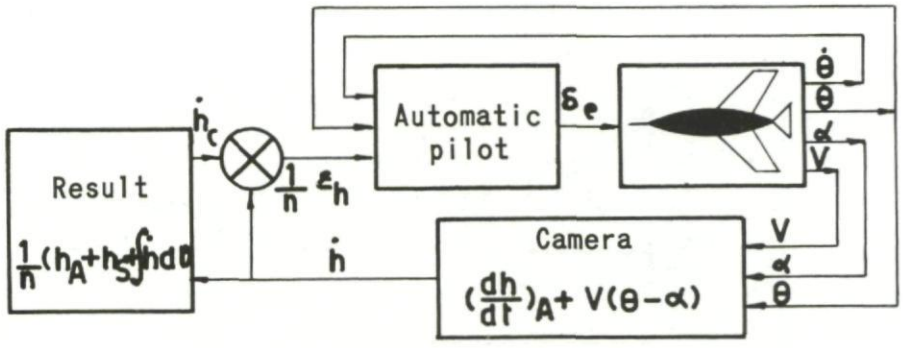

Fig.189 Automatic flare-out control; block diagram

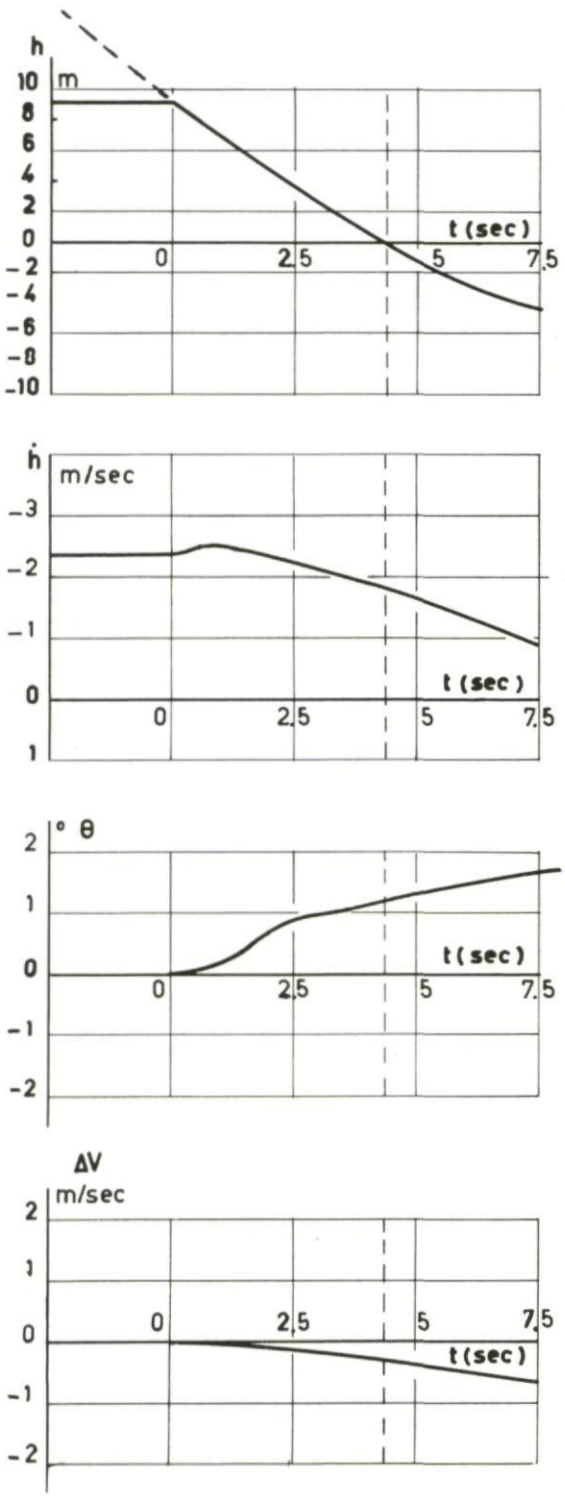

Fig. 190 Simulation of a flare-out

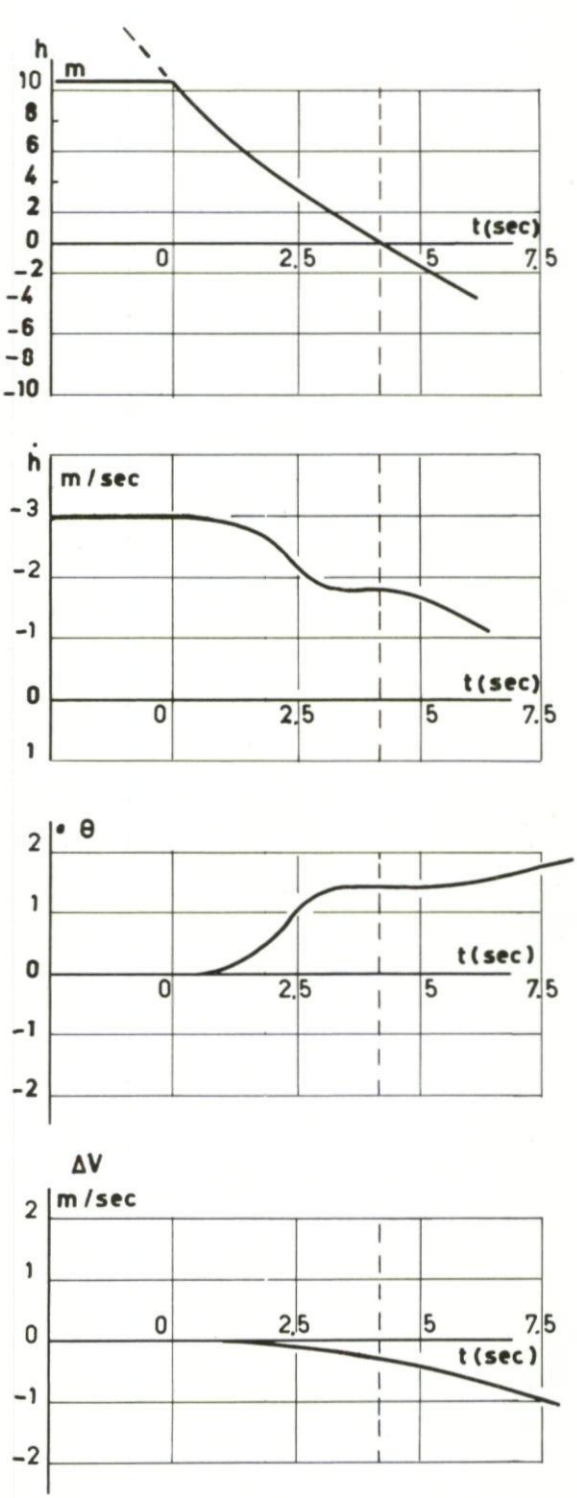

Fig. 191 Simulation of a flare-out

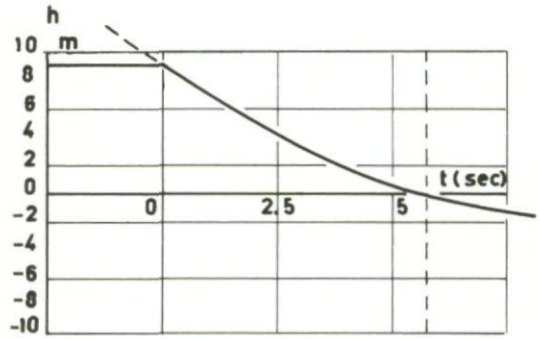

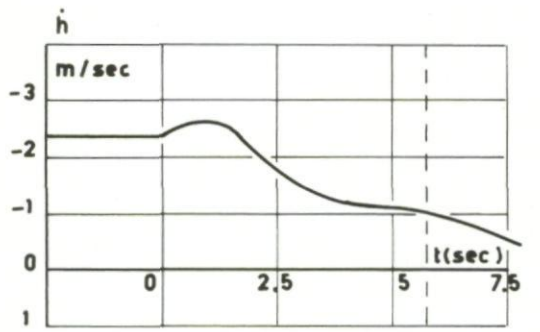

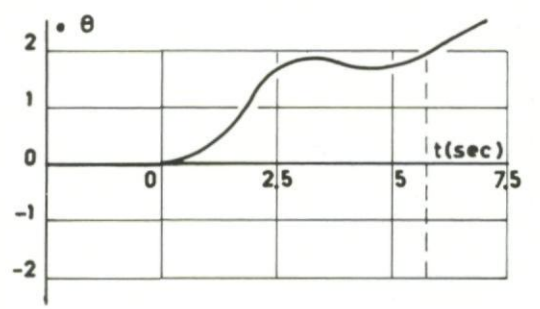

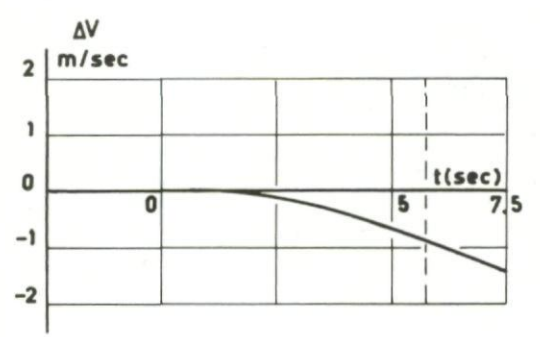

Fig.192 Simulation of a flare-out

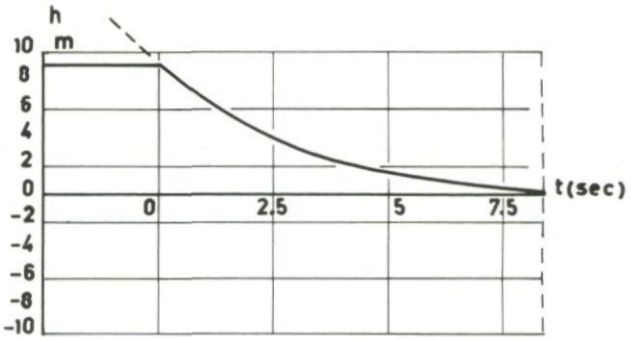

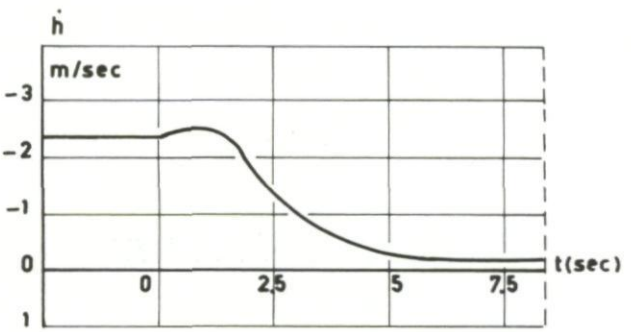

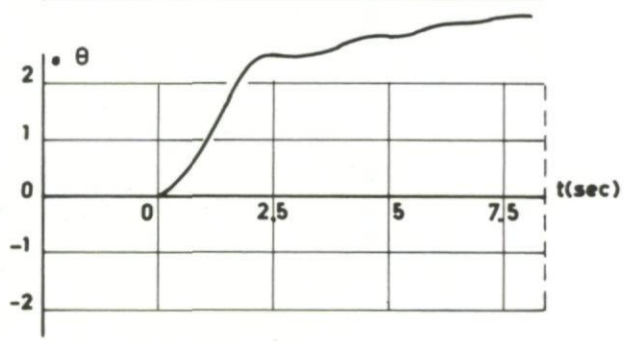

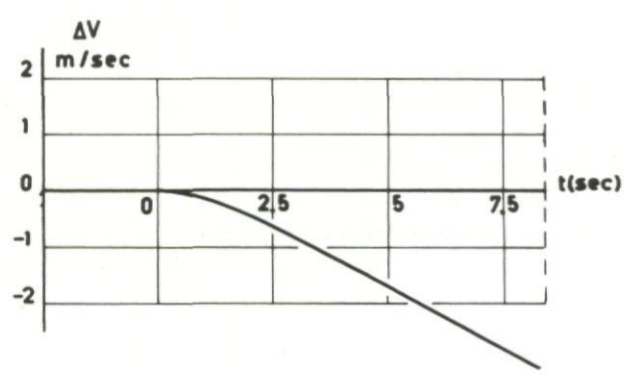

Fig.193 Simulation of a flare-out

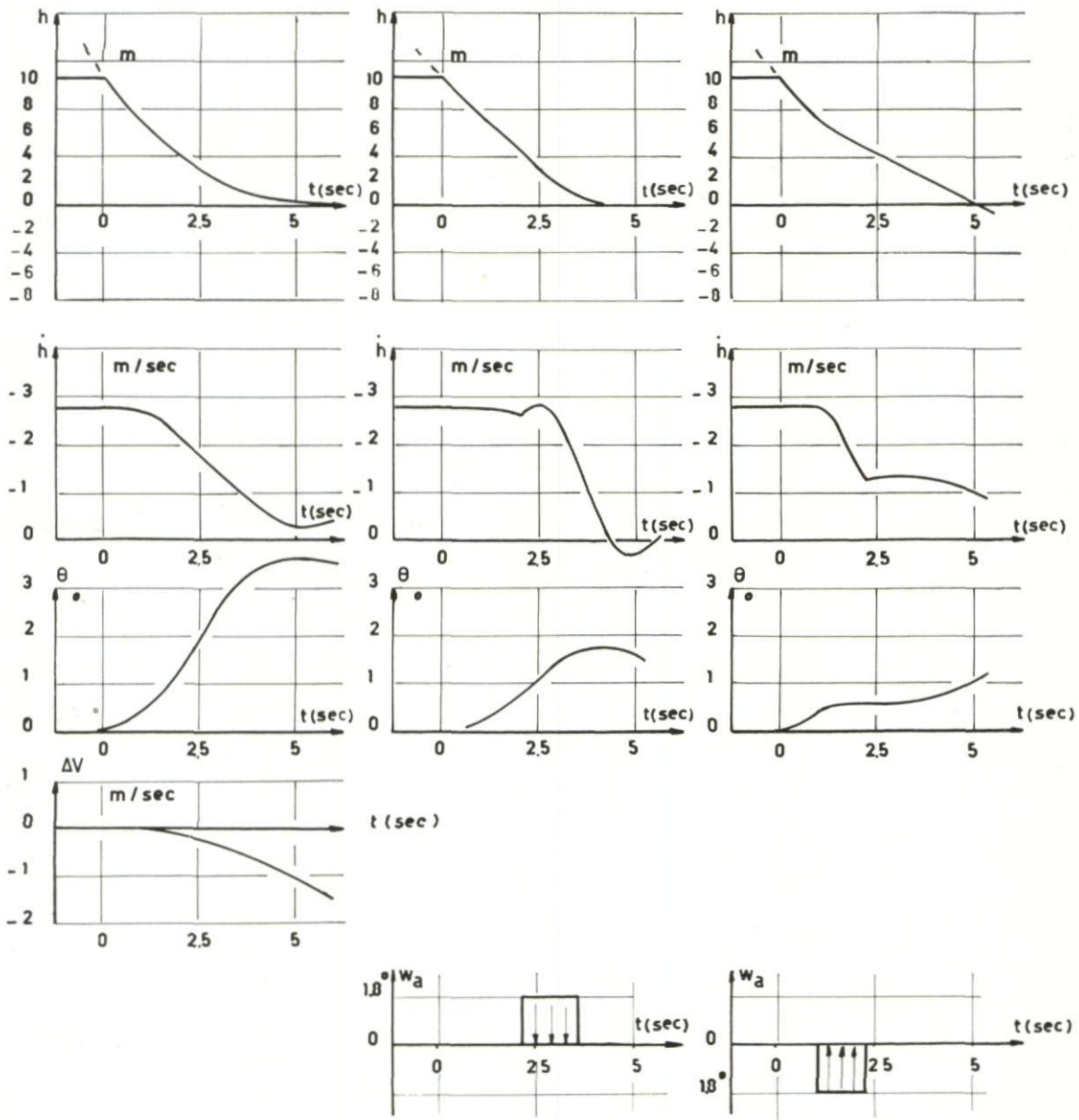

Fig.194 Simulation of a flare-out; action of a gust

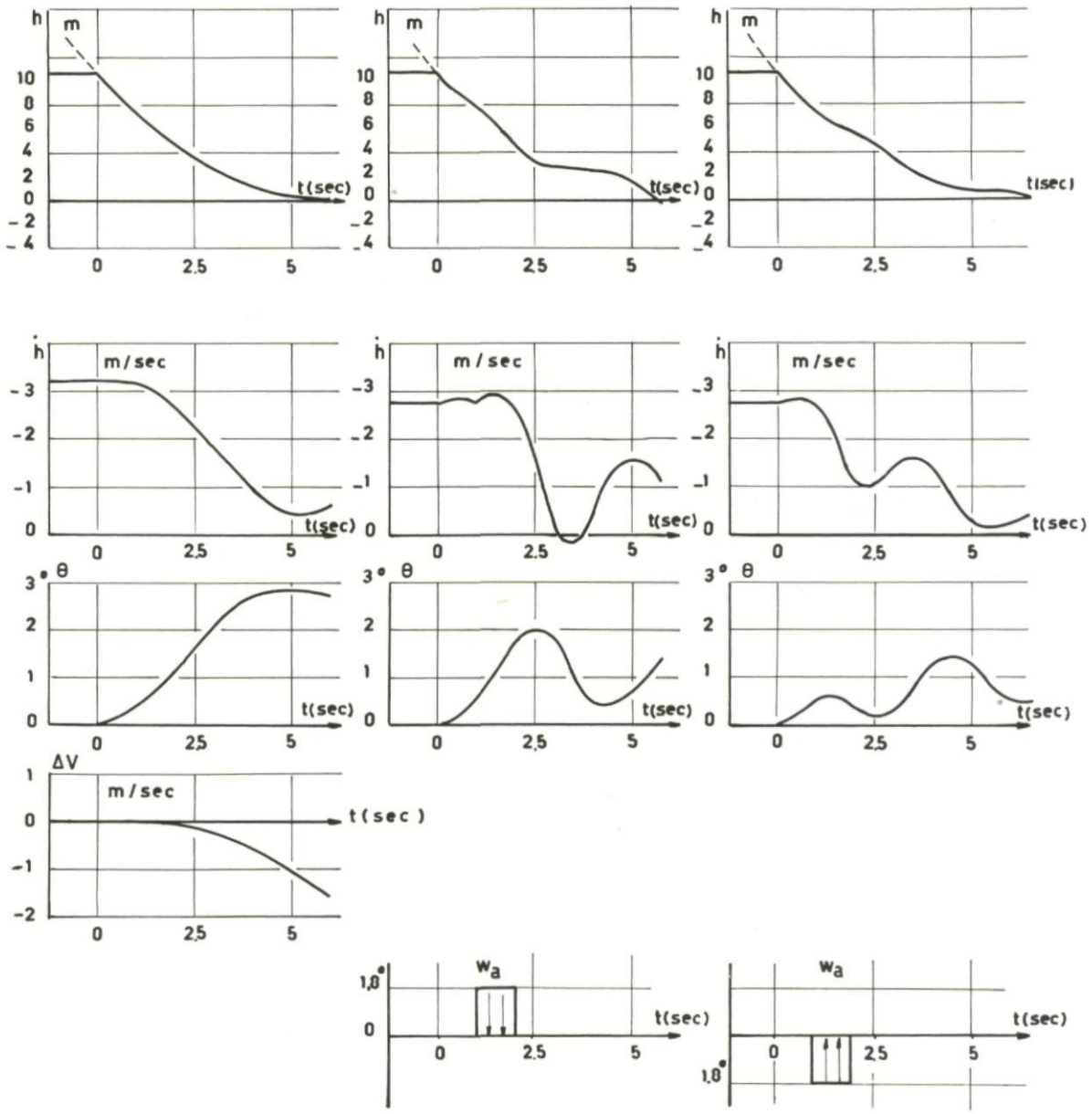

Fig.195 Simulation of a flare-out; action of a gust

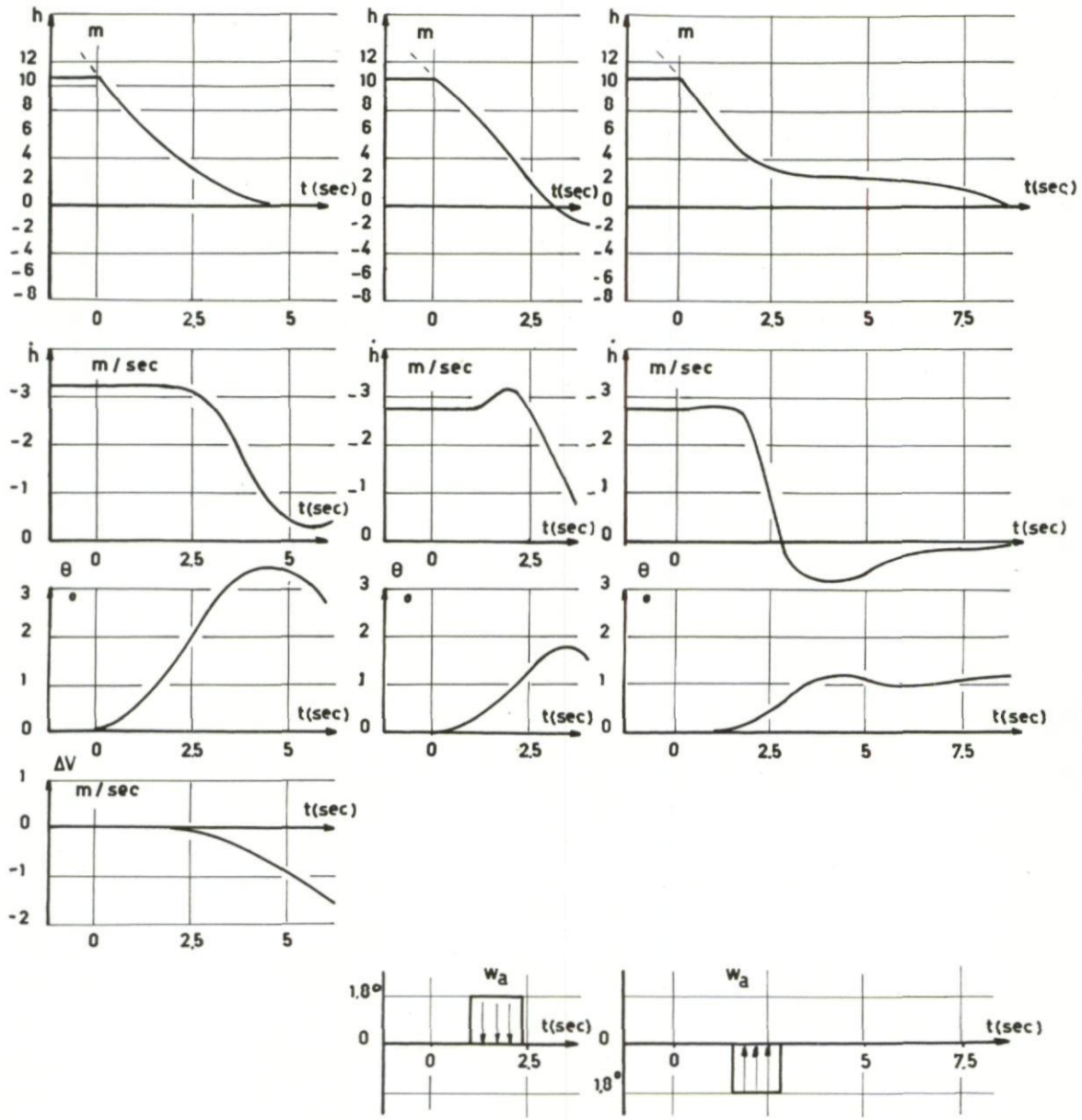

Fig.196 Simulation of a flare-out; action of a gust

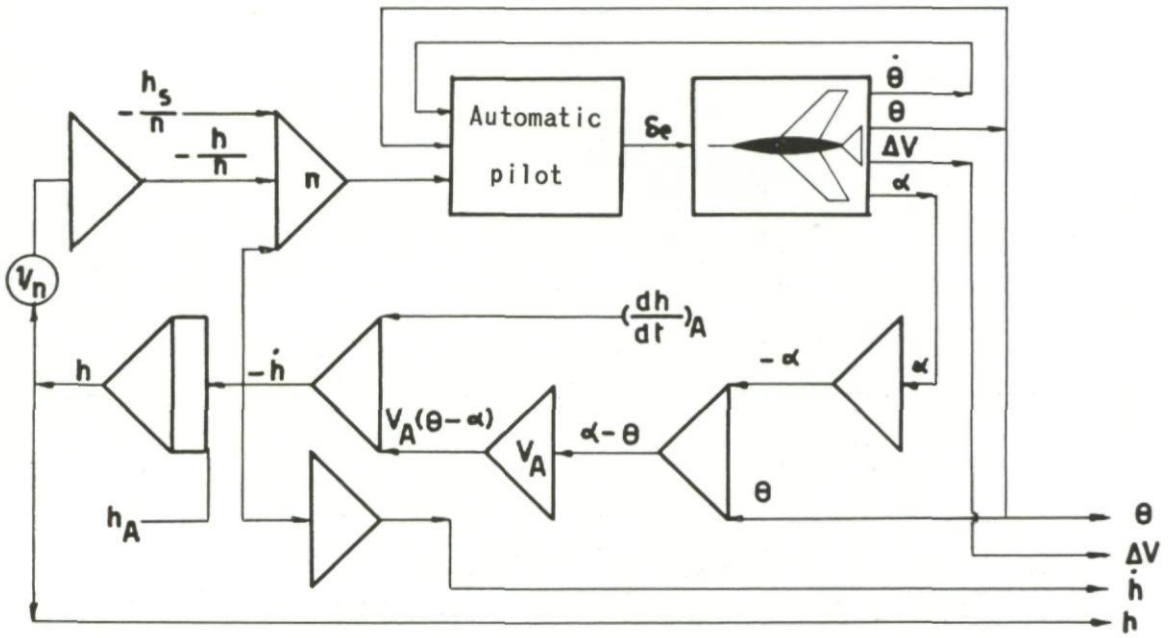

Fig.197 Simulation of an automatic flare-out and control; block diagram

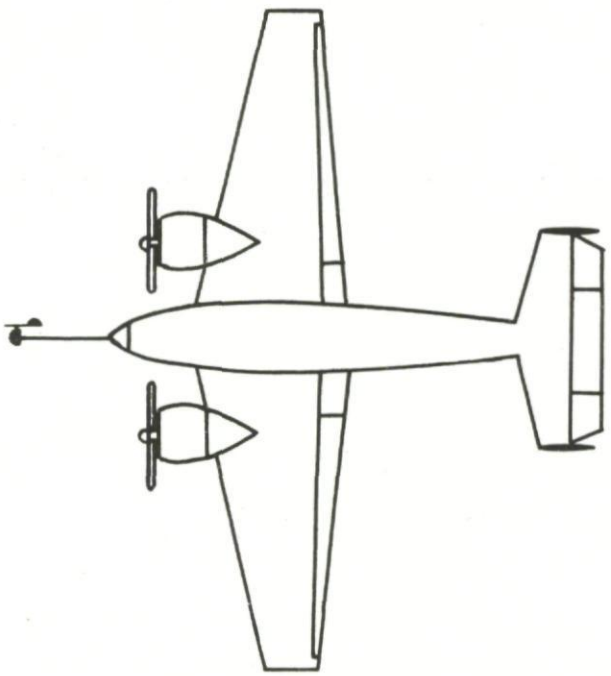

Fig.198 Aircraft fitted with gust alleviating device

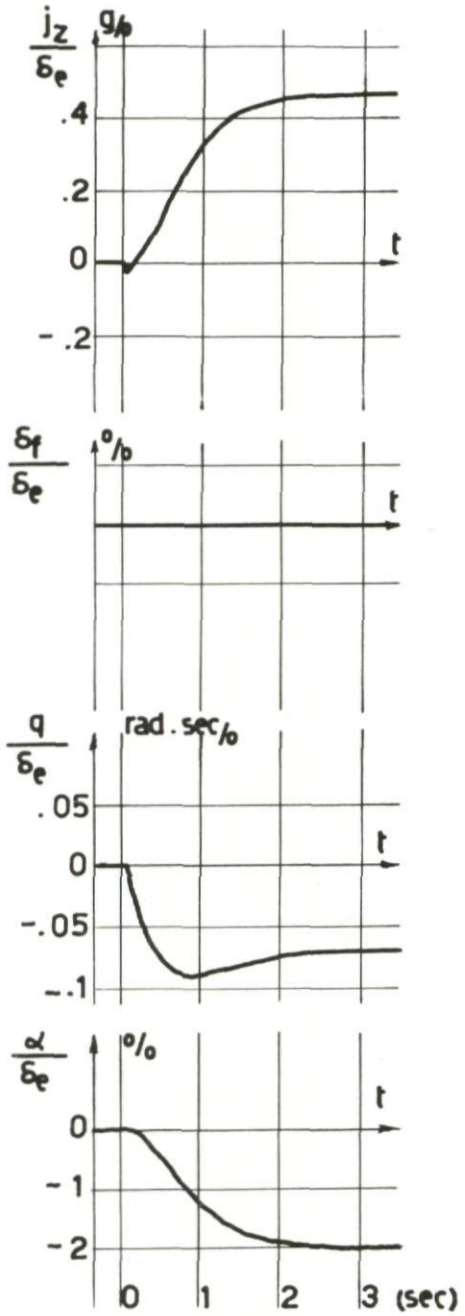

Fig. 199 Response to a δ_e step without gust alleviation

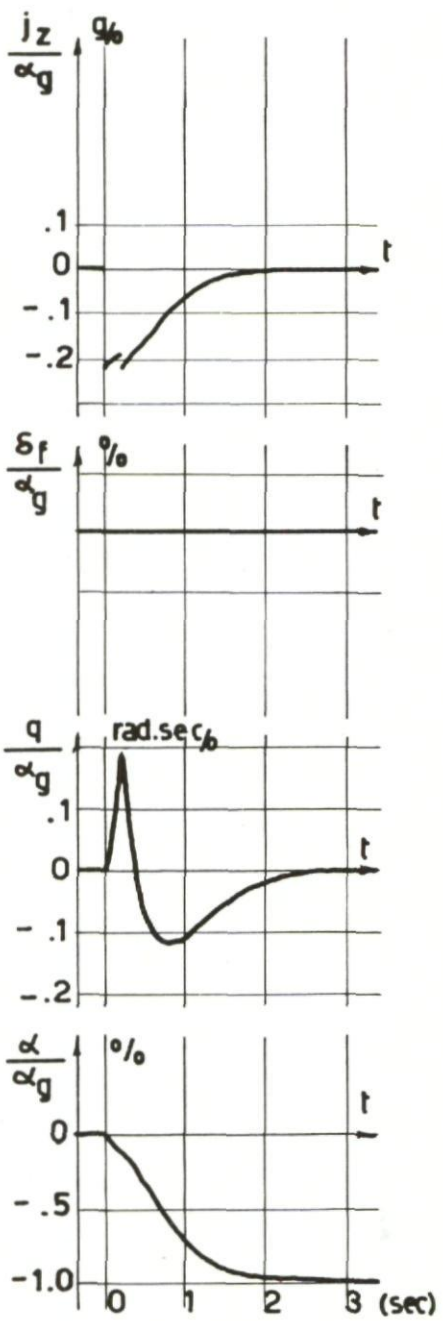

Fig. 200 Response to an α_g step without gust alleviation

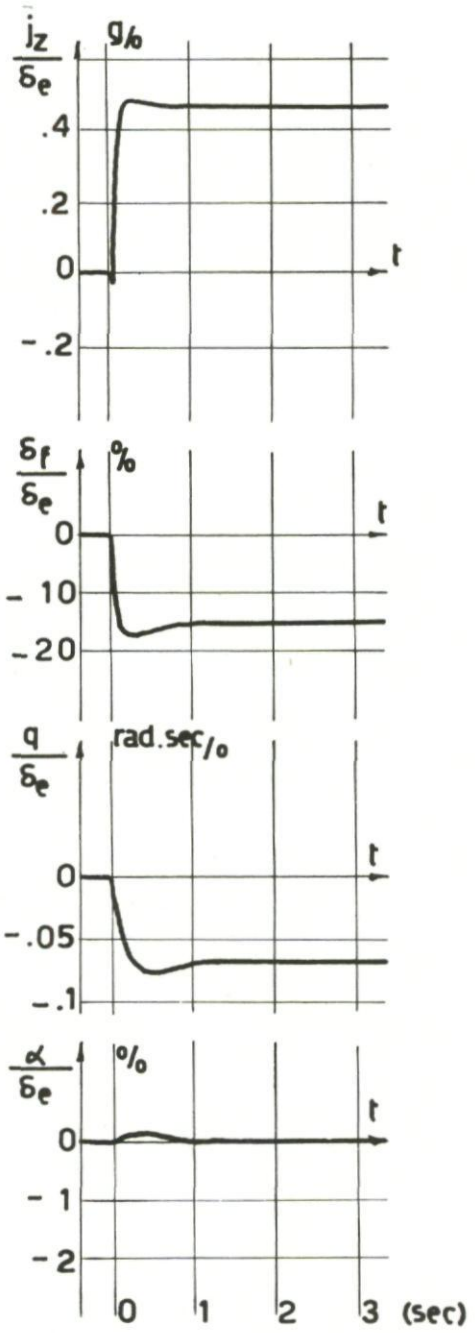

Fig. 201 Response to a δ_e step with gust alleviation

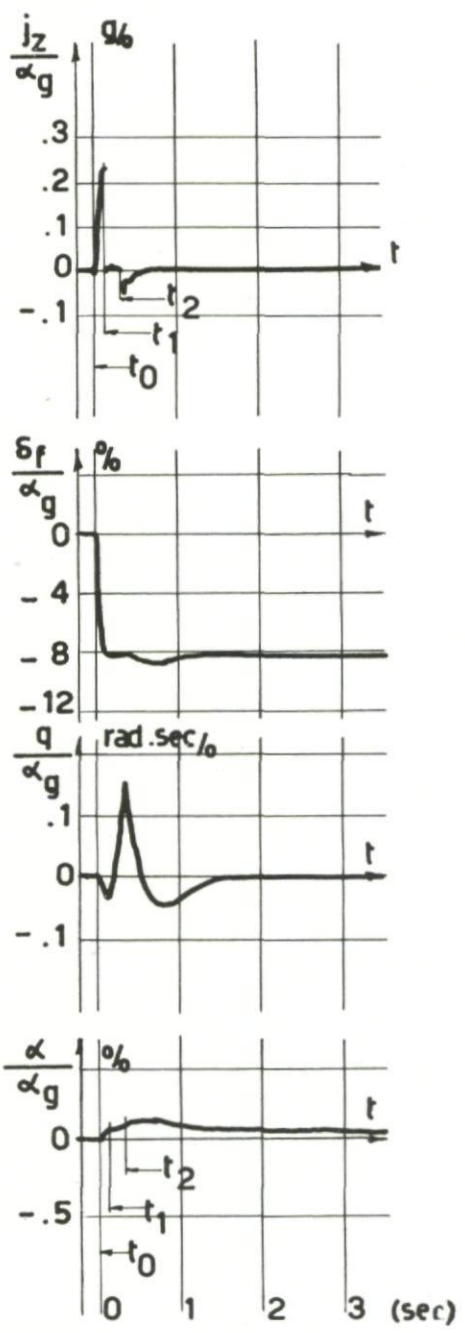

Fig. 202 Response to an α_g step with gust alleviation

PART IV - A CASE OF AEROPLANE GUIDANCE, AS AN EXAMPLE OF ANALOGUE COMPUTER UTILIZATION

F.C.Haus

CHAPTER 14

GENERAL DISCUSSION

14.1 THE PURPOSE OF THIS INVESTIGATION

Because of the ability to repeat tests, following a logical pattern, the analogue computer allows us to study the actual mechanism of a phenomenon and to investigate the action of different factors.

The present Part considers, in some detail, the problem of guiding an aeroplane during the approach stage of its landing.

The study reveals a large number of characteristics of the motion and is presented as an example of the possibilities offered by the analogue computer technique in the study of aircraft behaviour.

14.2 PROBLEM OF THE APPROACH PATH

The ideal approach path is provided by the intersection of the vertical plane passing through the axis of the runway and a plane perpendicular to it having a fixed slope with respect to the horizontal.

The vertical plane is the plane of the 'localizer' and the inclined plane is the plane of the 'glide path' making an angle ζ with the horizontal (Fig.203).

The intersection of the two planes cuts the runway at the ideal point of contact, i.e. the 'touch-down point'.

We shall consider here the problem of automatic guidance of the aeroplane to this point.

The position of the aeroplane during its approach will be defined with respect to a system of axes $OX_gY_gZ_g$ fixed relative to the ground, the origin being located on the intersection of the localizer and glide path planes at a distance D from the touch-down point. (This system of axes is different from the system B described in Section 1.1).

The axis OX_g lies along the line of intersection of the two planes, the axis OY_g is horizontal and directed towards the pilot's right, and the axis OZ_g is perpendicular to these two axes and directed downwards.

The position of the aeroplane during the approach will be determined by the three coordinates x, y, z, in which

y represents distance from the localizer plane

z represents distance from the glide-path plane.

14.3 BASIC CONSIDERATIONS OF THE INVESTIGATION

(1) Differences between the real and ideal approach paths are assumed to be small, so as to allow us to:

(a) Consider the longitudinal and lateral movements separately

(b) Simplify the kinematic relations defining the trajectory.

The longitudinal motion will be studied as if the aeroplane were moving in the localizer plane and the lateral motion as if the aeroplane were moving in the glide-path plane.

(2) In each of the investigations, we will use the equations of motion with respect to axes GXYZ fixed to the aeroplane. This coordinate system is fixed in the conventional way, and the usual sign system used for the forces X , Y , Z , the moments L , M , N , and the velocities u , v , w , p , q , r .

(3) The motion of the aeroplane following the ideal approach path in steady air is a well-defined steady-state motion.

The transient motion which the aeroplane describes when subjected to an initial disturbance is defined by a set of linear equations. In these equations the variables will be the deviations from the values for steady motion in still air.

(4) The aeroplane is fitted with four controls. Two of these (the elevator control and the engine throttle) govern the longitudinal motion; their displacements are represented by δ_e and δ_m . The other two (ailerons and rudder) govern the lateral motion and their displacements are represented by δ_a and δ_r .

With the usual sign convention, positive displacement of δ_e , δ_a and δ_r produce negative moments, while δ_m is positive when the displacement of the throttle lever increases the power.

With constant-speed propellers we can say, to a first approximation, that the power is proportional to the throttle opening.

Let W be the power supplied during a manoeuvre and W_0 the power supplied for trimmed motion in still air. Then δ_m is defined as follows:

$$\delta_m = \frac{W - W_0}{W_0}$$

(5) The displacement of the aeroplane will be investigated taking account of air movements in the surrounding atmosphere. The component velocities of the air along the axes GX , GY , GZ will be defined by u_a , v_a , w_a .

Note

It would have been more logical to define the components of velocity of the atmosphere with respect to ground axes like OX_g , OY_g , OZ_g , rather than to aeroplane axes, but the equations would be more complicated.

14.4 METHODS USED IN THE INVESTIGATION

Research into the problem of aeroplane control has been carried out with an analogue computer, using the aerodynamic characteristics of an existing aeroplane.

The necessary data come partly from wind tunnel investigation, and partly from simple evaluations.

The analogue computer work was done on several different occasions. It was started in September 1954 and it was possible, thanks to F.N.R.S.*, to use a computer which was temporarily installed in the industrial electronics laboratory of the University of Brussels.

The results obtained induced the Derveaux laboratories of Paris to place at our disposal, on three different occasions, a Djinn computer which permitted us to obtain the majority of the diagrams presented in this report. The last tests were made again at the University of Brussels.

The following presentation follows the reasoning we made at the time in order to find the best control equations.

Some time before our tests were completed we discovered that similar work had been carried out by R.E. Carroll and C.M. Tyler at the Bell Aircraft Corporation for the U.S.A.F.[28]

The report published by these researchers takes account of a great number of significant combinations; it recommends certain combinations of control equations but it is not possible to follow completely the successive tests on which these recommendations are based.

This report came into our possession in time for us to compare the control equations recommended by the American experimenters with our own, for the case of lateral motion. However, we were not able to make a similar comparison for the case of longitudinal motion, for reasons which will be seen later.

---

*Fonds National de la Recherche Scientifique

CHAPTER 15

EQUATIONS OF MOTION OF THE AEROPLANE

15.1 NOTATION SYSTEM

The equations of motion of the aeroplane have been written using the following variables:

Independent variable t

The time t is replaced by the aerodynamic time $\hat{t}$.

In the longitudinal motion, we define the specific mass as

$$\mu = \frac{2m}{\rho S c} \tag{15.1}$$

The unit of aerodynamic time τ is equal to $\mu c/V_0$ seconds.

In the lateral motion, we define the specific mass as

$$\mu' = \frac{2m}{\rho S b} \tag{15.2}$$

The unit of aerodynamic time τ is equal to $\mu' b/V_0$ seconds and is the same as for the longitudinal motion.

We shall call V_τ the displacement of the aeroplane per unit of aerodynamic time. Then we have:

$$V_\tau = V\left(\frac{\mu c}{V_0}\right) = V\left(\frac{\mu' b}{V_0}\right) \tag{15.3}$$

and, for the steady state:

$$V_{0,\tau} = \mu c = \mu' b \tag{15.4}$$

Dependent variables

The variables used are:

$$\left.\begin{aligned} \hat{u} &= \frac{u}{V_0} & \alpha &= \frac{w}{V_0} & \beta &= \frac{v}{V_0} \\ \hat{p} &= \frac{pb}{2V_0} & \hat{q} &= \frac{qc}{V_0} & \hat{r} &= \frac{rb}{2V_0} \end{aligned}\right\} \tag{15.5}$$

15.2 EQUATIONS OF MOTION

The longitudinal equations of motion are written taking the axes fixed to the chord:

$$\left.\begin{aligned}
&\frac{d\hat{u}}{d\hat{t}} - C_{x_u}\hat{u} - C_{x_\alpha}\alpha - \left(C_{x_q} - \mu\alpha_0\right)\hat{q} + C_L \cos\theta_0\,\theta \\
&\qquad = C_{x_{\delta_m}}\delta_m + C_{x_{\delta_e}}\delta_e - \left(C_{x_0} - \alpha_0 C_{x_\alpha}\right)\frac{u_a}{V_0} - C_{x_\alpha}\frac{w_a}{V_0} \\
&\frac{d\alpha}{d\hat{t}} - C_{z_u}\hat{u} - C_{z_\alpha}\alpha - \left(C_{z_q} + \mu\right)\hat{q} + C_L \sin\theta_0\,\theta \\
&\qquad = C_{z_{\delta_m}}\delta_m + C_{z_{\delta_e}}\delta_e - \left(C_{z_{\hat{u}}} - \alpha_0 C_{z_\alpha}\right)\frac{u_a}{V_0} - C_{z_\alpha}\frac{w_a}{V_0} \\
&\left(\frac{r_y}{c}\right)^2\frac{dq}{dt} - C_{m_u}\hat{u} - C_{m_\alpha}\alpha - \left(C_{m_q} + C_{m_{\dot{\alpha}}}\right)\hat{q} \\
&\qquad = C_{m_{\delta_m}}\delta_m + C_{m_{\delta_e}}\delta_e - \left(C_{m_u} - \alpha_0 C_{m_\alpha}\right)\frac{u_a}{V_0} - C_{m_\alpha}\frac{w_a}{V_0} \\
&\frac{d\theta}{d\hat{t}} - \mu\hat{q} = 0
\end{aligned}\right\} \qquad (15.6)$$

The displacement of the aeroplane is given by:

$$\left.\begin{aligned}
&\frac{dq}{d\hat{t}} - V_{0,\tau}(\alpha - \theta) = 0 \\
&\frac{dx}{d\hat{t}} - V_{0,\tau}(1 + \hat{u}) = 0
\end{aligned}\right\} \qquad (15.7)$$

The equation in z is the linearized form of the following equation:

$$\frac{dz}{dt} - V_{0,\tau}(1 + \hat{u})(\alpha - \theta) = 0$$

which is more exact, and has been used because it was possible to introduce products of variables in the computer.

The equations of lateral motion are written taking axes fixed to the principal axes of inertia:

$$\left.\begin{aligned}
&\frac{d\beta}{d\hat{t}} - C_{y_\beta}\beta - \left[C_{y_p} + 2\mu'(\alpha_0 - \alpha_p)\right]\hat{p} - \left[C_{y_r} - 2\mu'\right]\hat{r} + C_L \cos\varphi_0 \cos\theta_0\, \varphi \\
&\qquad = C_{y_{\delta_a}}\delta_a + C_{y_{\delta_r}}\delta_r - C_{y_\beta}\frac{v_a}{V_0} \\
&2\left(\frac{r_x}{b}\right)^2 \frac{d\hat{p}}{d\hat{t}} - C_{l_\beta}\beta - C_{l_p}\hat{p} - C_{l_r}\hat{r} \\
&\qquad = C_{l_{\delta_a}}\delta_a + C_{l_{\delta_r}}\delta_r - C_{l_\beta}\frac{v_a}{V_0} \\
&2\left(\frac{r_z}{b}\right)^2 \frac{d\hat{r}}{d\hat{t}} - C_{n_\beta}\beta - C_{n_p}\hat{p} - C_{n_r}\hat{r} \\
&\qquad = C_{n_{\delta_a}}\delta_a + C_{n_{\delta_r}}\delta_r - C_{n_\beta}\frac{v_a}{V_0} \\
&\frac{d\varphi}{d\hat{t}} - 2\mu'\hat{p} = 0 \\
&\frac{d\psi}{d\hat{t}} - 2\mu'\hat{r} = 0
\end{aligned}\right\} \qquad (15.8)$$

The displacement of the aeroplane in the glide path is given by

$$\frac{dy}{d\tau} - V_{0,\tau}(\beta + \psi) = 0 \qquad (15.9)$$

15.3 INPUT AND OUTPUT SIGNALS

In all that follows, the equations are written in a general form.

15.3.1 Longitudinal Motion

$$\left.\begin{aligned}
&\frac{\dot{u}}{V_0} + a_1\hat{u} + b_1\alpha + c_1\hat{q} + d_1\theta = h_1\delta_m + k_1\delta_e + (a_1 - \alpha_0 b_1)\frac{u_a}{V_0} + b_1\frac{w_a}{V_0}
\end{aligned}\right| \qquad (15.10)$$

$$
\left.\begin{aligned}
\dot{\alpha} + a_2\hat{u} + b_2\alpha + c_2\hat{q} + d_2\theta &= h_2\delta_m + k_2\delta_e + (a_2 - \alpha_0 b_2)\frac{u_a}{V_0} + b_2\frac{w_a}{V_0} \\
\dot{\hat{q}} + a_3\hat{u} + b_3\alpha + c_3\hat{q} &= h_3\delta_m + k_3\delta_e + (a_3 - \alpha_0 b_3)\frac{u_a}{V_0} + b_3\frac{w_a}{V_0} \\
\dot{\theta} + c_4\hat{q} &= 0 \\
\dot{z} + b_5\alpha + d_5\theta &= 0 \\
\dot{x} + a_6\hat{u} &= V_{0,\tau}
\end{aligned}\right\} \quad (15.10)
$$

15.3.2 Lateral Motion

$$
\left.\begin{aligned}
\dot{\beta} + a_1\beta + b_1\hat{p} + c_1\hat{r} + d_1\varphi &= h_1\delta_a + k_1\delta_r + a_1\frac{v_a}{V_0} \\
\dot{\hat{p}} + a_2\beta + b_2\hat{p} + c_2\hat{r} + d_2\varphi &= h_2\delta_a + k_2\delta_r + a_2\frac{v_a}{V_0} \\
\dot{\hat{r}} + a_3\beta + b_3\hat{p} + c_3\hat{r} &= h_3\delta_a + k_3\delta_a + a_3\frac{v_a}{V_0} \\
\dot{\varphi} + b_4\hat{p} &= 0 \\
\dot{\psi} + c_5\hat{r} &= 0 \\
\dot{y} + a_6\beta + e_6\psi &= 0
\end{aligned}\right\} \quad (15.11)
$$

The symbol $\cdot$ indicates a derivative with respect to aerodynamic time $\hat{t}$.

The control settings δ_e, δ_m, δ_a, δ_r and the velocity components u_a, v_a, w_a of the ambiant air, constitute the input signals, from which the aeroplane produces 12 output variables, viz.

$\hat{u}$	β	α
φ	θ	ψ
$\hat{p}$	$\hat{q}$	$\hat{r}$
x	y	z

These variables can be considered as the generalized coordinates of the aeroplane.

The input signals are of two different types: the wind velocity components u_a, v_a, w_a are random in nature.

The control displacements δ_e, δ_m, δ_a, δ_r are caused by the pilot and hence they can be predetermined. In the case of an automatic pilot, they are defined by the control equations.

15.4 MECHANICAL AND AERODYNAMIC CHARACTERISTICS OF THE AEROPLANE UNDER CONSIDERATION

The characteristics of the aeroplane were:

Total weight (G)		48,000 kg
Wing area		185.70 m^2
Wing span (b)		42.95 m
Chord (c)		4.31 m
Distance of tail-plane from centre of gravity		15.50 m
Radius of inertia:	r_x	5.48 m
	r_y	4.90 m
	r_z	7.34 m

The coefficients of lift and drag, C_L and C_D, are given in Figure 204, together with the ratios C_D/C_L and $C_D/C_L^{3/2}$.

The flight conditions under consideration are for a speed of V_0 = 60 m/sec, corresponding to a lift coefficient of 1.15.

Hence it can be seen that the angle of attack corresponds to the minimum value of C_D/C_L and this value is equal to 0.0914. This angle of attack, however, is less than that corresponding to the minimum value of $C_D/C_L^{3/2}$. Since the aeroplane is equipped with a constant-speed propeller, the useful power, corresponding to a constant value of δ_m, is constant and independent of the velocity of the aircraft.

The useful power supplied by the engines during the approach is known.

Let G be the weight of the aeroplane. The slope of the approach path is 2.5° or 0.0436 radian. To maintain these conditions a thrust of (0.0914 - 0.0436) G = 0.0478 G is required. The useful power to be supplied is then:

$$0.0478\ G\ V_0 \text{ Kg m/sec.}$$

The aeroplane flies under constant power and at an angle of attack smaller than that corresponding to minimum necessary power; all decrease in speed results in an increase of available power.

The following property comes out of the equations: any decrease in speed produces an increase in the propelling force, whilst a corresponding increase in angle of attack does not change the ratio C_D/C_L ; this retains its minimum value because of the assumption of linearization.

The following numerical values have been used:

$$\mu = 97.5 \qquad C_L = 1.15 \qquad \alpha_0 = 7^o = 0.122 \text{ rad}$$

$$\frac{r_y}{c} = 1.135 \qquad V_{0,\tau} = 424 \qquad \tau = 7.04 \text{ sec}$$

$C_{x_u} = -0.091$	$C_{x_\alpha} = +1.34$	$C_{x_q} = 0$	$C_{x_{\delta_m}} = +0.0635$	$C_{x_{\delta_e}} = 0$
$C_{z_u} = -1.773$	$C_{z_\alpha} = -5.19$	$C_{z_q} = 0$	$C_{z_{\delta_m}} = -0.10$	$C_{z_{\delta_e}} = -0.403$
$C_{m_u} = +0.11$	$C_{m_\alpha} = -0.90$	$C_{m_q} = -8.750$	$C_{m_{\delta_m}} = +0.0202$	$C_{m_{\delta_e}} = -1.375$
		$C_{m_{\dot\alpha}} = -2.020$		

The factor $C_{x_{\hat u}}$ incorporates the effect of variations of speed on the propelling force of the propeller.

Lateral Motion

$$\mu' = 9.82 \qquad C_L = 1.15 \qquad (\alpha_0 + \xi) = 4^o = 0.07 \text{ rad}$$

$$\frac{2r_x^2}{b^2} = 0.0327 \qquad \frac{2r_y^2}{b^2} = 0.0585 \qquad V_{0,\tau} = -424$$

$C_{y_\beta} = -0.756$	$C_{y_p} = +0.174$	$C_{y_r} = +0.170$	$C_{y_{\delta_a}} = 0$	$C_{y_{\delta_r}} = +0.20$
$C_{l_\beta} = -0.0755$	$C_{l_p} = -0.550$	$C_{l_r} = +0.304$	$C_{l_{\delta_a}} = -0.1$	$C_{l_{\delta_r}} = +0.01$
$C_{n_\beta} = +0.03$	$C_{n_p} = -0.092$	$C_{n_r} = -0.118$	$C_{n_{\delta_a}} = 0$	$C_{n_{\delta_r}} = -0.10$

With these values, the coefficients in the equations to be solved are given in the following table:

Longitudinal motion

	a	b	c	d	h	k	$a-\alpha_0 b$
1	+0.091	-1.34	+11.9	+1.15	+0.0635	0	+0.2544
2	+1.773	+5.19	-97.5	+0.0908	-0.10	-0.403	+1.141
3	-0.085	+0.697	+8.45	0	+0.0156	-1.065	-0.170
4			-97.5				
5		-424		+424			
6	-424						

Lateral motion

	a	b	c	d	e	h	k
1	+0.756	-1.55	+19.47	-1.15	0	0	+0.20
2	+2.32	+16.9	- 9.45	0	0	-3.07	+0.307
3	-0.516	+1.58	+ 2.03	0	0	0	-1.725
4		-19.64			0		
5			-19.64		0		
6	-424				-424		

CHAPTER 16

AUTOMATIC GUIDANCE

16.1 THE CONTROL EQUATIONS

Any relationship for determining the magnitude of the movement of a control as a function of the deviation of one or more variables from those corresponding to the required trajectory, constitutes a control equation.

We will try to find the control equations consistent with the aeroplane flying along the line of intersection of the localizer and glide-path planes.

We will suppose that it is possible to have a servo-mechanism which will satisfy the relationships between the deviations and the control settings.

16.1.1 Longitudinal Motion

$$\left.\begin{aligned} +\delta_e = {} & A_1\theta + A_2\left(\alpha - \frac{w_a}{V_0} + \alpha_0\frac{u_a}{V_0}\right) + A_3\left(\hat{u} - \frac{u_a}{V_0}\right) + A_4 z + \\ & + A_5\dot{\theta} + A_6\left(\dot{\alpha} - \frac{\dot{w}_a}{V_0} + \alpha_0\frac{\dot{u}_a}{V_0}\right) + A_7\frac{\dot{u}}{V_0} + A_8\dot{z} + A_9\int z\,dt \end{aligned}\right\} \quad (16.1)$$

$$\left.\begin{aligned} -\delta_m = {} & B_1\theta + B_2\left(\alpha - \frac{w_a}{V_0} + \alpha_0\frac{u_a}{V_0}\right) + B_3\left(\hat{u} - \frac{u_a}{V_0}\right) + B_4 z + \\ & + B_5\dot{\theta} + B_6\left(\dot{\alpha} - \frac{\dot{w}_a}{V_0} + \alpha_0\frac{\dot{u}_a}{V_0}\right) + B_7\frac{\dot{u}}{V_0} + B_8\dot{z} + B_{10}\int\hat{u}\,dt \end{aligned}\right\} \quad (16.2)$$

It can be seen that the term in A_2 depends on the geometric or aerodynamic angle of attack; the term in A_6 depends on the derivative of the term in A_2 ; the term in A_3 depends on the relative velocity; the term in A_7 depends on the derivative of the absolute velocity.

16.1.2 Lateral Motion

$$\left.\begin{aligned} +\delta_a = {} & A_1\psi + A_2\left(\beta - \frac{v_a}{V_0}\right) + A_3\varphi + A_4 y + \\ & + A_5\dot{\psi} + A_6\left(\dot{\beta} - \frac{\dot{v}_a}{V_0}\right) + A_7\dot{\varphi} + A_8\dot{y} \end{aligned}\right\} \quad (16.3)$$

$$+\delta_r = B_1\psi + B_2\left(\beta - \frac{v_a}{V_0}\right) + B_3\varphi + B_4 y + \\ + B_5\dot{\psi} + B_6\left(\dot{\beta} - \frac{\dot{v}_a}{V_0}\right) + B_7\dot{\varphi} + B_8\dot{y} \qquad (16.4)$$

16.2 CRITICISM OF THESE EQUATIONS

The simplified forms of the control equations are subject to the following objections:

(1) The assumption of proportionality between control movements and deviations never corresponds to reality;

(2) The method of measuring the error in z or y provided by ILS equipment does not provide us with a quantity which is always proportional to the deviation of z or y.

We can deal with the first objection by supplying the computer with information about the real properties of the servo-mechanisms.

We can progressively approach the real properties of the system in the following way:

(a) As a first step we represent the operation of the servo-mechanism by an equation of first order, of the type

$$\delta_e = A_1\theta_r \qquad (16.5)$$

where

$$a\frac{d\theta_r}{dt} + \theta_r = \theta \qquad (16.6)$$

giving, for a step in θ,

$$\delta_e = A_1\theta(1 - e^{-t/a}) \qquad (16.7)$$

or, in a general way,

$$\delta_e(s) = A_1\frac{1}{1 + as}\theta(s) \qquad (16.8)$$

This introduces a time constant a in the control equation.

(b) As we saw earlier, we can also represent the operation of the servo-mechanism by an equation of second order. Nevertheless, we use only the first approach in a certain number of cases where we introduce the time constant a.

The second objection arises from the characteristics of the transmissions from the ILS units.

The ideal guidance system would provide planes of constant signal parallel to the localizer and glide-path planes.

In this case the receiver on board the aircraft would provide a signal of strength proportional to the distance y separating the aircraft from the plane of the localizer and another signal of strength proportional to the distance z separating the aircraft from the glide-path plane, whatever might be the distance $D - x$ from the aircraft to the touch-down point.

This ideal guidance cannot be realized in practice, the real case always being different. The ILS transmitter provides a system of planes of equal signal strength and the strength of the signal for each point is proportional to the dihedral angle χ between the plane of reference (glide-path or localizer) and the signal plane passing through the aircraft centre of gravity (Fig.205).

These equi-signal planes determine, by intersection with the glide-path and localizer planes, a system of equi-signal lines.

The intensity of the received signal is proportional to the angle χ, provided this angle is sufficiently small ($\chi < 2.50^{\circ}$ or $\chi < 0.0436$ rad).

The received signal amounts to a certain number n micro-amperes. We have, for example, $n = 150$ micro-amperes for $\chi = 0.0436$ rad:

$$\operatorname{tg}\chi = 0.0436\left(\frac{n}{150}\right) = kn \qquad (16.9)$$

The transmitter producing the glide-path signals is situated on the side of the landing field close to the touch-down point, at a distance D from the origin of coordinates.

The distance z is related to the received signal by the relationship

$$z = (D - x)\operatorname{tg}\chi = (D - x)kn \qquad (16.10)$$

The same angle χ, i.e. the same received signal, corresponds to the distance z becoming proportionately smaller and smaller as x increases, i.e. as the transmitter is approached.

If it is desired to evaluate the linear deviation z from the signal n, everything will occur as if the sensibility of the receiver is increased in the proportion

$$\frac{D}{D - x} \quad \text{or} \quad \frac{D}{D - Vt} \qquad (16.11)$$

as the aircraft approaches the transmitter.

The simulation of the flight along the glide path requires a mechanical device performing the operation

$$\left.\begin{aligned} A_4 &= A_{4,0}\left[\frac{D}{D - Vt}\right] \\ B_4 &= B_{4,0}\left[\frac{D}{D - Vt}\right] \end{aligned}\right\} \qquad (16.12)$$

$A_{4,0}$ and $B_{4,0}$ representing the coefficients at time $t = 0$ and distance D.

Differentiating the equality

$$n = \frac{1}{k(D - Vt)} z$$

we have

$$\frac{dn}{dt} = \frac{1}{k(D - Vt)} \frac{dz}{dt} + \frac{z}{k(D - Vt)^2} V \qquad (16.13)$$

The derivative of z is only proportional to the derivative of the signal n when the aircraft is on the correct flight axis. This point is important if we wish to achieve automatic control using the terms $A_8\dot{z}$ or $B_8\dot{z}$.

The localizer signal obeys analogue laws. The deviation y is related to the received signal n by the relationship

$$y = (L - x)\mathrm{tg}\chi = (L - x)kn$$

but the distance L is always greater than D. The transmitter situated at the vertex of the angle χ is placed at the end of the landing strip furthest from the approaching aircraft, whilst the transmitter for the glide path is situated at the end nearest the aircraft.

There is, as before, an apparent increase in the sensitivity of the receiver in the ratio

$$\frac{L}{L - Vt}$$

16.3 IRREGULARITIES IN THE SIGNALS

Irregularities can exist in the lines of equal signal strength, causing these to become deformed from their ideal straight form (Fig.206).

In such a case it may happen that the guidance system gives an error signal when the aircraft actually lies exactly on the correct flight path.

Unless a second landing system is installed, such as the GCA or the AGCA, the pilot, whether human or automatic, cannot differentiate between an error signal n_A corresponding to a deviation of the aeroplane with respect to the required path and a signal n_B corresponding to an error of the signal-zero line (Fig.207).

It is not possible to prevent false orders from being given by signals such as n_B. The only thing that can be hoped for is that the aircraft will not respond fully to these signals if they are of sufficiently short duration.

If the duration of these false signals becomes appreciable, it must be accepted that the aeroplane will try to follow the signal $n = 0$ and describe an inexact trajectory, but means must be used to prevent the aeroplane from amplifying the distortion of the equi-signal line $n = 0$.

16.4 GENERAL REMARKS ON THE MOTION

The question as to what values to give to the coefficients $A_1 \ldots\ldots\ldots B_8$ is helped if we know:

(a) The behaviour of the aeroplane flying with controls fixed;

(b) The characteristics of artificial stability corresponding to the principal modes of elementary control, i.e. the effect of the coefficients $A_1 \ldots\ldots\ldots B_8$ taken singly.

(a) *Behaviour of the aeroplane in flight with controls fixed*

The controls-fixed flight corresponds to zero values of all the coefficients $A_1 \ldots B_8$. In still air (i.e. $du_a/dt = dv_a/dt = dw_a/dt = 0$), the characteristics of flight for fixed controls are completely defined by the matrix of coefficients of the first members of the equations:

$$\begin{vmatrix} a_1 & b_1 & c_1 & d_1 \\ a_2 & b_2 & c_2 & d_2 \\ a_3 & b_3 & c_3 & d_3 \\ a_4 & b_4 & c_4 & d_4 \end{vmatrix}$$

Much work has been done to determine these characteristics, knowing the matrix or the characteristic equation of the corresponding differential system. We can, in particular, calculate by analytical methods the response to a step unit affecting each of the inputs.

(b) *Elementary artificial stability*

The theory of servo-mechanisms gives methods of analysis which are useful in the study of elementary artificial stability.

The Nyquist criterion connects the artificial stability to the frequency response of the aircraft produced by the harmonic displacement of a control.

Before studying the application of this relationship, we should notice that the positive control settings δ_e , δ_a , δ_r produce negative displacements θ , φ , ψ . To retain the relationship in its usual form we can state that the control settings $-\delta_e$, $-\delta_a$, $-\delta_r$ produce positive angular displacements.

As an example, we will consider the effect of the rudder movement, $-\delta_r$, on the heading ψ .

Let ψ be the course, or heading, of the aeroplane

ψ_i be the required course.

The difference, $\epsilon = \psi_i - \psi$, is the error, furnished by a signal from an appropriate instrument.

The servo-control and the aeroplane form a loop system (Fig.208). The aeroplane constitutes system No.2 and the servo-control system No.1.

The input into the aeroplane is the control setting $-\delta_r$; the output is the course angle ψ .

The behaviour of the aeroplane can be defined by the frequency response of the output ψ to a sinusoidal input signal $-\delta_r$.

Let $R(\omega)$ be the frequency response. Any value of $R(\omega)$ corresponding to a particular value of ω has a modulus $|R(\omega)|$ and an out-of-phase angle ϕ .

The response $R(\omega)$ is given in cartesian coordinates in Figure 221. It can also be represented in polar coordinates and then provides a plot called admittance polar locus.

The servo-mechanism transforms an input signal, which is the error ϵ , into an output signal, viz., the displacement $-\delta_r$ of the control.

The frequency response of a servo-mechanism reduces to a simple numerical coefficient $B_1 = -\delta_r/\epsilon$ when the mechanism produces, without phase-shift, a control displacement which is proportional to the error signal.

Isolating the part of the system between A and B we have a system formed of two parts, 1 and 2, placed in an open loop.

The frequency response of the open loop system is the product of the frequency response of each of the two systems. The response of the open loop is then $B_1R(\omega)$.

Nyquist's theorem relates the stability of the closed loop system to the frequency response of the open loop system.

Whether the closed loop system is stable or not depends on the position of the point $x = -1$, $y = 0$ with respect to the admittance polar diagram.

Each time the polar locus of $B_1R(\omega)$ is made to pass through the point -1 due to variation of the characteristics of the system, the closed loop system passes from a condition of instability to stability or vice versa.

If there is a particular value of the frequency ω_n for which the function $R(\omega)$ has a phase shift ϕ of 180°, the point $B_1R(\omega)$ of the polar curve corresponding to this frequency ω_n will pass through the point -1, 0 when $B_1 = 1/|R(\omega_n)|$. Hence this value of B_1 will be critical.

The complete statement of Nyquist's theorem allows us to determine on which side of the locus the point -1 should come for the system to be stable. It is sufficient here to show that from the frequency response diagrams we can predetermine the existence of critical values in the coefficients of the control equations and calculate their values.

During calculations on basic artificial stability modes using an analogue computer, we have on several occasions passed from stable to unstable conditions by the variation of a control coefficient A or B . In each case, we ascertained that the critical value of this coefficient was the inverse of the frequency response modulus, for the frequency at which the out-of-phase angle was $\pm 180^o$.

(c) *Generalized artificial stability*

The root locus method can help us to predict the behaviour of artificially stabilized aeroplanes. Nevertheless, servo-mechanism theory does not give us a simple method of studying aircraft motions when the control equations are more complicated, particularly when the control settings depend on the errors of several variables.

The analogue computer cannot give us a general theory of aircraft artificial stability, but it provides the solution of stability problems in any particular case and allows us to solve these problems in a more or less experimental way.

Note

The angular frequency ω used later on expresses the frequency response in radians per unit of aerodynamic time τ .

CHAPTER 17

LATERAL BEHAVIOUR OF THE AEROPLANE

17.1 STABILITY WITH CONTROLS FIXED

The characteristic equation of the system is:

$$\begin{vmatrix} a_1 + \lambda & b_1 & c_1 & d_1 & 0 \\ a_2 & b_2 + \lambda & c_2 & 0 & 0 \\ a_3 & b_3 & c_3 + \lambda & 0 & 0 \\ 0 & b_4 & 0 & \lambda & 0 \\ 0 & 0 & c_5 & 0 & \lambda \end{vmatrix} = 0 \qquad (17.1a)$$

and can be written:

$$\lambda(\lambda^4 + K_3\lambda^3 + K_2\lambda^2 + K_1\lambda + K_0) = 0 \qquad (17.1b)$$

By inspection, one of the roots λ is zero. This comes from the fact that no exterior action on the aeroplane depends on ψ. The motion of the aeroplane is independent of its course or heading.

Neglecting the solution $\lambda = 0$, we see that the characteristic equation becomes an equation of fourth degree.

Substituting numerical values we see that the condition for spiral stability, viz.

$$K_0 = b_4 d_1 (a_2 c_3 - a_3 c_2) > 0 \qquad (17.2)$$

is not satisfied, since we have:

$$(a_2 c_3 - a_3 c_2) = 0.0088 - 0.0091 = -0.0003$$

and

$$b_4 d_1 > 0$$

The roots of the equation are:

$$\lambda = -16.2$$

$$\lambda = +1.75 \pm 4.16i$$

$$\lambda = +0.0139$$

The first real root defines an aperiodic motion in roll, strongly damped. The pair of complex roots defines the oscillatory motion, called the 'Dutch roll'. The

second real root defines the spiral motion, which is slightly unstable in this case. All deviations double at the end of:

$$\frac{ln\ 2}{0.0139} = \frac{0.692}{0.0139} \quad \text{units of time}$$

17.2 RESPONSE TO A STEP FUNCTION

The motion of the aeroplane following a control setting δ_a or δ_r depends on the flight characteristics with controls fixed.

We have determined the response to a step function for $-\delta_a = 0.002$ and $-\delta_r = 0.02$ radian by the Heaviside method of numerical calculation and by analogue calculation. The results show good agreement and are given in Figures 209 and 210.

The step response to a sudden excitation of $v_a = 0.1\ V_0$ (sharp lateral gust) has also been calculated by the Heaviside method and is given in Figure 258.

17.3 FREQUENCY RESPONSE

We have calculated the frequency response of 6 variables: β, $\hat{p}$, $\hat{r}$, φ, ψ, y, for sinusoidal excitations $-\delta_a$ and $-\delta_r$. These responses are shown in Figures 211 to 222. These diagrams show the actions caused by control movements $-\delta_a$ and $-\delta_r$.

At first sight, the comparison of each of the responses produced by the two excitations $-\delta_a$ and $-\delta_r$ does not give any indication of essential differences in the moduli, the differences being greater in the phases.

This seems to suggest that the two control movements are, to a slight extent, interchangeable, if we are satisfied with approximate control. However, we shall see that a choice has to be made between them if accurate control following a predetermined programme is required.

17.4 DIFFERENT DEGREES OF STABILITY

We will investigate the following control problems:

(1) The stabilization of a motion dependent on a 4th degree characteristic regardless of the aeroplane's course;

(2) The stabilization of the course direction as determined by the 5th order differential system;

(3) The control of the aircraft along a path fixed in position and direction, using a 6th order differential system.

For the first case, the stability obtained will return the aircraft, which is displaced from a steady flight path, to a new steady flight path, the course of which will be different from the former.

The stability for the second case ensures maintenance of the course direction, but the new trajectory will differ in position from the former.

The stability for the 3rd case brings the aircraft back to its initial trajectory in direction and position.

Whilst natural stability with an indeterminate final course can often be obtained by a convenient choice of the aerodynamic coefficients, stability in Cases (2) and (3) is only obtainable with a piloted aeroplane, i.e. an aeroplane in which the controls are moved in accordance with the errors of some generalized coordinates.

17.5 FIRST DEGREE STABILITY

First degree stability can be obtained by giving the aircraft appropriate aerodynamic characteristics. For our example it is sufficient to multiply a_2 or c_3 by 1.034 or to divide a_3 or c_2 by 1.034.

First degree artificial stability can also be obtained by automatic control. A control equation $+\delta_r = B_5\dot{\psi}$ with the condition $B_5 > 0$ is realized by using a yaw damper, which, in fact, increases the coefficient c_3 .

Control characterized by the factors A_2 and B_2 is possible and can lead to stability when $A_2 > 0$ or $B_2 > 0$. It does nothing but change the terms a_2 or a_3 of the determinant (17.1) and presents the same possibilities as the modification of the aerodynamic characteristics of the aeroplane by configuration changes.

Control based on the angle of side-slip should only be used in exceptional circumstances since the detection of side-slip angle is difficult.

Control according to the relationship: $\delta_a = A_3\varphi$, with $A_3 > 0$, has the same effect as the action of a human pilot who displaces the ailerons to correct a banking error he perceives by visual aids.

Figures 223a and 223c show the motion of the aircraft when, at time $t = 0$, the automatic pilot is suddenly put into service for an initial condition $\varphi_0 = -0.06$. The values of A_3 are respectively 0.5 and 2.

The initial displacement φ_0 becomes zero, but the aeroplane does not return to its original course and the deviation y from the trajectory at time $t = 0$ increases continually.

The control for $B_3 > 0$ is characterized by the pilot turning the rudder proportionally to the bank angle. Figures 223c and 223d represent the motion of the aircraft under control conditions defined by:

$$B_3 = 0.5$$

$$B_3 = 1$$

It can be seen that for $B_3 = 0.5$ the aircraft can return to linear flight without bank, while for $B_3 = 1$ the aircraft is unstable.

This result is in agreement with the indications given by the frequency response φ of the aircraft, produced by an excitation δ_r. In effect, at the frequency $\omega = 5.2$, the modulus $\varphi/(-\delta_r)$ is 1.4 and the out-of-phase angle is $\pm 180^{\circ}$. The critical value of the coefficient B_3 is then

$$B_3 = \frac{1}{1.4} = 0.715$$

which is compatible with the results obtained on the computer.

Note

Control for A_3 or B_3 is obtained by putting terms d_2 and d_3 in place of the zeros in the determinant (17.1).

17.6 SECOND DEGREE STABILITY

Directional stability can only be introduced by adding terms e_2 and e_3 in the determinant. These terms will be obtained by pilot action producing:

$$+\delta_a = A_1\psi$$

$$+\delta_r = B_1\psi$$

This control equation leads to a characteristic equation of the 5th degree.

The introduction of a term $A_1 > 0$ makes the system completely unstable in our particular case.

The control characterized by $B_1 > 0$, on the contrary, leads to stability as soon as B_1 has a sufficiently large value. The resulting stability includes directional stability.

The characteristic equation of the 5th degree has been solved and has two pairs of complex roots and one real root. The numerical values are as follows:

B_1	*Real root* (λ)	*Short oscillation or Dutch roll* (λ)	*Spiral motion or long oscillation* (λ)
0	-16.2	-1.75 ± 4.16i	+0.0139 and 9
0.2	-16.207	-1.71 ± 4.82i	-0.026 ± 0.9i
0.5	-16.246	-1.62 ± 5.78i	-0.103 ± 1.19i
1	-16.304	-1.53 ± 7.1i	-0.1735 ± 1.54i
2	-16.399	-1.42 ± 9.2i	-0.2425 ± 1.54i

The roots correspond to oscillations for which the damping time to half amplitude $T_{½}$, and the period T , expressed in units of aerodynamic time, are:

B_1	*Short oscillation*		*Long oscillation*	
	$T_{½}$	T	$T_{½}$	T
0.2	0.403	1.31	26.8	7.00
0.5	0.426	1.085	6.9	5.28
1	0.45	0.885	4	4.55
2	0.485	0.684	2.85	4.13

Using the analogue computer we find for the differential system the curves $\psi(\hat{t})$ given in Figure 224 for an initial deviation $\psi_0 = 0.008$. These diagrams also show the two oscillations corresponding to two pairs of complex roots.

For small values of the gain B_1 , the long-period oscillation, which is only slightly damped, predominates.

When the gain B_1 increases, a short-period oscillation develops progressively and is much more quickly damped. For $B_1 = 5$ the long-period oscillation has nearly disappeared.

There is agreement between the characteristics of the oscillations given by the diagrams and the results of calculation.

The plot of the admittance locus agrees with the results given by the analogue computer. The polar diagrams of the admittance locus for ψ produced by $-\delta_a$ and $-\delta_r$ are given in Figure 225.

At the frequency $\omega = 0.65$, the response to the excitation $-\delta_r$ has a modulus of 8 and an out-of-phase angle of 180°.

The intersection will be brought back to the point -1 by a control factor $B_1 = 1 \div 8 = 0.125$. At this point the stability of the aeroplane will be neutral.

This conclusion agrees with results given by the analogue computer, which shows that there is instability for $B_1 = 0$ and stability for $B_1 = 0.20$.

On the other hand, the impedance locus of ψ produced by $-\delta_a$ will remain on the same side of -1 , whatever may be the positive value of A_1 by which the modulus is multiplied.

Since there is instability for $A_1 = 0$, there will also be instability for all positive values of A_1 .

17.7 COMBINATION OF TWO ERROR SIGNALS

We will examine here the basic control conditions for the second stability case. The results are presented graphically in Figure 226.

(a) *The combination* $A_1 + B_1$

The stability caused by the control B_1 can counterbalance the instability caused by A_1, if A_1 is sufficiently small.

The combination $A_1 = 1$ and $B_1 = 1$ is stable;

The combination $A_1 = 2$ and $B_1 = 1$ is unstable. The curves a and c show the changes in ψ for this case.

For control conditions $A_1 = -2$ and $B_1 = 1$, with the aileron control crossed, the simulator shows that there is stability (curve b), but the aeroplane is less stable than if it were piloted by B_1 alone.

(b) *The combination* $A_3 + B_1$

For A_3 the aeroplane is strongly stabilized for the first control case.

If a control B_1 is added for directional stability, a very stable motion is obtained. Curve d shows the effect of a deviation $\psi = 0.08$ on an aircraft controlled by $A_3 = 1$ and $B_1 = 1$.

(c) *The combination* $A_3 + A_1$

The stabilizing effect of A_3 is such that it permits the utilization of ailerons to correct a heading error, without having to use the rudder control.

However, the motion becomes very oscillatory and even unstable if A_1 is too large. Curves e, f, g show the motion following a deviation ψ_0 for the three combinations:

$A_3 = 4$ $\quad$ $A_1 = 2$

$A_3 = 4$ $\quad$ $A_1 = 3$

$A_3 = 4$ $\quad$ $A_1 = 4$

17.8 THIRD DEGREE STABILITY

Position stabilization necessitates the detection of the displacement y and its introduction into the control conditions by the terms in A_4 or B_4.

However, these terms when used alone always lead to instability; hence we must investigate their effect in combination with a stabilizing term. For this purpose we have chosen the term B_1.

The trajectories $y = f(\hat{t})$ following an initial displacement $y_0 = 50$ m, $\psi_0 = 0$, are given in Figure 227 for the following combinations:

	$B_1 = 4$	$B_1 = 2$
$A_4 = 0.44 \times 10^{-3}$ $A_4 = 0.88 \times 10^{-3}$ $A_4 = 1.75 \times 10^{-3}$	Group a	Group b
$B_4 = 0.44 \times 10^{-3}$ $B_4 = 0.88 \times 10^{-3}$ $B_4 = 1.75 \times 10^{-3}$	Group c	Group d

The components A_4 and B_4 tend to produce an oscillatory motion. The component B_1 damps this oscillation to some extent.

The aeroplane is more rapidly brought back to its correct approach path ($y = 0$) when the displacement y is used to control the ailerons (i.e. control conditions for A_4), than when it is used to control the rudder (i.e. control condition B_4), but the trajectories are more difficult to stabilize in the first case.

For $B_4 = 1.75 \times 10^{-3}$ and $B_1 = 2$, the motion was so unstable as to be impossible to record.

17.9 MORE COMPLEX CONDITIONS FOR OBTAINING THIRD DEGREE STABILITY

As the control factor A_3 has a strong stabilizing effect, we will introduce it in any control equation intended to perform 3rd degree stabilization.

A component $A_3 = 1$ can modify things in such a way that it is possible to have much larger values of A_4 without leading to instability.

The curves shown in Figure 228(a) give the trajectories $y = f(\tau)$ for the combinations:

$$B_1 = 2$$

$$A_3 = 1$$

$$A_4 = \begin{cases} 0.88 \times 10^{-3} \\ 1.75 \times 10^{-3} \\ 2.64 \times 10^{-3} \end{cases}$$

Tests have shown that numerous combinations of the variables $B_1\psi$, $A_3\varphi$, $A_4 y$ are possible and permit an aeroplane displaced by y_0 from the correct approach path to return to this path.

A second group of possible combinations occurs. This is a group where the second case of stabilization is obtained by the action of $A_1\psi + A_3\varphi$ and the position maintained by $A_4 y$.

Because of the destabilizing action of $A_1\psi$, the component $A_3\varphi$ must be larger than in the previous case and A_3 was found to be equal to 3 or 4.

On the other hand, the gain of the loop for A_4 must be higher in order to bring the aeroplane back on to the correct approach path.

It is possible to obtain trajectories which are close to those defined in the previous case. The combinations:

$$A_1 = 3$$

$$A_3 = 4$$

$$A_4 = \begin{cases} 2.62 \times 10^{-3} \\ 5.25 \times 10^{-3} \\ 7.87 \times 10^{-3} \end{cases}$$

give the trajectories presented in Figure 228(b), where A_4 is the variable element. In the combination $A_1\psi$, $A_3\varphi$, $A_4 y$, the increase in the term A_4 produces a long-period oscillation. Further increase in A_4 would lead to instability.

However, the term A_1 can act as a stabilizing element against A_4 when A_3 is sufficiently great to eliminate the instability of the oscillation of smaller period that would be caused by A_1 in the absence of A_3 .

The trajectories of Figure 228(c), where A_1 is the variable element, establish this fact.

17.10 CONTINUOUS VARIATION OF A_4

We will now consider how the convergence of the equi-signal lines to the transmitter modifies the trajectories.

Consider the aeroplane at time $\hat{t} = 0$, in position A (see Fig. 229), at a distance of 6.345 m from the transmitter, and let it be at position B , distance 2.125 m from the transmitter, at time $\hat{t} = 10$.

During the flight from A to B , the convergence of the equi-signal increases the gain, A_4 , of the automatic pilot.

The initial value of the gain is multiplied by an increasing factor, the final value of which, at B , is 3.

Tests have been made to study this variable gain by using a potentiometer which introduced a continuously variable A_4 into the circuit.

Trajectories for constant gain are given in Figures 228(a) and (b); they correspond to values of A_4 in the ratios 1:2:3.

On each of these diagrams the records obtained for variable gain A_4 have been plotted (dashed line). This value of gain has its smallest value at time $\hat{t} = 0$ and a value of three times this at time $\hat{t} = 10$.

The trajectory for variable gain separates progressively from the trajectory for the minimum constant gain and converges to the axis without crossing it, as is the case for maximum constant gain (Fig.229).

These tests indicate that it is possible to use an increased gain at the end of the approach path, but we have to satisfy the important condition that the increase of gain, due to the convergence, cannot lead, at the period just before touch-down, to instability. However, progressive variation of the gain allows us to approach this limit more closely than if the increased gain existed from the start of the approach.

This fact reduces the problems imposed by the convergence of the equi-signal lines.

It has only been possible to study all the variables of trajectories with variable gain in a few cases; these will be discussed in Section 19.2.

Nevertheless, a detailed study of many different trajectories for constant gain gives indications which permit us to make a judicious choice between the different possible combinations of available error signals.

CHAPTER 18

GUIDANCE IN THE LOCALIZER PLANE

18.1 CONTENTS OF THIS CHAPTER

The present chapter is devoted to the study of the combinations A_1 ..... B_n , to provide convenient localizer characteristics.

In the whole of the discussion, the factors A_4 , B_4 , A_8 and B_8 are assumed constant, which means that the sensitivity of the displacement detector is independent of distance.

We will compare the combinations for three types of different initial conditions, acting independently:

$$y_0 = - 50 \text{ m}$$

$$\psi_0 = 0.08 \text{ rad}$$

$$v_a = 0.1 \, V_0$$

The initial condition $y_0 \neq 0$, all other variables being zero, corresponds to the following practical case: The aeroplane is flying normally ($\beta = \varphi = p = r = 0$) on a course parallel to the runway direction but at a distance $y_0 \neq 0$ from the axis of the correct approach path. At the time $\hat{t} = 0$, the servo-mechanism is put into service.

The initial condition $\psi_0 \neq 0$, all other variables being zero, corresponds to the automatic pilot being put into service at a moment when the aeroplane is on the axis of the correct approach path ($y_0 = 0$) , but where its trajectory cuts this axis at an angle ψ_0 .

The initial condition $v_a = 0$, all other variables being zero, corresponds to a cross-wind developing when the aeroplane is following the correct approach path under the control of the automatic pilot.

For each case the motion is described by the 6 variables y , β , φ , ψ , δ_a , δ_r .

18.2 CONTROL SUBJECT TO THREE ERROR SIGNALS

We will limit ourselves in this chapter to combinations where the y displacement error signal acts only on the ailerons. In all cases we have:

$$A_4 \neq 0$$

$$B_4 = 0$$

except in the case of the coupling of the two controls.

In Chapter 17 we saw that two types of 3-error combinations are of interest. These are:

$$B_1 \quad A_3 \quad A_4$$

$$A_1 \quad A_3 \quad A_4$$

We will group together, as systematically as possible, the results of the tests calculated on the computer.

The initial condition $y_0 = -50$ m was used to make a first selection of the combinations tried; the action of satisfactory combinations was then examined for conditions $\psi_0 = 0.08$ and $v_a = 0.1\ V_0$.

A first group of combinations corresponds to the following control conditions:

Case	A_1	A_3	$A_4 \times 10^3$	B_1	Figure No.
a	0	1.5	3.50	2	230
b	0	1	1.75	2	231
c	3	4	5.25	0	232
d	3	3	3.50	0	239

Examination of these results shows that Cases a and b (using B_1) and Cases c and d (using A_1) lead to very different characteristics, although the projections of the trajectories on the ground are similar.

In the first two cases the rudder displacement ($\delta_r = +B_1\psi$) counteracts important variations in the course or heading, but does not prevent a strong side-slip to the right. In fact, in the equation

$$y = \int V_0(\psi + \beta)\ dt \qquad (18.1)$$

the effect of β is preponderant.

The aeroplane is displaced laterally in side-slipping to the right. The control displacements δ_a and δ_r are in the opposite sense; they correspond to what a pilot would do if he wanted to move the aeroplane laterally by side-slipping.

In the last two cases, the correction determined from the directional deviation is applied to the ailerons; the aeroplane does not hold to its original course so closely and is allowed to turn in order to realize the desired transverse displacement.

However, this turn, following a bank, must be obtained without recourse to the rudder, and hence will always be accompanied by side-slip. Records show that this side-slip is oscillatory.

The part produced by the term in ψ is predominant in the formation of y. The effect of β is practically zero, because of the oscillatory nature of the side-slip.

The occurrence of inverse yaw at the beginning of the motion should be noted: this delays the decrease of the initial error.

Manoeuvres of types a and b are completely different from those of types c and d.

It is inadvisable to side-slip an aeroplane in conditions of no visibility. This again restricts the field of study and forces us to limit the investigation to conditions which are derived from types c and d.

18.3 DETAILED DISCUSSION OF CERTAIN COMBINATIONS

We will modify the conditions for combinations c and d. The following table gives the control coefficients used and refers to the Figures describing the motion.

Control Conditions Derived from Case c

Case	*Fig.No.*	A_1	A_3	$A_4 \times 10^3$	$A_8 \times 10^3$	B_5	B_1	B_2	B_3	$B_4 \times 10^3$
c	232	3	4	5.25						
e	234	-	4	5.25	7.08					
f	235	3	4	5.25				-2		
g	236	3	4	5.25			0.798		1.064	1.40
h	233	3	4	5.25		0.051				

Case e is a variant of case c, where the component A_1 is replaced by the component A_8.

Now

$$\dot{y} = V_0(\psi + \beta)$$

$$A_8\dot{y} = A_8V_0\psi + A_8V_0\beta$$

and the control term A_8y is equivalent to the superposition of conditions

$$A_8V\psi = A_1\psi$$

$$A_8V\beta = A_2\beta$$

Case e corresponds to $A_8 = 7.08 \times 10^{-3}$, which leads to: $A_1 = A_2 = 7.08 \times 10^{-3} \times 424 = 3$.

The replacement of A_1 by A_8 adds, in fact, an effect $A_2 > 0$, which is analogous to an increase in dihedral; it slightly modifies the trajectory.

The use of A_1 or A_8 corresponds to two very different physical conditions.

In the first case, we must know the direction of the landing strip and measure the angular deviation between the landing strip and the aeroplane. This is done by using a directional gyro, an instrument which is accurate, but whose use will lead to complications if there is a cross-wind, and this necessitates a correction due to drift.

In the second case, the derivative of the distance y must be computed. Differential analysers are not very precise and they amplify all the irregularities of the quantity to be derived, notably the noise, which is a serious inconvenience, but the reference y can be used without correction in the case of a cross-wind.

The complete elimination of side-slip would be an improvement. One may try to attain this result by proper use of the rudder. This leads to other changes in the control equation. Two methods of aileron control may be envisaged:

Case f. Adding rudder movement as a function of side-slip.

$\delta_r = B_2\beta$ with $B_2 < 0$, corresponding to an increase of weathercock stability.

Case g. Linking the rudder to the ailerons in order to obtain a rudder deflection which should be a definite fraction of the aileron deflection.

Tests have shown that Case f results in the formation of strong oscillations of short period and is inadvisable. The conditions of Case g have been tested for different proportionality coefficients, one of which, viz. $\delta_r = 0.266\ \delta_a$, will be considered here. This corresponds to values of B_1, B_3 and B_4 of $0.266\ A_1$, $0.266\ A_3$, and $0.266\ A_4$, respectively.

These control conditions are very good; the side-slip is reduced and the opposing yaw is suppressed.

For Case h, a light damping of the yaw is set up by moving the rudder control in proportion to the angular velocity of the yaw.

This action does not in any way decrease the initial side-slip or the inverse yaw, but clearly reduces the oscillations.

The trajectories are less irregular than for the fundamental Case c. A greater effect would probably be obtained by using larger values of A_6. Further modifications of Case c (see Figs. 237 and 238) will be discussed in Section 19.4.

A second group of modifications to be considered here consists of variants of Case d. These are given in the following table:

Case	*Fig.No.*	A_1	A_3	$A_4 \times 10^3$	$A_8 \times 10^3$	B_1	B_3	$B_4 \times 10^5$	$B_8 \times 10^{-5}$
d	239	3	3	3.5	-	-	-	-	-
i	240	-	3	3.5	7.08	-	-	-	-
j	241	3	3	3.5	-	0.804	0.804	0.93	-
k	242	-	3	3.5	7.08	-	0.804	0.93	1.88

Because we use a factor A_4 which is smaller than in the preceding cases the time necessary to reach the axis $y = 0$ is always greater.

Case i differs from Case d by the substitution of A_8 for A_1 ; Case j differs from Case d by the introduction of a rudder movement, which is given by

$$\delta_r = 0.266\delta_a$$

Finally, Case k allows both the two preceding modifications to be made: substitution of A_5 for A_1 and linkage between rudder and aileron controls.

Figure 242 shows that such conditions nearly eliminate the side-slip.

18.4 INITIAL DISPLACEMENT OF ψ

In order to facilitate reference to the Figures, the numbers of the Figures giving t behaviour of the system for three different initial conditions appear in the table below:

Case	*Perturbation*		
	y_0	ψ_0	v_a
Controls fixed	-	-	258
a	230	246	-
b	231	247	-
c	232	248	259
h	233	249	260
e	234	250	261
f	235	251	262
g	236	252	263
d	239	253	264
i	240	254	265
j	241	255	266
k	242	256	267

The initial displacement $\psi_0 \neq 0$, all other variables being zero, corresponds to the case where the automatic pilot is put into service at the moment when the aeroplane, flying on a straight course, cuts the required course direction at an angle ψ_0 .

We have investigated the effect of a displacement $\psi_0 = 0.08$ in a certain number of the preceding cases. The aeroplane makes a small angle with the localizer axis and to the right of it, and finally is made to fly along the axis following the course $\psi = 0$.

In all cases, the aeroplane starts to move away from the axis (y increases to the right), but is brought back as a consequence of the effect of the displacement y on the controls.

The Figures are self-explanatory.

18.5 EFFECT OF A SIDE GUST

Let us suppose that the aeroplane suddenly meets a transverse gust of intensity $v_a = 0.1V_0$, directed towards the right, and that it remains in this condition.

The case has been considered for an aeroplane with controls fixed and for a certain number of control conditions.

The diagrams of β give the true or aerodynamic side-slip $(\beta - v_a/V_0)$ if the O-axis is taken as reference. If an axis passing through 0.10 is taken as reference then the curves give the apparent side-slip.

For controls fixed, the gust v_a produces, at time $\hat{t} = 0$, a side-slip towards the left of $\beta = -0.10$, which has three effects:

(a) The aeroplane tends to face the relative wind by a rotation in yaw. This means $d\psi/dt < 0$;

(b) The aeroplane tends to roll to the right: $d\varphi/dt < 0$;

(c) The aeroplane tends to be carried by the cross-wind towards the right, thus reducing the aerodynamic side-slip.

These initial motions, together with the resultant motion, are represented in Figure 254. The results have been calculated by Heaviside's method.

The purpose of the control is to bring the aeroplane on to the axis OX after a given time. The ideal final conditions are:

$$\psi = -0.10 \qquad \text{and} \qquad \beta = +0.10$$

all other variables being zero and the controls being in a neutral position.

This means that the aeroplane would fly 'crabwise' with respect to the ground, but without side-slip relative to the air and without bank.

It is clear that any control equation where ψ appears leads to a residual error in y. Calculations using the analogue computer confirm this. The residual error y can be easily calculated as a function of the speed v_a, using simple algebraic equations.

Where y and ψ act on the same control, we obtain finally:

$$+\delta_a = A_1\psi + A_4 y = 0$$

The action of the directional error tending to lift the right wing is counterbalanced by the distance error, which tends to lift the left wing.

In its final state the aeroplane has neither side-slip nor bank and is displaced parallel to the correct approach path by a distance $y = -(A_1/A_4)\,\psi$.

When y and ψ are not applied to the same control, the final path is also a straight line but there can be side-slip β, bank φ and permanent settings of the controls. These conditions were considered undesirable and hence the case was not investigated further.

We can avoid the appearance of the residual error y by replacing the detection of the heading error ψ by that of the derivative $\dot{y}$.

For these conditions no signal is produced as soon as a trajectory parallel to the correct approach path is obtained, whatever may be the course of the aeroplane and its distance from the axis.

The control dependent on y can then act without opposition until the aeroplane is flying on the required axis.

All calculations on the computer confirm this. When $A_1\psi$ is replaced by $A_8\dot{y}$, the aeroplane is brought back quickly to the axis.

18.6 COMPARISON WITH AMERICAN RESEARCH

We had reached the present stage in our investigations when American work on this subject came to our notice (see Section 14.4).

We have stated that their optimum control conditions were appreciably more complicated than ours, the last of ours being considered the most satisfactory.

Although the work of Carroll and Tyler was for the control of aeroplanes of a different type from that considered by us, we have studied the conditions recommended by these authors. The basic data are given below:

Ailerons	*Rudder*
$A_3 = 2$	$B_2 = -2$
$A_4 \times 10^3 = 7.18$	$B_6 = 0.28$
$A_8 \times 10^3 = 7.08$	$\delta_r = 0.50\ \delta_a$
$A_7 \times 10^3 = 3.57$	(i.e. values of B_3, B_4, B_8 and B_7 are half of the corresponding A values)

These conditions constitute Case 1.

The response to the perturbation y_0 , ψ_0 , v_a is shown in Figures 243, 257, 268 respectively.

The responses to displacement y_0 and ψ_0 are a little more rapid than those for our case (case k), but the response to the gust v_a is the same.

We tried to find the reason for the existence of the additional factors contained in the control conditions.

To do this we started with the American values of A_3 , A_4 and A_5 and added the other components one by one (Case l_1 in the following table).

Case	A_3	$A_4 \times 10^3$	$A_8 \times 10^3$	$A_7 \times 10^3$	*Rudder aileron coupling*	B_2	B_6	*Figure No. for*		
								y_0	ψ_0	v_a
1	2	7.18	7.08	3.57	0.50	-2	-0.28	243	257	268
l_1	2	7.18	7.08	-	0	-	-	244		269
l_2	2	7.18	7.08	3.57	0	-	-	245		270
l_3	2	7.18	7.08	3.57	0.50	-	-			271
l_3	2	7.18	7.08	3.57	0.50	-2	-			272
l_4	2	7.18	7.08	3.57	0.50	-	-0.28			273

The starting condition, case l_1, gives a rapid response to an error in y_0 , but large oscillations because of the high value of A_4 .

The addition of a term in A_7 corresponds to an increase of damping in roll and changes practically nothing: this fact is not surprising since the damping term $\partial C_L/\partial p$ is generally sufficient when the stalling conditions are not reached.

The effect of the coupling $\delta_r = 0.50\delta_a$ is favourable and will not be discussed further.

The introduction of the term in B_2 causes a rapid oscillation (see Fig.267), which is undesirable and confirms the result obtained previously.

The factor $B_6\dot{\beta}$ strongly damps the motion, as is seen in Figure 273. It is clear that $B_6\dot{\beta}$, in the conditions proposed by the American investigators, cancels the disturbing effect of $B_2\beta$ and makes the use of this signal acceptable. (Curves 272 behave as curves 268 for the particular conditions recommended).

Reference to the work of Carroll and Tayler has been made to show the great variety of possible control conditions.

Only with an analogue computer can the study of these problems be made.

Note

Case 1 necessitates the detection of six variables, whilst Case k requires only three. The response to the initial condition v_a is exactly the same in both cases; the response to the two other initial conditions is a little better in Case 1 than in Case k.

We do not intend to discuss here whether the small improvement obtained justifies the necessity of measuring three extra variables.

CHAPTER 19

REMARKS ON THE LATERAL MOTION

19.1 EFFECT OF TIME IN CONTROL MOVEMENT

The assumption of proportionality between the detected displacement and the control setting does not take account of the actual behaviour of the control system. The response to a sudden displacement y_0 cannot cause a control movement $\delta_a = A_4 y$ to occur instantaneously. The control move must be progressive and depends on the characteristics of the mechanisms utilized.

The results already obtained give a good indication of the phenomena produced, but do not give exact values of the development of the variables.

In order to get an idea of this control time delay, we have considered several cases where the action of the displacement y has been slowed down.

The most simple case is given by the first order relationship already defined. We assume:

$$\delta_a = +A_4 y(1 - e^{-t/a})$$

where the time constant, a, has been taken equal to 3 seconds, i.e. $3/7.05 = 0.425$ unit of non-dimensional time.

19.2 MOTION WITH VARIABLE GAIN OF y

We have done a certain number of tests with continuous variation of the gain of the receiver on the displacement y, all the variables being recorded. The following notation has been used (see Fig.274):

A , position of aeroplane at time $\hat{t} = 0$

F , transmitter

B , point half way between A and E

E , end of landing strip nearest to approaching aeroplane.

The distance L between A and F , is taken as 10,000 meters. The distance EF is 2500 meters. Hence the gain increases from 1 to 2 between A and B and from 1 to 4 between A and E .

We have considered Cases a and c, modified as follows to become Cases a′ and c′.

(1) The value of A_4 at position A is half that for the corresponding case of constant gain, but the values of A_1 , A_3 and B_1 are unchanged.

	A_1	A_3	A_4 *variable*	B_1
Case a′ at A	0	1.5	1.75	2
B			3.50	
C			7.00	
Case c′ at A	3	4	2.62	0
B			5.25	
C			10.50	

(2) We have introduced the time constant into the control term $A_4 y$. The two causes which reduce the effectiveness of the readjustment to an error (i.e. reduction by half of A_4 and the time constant) have been introduced simultaneously, resulting in the reactions of the aeroplane being slower than for Cases a and c .

We have, therefore, investigated the response to the initial condition $y_0 = 100$ m , in order to compare the diagrams.

The same scale as for the preceding diagrams has been used in Figures 275 and 276. The peaks in the δ_a-curve have been suppressed; the trajectories have the same fundamental characteristics as in the preceding cases.

Case a′ (Fig.275) results in a trajectory having little variation in course and having lateral displacement due to side-slip. This side-slip to the right is caused by the rudder being moved to the left and the ailerons inclining the aeroplane to the right.

Case c′ (Fig.276) leads to an appreciable change of course, in the required direction, but there is also an oscillatory side-slip.

19.3 DISTORTION EFFECTS

The effect of irregularities in the beam field generated by the localizer has been studied.

We have arbitrarily chosen the following conditions. A deviation of 0.25° starting at C , 1500 m before the touch-down point, which is continued for 480 m, up to D.

After the point D , i.e. 1020 m before touch-down, the normal beam is re-established (Fig.277(a)).

This irregularity exceeds the distortions generally encountered in practice and for purposes of comparison we have reproduced in Figure 277(b) a typical deflection diagram for the localizer beam at San Francisco Airport as it was in 1952 (Ref.30).

The distance CD is covered by the aeroplane in 8 seconds, i.e. 1.2 units of non-dimensional time.

These results have been incorporated in the preceding problem.

In the zone CD , the gain in z is larger than for the normal cases a and c, but is far from having a value corresponding to instability.

Figures 278 and 279 show the trajectories and the characteristics of the different variables for the controlled aeroplane in cases a′ and c′.

One cannot expect the receiver to discern between erroneous and exact signals; the guidance system can do nothing but tend to guide the aeroplane to the zero signal axis. However, this process is slow, the aeroplane deviates from its trajectory at C , continues to diverge from the axis after the point D in spite of the fact that the zero signal line is returned to the correct landing strip axis, causing the aeroplane to receive a strong recall signal. The duration of the erroneous signal (8 seconds) is such that the aeroplane follows a trajectory which amplifies the distortion of the zero signal line.

The different types of control possible may be classified according to the perturbation considered. A perturbation of the beam may be considered as a new form of excitation.

It would be of interest to define a type of perturbation of the beam and compare the effect of the different control conditions for this excitation. The aeroplane must necessarily react to the error signal produced by the deviation of the zero signal line, but it should be arranged that the amplifications of this signal be as small as possible.

19.4 EFFECT OF B_4

The effect of B_4 on the control was not considered at the beginning of Chapter 18; the results of the two tests given below explain why it was not considered.

We introduced $B_4 = 1.4 \times 10^{-3}$ into Case c to have the condition of Case m:

$$A_1 = 3 \quad A_3 = 4 \quad A_4 = 5.25 \times 10^{-3} \quad B_4 = 1.4 \times 10^{-3}$$

and have applied the initial condition $y_0 = -50$.

The results given in Figure 237 show that there occurs a change of heading in the required direction which is much larger than for the preceding cases but the effect of changes in heading on the lateral displacement is cancelled out by an opposing side-slip of considerable magnitude. Hence we see that the introduction of $B_4 y$ is undesirable.

The excellent conditions of Case g included a term in $B_4 y$ of the same value, but there were also terms in $B_1 \psi$ and $B_3 \varphi$.

We have established that the initial deflection of the rudder for both Cases g and m is of the same sign and the same order of magnitude, but it is too prolonged for Case m. For Case g, the effect of the terms in B_1 and B_3 is to stop the positive rudder displacement after a very short time.

To summarize, it can be stated that the term B_4 is undesirable when employed alone, but is favourable when used in conjunction with B_1 and B_3 .

We also considered a case for $B_4 = -1.4 \times 10^{-3}$ added to the conditions of Case c. The result is just as bad: strong side-slip, tending to bring the aeroplane back to the correct approach path, is produced, but is opposed by a change of heading in the wrong direction (Fig.238).

19.5 SEMI-AUTOMATIC CONTROL

There are instruments for aeroplanes which will perform the addition of signals:

$$A_1\psi + A_3\varphi + A_4 y = D$$

giving a direct indication of D to the pilot.

The most well known instrument of this type is the Sperry Zero Reader. A vertical pointer moves in front of a graduated scale, giving a deviation proportional to D . It is possible to measure on actual instruments the respective values of A_1 , A_3 , A_4 , which are incorporated in Zero Readers in use.

An instrument, calibrated by the maker for a twin-engined aeroplane, has been analysed on the ground. It was found that a deflection of the pointer of 10 mm corresponded to any of the following displacements, applied independently:

$$d\varphi = 12^{o}$$

$$d\psi = 10^{o}$$

$$d\chi = -1.4^{o}$$

χ being the angle at the apex of the equi-signal lines.

At a distance of 10 km from the radio transmitter, this angle corresponded to a displacement $dy = -244$ m . Hence we have:

$$A_1\left[\frac{10}{57.3}\right] = A_3\left[\frac{12}{57.3}\right] = A_4 \times 244$$

The coefficients of the control equation were in the ratio

$$\frac{A_3}{A_1} = 0.834$$

$$\frac{A_4 \times 10^3}{A_1} = 0.715$$

while the conditions utilized by us for Case c′ corresponded to

$$\frac{A_3}{A_1} = 1.33$$

$$\frac{A_4 \times 10^3}{A_1} = 0.875$$

One can imagine that the pilot should be able to move the aileron controls in proportion to the reading D.

The pilot, then, constitutes the servo-mechanism of the above system. A semi-automatic control subject to the above conditions should be possible if the pilot could move his controls in proportion to the reading D, which is somewhat doubtful.

However, the technique of using the instrument is different from this and is based on the fact that the aeroplane, displaced from its correct approach path, returns to it tangentially if the reading D is kept at zero during this motion.

The control setting $\delta_a = f(\hat{t})$ for this manoeuvre is not indicated by the instrument, which serves only to tell the pilot when the condition $D = 0$ is not satisfied, i.e. the technique to find the correct value of $\delta_a = f(\hat{t})$ relies more or less on tentative control movements performed by the pilot.

However, the sign of the correction to be applied is indicated in any case by the sign of $D \neq 0$, i.e. by the sense of displacement of the pointer of the instrument.

19.6 FINAL REMARKS

The analogue computer permits us to make a very precise study of the phenomena of lateral control.

The analysis has shown that many points are worth studying. The introduction of real behaviour of servo-mechanisms opens up the field for a new series of researches.

One conclusion which has already been stated, but which will be mentioned again, is that the replacing of A_1 by A_8 has been shown to have many advantages, when we take account of the cross-wind v_a.

In a very careful practical study of automatic approach Mercer[29] arrived at an opposite conclusion. He stated that control relying on ψ signals was better than the one using $\dot{y}$ signals.

This contradiction appears to us to result from the following facts:

(a) Tests were made at airports where the beam suffered from many irregularities;

(b) Construction of equipment using the A_8 signal being more difficult because of the necessity of performing a derivation. Nevertheless, recent American equipment uses the $A_8\dot{y}$ factor. This leads us to believe that the difficulties encountered by Mercer in his practical tests have been overcome.

CHAPTER 20

LONGITUDINAL BEHAVIOUR OF THE AEROPLANE

20.1 STABILITY WITH CONTROLS FIXED

The characteristic equation of the system is:

$$\begin{vmatrix} a_1 + \lambda & b_1 & c_1 & d_1 \\ a_2 & b_2 + \lambda & c_2 & d_2 \\ a_3 & b_3 & c_3 + \lambda & 0 \\ 0 & 0 & c_4 & +\lambda \end{vmatrix} = 0$$

i.e.
$$\lambda^4 + K_3\lambda^3 + K_2\lambda^2 + K_1\lambda + K_0 = 0 \qquad (20.1)$$

This equation has been studied extensively. It has normally two pairs of complex roots which define:

(i) A rapid oscillation, very damped, about the centre of gravity;

(ii) A slow oscillation (sometimes called the phugoid motion), slightly damped.

For the numerical values used in this study, the roots are:

$$\lambda = -0.095 \pm 1.282i$$

$$\lambda = -6.77 \pm 8.195i$$

The corresponding periods, T, and the times of half amplitude, $T_{½}$, are:

$$T = \frac{6.28}{6.77} = 0.9 \qquad T = \frac{6.28}{1.282} = 4.905$$

$$T_{½} = \frac{.692}{8.195} = 0.0845 \qquad T_{½} = \frac{0.692}{0.095} = 7.28$$

20.2 RESPONSE TO A STEP FUNCTION

The motion of the aeroplane following an elevator control setting δ_e or a throttle manoeuvre δ_t has been determined on a computer. The responses produced for:

$$\delta_e = -0.016$$

$$\delta_m = 0.20$$

have been investigated on the analogue computer and are given in Figures 280 and 281. The curves clearly show the existence of the phugoid oscillation, which affects principally the variables θ, z and ν.

Figure 281 shows that the increase of thrust produces, at the outset, an acceleration of the aeroplane, as well as a nose-up pitching motion. This pitching stops the acceleration rapidly and causes the aeroplane to decelerate.

The responses to sharp gusts:

$$u_e = 0.125\ V_0$$

$$w_e = 0.020\ V_0$$

have been determined and are given in Figures 325 and 330.

20.3 FREQUENCY RESPONSE

The frequency responses of the variables α, ν, θ, γ, z have been calculated and are given in Figures 282 to 291. The angle $\gamma = \theta - \alpha$ is the inclination of the trajectory with respect to the desired direction.

20.4 DIFFERENT DEGREES OF STABILITY

The calculations we have made do not take account of the decrease in density of the atmosphere with increasing altitude.

Under these conditions, the characteristic equation of the 4th degree determines the longitudinal stability, but does not include any term representing the altitude.

The addition of one of Equations (16.1) or (16.2) to the equations of the system (15.10) only permits stabilization of the aeroplane at altitude if one of the controls is made dependent on the error signal in z.

20.5 STABILITY WITH NO ACCOUNT TAKEN OF ALTITUDE

The longitudinal stability for controls fixed is a theoretical concept which does not correspond to the practical consideration of an aeroplane fitted with reversible controls. For this type of aeroplane the controls-free stability is the most important consideration.

The behaviour of a controls-free aeroplane can be considered as the behaviour of a controlled plane, where the setting of the elevator assumes, at any time, a value such that its hinge moment is zero, account being taken of the aerodynamic forces, the acceleration and the gravity forces.

However, it has been found that controls-free stability is never sufficient to control the aeroplane in atmosphere which has slight perturbations.

Many automatic devices have been made. Let us recall the well known properties of the artificial stability produced by a basic type of automatic pilot utilizing the error signals in θ , α , $\hat{u}$, q . We will consider these separately:

(a) *Error signal in* θ

The most simple of the devices is the control condition

$$+\delta_e = A_1\theta$$

where the control setting is governed by the attitude error θ .

Control by A_1 necessitates including in the characteristic determinant a term in d_3 proportional to $-(\partial C_m/\partial \delta_e)(d\delta_e/d\theta)$ or proportional to $-A_1(\partial C_m/\partial \delta_e)$.

Such a term does not increase the total available damping. The total available damping is, in effect, equal to the sum of the roots, i.e. equal to $-k_3$ or $+(a_1 + b_2 + c_3 + d_4)$.

The introduction of the term d_3 can only modify the distribution of a constant $-k_3$ between the real parts of the two roots.

It is well known that control by A_1 considerably improves the damping of the phugoid, but the increase of the real part of the root representing the phugoid is lost by the root representing the rapid oscillation.

(b) *Error signal in* α

The control in terms of A_2 characterized by $+\delta_e = A_2\alpha$ $(A_2 > 0)$ only produces an increase in the static stability $\partial C_m/\partial \alpha$.

An excess of static stability decreases the damping of the phugoid, but this effect is negligible for moderate increase of stability.

(c) *Error signal* $\hat{u}$

Control as a function of $\hat{u}$, which causes the plane to dive when $\hat{u}$ decreases in order to maintain the velocity, is defined by: $+\delta_e = A_3\hat{u}$, for $A_3 < 0$.

It is inadvisable to use this control equation alone as it strongly reduces the damping of the phugoid.

(d) *Error signal in* q *(or* $\dot{\theta}$*)*

The control $+\delta_e = A_6\dot{\theta}$ increases the term c_3 of the determinant and also increases the total available damping.

This increase of damping is utilized much more for the rapid oscillation than for the phugoid oscillation.

20.6 SECOND DEGREE OF STABILITY

The maintenance of a constant altitude z constitutes a supplementary requirement and involves using an error signal in z .

This signal can act on the elevator control $(A_u < 0)$ or the power control $(B_u < 0)$.

Figure 292 shows the motion of the aeroplane following initial conditions

$$z_0 = 50 \text{ m (downwards)}$$

$$\hat{u}_0 = \alpha_0 = \theta_0 = 0$$

under the action of a control $\delta_e = A_u z$.

The computer has shown that for $A_u = -0.28 \times 10^{-3}$ the aeroplane is brought back very slowly to the altitude $z = 0$ by a sustained oscillatory motion.

For $|A_u| < 0.28 \times 10^{-3}$ the change in altitude is slower, but the oscillations are damped.

For $|A_u| > 0.28 \times 10^{-3}$ the change in altitude is more rapid, but the oscillations increase and the motion is unstable.

The behaviour of the aeroplane under the effect of a change in power is similar.

Figure 293 shows the trajectory produced by $B_u = -4.52 \times 10^{-3}$. The oscillatory motion is almost undamped; the gain of altitude is very slow. Smaller or larger values of B_u produce the same effect as changes in A_u .

Hence we see that control as a function of altitude alone is not satisfactory; it leads to instability as soon as the gain of the control signal passes a limit which is too weak for practical purposes.

The admittance loci of z , produced by $-\delta_e$ or $+\delta_m$, allows us to verify this property. These show that when z is out of phase by $\pm 180^o$ the corresponding moduli are respectively equal to 3500 and 200. The critical values of A_u and B_u must be the inverse of these moduli.

The values $A_u = -0.28 \times 10^{-3}$ and $B_u = -4.52 \times 10^{-3}$ have been found by approximate experiments and are not the exact critical values.

It can be seen that the value of B_u corresponding to Figure 293 is a little too small; the oscillation is slightly damped. In these conditions, the values

$$A_u = \frac{1}{3500} \quad \text{and} \quad B_u = \frac{1}{200}$$

give satisfactory correlation.

20.7 THE LONG-PERIOD OSCILLATION

Figures 280 and 281 show that the period of the phugoid is equal to 5τ . Figures 292 and 293 show that the period of the long-period oscillation, produced by control as a function of the displacement in altitude, is 4.25τ .

We do not want to discuss here the characteristics common to this oscillation and the phugoid, but there is a difference which can be seen immediately.

The phugoid oscillation is not important in the case of manual control, or in automatic control in the first stabilization program (except for control in $A_3\hat{u}$), whilst the long-period oscillation produced by $A_4 z$ controls is important and becomes easily unstable. Its study cannot be neglected. Many serious errors have resulted from introducing the error signal in z into the automatic pilot without sufficient study of the problems involved.

The use of z as a control reference is only possible if we introduce into the control equations terms to damp the oscillations.

To do this, we must superimpose on to the signals $\delta_e = A_4 z$, signals which are out of phase by 90° (or about 90°) with respect to them. These signals will be supplied by the detection of the displacements of variables which are, to a considerable extent, in quadrature with the variable z . The variables θ , $\dot{z}$ and $\dot{u}/V_0$ satisfy this requirement; θ lags and $\dot{z}$, $\dot{u}/V_0$ lead on δ_e .

20.8 DAMPING BY A TERM $\delta_e = A_1\theta$

The addition in the control equation of a term $A_1\theta$ (or $B_1\theta$) with $A_1 > 0$, effectively damps the oscillation.

In Figure 294 the original results recorded are presented; these describe the trajectories following an initial displacement z_0 . The records correspond to the following cases:

a $A_4 = -0.14 \times 10^{-3}$ stable

b $A_4 = -0.28 \times 10^{-3}$ undamped; case of Figure 292

c $A_4 = -0.42 \times 10^{-3}$ unstable

d $A_4 = -0.42 \times 10^{-3}$ undamped, stabilized by $A_1 = +0.028$

e $A_4 = -0.42 \times 10^{-3}$ undamped, stabilized by $B_1 = +0.48$

We have attempted to bring the unstable oscillation (Case c) to the condition of a simple undamped oscillation. This was done by adding a term $A_1 = +0.028$ or $B_1 = +0.48$.

Later, (Fig.299), an example of control for a higher gain is given, i.e. $A_4 = -2.54 \times 10^{-3}$, stabilized by $A_1 = +0.406$. Analogue results (not given here) have been obtained for the case of altitude control by the term in B_4 .

20.9 OTHER POSSIBILITIES OF DAMPING

We have investigated the damping effect of terms in $A_5\dot{\theta}$, $A_8\dot{z}$ and $A_7(\dot{u}/V_0)$ on the pure phugoid, not excited by the signals A_4 or $B_4 < 0$.

We have reconsidered the calculation of the trajectory following an elevator displacement δ_e of the control (Fig.280) and have added successively control commands which are functions of the variables.

$$\delta_e = A_5\dot{\theta} \quad \text{where} \quad A_5 = +0.093 \quad \text{(Fig.295)}$$

$$\delta_e = A_8\dot{z} \quad \text{where} \quad A_8 = -0.946 \times 10^{-3} \quad \text{(Fig.296)}$$

$$\delta_e = A_7(\dot{u}/V_0) \quad \text{where} \quad A_7 = -0.64 \quad \text{(Fig.297)}$$

The control by A_5 results in an increase in the damping in pitch but the greatest effect is on the rapid oscillation; the improvement in the phugoid is small.

On the contrary, controls by A_7 and A_8 are very effective from the point of view of the damping of the phugoid. Two characteristics can be pointed out:

(i) The effect of the control for A_8 is related to the term in A_1 . We have:

$$\dot{z} = V_\tau(\alpha - \theta)$$

$$A_8\dot{z} = -A_8V_\tau\theta + A_8V_\tau\alpha$$

The control in $A_8\dot{z}$ is then equivalent to the simultaneous use of a control in θ and α where:

$$A_1\theta = -A_8V_\tau\theta$$

$$A_2\alpha = +A_8V_\tau\alpha$$

A_8 is chosen to be -0.946×10^{-3} . The control conditions can be considered as being:

$$A_1 = +0.946 \times 10^{-3} \times V_\tau = +0.4$$

$$A_2 = -0.946 \times 10^{-3} \times V_\tau = -0.4$$

acting simultaneously.

(ii) The use of the control condition A_7 causes practical problems which will be discussed later on.

It can be mentioned here that the effect of the signals in A_8 and A_7 decreases if the signals are applied with a time lag.

(a) We have applied a time constant to the signal A_7 equal to half a unit of aerodynamic time and obtained the curves shown in Figure 298, which shows much less damping than those in Figure 297.

(b) During our tests we used two control equations containing A_8 differing only by a time constant applied to A_8 (Figs.309 and 310).

The trajectory defined with the time constant, in Figure 310, is less damped than that in Figure 309.

CHAPTER 21

MAINTENANCE OF THE GLIDE PATH

21.1 CONTENTS OF THIS CHAPTER

This chapter is devoted to the investigations of combinations of A_1 , A_n , B_1 , B_n , which lead to satisfactory holding of the required trajectory making an angle of -2.5^o (-0.0436 rad) with the horizontal.

We will compare these combinations for four types of initial conditions, acting independently:

$$z_0 = 50 \text{ m}$$

$$\zeta_0 = +2.5^o \text{ (or 0.0436 rad)}$$

$$u_a = 0.125V_0$$

$$w_a = 0.02V_0$$

These conditions correspond to the following cases:

(a) An aeroplane fyling parallel to, but 50 m below, the glide path, at the moment when the automatic pilot is put into action;

(b) An aeroplane flying horizontally, where the automatic pilot is put into action at the moment when it cuts the glide path;

(c) An aeroplane following the glide path with the automatic pilot in action but encountering a tail gust at time $\tau = 0$;

(d) An aeroplane following the glide path with the automatic pilot in action, but subjected to a down gust at time $\tau = 0$.

We recorded the values of the variables α , ν , θ , z , δ_e , δ_m .

The analogue computer was not set up to measure γ (the slope of the trajectory) nor $n = V(d\gamma/dt)$, the normal acceleration.

The curve $\gamma = \theta - \alpha$ has, nevertheless, been calculated and plotted. It is indicated by dotted lines.

It was considered too inaccurate to obtain the normal accelerations by deriving the curve of γ .

In all our calculations we have assumed A_4 and B_4 constant along the trajectory.

21.2 BASIC CONDITIONS

To find more rapid changes in altitude than in the preceding chapter, we have taken a value of $A_4 = -2.54 \times 10^{-3}$ and have tried to stabilize the motion by using a control setting which is a function of θ or $\dot{z}$.

We have successively combined the control setting $A_4 z$ indicated above with:

$$A_1\theta = 0.406\theta \qquad \text{(Fig.299)}$$

$$A_8\dot{z} = -0.946 \times 10^{-3}\dot{z} \qquad \text{(Fig.300)}$$

The introduction of $A_8\dot{z} = -0.946 \times 10^{-3}\dot{z}$ is equivalent to the use of $A_1\theta + A_2\alpha$ with:

$$A_1 = -A_8 V_{0,\tau} = +0.406$$

$$A_2 = +A_8 V_{0,\tau} = -0.406$$

Comparing the Figures, we can see that the curves for z and γ differ only slightly, but the curves for θ and α have appreciable differences.

The term $A_2 = -0.406$ decreases the static stability.

The amplitude of the changes in α and θ is bigger when this destabilizing term is introduced.

The analogue computer shows us that if a term in $A_4 z$ or $B_4 z$ of sufficient magnitude is used to produce the desired change in altitude in a short enough time, the terms in $A_1\theta$ or $A_8\dot{z}$ can hardly stabilize the motion in a suitable manner.

The control conditions where the term in A_4 or B_4 is stabilized by a term in A_5 acting alone have not furnished us with any satisfactory results and hence are not included in this report. Other conditions must be investigated.

21.3 MORE COMPLEX CONDITIONS

The analogue computer shows us that the use of $A_7(\dot{u}/V_0)$ results in strong damping of the phugoid without affecting the changes in altitude z as much as the terms A_1 and A_8.

All control conditions considered from now on will contain a term in A_7.

After a number of tentative efforts we established the condition (Case a):

$$+\delta_e = A_4 z + A_5\dot{\theta} + A_7\dot{\nu}$$

where

$$A_4 = -2.52 \times 10^{-3}$$

$$A_5 = +13.7 \times 10^{-3}$$

$$A_7 = -0.64$$

The control equation gives the trajectory shown in Figure 301. It is curious to note that the aeroplane gains 42 metres in altitude in the first 2 units of time, after which it only climbs very slowly.

This objectionable characteristic is removed by the addition in the control conditions of a term in A_3, viz.

$$A_3 = +0.24$$

the action of which is to pitch the aeroplane up when the speed is less than it should be. The control equation then becomes

$$+\delta_e = A_3\left(\hat{u} - \frac{u_a}{V_0}\right) + A_4 z + A_7 \frac{\dot{u}}{V_0} + A_5\dot{\theta}$$

where

$$A_3 = +0.24$$

$$A_4 = -2.52 \times 10^{-3}$$

$$A_5 = +13.7 \times 10^{-3}$$

$$A_7 = -0.64$$

and will be completely studied (it will be called Case b).

The motion for an initial displacement of $z = +50$ m is shown in Figure 302.

The correct altitude is regained in 1.6 units of time, i.e. 11 seconds, but the aeroplane is slowed down by the amount $\Delta\hat{u} = -0.14$. The work done in the change of height is 50 G kilogram-metres, where G represents the weight of the aeroplane. The energy liberated by the loss in speed is:

$$\frac{1}{2}\frac{G}{g} V^2[1 - (1 - \hat{u})^2]$$

$$= \frac{G}{2 \times 9.81} \times 3600\ (1 - 0.74) = 47.7\ G \text{ kilogram-metres}$$

The increase of incidence during this interval of time reduces the power necessary for level flight. From the curve of $C_D/C_L^{3/2}$ given in Figure 204 we can see that the corresponding reduction of work is 2.3 G kilogram-metres.

21.4 POWER CONTROL

It is useful to alter the power when a change in altitude is wanted. Two methods of control are possible: control by change in the relative velocity $(\hat{u} - u_a/V)$ or directly by the displacement of altitude z.

For the system where the velocity change controls the power, we chose the following conditions (Case c):

$$+\delta_e = A_4 z + A_5 \dot{\theta} + A_7(\dot{u}/V_0)$$

$$-\delta_m = B_3\left(\hat{u} - \frac{u_a}{V}\right)$$

where

$$A_4 = -2.52 \times 10^{-3}$$

$$A_5 = 13.7 \times 10^{-3}$$

$$A_7 = -0.64$$

$$B_3 = 3.72$$

The elevator control is exactly the same as for Case a, but a power control term δ_m is added.

Figure 303 shows the effect of an initial displacement z_0. This displacement causes the elevator to give the aeroplane a pitching-up moment, resulting in a deceleration which brings the power control into action. These conditions (Case c) do not alter the maximum velocity and incidence changes which were found in Case a, but the recovery of altitude is more rapid and these changes have a shorter duration.

For the control conditions where the displacement z controls the power directly, we chose the following combination (Case d):

$$+\delta_e = A_5 \dot{\theta} + A_7(\dot{u}/V_0)$$

$$-\delta_m = B_4 z$$

where

$$A_5 = +0.093$$

$$A_7 = -0.64$$

$$B_4 = -0.042$$

The elevator is only acted on by terms which contribute to the damping. The control effects for these conditions are shown in Figure 304.

The motion has changes of velocity and incidence which are much smaller than for the preceding case, but the aeroplane only approaches the desired flight path asymptotically. The displacements of the elevator are very small.

Before going further, let us investigate what happens when the aeroplane is at a considerable distance from the transmitter.

The terms A_4 and B_4 are smaller, but the other coefficients of the control equations retain their values.

Let us reduce the value of A_4 to one-sixth of its value to form cases which we will call a′ , b′ , c′ (see the following table).

By reducing B_4 to one-sixth of its value in Case d we have Case d′. The damping terms become too large and reduce the rapidity of response. Figures 305, 306 and 307 show the motion corresponding to an initial condition $z_0 = 50$ m .

Case	A_3	$A_4 \times 10^3$	$A_5 \times 10^3$	A_7	B_3	$B_4 \times 10^3$	Fig.No.
a		-2.52	13.7	-0.64			301
b	0.24	-2.52	13.7	-0.64			302
b′	0.24	-0.42	13.7	-0.64			305
c		-2.52	13.7	-0.64	3.72		303
c′		-0.42	13.7	-0.64	3.72		306
d			93	-0.64		- 42	304
d′			93	-0.64		- 7	307

21.5 SUPERPOSITION OF THE EFFECTS OF B_3 AND B_4

The control of power by B_3 and B_4 results in different effects and we have investigated whether or not the addition of these terms produces favourable results.

However, we must increase the damping and to do this we decided to make use of the 3 stabilizing components $A_5\dot{\theta}$, $A_7(\dot{u}/V_0)$, $A_8\dot{z}$. The control conditions are then (Case e):

$$\delta_e = A_4 z + A_5\dot{\theta} + A_7(\dot{u}/V) + A_8\dot{z}$$

$$-\delta_m = B_3\left(\hat{u} - \frac{u_a}{V_0}\right) + B_4 z$$

where $A_4 = -2.52 \times 10^{-3}$ $\quad B_3 = +3.72$

$A_5 = +0.093$ $\quad B_4 = -42 \times 10^{-3}$

$A_7 = -0.64$

$A_8 = -0.946 \times 10^{-3}$

Figure 308 shows the motion following an initial condition $z_0 = 50$ m .

A very rapid recovery of altitude is obtained, but the aeroplane goes slightly above the intended flight path before regaining it.

The increase of incidence at the start of the motion is relatively high, the decrease of velocity small.

The numerical values of the damping terms were guessed at. Once a convenient choice of conditions had been found, we did not further investigate the division of the damping contribution between the 3 damping terms and hence we reduced the numbers of cases to be considered. Perhaps the values chosen are not the best.

We could also have used $A_1\theta$ (or $B_1\theta$), but we did not consider this variable since its introduction into the control equation may contribute to the formation of a static error in the final equilibrium conditions for initial perturbances to be considered later.

Case e has been taken as the starting point for a series of modifications defined in the following table:

Case	$A_4 \times 10^3$	$A_5 \times 10^3$	A_7	$A_8 \times 10^3$	B_3	$B_4 \times 10^3$	Fig.No.
e	-2.52	93	-0.64	-0.946	3.72	-42	308
f	-2.52	93	-0.64	-0.946	3.72(x)	-42(x)	309
g	-2.52	93	-0.64	-0.946(x)	3.72(x)	-42(x)	310
g′	-0.42	93	-0.64	-0.946(x)	3.72(x)	- 7(x)	311
h (A_2 = +4)	-2.52	93	-0.64	-0.946(x)	3.72(x)	-42(x)	312
i (A_1 = -0.74)	-2.52	93	-0.64	-0.946(x)	3.72(x)	-42(x)	313
j (with term in j′ $Aq\int zdt$)	-2.52	93	-0.64	-0.946(x)	3.72(x)	-42(x)	314
	-0.42	93	-0.64	-0.946(x)	3.72(x)	- 7(x)	315

(x) indicates a time constant in the term.

We are very close to a critical case, as far as damping is concerned, and certain modifications make the conditions unsuitable. The following remarks can be made about these modifications:

(1) *Introduction of a time constant in the terms* B_4z *and* $B_3(\hat{u} - u_a/V_0)$

For a first study of the problem we have assumed linear conditions, assuming that at the moment of detection of the displacement z_0 there is an instantaneous motion of the controls.

This assumption cannot be realized in practice and all calculations should be made taking account of the real properties of the control mechanisms and at least, a time constant should be introduced.

The results obtained up to the present do not correspond to cases which are possible in practice. Nevertheless, they allow us to explain the various effects of the different components in the control conditions.

The greatest objection to the assumption is in the case of the power control, where, according to Figure 308, the power is increased by 210% in zero time, which is clearly impossible.

To investigate the effect of a more progressive control we have introduced a time constant of 1 unit of aerodynamic time in the term δ_m . This corresponds to

$$\delta_m = \frac{1}{1 + s}\left[B_3\left(\nu - \frac{u_a}{V}\right) + B_4 z\right]$$

in symbolic representation.

Figure 229 shows that there is a time lag in the development of power and that the increased power is maintained for too long a time. The climb is less rapid and the aeroplane overshoots the reference altitude by a considerable amount. The introduction of a delayed term B_4 tends to diminish the oscillation present in Case e.

(2) *Introduction of a time constant for the term* A_8

The measurement of $\dot{z}$ can be made from the rate-of-climb indicator, which is an instrument having a considerable time lag. To take account of this fact, we have added to the damping term in A_8 a time constant equal to $\frac{1}{2}\tau$. The control conditions then become:

$$\delta_e = A_1\theta + A_4 z + A_5\dot{\theta} + A_7(\dot{u}/V_0) + \frac{1}{1 + 0.5s} A_8\dot{z}$$

The introduction of this time constant reduces the damping.

This case (Case g) is defined in the last table and the response to an initial condition of $z_0 = 50$ m is given in Figure 310. It can be seen that there is an oscillation.

(3) *Reduction of the terms* A_4 *and* B_4

We form Case g′ by reducing the terms A_4 and B_4 , which are included in Case g, to one-sixth of their respective values. The response to a displacement $z_0 = 50$ m is much slower but is no longer oscillatory.

(4) *Addition of a term in* A_2

We have considered the effect of the increase in static stability corresponding to a term $A_2 > 0$, the term being introduced in Case g .

For a value of $A_2 = 4$, corresponding to an appreciable increase in static stability produced by a setting of the elevator proportional to the deviation of α , the motion becomes quite oscillatory.

Figure 312 (compare with 310) gives the motion following a displacement z_0 .

(5) *A destabilizing term in* A_1

For reasons which will be discussed in the following chapter, we have considered a Case i, derived from Case g by the addition of a destabilizing term $A_1\theta = -0.74\theta$. The motion is clearly oscillatory.

(6) *Integral term in* z

In the following chapter we will give reasons which justify the introduction of an integral term in z and the resulting inconveniences.

21.6 COMBINATIONS INVESTIGATED FOR OTHER INITIAL DEFLECTIONS

Some of the preceding cases have been studied with other initial displacements. The following table gives the Figure numbers corresponding to these various conditions.

	Initial error in			
Case	z_0	ζ_0	u_e	w_a
Locked controls	-	-	325	330
Case b	302	316	326	331
b′	305	320	-	-
c	303	317	327	332
c′	306	321	-	-
d	304	318	328	333
d′	307	322	-	-
g	310	319	329	334
g′	311	323	-	-
j	314	-	-	-
j′	315	324	-	-

21.7 INITIAL CONDITION ζ_0 (OR ENTERING THE GLIDE PATH)

During approach, the aeroplane, flying horizontally, encounters the axis of the glide path. At the moment of this intersection, the aeroplane is required to change its trajectory and to follow the glide path, which is inclined at -2.5° to the horizontal.

In the horizontal flight, before the intersection with the glide path, the aeroplane must ignore the inclined axes.

Manual or automatic control, using error signals of altitude h, assures level flight. When the aeroplane reaches the glide path, the distance z, measured from the glide path, must become the essential control factor.

The receiver of the z-signal must be switched on at this moment. The aeroplane, flying horizontally, will rise too high if it maintains its straight trajectory after crossing the glide path, and an error signal in z, becoming more and more negative, will be received.

In our calculations, the order given to the servo-mechanism by the chief pilot will be simulated by the introduction of ζ_0 in the equation:

$$\dot{z} = V_\tau(\alpha - \theta - \zeta_0)$$

where $\zeta_0 = +2.5^{\circ} = +0.0436$ rad.

This means that the axis forming the origin of the z-variable is rotated downwards about $\zeta_0 = +2.5^{\circ}$.

The θ and γ values, given by the computer, indicate nevertheless the displacements of attitude and trajectory with respect to the original reference lines.

Let us examine the results obtained with the control equations which we considered.

The term $A_4 z$ is going to put the aeroplane into a dive, resulting in an increase of velocity and a steeper trajectory.

The power available is too great for this new trajectory.

In Case b, when the throttle control is not changed, the excess of power must be compensated for by less economical flight conditions, resulting in greater speed and smaller incidence, the increase of speed being considerable (Fig.316).

If a term B_3 (Case c) is included in the control conditions, the increase of speed will decrease the available power and hence the increase of speed will not be so great (Fig.317).

For Case d, i.e. where we have the control term $B_4 z$ acting on the throttle, the error in z leads also to a decrease in power (Fig.318).

In all these cases, the aeroplane tends to move to a position of equilibrium above the glide path, and flies faster at a smaller incidence along a trajectory parallel to the glide path, the final value of γ being equal to -0.0436 rad or -2.5°.

The aeroplane is displaced 11 to 12 metres above the glide path in Cases b and c, and 16 metres above it in Case d. The numerical value of B_4 is too small to have a great effect; however, it does limit any excess of velocity.

Case g (Fig.319), which entails a combination of different effects, gives a smaller final error in z . However, the control conditions adopted do not give sufficient decrease in power and hence an increase in velocity is still necessary to absorb the excess power. All the control equations lead to a static error.

The cases where the gain of A_4 or B_4 is one-sixth of their preceding values result in final errors in z which are 6 times larger; hence they will not suitably guide the aeroplane along the glide path (Figs.320 to 323).

In an actual approach, because of the increase of the gain in A_4 and B_4 during the descent, the static error in z will not be the same at the end as at the beginning of the descent. The final error in z will correspond to the larger gains realized there. However, we must consider that the response of the automatic pilot to an order to change the gradient of its flight path is not satisfactory for the control conditions studied here.

Note

(1) Let W_0 be the necessary power for horizontal flight

W_ζ be the necessary power for flight along a descending trajectory.

In supposing that, in the two assumptions, the curves of C_L and C_D as a function of α are the same, we find, in the case considered:

$$W_\zeta = 0.522\ W_0$$

The coefficients B define the changes in power in the form of a fraction δ_m of the power W_ζ .

If we want to represent this change as a fraction of the power in horizontal flight, these changes will be fractions δ'_m of the power W_0 , where $\delta'_m = 0.522\ \delta_m$.

(2) We did not use, in the control equation, terms proportional to an error in θ or in γ .

The reason is that the final trim position along the glide path results in values of θ and γ other than those corresponding to the horizontal path.

Using θ-control without changing the reference or zero value at the entrance of the glide path would increase the static error in z .

(3) At the moment of intersection with the glide path, an action of the pilot is necessary to change the control settings, and to put into action the sensors of error z.

This unavoidable action could be also used in the following ways:

(a) By changing the zero value of θ, which would provide the opportunity to use the stabilizing term $A_1\theta$ in the control equation;

(b) By operating the thrust control to produce the necessary reduction of δ_m without having to rely on the action of the terms $B_3\hat{u}$ and $B_4 z$.

(4) Another way to suppress the static error in z would be to introduce an integral term $A_q\int z\, d\hat{t}$ in the control equation.

The action of such a term could overcome the unfavourable effect of A_1.

21.8 THE GUST u_a

The aeroplane, flying in a descending path of slope 2.5^o, receives a gust u_a from the rear. We will assume that this gust occurs suddenly and that it has a magnitude of $0.125\ V_0$.

The calculation has been made for a gust u_a acting parallel to the axis OX of the aeroplane, and not for a horizontal gust. This case is somewhat artificial, since the direction of the gust, instead of being constant, changes with the direction of the aeroplane.

A gust acting parallel to the aeroplane chord can be divided into two components u_{ag} and w_{ag} related to the horizontal and vertical axes: these components would be:

$$u_{ag} = +0.125V_0 \cos(4.5^o + \theta)$$

$$w_{ag} = -0.125V_0 \sin(4.5^o + \theta)$$

In Figures 325 and following, the diagram of $\hat{u}$ agrees with the absolute velocity when read with respect to the origin and give the relative velocity $(\hat{u} - u_a/V_0)$ if read with respect to the broken line.

The gust produces transient effects, which we can study for the case of an aeroplane with locked controls (Fig.325). The tail gust decreases the relative velocity of the aeroplane and causes it to dive. This results in a series of oscillations which resemble the phugoid, but which are, in fact, a little different because of the introduction of the excitation w_{ag}.

The component w_{ag}, which is a function of θ, has an important effect on the aeroplane altitude; it tends to deviate the aeroplane upwards from the initial path with increasing time.

The diagram of α gives the apparent angle of attack. The real angle of attack

$$\alpha_r = \alpha - \frac{w_a}{V_0} + \alpha_0 \frac{u_a}{V_0}$$

is larger than the apparent angle of attack α by the amount $\alpha_0(u_a/V_0) = 0.0153$ rad. The final value of the real angle of attack about which the aeroplane oscillates is 0°.

The state of affairs is changed when the aeroplane is controlled by the servo-mechanism we studied earlier.

In Case b (Fig.326), the initial decrease in altitude due to insufficient velocity is unimportant. The automatic pilot raises the nose of the aeroplane and the incidence increases. This pitch-up control changes during the motion and becomes a pitch-down control.

Because of the added velocity u_a the slope of the flight path would become smaller than the required slope if the pilot did not intervene. The aeroplane can fly again in a steady state along a trajectory with the correct slope if there is a decrease in power. If the control conditions do not include a power control, the excess of power must be absorbed by the aeroplane flying faster.

The automatic pilot for Case b can only cause this to happen if it receives a signal in z, i.e. if the aeroplane is above the correct approach path. With the control conditions adopted, this residual displacement z is quite small.

In Case c (Fig.327), any increase in the relative velocity produces a decrease in the power and vice-versa.

As a result of these power variations, the establishment of the final conditions necessitates a smaller increase of velocity.

In Case d (Fig.328), the aeroplane loses height at the beginning of the motion. The control $-\delta_t = B_4 z$ supplies temporary, supplementary power, but changes sign when the displacement z changes sign.

The decrease in power for the final conditions is necessarily related to the distance z, i.e. to the height of the aeroplane above the correct flight path.

Case g (Fig.329) has the two effects B_3 and B_4 with a time constant included.

In Cases b', c', d', g' (sensitivity of the control in z being one-sixth its normal value) we have similar effects, but the residual displacements in z are 6 times as large. The figures have not been reproduced in this report.

21.9 THE GUST w_a

We have investigated the effect of a gust normal to the axis OX and directed downwards. The gust is assumed to occur suddenly and has a magnitude

$$w_a = 0.02\ V_0 \text{ , i.e. } 1.2 \text{ m/sec}$$

The transient effects of the gust on the aeroplane, flying with locked controls, are shown in Figure 330. On this and the following figures the curve α gives the angle between the axis OX and the absolute velocity if it is read with respect to the abscissa: if it is read with respect to the broken line the curve gives the aerodynamic angle of attack $(\alpha - w_a/V_0)$.

The curve of $\gamma = \theta - \alpha$ represents the slope of the trajectory with respect to the correct approach path.

The angle of incidence being reduced by the gust, the aeroplane, when flying with locked controls, pitches up slightly because of static stability. However, the aeroplane is involved in a downward motion and diverges steadily from the correct approach path. The amplitude of the oscillations which accompany this motion is small.

The aeroplane maintains a course close to the correct approach path for the control conditions which we have studied.

In Case b we have established (Fig.331) that the aeroplane does not pitch up due to the effect of the gust: the first reaction of the auto-pilot is to put the aeroplane into a nose-down attitude, but this motion, due to the term $A_7(\dot{u}/V_0)$ does not last and rapidly changes its sense because of the intervention of the term in $A_4 z$.

The angle of incidence of the aeroplane increases, its velocity decreases and the excess of power made available by this effect opposes the action of the wind velocity. The aeroplane then flies along a trajectory parallel to the correct approach path, but is always lower.

In Case c (Fig.332), extra power is produced in proportion to the reduction in velocity of the aeroplane. A decrease of velocity is necessary, but is less than in the previous case. The motion of the elevator is similar.

In Case d (Fig.333), the power is produced in proportion to the displacement z until the excess power so produced cancels the effect of the downward wind. The elevator has very little effect, it being used only at the start of the motion to control the nose-down attitude.

Case g (Fig.334), showing the two effects on δ_m with a time constant, does not have any peculiarity. It leads to a minimum displacement in z , which is normal.

Cases b′, c′, d′ and g′ for small gain in the displacement z have been investigated, but the results are not given in this report, since they have the same characteristics.

The aeroplane does not fly so close to the correct approach path, but moves away from it, the final error in distance being six times as great.

Note

The component in $A_7(\dot{u}/V_0)$, common to the control equations studied, produces an unexpected effect; this is due to the slight nose-down attitude which can be seen in the diagrams.

CHAPTER 22

REMARKS ON THE LONGITUDINAL MOTION

22.1 PROGRESSIVE VARIATION OF THE GAIN IN A_4 OR B_4

We have not made tests with progressive variation in the gain, in the case of longitudinal motion, as we did in the case of lateral motion. The set-up for this purpose was prepared but not used.

We considered it more useful to collect together the information necessary to having an idea of the phenomena, considering only simple cases with constant coefficients, than to simulate completely real cases with variable coefficients.

To have an idea where the instability regions are is very useful, for the consequences of an increase in gain of the ILS receiver is more serious for longitudinal motion than for lateral motion.

The glide-path transmitter is, in effect, placed at the entry of the landing strip, at the touch-down point, whilst the localizer transmitter is placed at the exit end of the landing strip.

Hence the gain of the receiver tends to infinity at the touch-down point. The aeroplane must, therefore, cease to use this signal before touch-down, whereas the localizer signal can be used right up to touch-down.

This is not an irremediable drawback, for in the present flight technique the pilot has to see the landing-strip approach lights at about 200 feet or 60 metres above the ground, and has to pilot manually from that point.

Considering that the aeroplane is flying at an altitude of about 360 metres before entering the glide path, the gain is going to vary from 1 to 6 between the beginning of the descending flight and the point where the pilot must resume manual control. This explains why we have considered cases where the gain varied in such a manner.

The minimum requirements will be: (1) enough stability for the high-gain case, in order to secure some margin of safety if the auto-pilot is switched off later than foreseen, and (2) sufficient effectiveness for the low-gain case.

The proposed control equations do not give an adequate effectiveness in the latter case; this shows the difficulty of the problems and the utility of devices which reduce the gain in proportion to the time elapsed from the moment of entry into the glide path. These devices are incorporated in certain existing automatic pilots.

22.2 INTEGRAL CONTROL

The static error z is unavoidable in cases with initial conditions ζ_0 , u_a , w_a .

Theoretically, it exists also for an initial condition in z_0 , but becomes infinitely small and can be neglected in that case.

It can be suppressed by a control component proportional to the integral of z .

The general theory of control explains this fact, and give the effect of such a component.

We have investigated two cases, introducing the integral of z to be added to Case g:

$$+\delta_e = +A_4 z + A_5 \dot{\theta} + A_7 \frac{\dot{u}}{V_0} + \frac{1}{1 + ap} A_8 \dot{z} - 0.00192 \int z \, d\hat{t}$$

which becomes Case j.

For Case g′ we have:

$$+\delta_e = +A_4 z + A_5 \dot{\theta} + A_7 \frac{\dot{u}}{V_0} + \frac{1}{1 + ap} A_8 \dot{z} - 0.00032 \int z \, d\hat{t}$$

which becomes Case j′.

The response to an initial displacement z_0 is shown in Figures 314 and 315.

When the initial condition is a displacement z_0 , the introduction of an integral control term is far from being favourable. The aeroplane crosses the correct approach path several times and residual oscillations with very long periods occur.

It can be shown easily that the integral control condition suppresses the static error z following an initial perturbation of ζ , u_a or w_a . These errors are corrected: the aeroplane is brought back to fly along the correct approach path, but the process is very slow. The aeroplane establishes itself in a régime imposed by the equilibrium conditions.

We will indicate the response to an initial displacement ζ in Case j′ (Fig.324) which can be compared with the response to the same displacement in Case g′ (Fig.323).

Without integral control conditions, the aeroplane flies at 35 metres above the correct approach path; for an increase of speed of +0.095 and a reduction of power $\delta_m = -0.60$. With integral control conditions, the aeroplane will be made to fly along the correct approach path, but with an excess speed of +0.130 and a reduction of power of $\delta_m = -0.38$.

22.3 IMPROVING THE DAMPING

The variables which produce damping when their errors are introduced in the control equation are θ , $\dot{\theta}$, $\dot{u}/V_0$, $\dot{z}$.

The term $A_1\theta$ has not been proposed because it contributes to the building up of a static error at entry to the glide path, unless an adjustment is made in the setting of the zero value for θ.

This drawback can nevertheless be suppressed if we use integral control.

The term $A_5\theta$ damps the short-period oscillation but has only little effect on the long-period oscillation.

The use of terms $A_8\dot{z}$ and $A_7(\dot{u}/V_0)$ is subject to drawbacks that will be discussed later.

The determination of the variables $\dot{z}$ and $\dot{u}/V_0$ raises certain problems and it is necessary to investigate the physical reality to which these variables correspond.

Variable $\dot{z}$

Two methods are available for measuring $\dot{z}$:

(a) We may obtain the derivative of z directly, but this suffers from the disadvantage that all irregularities affecting z are amplified.

(b) The derivative $\dot{z}$ can be computed in the following way: let h be the altitude of the aeroplane, measured positive upwards, and ζ the slope of the correct approach path, measured positive downwards. Then we have:

$$\dot{h} = -\dot{z} - V_\tau\zeta$$

The measurement of $\dot{h}$ is given by the rate-of-climb indicator and permits us to obtain $\dot{z}$, knowing V_τ and ζ.

This is an indirect measurement and is affected by the unavoidable time lag in the rate-of-climb indicator.

Variable $\dot{u}/V_0$

In our equations, $\dot{u}/V_0$ is a measure of the absolute acceleration.

The classical type of accelerometer is sensitive to absolute acceleration and to the attitude of the aeroplane. A longitudinal accelerometer measures the value of

$$\frac{du}{dt} + g \sin\theta$$

which, expressed non-dimensionally, is in our case:

$$\dot{u} + 7.05\, g \sin\theta$$

Let us call the reading of the accelerometer $\mathfrak{R}$. This reading is related to the true acceleration $\dot{u}/V_0$ by:

$$\mathcal{R} = \frac{\dot{u}}{V_0} + k\theta$$

and for our case:

$$k = \frac{7.05\ g}{V_0} = \frac{7.05 \times 9.81}{60} = 1.15$$

We can at this point envisage three different solutions:

(a) By utilizing the error of the variable $\dot{u}/V_0$ defined above, measuring the variable $\mathcal{R}$, introducing the correction k and obtaining:

$$\frac{\dot{u}}{V_0} = \mathcal{R} - k\theta$$

θ being measured by a position gyroscope.

(b) By accepting control of the aeroplane using $A_7\mathcal{R}$ instead of $A_7(\dot{u}/V_0)$.

(c) By trying to derive $\dot{u}/V_0$ from measurements of the air speed.

Each solution has its drawbacks: the first obviously leads to mechanical complication; the second is unsound; the third alters the principle of the control.

We will investigate these conditions in the following sections.

22.4 THE USE OF AN ACCELEROMETER

The horizontal accelerometer reading gives us: $\mathcal{R} = \dot{u}/V_0 + k\theta$. If we use $A_7\mathcal{R}$ instead of $A_7(\dot{u}/V_0)$, we add a term $A_1 = k\,A_7$ in the control equation.

The value of A_1 is: $A_1 = -1.15\ A_7 = -0.74$.

This has been done for Case g, which, with this addition, becomes Case i.

A term in A_1, with a negative coefficient, adversely affects the stability to a considerable extent. A calculation made for an initial displacement Z_0 gives us the result shown in Figure 313.

The motion is definitely oscillatory, which shows us that control depending on the value of $\mathcal{R}$ taken from a horizontal accelerometer is unsuitable.

The third solution will be studied in some detail.

22.5 USE OF THE AIR-SPEED INDICATOR

If the derivative of the air-speed indicator reading can be obtained exactly, we can replace $A_7(\dot{u}/V_0)$ in the control equation by $A_7(\dot{u}-\dot{u}_a)/V_0$.

As long as there is no variation in u_a , the response will be the same as when the absolute acceleration $\dot{u}/V_0$ is used, but the response to a gust u_a will be different.

During a motion following a sharp-edged gust u_a , the relative and absolute velocities vary according to the curves 1 and 2 in Figure 335. At any instant $t \neq 0$, the two derivatives are the same, but at time $t = 0$ the relative velocity changes abruptly by u_a/V_0 . Its derivative changes in the form of a pulse:

$$\frac{\dot{u} - \dot{u}_a}{V_0} = \frac{\dot{u}}{V_0} - \mathcal{Y}(\hat{t}) \frac{u_a}{V_0}$$

where $\mathcal{Y}(\hat{t})$ is the Dirac function.

The pulse in u_a/V is introduced into the automatic pilot by:

$$+\delta_e = A_7\left(\frac{\dot{u} - \dot{u}_a}{V_0}\right)$$

and produces theoretically a pulse in the control setting:

$$+\delta_e(\hat{t}) = -A_7 \mathcal{Y}(\hat{t}) \frac{u_a}{V_0}$$

If the derivation of (u_a/V_0) were performed correctly, and if all the servo-mechanisms functioned without inertia, the aeroplane would be subjected to an impulsive pitching moment corresponding to a pulse in the control setting

$$\delta_e(\hat{t}) = (-0.64)(-0.125)\mathcal{Y}(\hat{t}) = 0.08\mathcal{Y}(\hat{t})$$

The theoretical effect of this impulsive control setting can be determined on the simulator.

The output variables α , $\hat{u}$, θ produced by a pulse are the derivatives of the same output variables when the excitation is a step function having the same input value.

Consequently, it is sufficient to determine the derivatives $d\alpha/d\hat{t}$, $d\nu/d\hat{t}$, $d\theta/d\hat{t}$ for a step displacement of the control equal to $(\delta_e) = +0.08$. This has been done for the control conditions of Cases b, c and d, by recording voltages in the computer corresponding to these derivatives. The results are all very much alike and only one of them has been reproduced in this report (Fig.336).

The impulsive control setting produces important peaks in the α and θ diagrams. It causes first pitch-down and then pitch-up of the aeroplane. A nose gust $(u_a < 0)$ would produce opposite effects.

The response of the aeroplane to a gust u_a could be obtained when the automatic pilot is sensitive to $(\dot{u} - \dot{u}_a)/V_0$ instead of to $\dot{u}/V_0$, by adding the correction defined above to the response calculated for a signal in $\dot{u}/V_0$.

The impulse is a purely theoretical idea, but it has some practical significance, for the response to the impulse allows us, by calculation or by simple graphical construction, to calculate the response to an action of the same type, acting for a finite interval of time.

The transfer functions of the different components affecting the controls, air-speed indicator, servo-motor, and the imperfect derivative network will, however, transform the response.

The quantity $\delta_e(\hat{t})$ resulting from the impulse in the relative velocity will lose its discontinuous form and become a slower motion, of which the action in the motion of the aeroplane can be established after the impulsive response.

Such an operation considerably decreases the importance of the peaks in the diagrams of α and θ, but the result of the calculation will depend entirely on the assumptions made about the characteristics of the control components.

Some additional tests have been made in this way. In the tests already described, the voltage representing $\dot{u}/V_0$ was measured in the loop, after summing the terms $-a_1\hat{u}$, $-b_1\alpha$, etc., but before integration. This voltage multiplied by A_7 was then introduced in the summation, giving $+\delta_e$.

Another set-up has been prepared: the voltage representing $(\hat{u} - u_a/V)$ was obtained by integration of $\int(\dot{u}/V_0)d\hat{t}$ and summation with $-u_a/V$; its derivative was calculated by a derivator network.

The derivative was deliberately chosen to be imperfect; the imperfection resulted in the introduction of a time constant a in the resulting derivative of $(\hat{u} - u_a/V_0)$.

Tests with a step unit disturbance in u_a/V_0 were made for Case g. The replacement of $A_7s\hat{u}$ by $A_7[s/(1+as)(\hat{u}-u_a/V_0)]$ introduced also a time constant a in the term $A_7(\dot{u}/V_0)$ and reduced its stabilizing action.

We made the calculation for various values of the time constant a: 0.05, 0.10, 0.20, 0.50. We give, in Figures 337 and 338, the results for the values $a = 0.05$ and $a = 0.20$. The curves may be compared with those of the true Case g given in Figure 329. There is still a peak in δ_e at the beginning of the response. There are corresponding peaks in α, θ and $\hat{u}$. They are of the same sign as those predicted theoretically and represented in Figure 336, but are smaller, due to the imperfect derivation.

The loss of the stabilizing effect of $A_7(\dot{u}/V_0)$ due to the time constant affecting this term is clearly seen. It is still greater for the case $a = 0.50$, which is not reproduced here.

The peaks will, of course, be reduced if the sharpness of the gust decreases and will be reduced a second time if we take account of the real inertia characteristics of the servo-mechanism.

The effects of replacing $A_7(\dot{u}/V_0)$ by $A_7(\dot{u}-\dot{u}_a/V_0)$ lead nevertheless to unfavourable characteristics, as any time lag, or time constant corresponding to the derivation, which is incorporated to eliminate the initial peaks produced by $\dot{u}_a/V_0$, will decrease the stabilizing effect of A_7.

Note

It must be remembered that the time constants already existing in Case g, i.e.

$$a = 0.5 \text{ acting on } A_8\dot{z}$$

$$a = 1 \text{ acting on } (\beta_3(\dot{u}/V_0) + B_4\dot{z})$$

are maintained and added to the time constant affecting A_7 .

22.6 MORE ELABORATE CASES

The tests analyzed in this report were intended to show clearly the effect of the most important terms entering into the control equations.

The control equations were kept relatively simple. Other tests, with more intricate control laws, have been made.

The question of how to mix the stabilizing terms in order to improve the aircraft motion remains open. As $A_7(\dot{u}-\dot{u}_a)/V_0$ has some drawbacks, we tried to keep A_7 small and to use $A_1\theta$ to increase stability. This is possible when the static error in z is suppressed by an integrating term.

We calculated the responses to the 4 initial conditions, for such combinations. The results of one of them are given in Figures 339 to 342 as an example of the results that can be obtained.

The control coefficients were:

$$A_1 = 1 \qquad A_3 = 0.4 \qquad A_4 = -4 \times 10^{-3} \qquad A_5 = 0.16 \times 10^{-3}$$

$$A_7 = -0.5 \qquad A_8 = 2 \times 10^{-3} \qquad A_9 = 0.5 \times 10^{-3}$$

$$B_3 = 8 \qquad B_4 = 50 \times 10^{-3}$$

This control equation reduces the drawbacks of the integrating term $A_9\int z\, d\hat{t}$, although, during the response to a displacement z_0 , the distance z exceeds its final value by 20% of the initial error (Fig.339).

The static error in z is zero after 4 units of time when simulating the entrance in the glide path (Fig.340). The final value of ν is 0.08, due to an insufficient decrease in thrust.

A final value $\nu = 0$ could nevertheless be obtained. To do this, an integral term $B_{10}\int\nu\, d\hat{t}$, with $B_{10} > 0$, should be added to the thrust control. This opens the way to new and still more elaborate control equations.

The introduction of $B_{10}\int\nu\, d\hat{t}$ into the control equation will produce an oscillation of very long period. We ascertained that it was possible to effect reasonable damping of this oscillation by a strong increase in the term $B_3(\nu - u_a/V_0)$ but a long time will be necessary to cancel the static errors.

A control equation using the same terms A as those of the preceding combination, and using:

$$B_3 = 20 \qquad B_4 = 50 \times 10^{-3} \qquad B_{10} = 1$$

gave the results which are described in Figures 343 to 346.

During the response to z_0, the displacement z exceeds its final value by more than 30% (Fig.343).

While entering the glide path, the static error in z disappears only after 8 time units; the error in ν vanishes also, but only after 16 time units. Although there is no static error in ν, the final value of α is quite different from the initial one (Fig.344).

This results from the reduction of δ_t, as account is taken in the aerodynamic aircraft characteristics of the variation of the lift coefficient with δ_m.

The response to a front gust u_a (Fig.345) leads in 10 time units to an absolute speed equal to $(\nu + u_a/V_0)$, which means the cancellation of any static error in speed.

The initial peaks of the responses, produced by $A_7(\dot{u}_a/V_0)$, still present, are reduced.

The response to the gust w_a does not need any comment (Fig.346).

22.7 COMPARISON WITH CAROLL AND TYLER TESTS

There is no similarity between the control conditions considered by us and those recommended by Caroll and Tyler.

We have tolerated slow motions and made systematic efforts to keep the values of the control coefficients as small as possible.

Caroll and Tyler required a quick return to the correct flight path after disturbance but accepted relatively higher values of the control coefficients.

They arrived at control equations of the type

$$+\delta_e = A_1\theta + A_2\left(\alpha - \frac{w_a}{V_0}\right) + A_4 z + A_5\dot{\theta} + A_8\dot{z}$$

$$-\delta_m = B_3\left(\nu - \frac{u_a}{V_0}\right) + B_4 z + B_8\dot{z}$$

having a time constant in the term in $A_8\dot{z}$.

The set-up used in our calculations would not have permitted us to introduce, into the computer, values of the coefficients A_1 ..... B_n as high as those used by Caroll and Tyler, without changing the scales and the whole set-up.

The time at our disposal did not allow us to do this. We did not, therefore, try to find out why their control equations differed from those which gave us good results.

22.8 FINAL REMARKS

The study of longitudinal control clearly shows the possibilities of analysis offered by the analogue computer.

The test results given are not for the purpose of formally recommending a particular type of control condition. Their purpose is to show that the effects of the choice of control coefficients can be completely foreseen and computed by an analogue computer.

LIST OF FIGURES

		Page
Fig.203	Localizer and glide path axes	402
Fig.204	Lift and drag coefficients used for calculation	402
Fig.205	Planes of equal-signal strength	403
Fig.206	Deformation of equi-signal strength line	403
Fig.207	Two different meanings of the same error signal	404
Fig.208	Closed-loop autopilot and aeroplane	404
Fig.209	Lateral motion; response to a step $\delta_a = -0.002$	405
Fig.210	Lateral motion; response to a step $\delta_r = -0.02$	406
Fig.211	(a) Frequency response; β produced by $-\delta_a$, amplitude	407
	(b) Frequency response; β produced by $-\delta_a$, phase	407
Fig.212	(a) Frequency response; p produced by $-\delta_a$, amplitude	408
	(b) Frequency response; p produced by $-\delta_a$, phase	408
Fig.213	(a) Frequency response; r produced by $-\delta_a$, amplitude	409
	(b) Frequency response; r produced by $-\delta_a$, phase	409
Fig.214	(a) Frequency response; φ produced by $-\delta_a$, amplitude	410
	(b) Frequency response; φ produced by $-\delta_a$, phase	410
Fig.215	(a) Frequency response; ψ produced by $-\delta_a$, amplitude	411
	(b) Frequency response; ψ produced by $-\delta_a$, phase	411
Fig.216	(a) Frequency response; y produced by $-\delta_a$, amplitude	412
	(b) Frequency response; y produced by $-\delta_a$, phase	412
Fig.217	(a) Frequency response; β produced by $-\delta_r$, amplitude	413
	(b) Frequency response; β produced by $-\delta_r$, phase	413
Fig.218	(a) Frequency response; p produced by $-\delta_r$, amplitude	414
	(b) Frequency response; p produced by $-\delta_r$, phase	414

		Page
Fig.219	(a) Frequency response; r produced by $-\delta_r$, amplitude	415
	(b) Frequency response; r produced by $-\delta_r$, phase	415
Fig.220	(a) Frequency response; φ produced by $-\delta_r$, amplitude	416
	(b) Frequency response; φ produced by $-\delta_r$, phase	416
Fig.221	(a) Frequency response; ψ produced by $-\delta_r$, amplitude	417
	(b) Frequency response; ψ produced by $-\delta_r$, phase	417
Fig.222	(a) Frequency response; y produced by $-\delta_r$, amplitude	418
	(b) Frequency response; y produced by $-\delta_r$, phase	418
Fig.223	(a) Response of an aircraft controlled by $\delta_a = A_3\varphi$	419
	(b) Response of an aircraft controlled by $\delta_a = A_3\varphi$	419
	(c) Response of an aircraft controlled by $\delta_r = B_3\varphi$	419
	(d) Response of an aircraft controlled by $\delta_r = B_3\varphi$	419
Fig.224	Deviation of ψ for an aircraft controlled by $\delta_r = A_3\varphi$	420
Fig.225	Polar plot of the frequency response in ψ, for δ_a and δ_r inputs	421
Fig.226	Deviation of ψ for the aeroplane piloted by various control equations	422
Fig.227	Deviation of y for a control equation involving terms in A_4, B_4	423
Fig.228	Deviation of y for a control equation involving terms in A_4, B_4	424
Fig.229	Steady variation of coefficients A_4 and B_4	425
Fig.230	Aircraft response to an initial error y = 50 m, case a	426
Fig.231	Aircraft response to an initial error y = 50 m, case b	427
Fig.232	Aircraft response to an initial error y = 50 m, case c	428
Fig.233	Aircraft response to an initial error y = 50 m, case h	429
Fig.234	Aircraft response to an initial error y = 50 m, case e	430
Fig.235	Aircraft response to an initial error y = 50 m, case f	431

		Page
Fig.236	Aircraft response to an initial error y = 50m, case g	432
Fig.237	Aircraft response to an initial error y = 50m, modified case c	433
Fig.238	Aircraft response to an initial error y = 50m, modified case c	434
Fig.239	Aircraft response to an initial error y = 50m, case d	435
Fig.240	Aircraft response to an initial error y = 50m, case i	436
Fig.241	Aircraft response to an initial error y = 50m, case j	437
Fig.242	Aircraft response to an initial error y = 50m, case k	438
Fig.243	Aircraft response to an initial error y = 50m, case l	439
Fig.244	Aircraft response to an initial error y = 50m, case l_1	440
Fig.245	Aircraft response to an initial error y = 50m, case l_2	441
Fig.246	Aircraft response to an initial error ψ = 0.08 rad., case a	442
Fig.247	Aircraft response to an initial error ψ = 0.08 rad., case b	443
Fig.248	Aircraft response to an initial error ψ = 0.08 rad., case c	444
Fig.249	Aircraft response to an initial error ψ = 0.08 rad., case h	445
Fig.250	Aircraft response to an initial error ψ = 0.08 rad., case e	446
Fig.251	Aircraft response to an initial error ψ = 0.08 rad., case f	447
Fig.252	Aircraft response to an initial error ψ = 0.08 rad., case g	448
Fig.253	Aircraft response to an initial error ψ = 0.08 rad., case d	449
Fig.254	Aircraft response to an initial error ψ = 0.08 rad., case i	450
Fig.255	Aircraft response to an initial error ψ = 0.08 rad., case j	451
Fig.256	Aircraft response to an initial error ψ = 0.08 rad., case k	452
Fig.257	Aircraft response to an initial error ψ = 0.08 rad., case l	453
Fig.258	Aircraft response to a side gust v_a, locked controls	454
Fig.259	Aircraft response to a side gust v_a, case c	455
Fig.260	Aircraft response to a side gust v_a, case h	456

Page

Fig.261 Aircraft response to a side gust v_a, case e 457

Fig.262 Aircraft response to a side gust v_a, case f 458

Fig.263 Aircraft response to a side gust v_a, case g 459

Fig.264 Aircraft response to a side gust v_a, case d 460

Fig.265 Aircraft response to a side gust v_a, case i 461

Fig.266 Aircraft response to a side gust v_a, case j 462

Fig.267 Aircraft response to a side gust v_a, case k 463

Fig.268 Aircraft response to a side gust v_a, case l 464

Fig.269 Aircraft response to a side gust v_a, case l_1 465

Fig.270 Aircraft response to a side gust v_a, case l_2 466

Fig.271 Aircraft response to a side gust v_a, case l_3 467

Fig.272 Aircraft response to a side gust v_a, case l_3' 468

Fig.273 Aircraft response to a side gust v_a, case l_4 469

Fig.274 Definition of some points of the approach path 470

Fig.275 Aircraft response to an initial error y = 100m, case a′ 471

Fig.276 Aircraft response to an initial error y = 100m, case c′ 472

Fig.277 (a) Schematic distortion of the beam 473

(b) Typical localizer beam 473

Fig.278 Aircraft response with distortion of the beam, case a′ 474

Fig.279 Aircraft response with distortion of the beam, case c′ 475

Fig.280 Longitudinal motion; response to a step input $\delta_e = -0.016$ 477

Fig.281 Longitudinal motion; response to a step input $\delta_m = +0.20$ 479

Fig.282 (a) Frequency response; $\hat{u}$ produced by $-\delta_e$, amplitude 481

(b) Frequency response; $\hat{u}$ produced by $-\delta_e$, phase 481

Fig.283 (a) Frequency response; α produced by $-\delta_e$, amplitude 482

		Page
Fig.283	(b) Frequency response; α produced by $-\delta_e$, phase	482
Fig.284	(a) Frequency response; θ produced by $-\delta_e$, amplitude	483
	(b) Frequency response; θ produced by $-\delta_e$, phase	483
Fig.285	(a) Frequency response; γ produced by $-\delta_e$, amplitude	484
	(b) Frequency response; γ produced by $-\delta_e$, phase	484
Fig.286	(a) Frequency response; z produced by $-\delta_e$, amplitude	485
	(b) Frequency response; z produced by $-\delta_e$, phase	485
Fig.287	(a) Frequency response; $\hat{u}$ produced by δ_m, amplitude	486
	(b) Frequency response; $\hat{u}$ produced by δ_m, phase	486
Fig.288	(a) Frequency response; α produced by δ_m, amplitude	487
	(b) Frequency response; α produced by δ_m, phase	487
Fig.289	(a) Frequency response; θ produced by δ_m, amplitude	488
	(b) Frequency response; θ produced by δ_m, phase	488
Fig.290	(a) Frequency response; γ produced by δ_m, amplitude	489
	(b) Frequency response; γ produced by δ_m, phase	489
Fig.291	(a) Frequency response; z produced by δ_m, amplitude	490
	(b) Frequency response; z produced by δ_m, phase	490
Fig.292	Aircraft response to an initial error z = 50m, for $\delta_e = A_4 z$	491
Fig.293	Aircraft response to an initial error z = 50m, for $\delta_m = B_4 z$	493
Fig.294	Response to an initial error z = 50m for $\delta_e = A_4 z$ with and without stabilizing terms	495
Fig.295	Response to step input δ_e = -0.016 damped $A_5\dot{\theta}$	497
Fig.296	Response to step input δ_e = -0.016 damped by $A_8\dot{z}$	498
Fig.297	Response to step input δ_e = -0.016 damped by $A_7\dot{u}$	499
Fig.298	Response to a step input δ_e = -0.016 damped by $A_7\dot{u}$ with time constant	500
Fig.299	Response to initial error z = 50m	501

		Page
Fig.300	Response to initial error z = 50m	502
Fig.301	Response to initial error z = 50m, case a	503
Fig.302	Response to initial error z = 50m, case b	504
Fig.303	Response to initial error z = 50m, case c	505
Fig.304	Response to initial error z = 50m, case d	506
Fig.305	Response to initial error z = 50m, case b′	507
Fig.306	Response to initial error z = 50m, case c′	509
Fig.307	Response to initial error z = 50m, case d′	510
Fig.308	Response to initial error z = 50m, case e	511
Fig.309	Response to initial error z = 50m, case f	512
Fig.310	Response to initial error z = 50m, case g	513
Fig.311	Response to initial error z = 50m, case g′	514
Fig.312	Response to initial error z = 50m, case h	515
Fig.313	Response to initial error z = 50m, case i	516
Fig.314	Response to initial error z = 50m, case j	517
Fig.315	Response to initial error z = 50m, case j′	518
Fig.316	Aircraft response to an initial error γ, case b	519
Fig.317	Aircraft response to an initial error γ, case c	520
Fig.318	Aircraft response to an initial error γ, case d	521
Fig.319	Aircraft response to an initial error γ, case g	522
Fig.320	Aircraft response to an initial error γ, case b′	523
Fig.321	Aircraft response to an initial error γ, case c′	524
Fig.322	Aircraft response to an initial error γ, case d′	525
Fig.323	Aircraft response to an initial error γ, case g′	526

		Page
Fig.324	Aircraft response to an initial error γ, case j'	527
Fig.325	Aircraft response to a gust u_a, locked controls	528
Fig.326	Aircraft response to a gust u_a, case b	529
Fig.327	Aircraft response to a gust u_a, case c	530
Fig.328	Aircraft response to a gust u_a, case d	531
Fig.329	Aircraft response to a gust u_a, case g	532
Fig.330	Aircraft response to a gust w_a, locked controls	533
Fig.331	Aircraft response to a gust w_a, case b	534
Fig.332	Aircraft response to a gust w_a, case c	535
Fig.333	Aircraft response to a gust w_a, case d	536
Fig.334	Aircraft response to a gust w_a, case g	537
Fig.335	Influence of u_a on the absolute and relative velocities	538
Fig.336	Response to a pulse in $\dot{u}_a/V_0$	538
Fig.337	Response to a gust u_a involving a pulse in $\dot{u}_a/V_0$	539
Fig.338	Response to a gust u_a involving a pulse in $\dot{u}_a/V_0$	540
Fig.339	Response to an initial error z, with integral control	541
Fig.340	Response to an initial error γ, with integral control	542
Fig.341	Response to a gust u_a, with integral control	543
Fig.342	Response to a gust w_a, with integral control	544
Fig.343	Response to an initial error z, with integral control	545

Page

Fig.344 Response to an initial error γ, with integral control 546

Fig.345 Response to a gust u_a, with integral control 547

Fig.346 Response to a gust w_a, with integral control 548

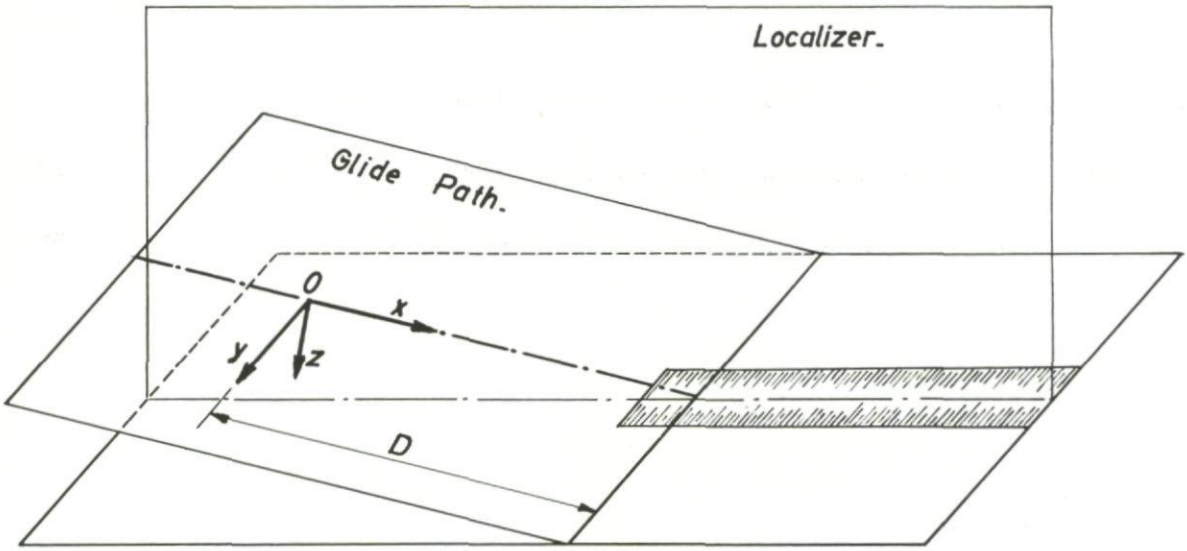

Fig. 203 Localizer and glide path axes

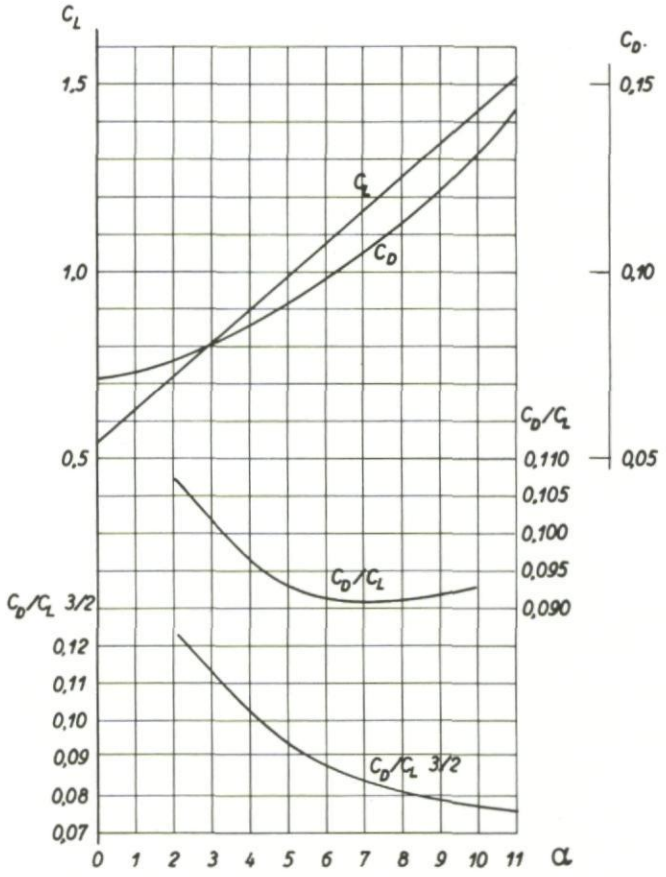

Fig. 204 Lift and drag coefficients used for calculation

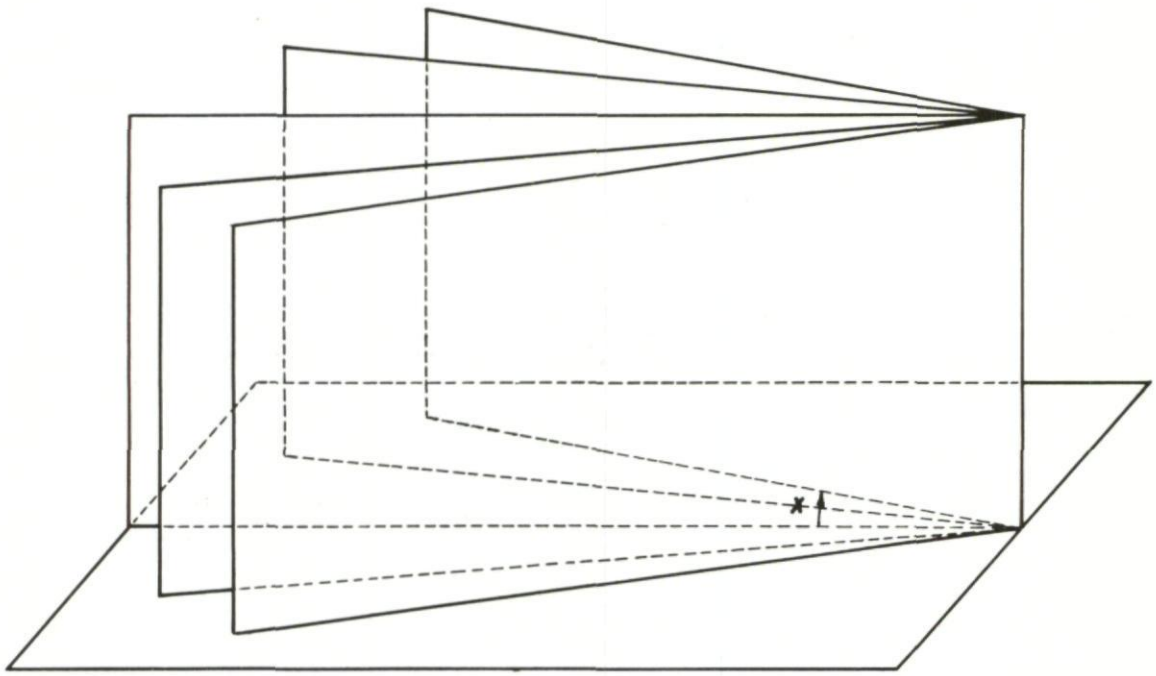

Fig.205 Planes of equal signal strength

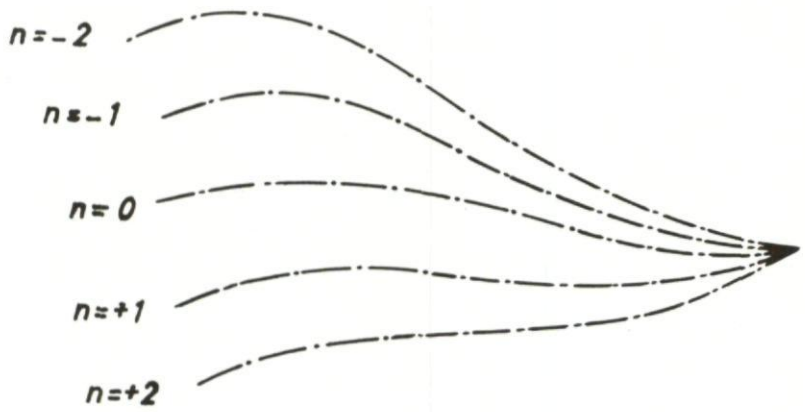

Fig.206 Deformation of equi-signal strength line

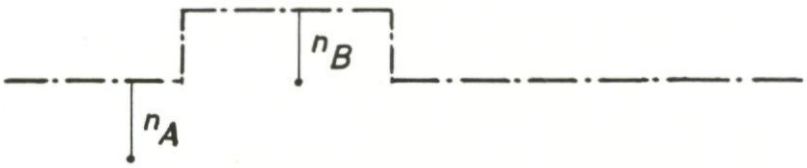

Fig.207 Two different meanings of the same error signal

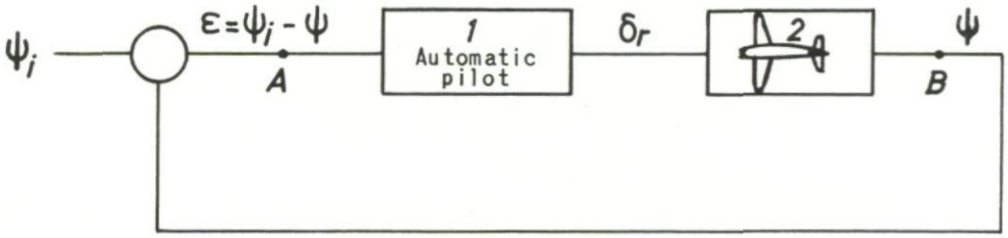

Fig.208 Closed-loop autopilot and aeroplane

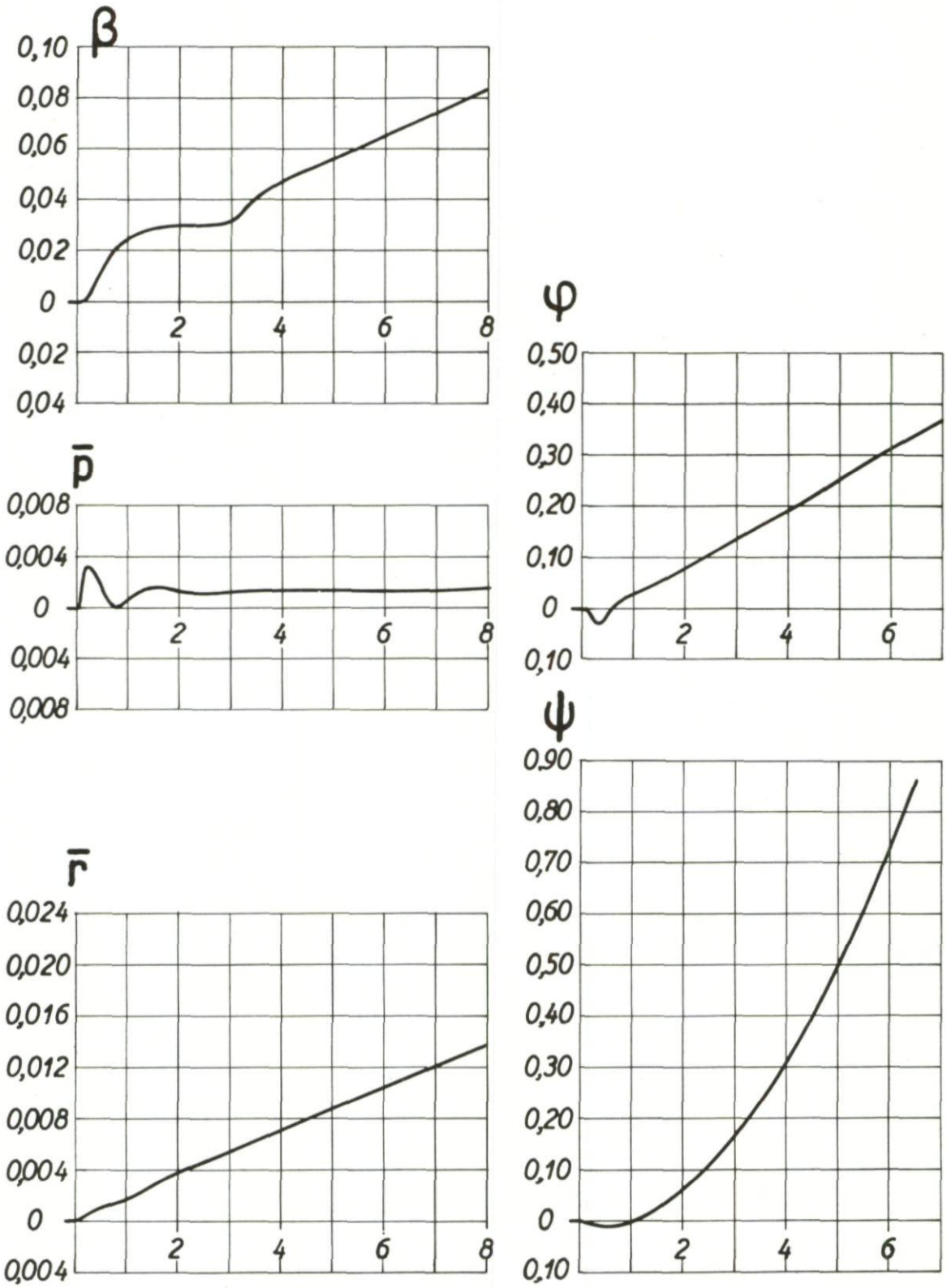

Fig.209 Lateral motion; response to a step $\delta_a = -0,002$

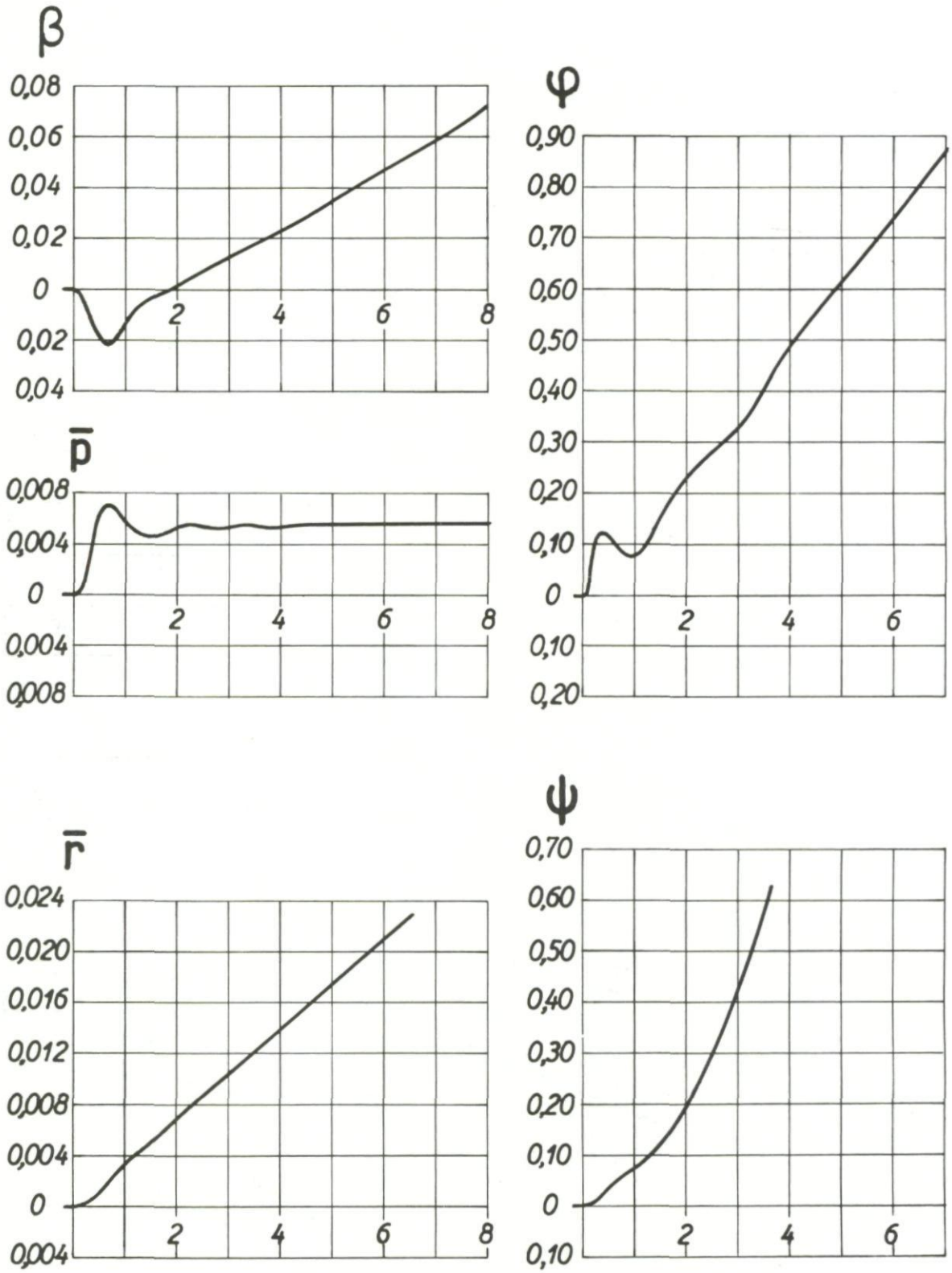

Fig.210 Lateral motion; response to a step $\delta_r = -0.02$

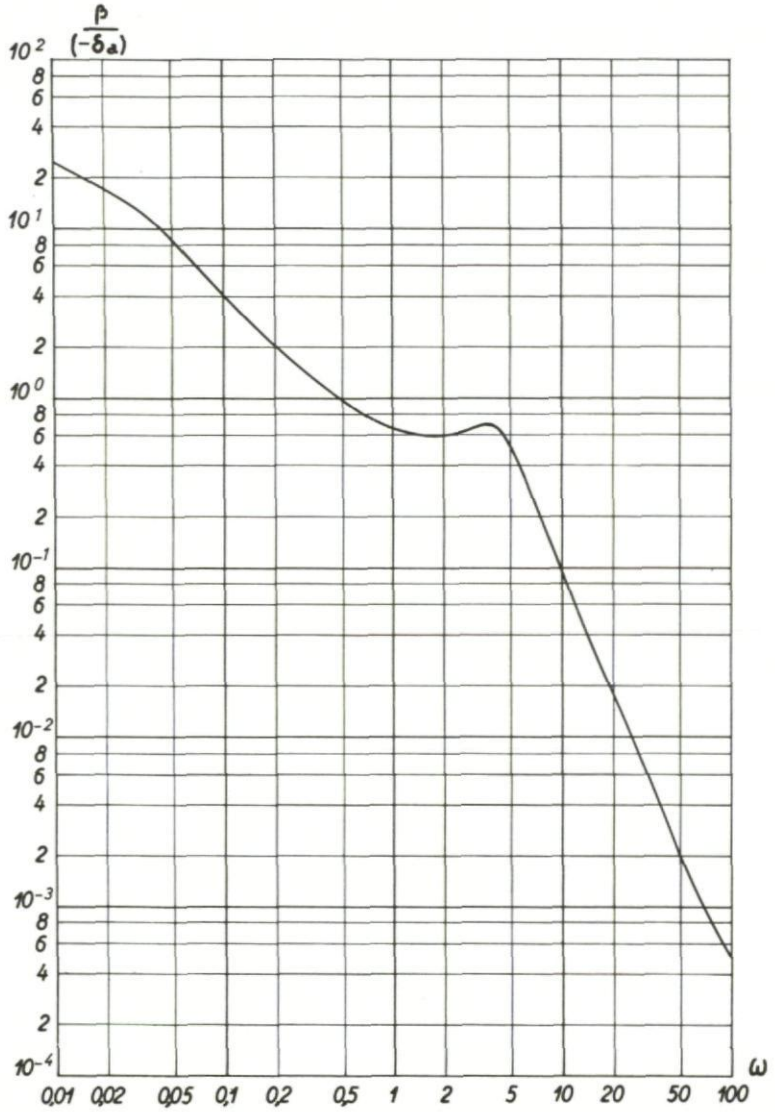

Fig.211(a) Frequency response; β produced by $-\delta_a$, amplitude

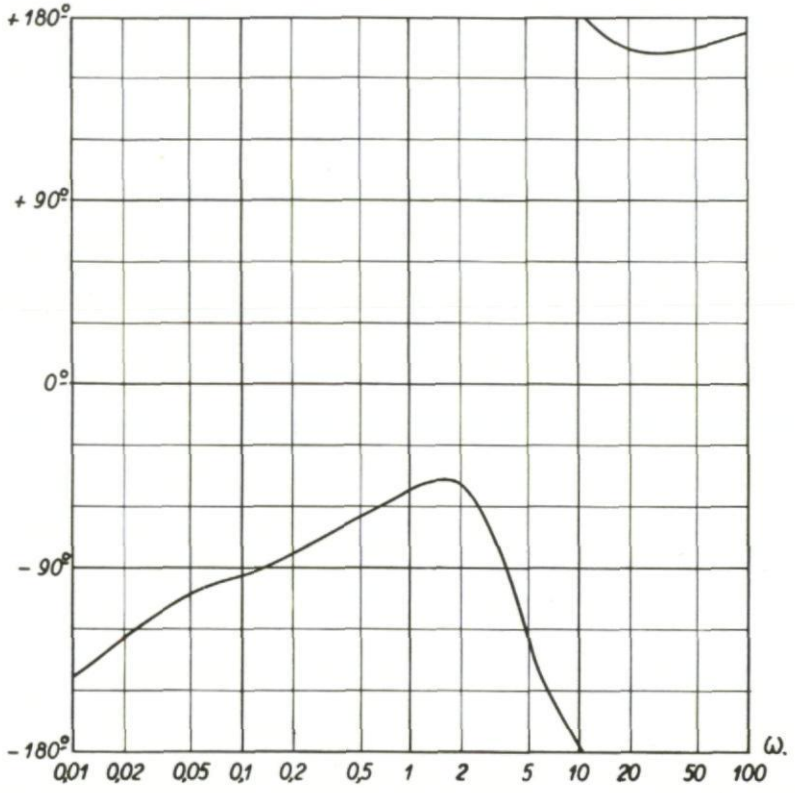

Fig.211(b) Frequency response; β produced by $-\delta_a$, phase

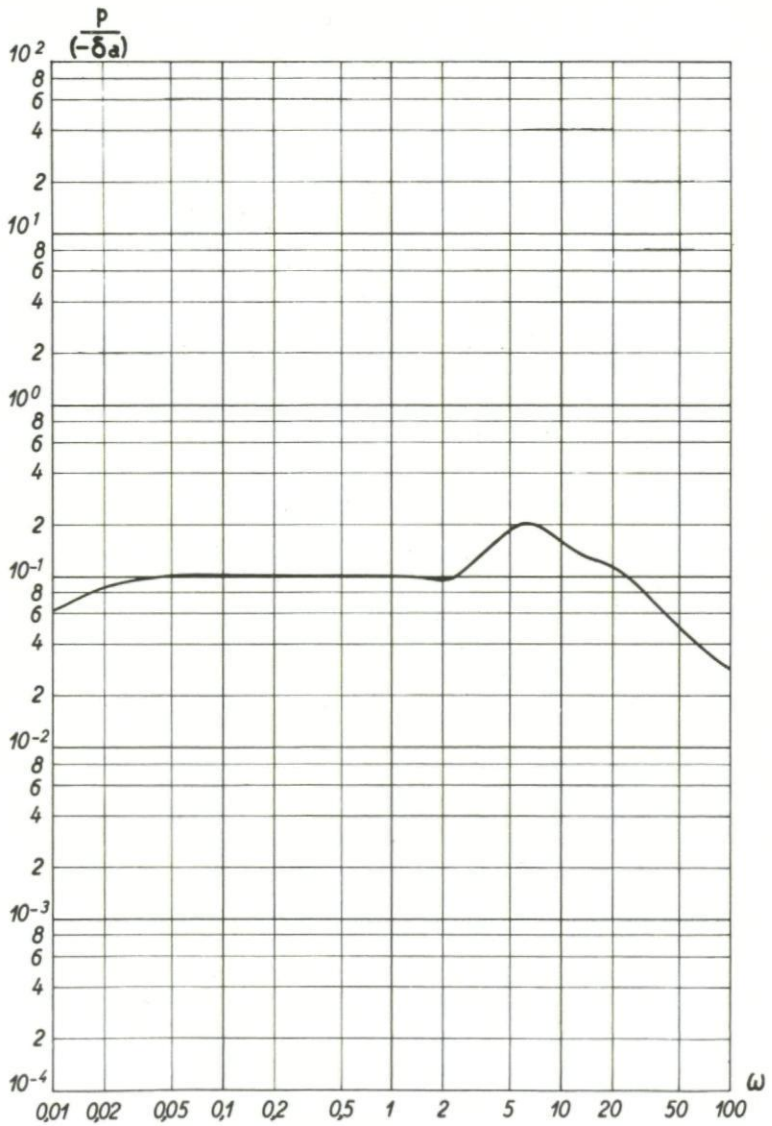

Fig. 212(a) Frequency response; p produced by $-\delta_a$, amplitude

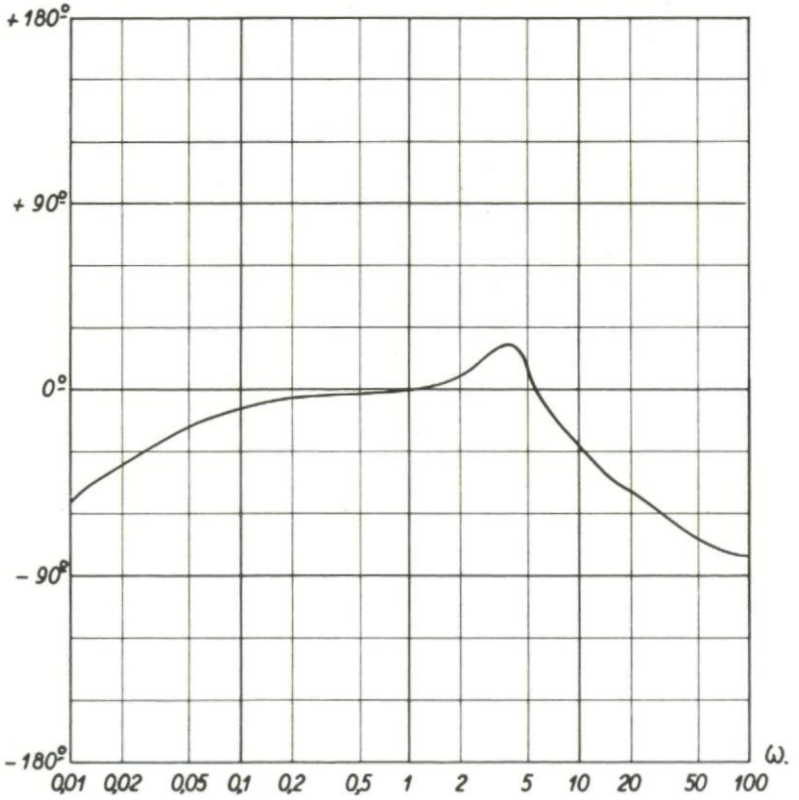

Fig. 212(b) Frequency response; p produced by $-\delta_a$, phase

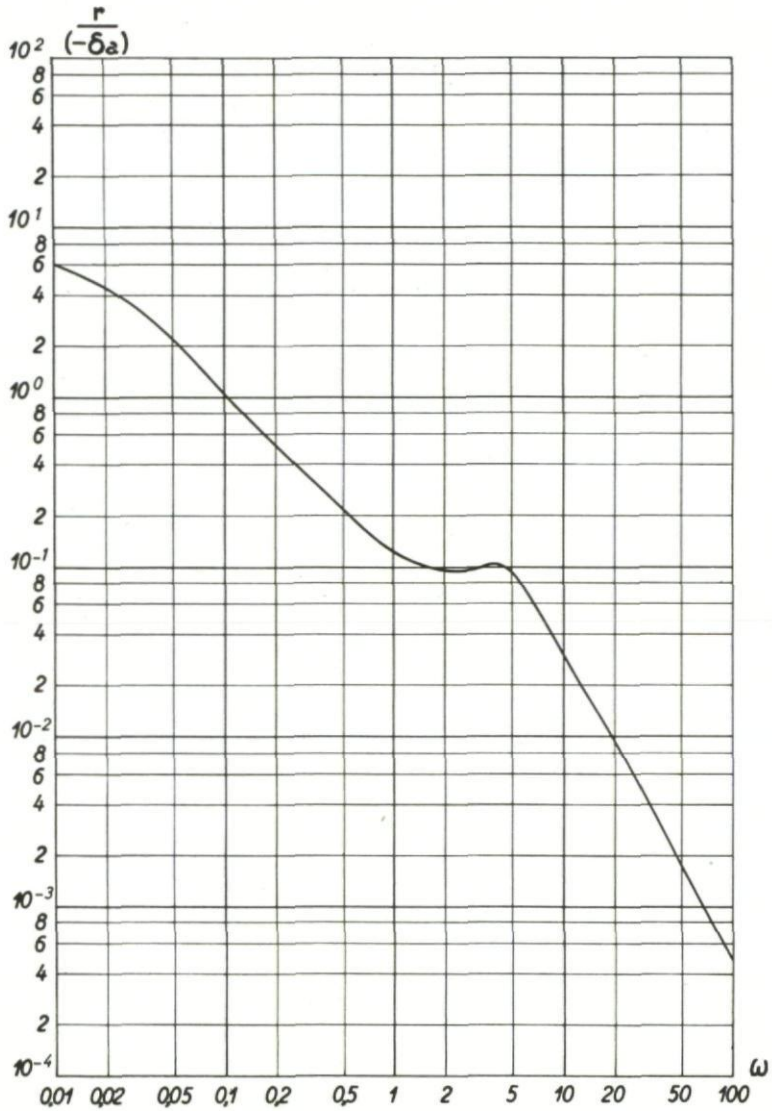

Fig. 213(a) Frequency response; r produced by $-\delta_a$, amplitude

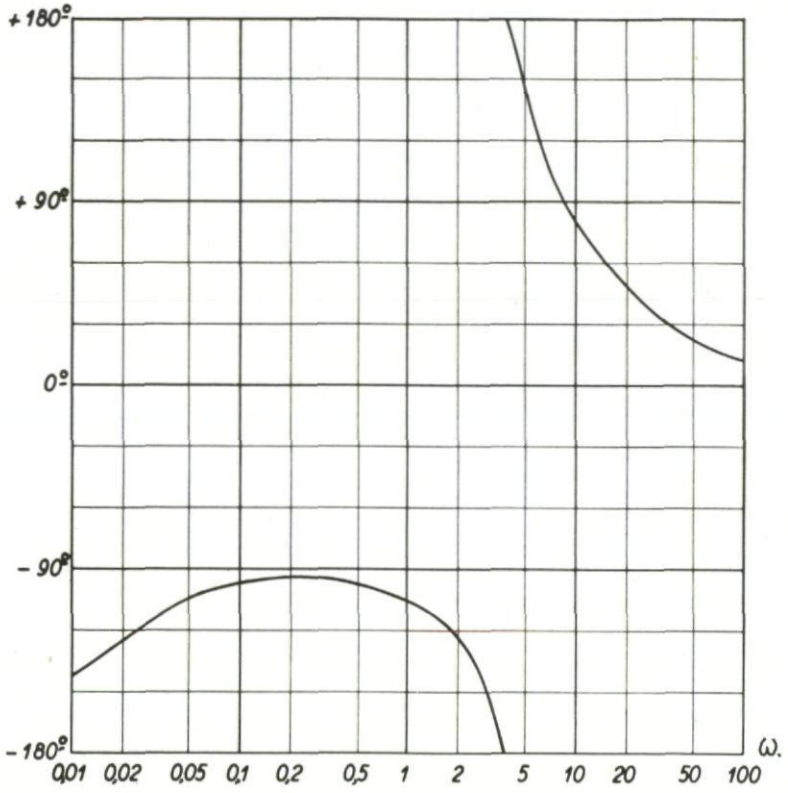

Fig. 213(b) Frequency response; r produced by $-\delta_a$, phase

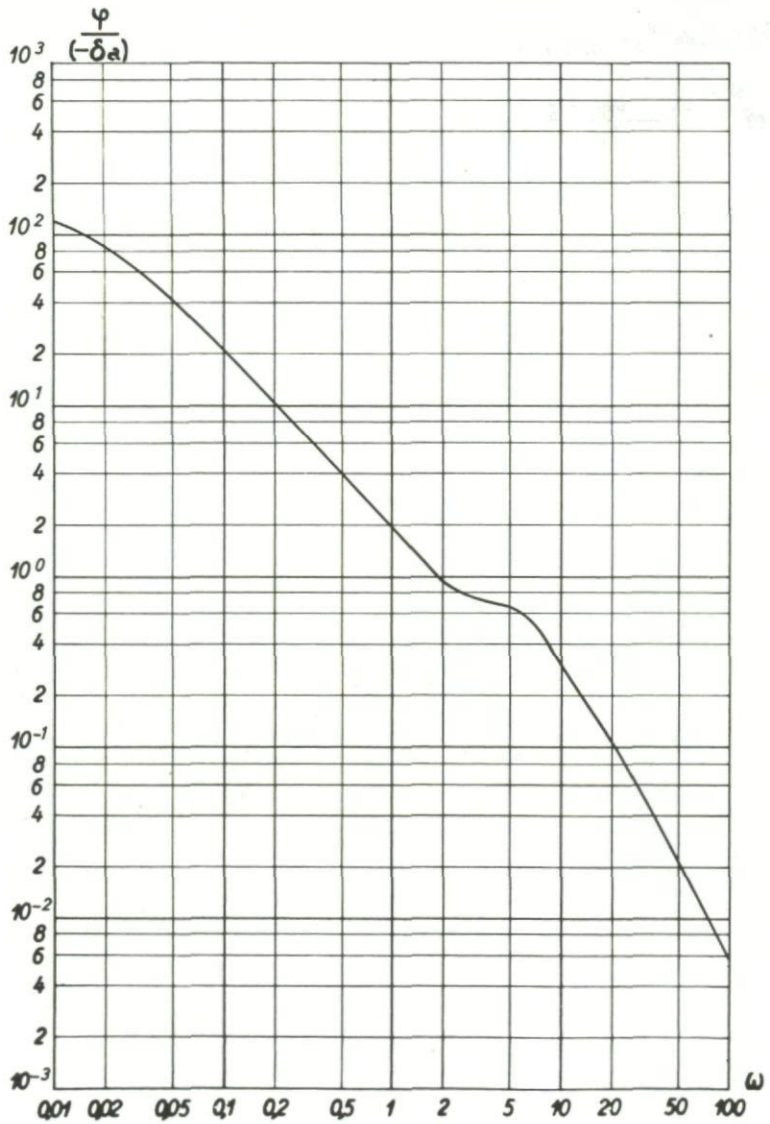

Fig. 214(a) Frequency response; φ produced by $-\delta_a$, amplitude

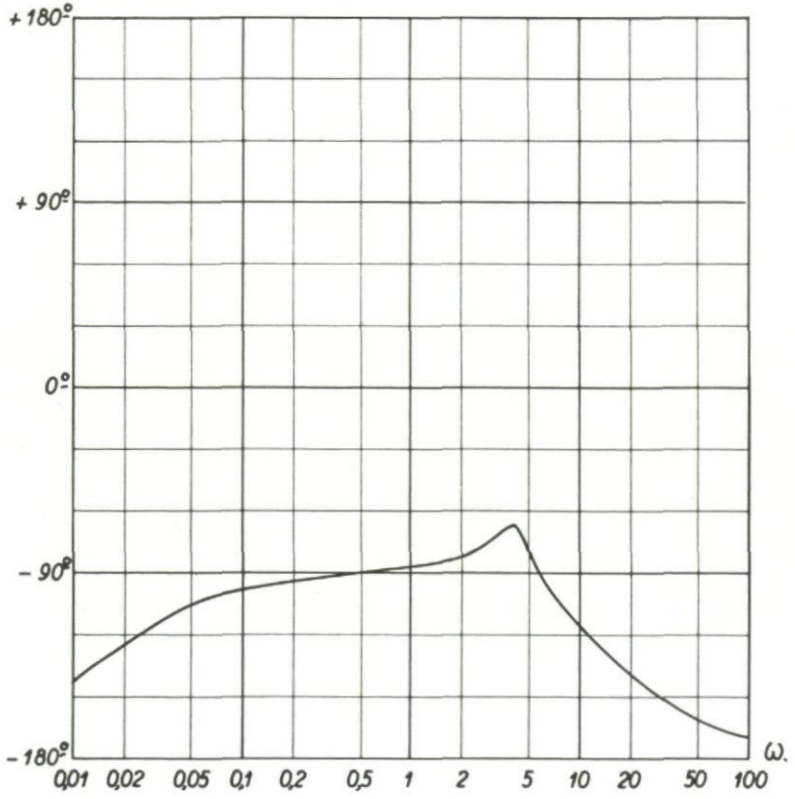

Fig. 214(b) Frequency response; φ produced by $-\delta_a$, phase

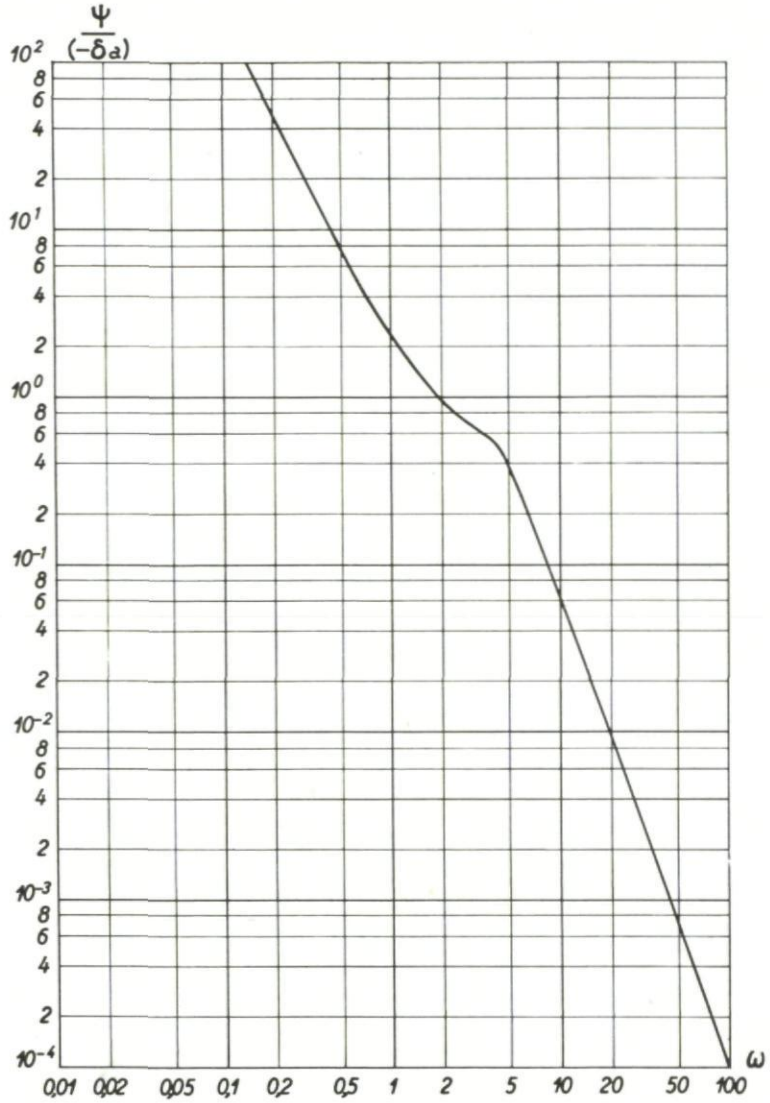

Fig. 215(a) Frequency response; ψ produced by $-\delta_a$, amplitude

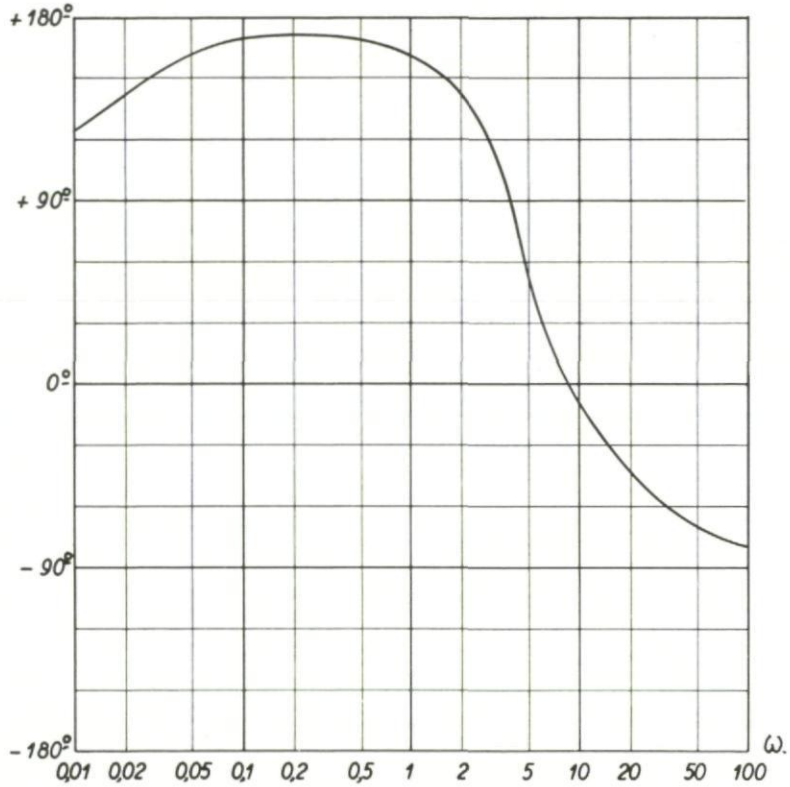

Fig. 215(b) Frequency response; ψ produced by $-\delta_a$, phase

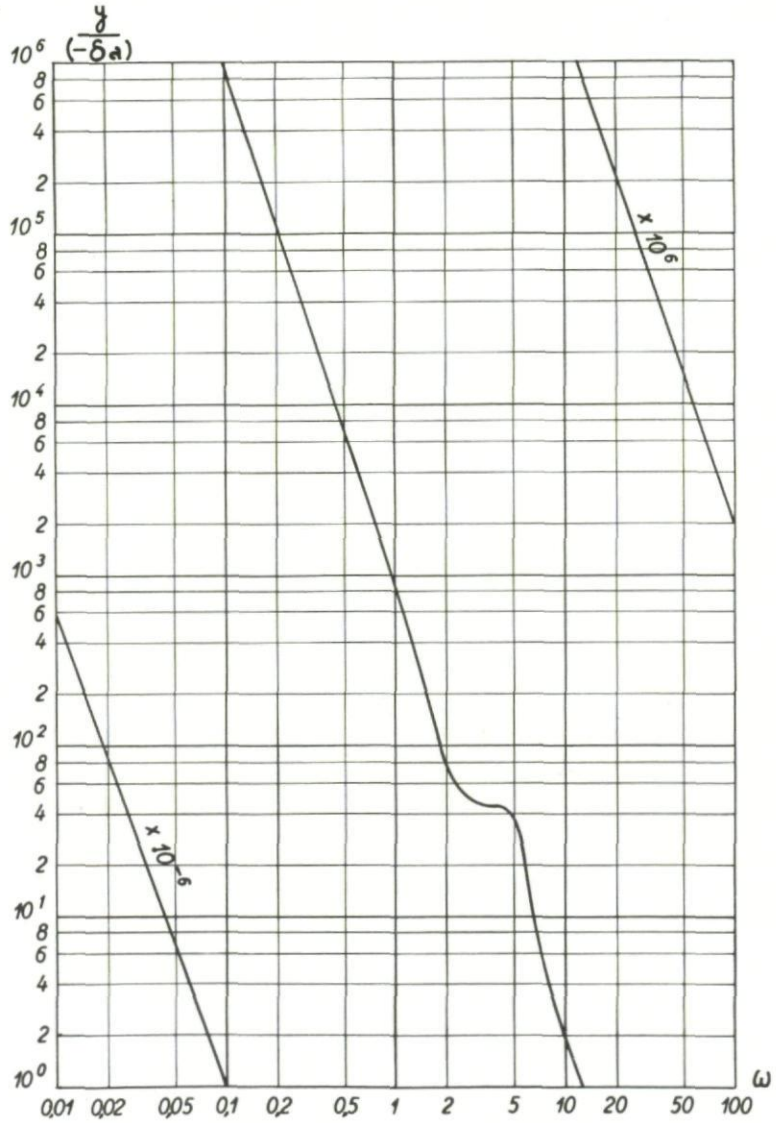

Fig.216(a) Frequency response; y produced by $-\delta_a$, amplitude

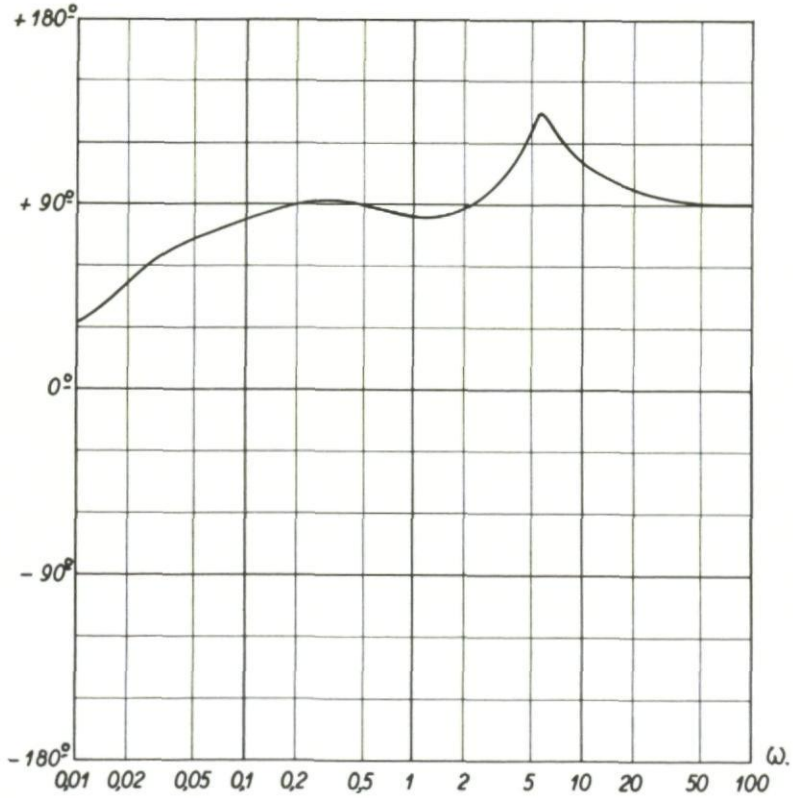

Fig.216(b) Frequency response; y produced by $-\delta_a$, phase

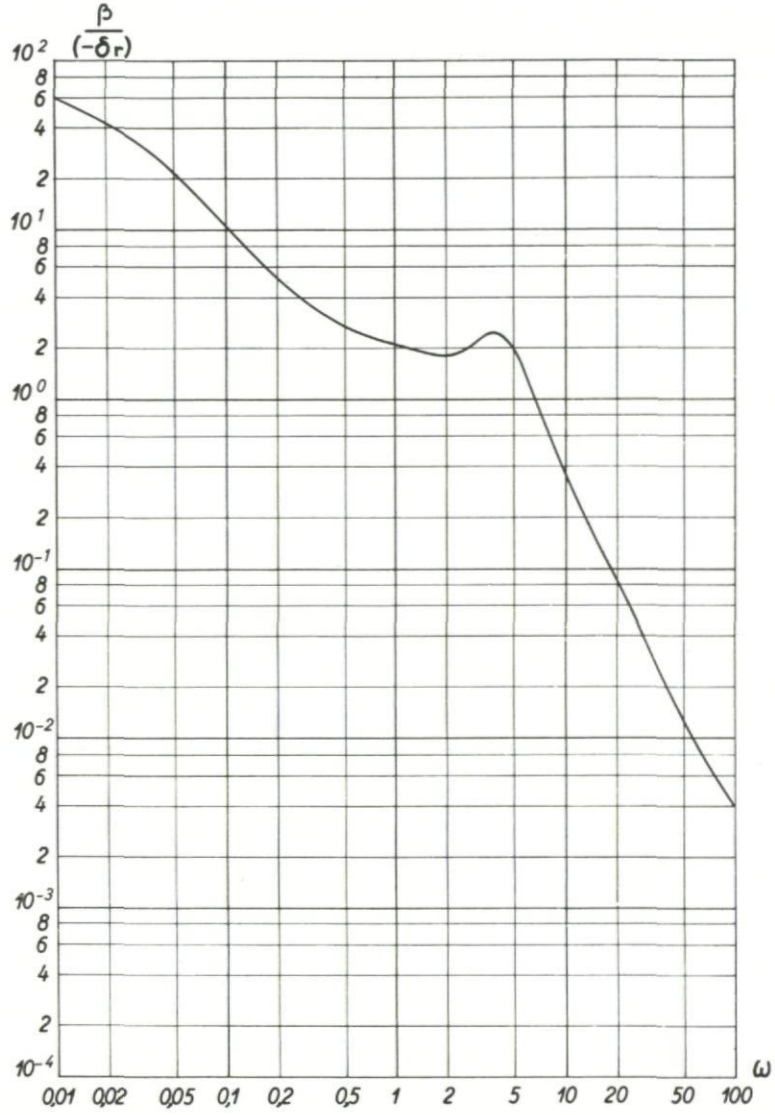

Fig. 217(a) Frequency response; β produced by $-\delta_r$, amplitude

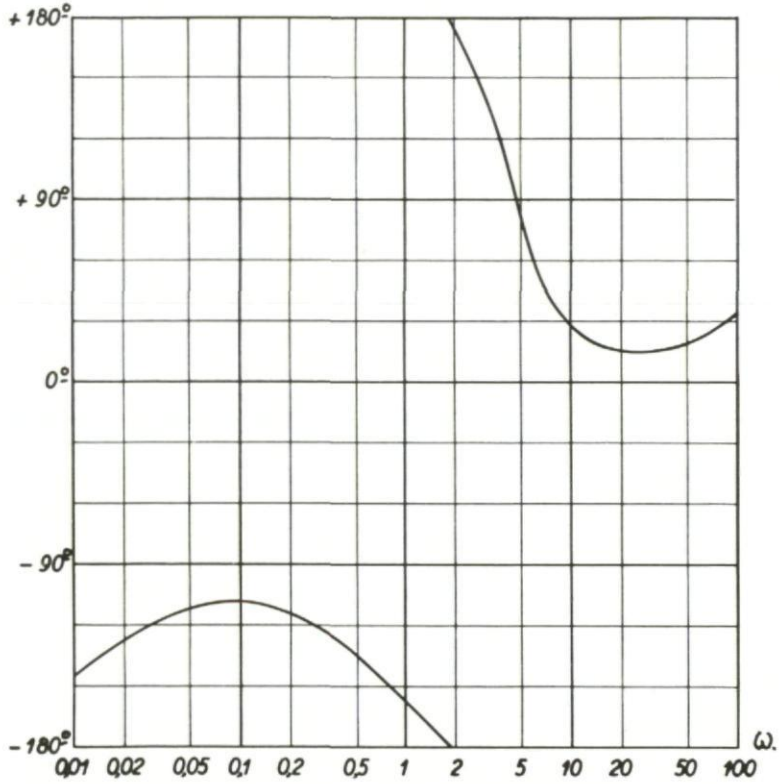

Fig. 217(b) Frequency response; β produced by $-\delta_r$, phase

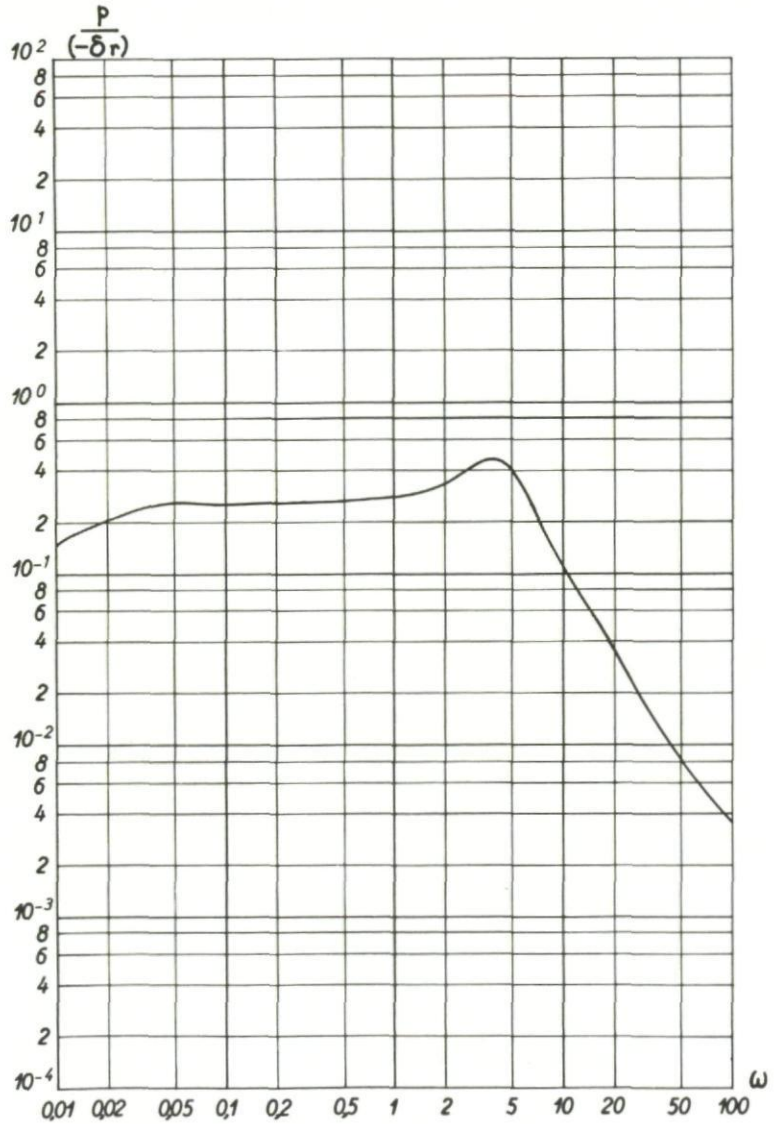

Fig. 218(a) Frequency response; p produced by $-\delta_r$, amplitude

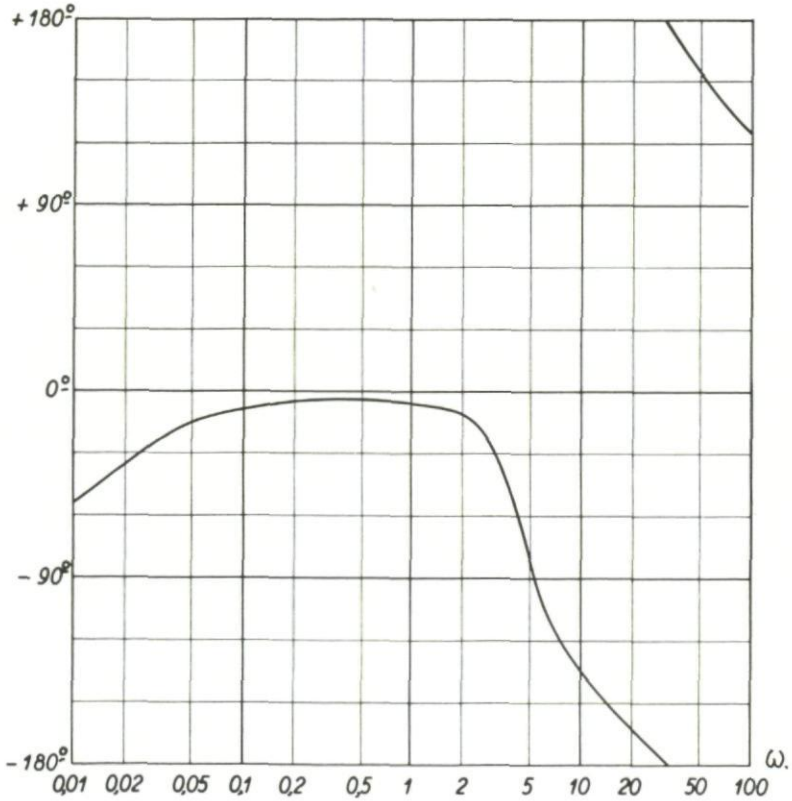

Fig. 218(b) Frequency response; p produced by $-\delta_r$, phase

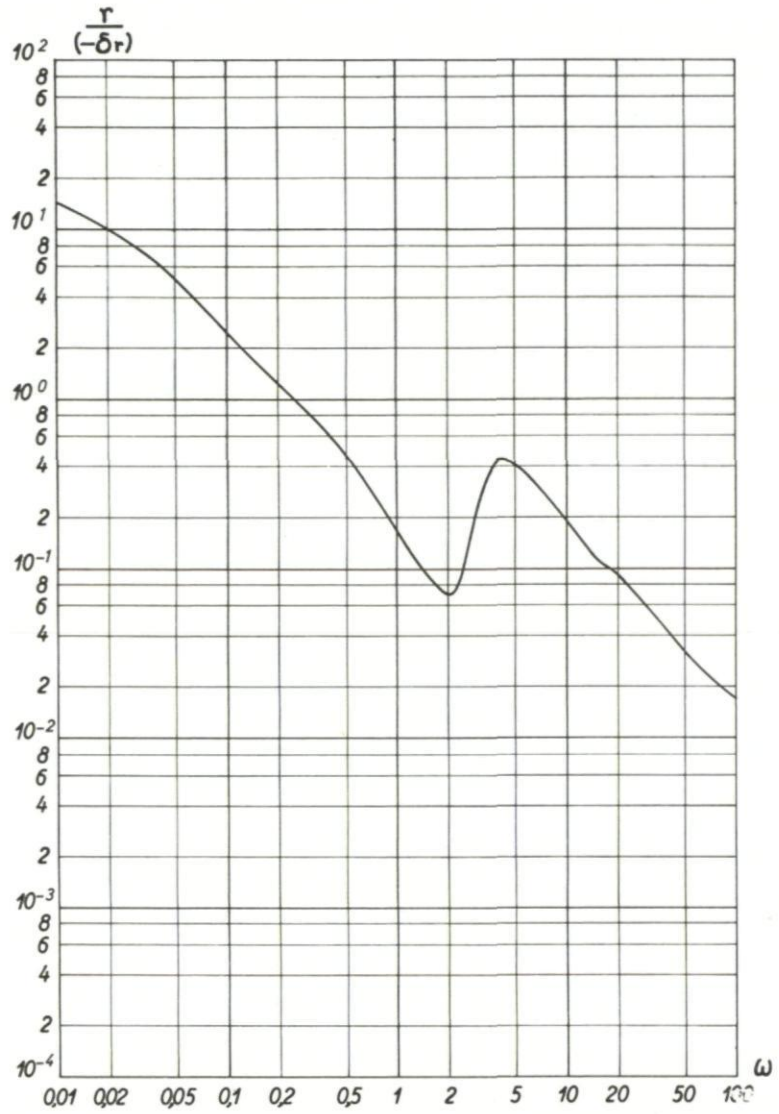

Fig. 219(a) Frequency response; r produced by $-\delta_r$, amplitude

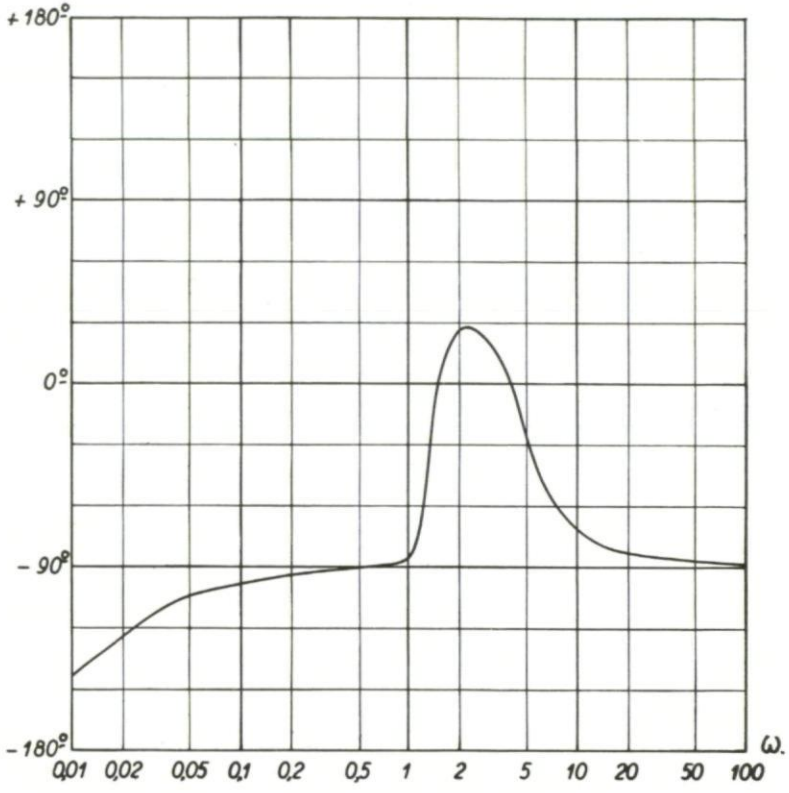

Fig. 219(b) Frequency response; r produced by $-\delta_r$, phase

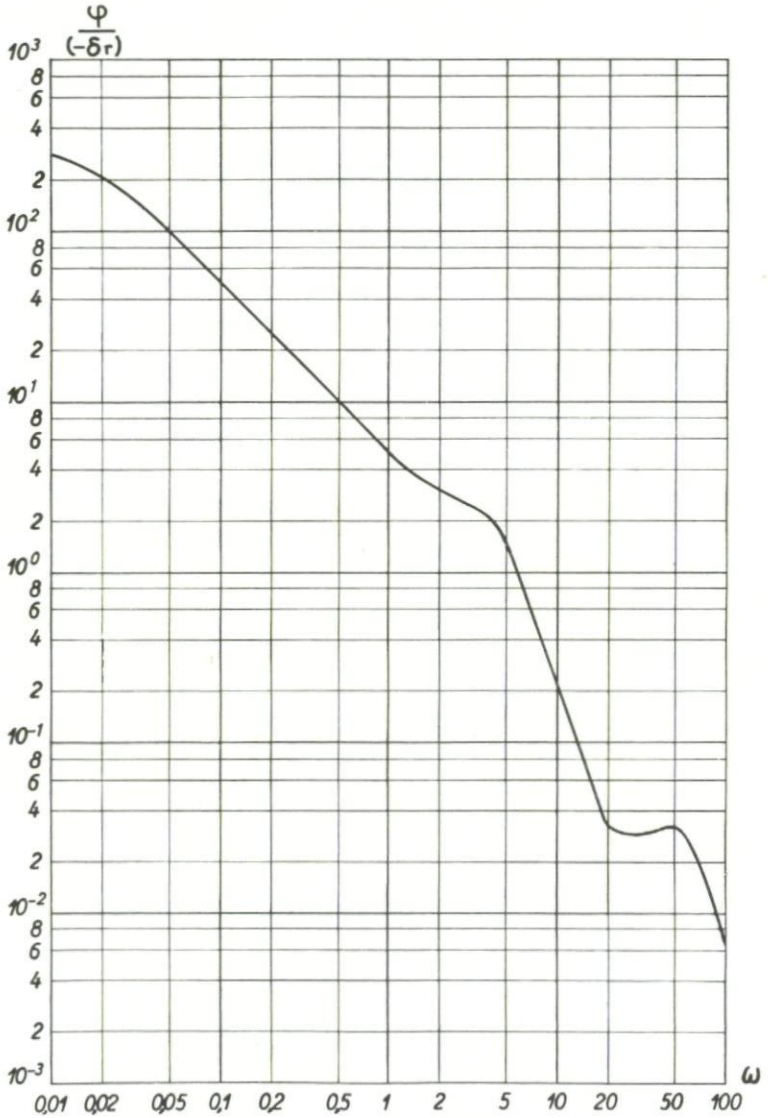

Fig. 220(a) Frequency response; φ produced by $-\delta_r$, amplitude

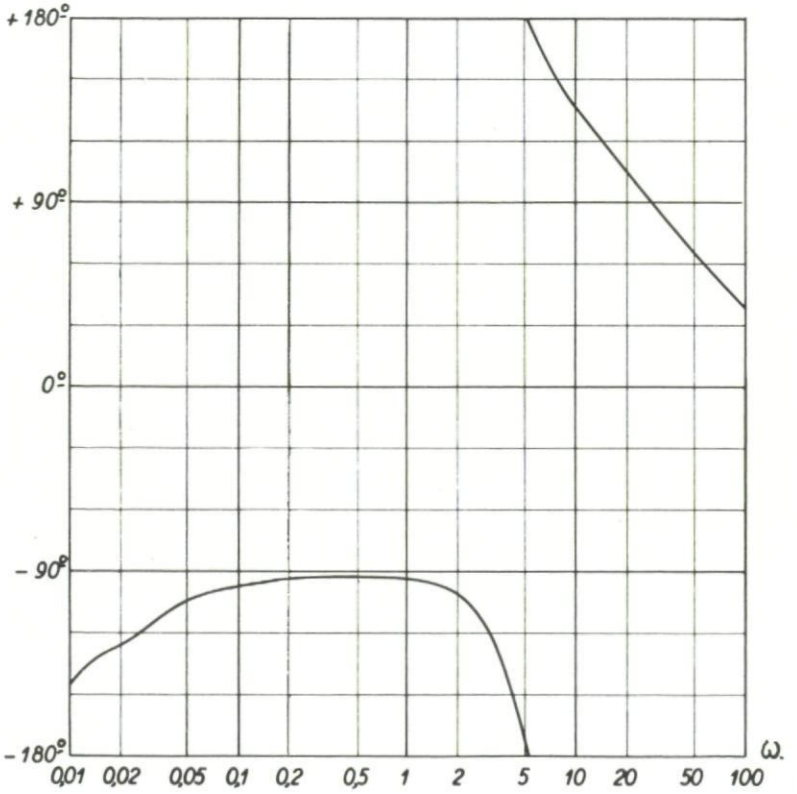

Fig. 220(b) Frequency response; φ produced by $-\delta_r$, phase

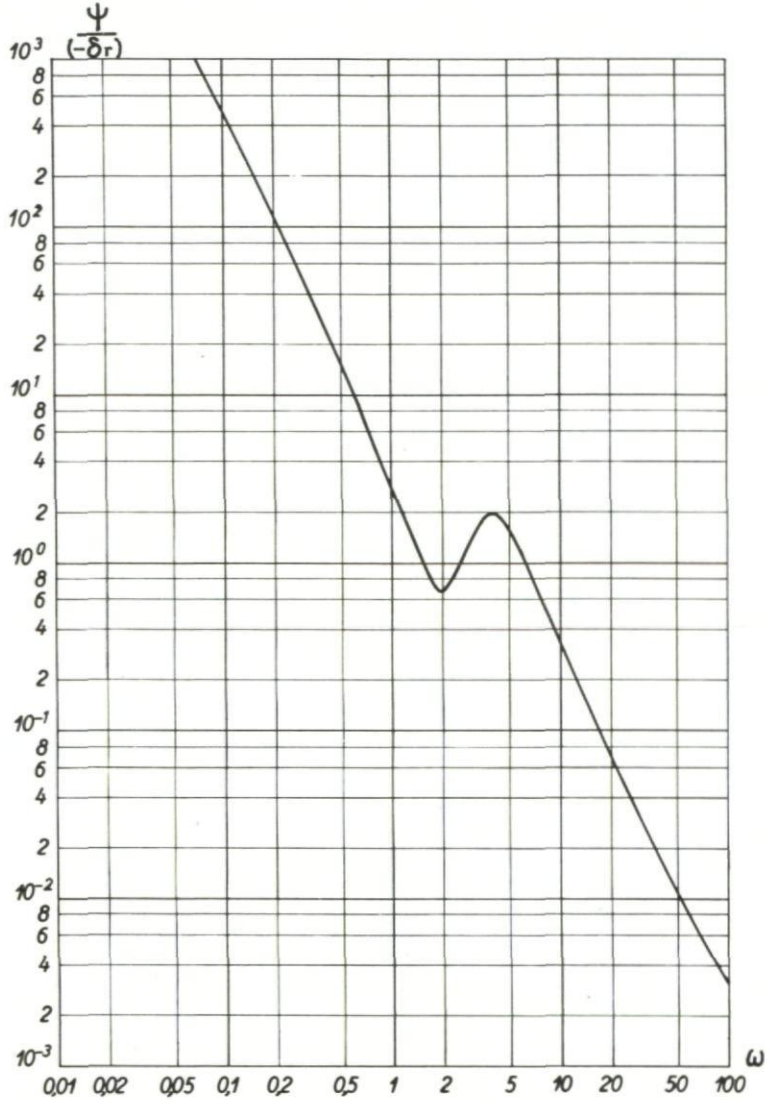

Fig. 221(a) Frequency response; ψ produced by $-\delta_r$, amplitude

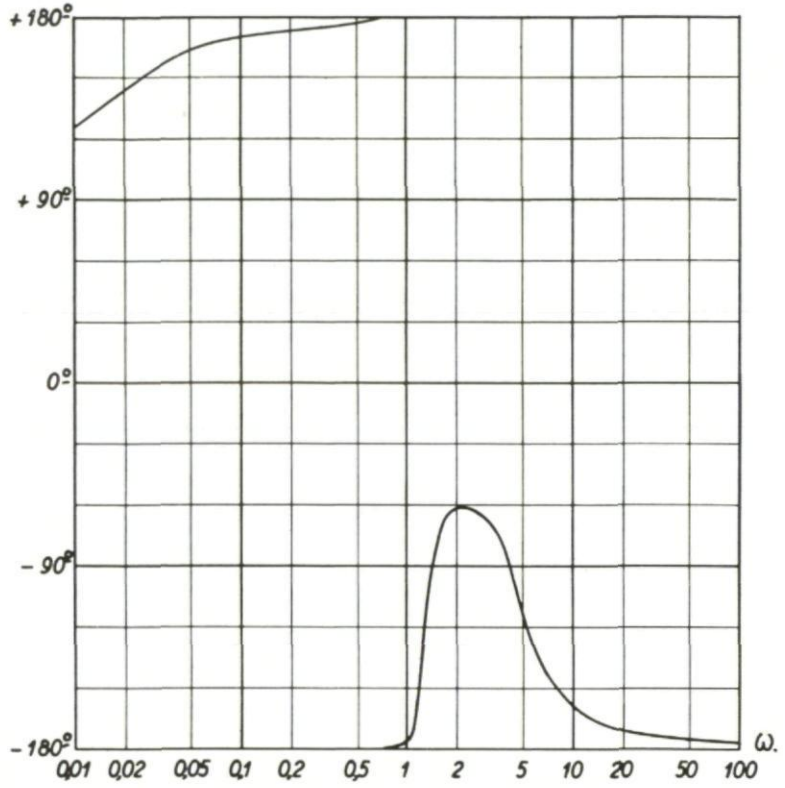

Fig. 221(b) Frequency response; ψ produced by $-\delta_r$, phase

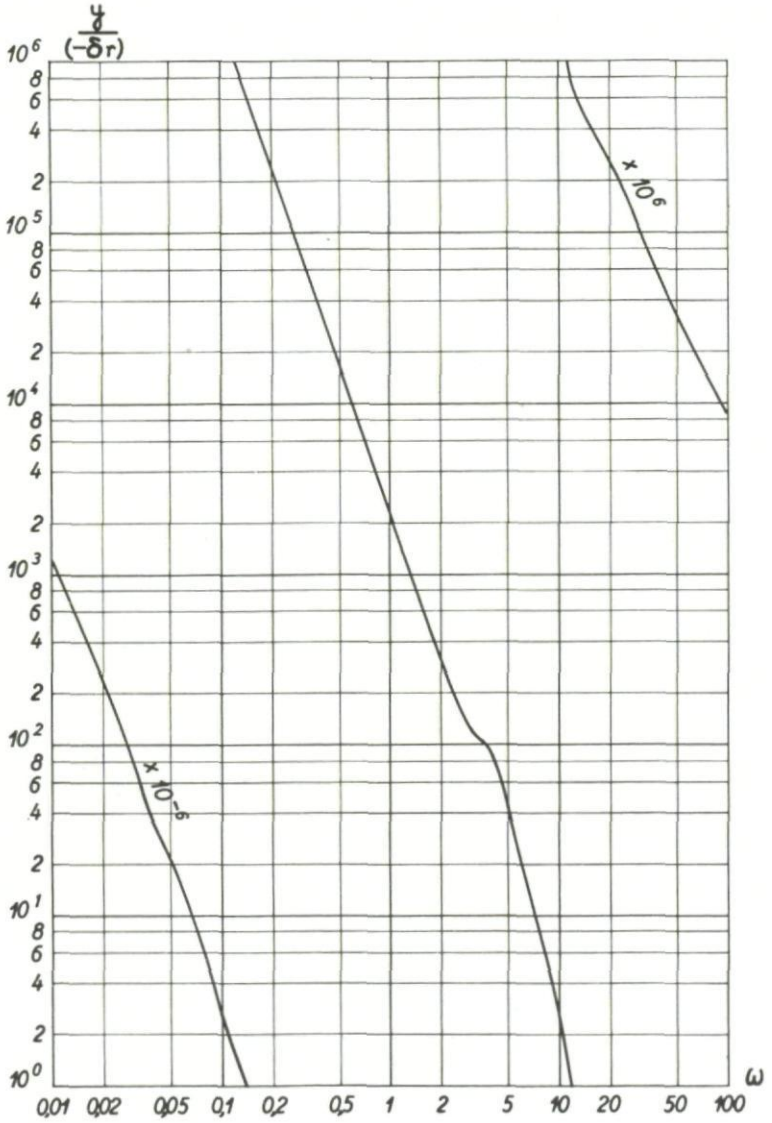

Fig. 222(a) Frequency response; y produced by $-\delta_r$, amplitude

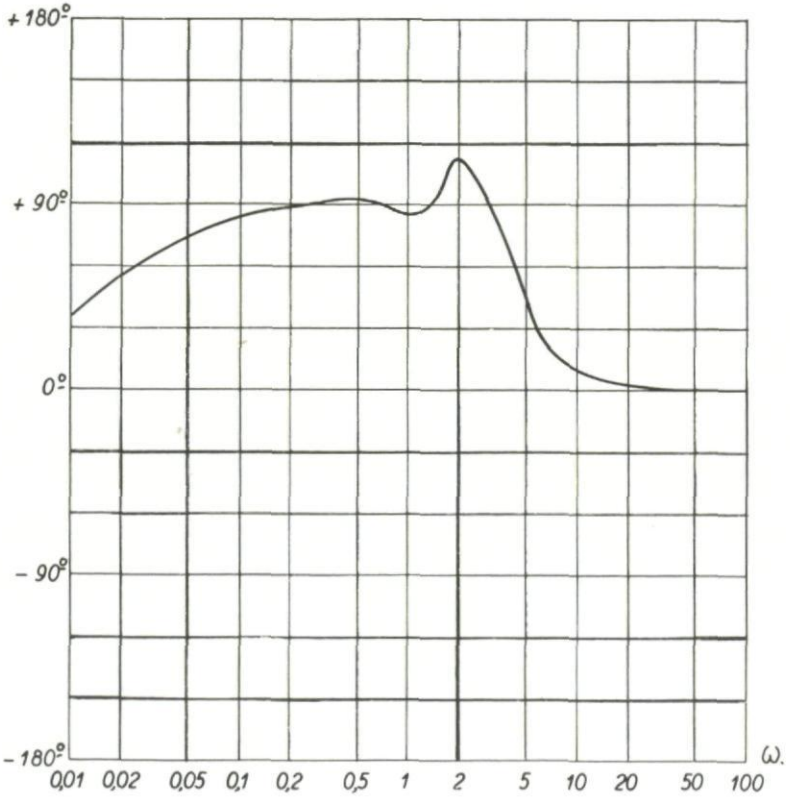

Fig. 222(b) Frequency response; y produced by $-\delta_r$, phase

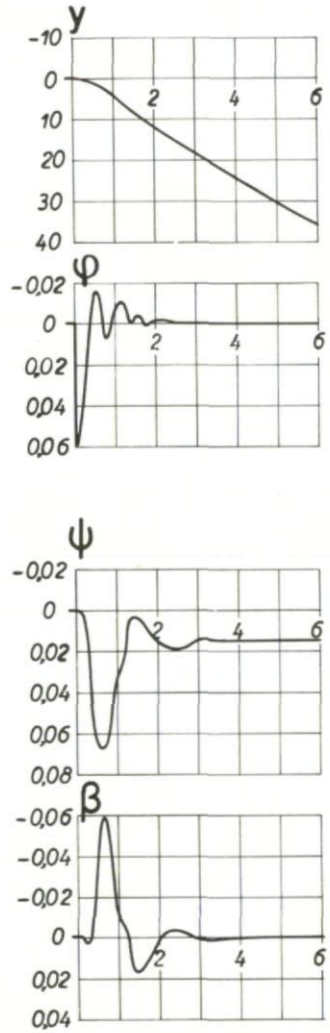

Fig. 223(a) Response of an aircraft controlled by $\delta_a = A_3\varphi$

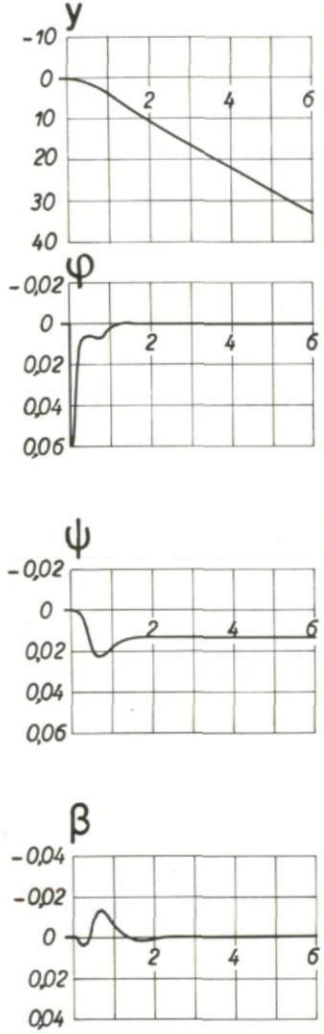

Fig. 223(b) Response of an aircraft controlled by $\delta_a = A_3\varphi$

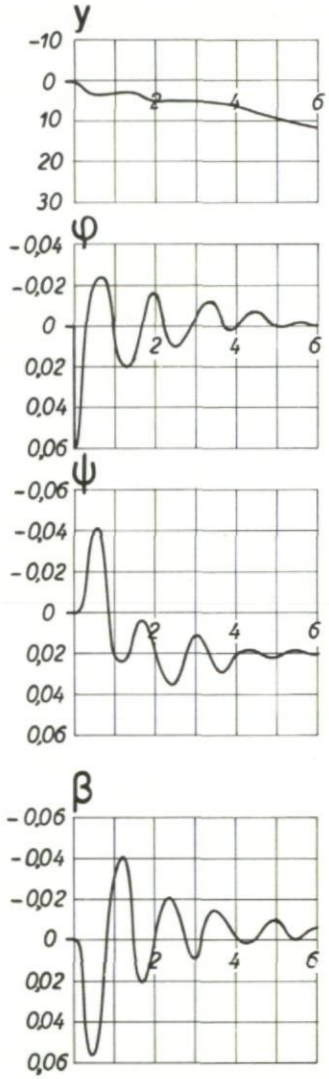

Fig. 223(c) Response of an aircraft controlled by $\delta_r = B_3\varphi$

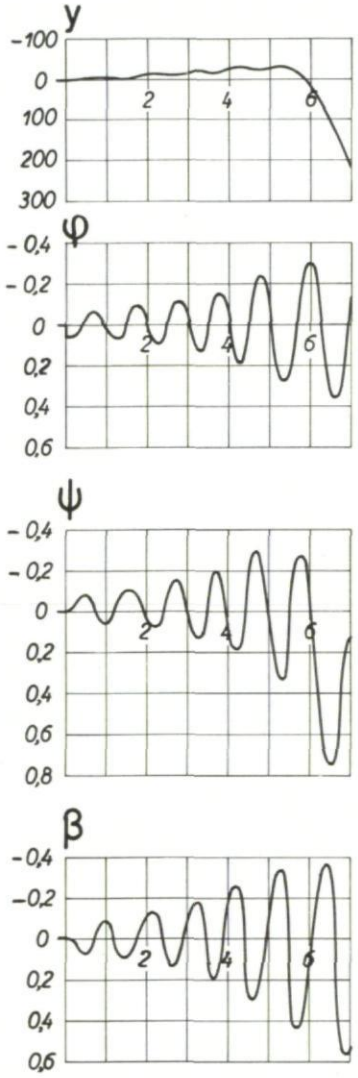

Fig. 223(d) Response of an aircraft controlled by $\delta_r = B_3\varphi$

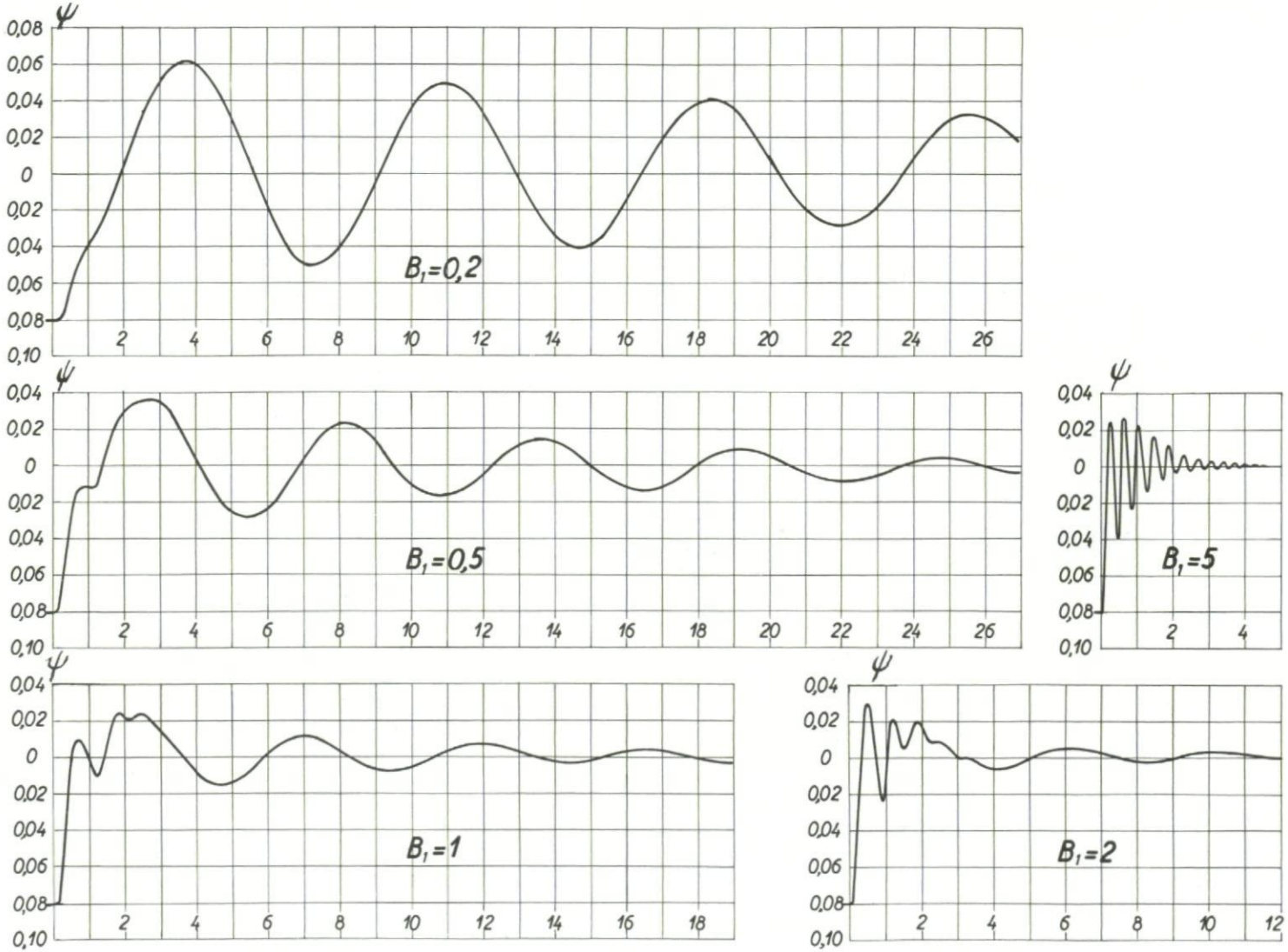

Fig.224 controlled by $\delta_r = B_3\varphi$ craft controlled by $\delta_r = A_3\varphi$

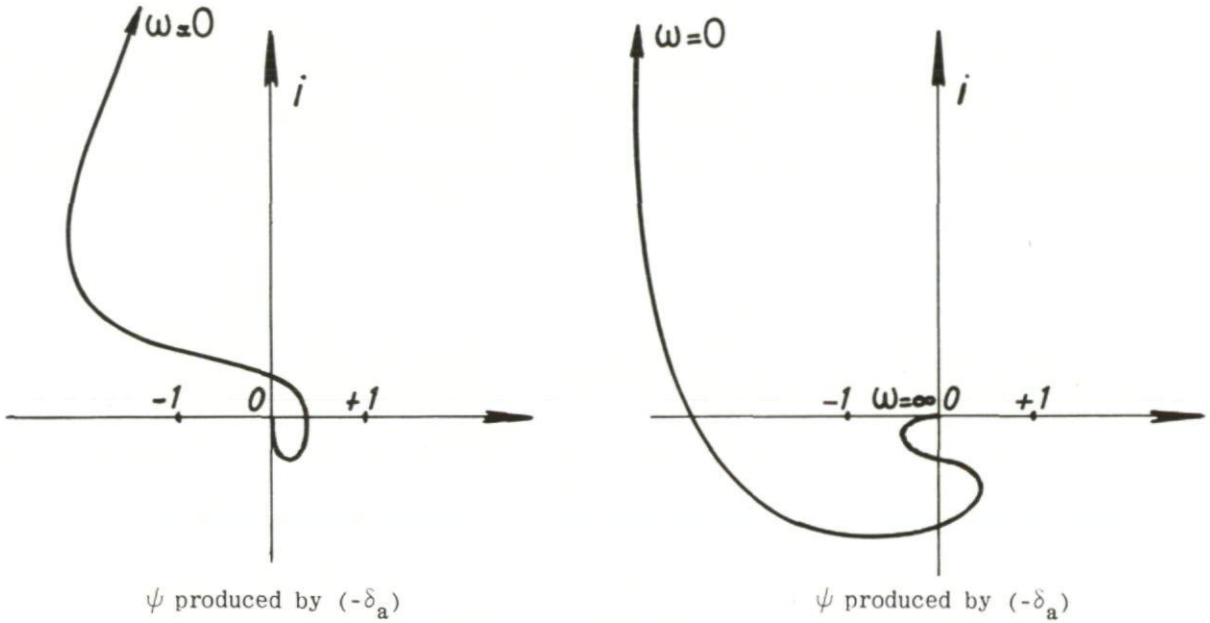

Fig.225 Polar plot of the frequency response in ψ, for δ_a and δ_r inputs

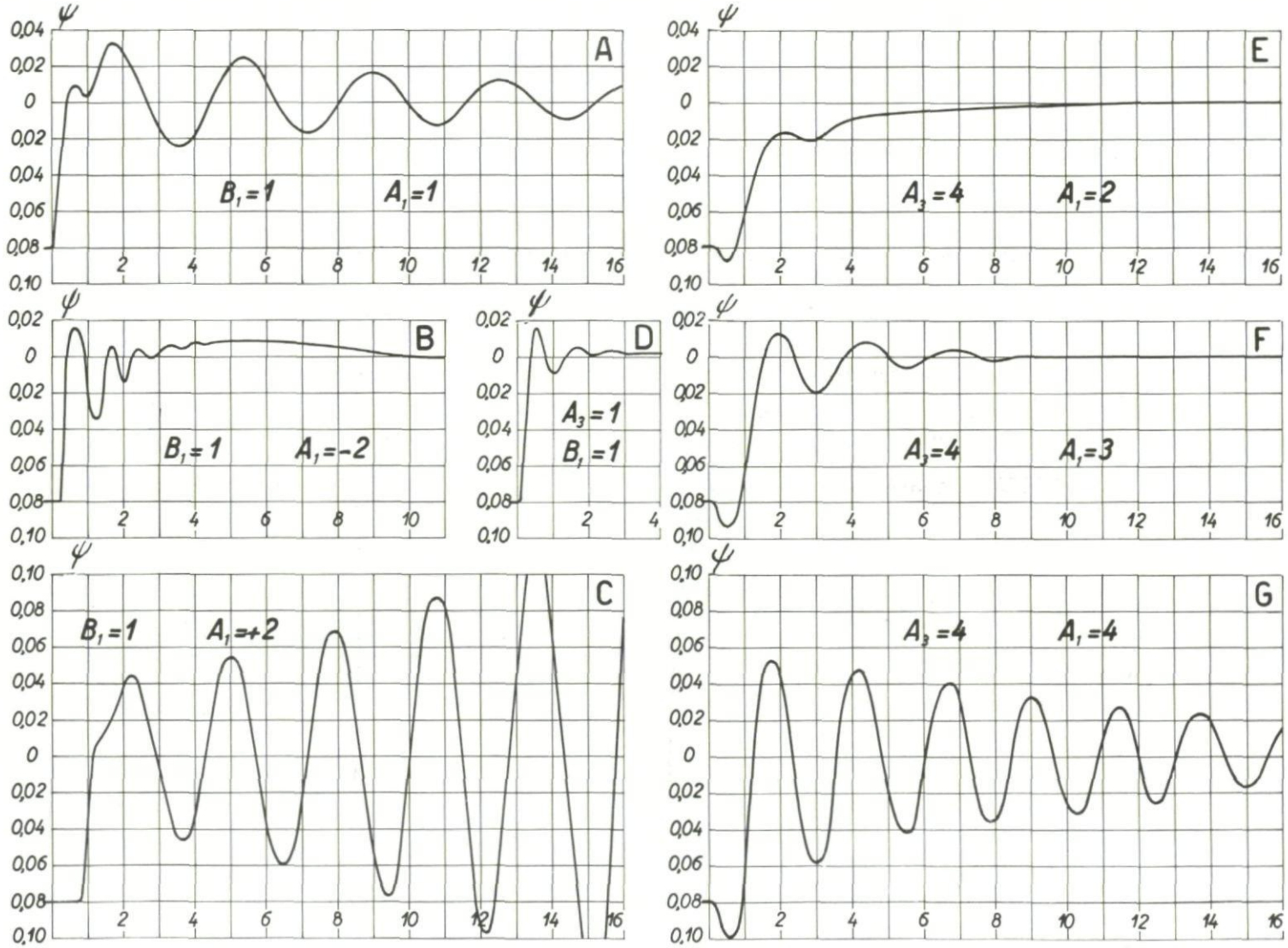

Fig. 226 Deviation of ψ for the aeroplane piloted by various control equations

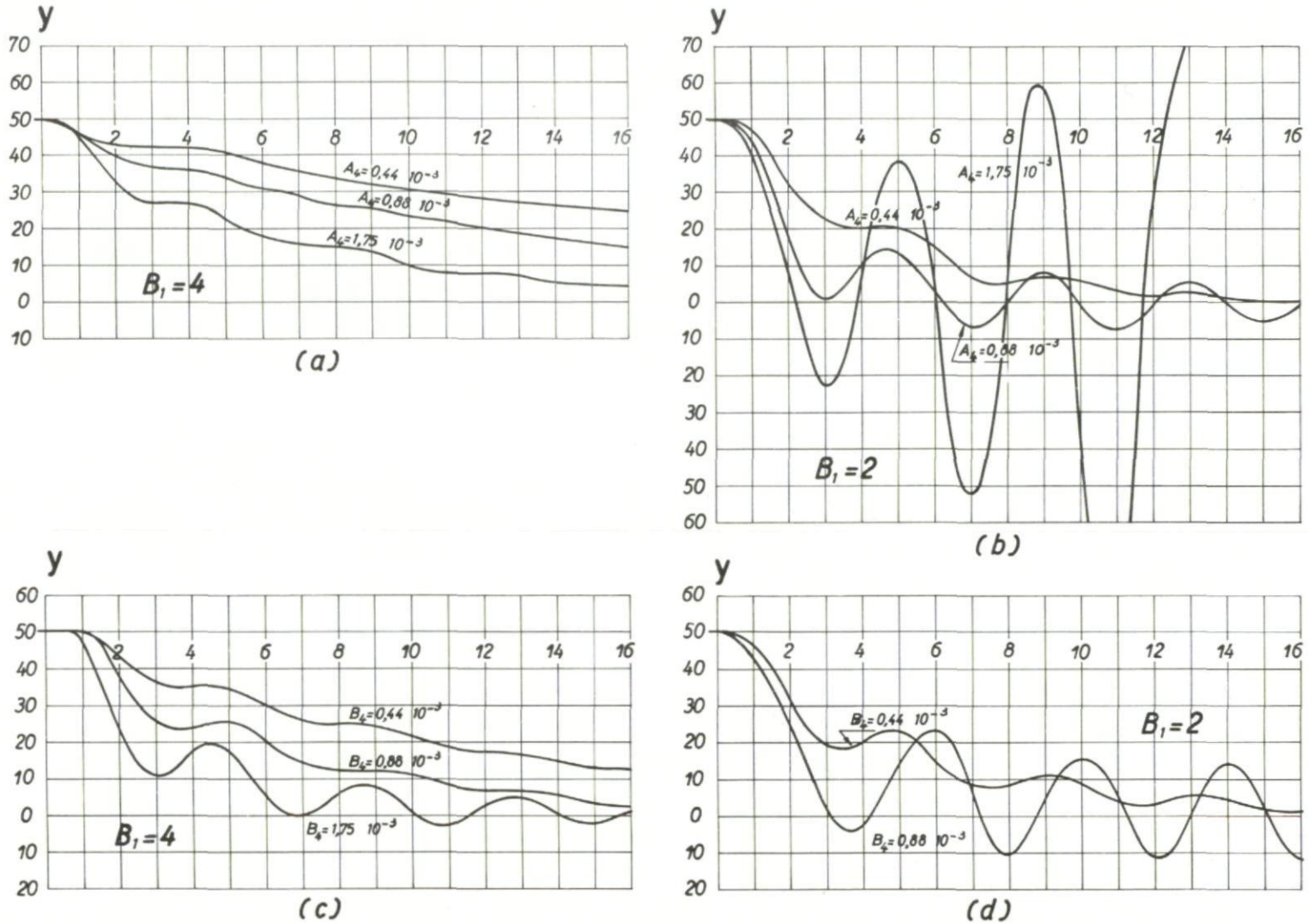

Fig. 227 Deviation of y for a control equation involving terms in A_4, B_4

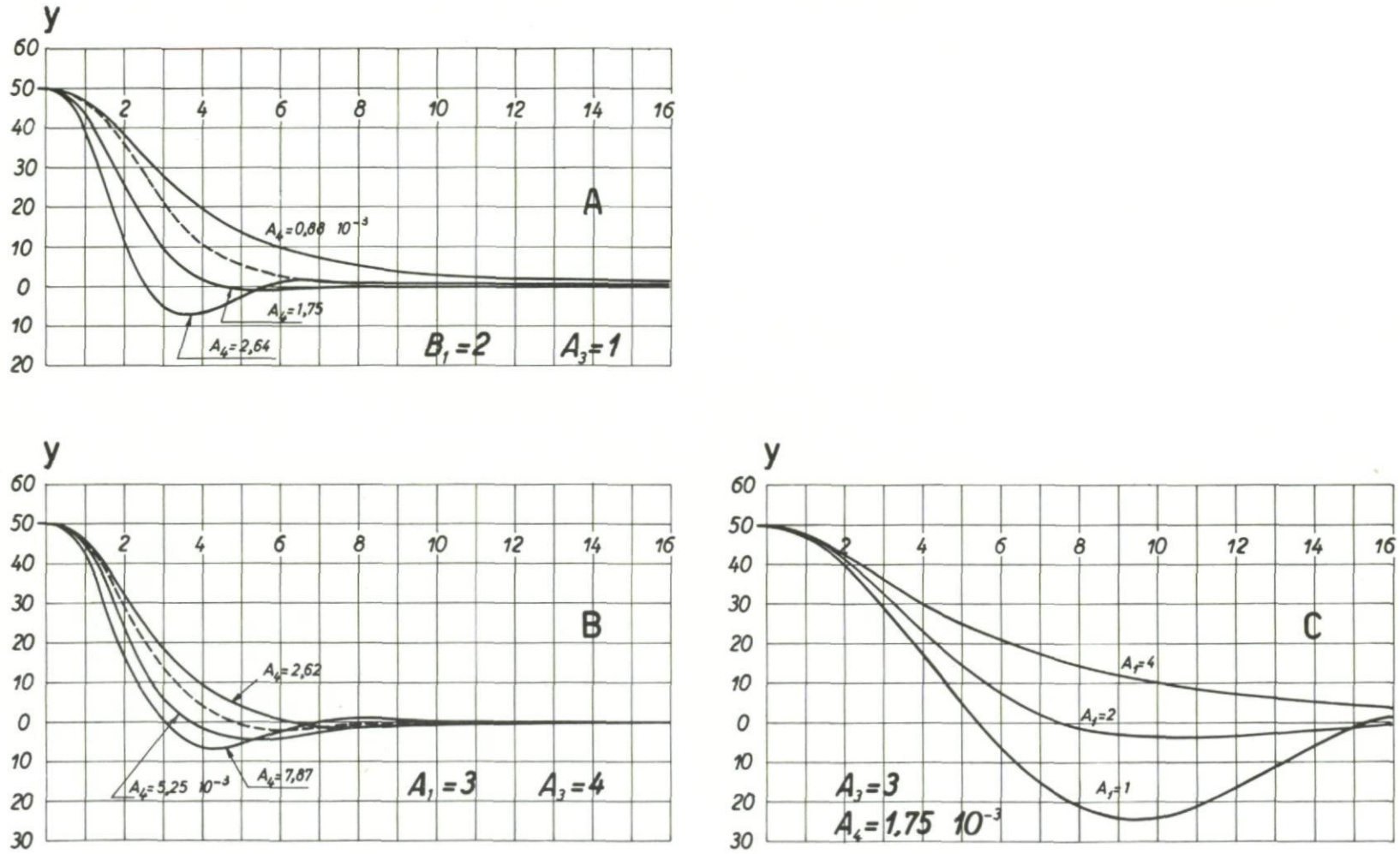

Fig. 228 Deviation of y for a control equation involving terms in A_4, B_4

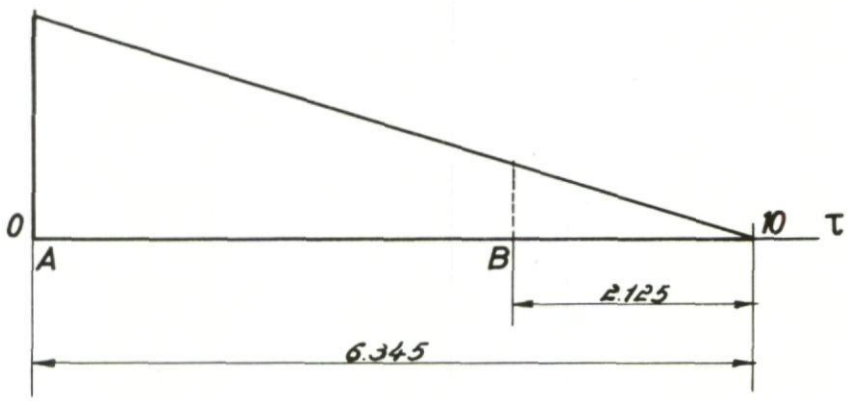

Fig. 229 Steady variation of coefficients $A_ц$ and $B_ц$

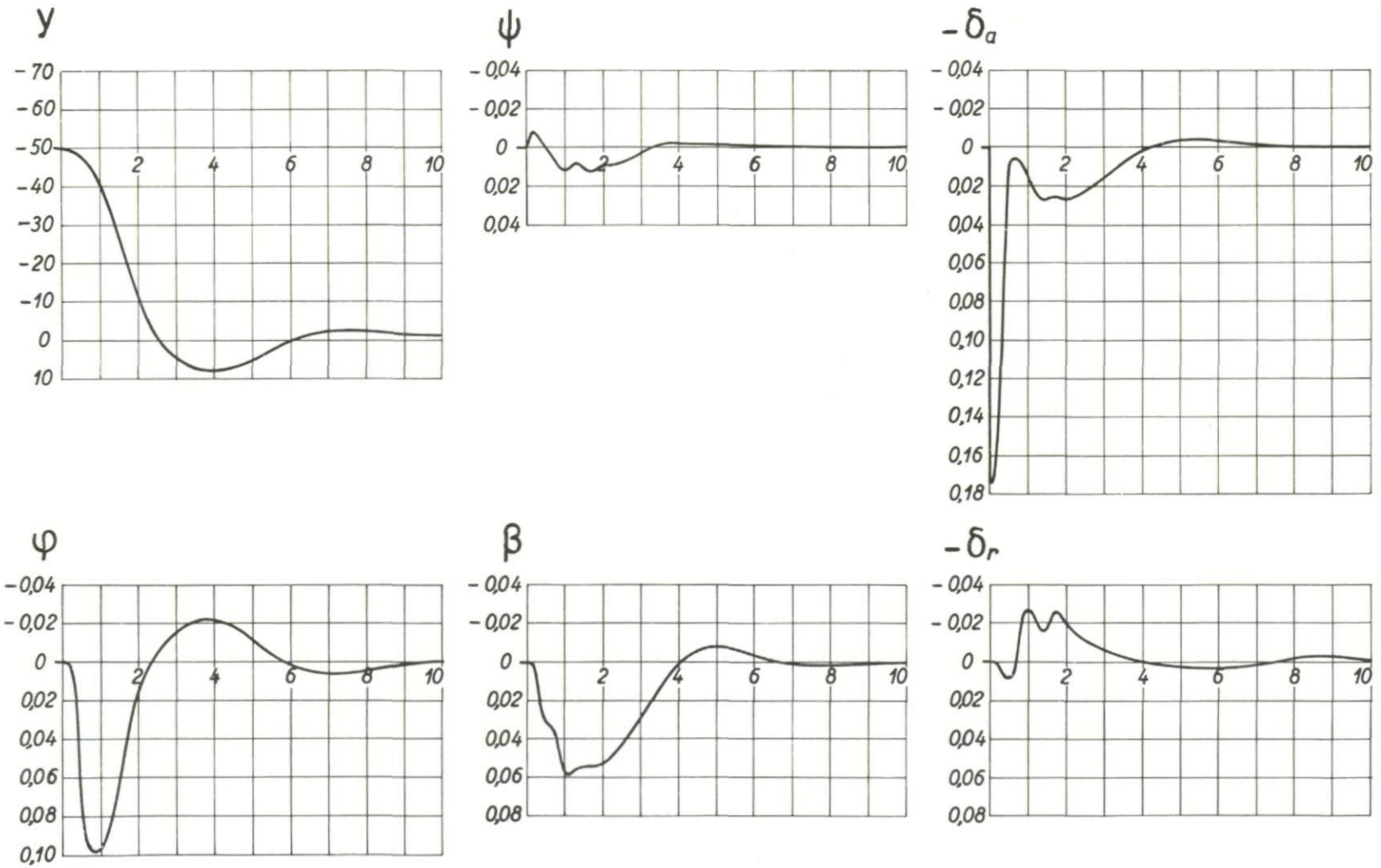

Fig.230 Aircraft response to an initial error y = 50m, case a

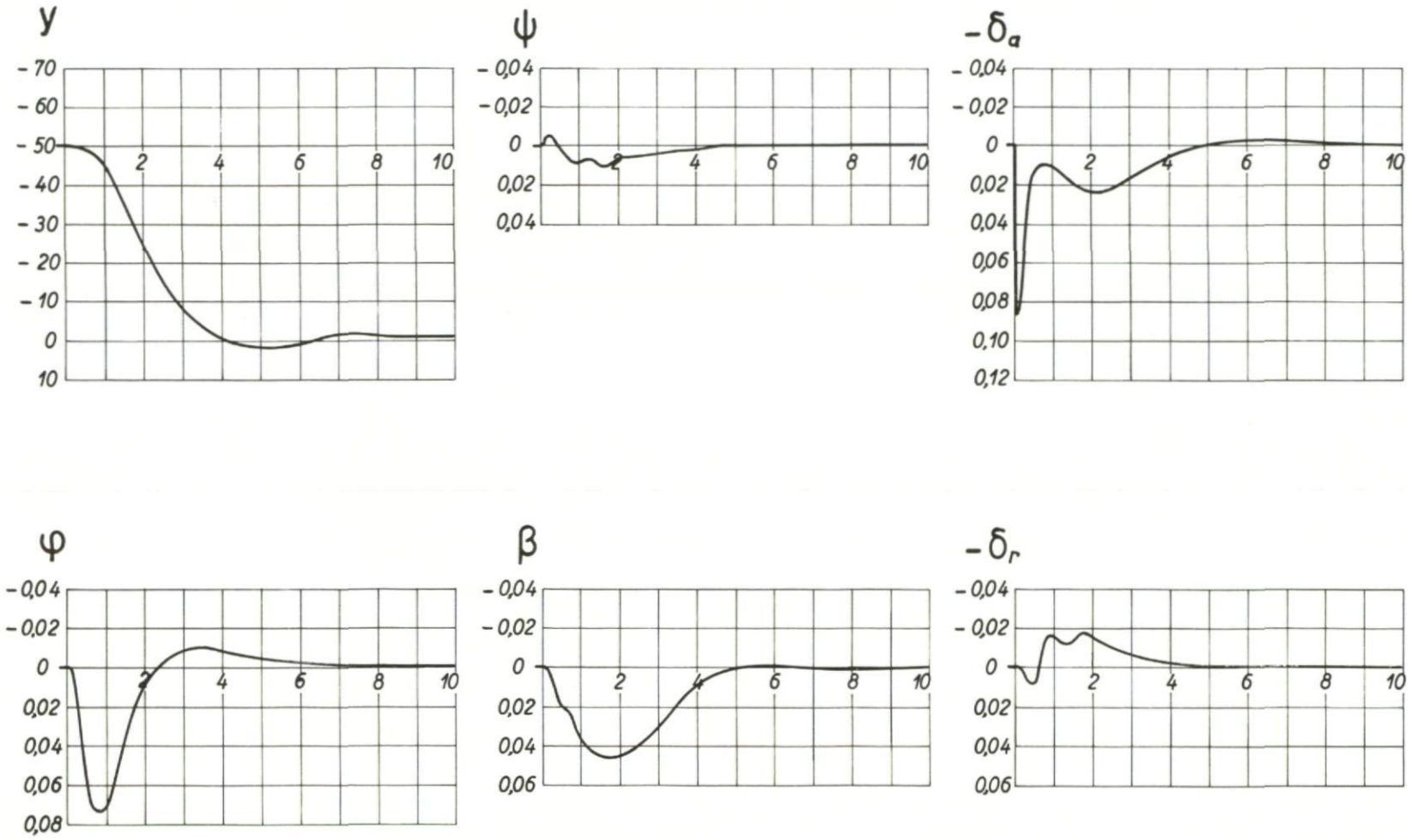

Fig.231 Aircraft response to an initial error y = 50m, case b

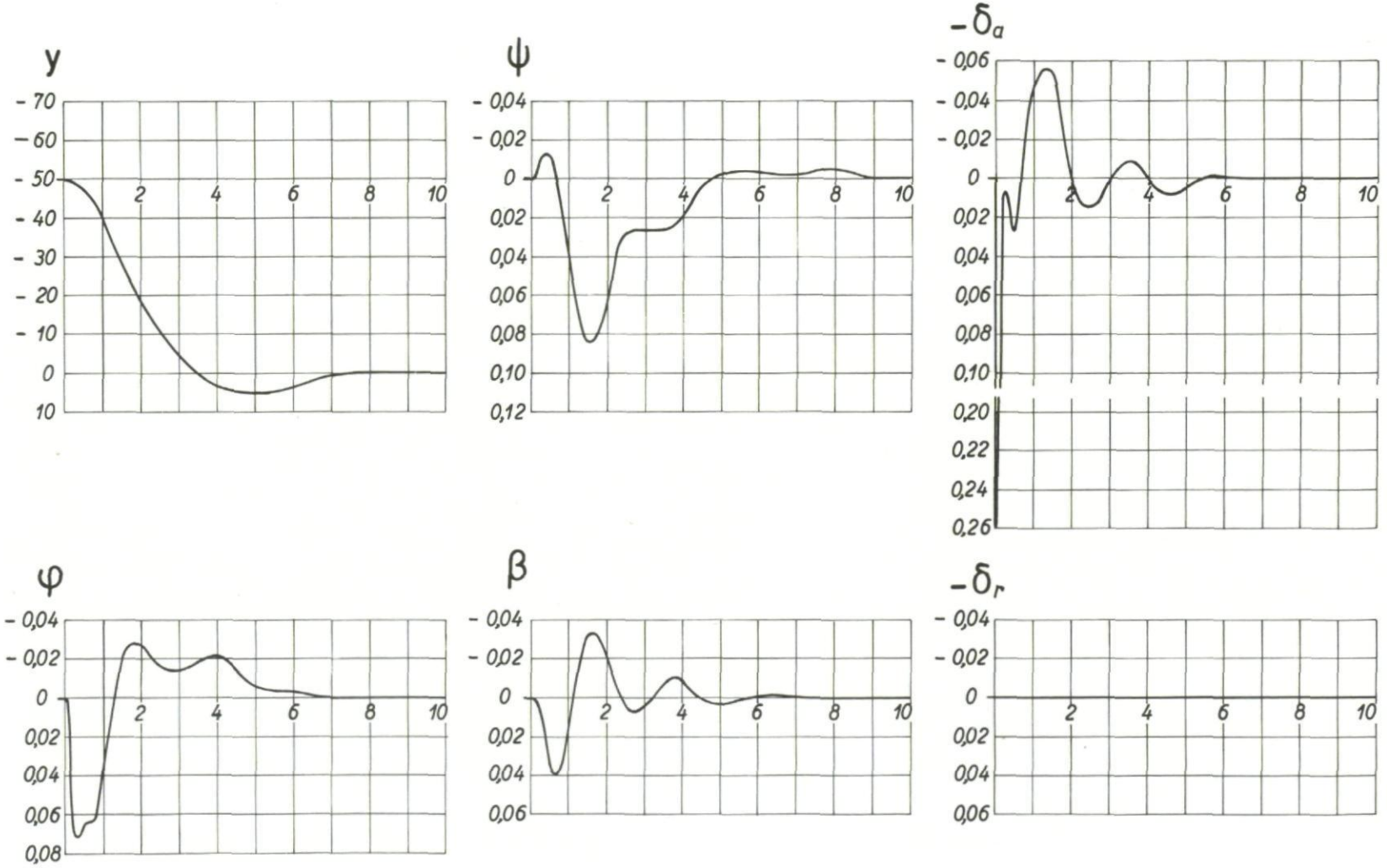

Fig. 232 Aircraft response to an initial error y = 50m, case c

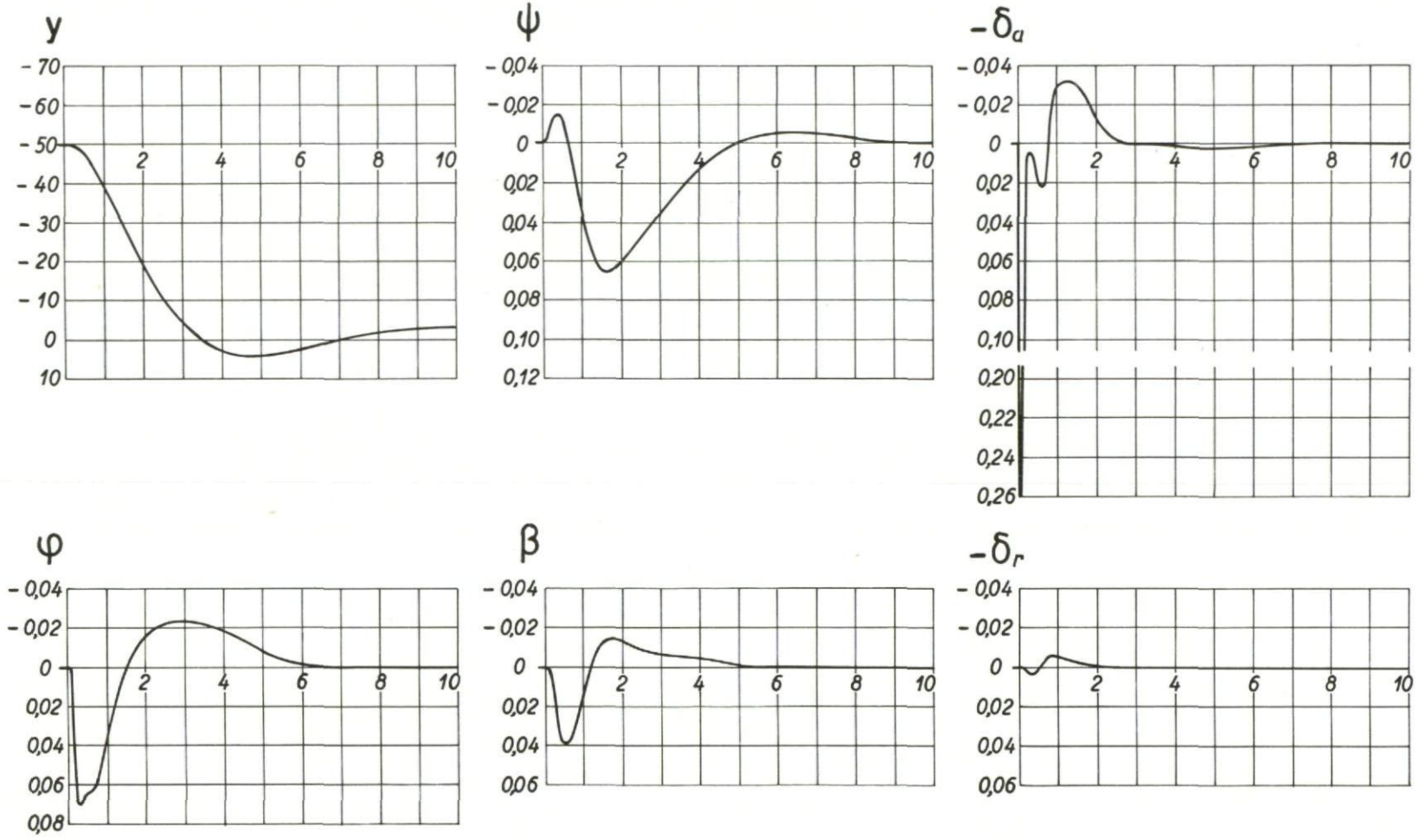

Fig.233 Aircraft response to an initial error y = 50m, case h

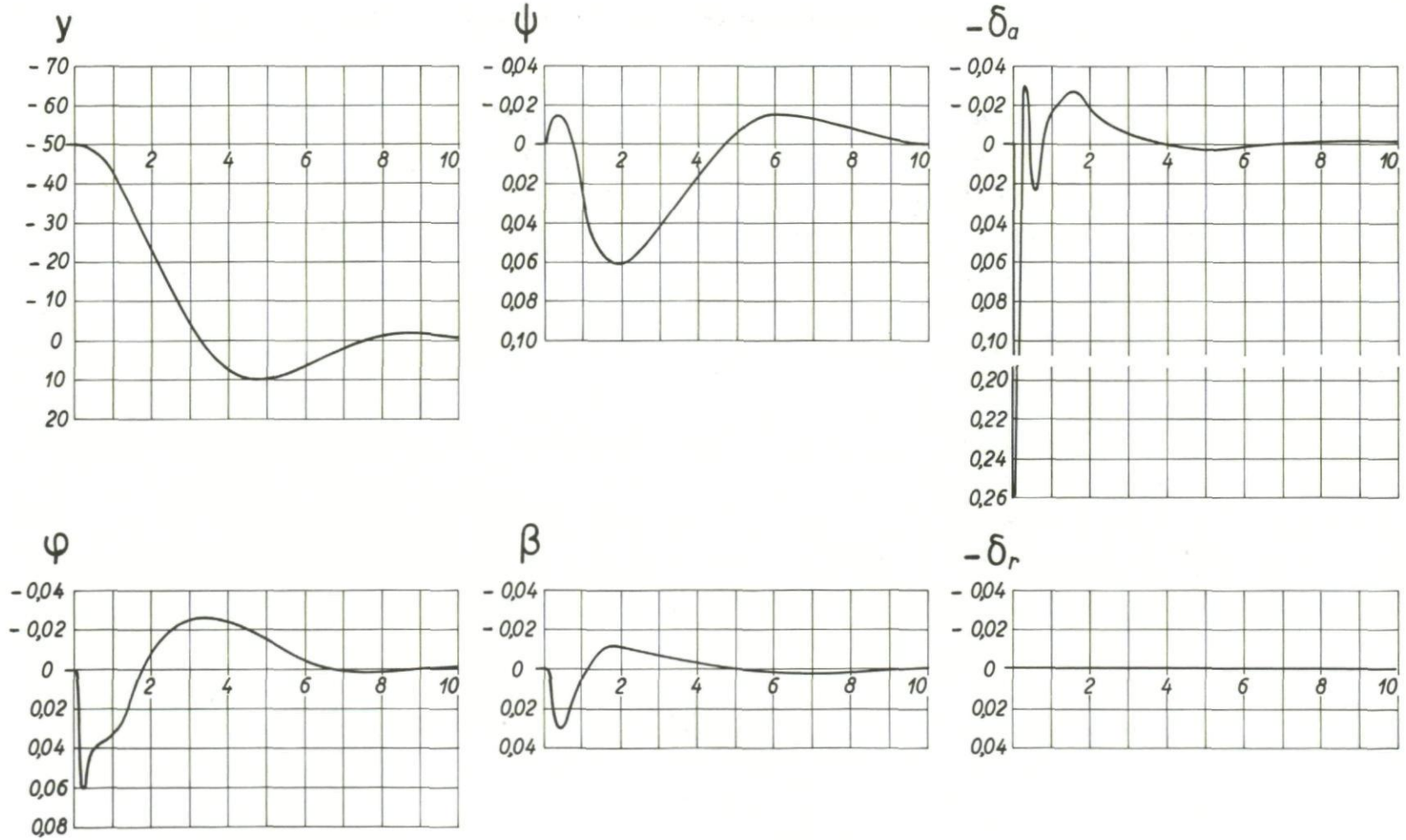

Fig.234 Aircraft response to an initial error y = 50m, case e

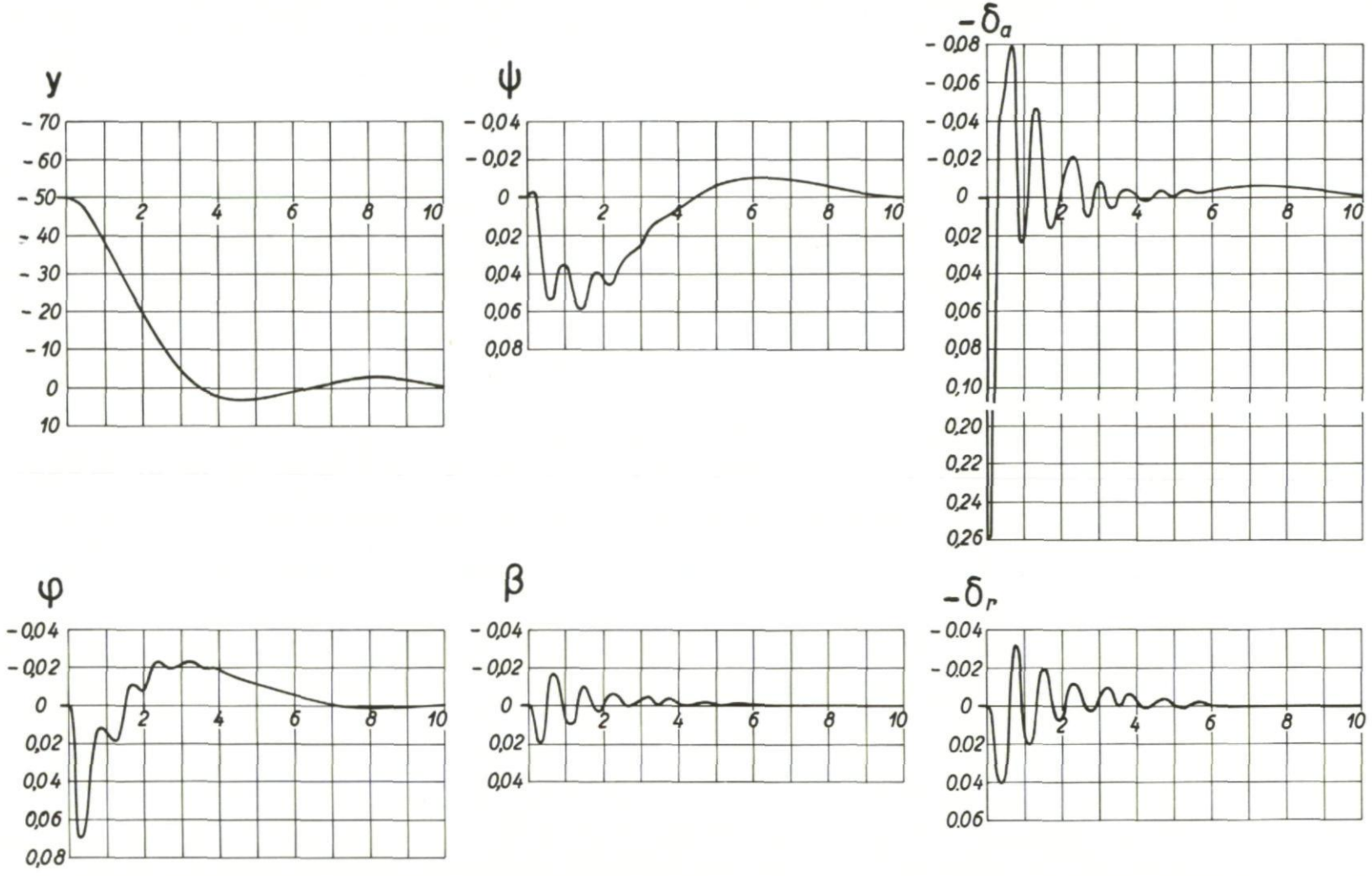

Fig. 235 Aircraft response to an initial error y = 50m, case f

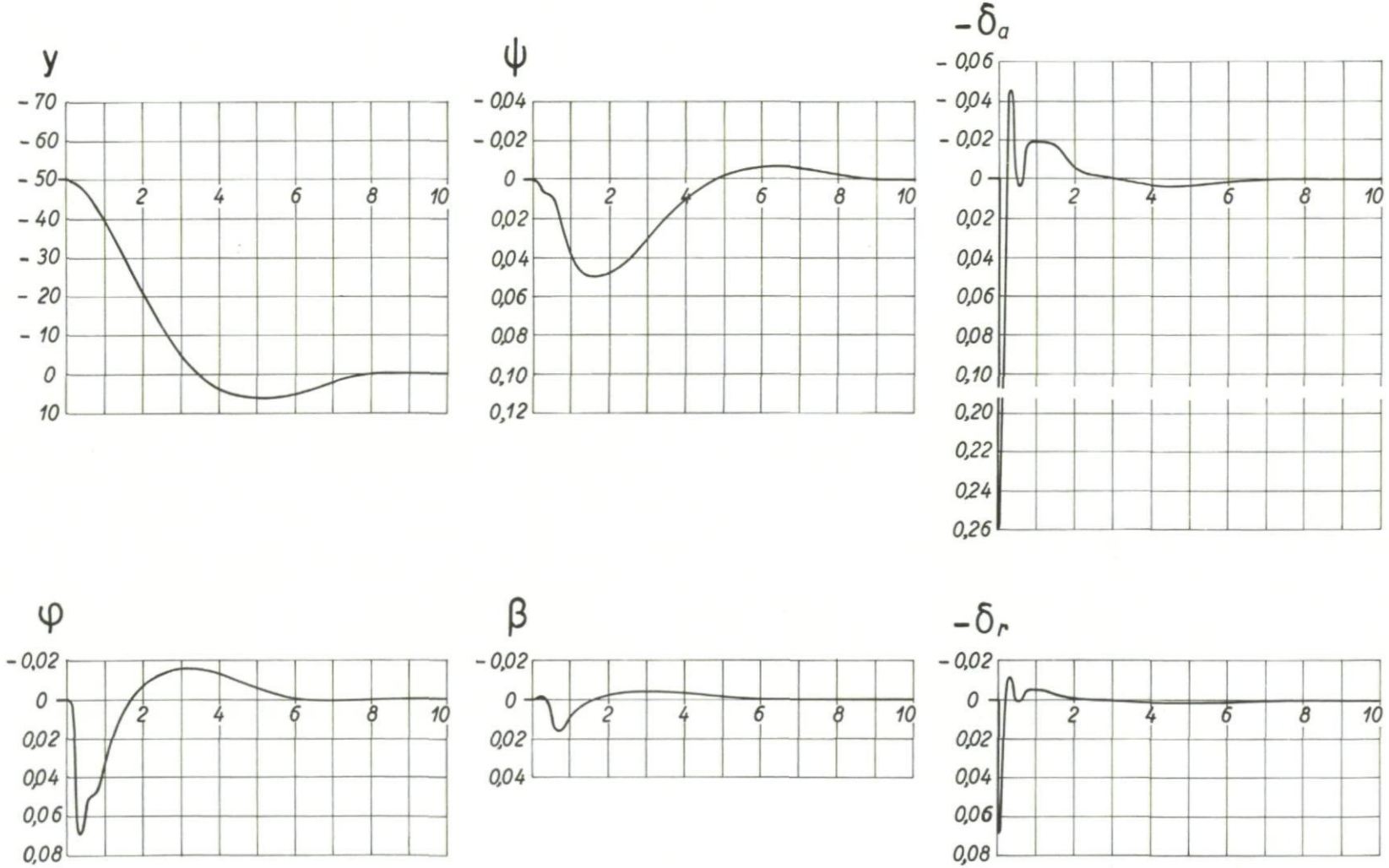

Fig.236 Aircraft response to an initial error y = 50m, case g

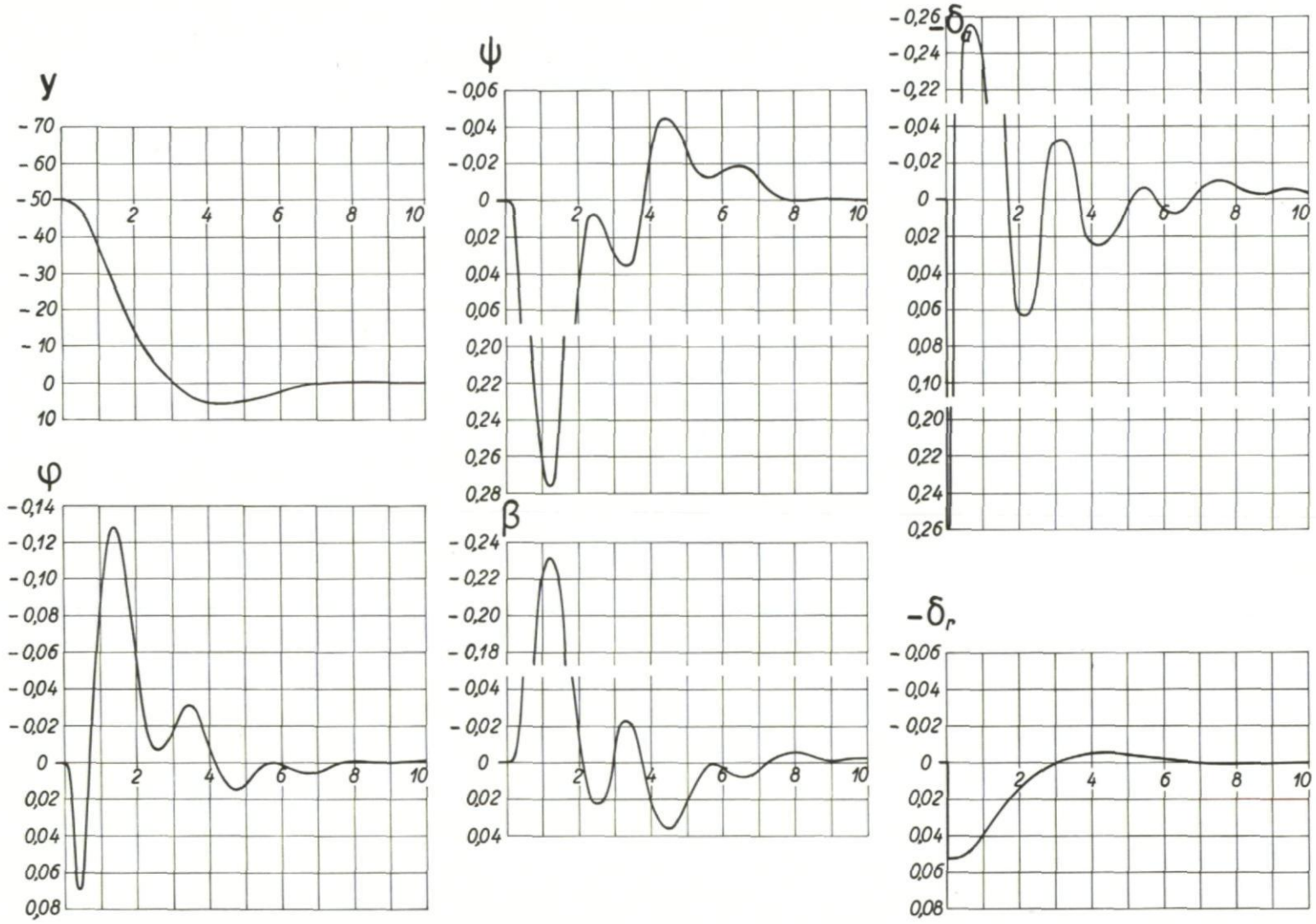

Fig. 237 Aircraft response to an initial error y = 50m, modified case c

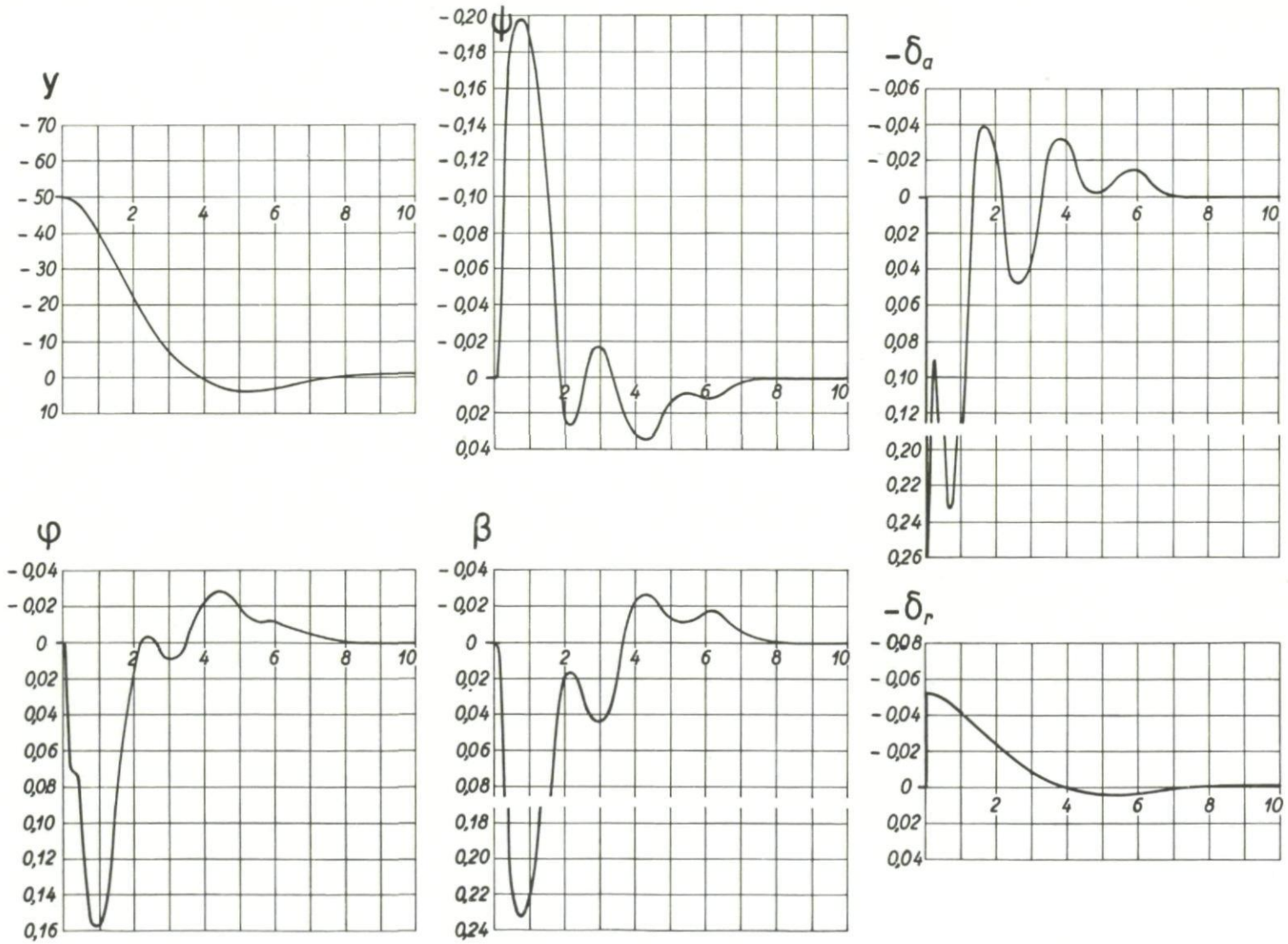

Fig.238 Aircraft response to an initial error y = 50m, modified case c

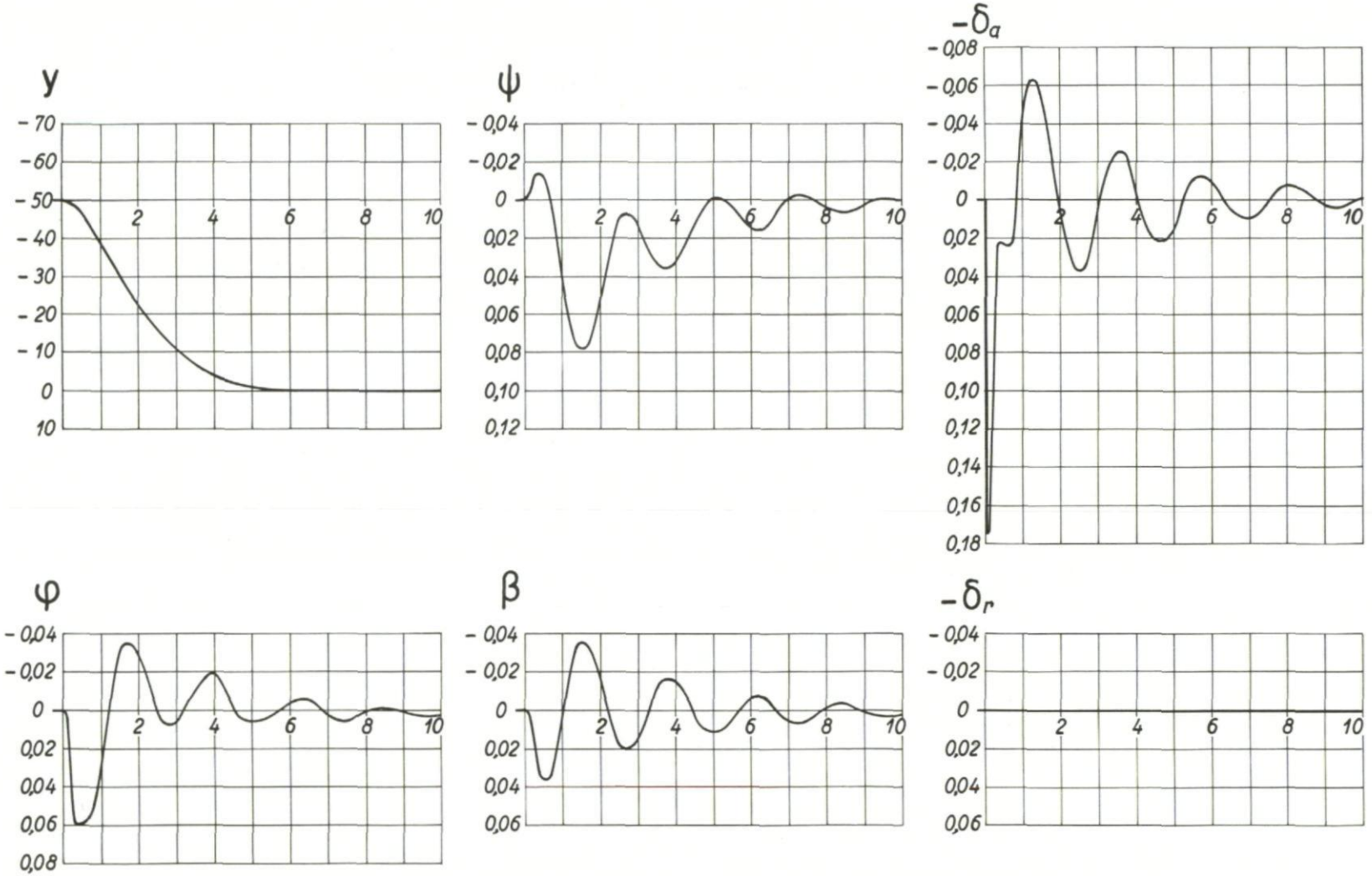

Fig.239 Aircraft response to an initial error y = 50m, case d

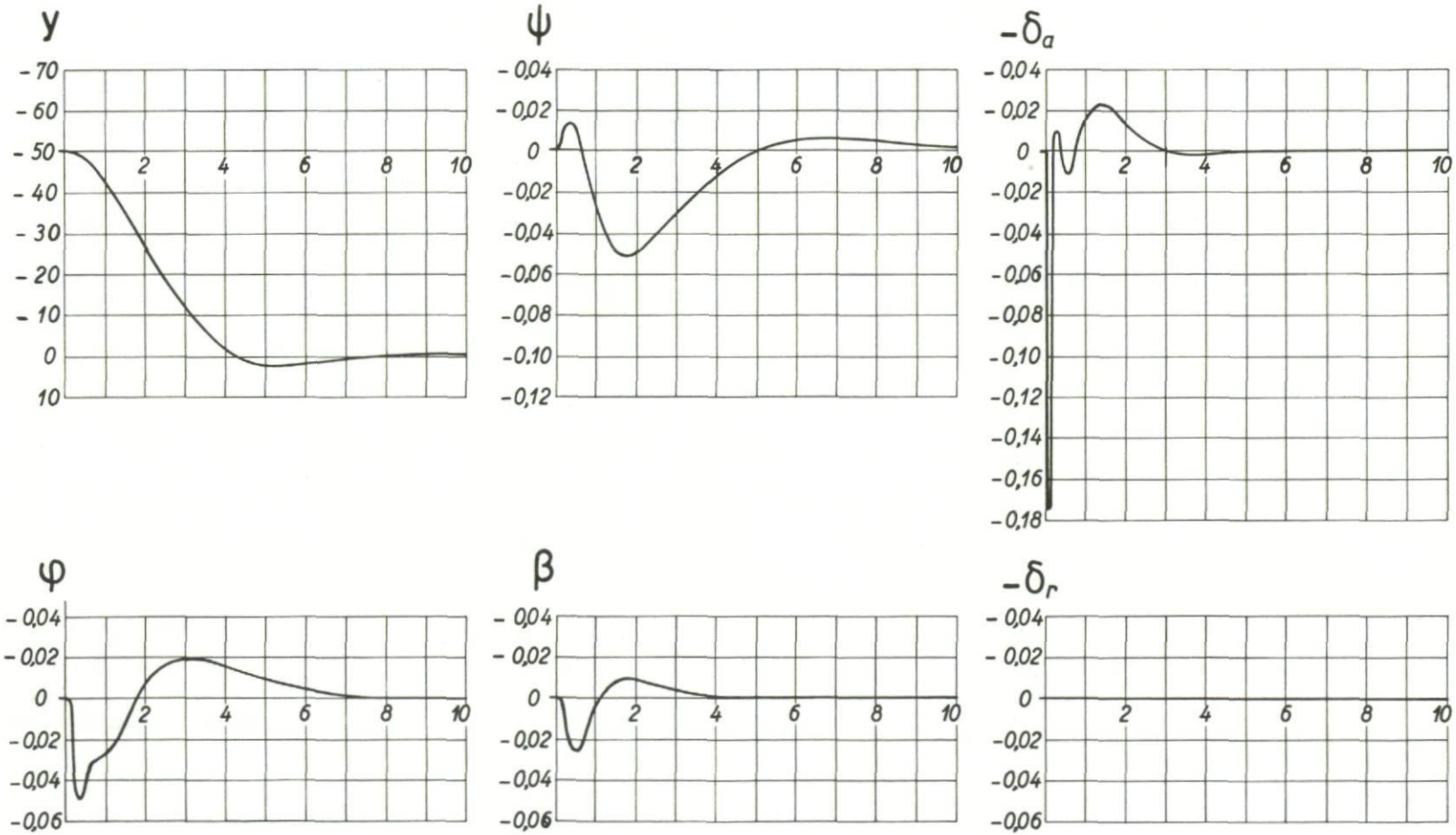

Fig.240 Aircraft response to an initial error y = 50m, case i

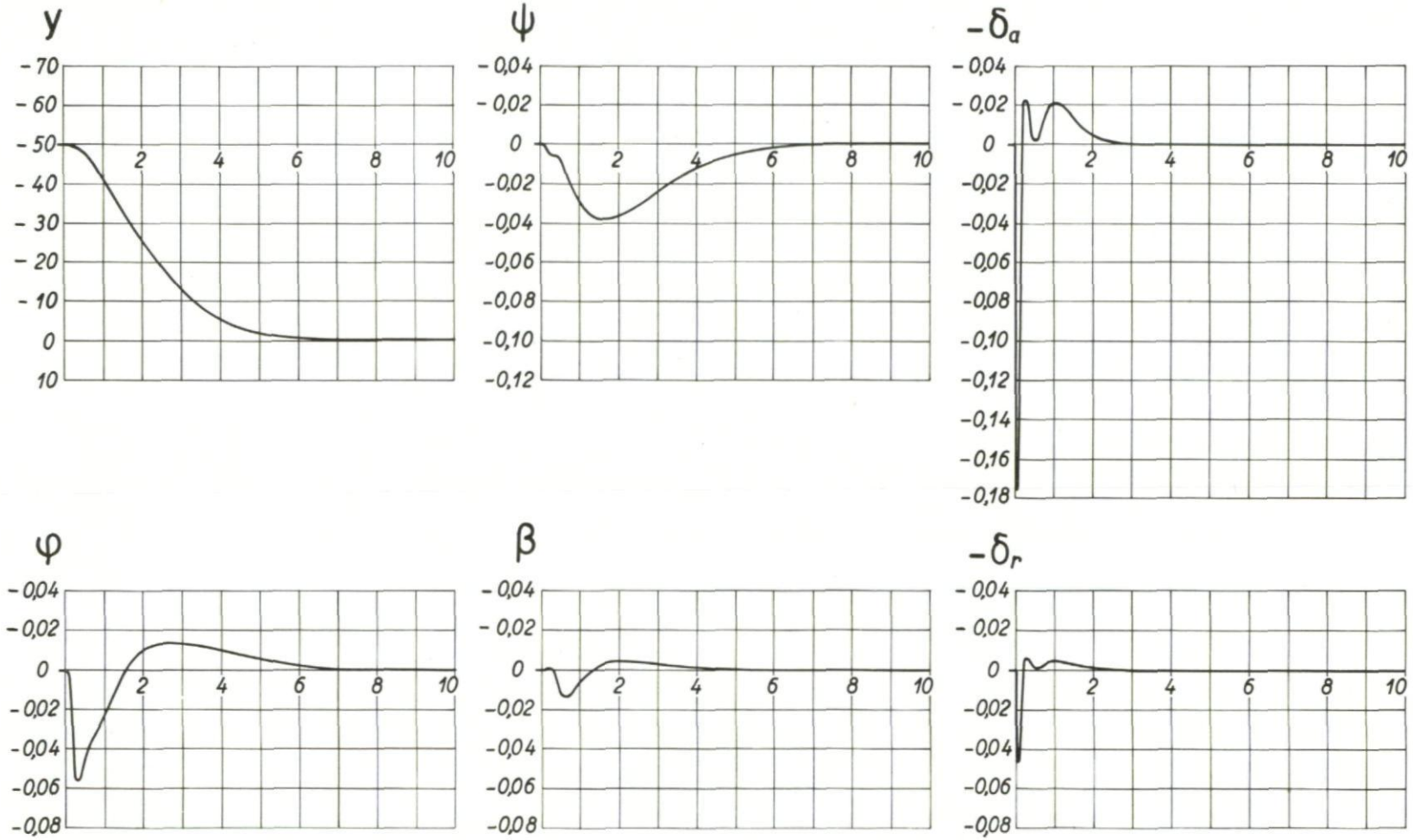

Fig.241 Aircraft response to an initial error y = 50m, case j

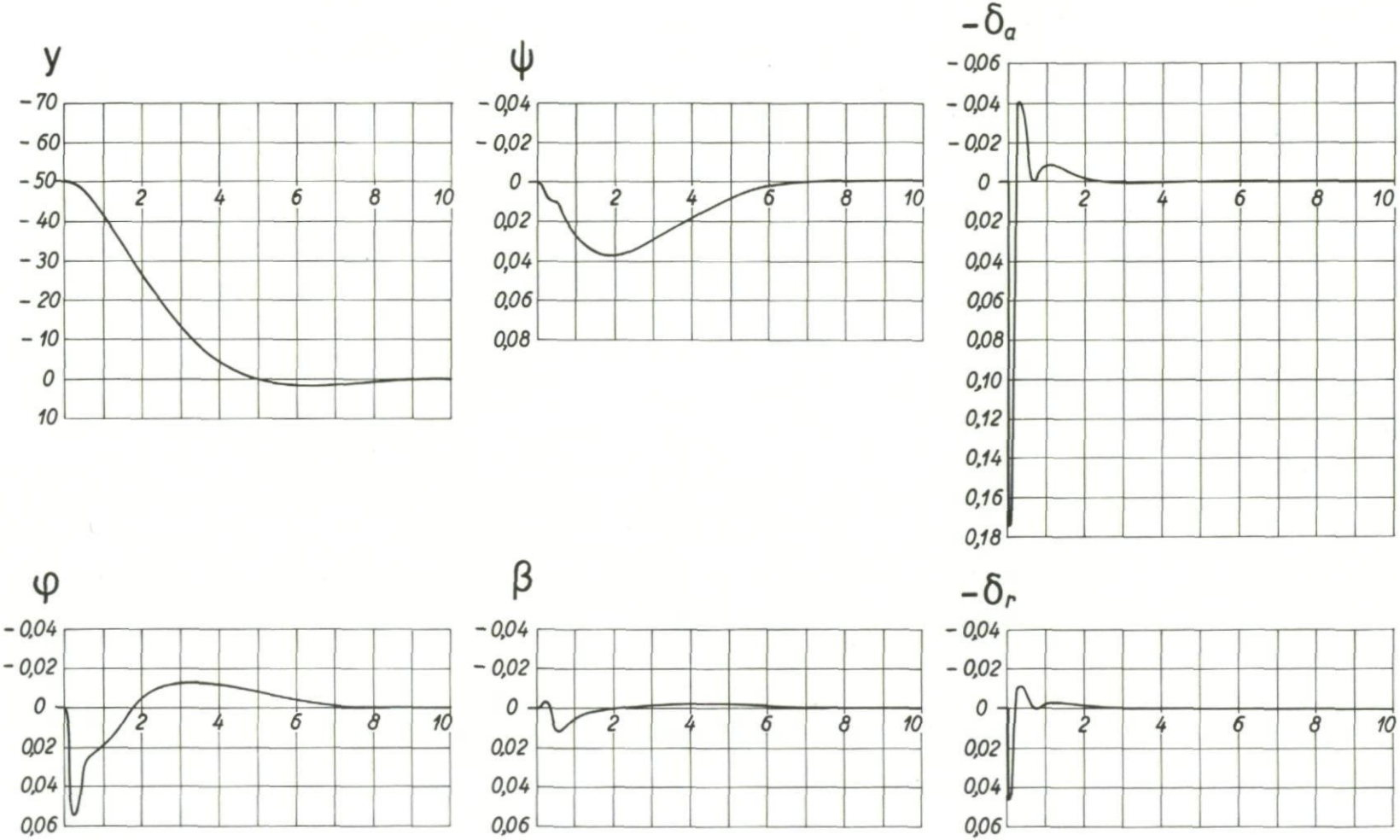

Fig. 242 Aircraft response to an initial error y = 50m, case k

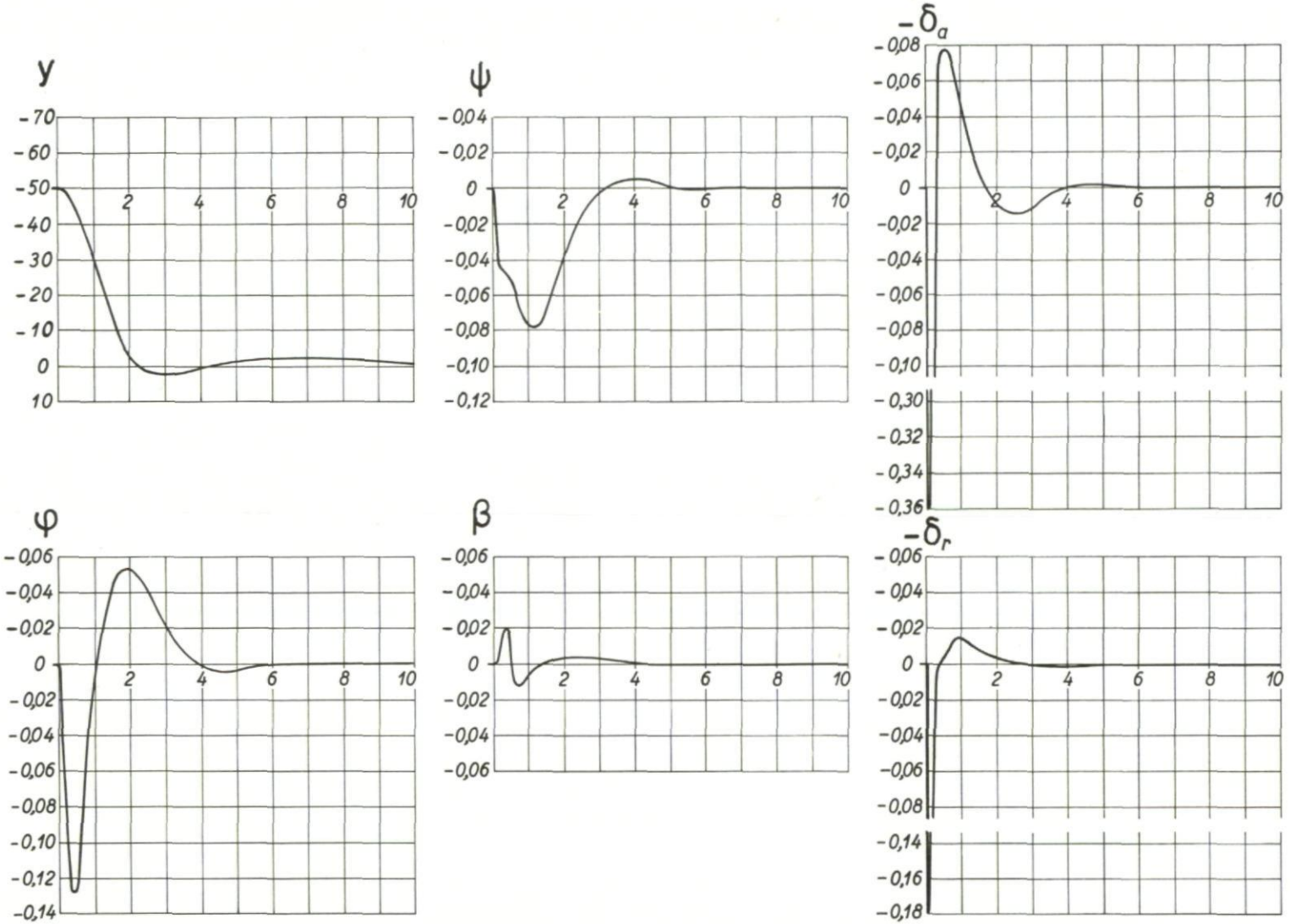

Fig.243 Aircraft response to an initial error y = 50m, case *l*

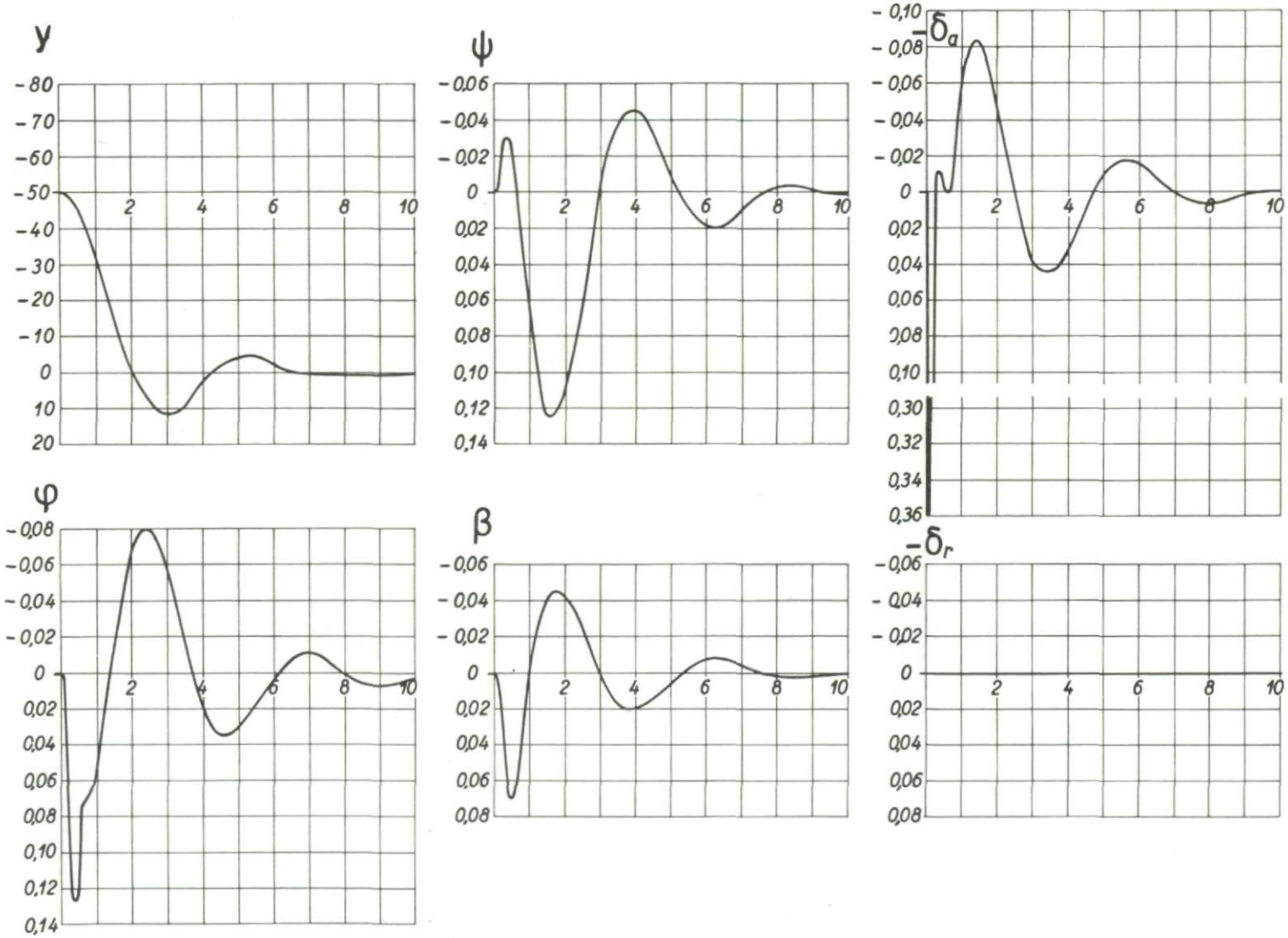

Fig.244 Aircraft response to an initial error y = 50m, case l_1

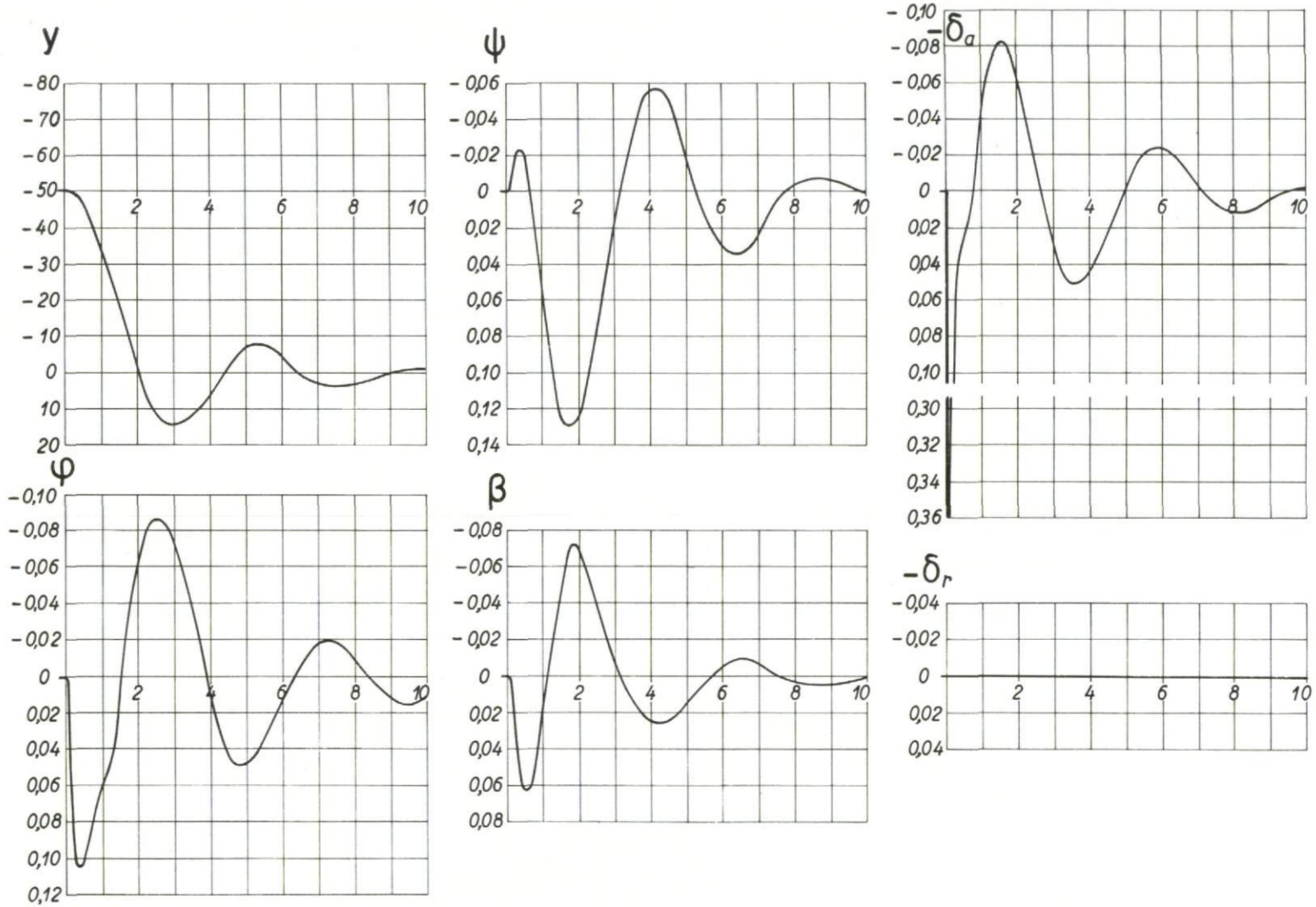

Fig.245 Aircraft response to an initial error y = 50m, case l_2

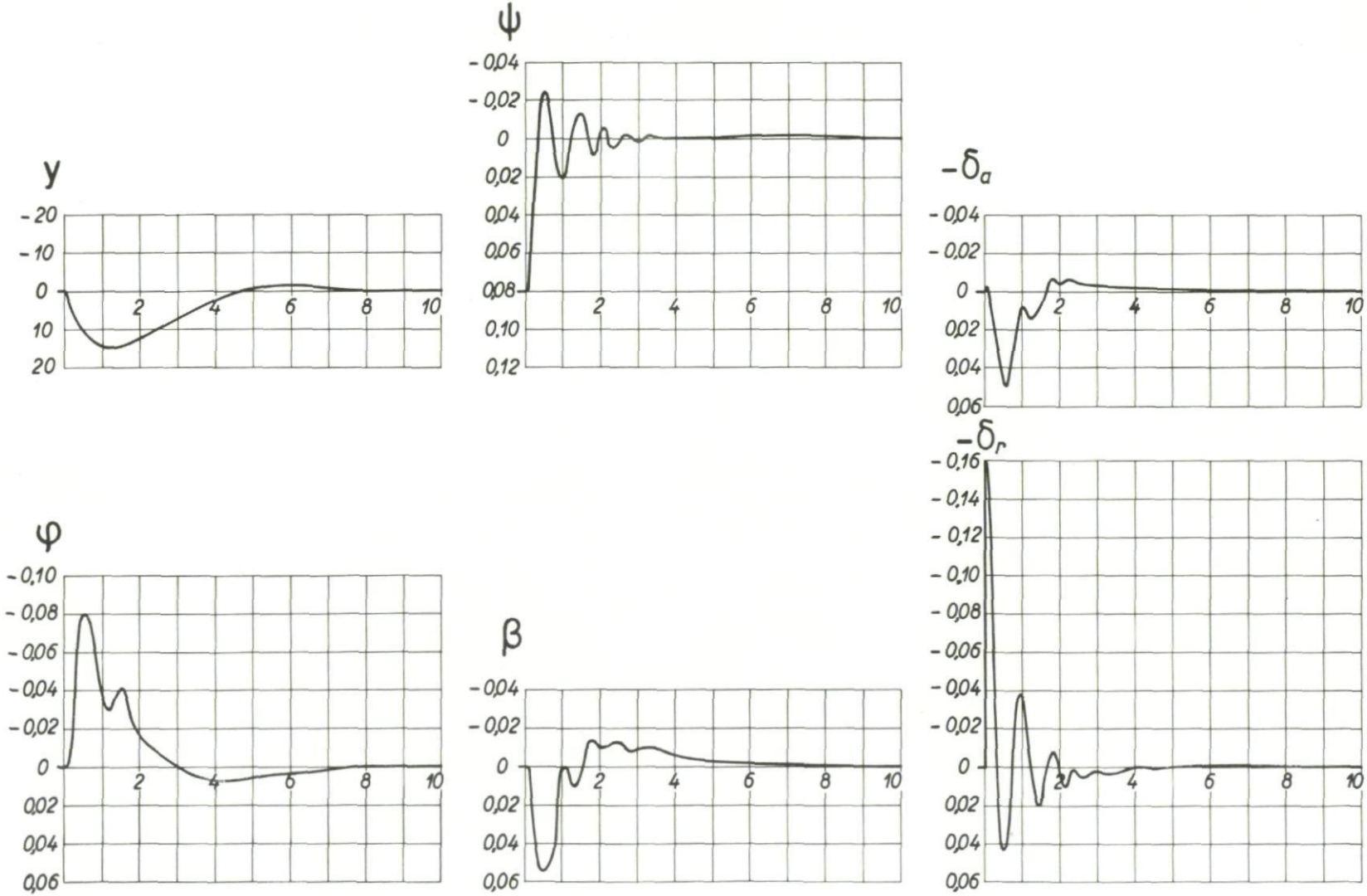

Fig. 246 Aircraft response to an initial error $\psi = 0.08$ rad., case a

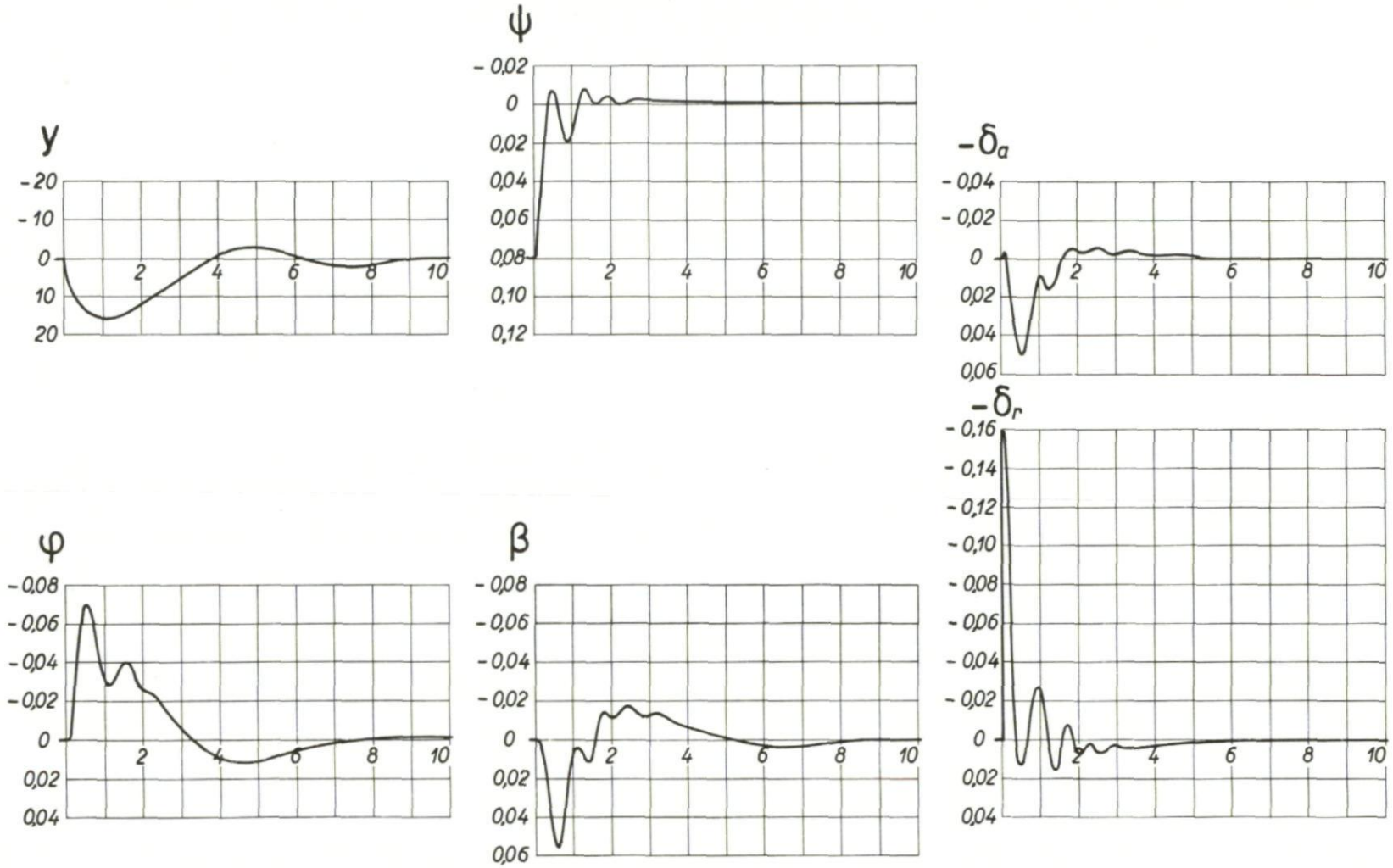

Fig. 247 Aircraft response to an initial error $\psi = 0.08$ rad., case b

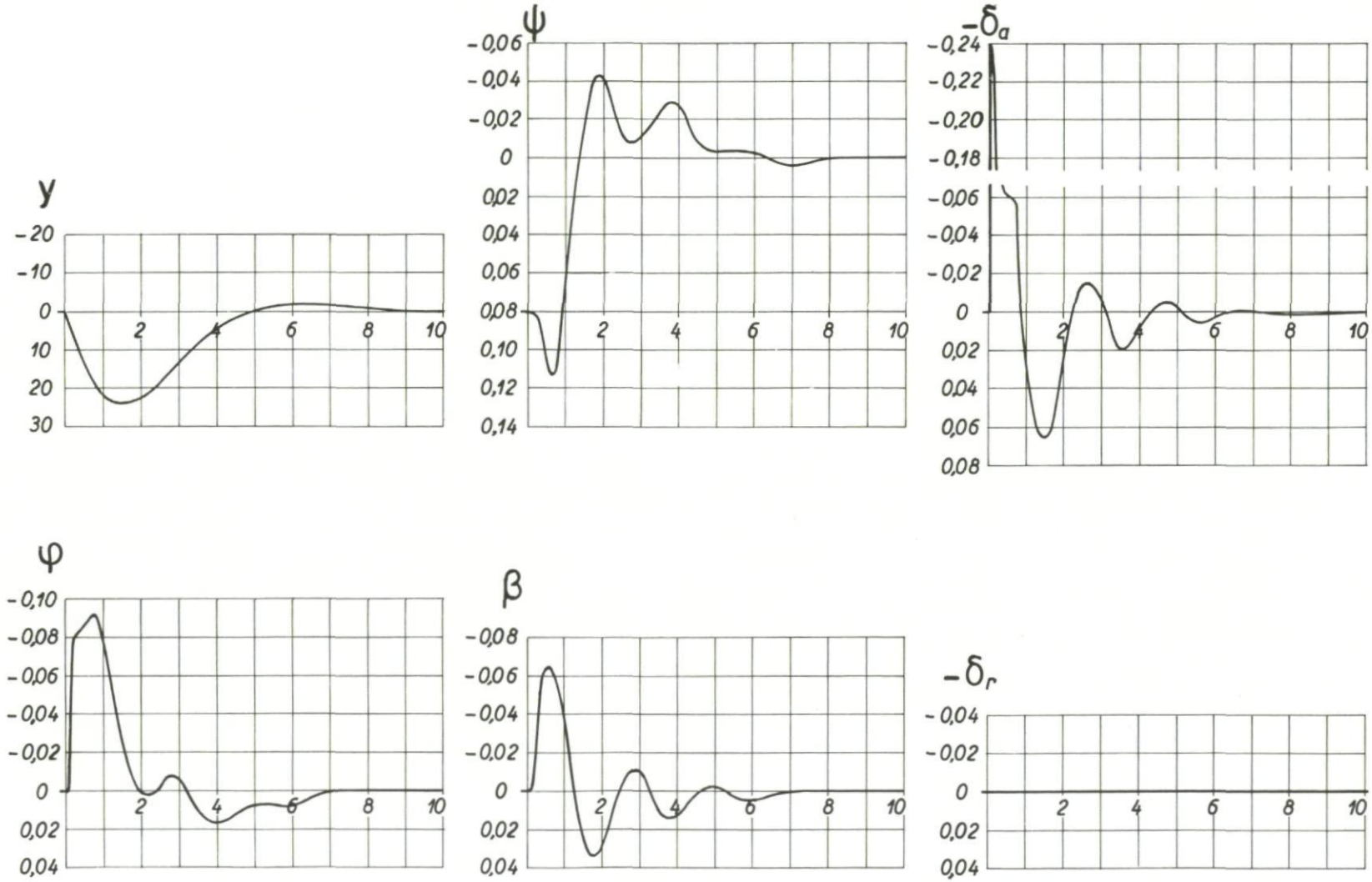

Fig.248 Aircraft response to an initial error ψ = 0.08 rad., case c

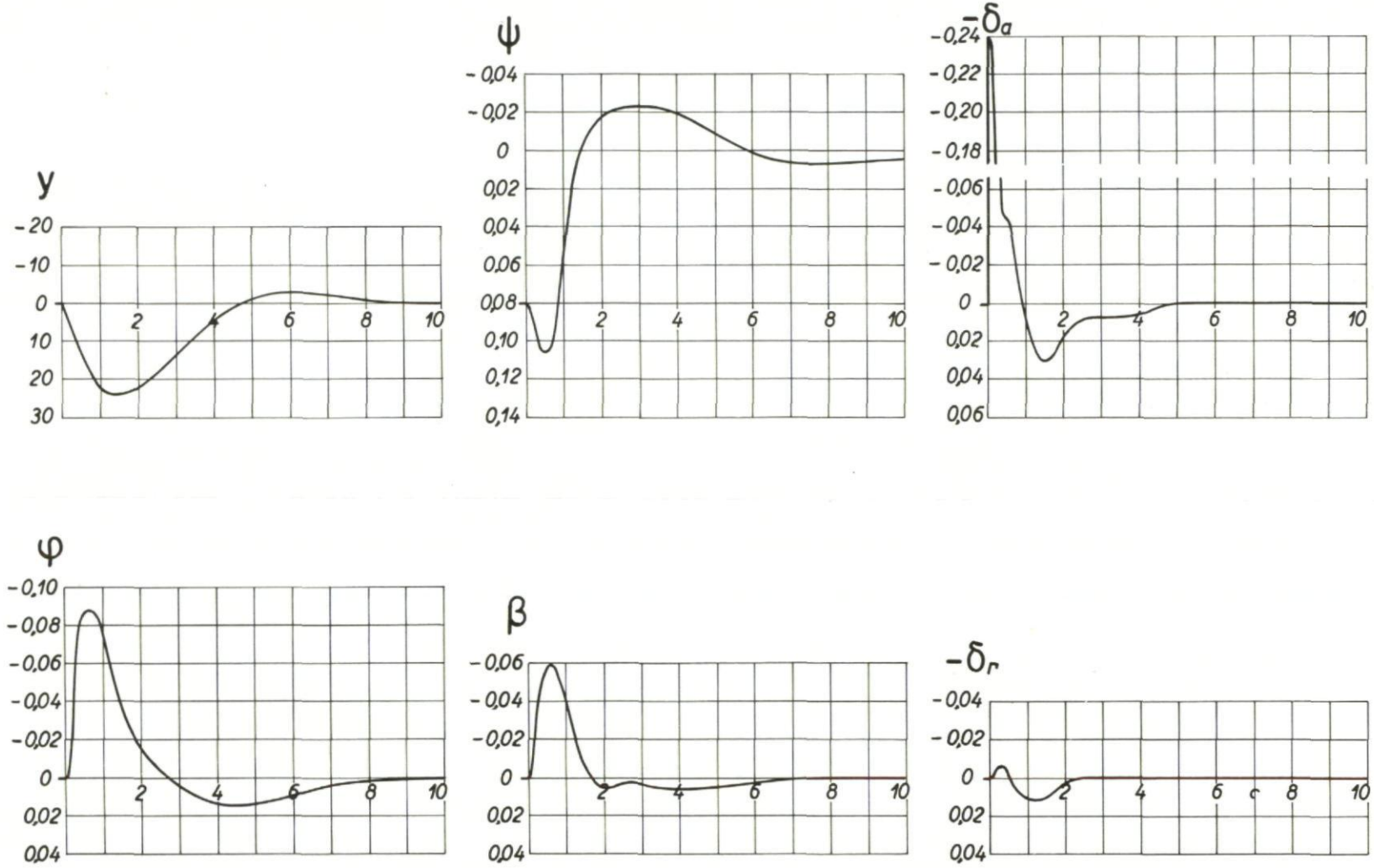

Fig.249 Aircraft response to an initial error ψ = 0.08 rad., case h

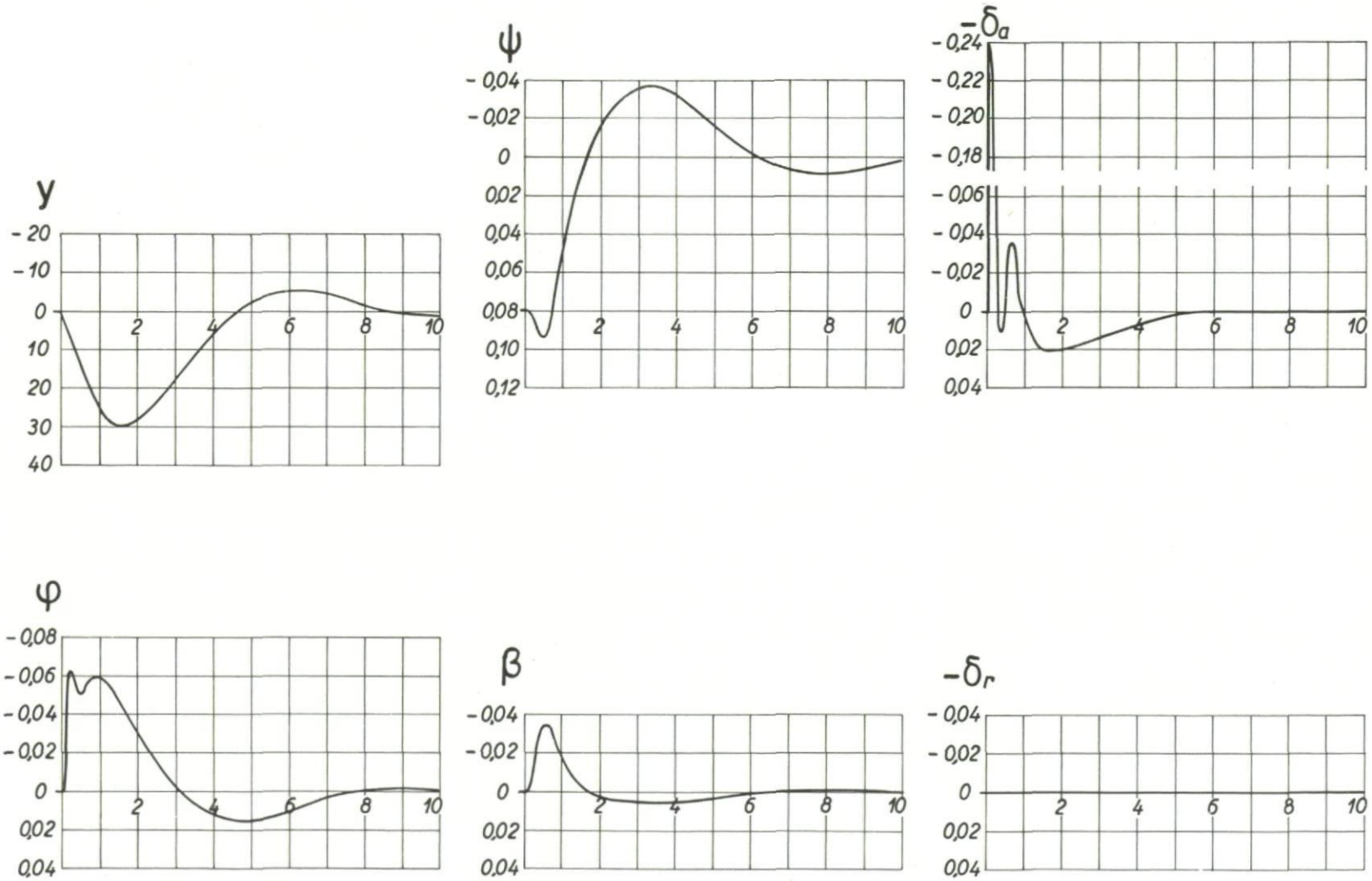

Fig.250 Aircraft response to an initial error $\psi = 0.08$ rad., case e

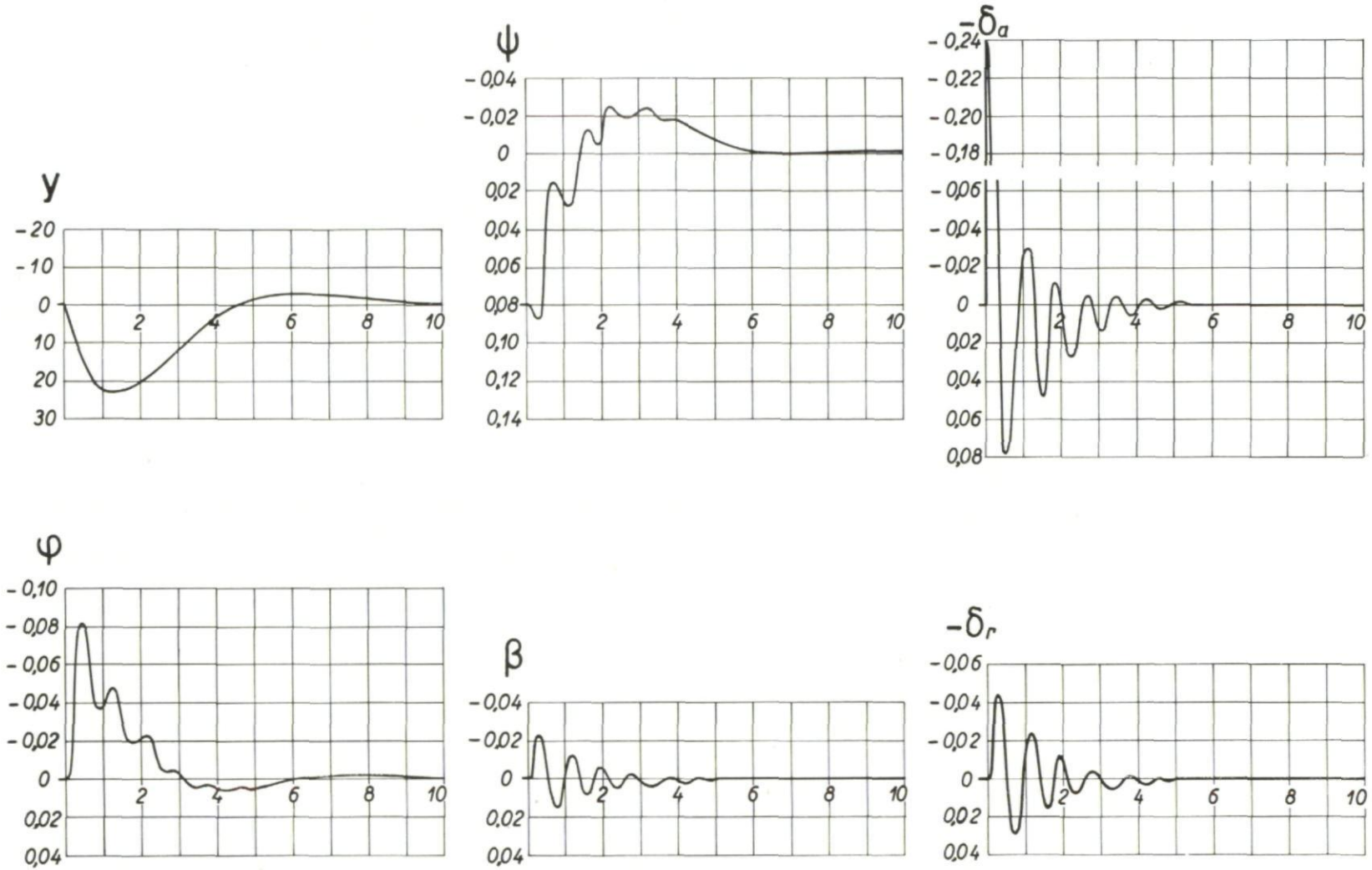

Fig. 251 Aircraft response to an initial error $\psi = 0.08$ rad., case f

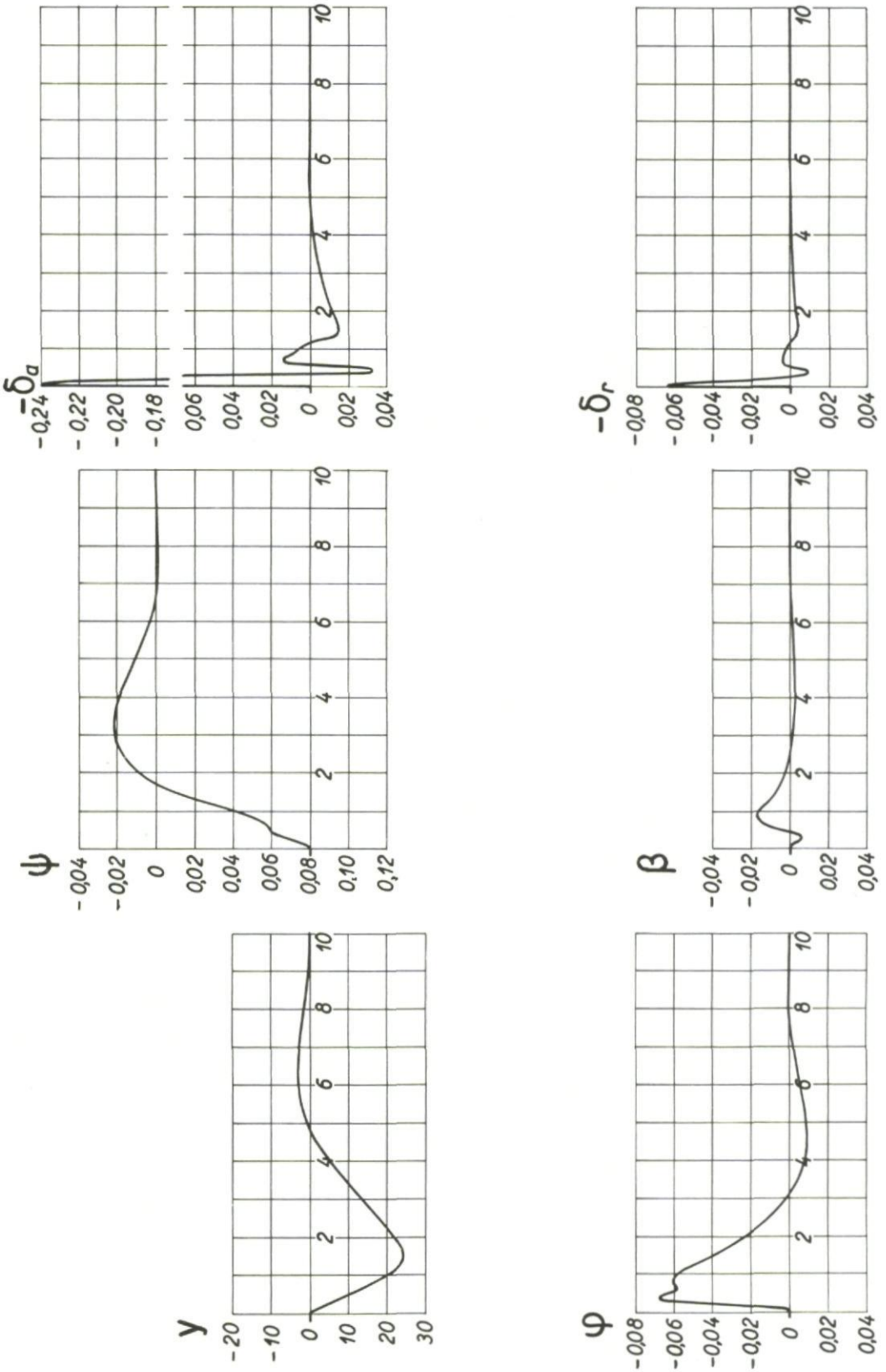

Fig.252 Aircraft response to an initial error $\psi = 0.08$ rad., case g

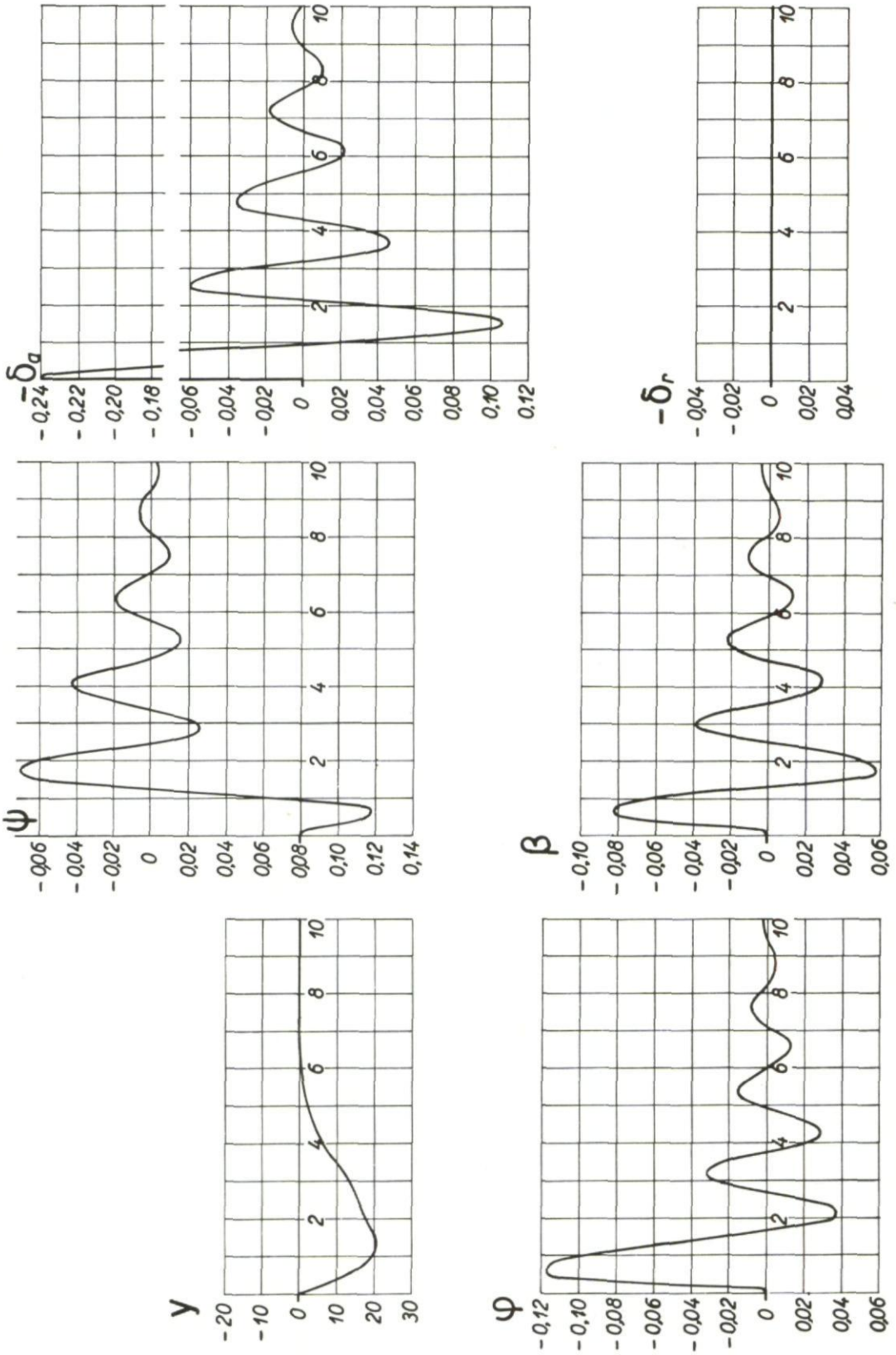

Fig.253 Aircraft response to an initial error $\psi = 0.08$ rad., case d

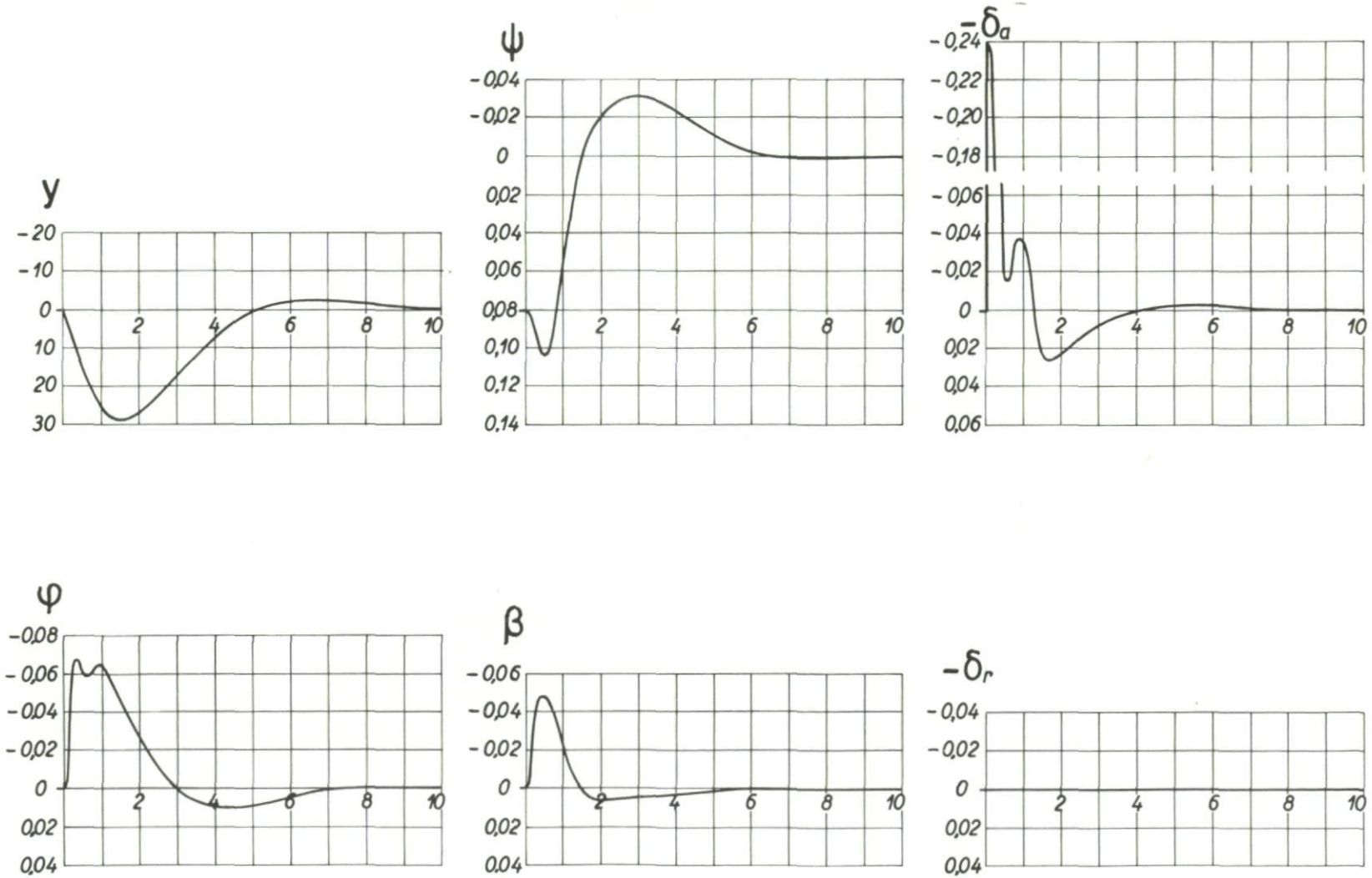

Fig. 254 Aircraft response to an initial error $\psi = 0.08$ rad., case i

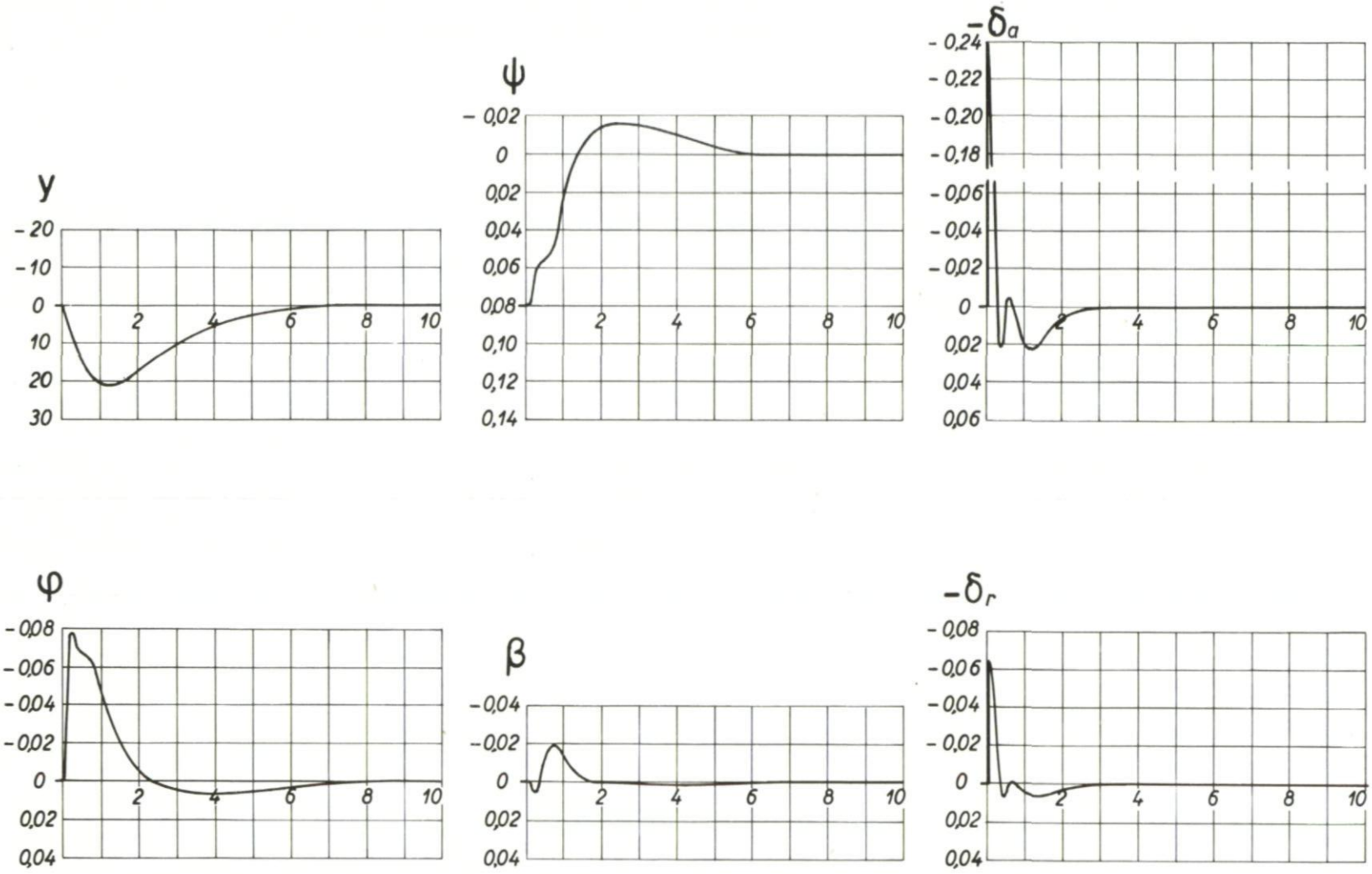

Fig.255 Aircraft response to an initial error $\psi = 0.08$ rad., case j

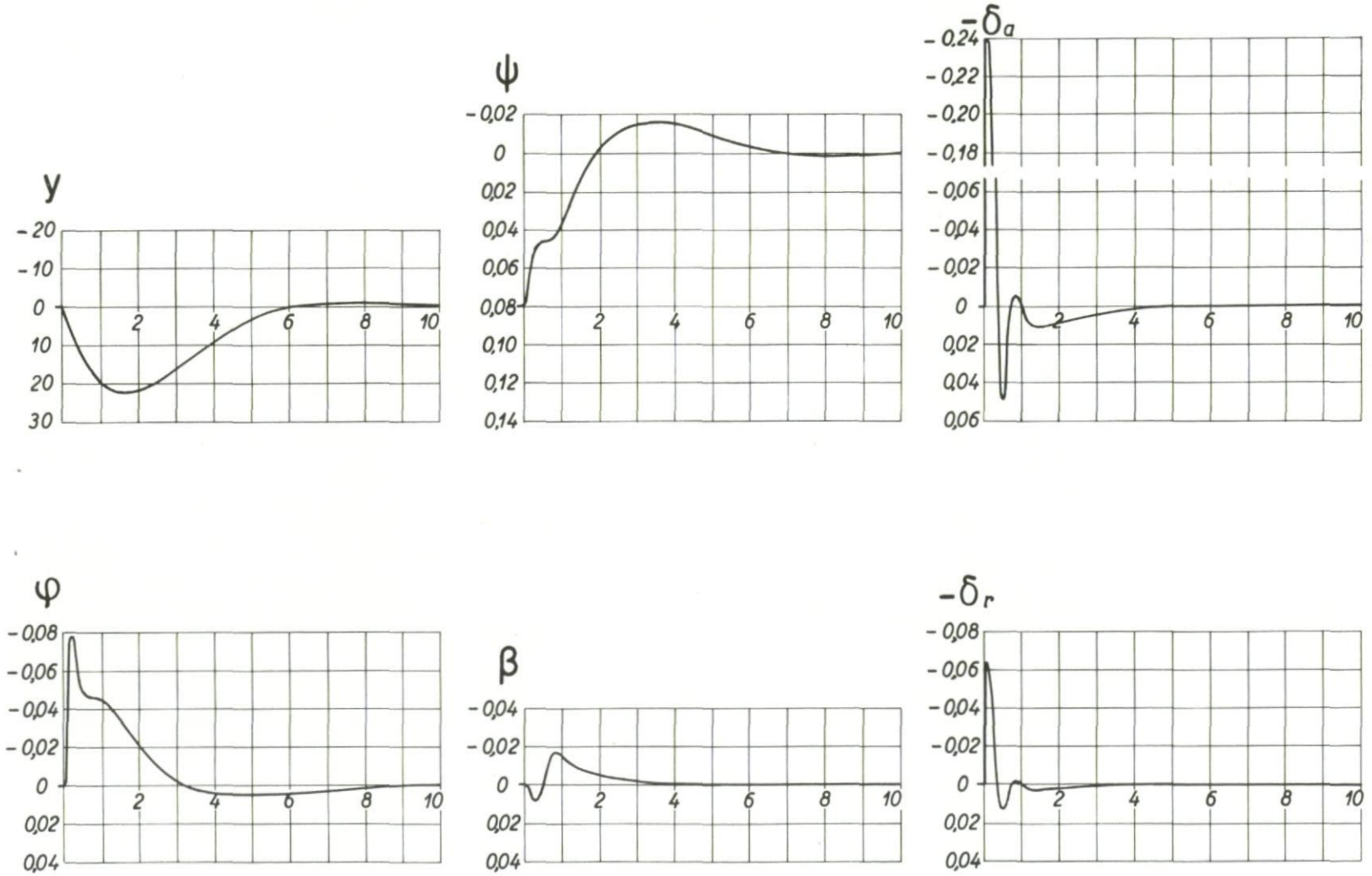

Fig.256 Aircraft response to an initial error ψ = 0.08 rad., case k

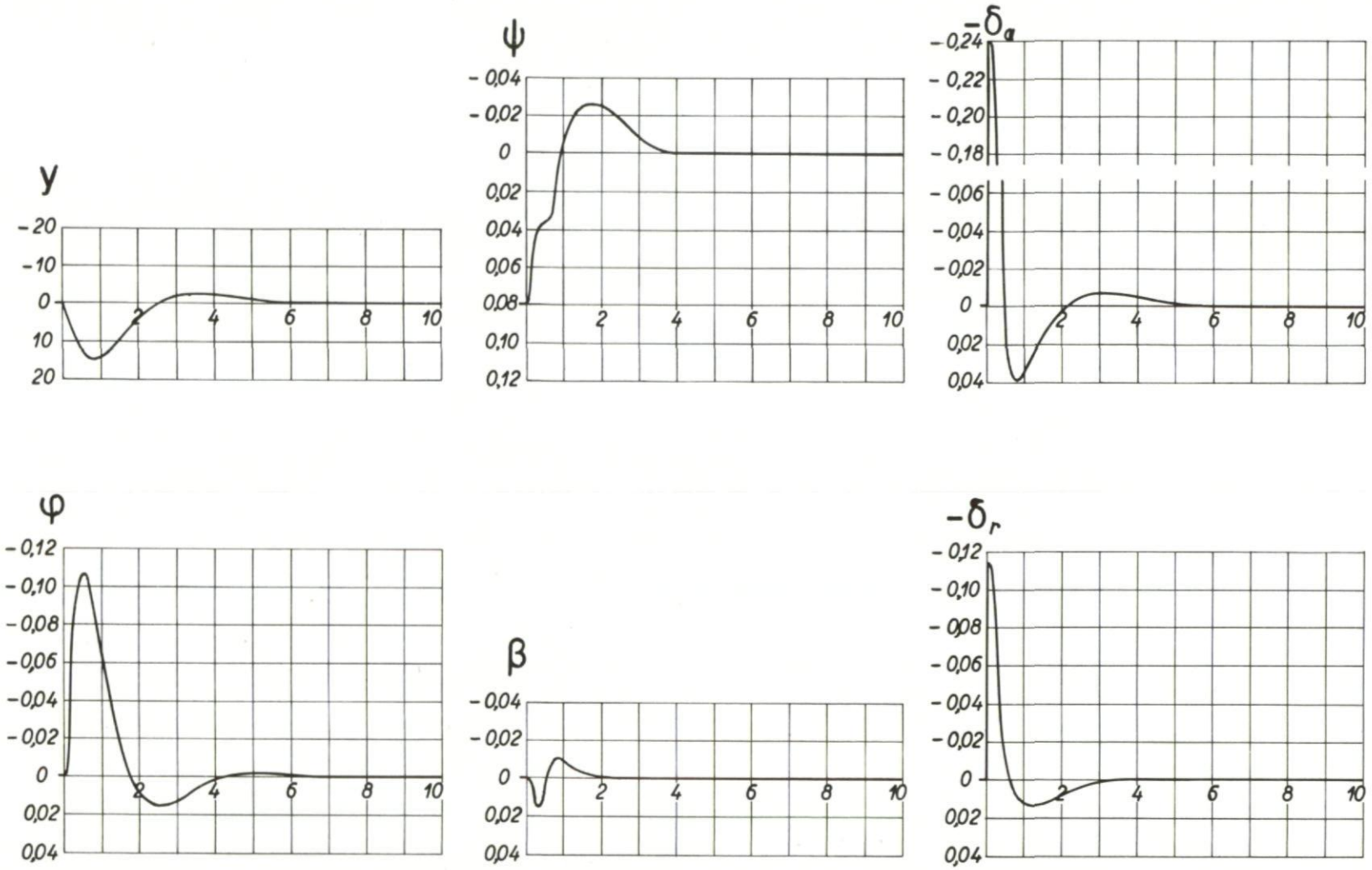

Fig.257 Aircraft response to an initial error ψ = 0.08 rad., case *l*

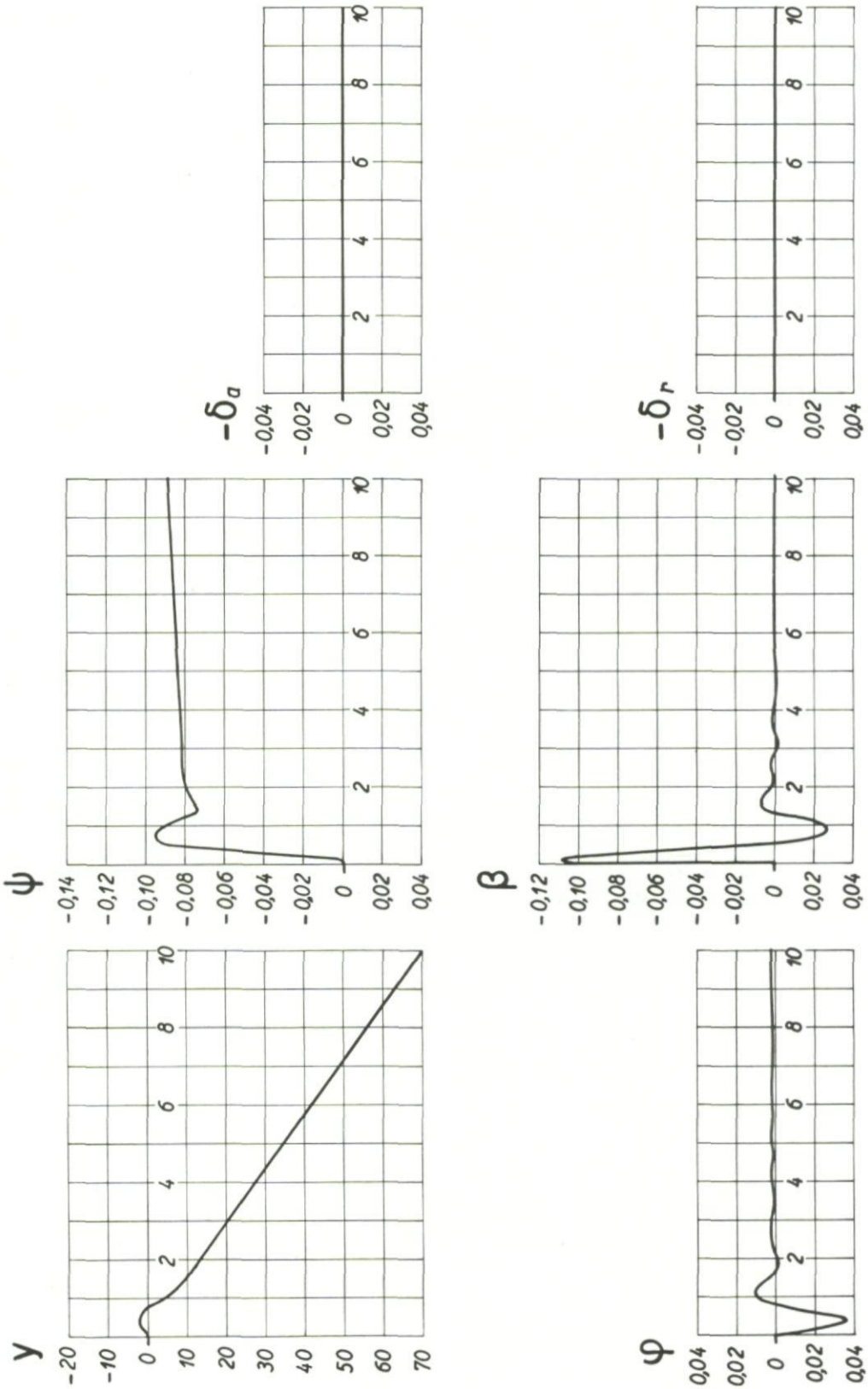

Fig.258 Aircraft response to a side gust v_a, locked controls

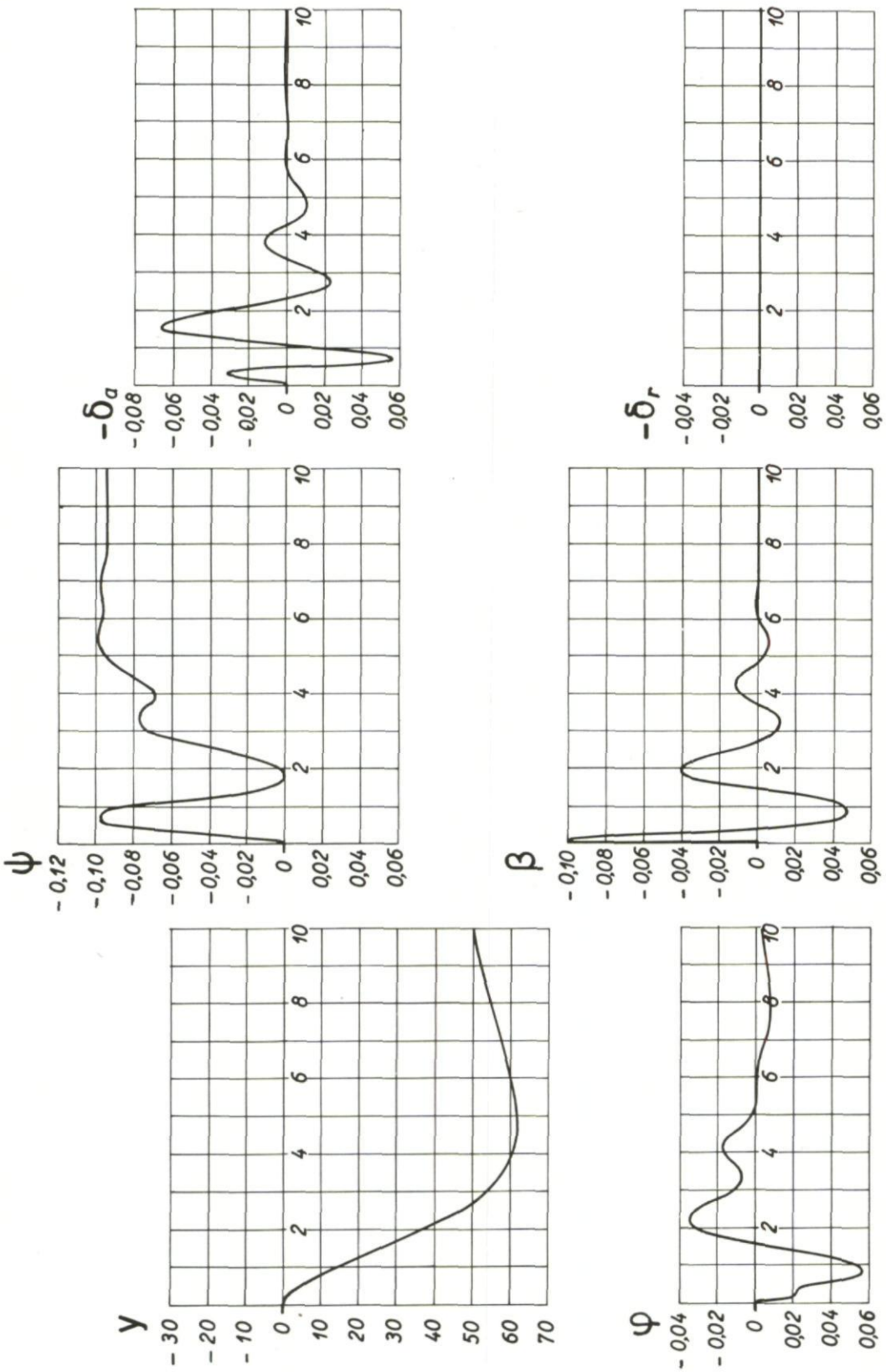

Fig.259 Aircraft response to a side gust v_a, case c

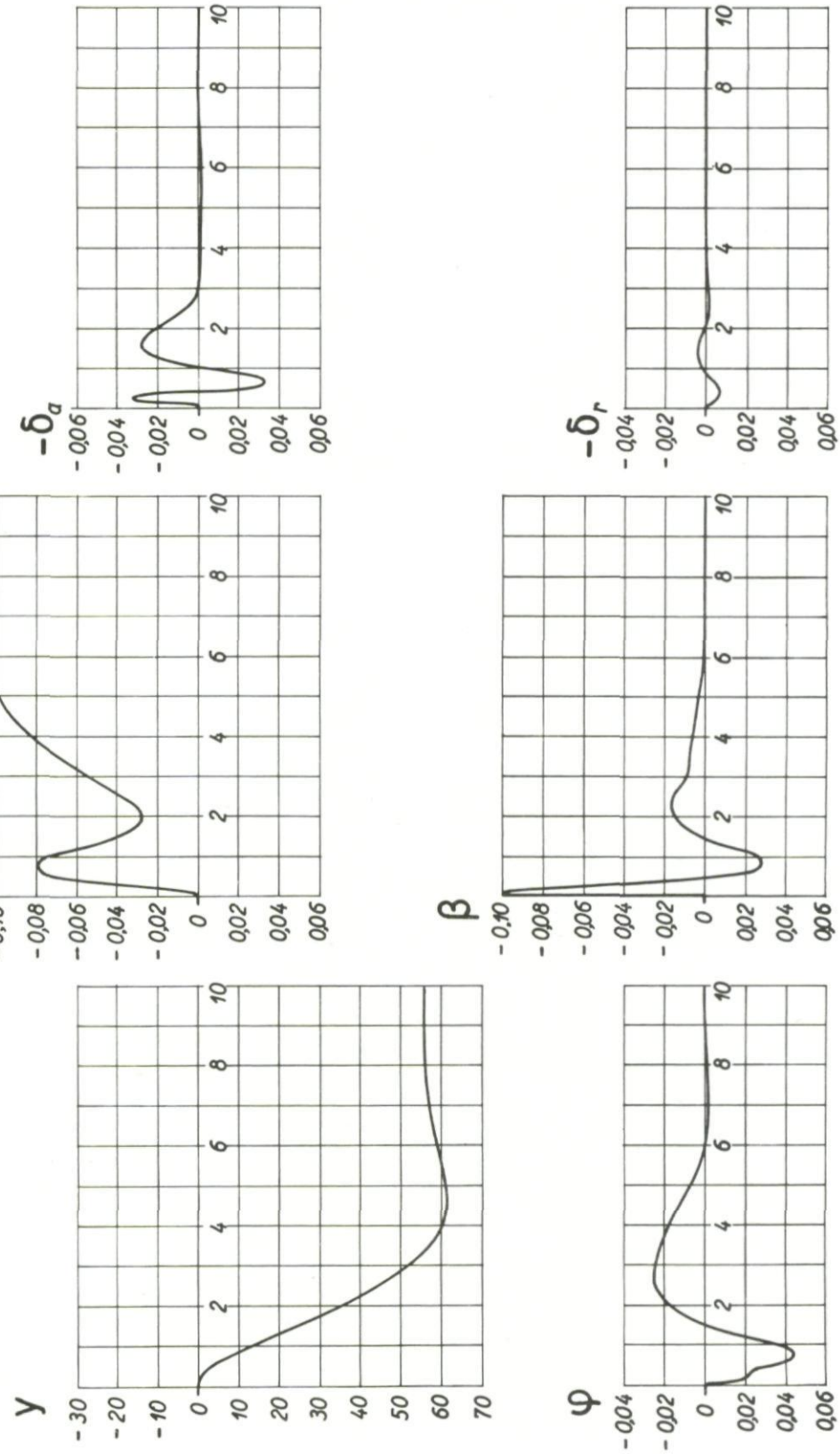

Fig.260 Aircraft response to a side gust v_a, case h

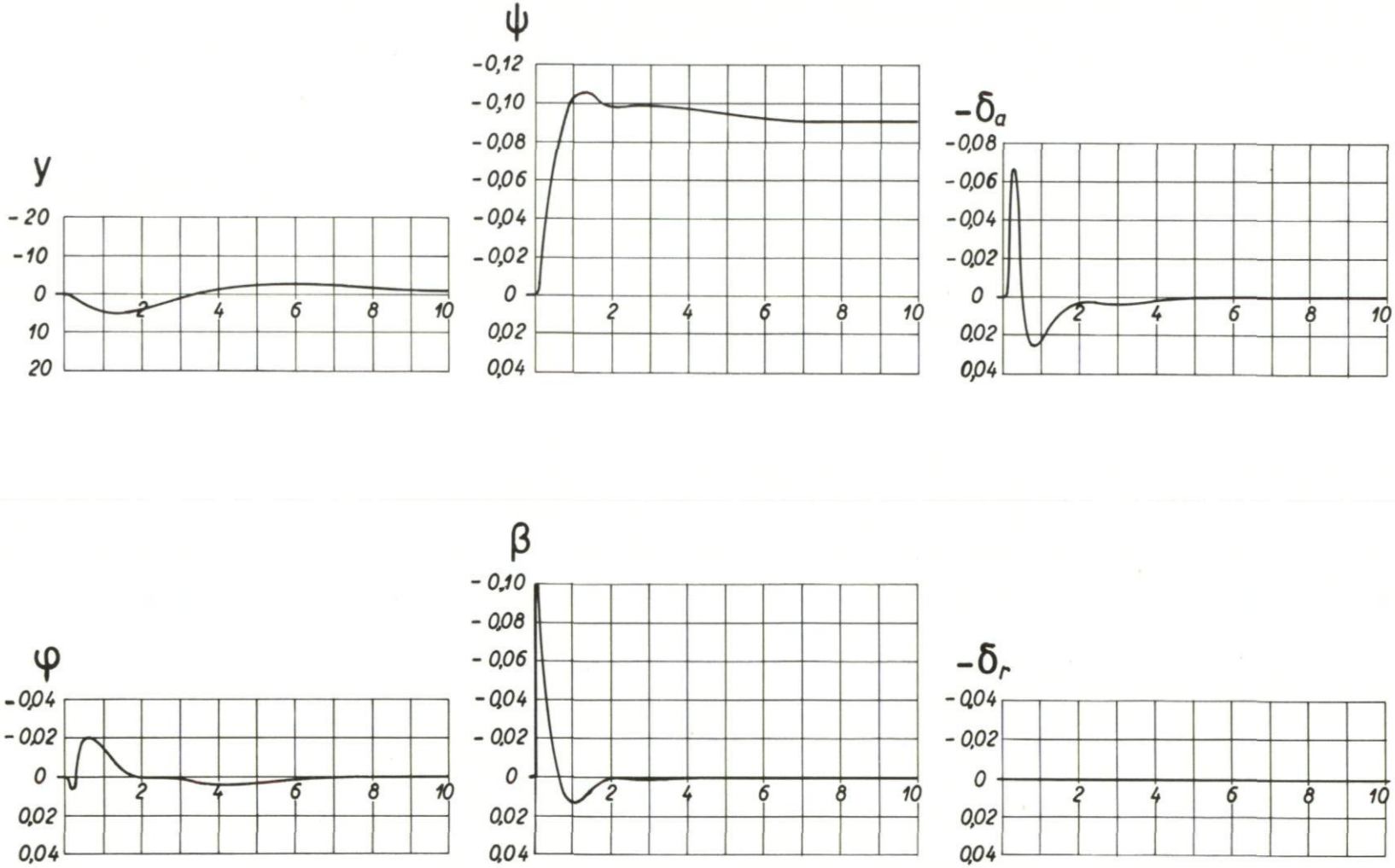

Fig.261 Aircraft response to a side gust v_a, case e

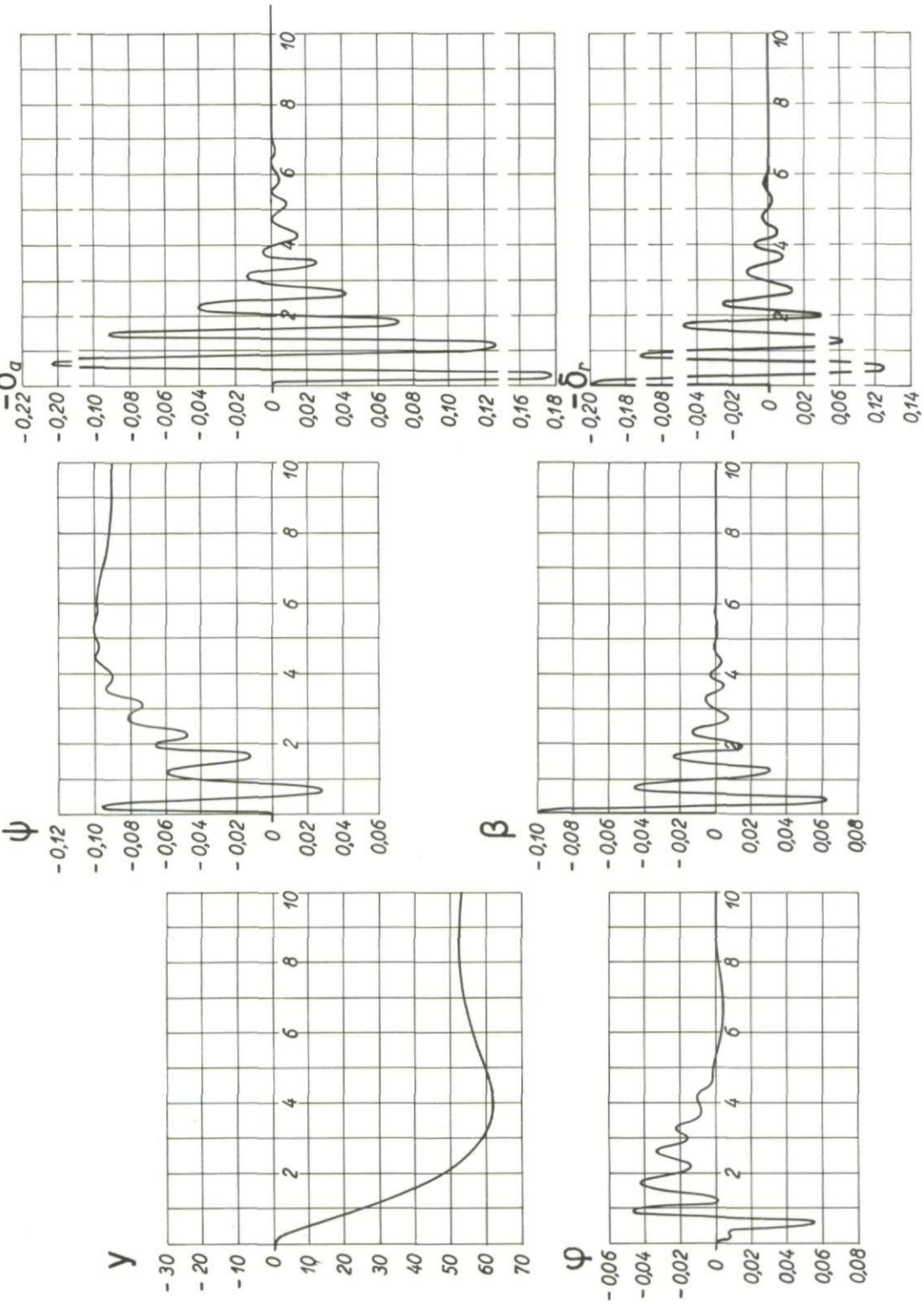

Fig.262 Aircraft response to a side gust v_a, case f

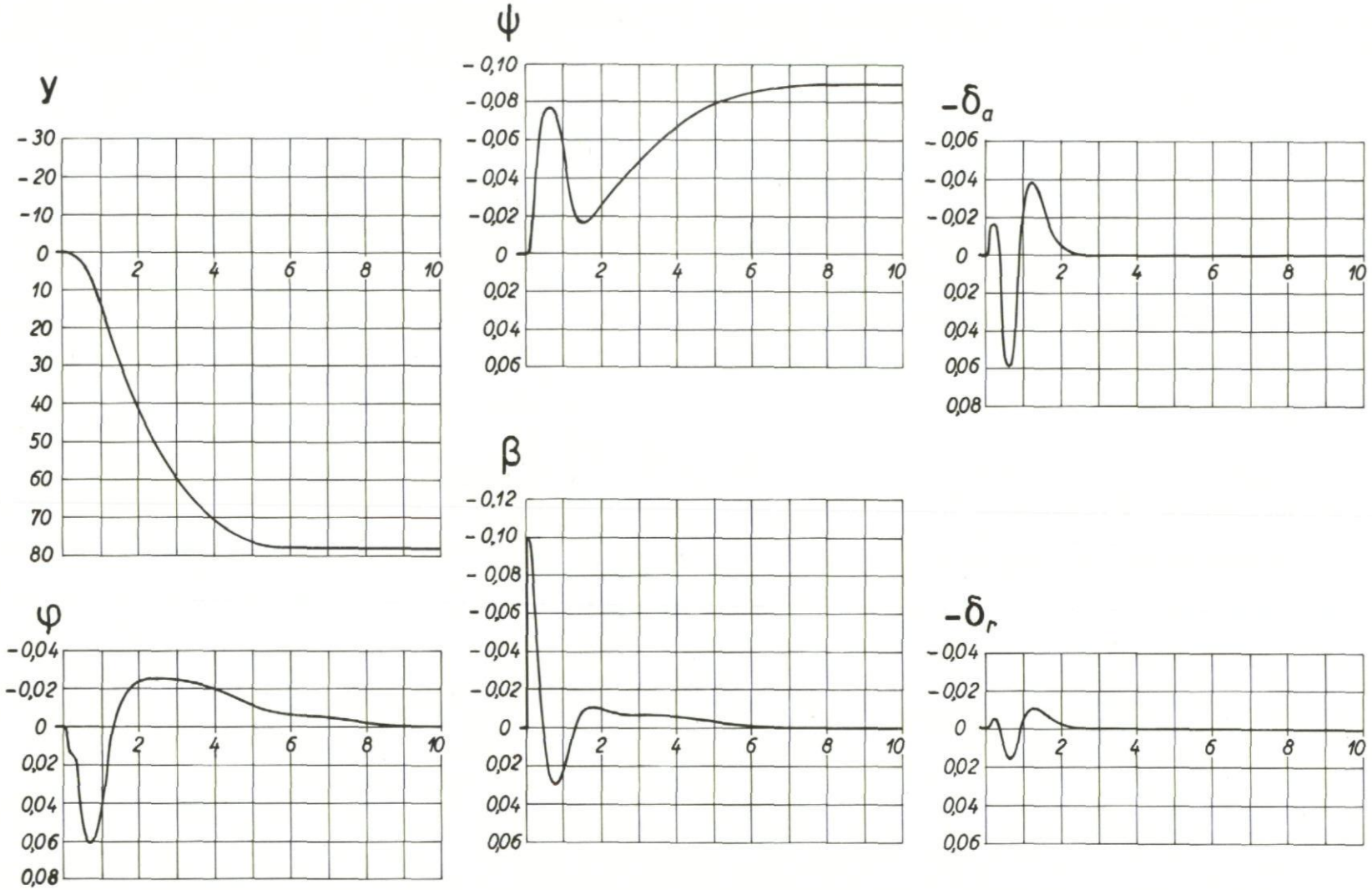

Fig. 263 Aircraft response to a side gust v_a, case g

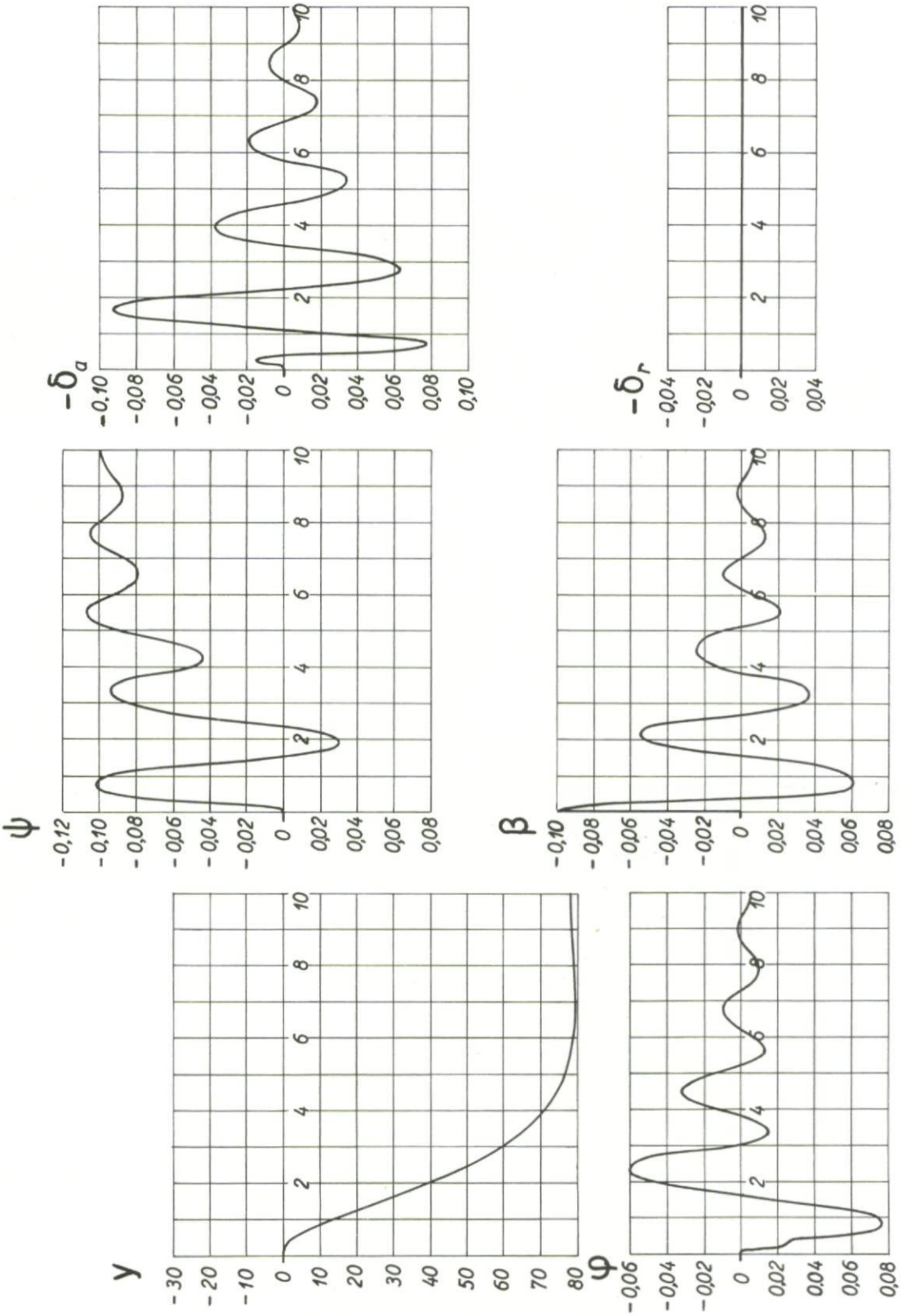

Fig.264 Aircraft response to a side gust v_a, case d

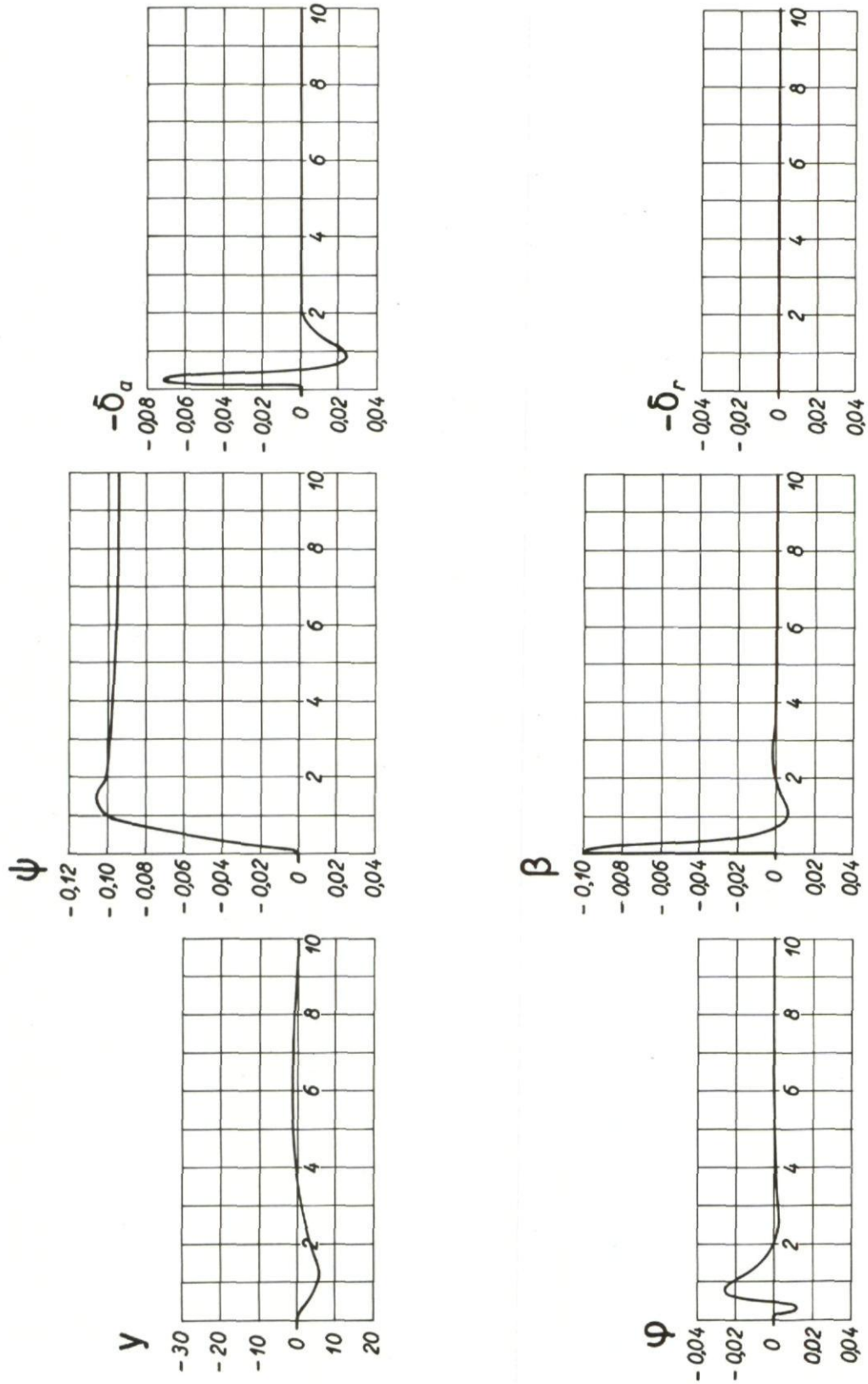

Fig.265 Aircraft response to a side gust v_a, case i

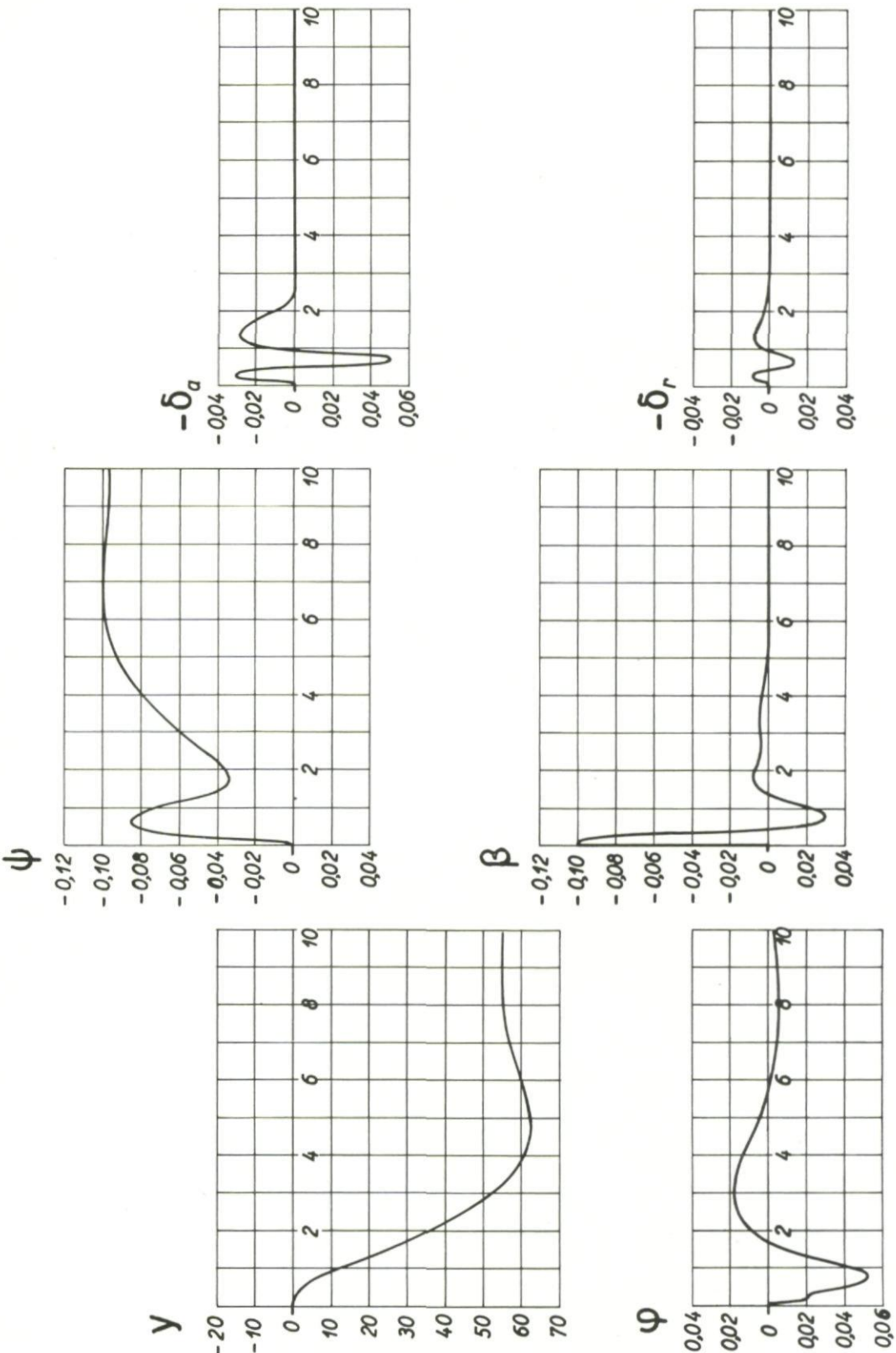

Fig.266 Aircraft response to a side gust v_a, case j

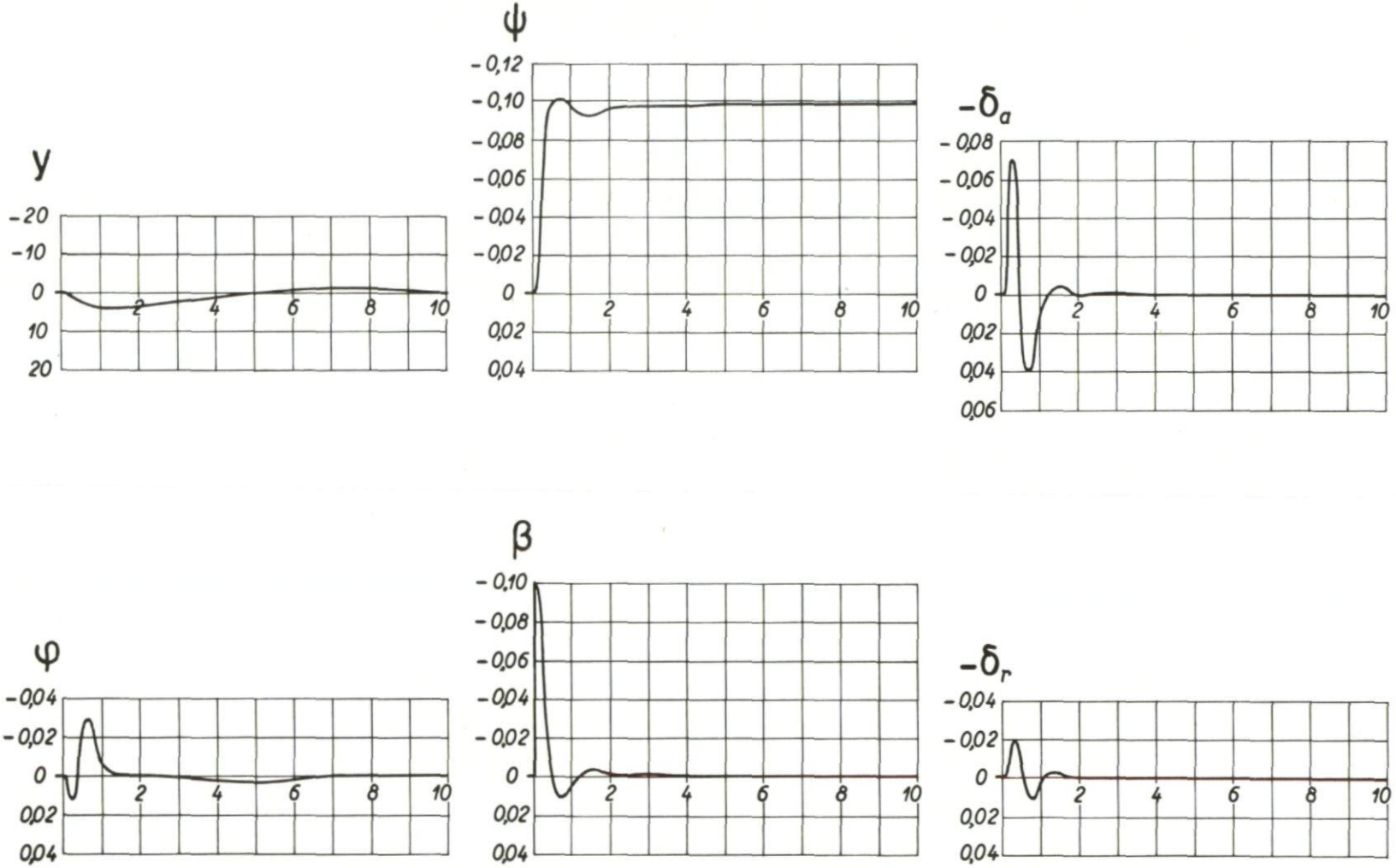

Fig.267 Aircraft response to a side gust v_a, case k

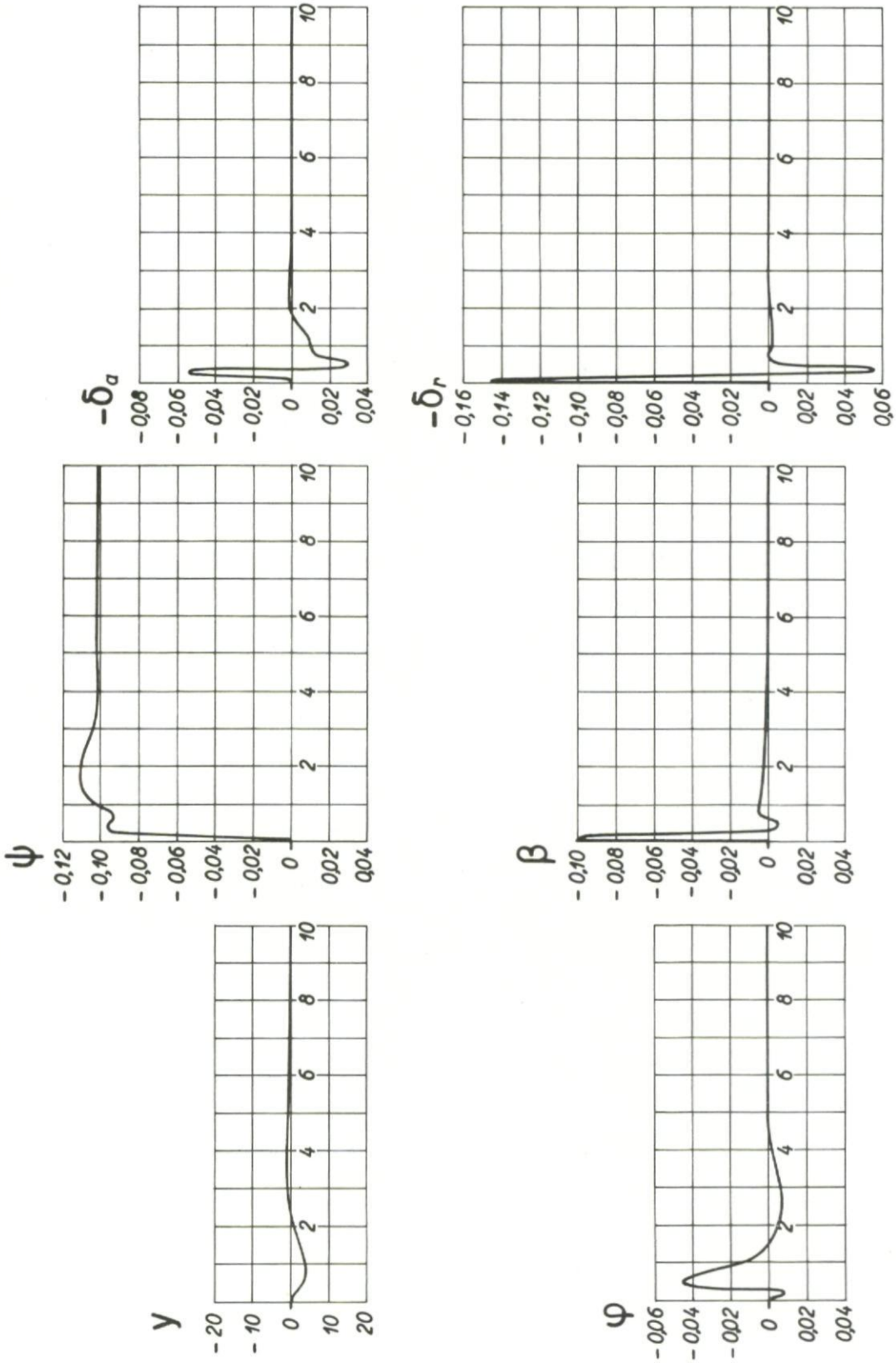

Fig.268 Aircraft response to a side gust v_a, case *l*

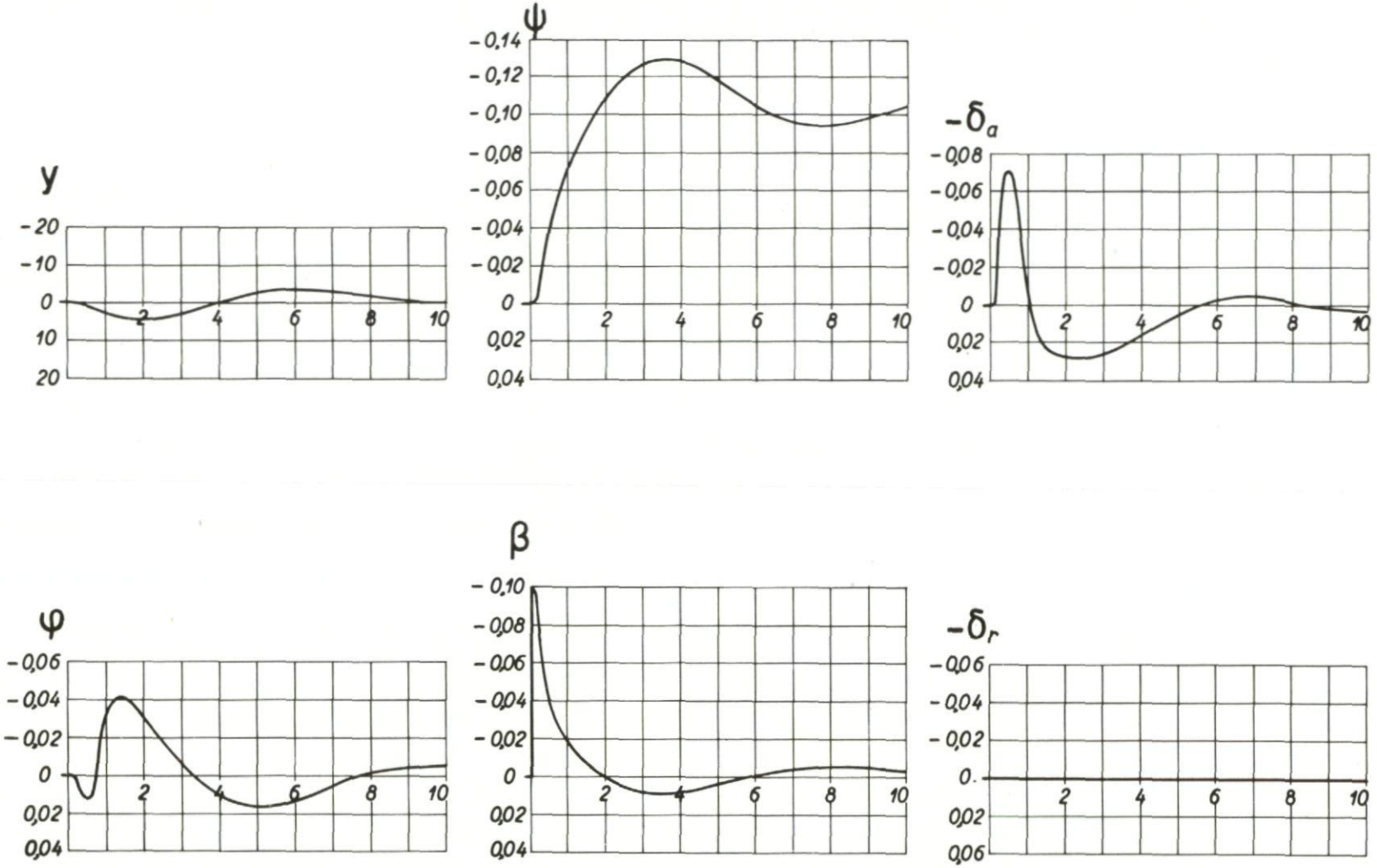

Fig. 269 Aircraft response to a side gust v_a, case l_1

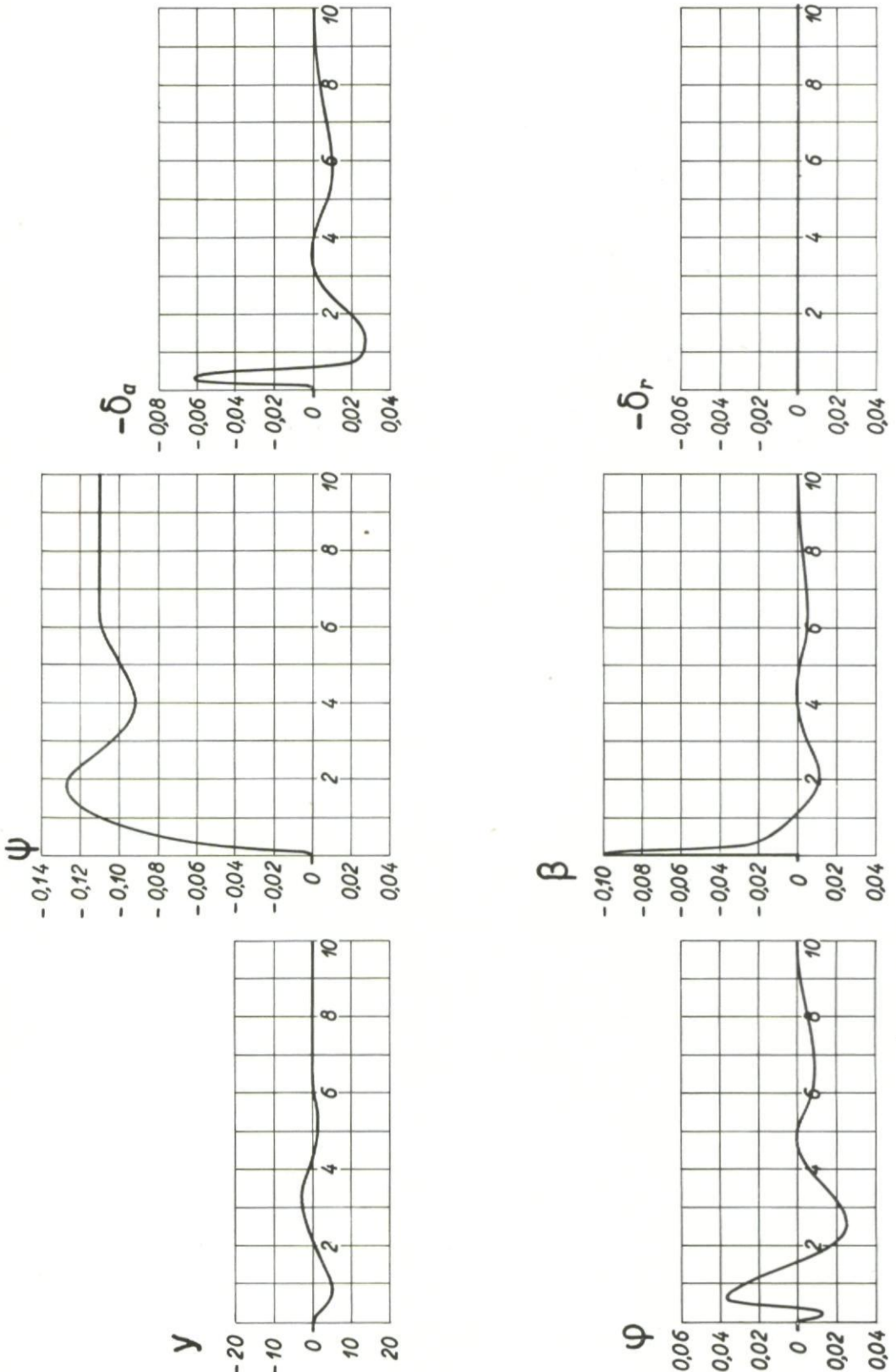

Fig.270 Aircraft response to a side gust v_a, case l_2

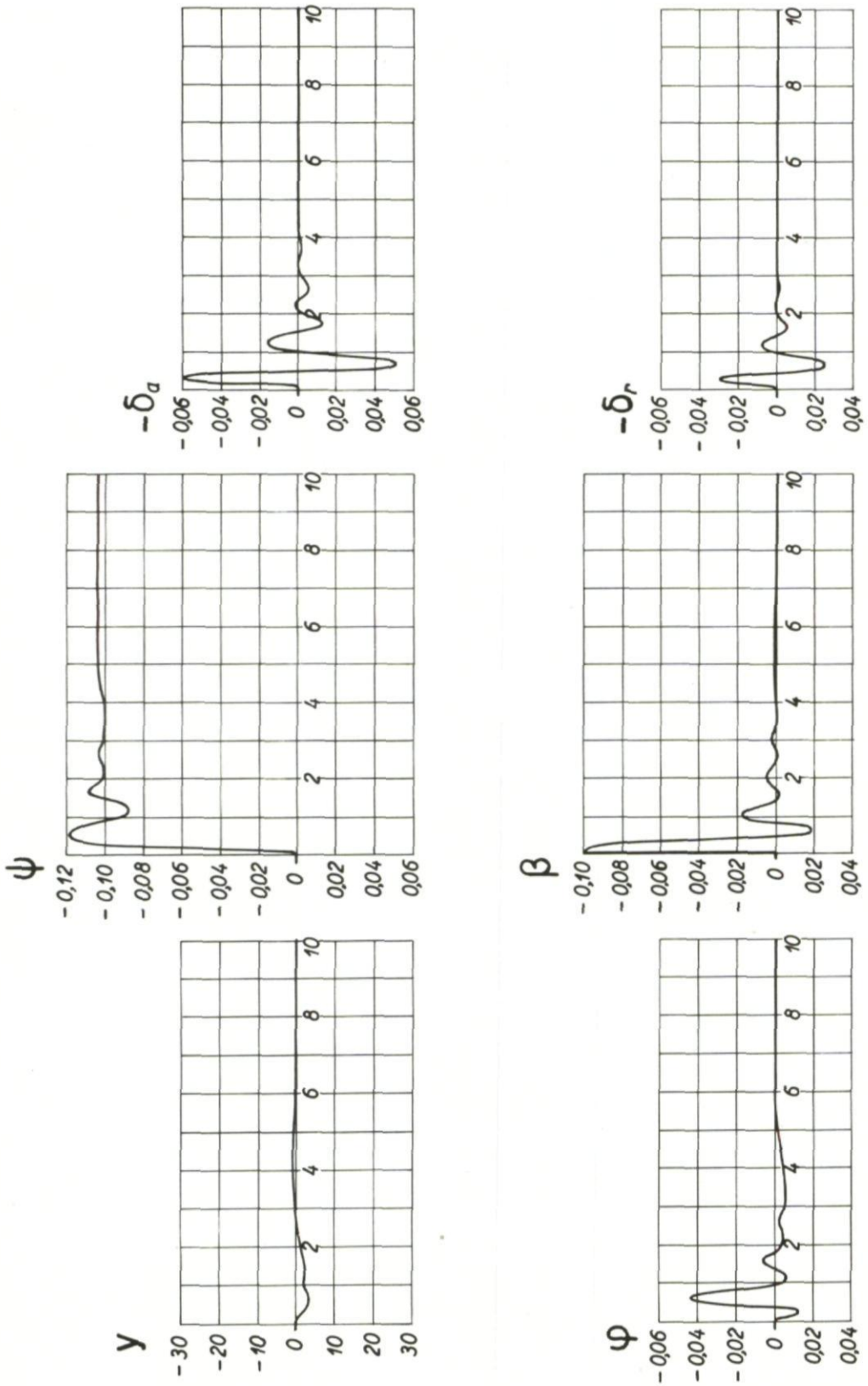

Fig.271 Aircraft response to a side gust v_a, case l_3

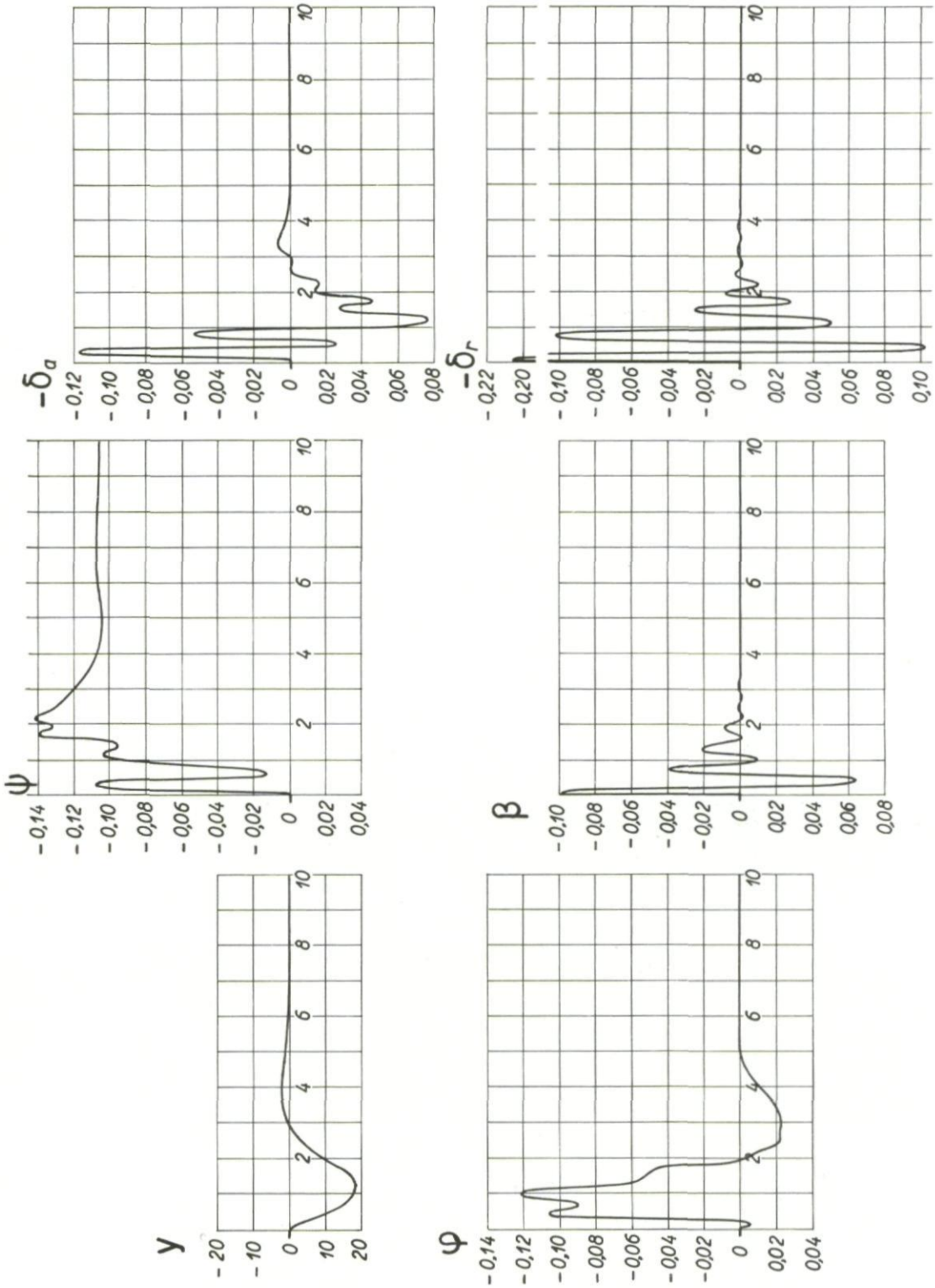

Fig.272 Aircraft response to a side gust v_a, case l'_3

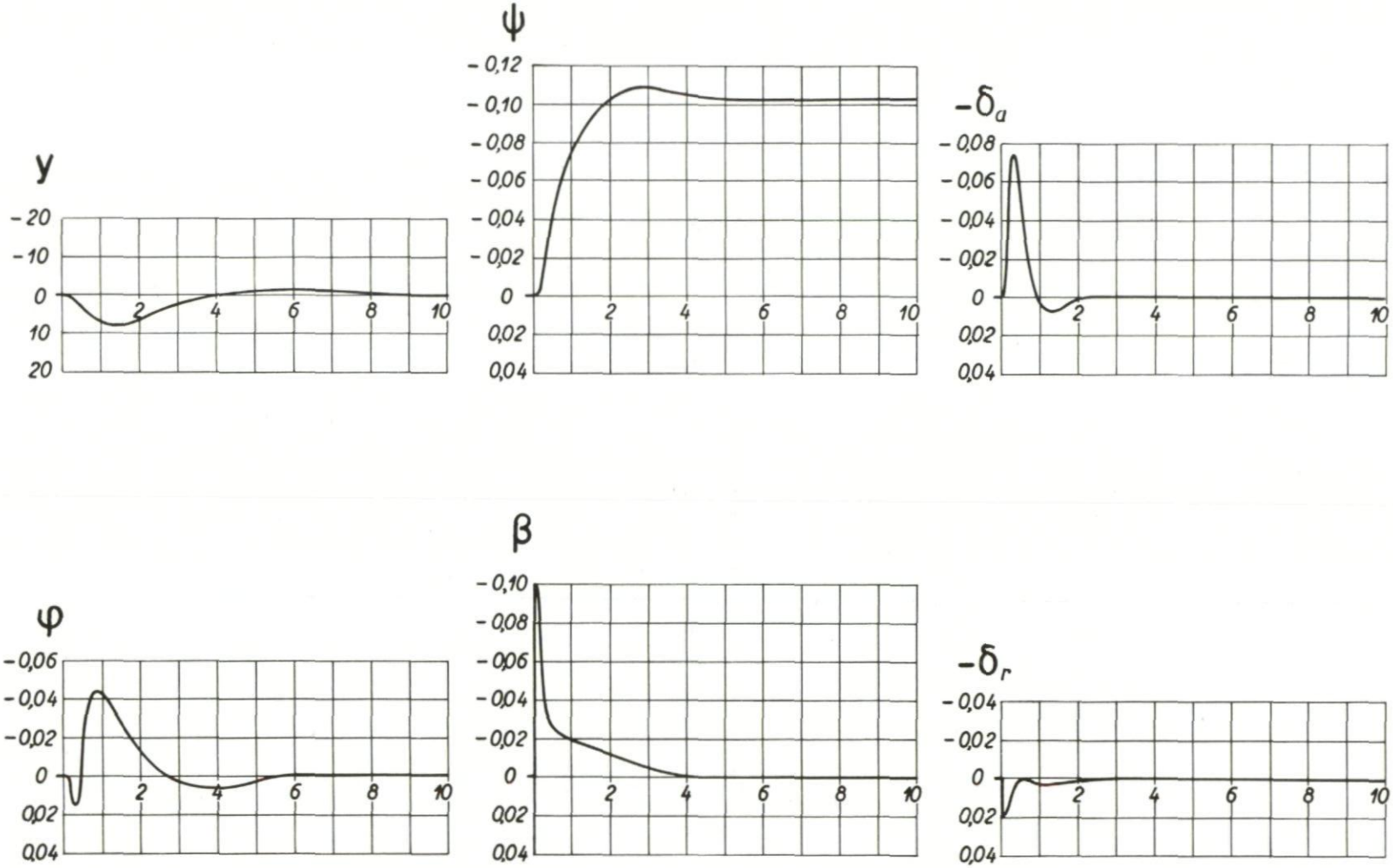

Fig. 273 Aircraft response to a side gust v_a, case l_4

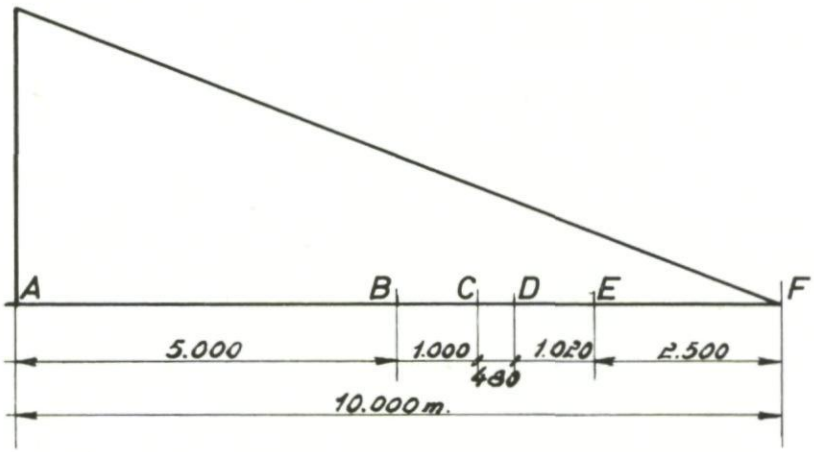

Fig.274 Definition of some points of the approach path

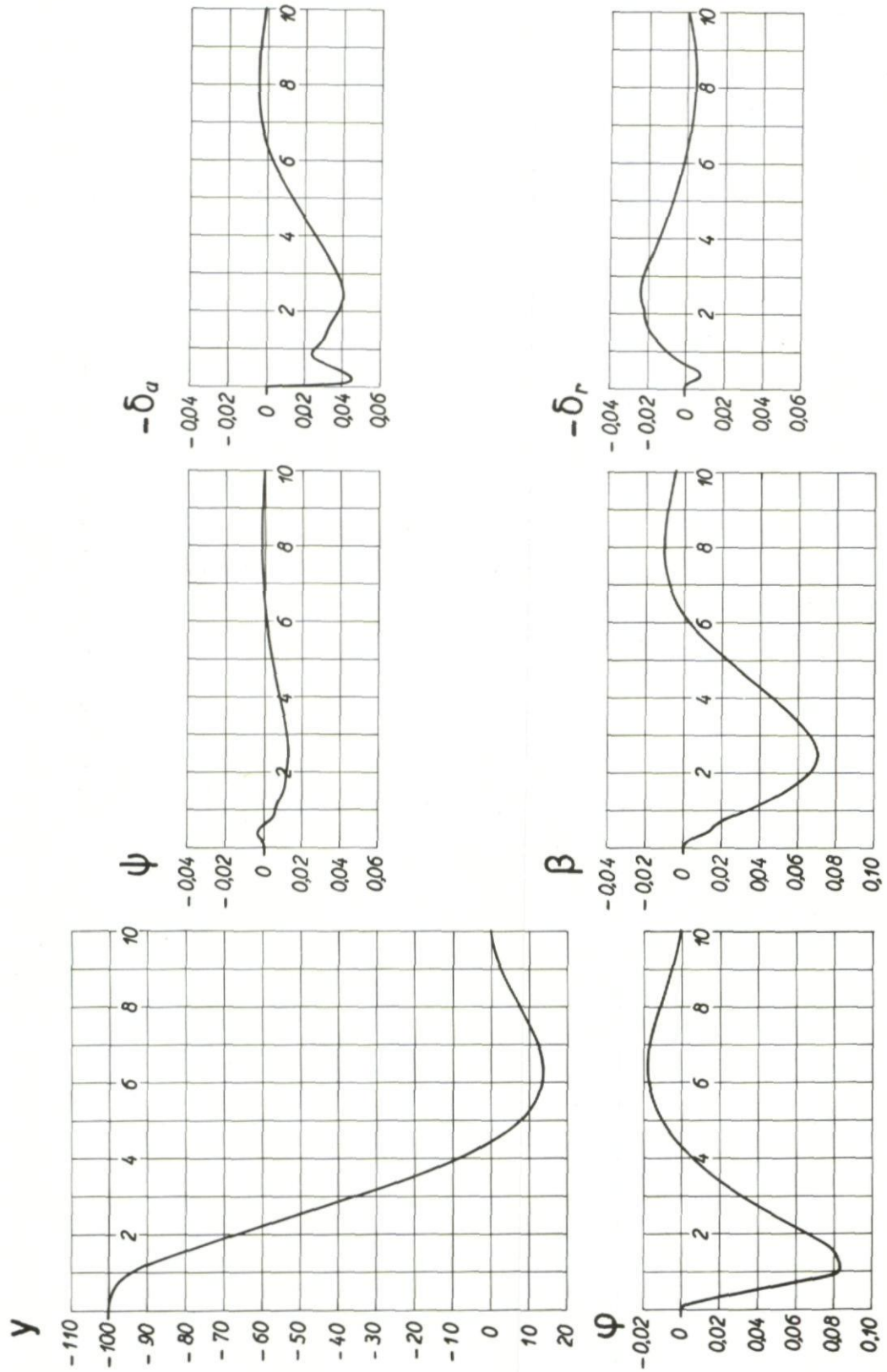

Fig.275 Aircraft response to an initial error y = 100m, case a'

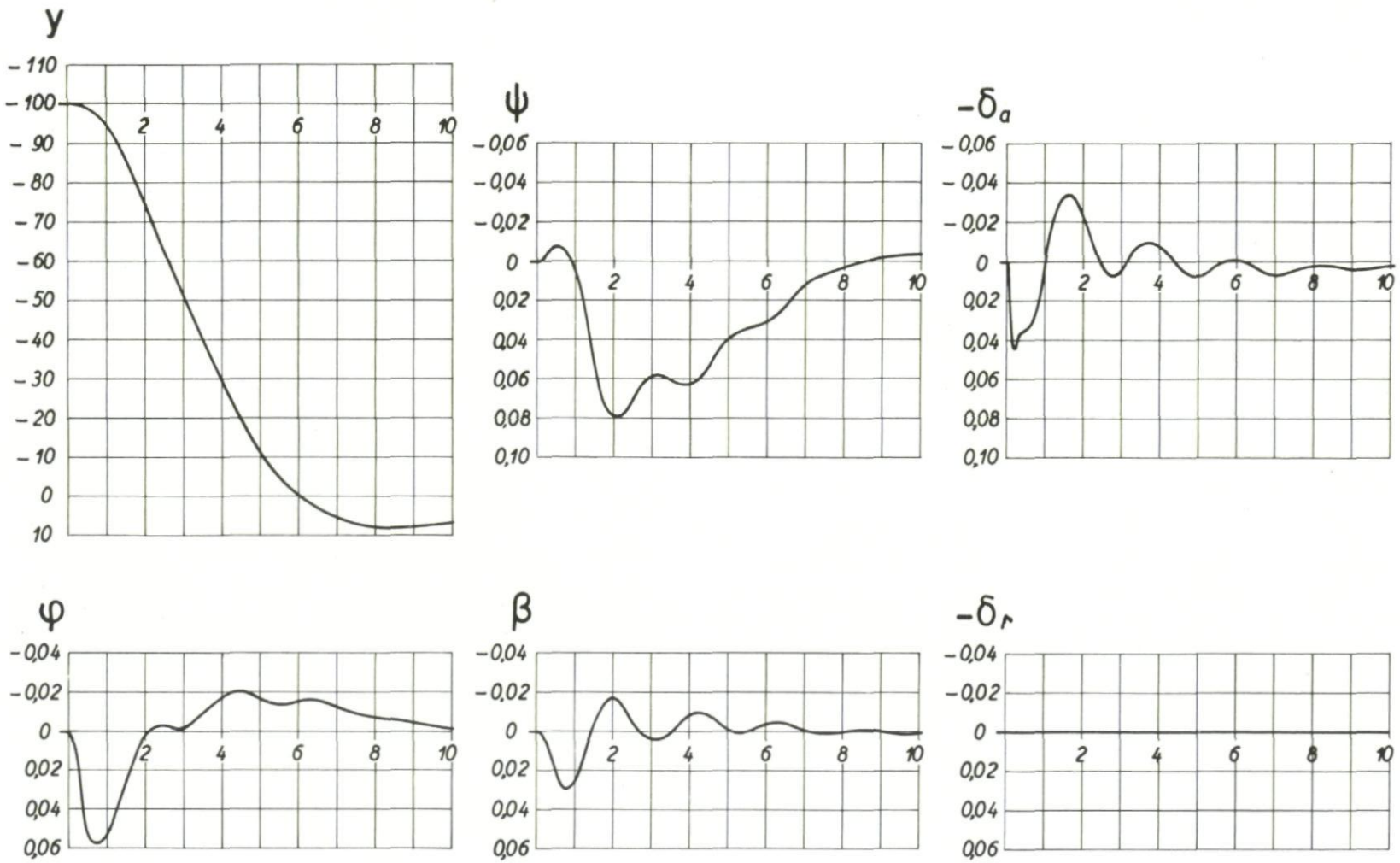

Fig.276 Aircraft response to an initial error y = 100m, case c'

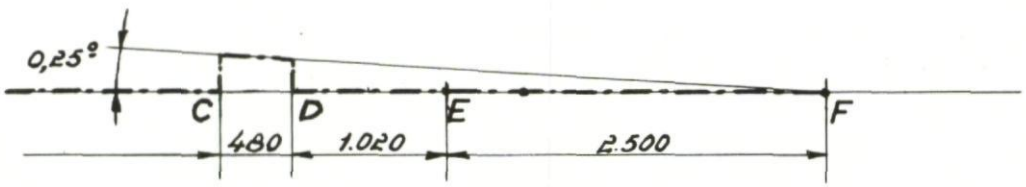

Fig.277(a) Schematic distortion of the beam

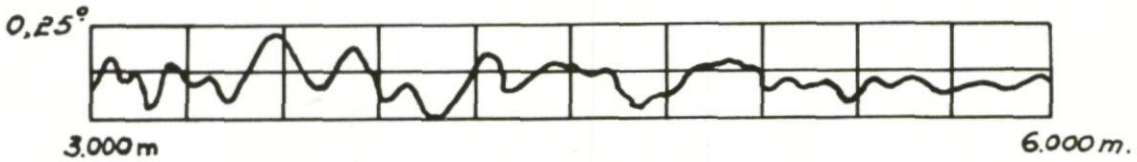

Fig.277(b) Typical localizer beam

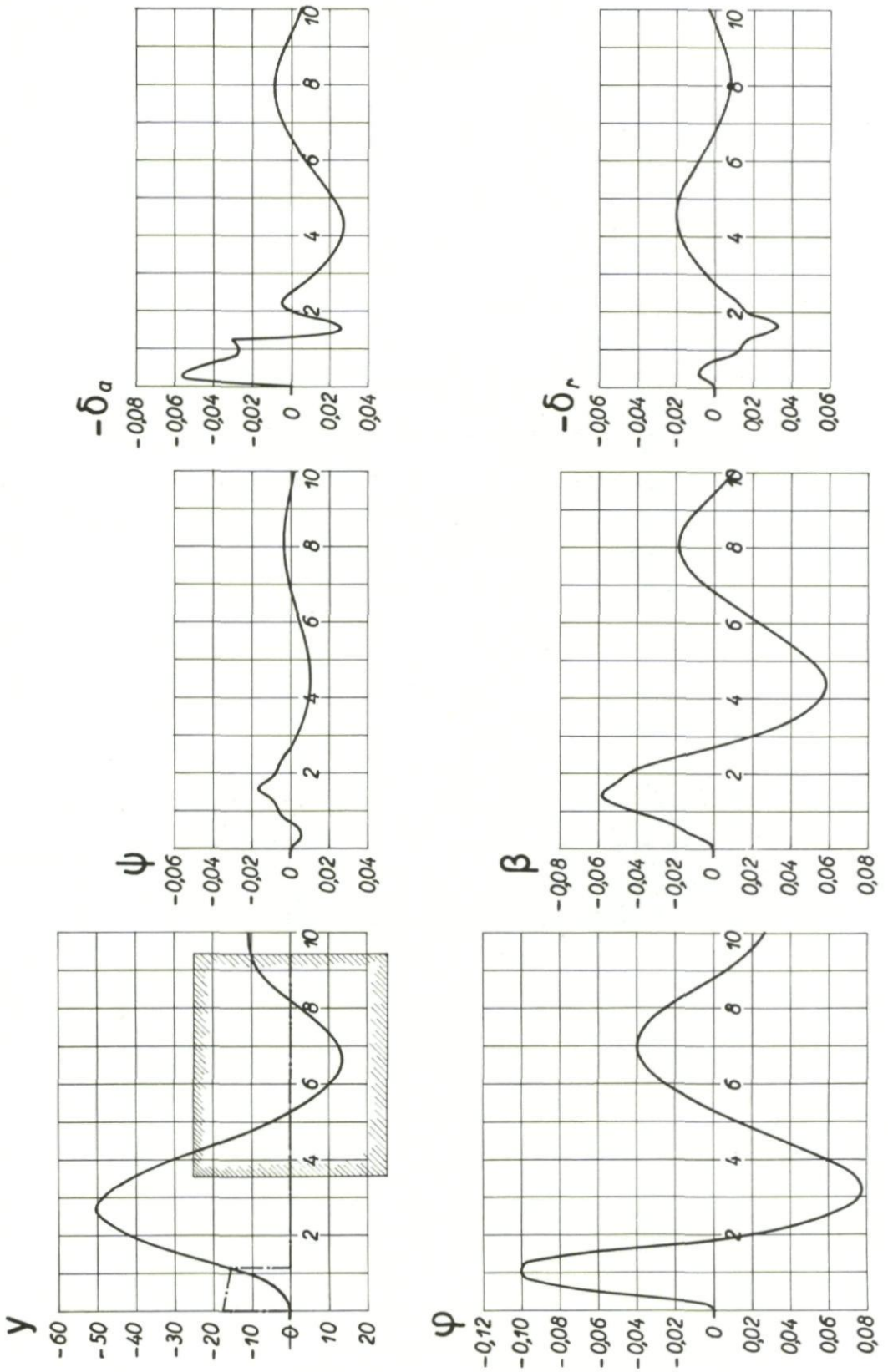

Fig.278 Aircraft response with distortion of the beam, case a'

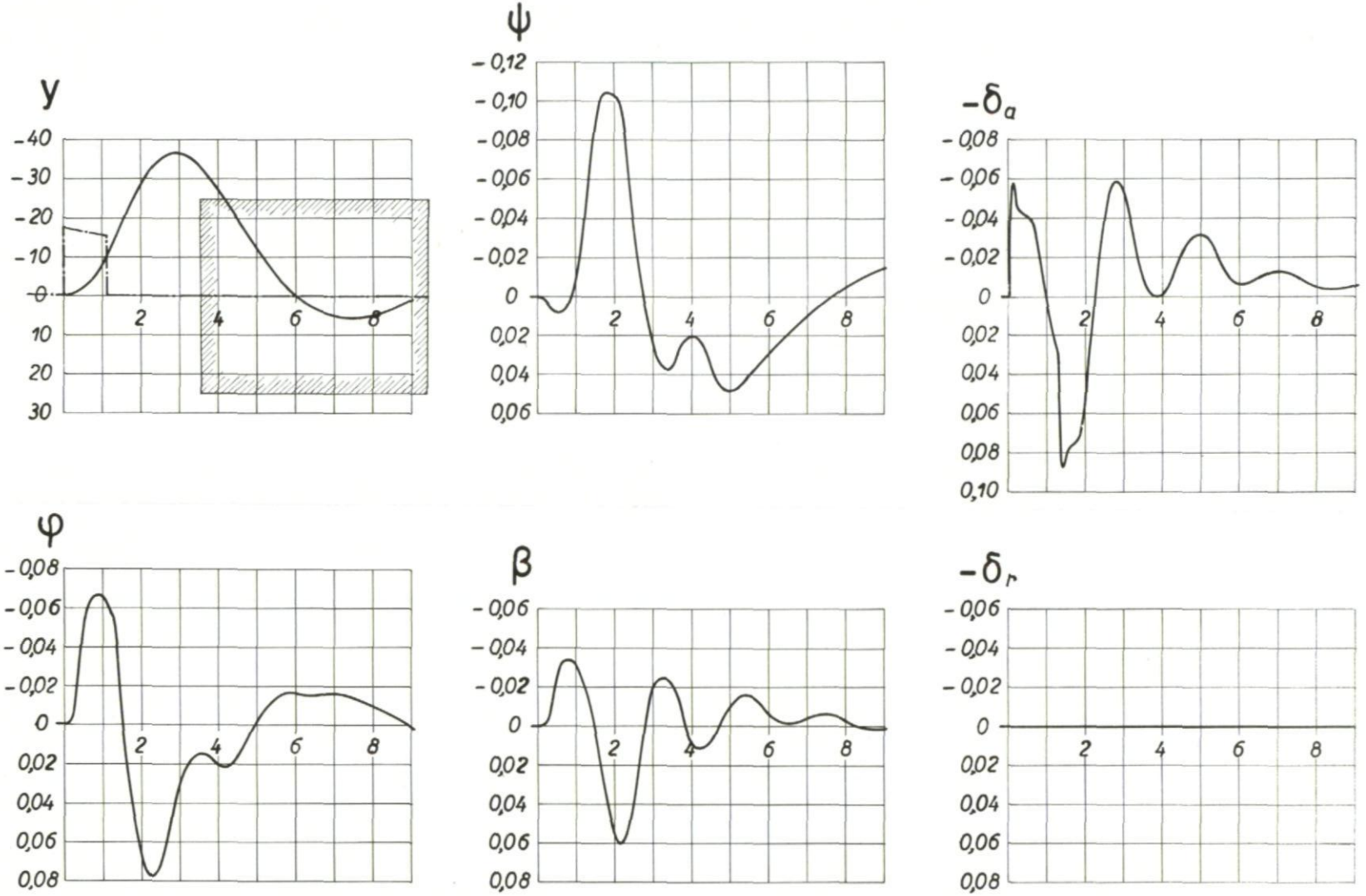

Fig.279 Aircraft response with distortion of the beam, case c′

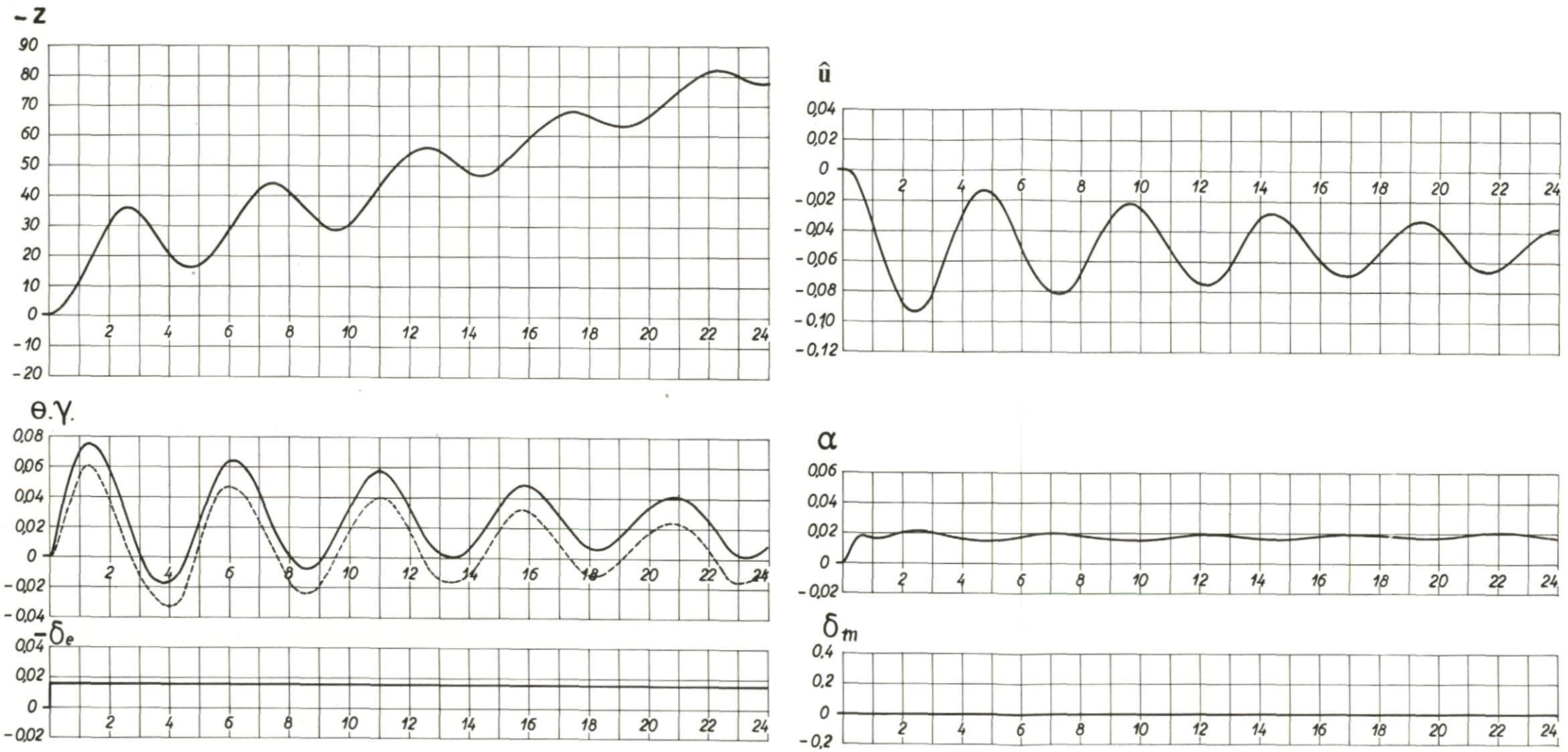

Fig.280 Longitudinal motion; response to a step input $\delta_e = -0.016$

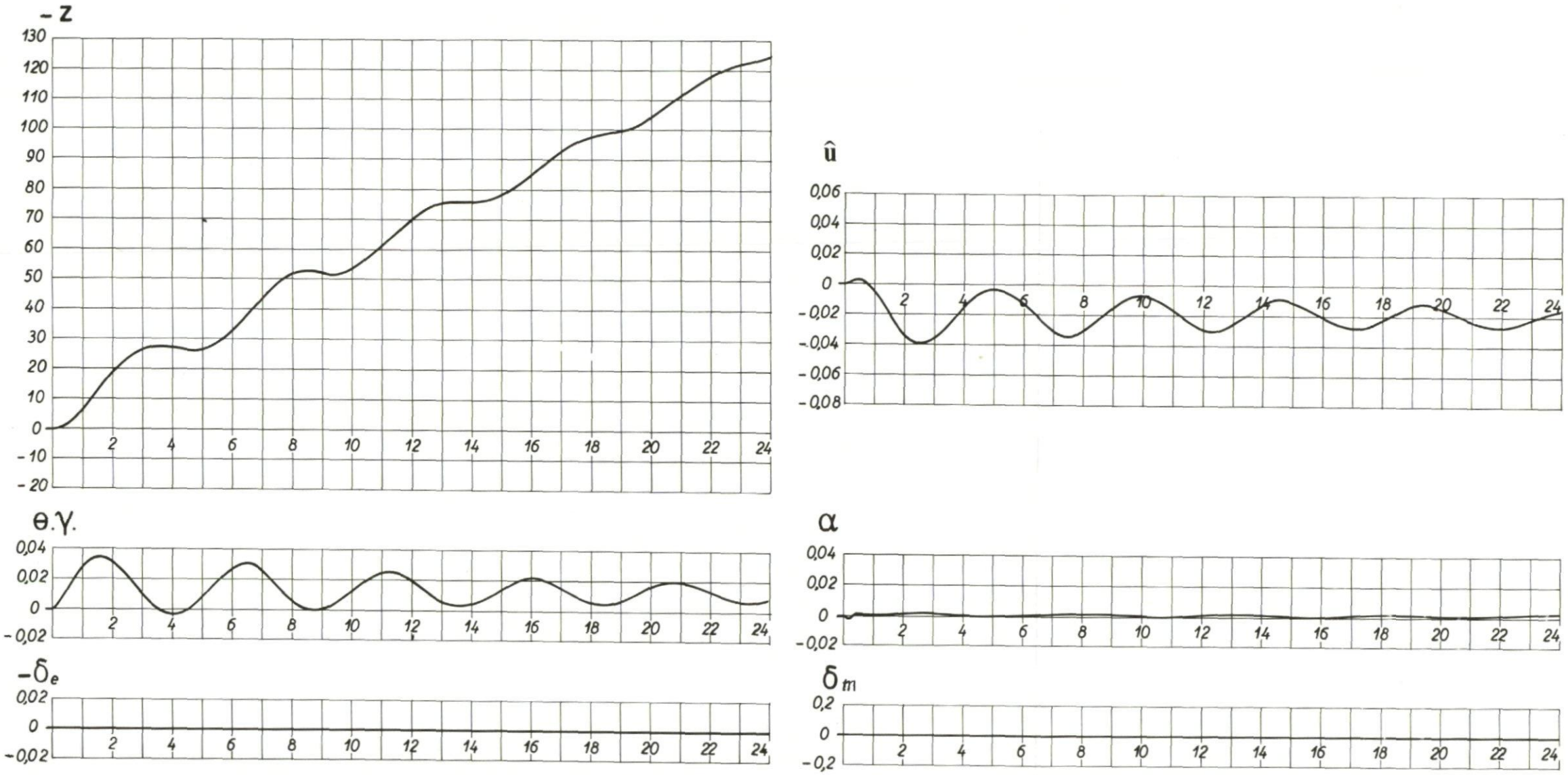

Fig.281 Longitudinal motion; response to a step input δ_m = +0.20

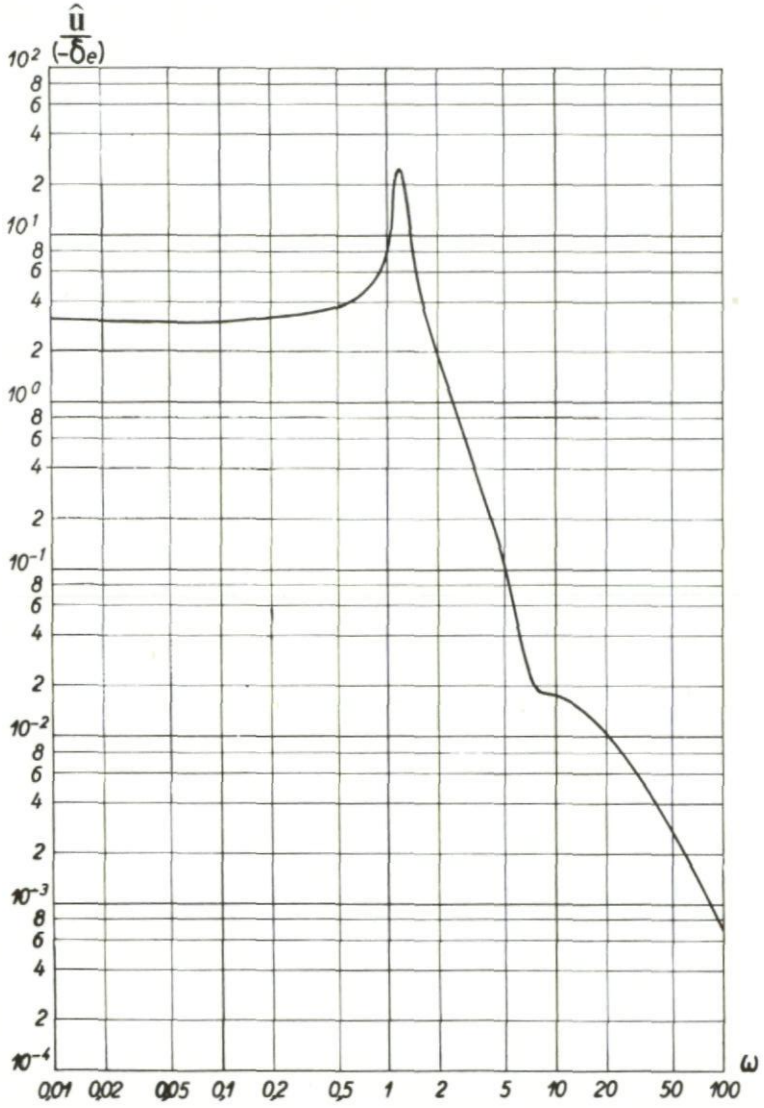

Fig.282(a) Frequency response; $\hat{u}$ produced by $-\delta_e$, amplitude

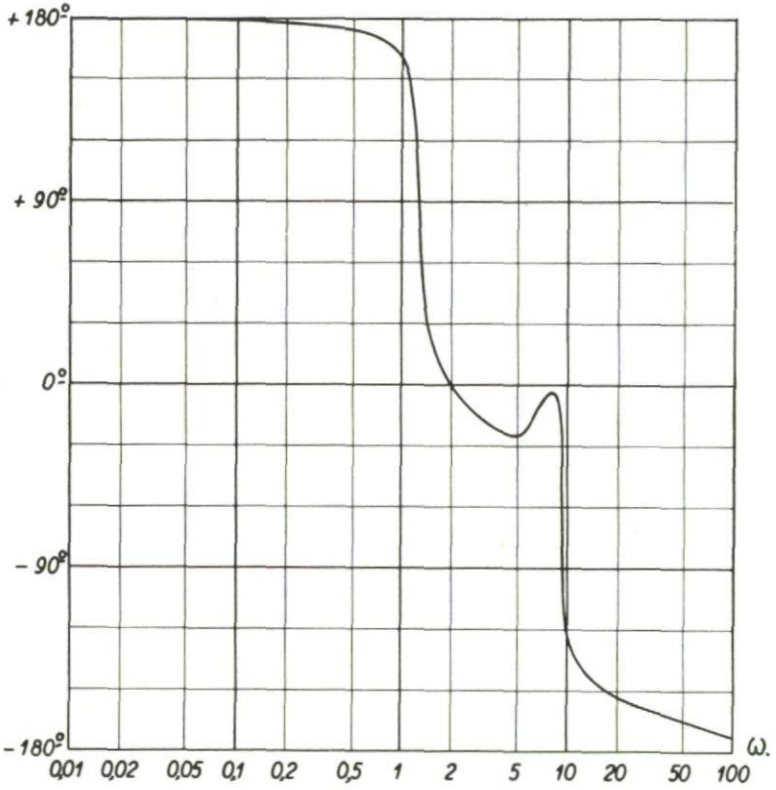

Fig.282(b) Frequency response; $\hat{u}$ produced by $-\delta_e$, phase

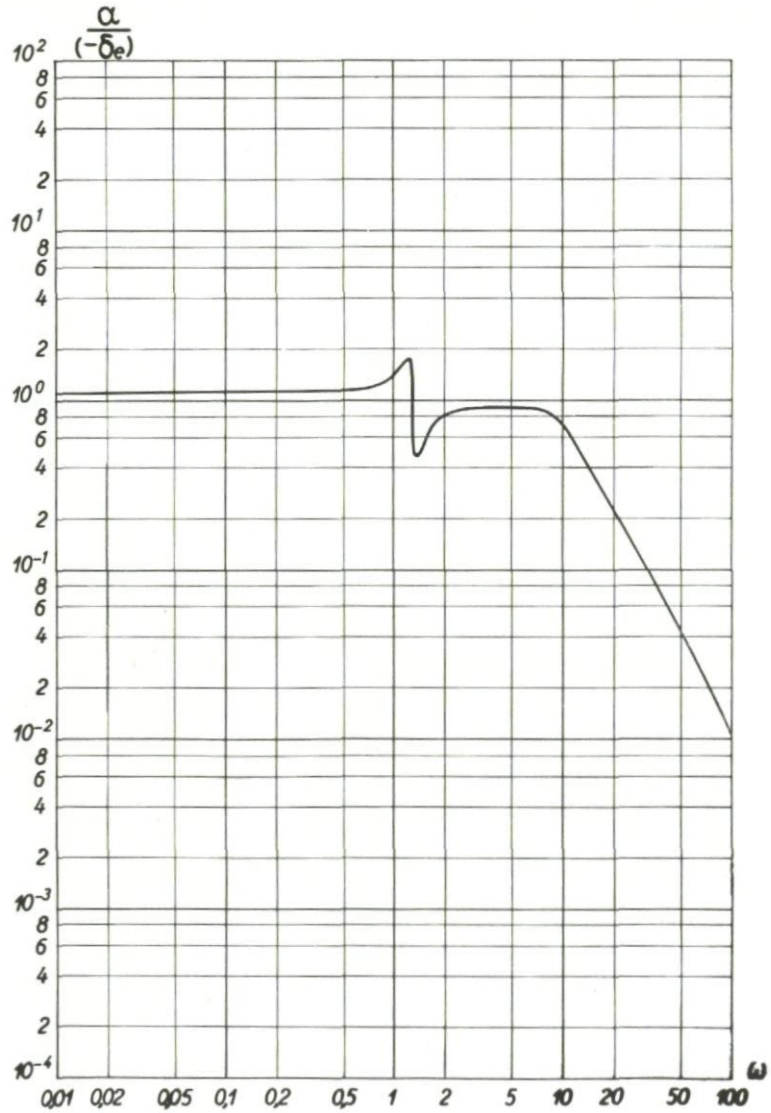

Fig.283(a) Frequency response; α produced by $-\delta_e$, amplitude

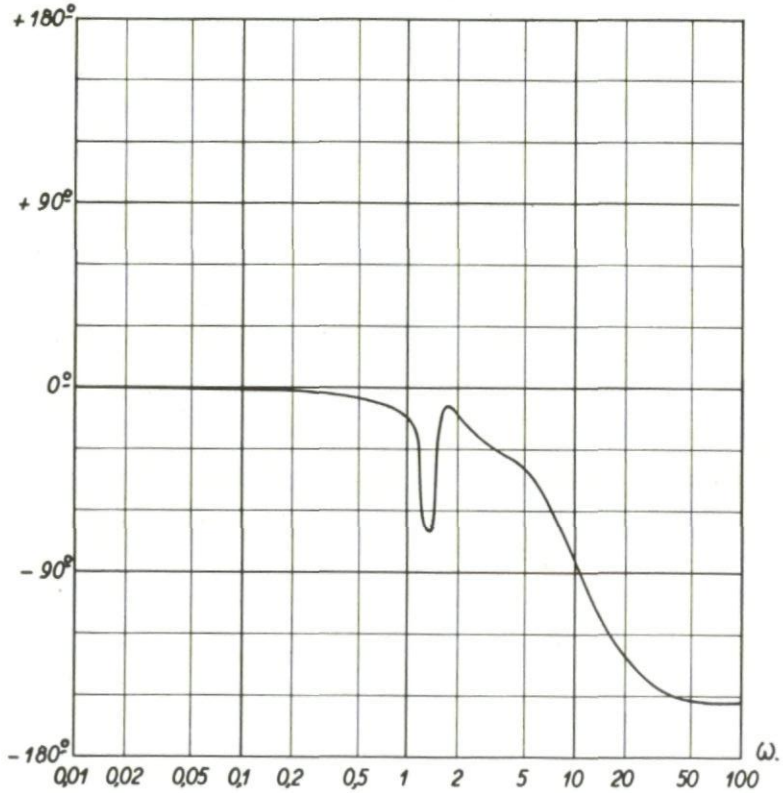

Fig.283(b) Frequency response; α produced by $-\delta_e$, phase

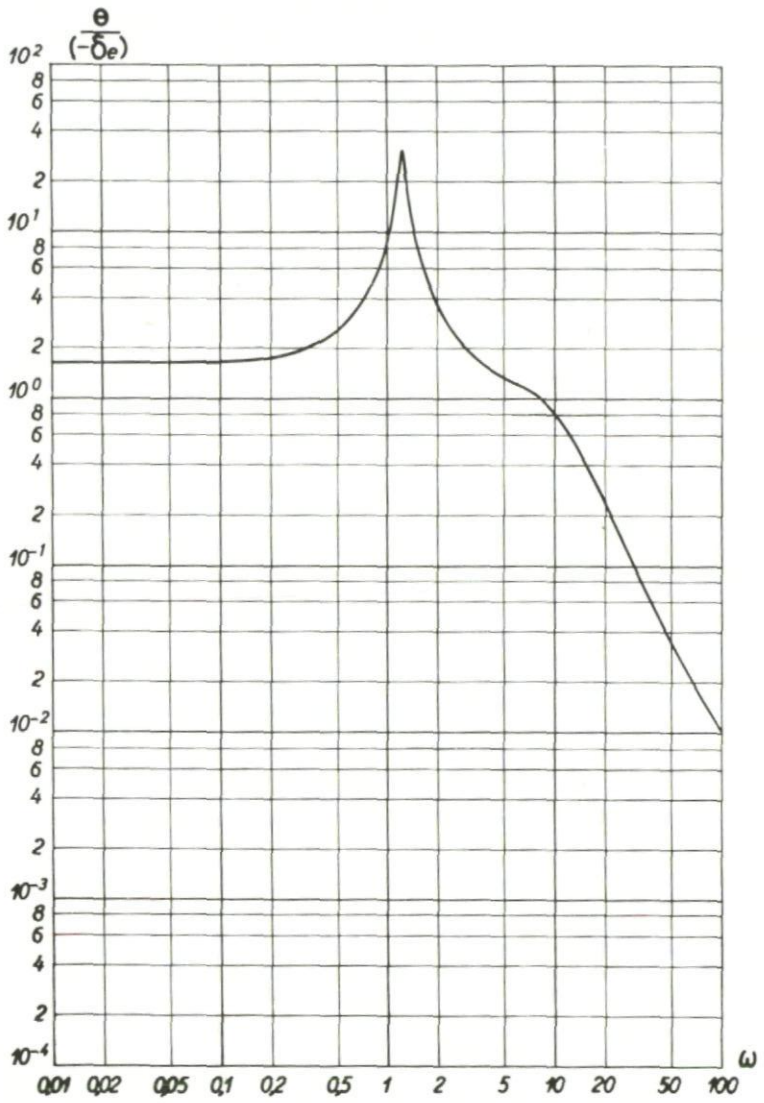

Fig. 284(a) Frequency response; θ produced by $-\delta_e$, amplitude

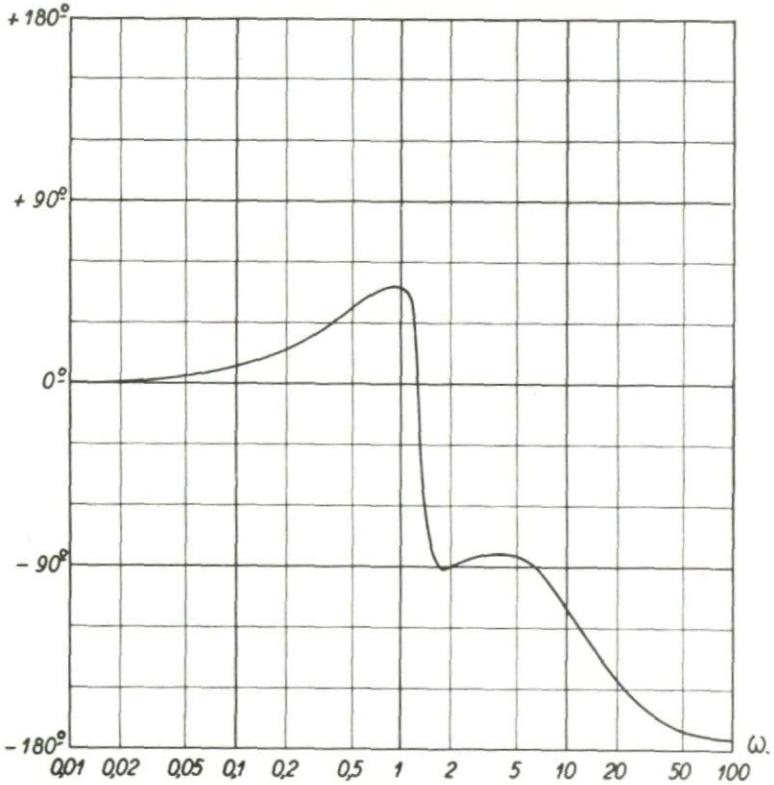

Fig. 284(b) Frequency response; θ produced by $-\delta_e$, phase

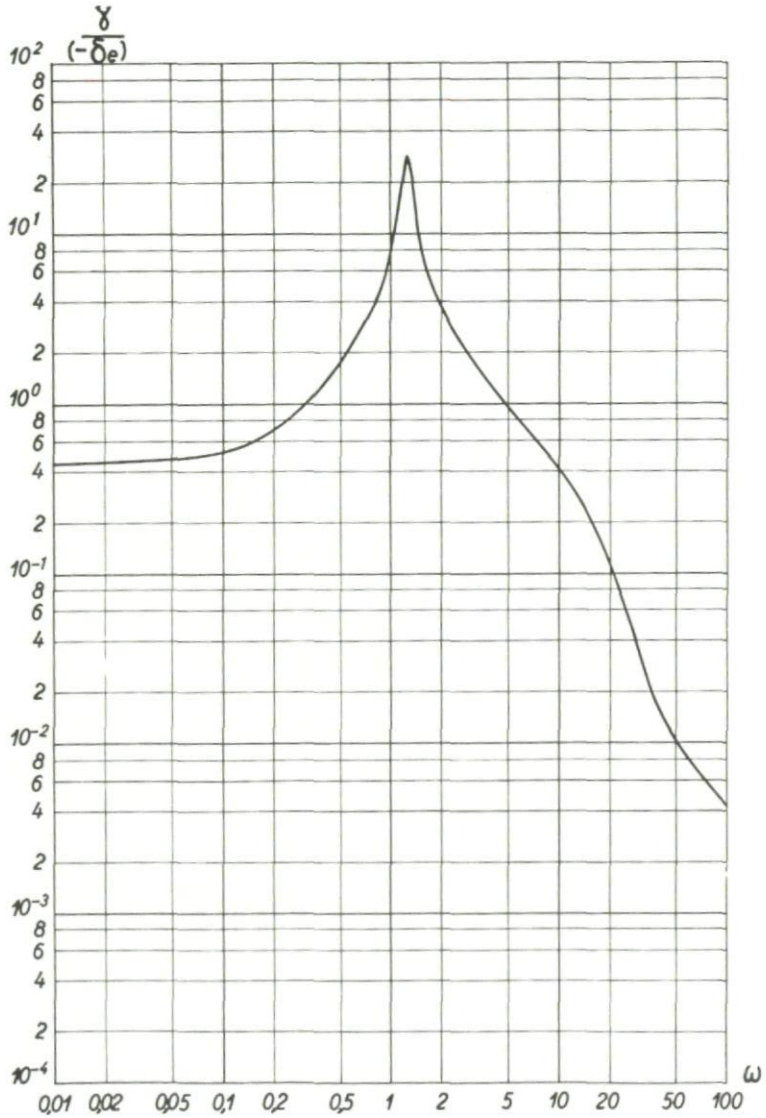

Fig. 285(a) Frequency response; γ produced by $-\delta_e$, amplitude

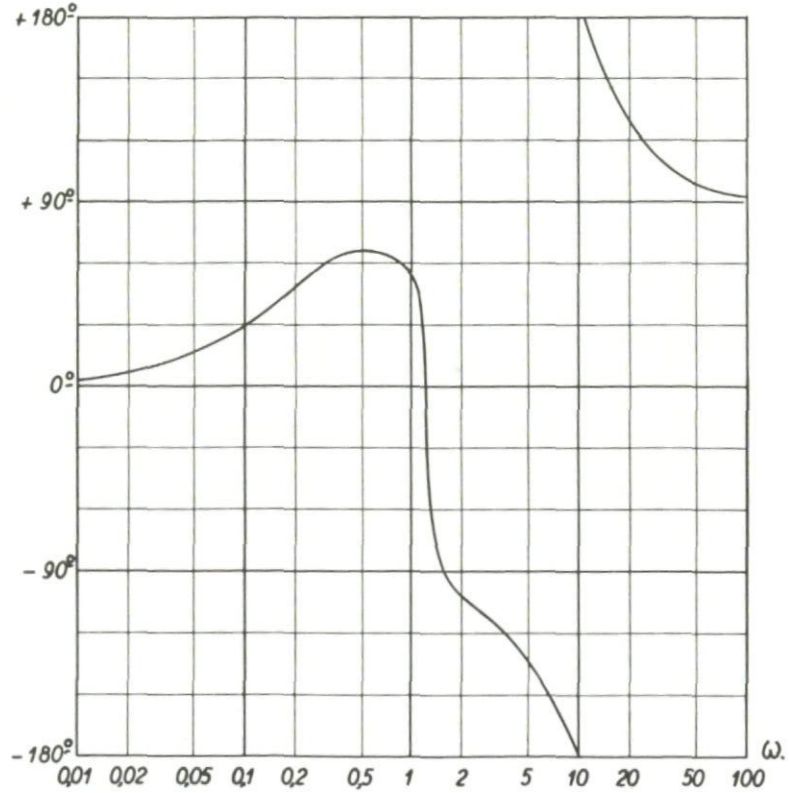

Fig. 285(b) Frequency response; γ produced by $-\delta_e$, phase

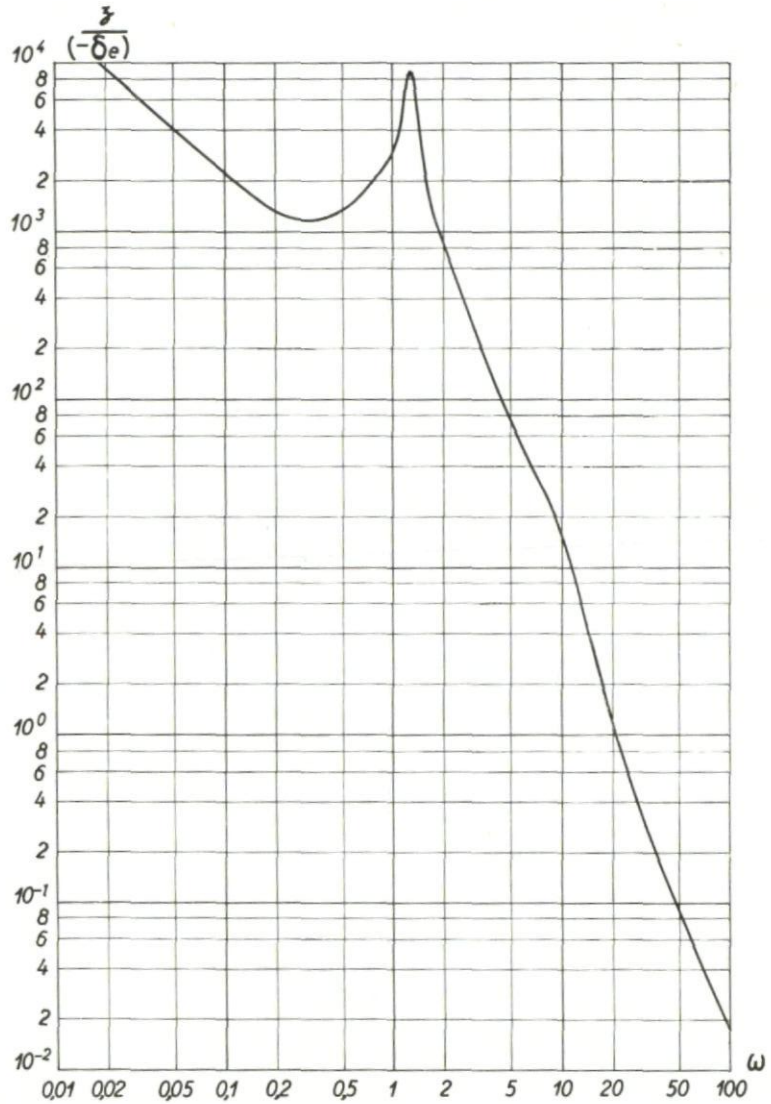

Fig. 286(a) Frequency response; z produced by $-\delta_e$, amplitude

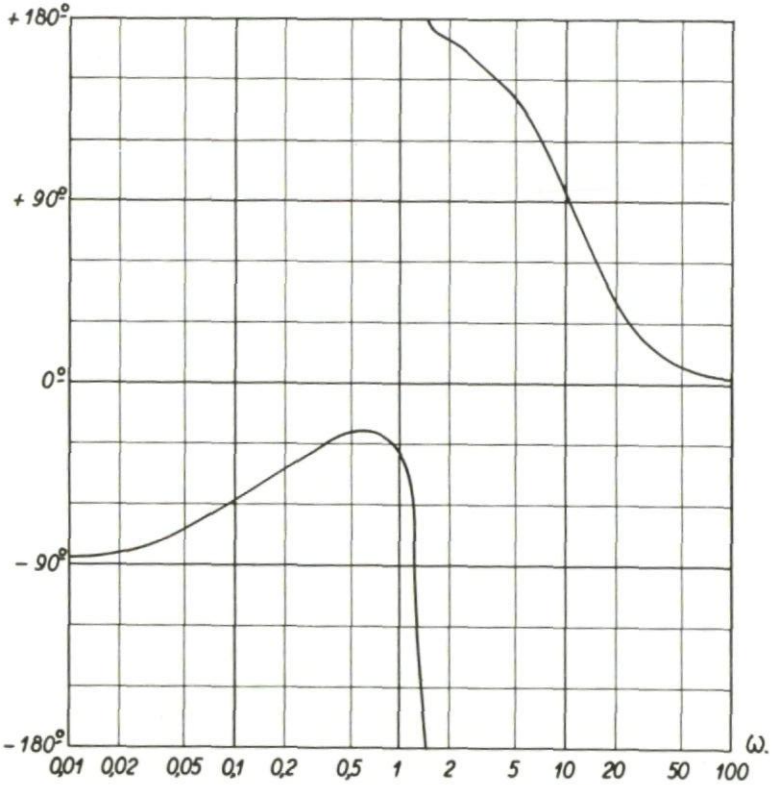

Fig. 286(b) Frequency response; z produced by $-\delta_e$, phase

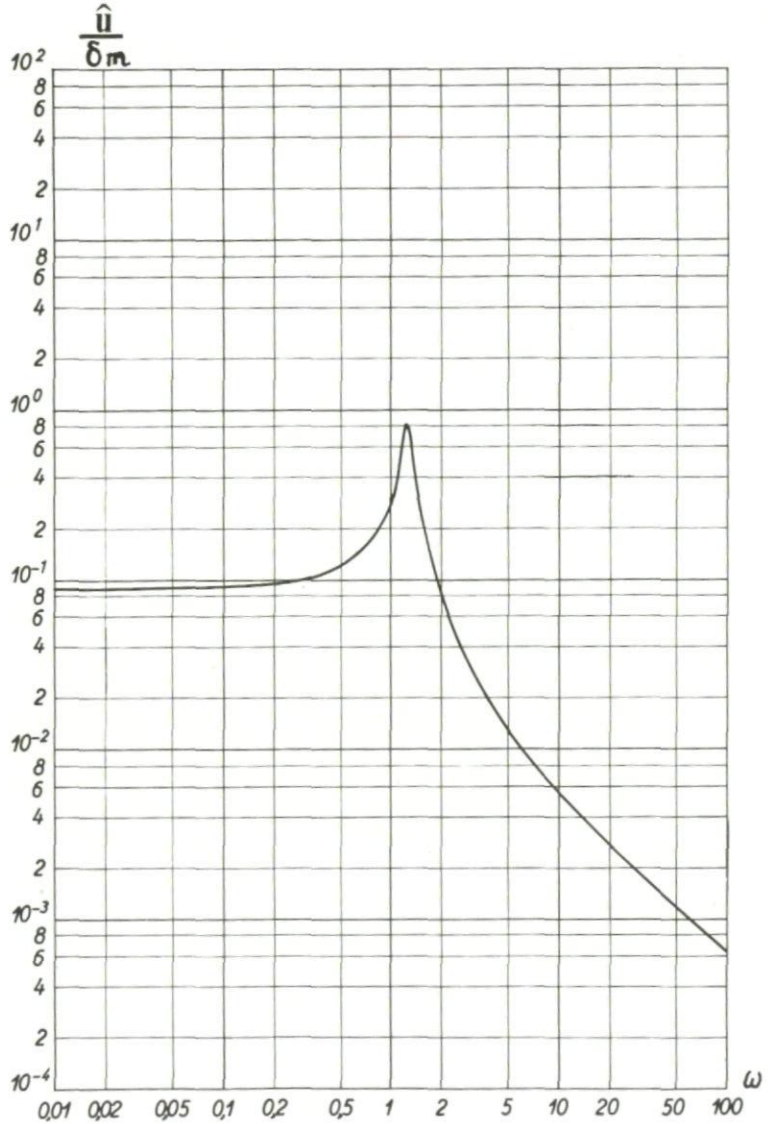

Fig.287(a) Frequency response; $\hat{u}$ produced by δ_m, amplitude

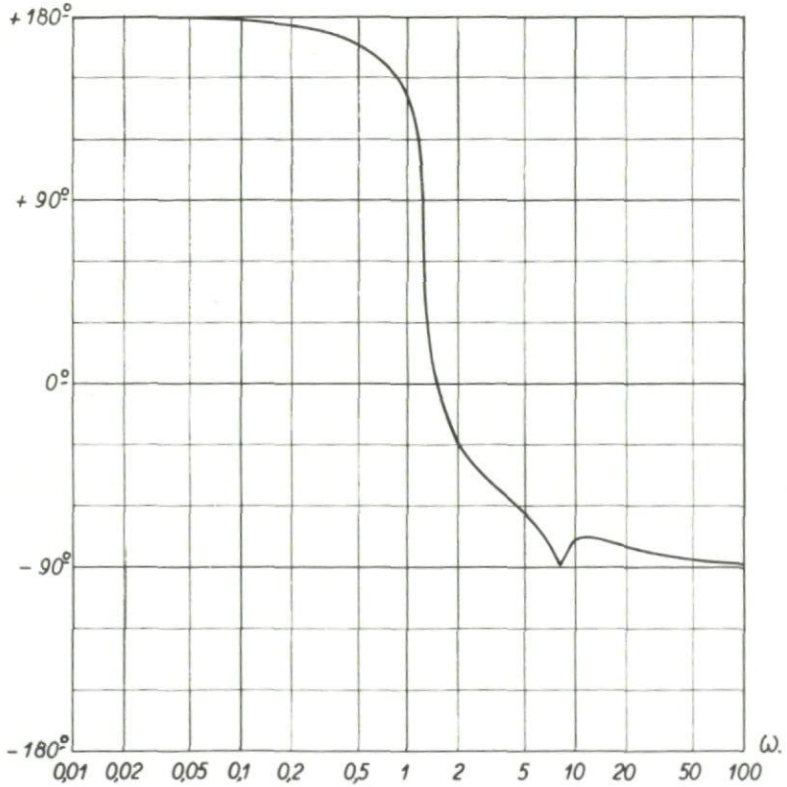

Fig.287(b) Frequency response; $\hat{u}$ produced by δ_m, phase

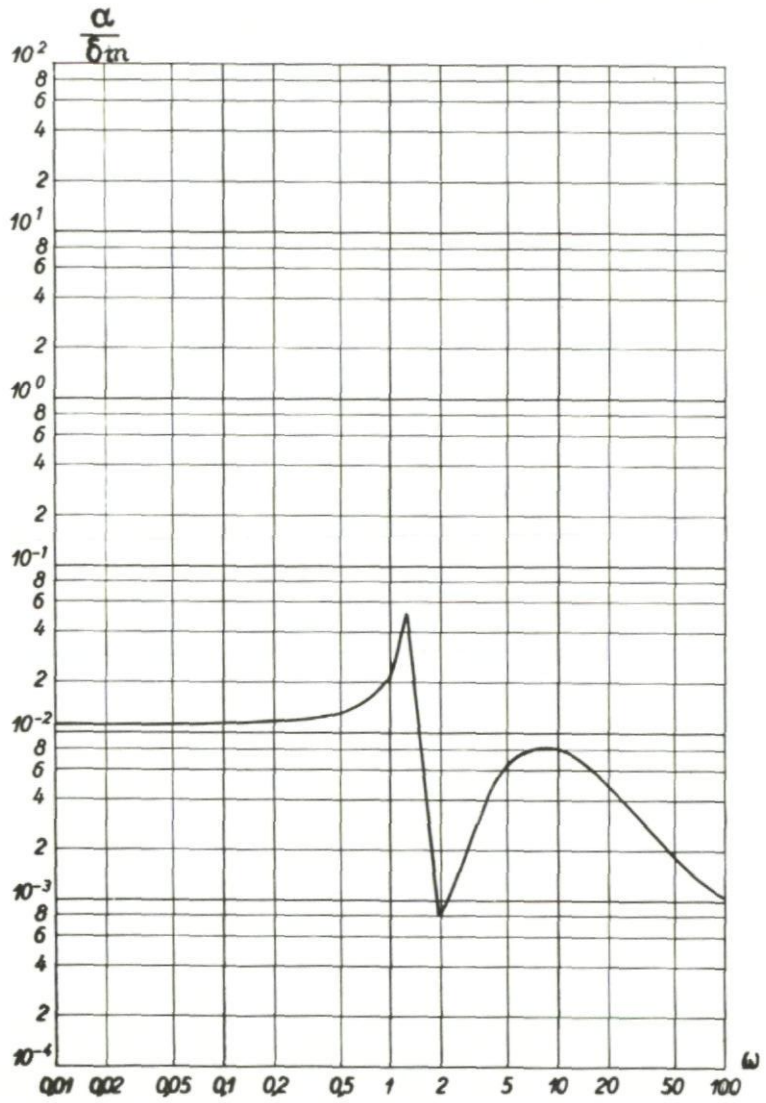

Fig. 288(a) Frequency response; α produced by δ_m, amplitude

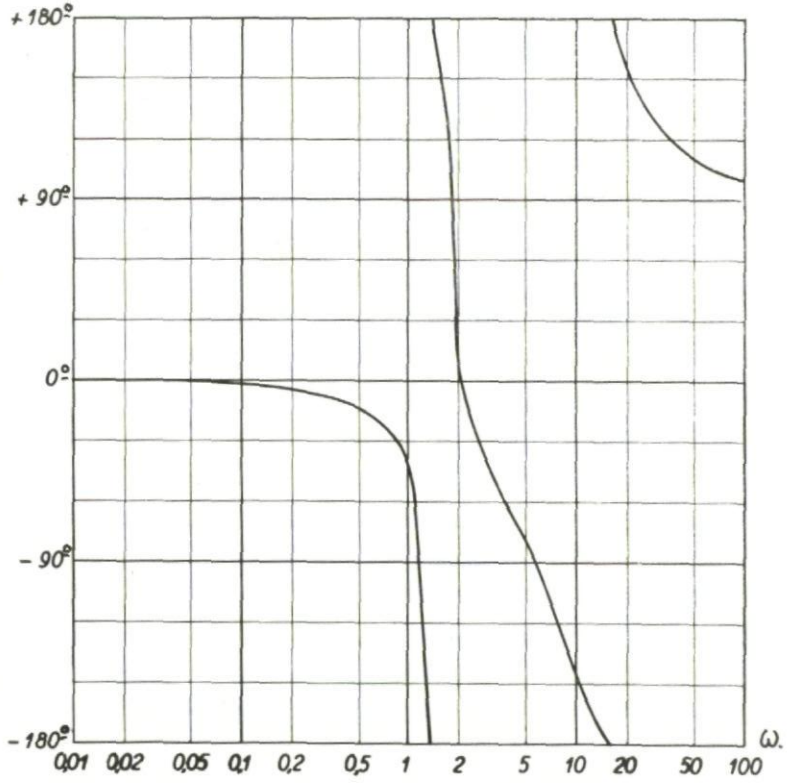

Fig. 288(b) Frequency response; α produced by δ_m, phase

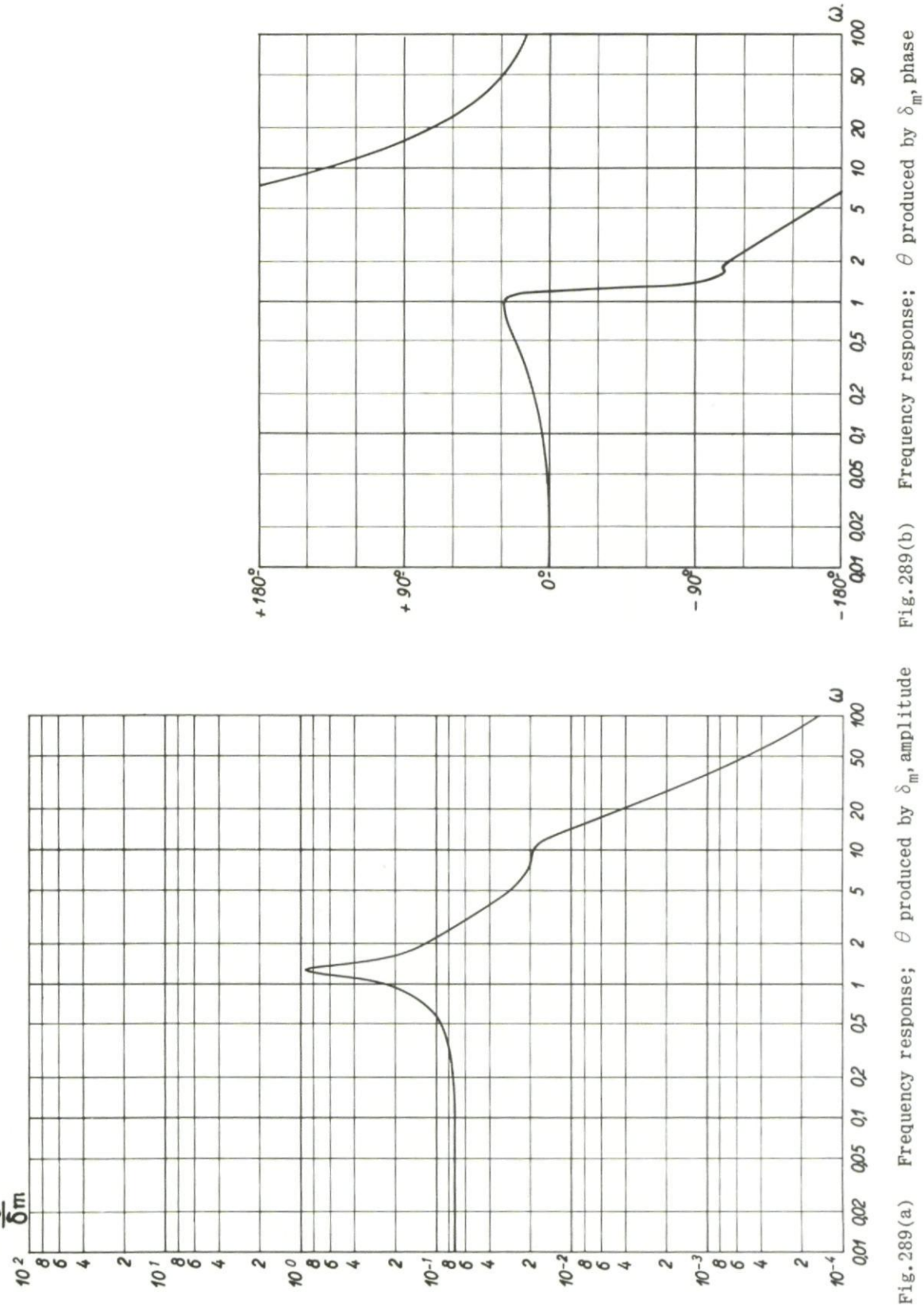

Fig.289(a) Frequency response; θ produced by δ_m, amplitude

Fig.289(b) Frequency response; θ produced by δ_m, phase

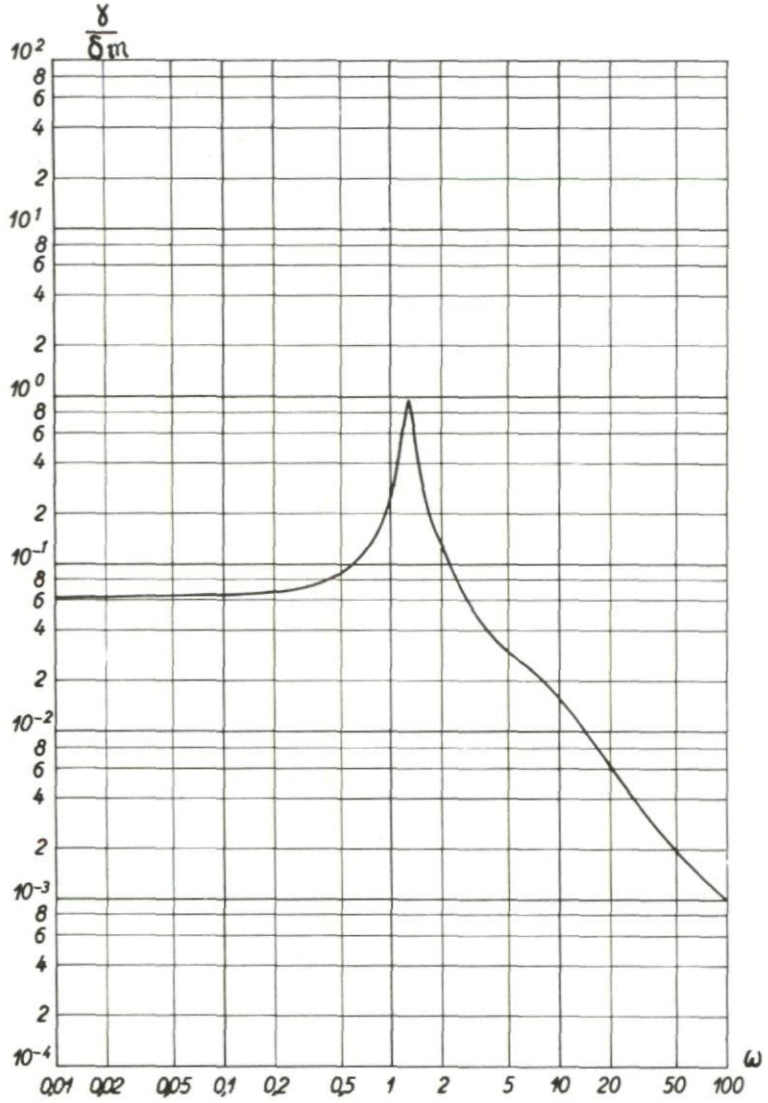

Fig. 290(a) Frequency response; γ produced by δ_m, amplitude

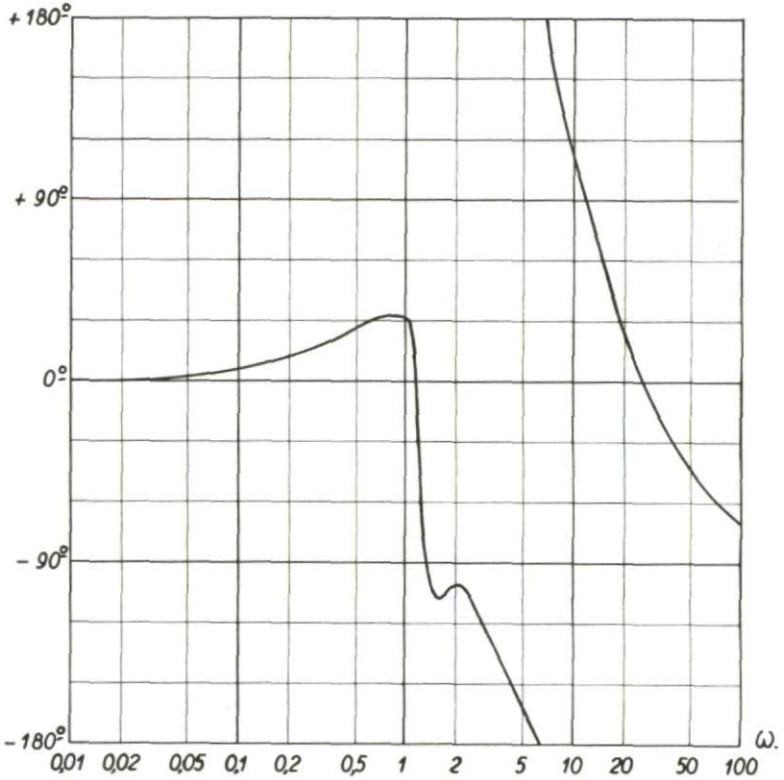

Fig. 290(b) Frequency response; γ produced by δ_m, phase

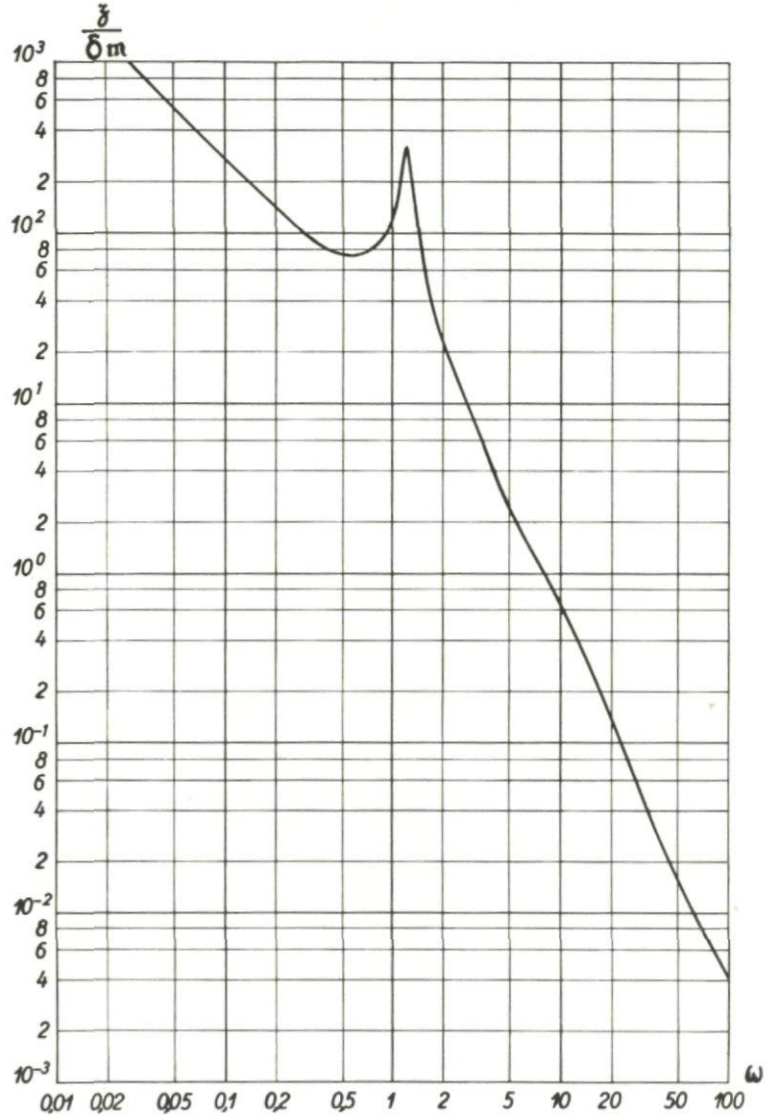

Fig. 291(a) Frequency response; z produced by δ_m, amplitude

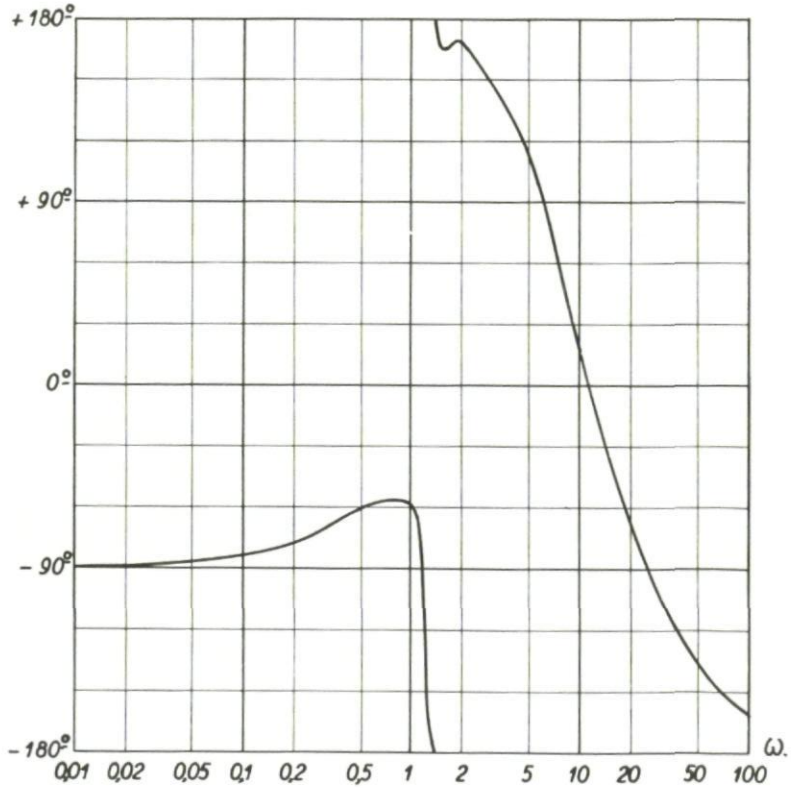

Fig. 291(b) Frequency response; z produced by δ_m, phase

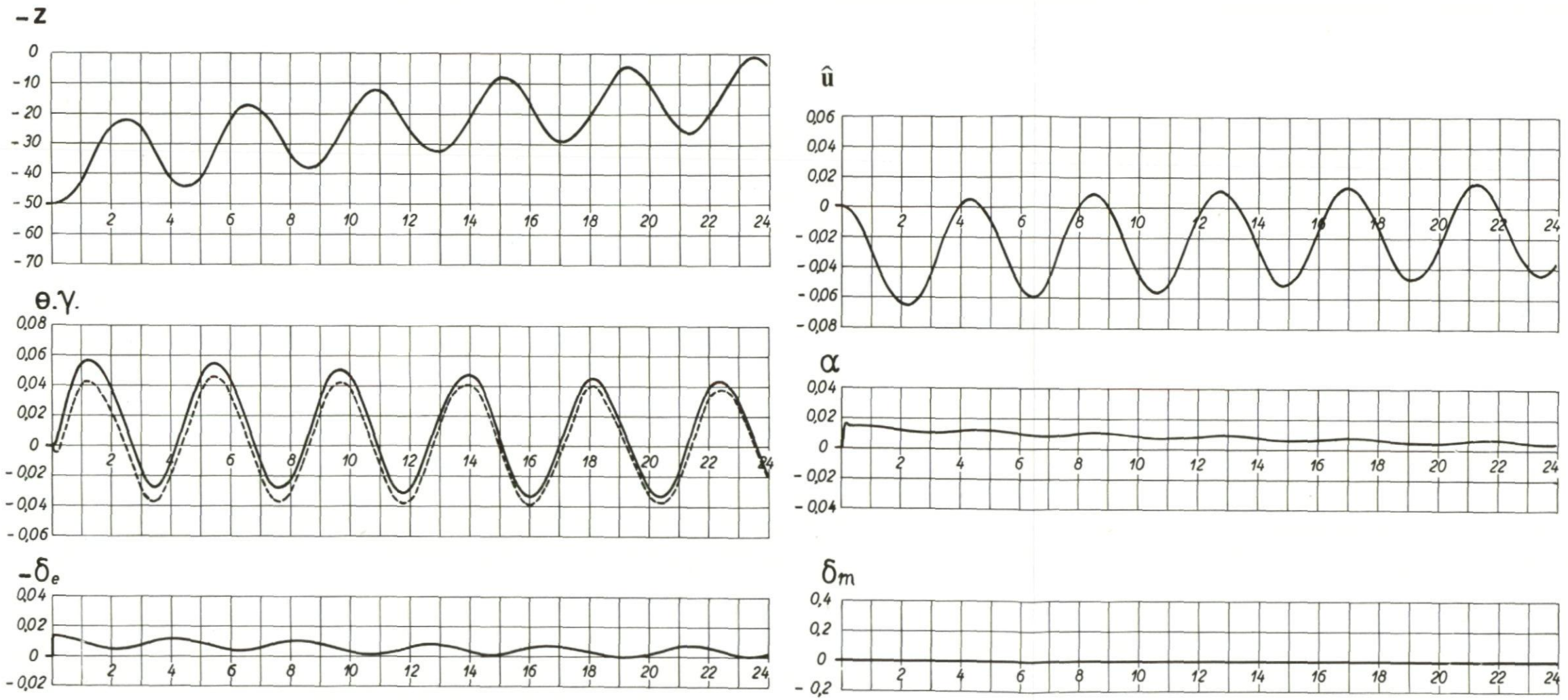

Fig.292 Aircraft response to an initial error z = 50 m, for $\delta_e = A_4 z$

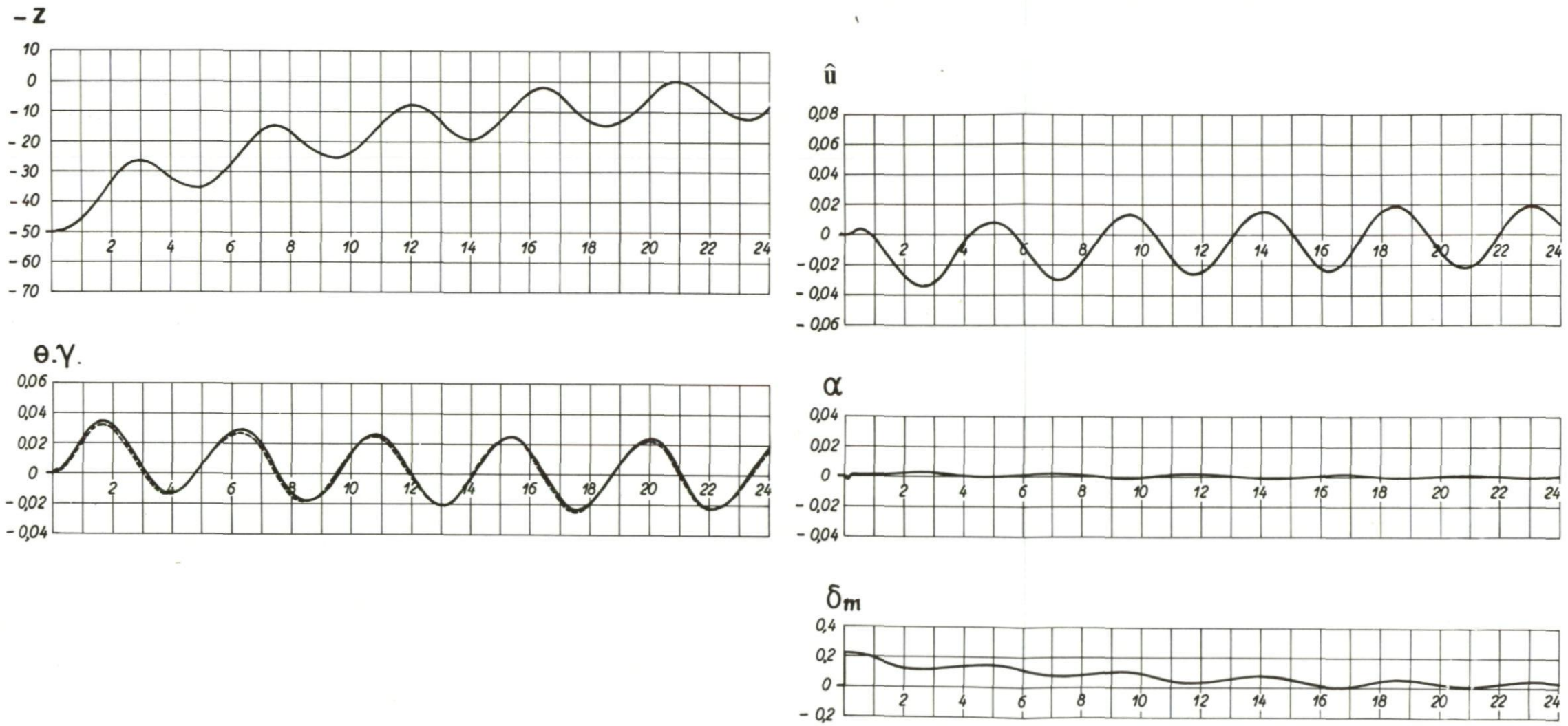

Fig.293 Aircraft response to an initial error z = 50 m, for $\delta_m = B_4 z$

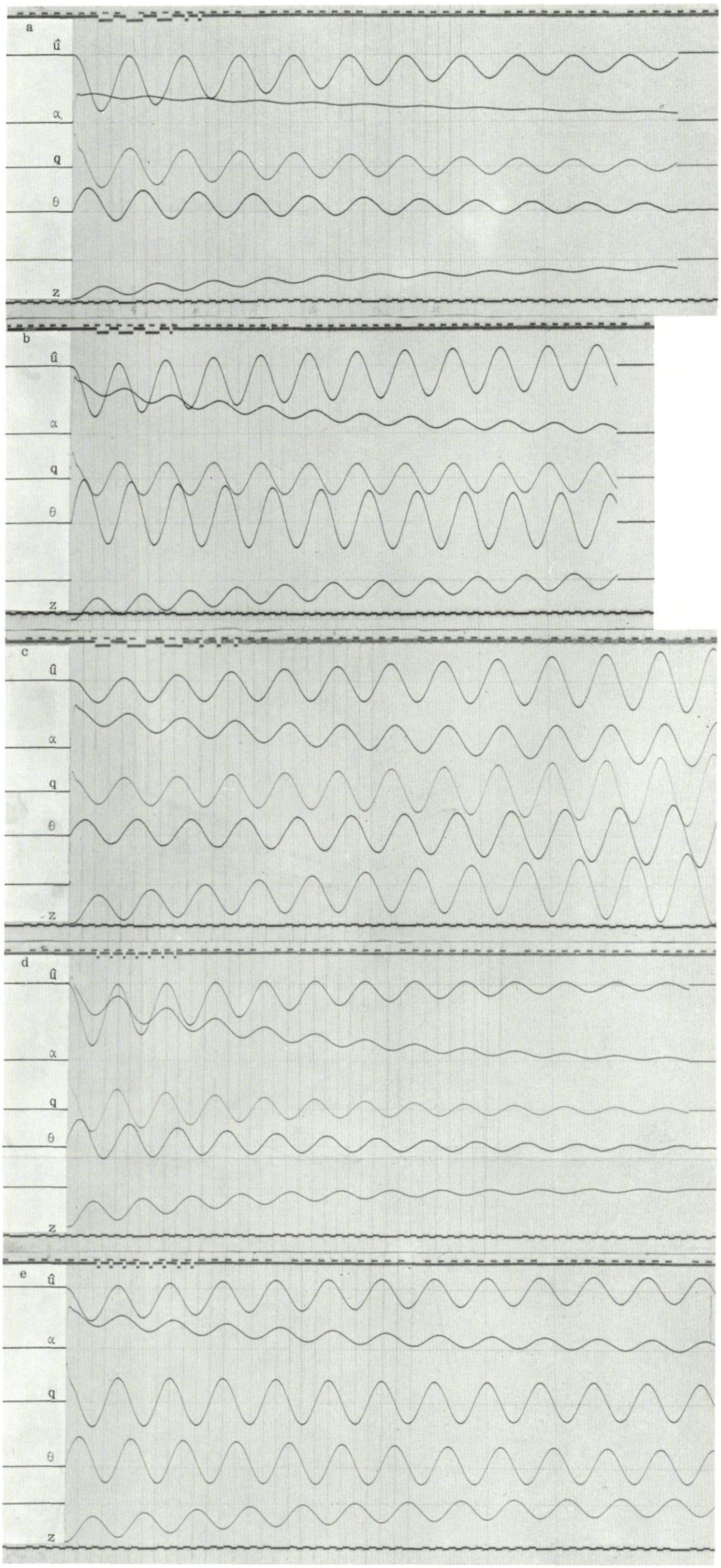

Fig.294 Response to an initial error z = 50m for $\delta_e = A_u Z$ with and without stabilizing terms

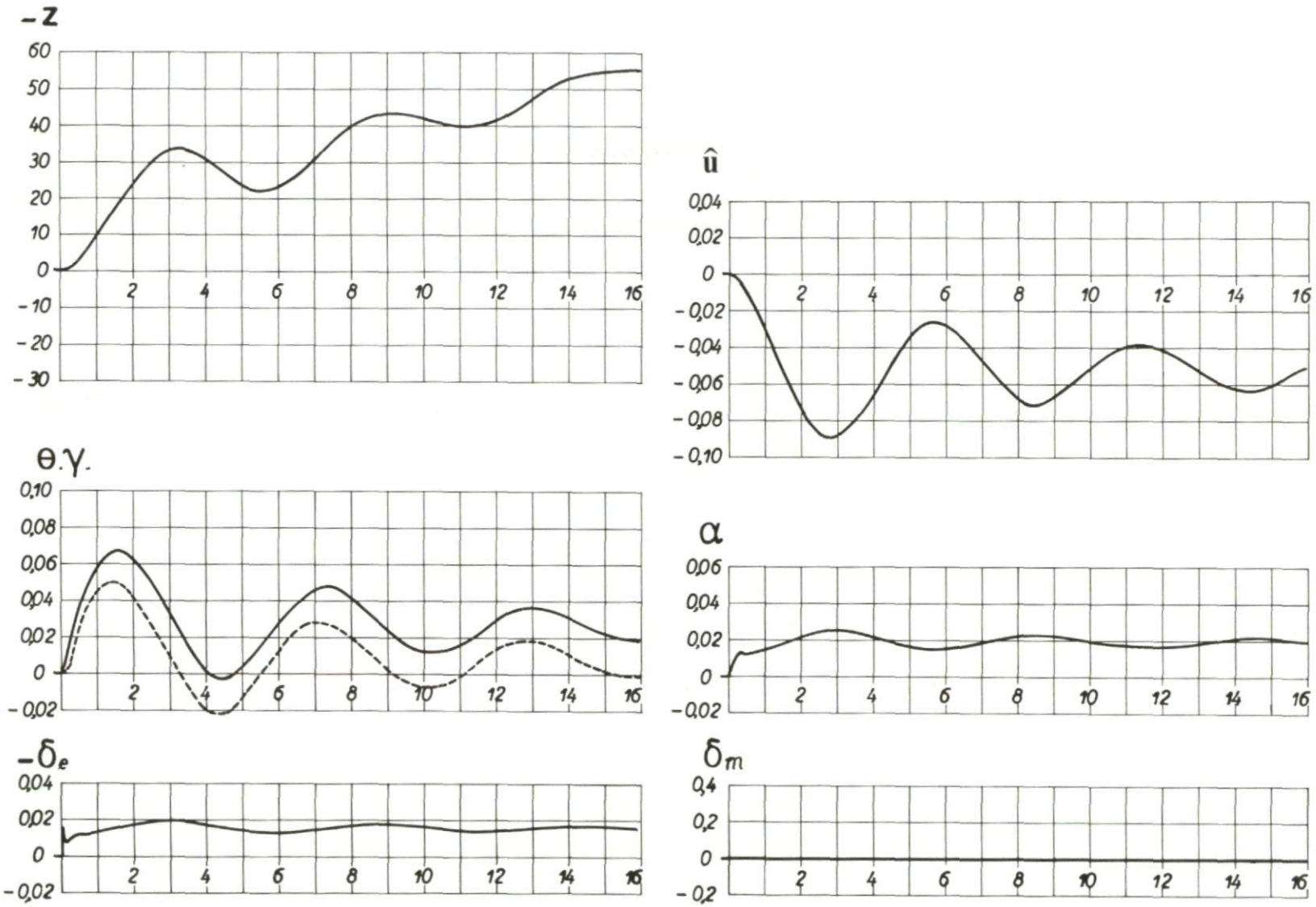

Fig.295 Response to step input δ_e = -0.016 damped by $A_5\dot{\theta}$

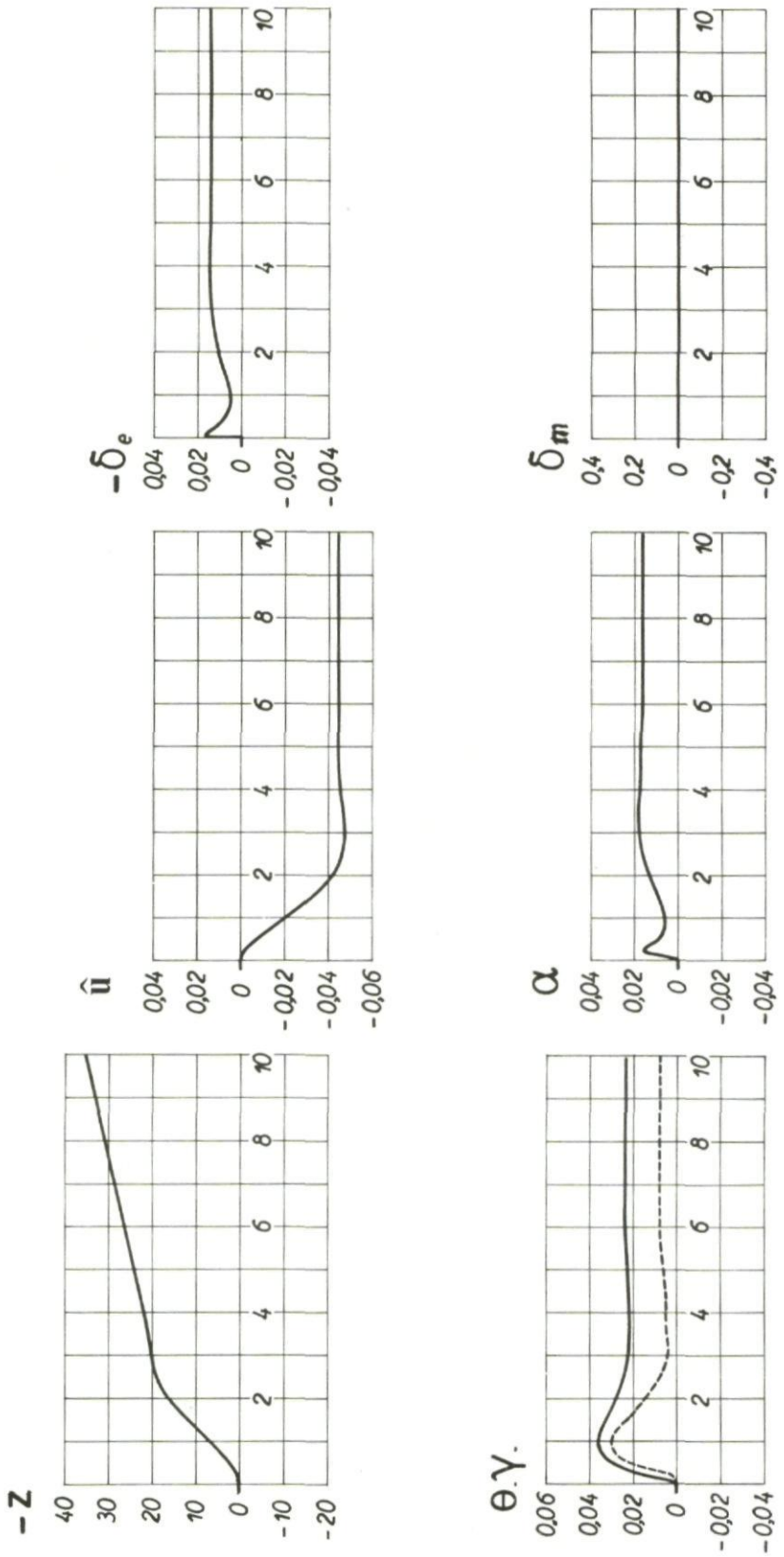

Fig.296 Response to step input δ_e = -0.016 damped by $A_8\dot{z}$

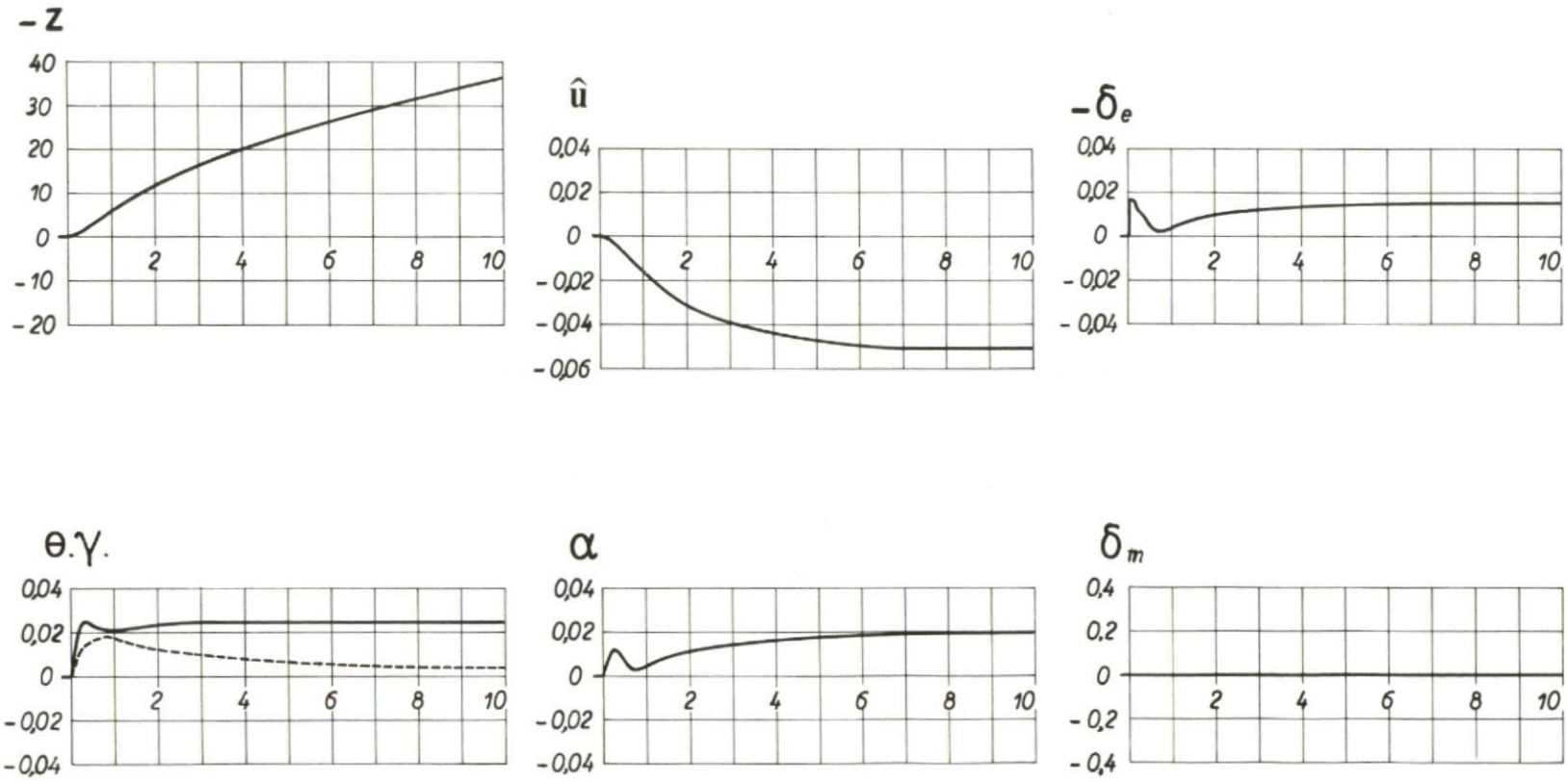

Fig.297 Response to step input δ_e = -0.016 damped by $A_7\dot{u}$

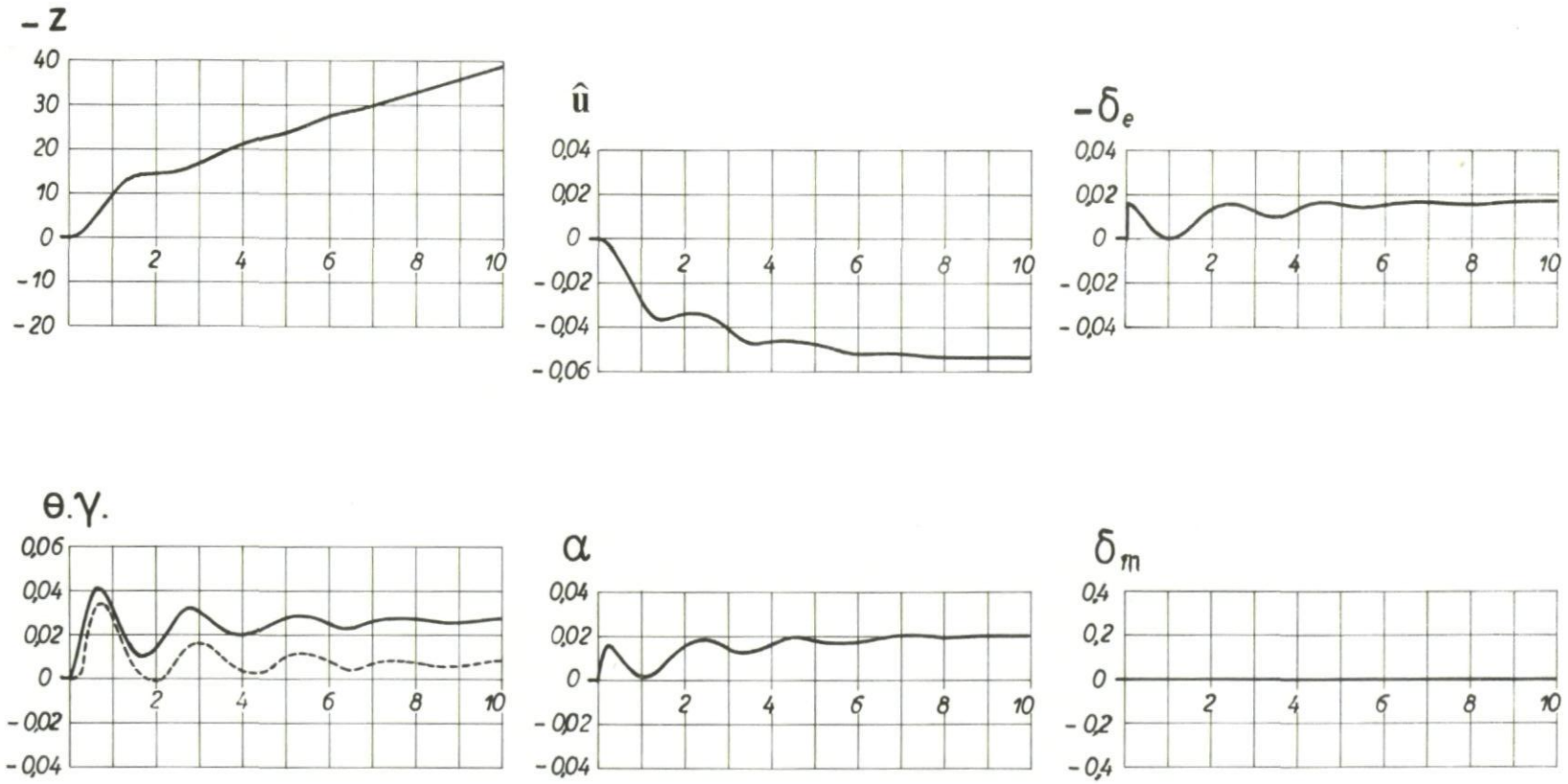

Fig.298 Response to step input δ_e = -0.016 damped by $A_7\dot{u}$ with time constant

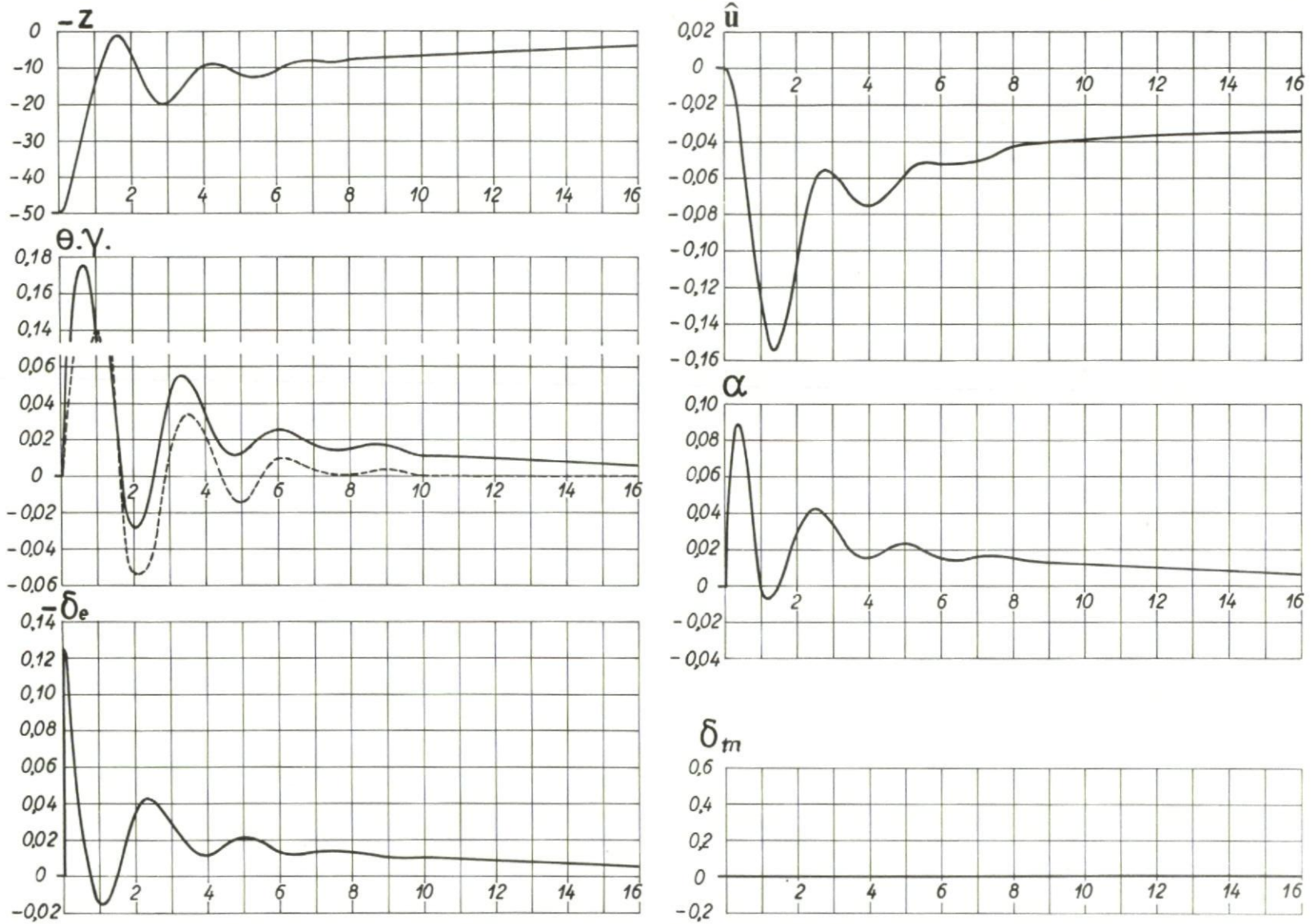

Fig.299 Response to initial error z = 50m

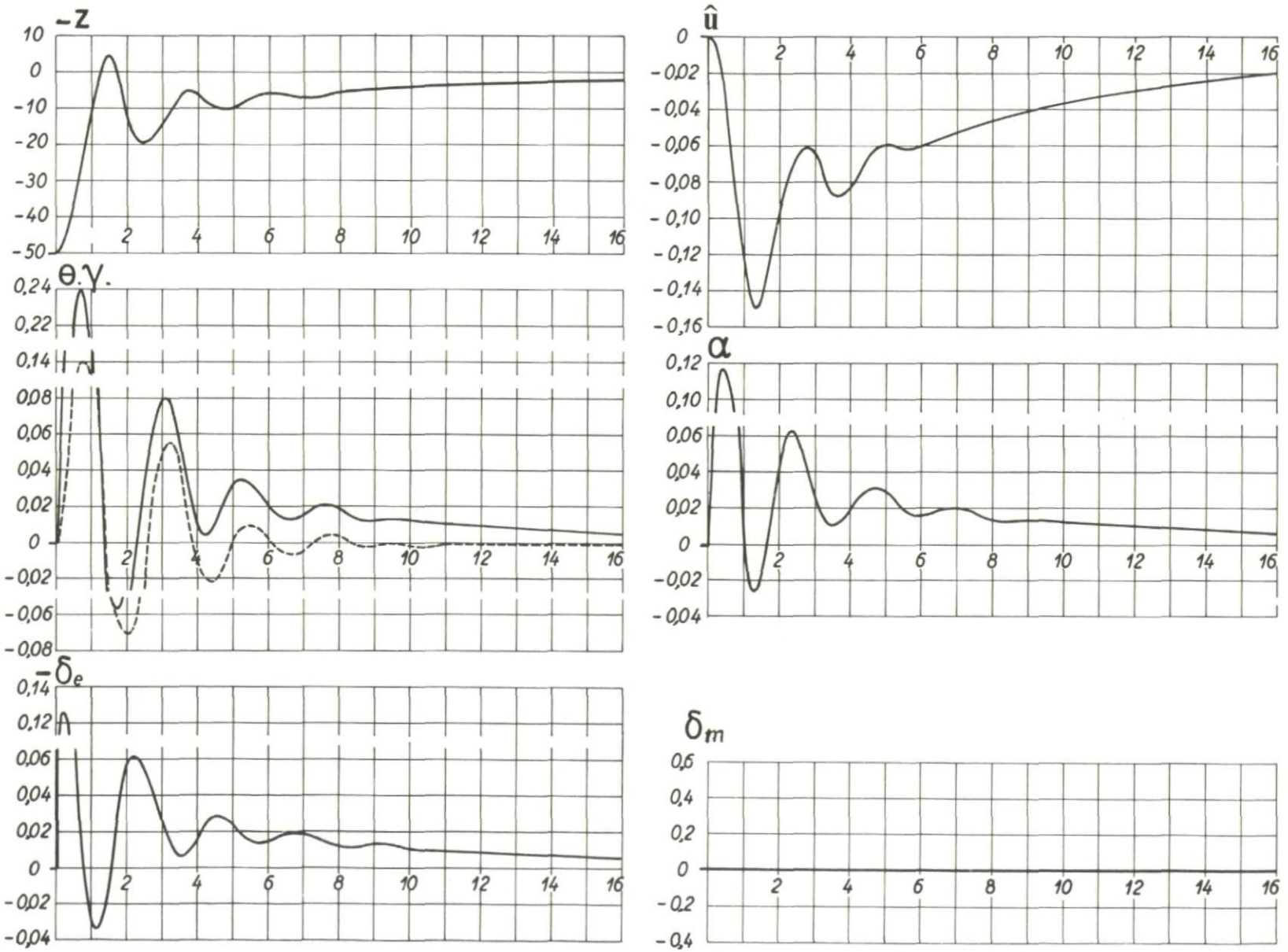

Fig.300 Response to initial error z = 50m

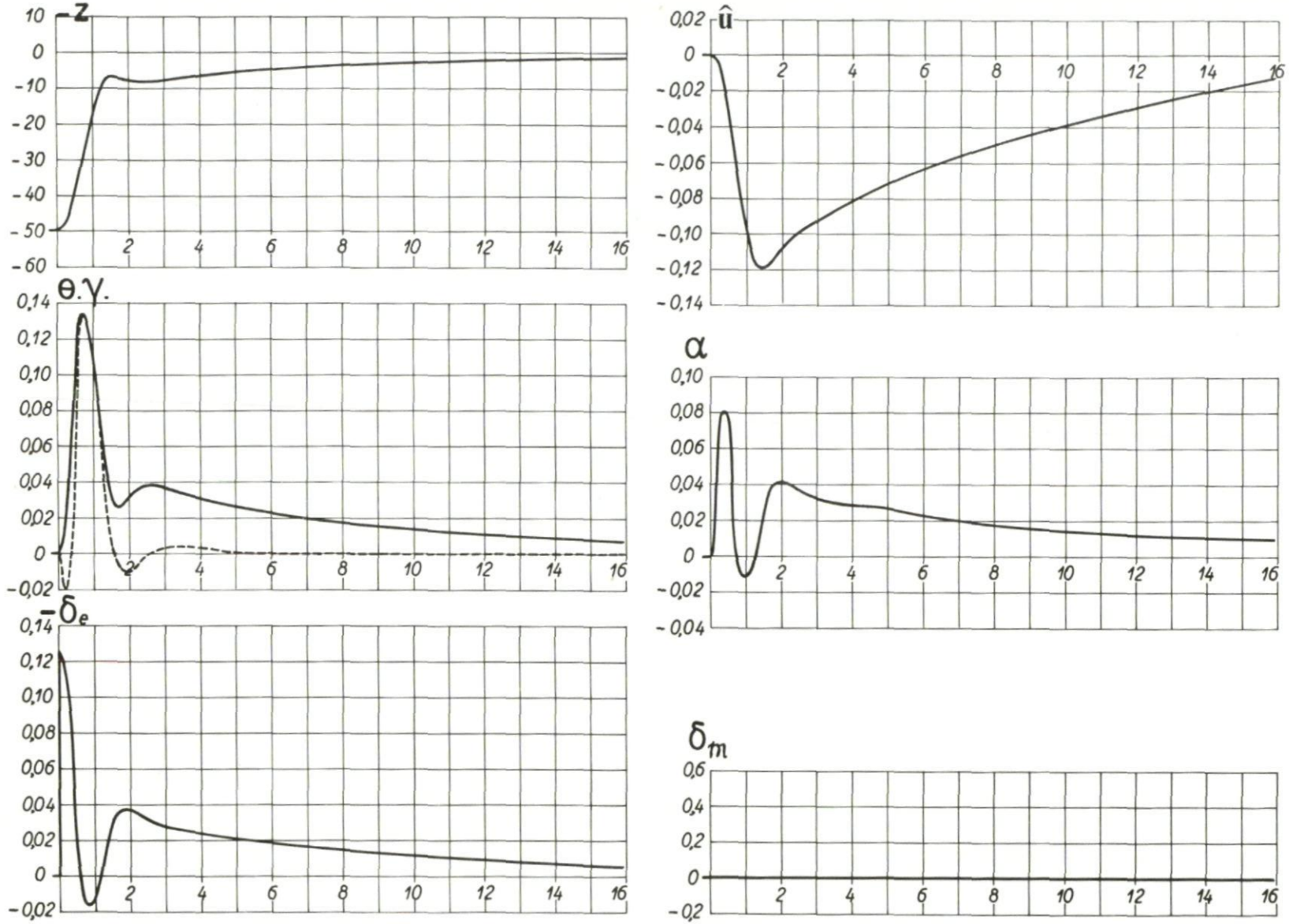

Fig.301 Response to initial error z = 50m, case a

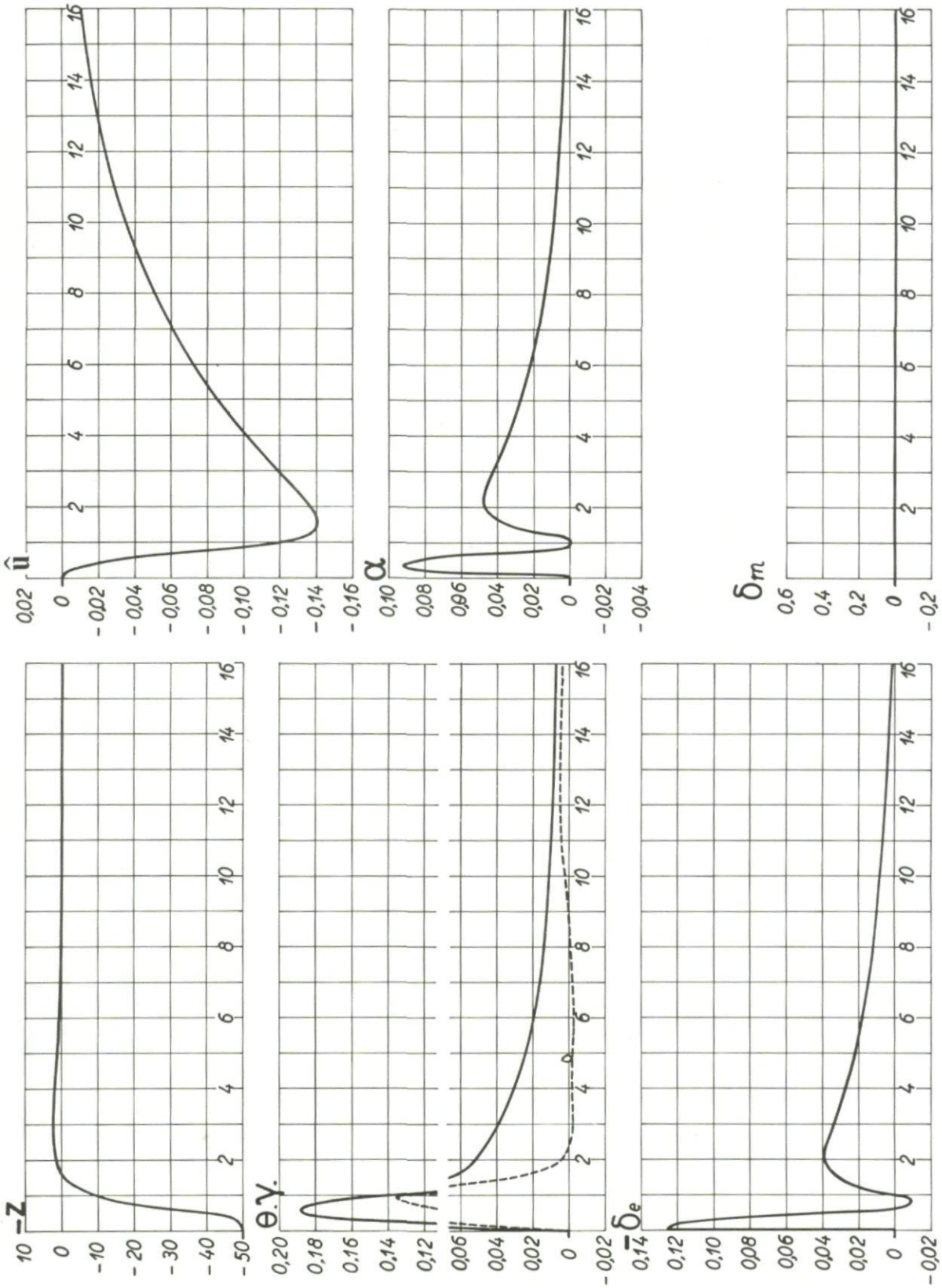

Fig.302 Response to initial error z = 50m, case b

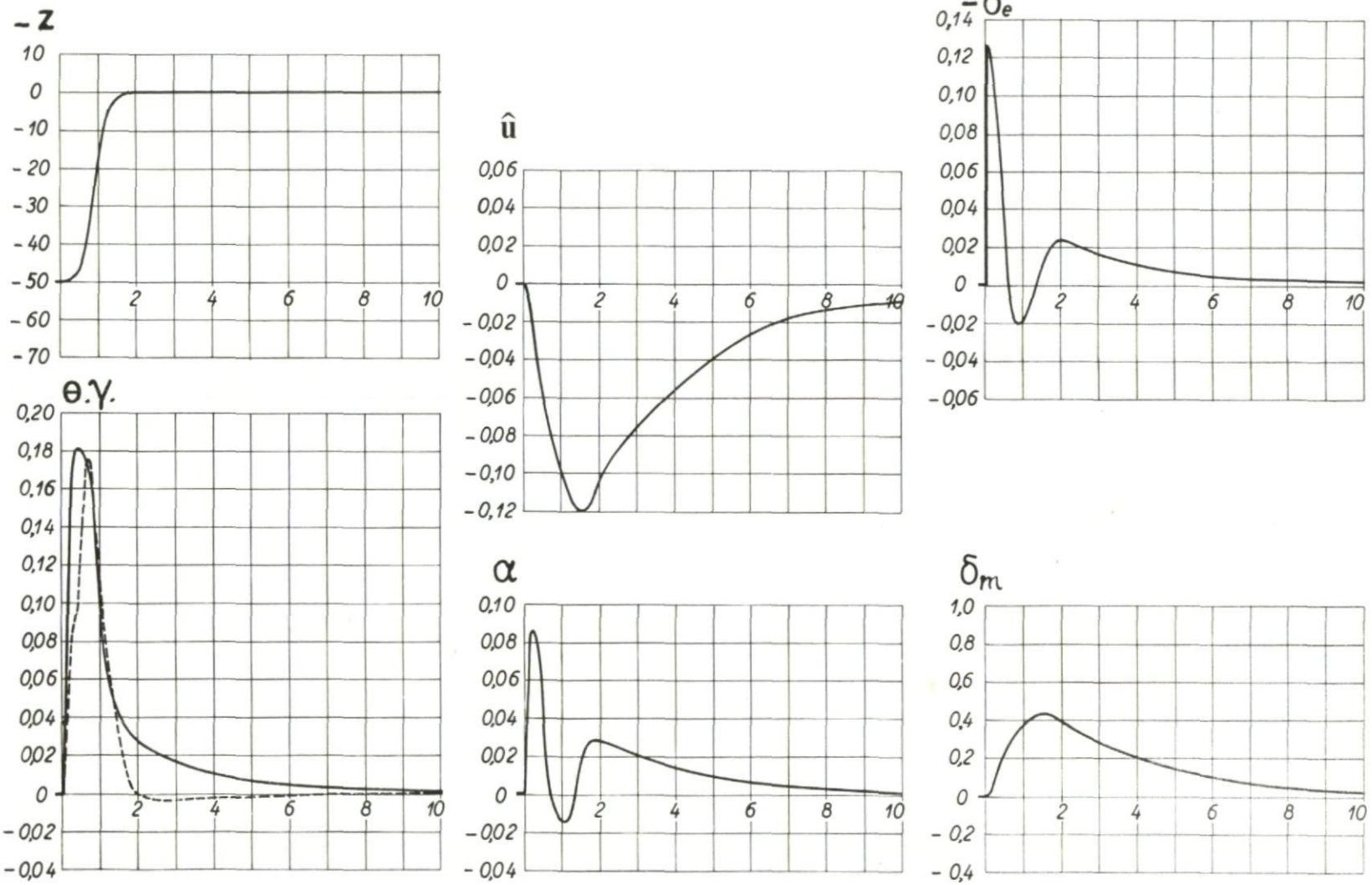

Fig.303 Response to initial error z = 50m, case c

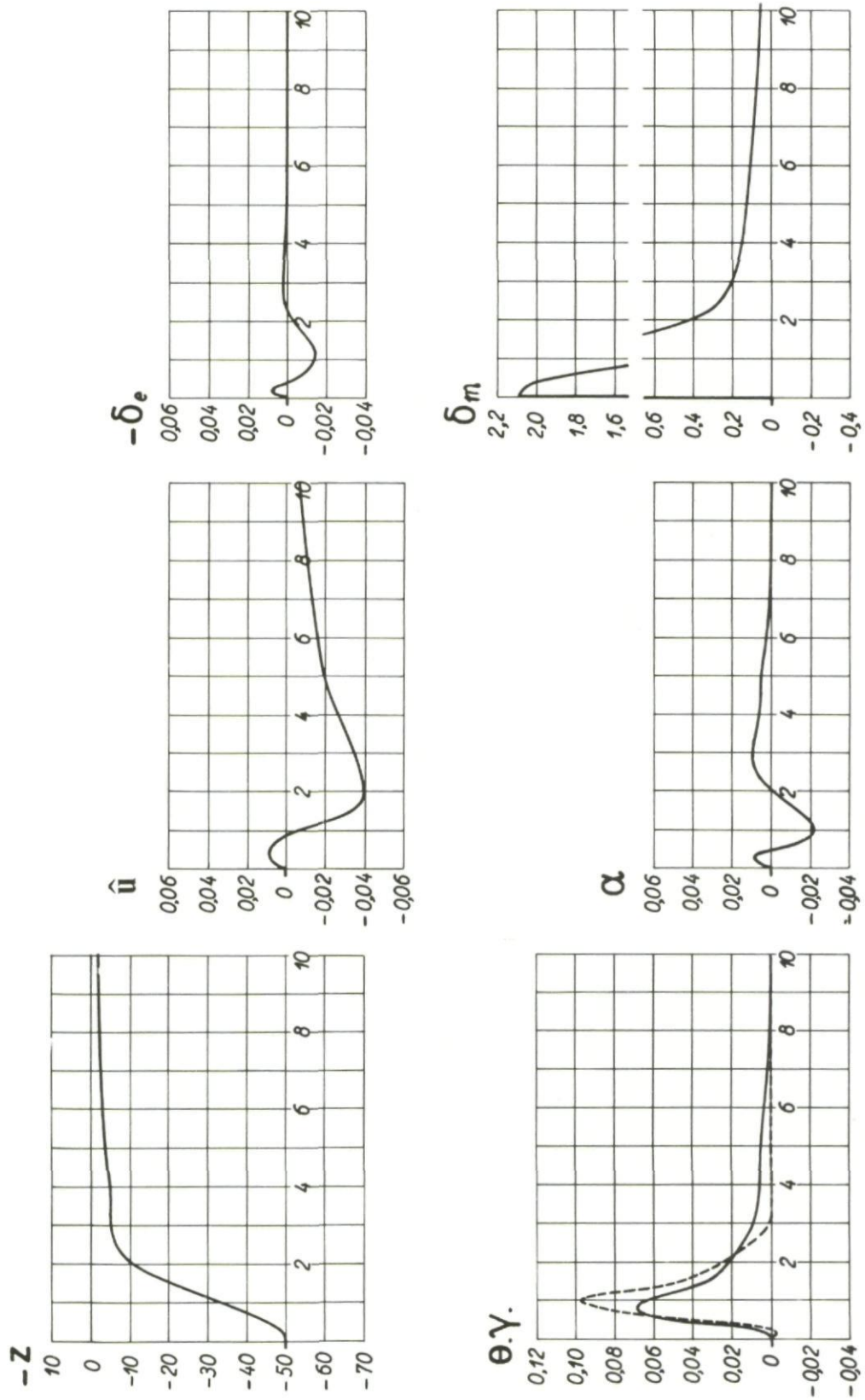

Fig.304 Response to initial error z = 50m, case d

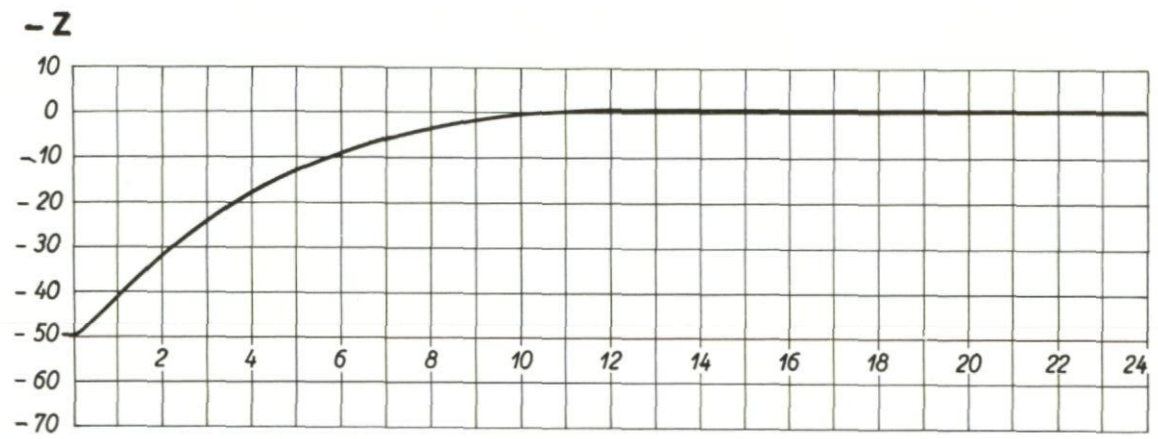

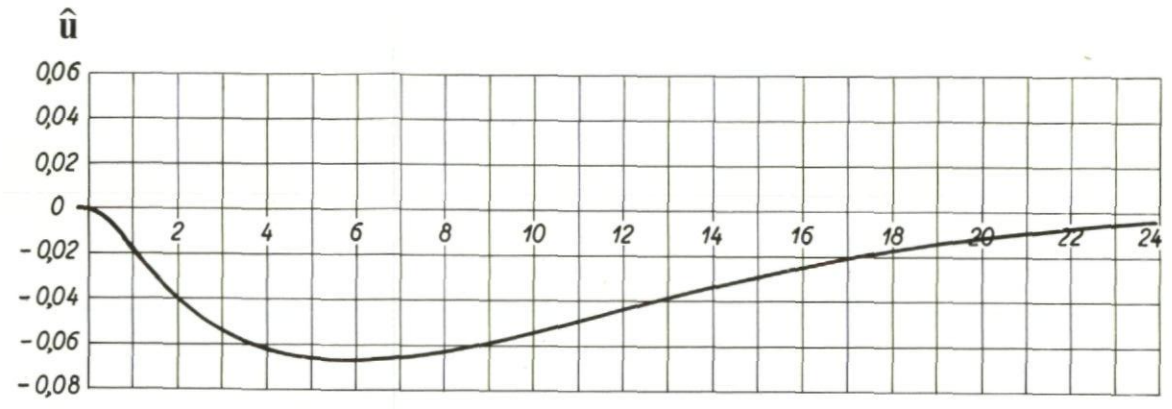

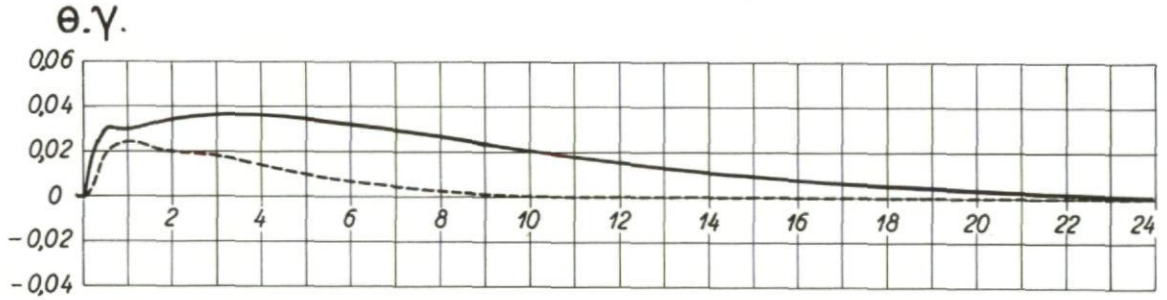

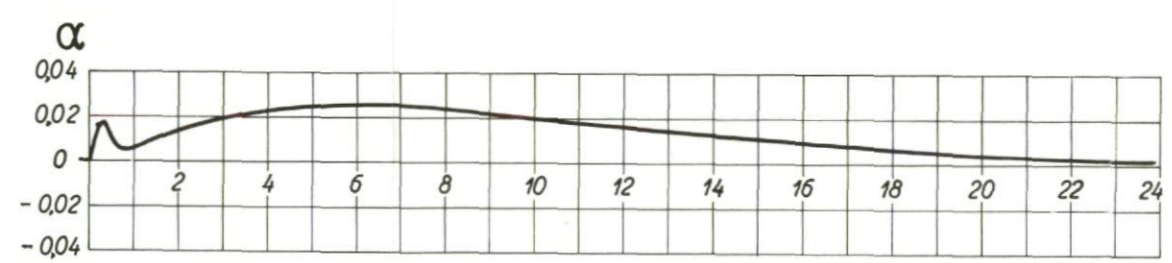

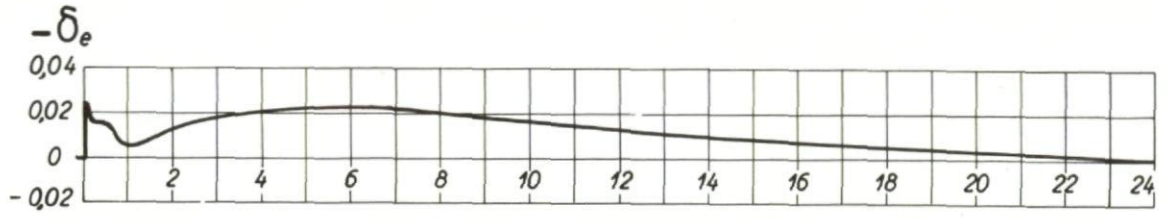

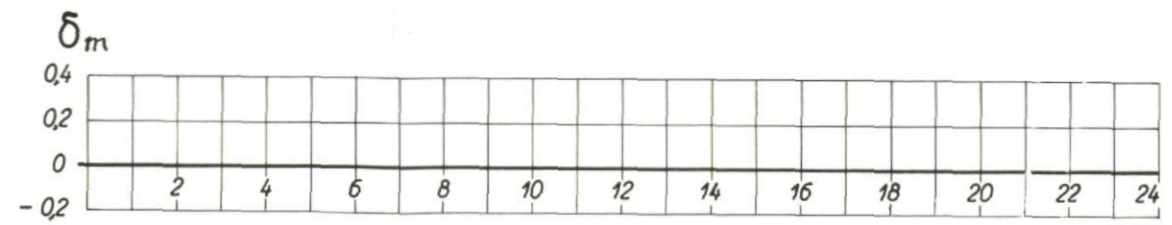

Fig.305 Response to initial error z = 50m, case b'

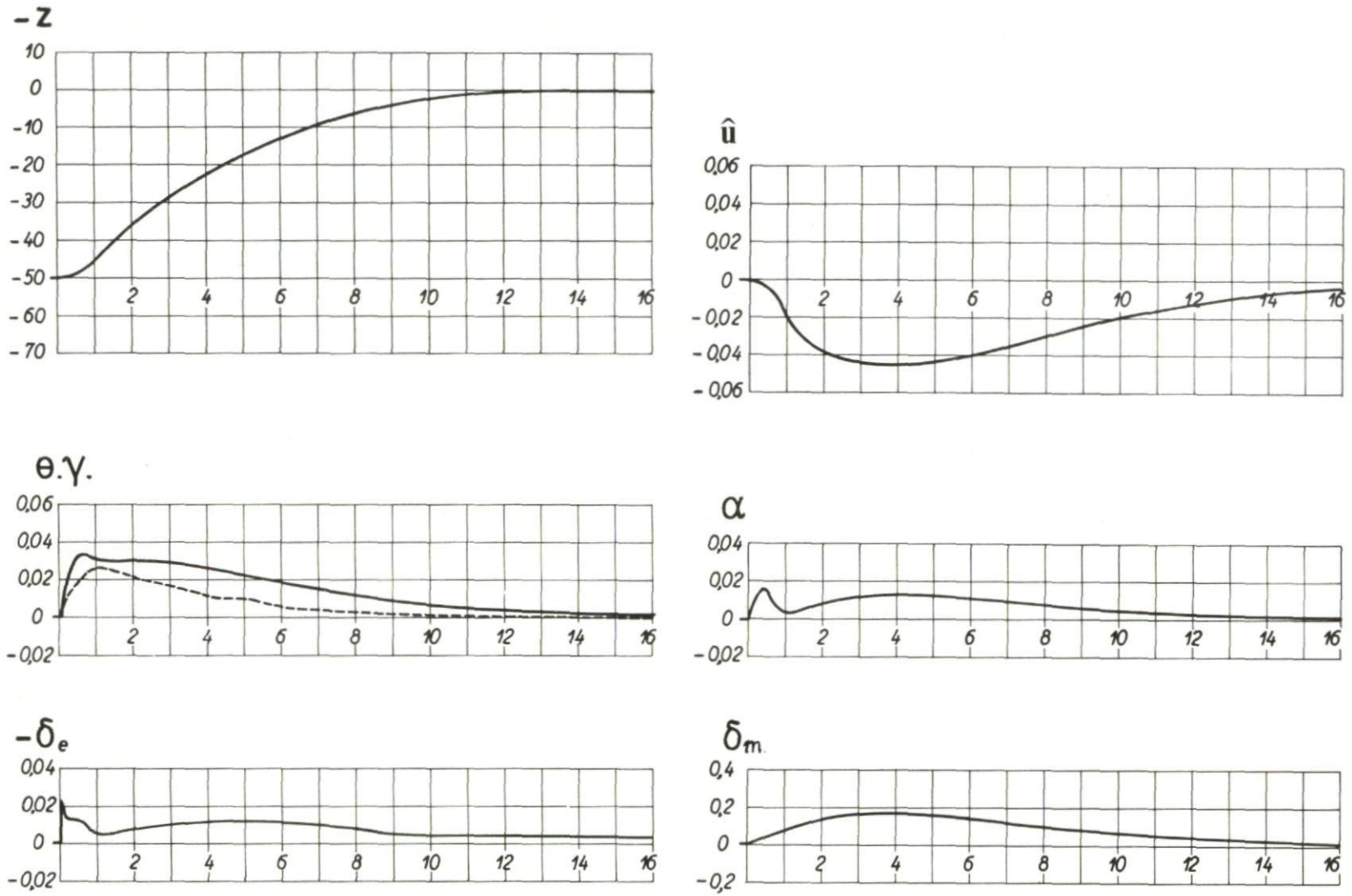

Fig. 306 Response to initial error z = 50m, case c'

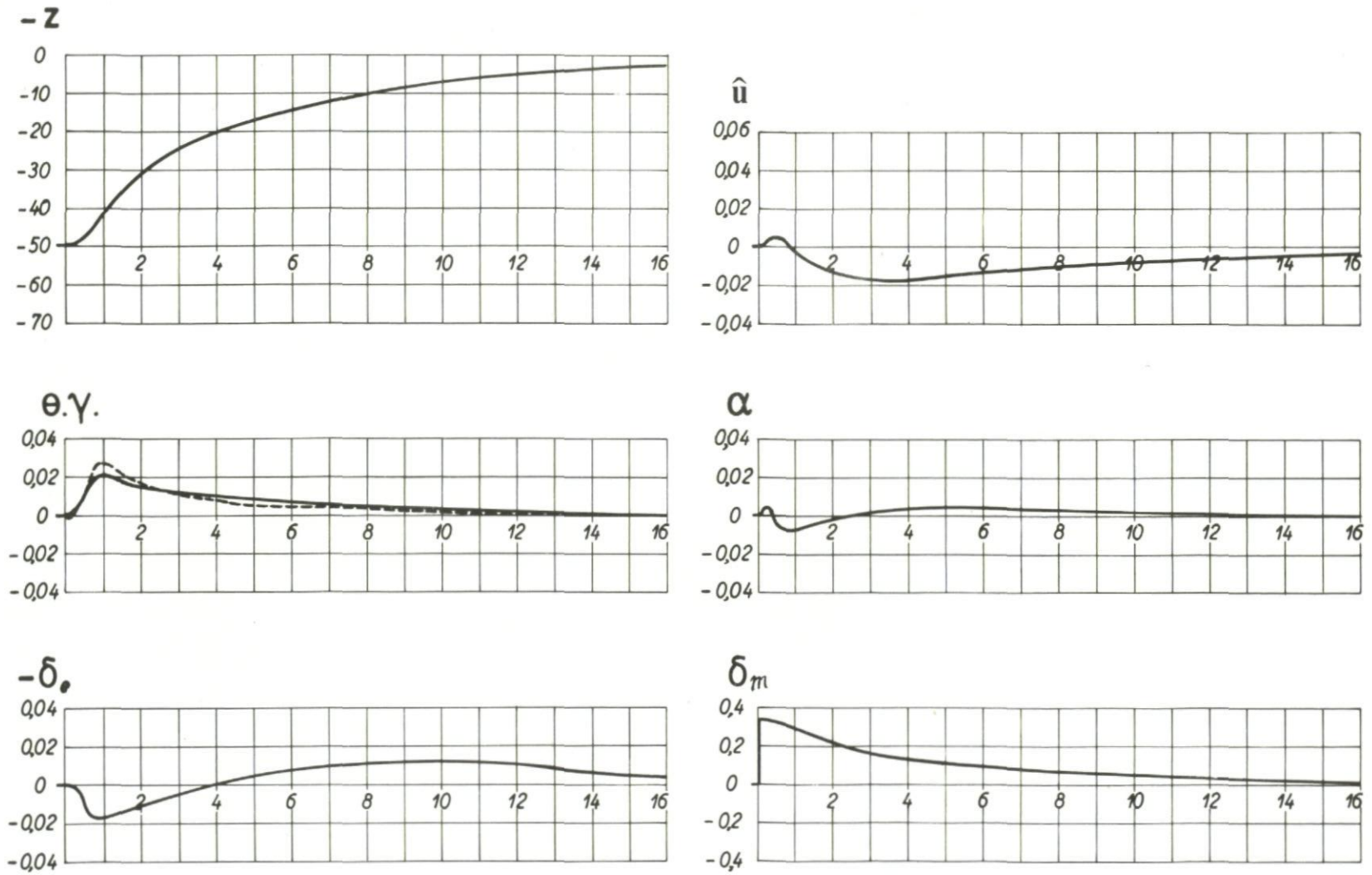

Fig. 307 Response to initial error z = 50m, case d'

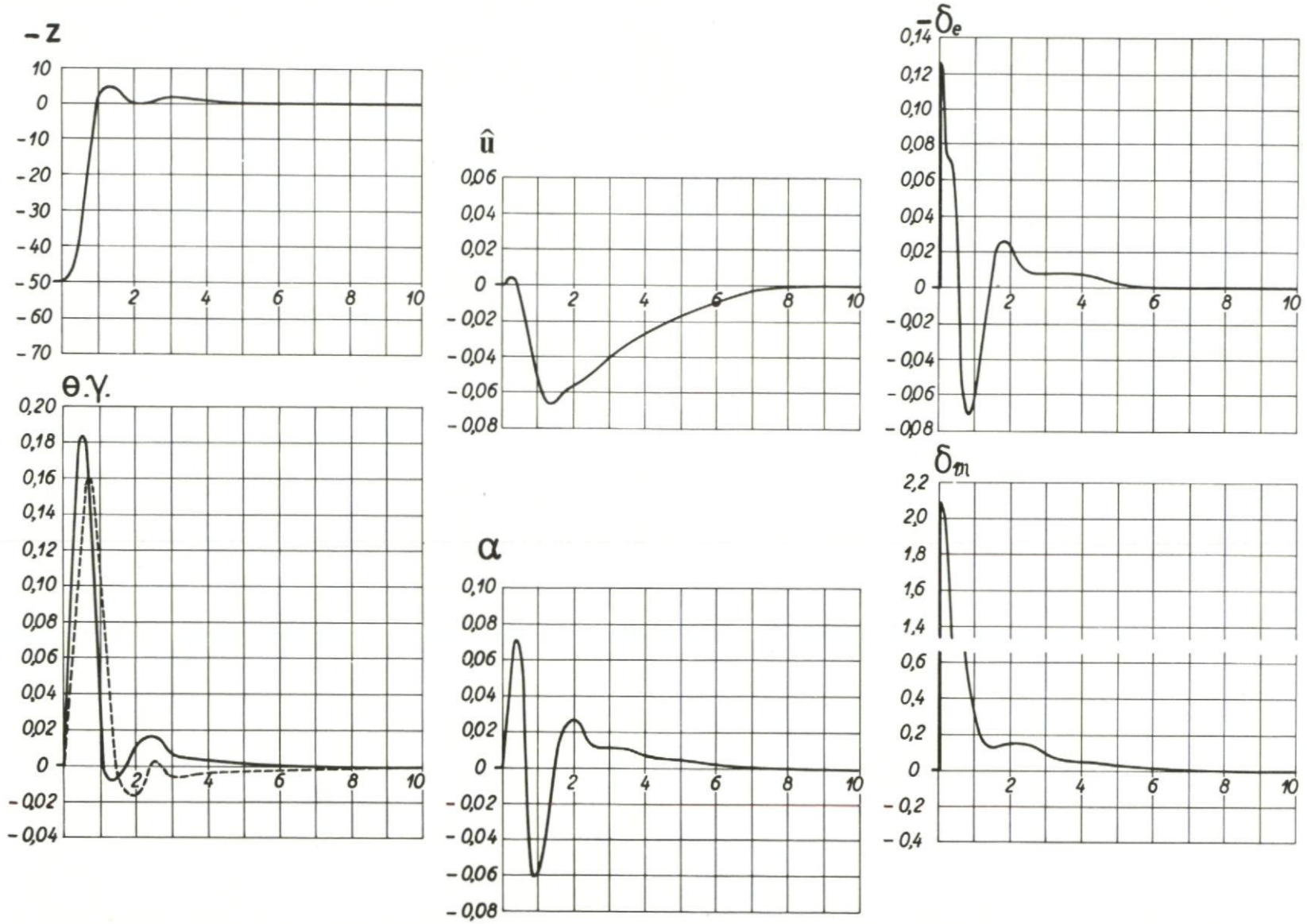

Fig. 308 Response to initial error z = 50m, case e

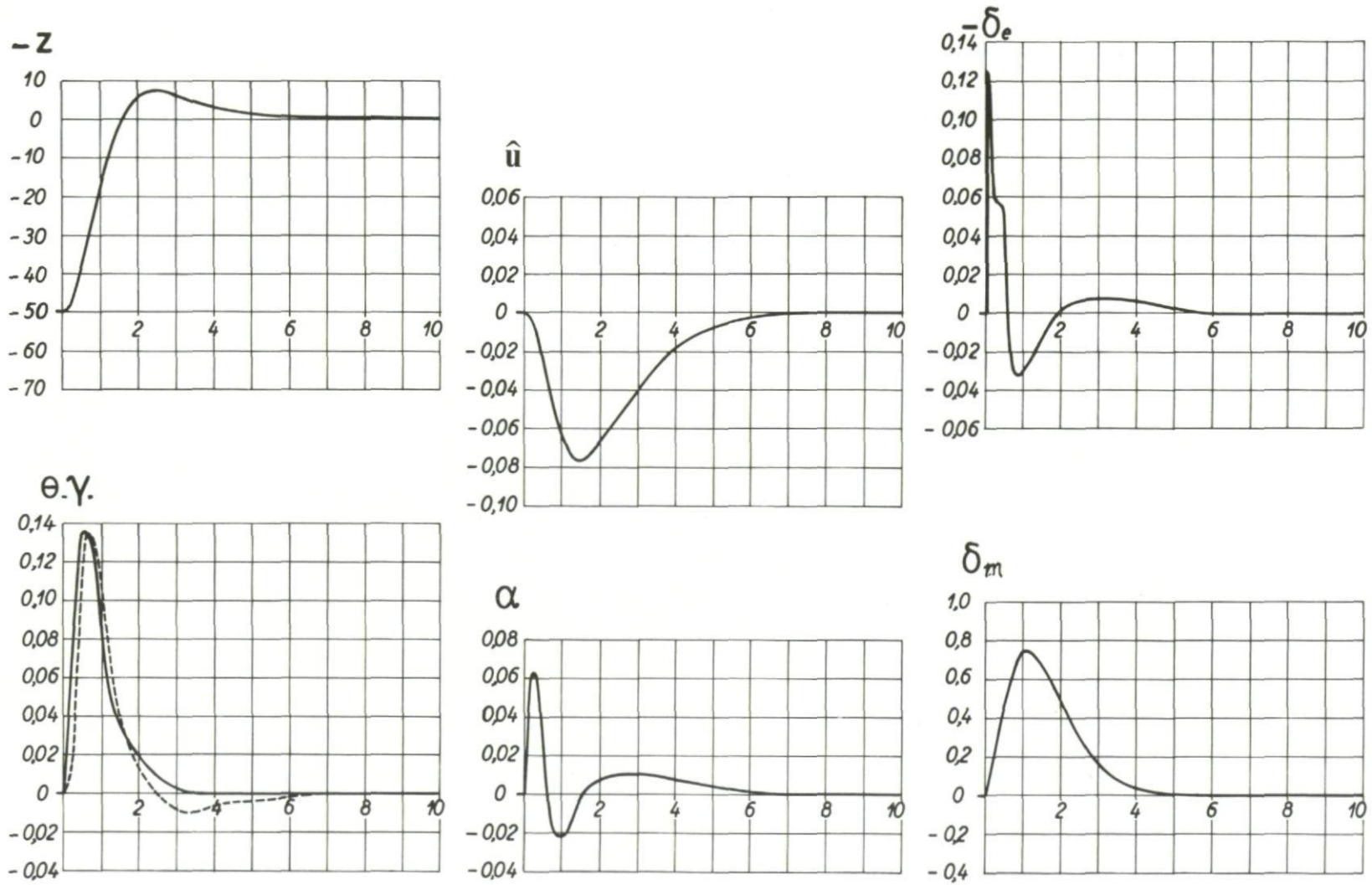

Fig.309 Response to initial error z = 50m, case f

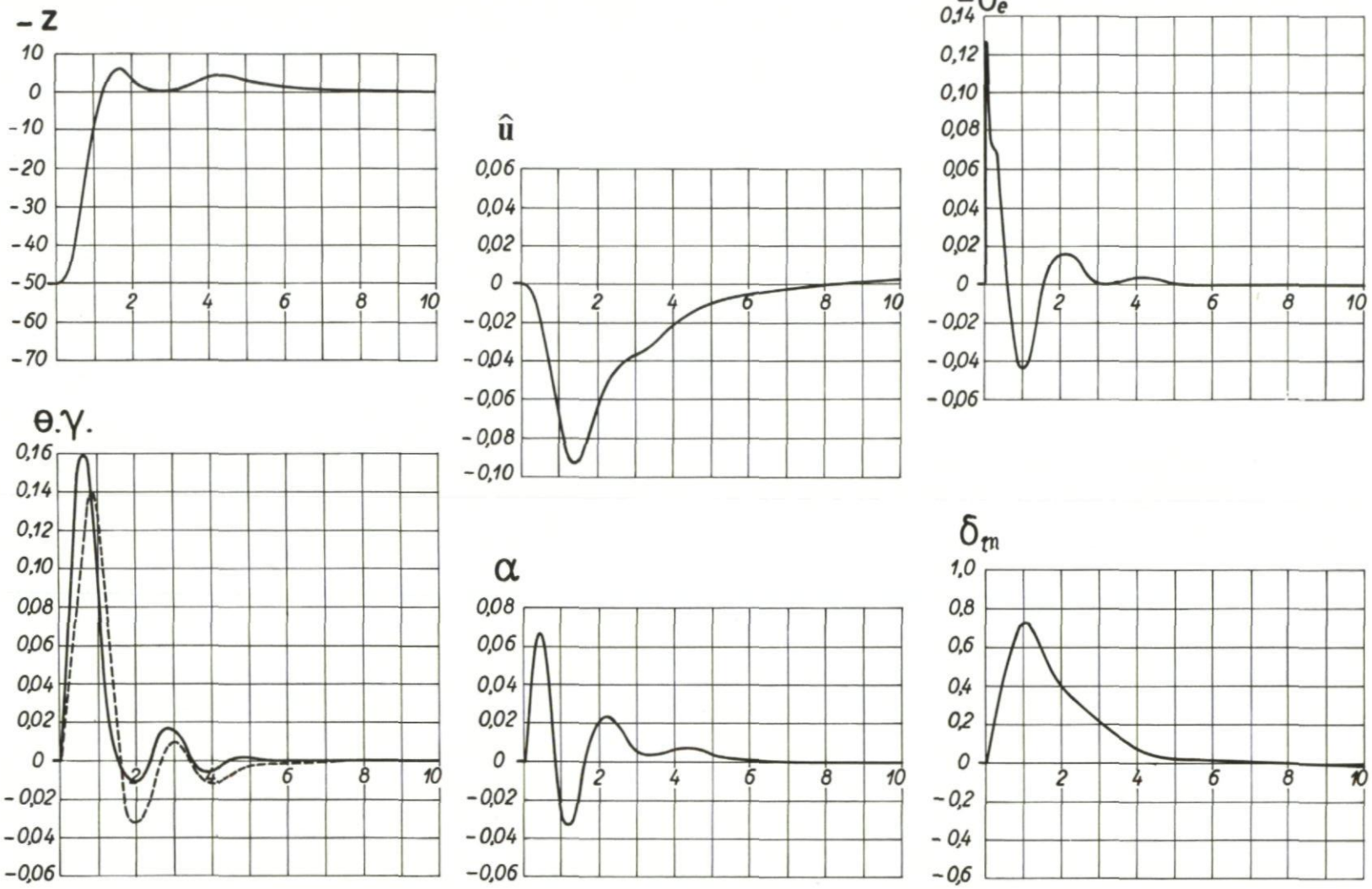

Fig.310 Response to initial error z = 50m, case g

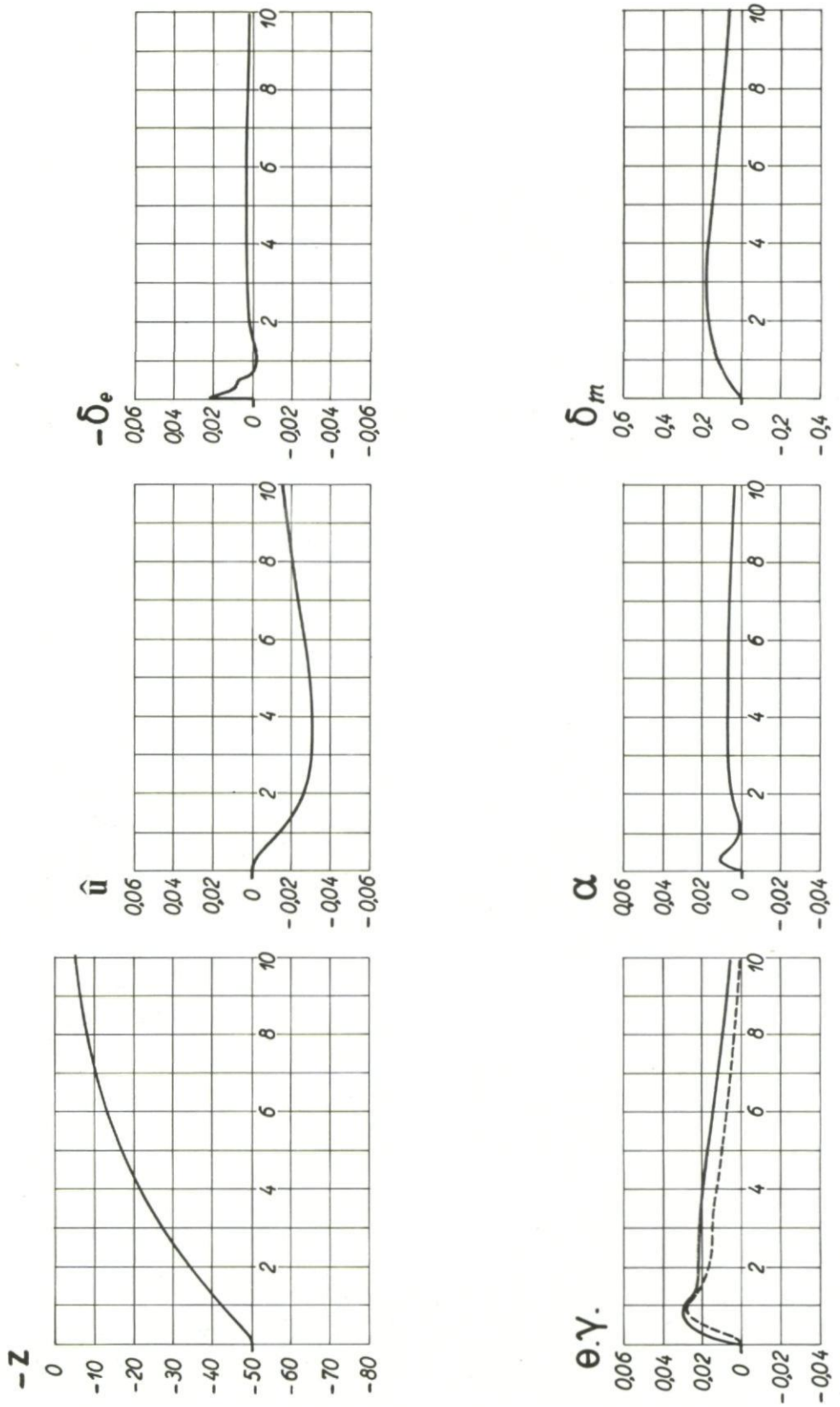

Fig.311 Response to initial error z = 50m, case g'

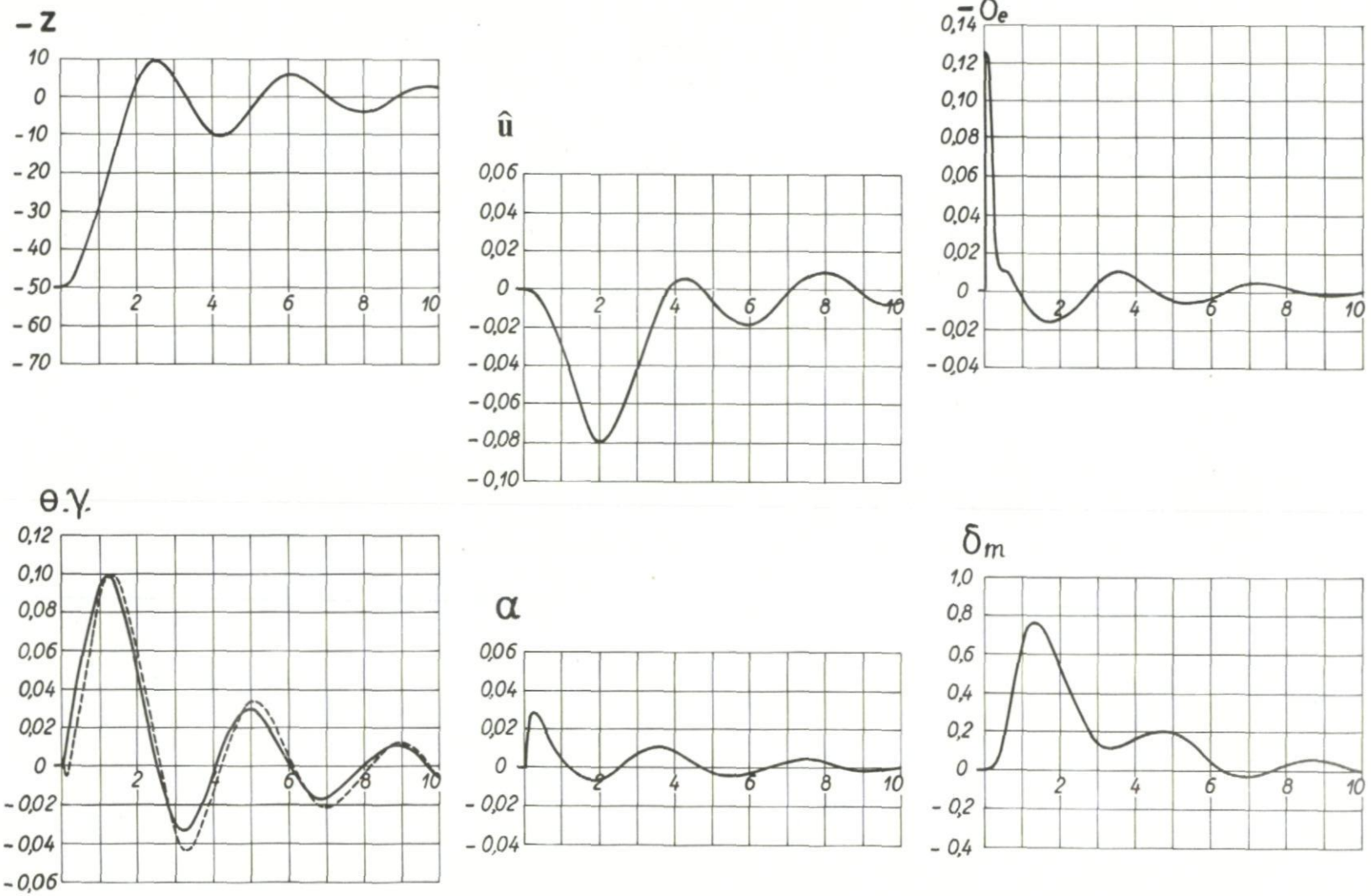

Fig.312 Response to initial error z = 50m, case h

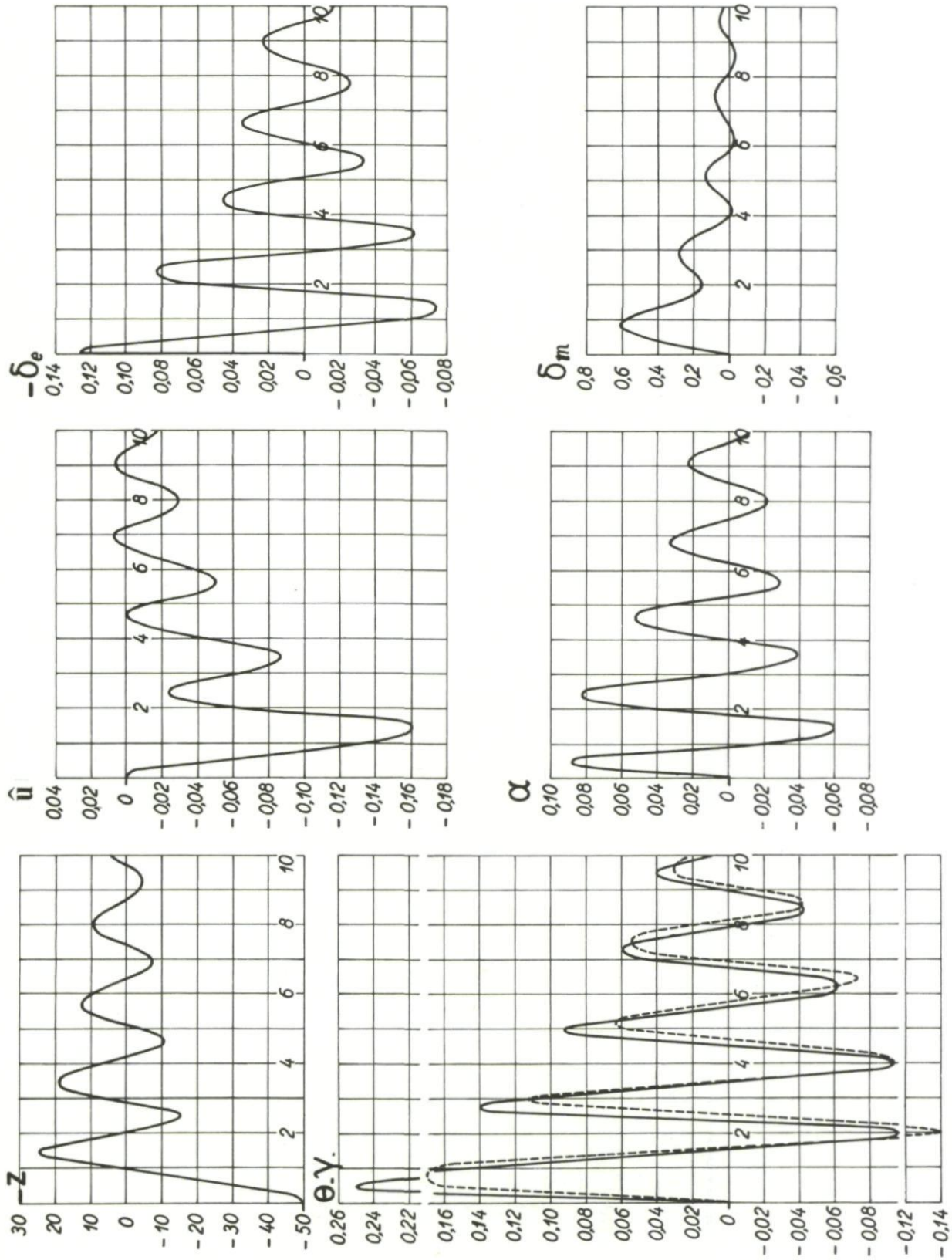

Fig.313 Response to initial error z = 50m, case 1

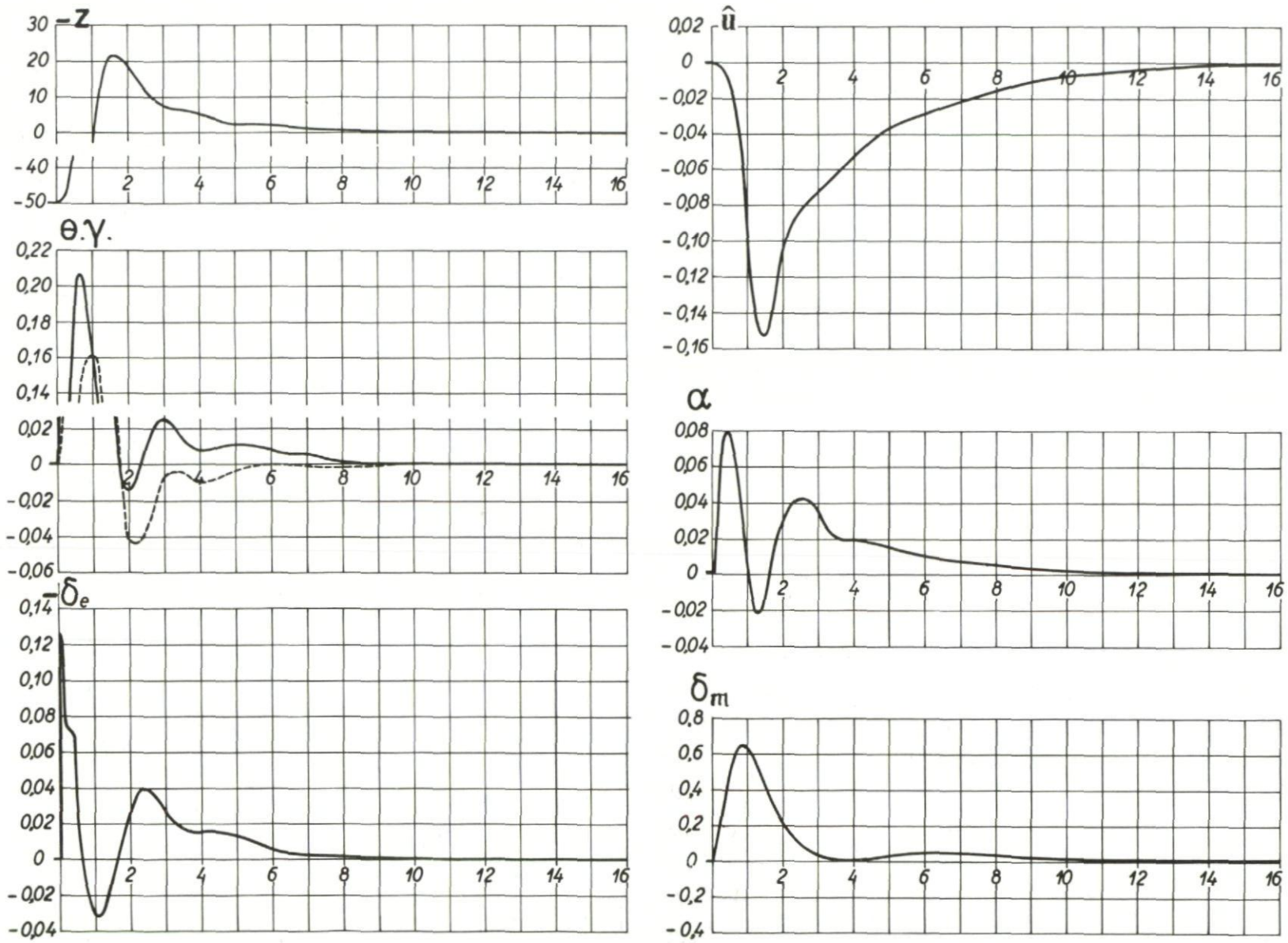

Fig.314 Response to initial error z = 50m, case j

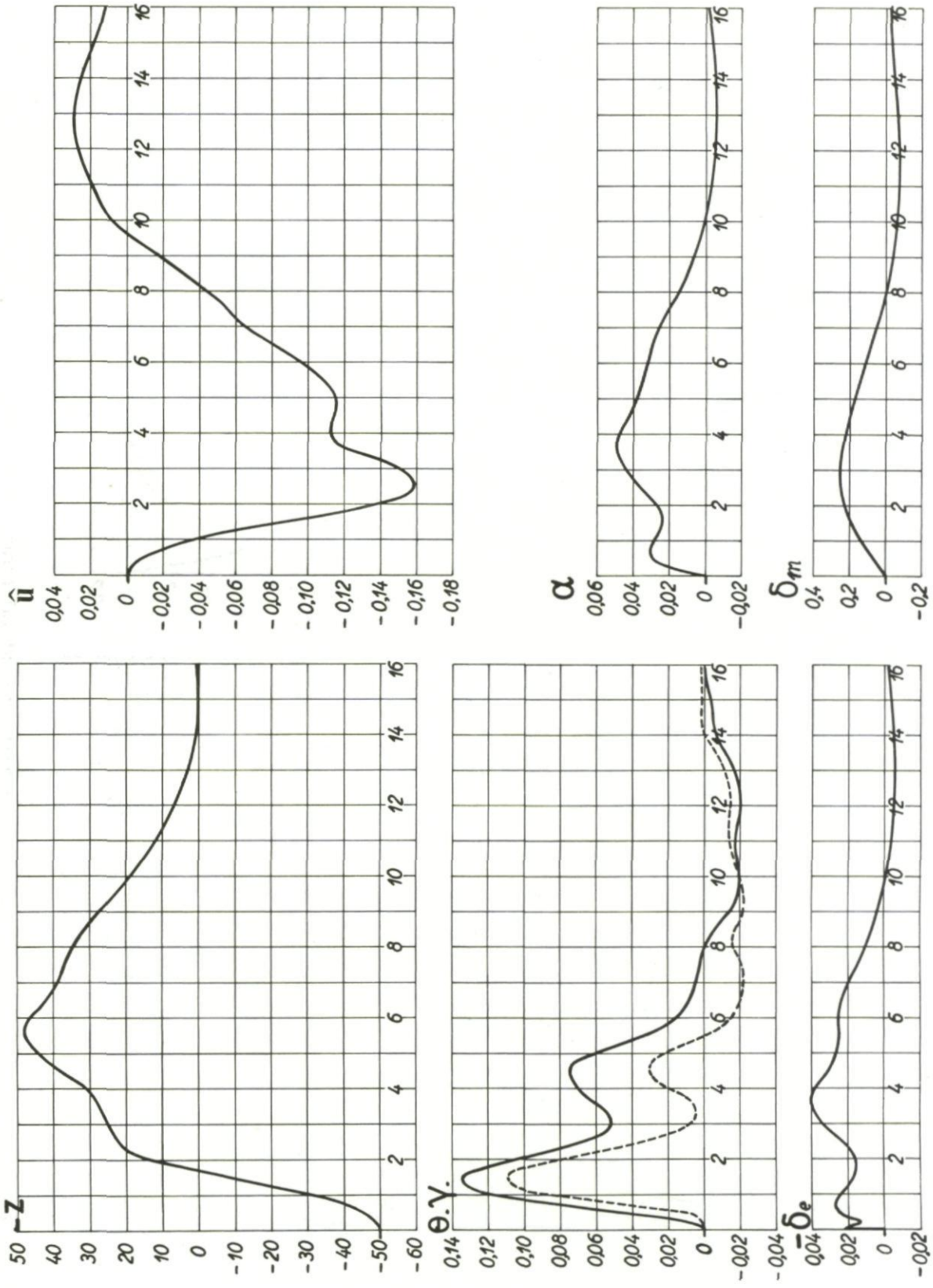

Fig.315 Response to initial error z = 50m, case j'

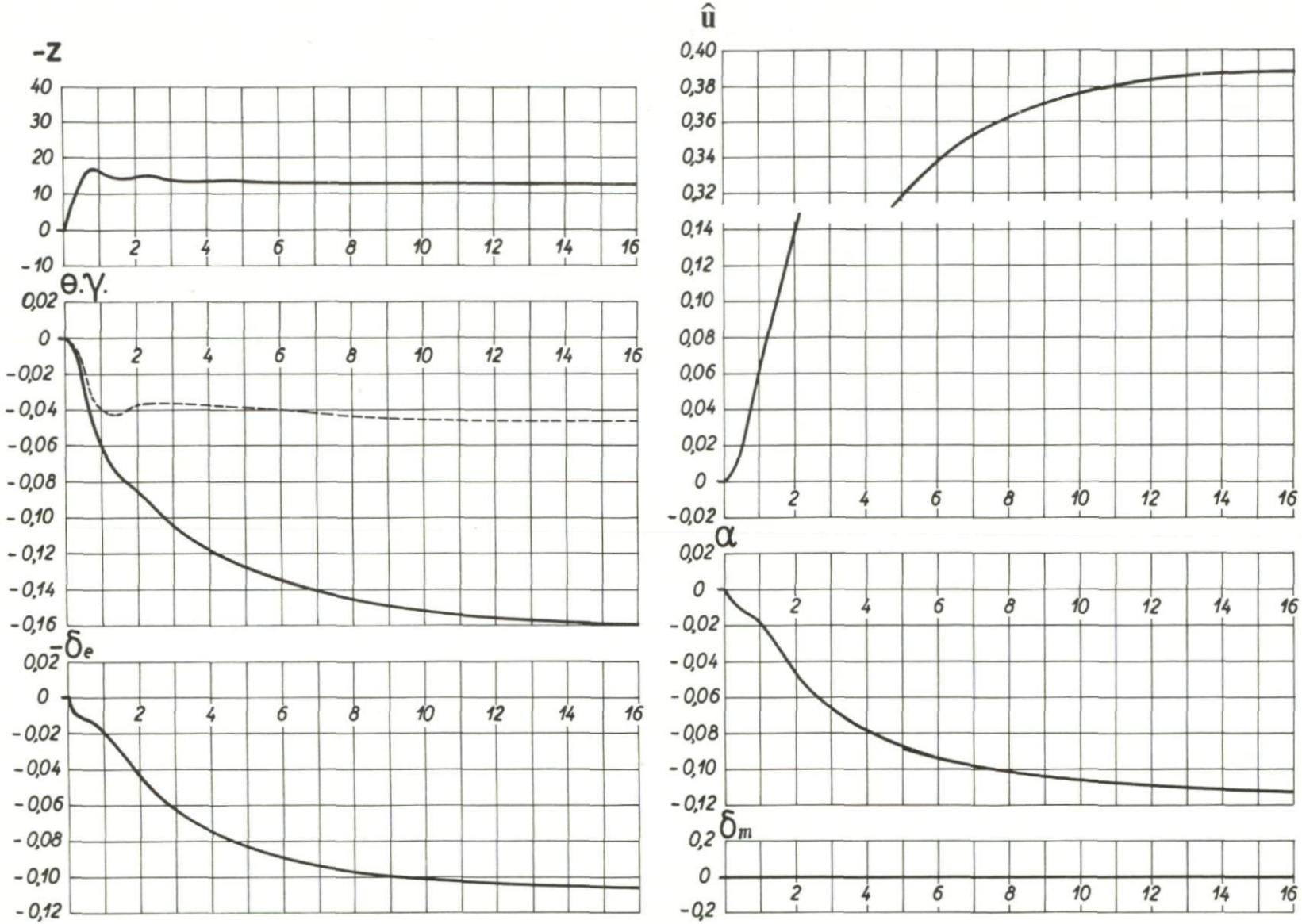

Fig. 316 Aircraft response to an initial error γ, case b

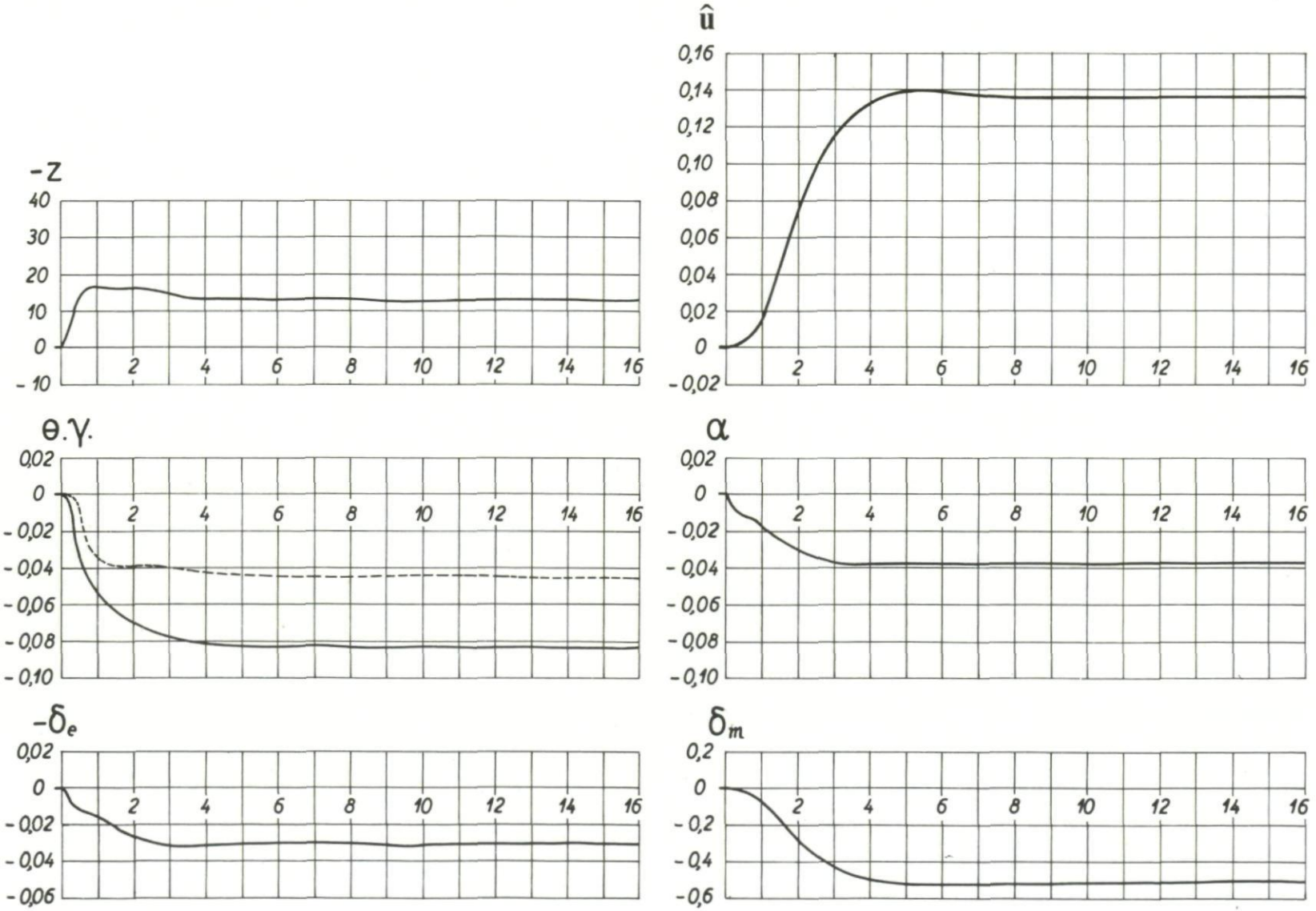

Fig.317 Aircraft response to an initial error γ, case c

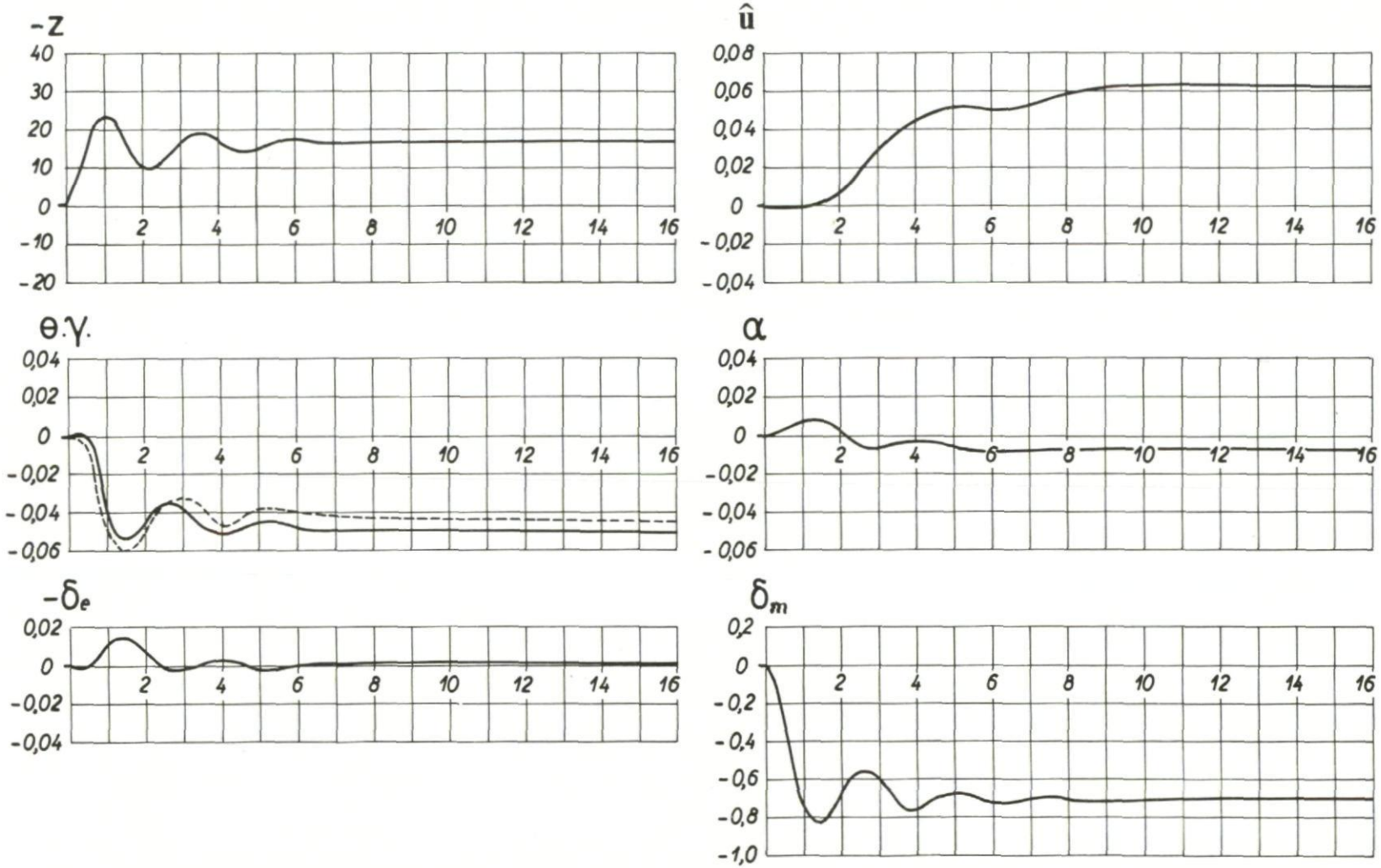

Fig.318 Aircraft response to an initial error γ, case d

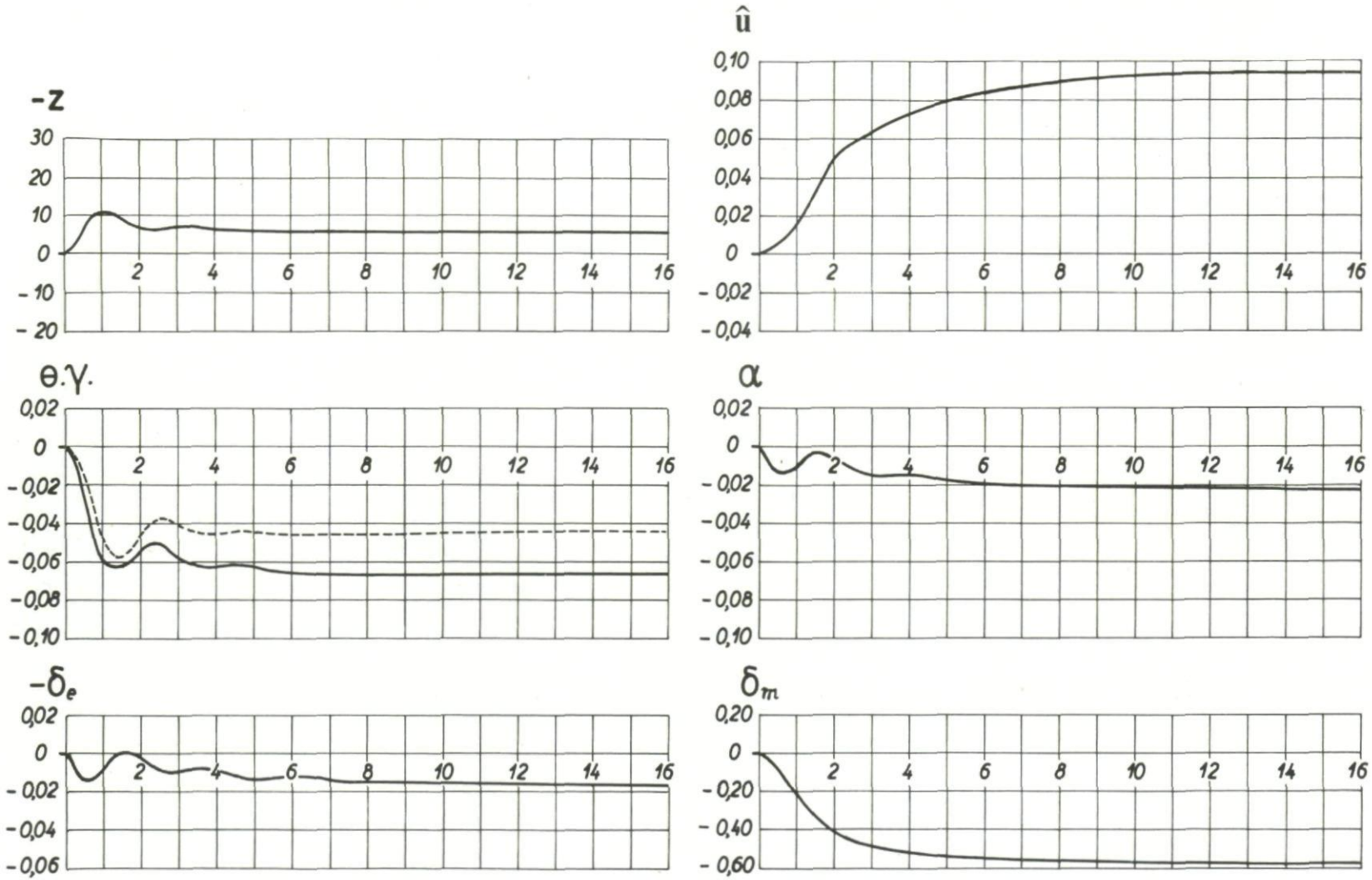

Fig. 319 Aircraft response to an initial error γ, case g

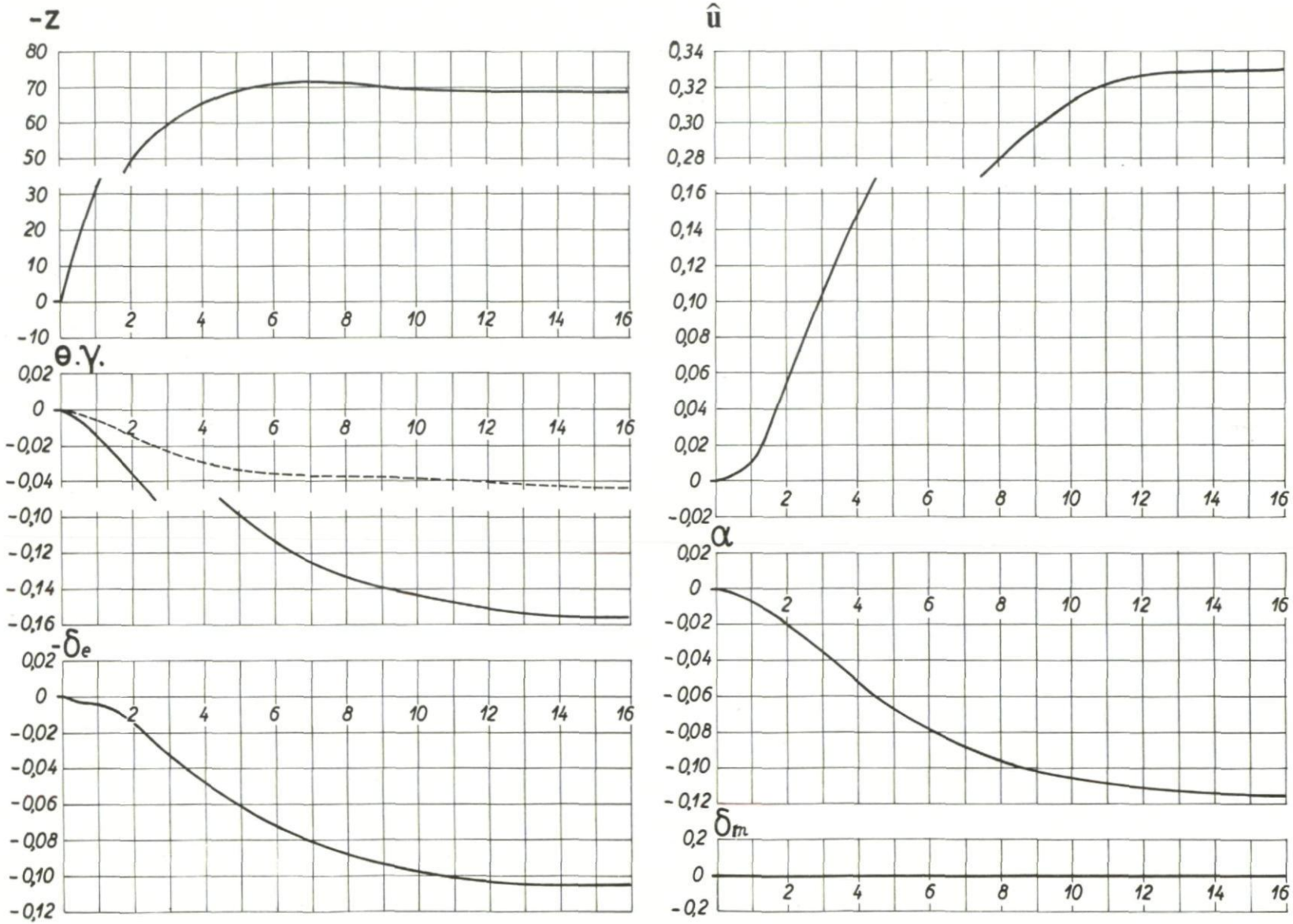

Fig. 320 Aircraft response to an initial error γ, case b'

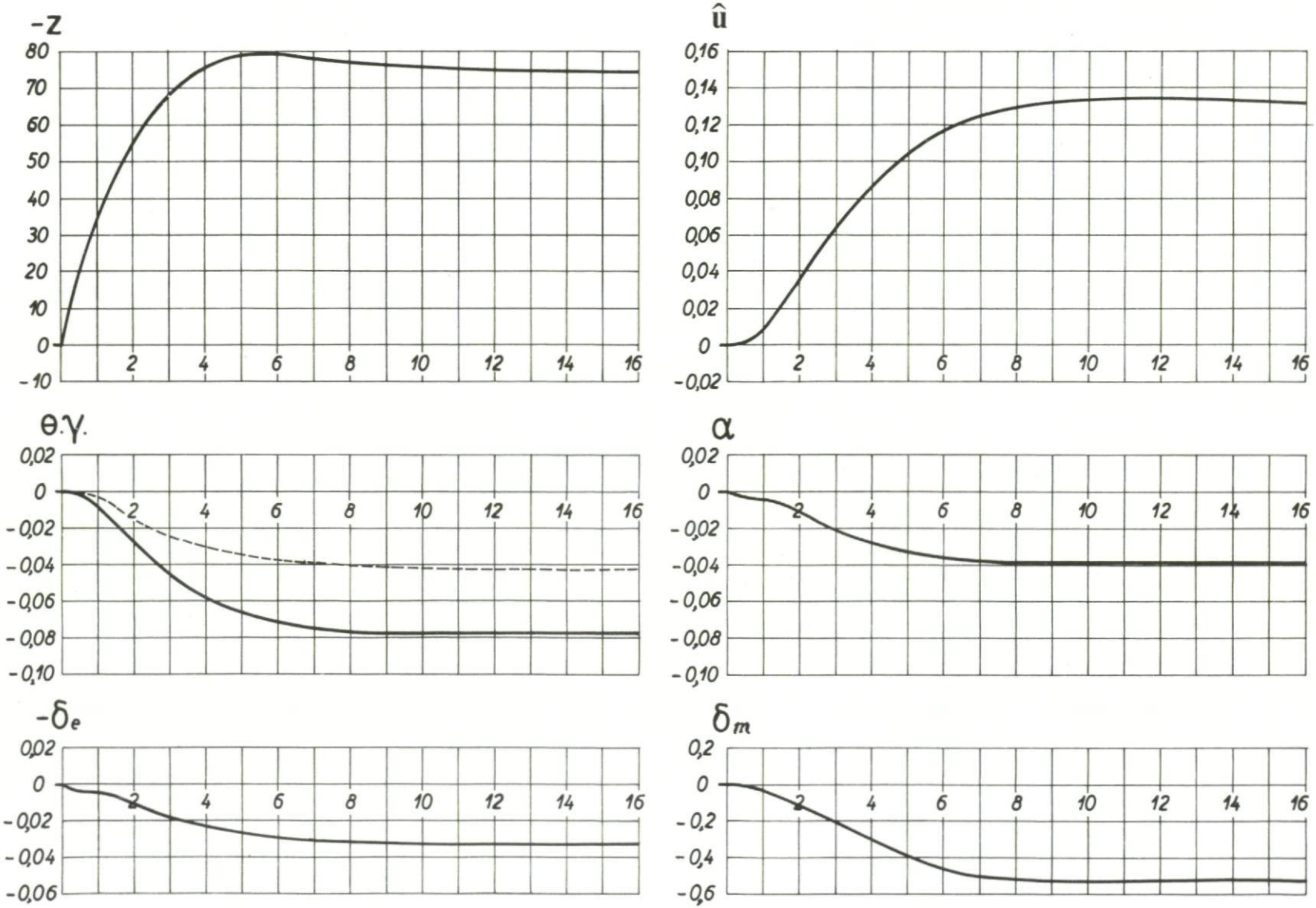

Fig.321 Aircraft response to an initial error γ, case c'

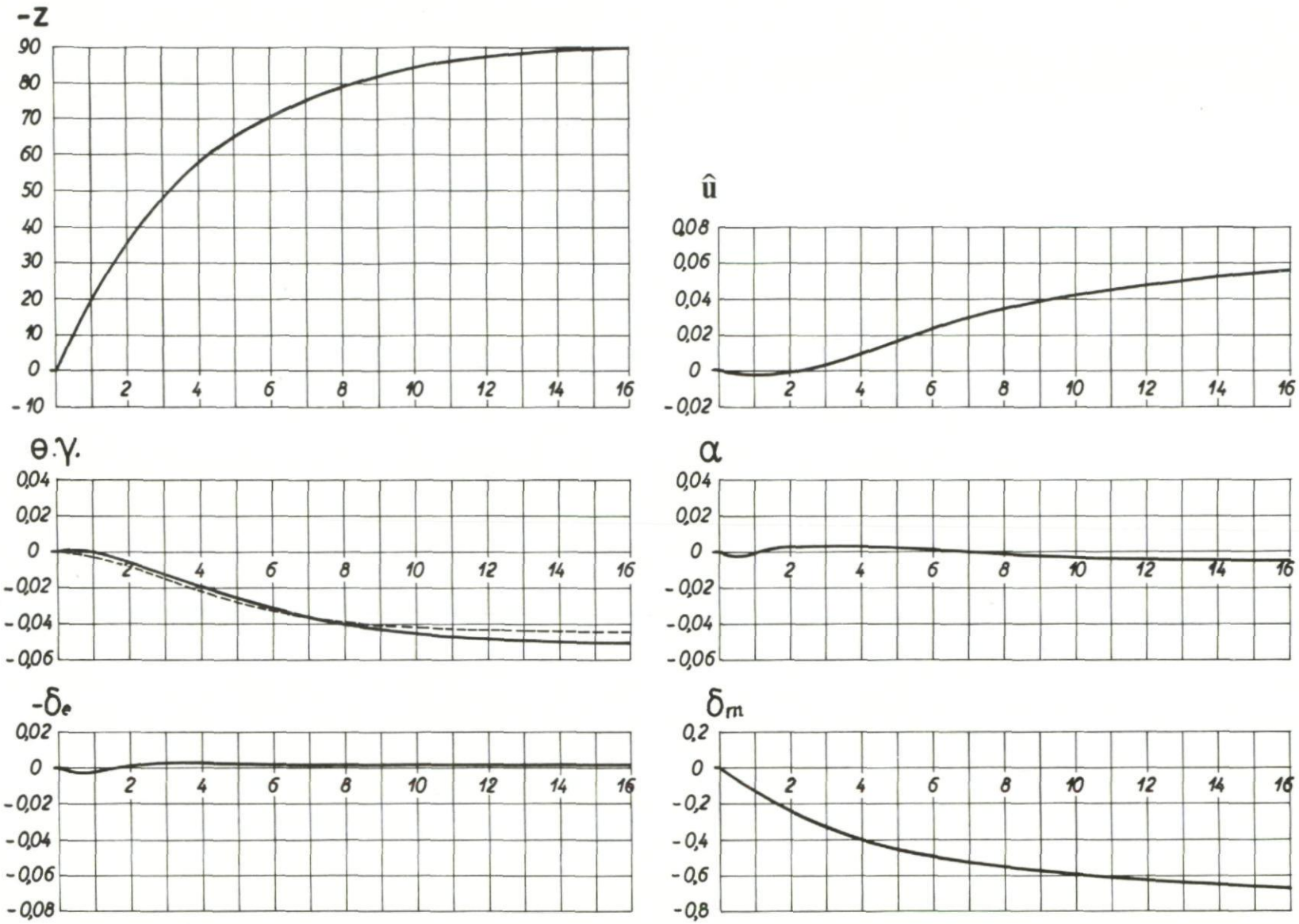

Fig. 322 Aircraft response to an initial error γ, case d′

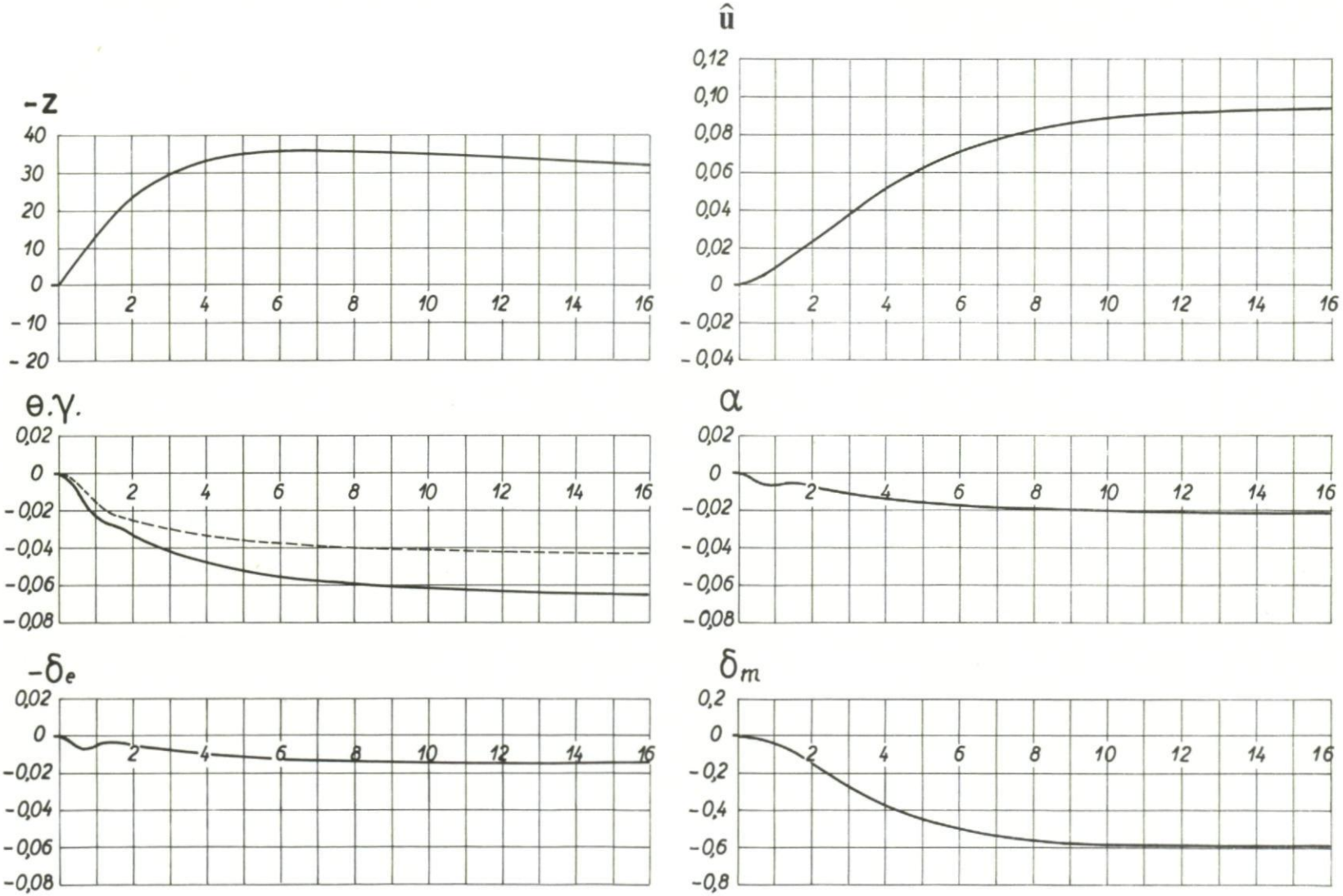

Fig.323 Aircraft response to an initial error γ, case g'

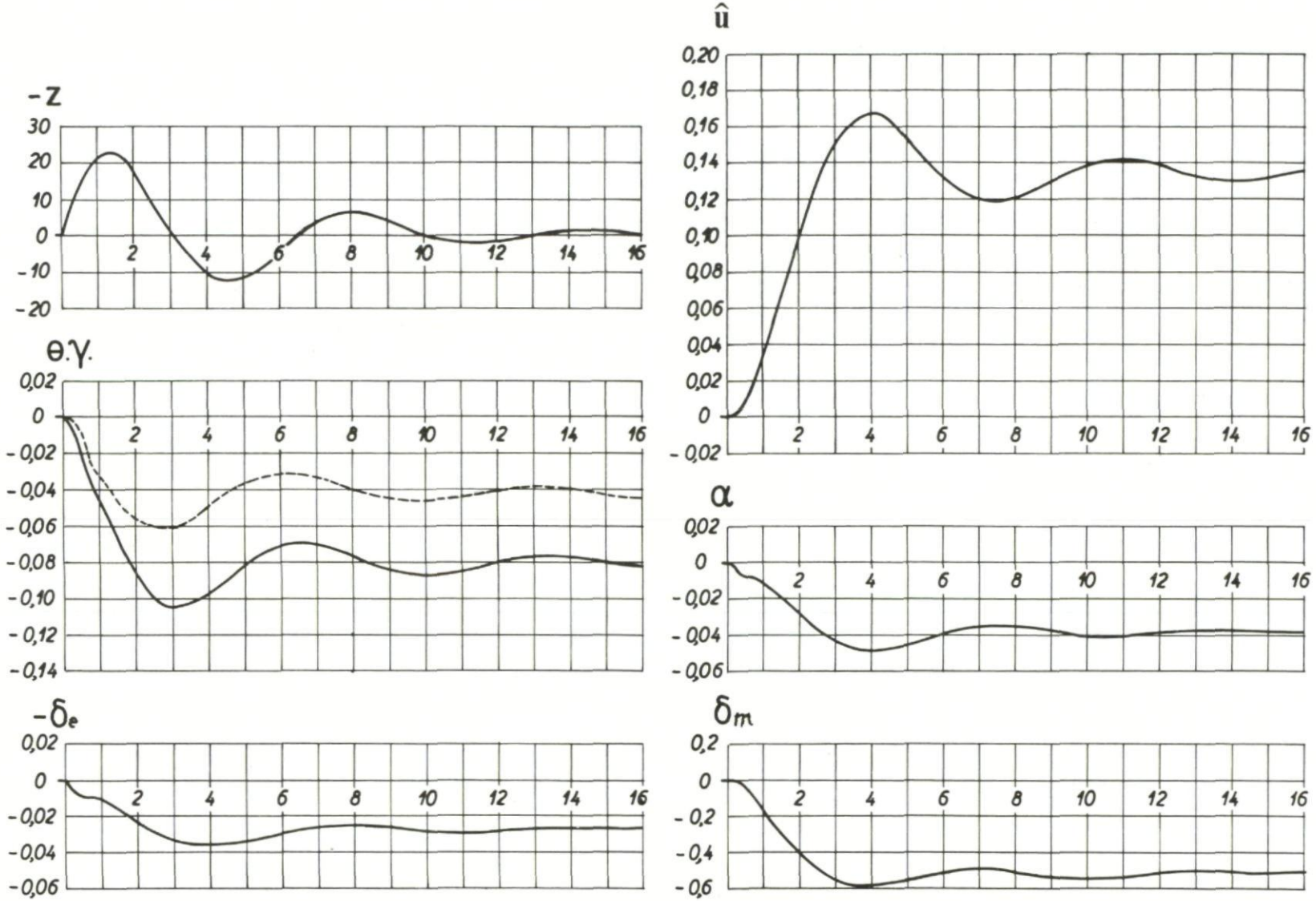

Fig.324 Aircraft response to an initial error γ, case j'

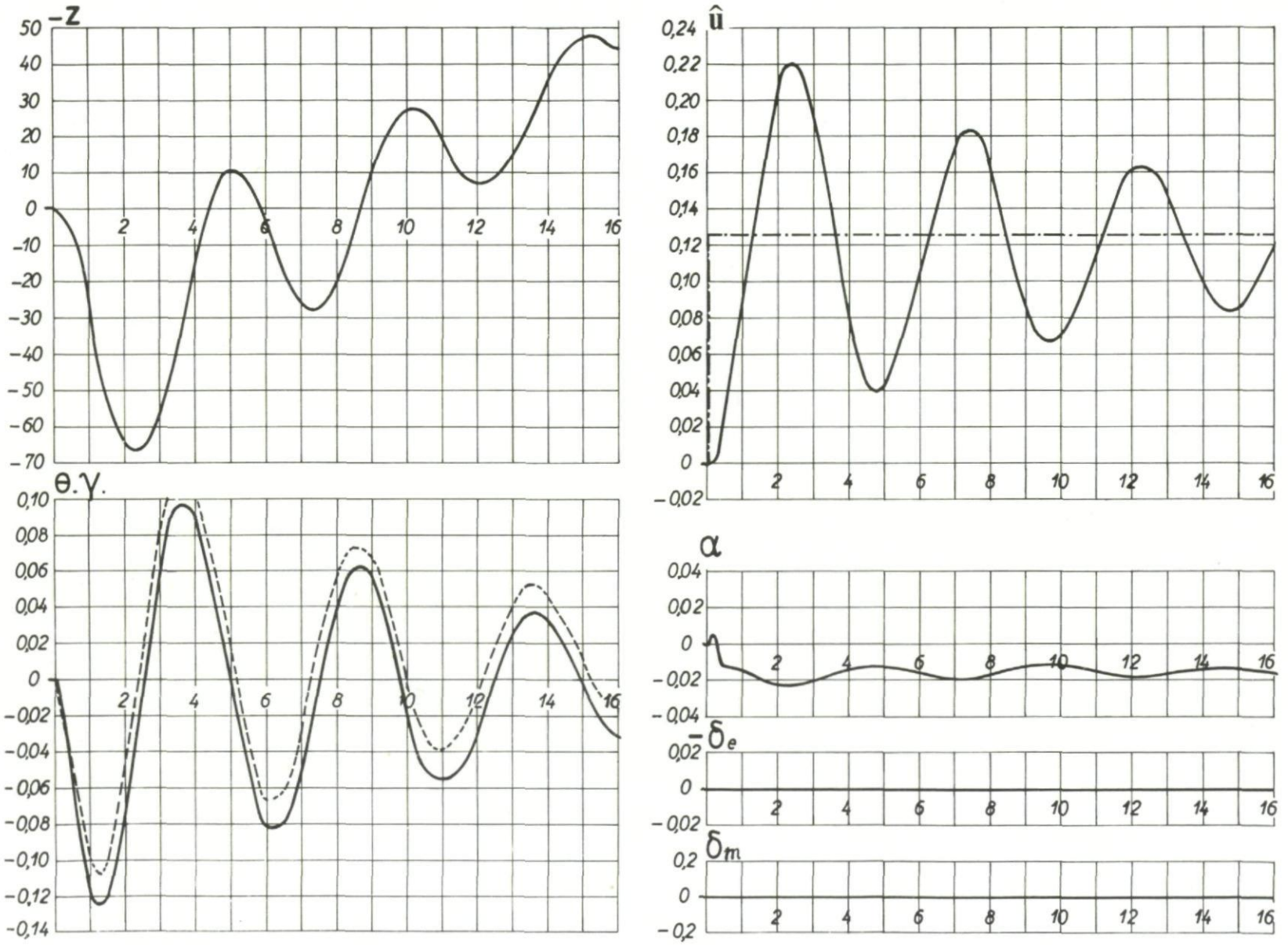

Fig.325 Aircraft response to a gust u_a, locked controls

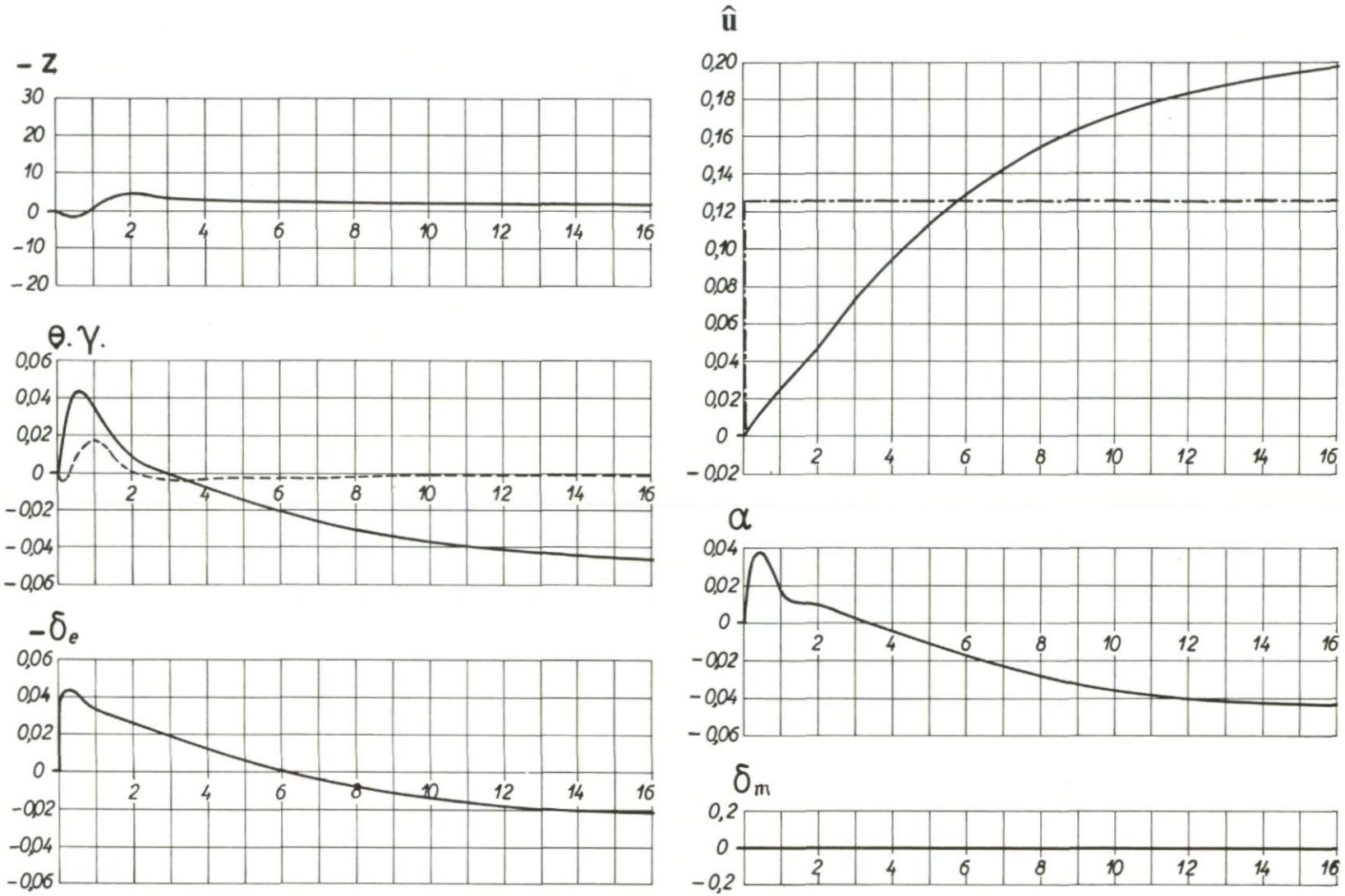

Fig.326 Aircraft response to a gust u_a, case b

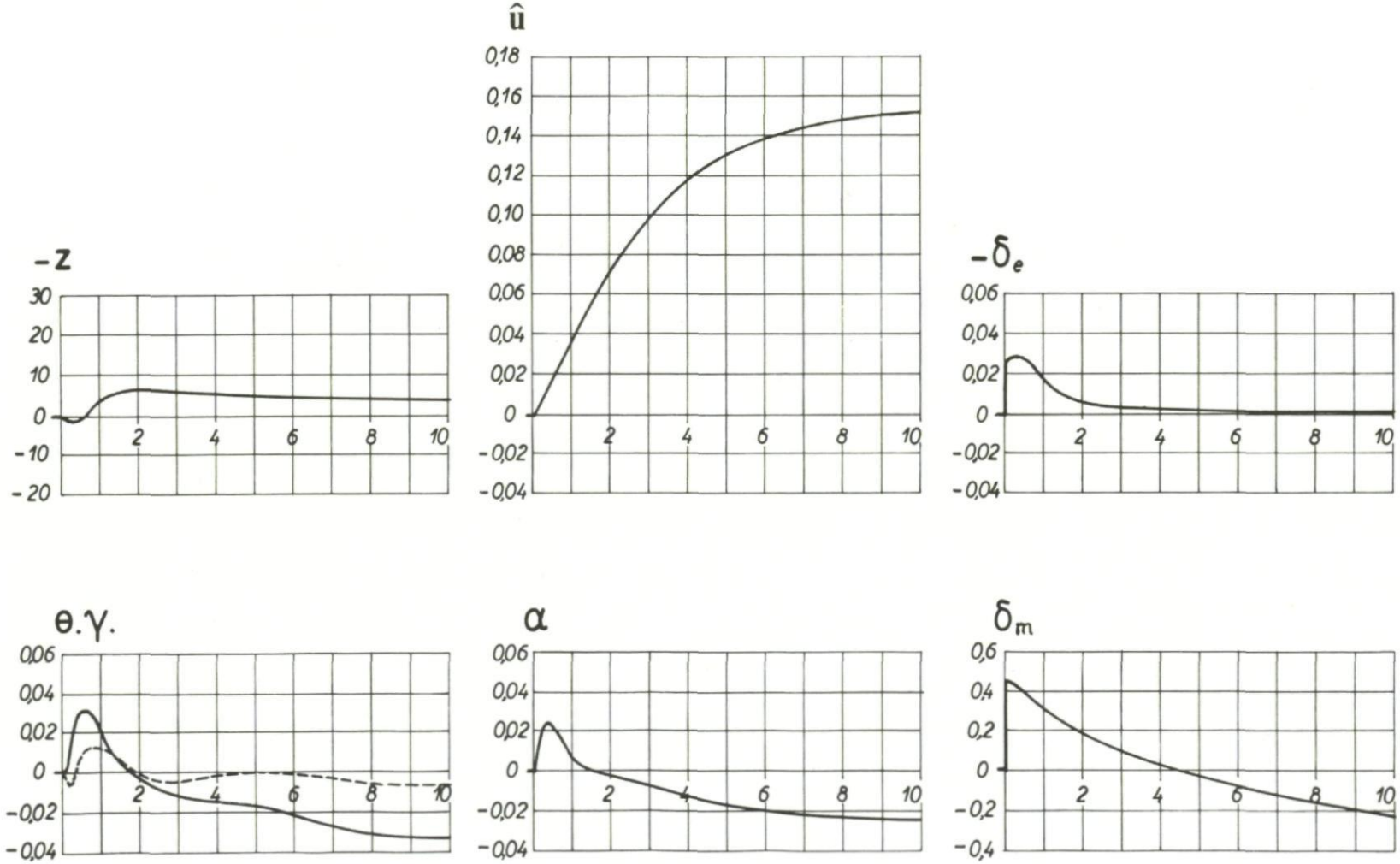

Fig. 327 Aircraft response to a gust u_a, case c

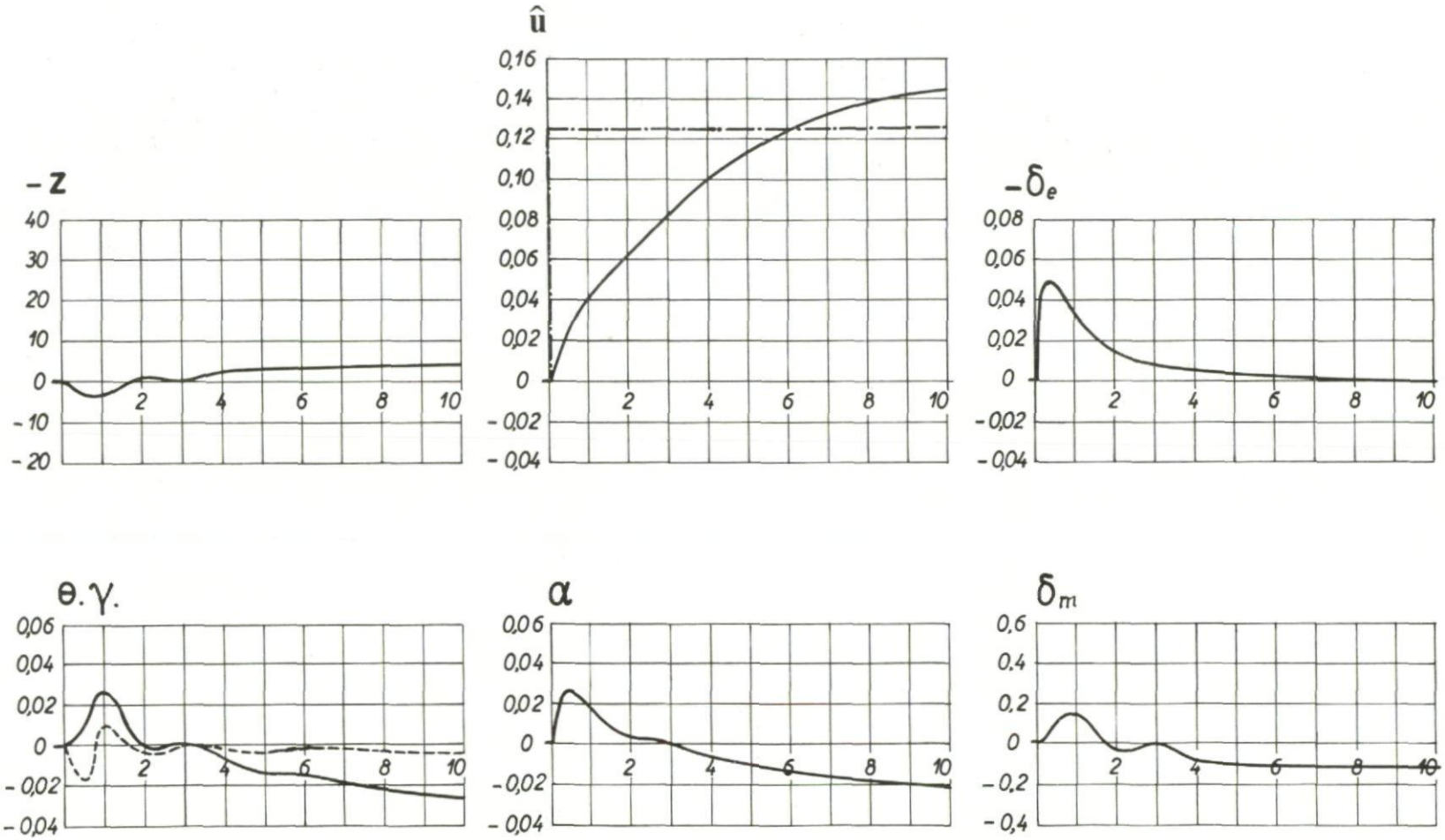

Fig.328 Aircraft response to a gust u_a, case d

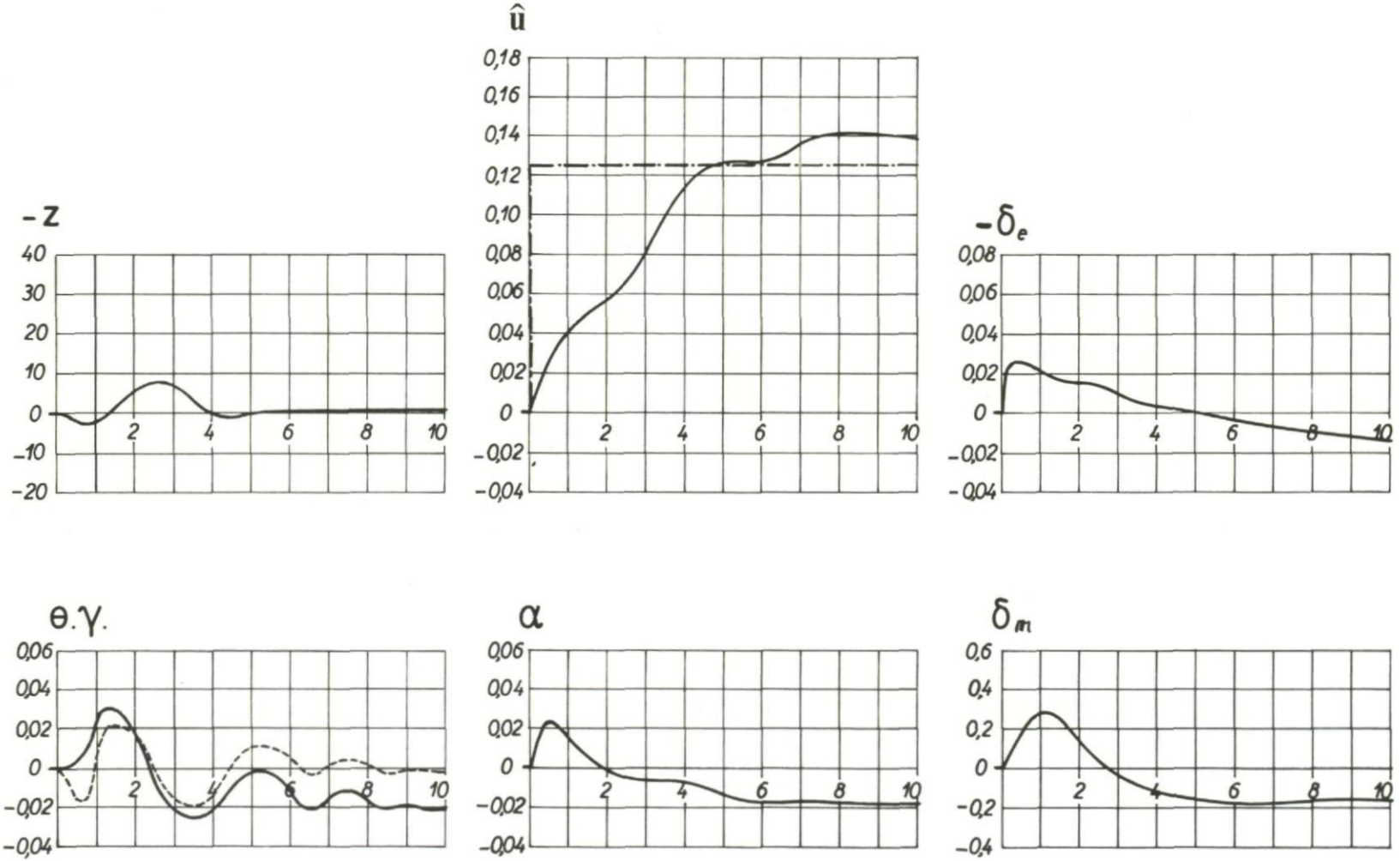

Fig.329 Aircraft response to a gust u_a, case g

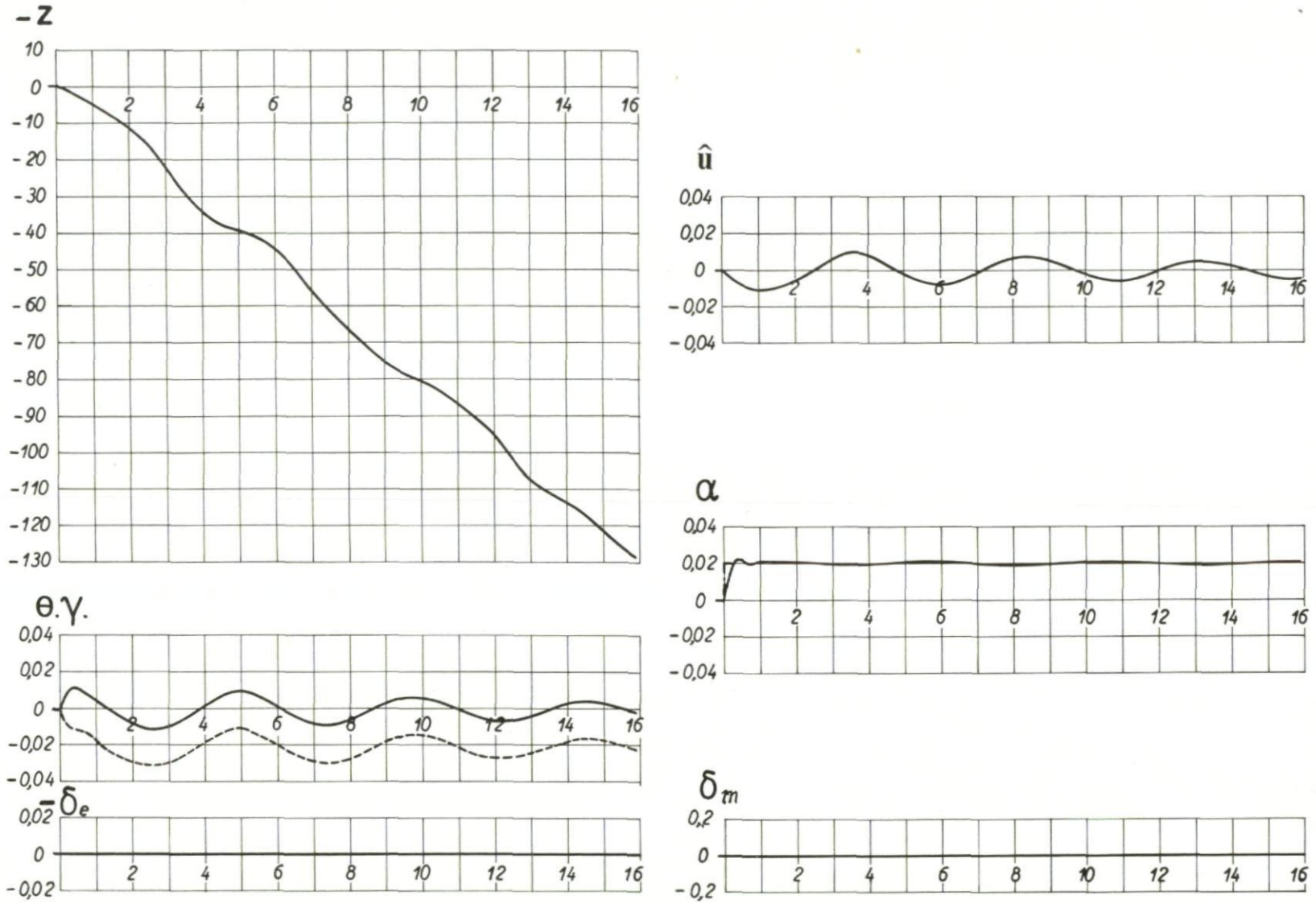

Fig.330 Aircraft response to a gust w_a, locked controls

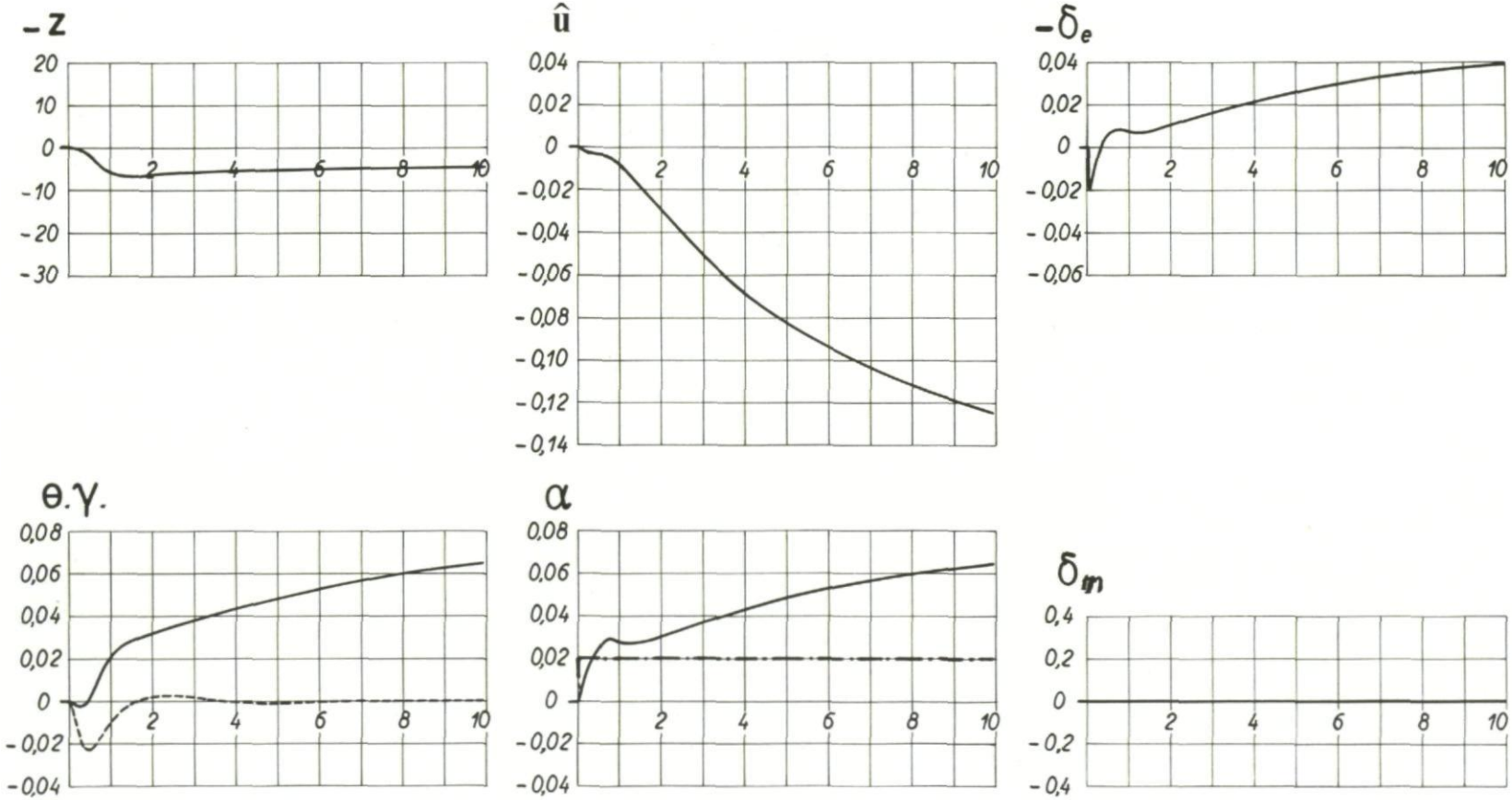

Fig.331 Aircraft response to a gust w_a, case b

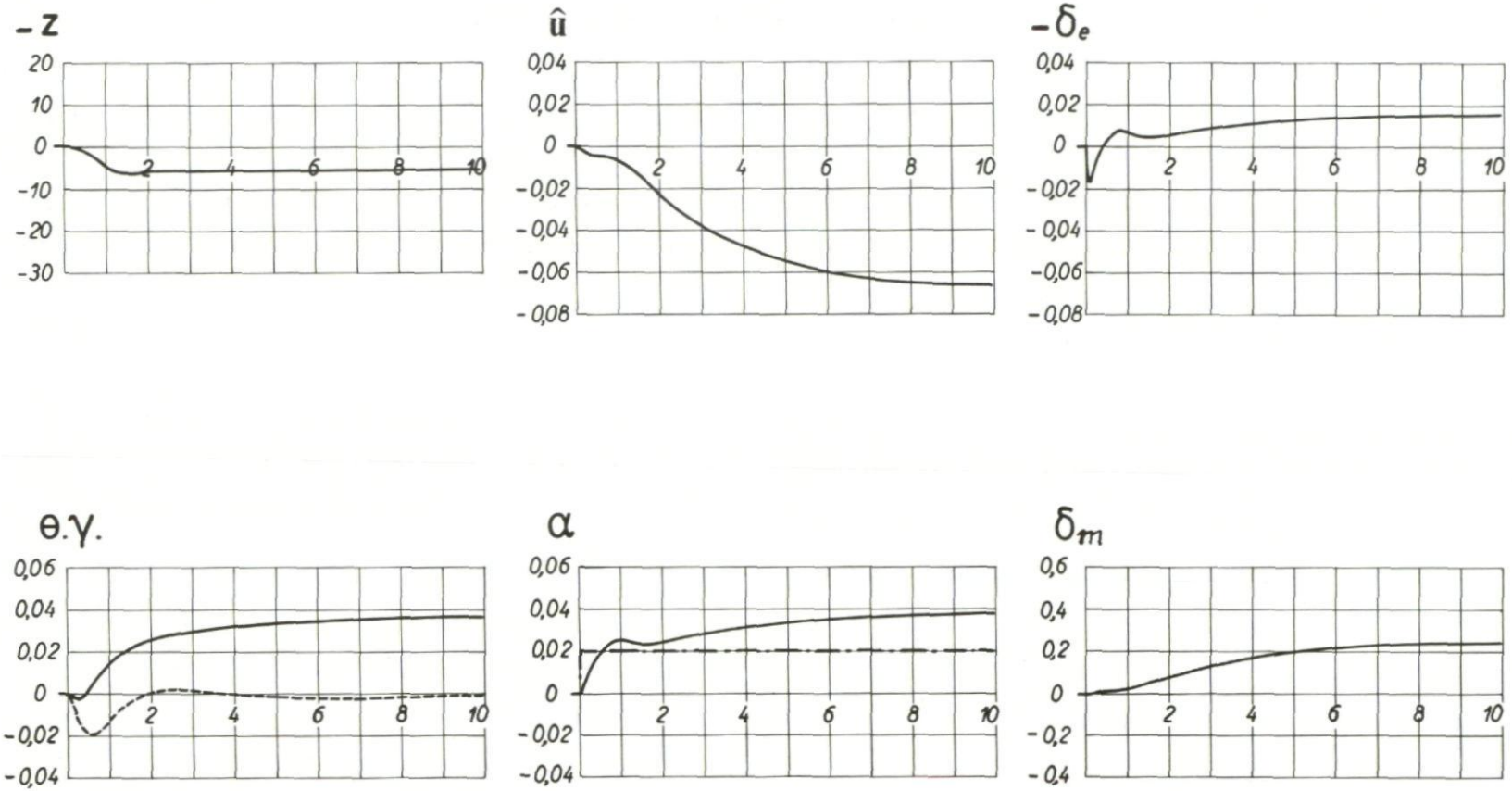

Fig.332 Aircraft response to a gust w_a, case c

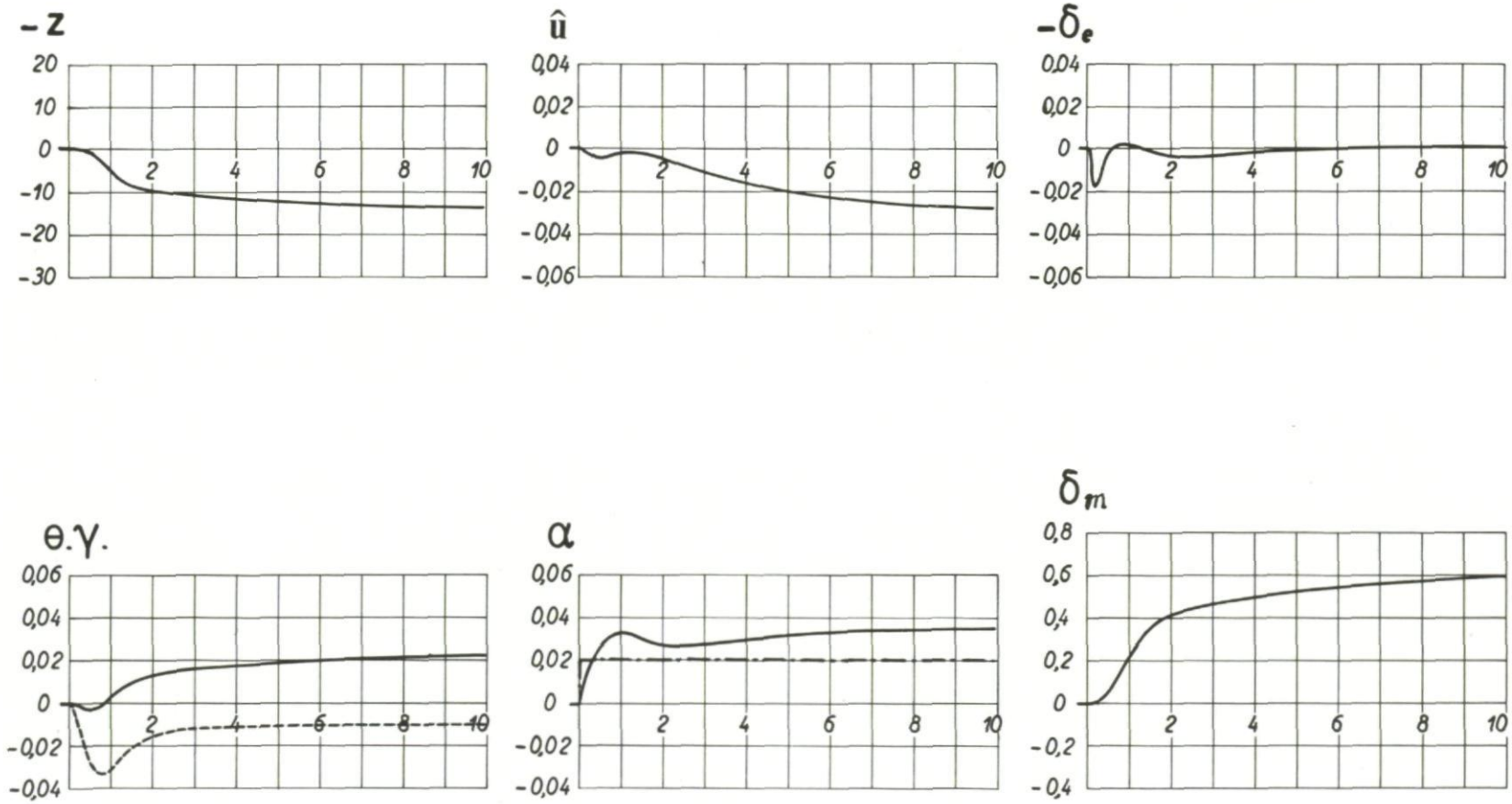

Fig.333 Aircraft response to a gust w_a, case d

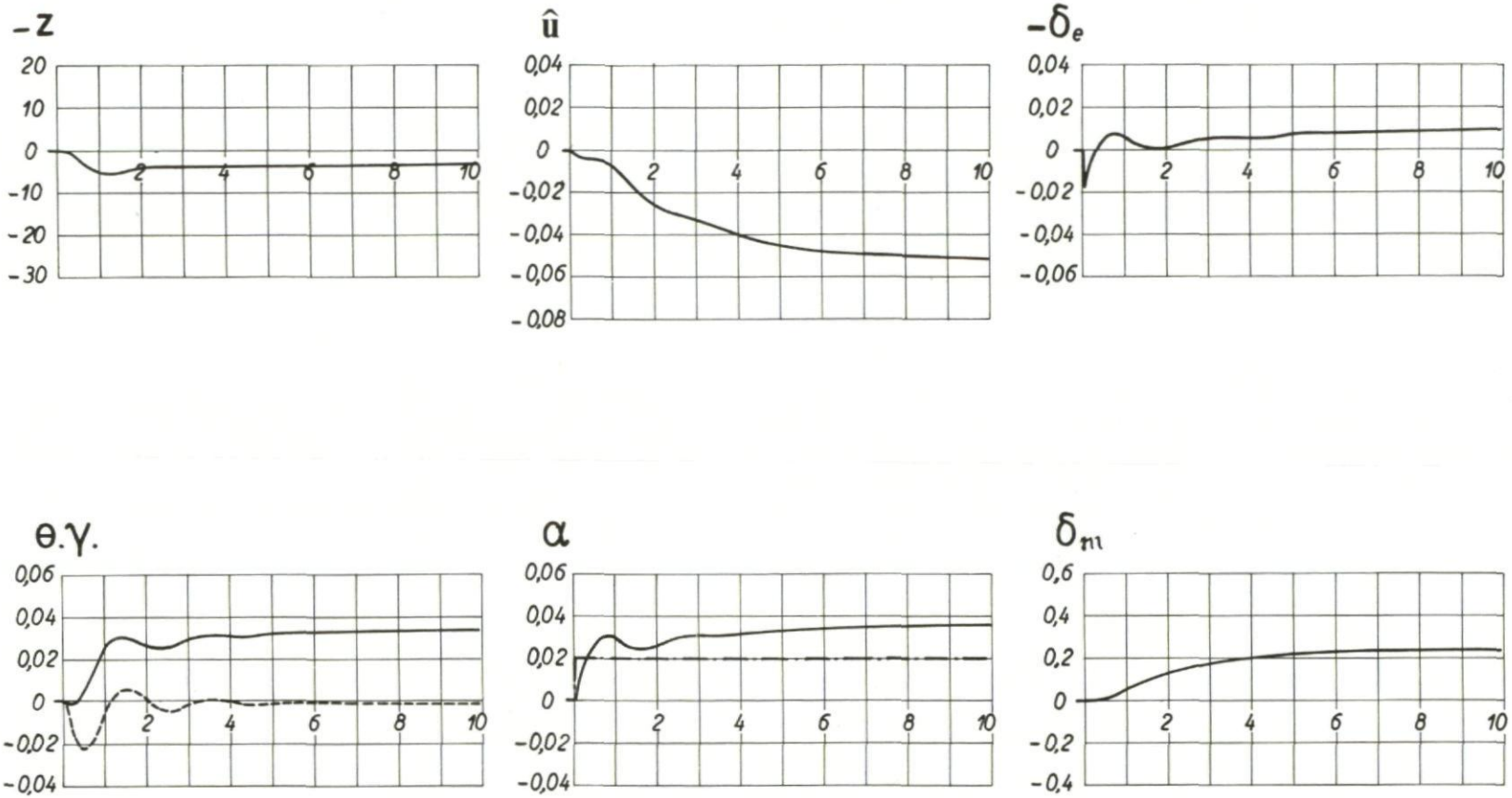

Fig. 334 Aircraft response to a gust w_a, case g

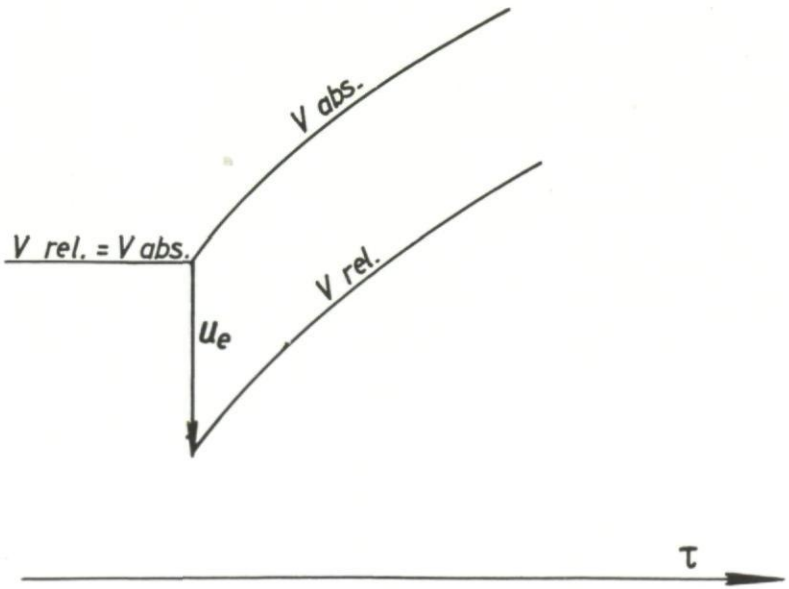

Fig. 335 Influence of u_a on the absolute and relative velocities

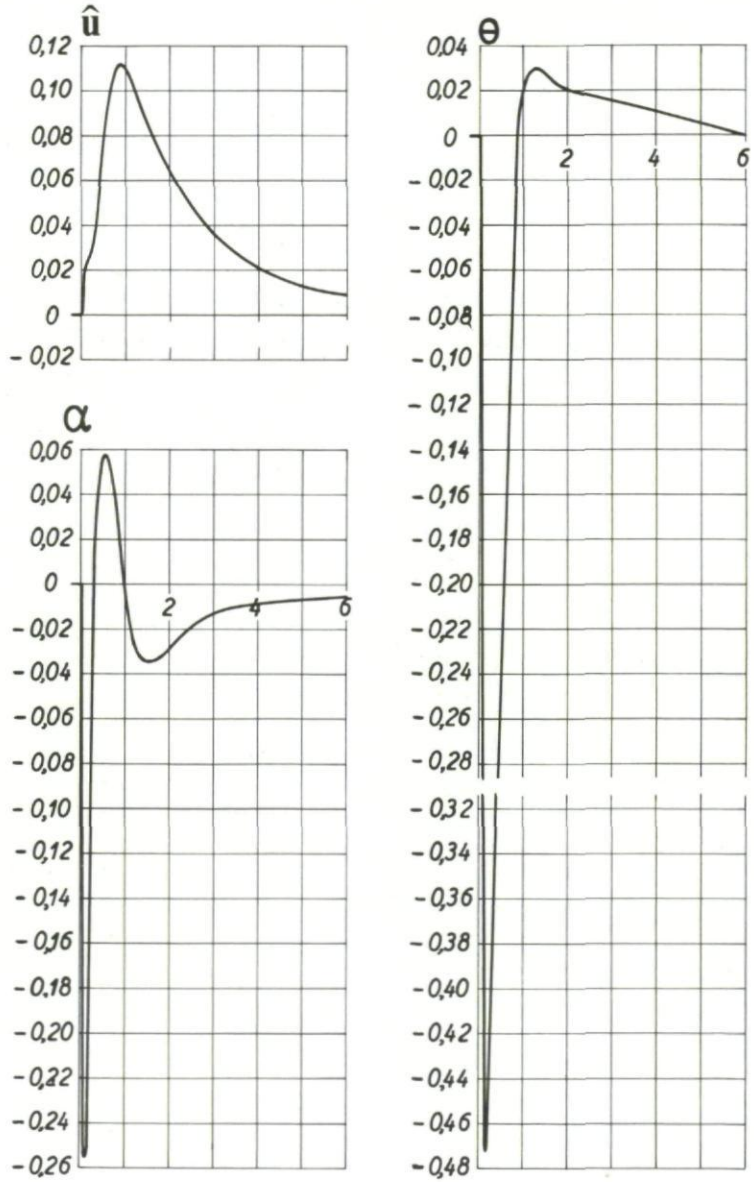

Fig. 336 Response to a pulse in $\dot{u}_a/V_0$

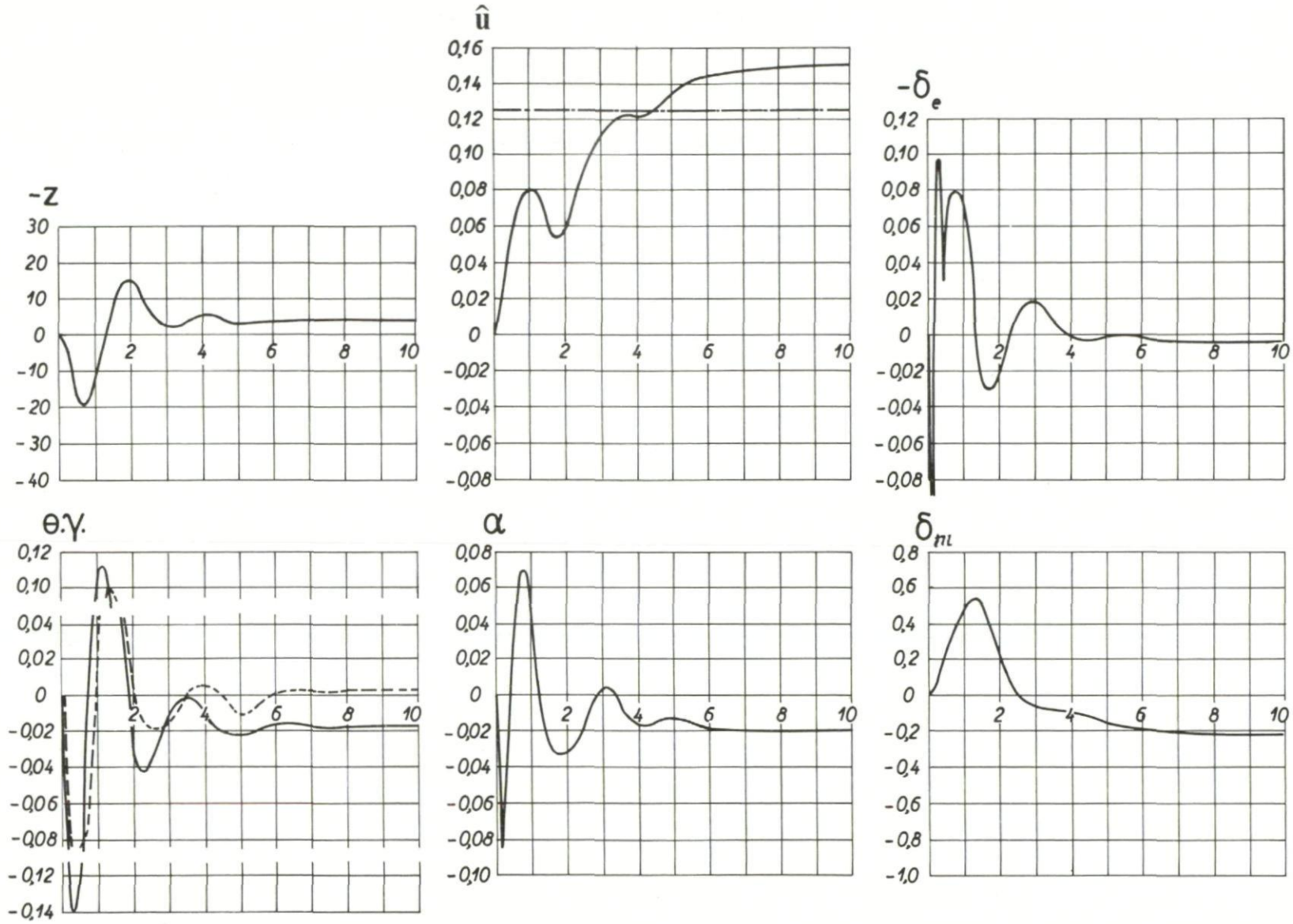

Fig. 337 Response to a gust u_a involving a pulse in $\dot{u}_a/V_0$

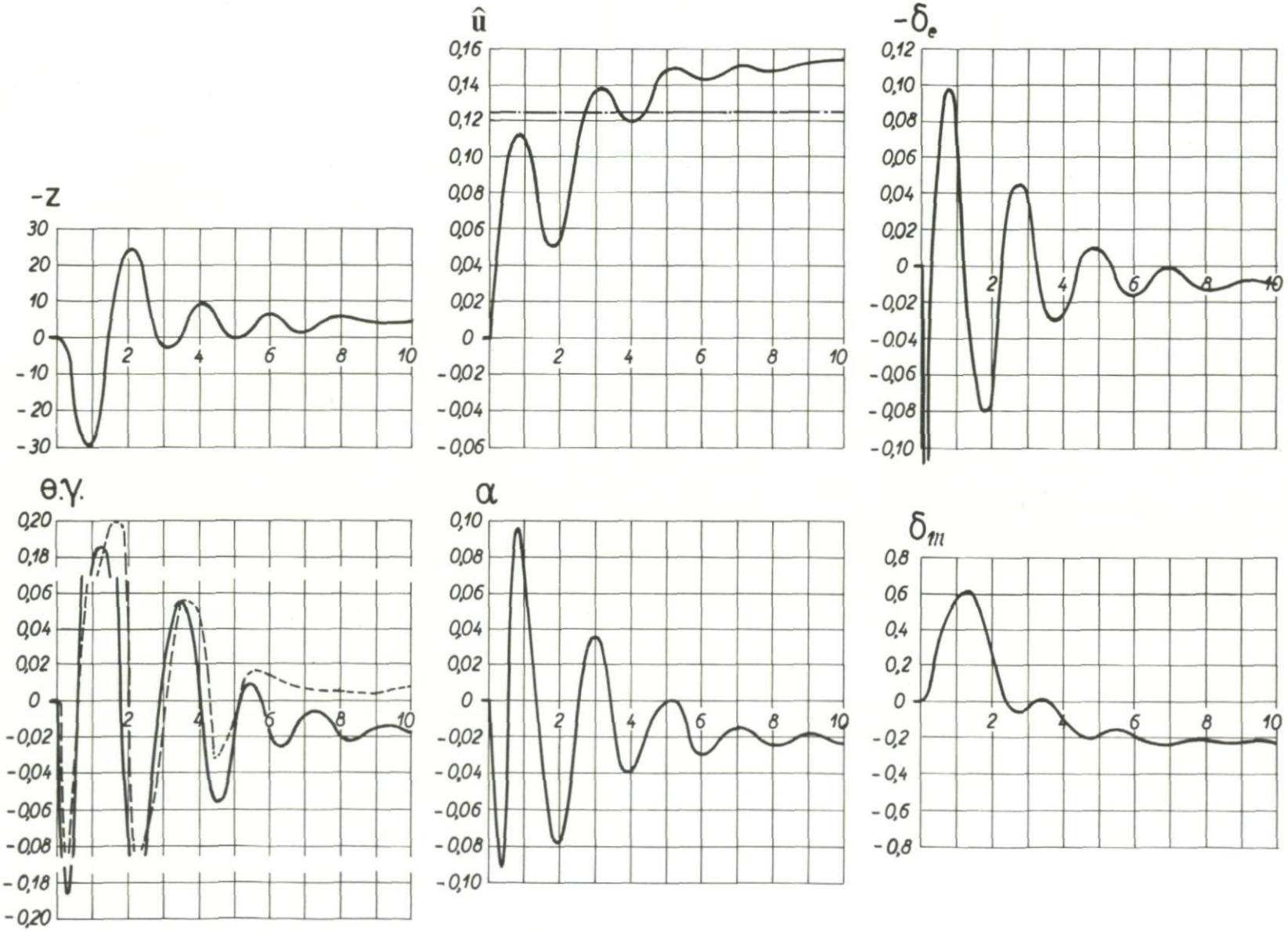

Fig.338 Response to a gust u_a involving a pulse in $\dot{u}_a/V_0$

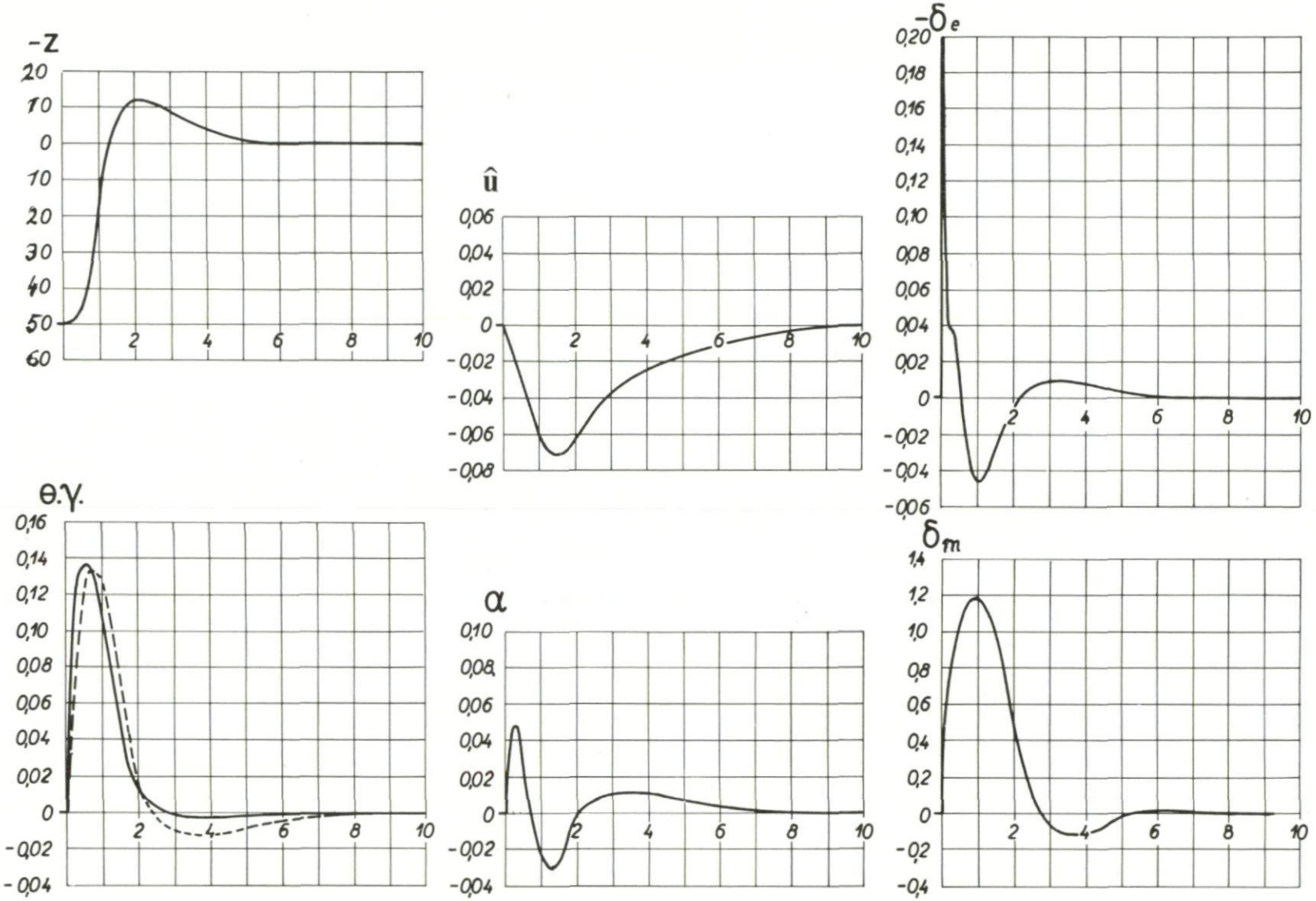

Fig.339 Response to an initial error z, with integral control

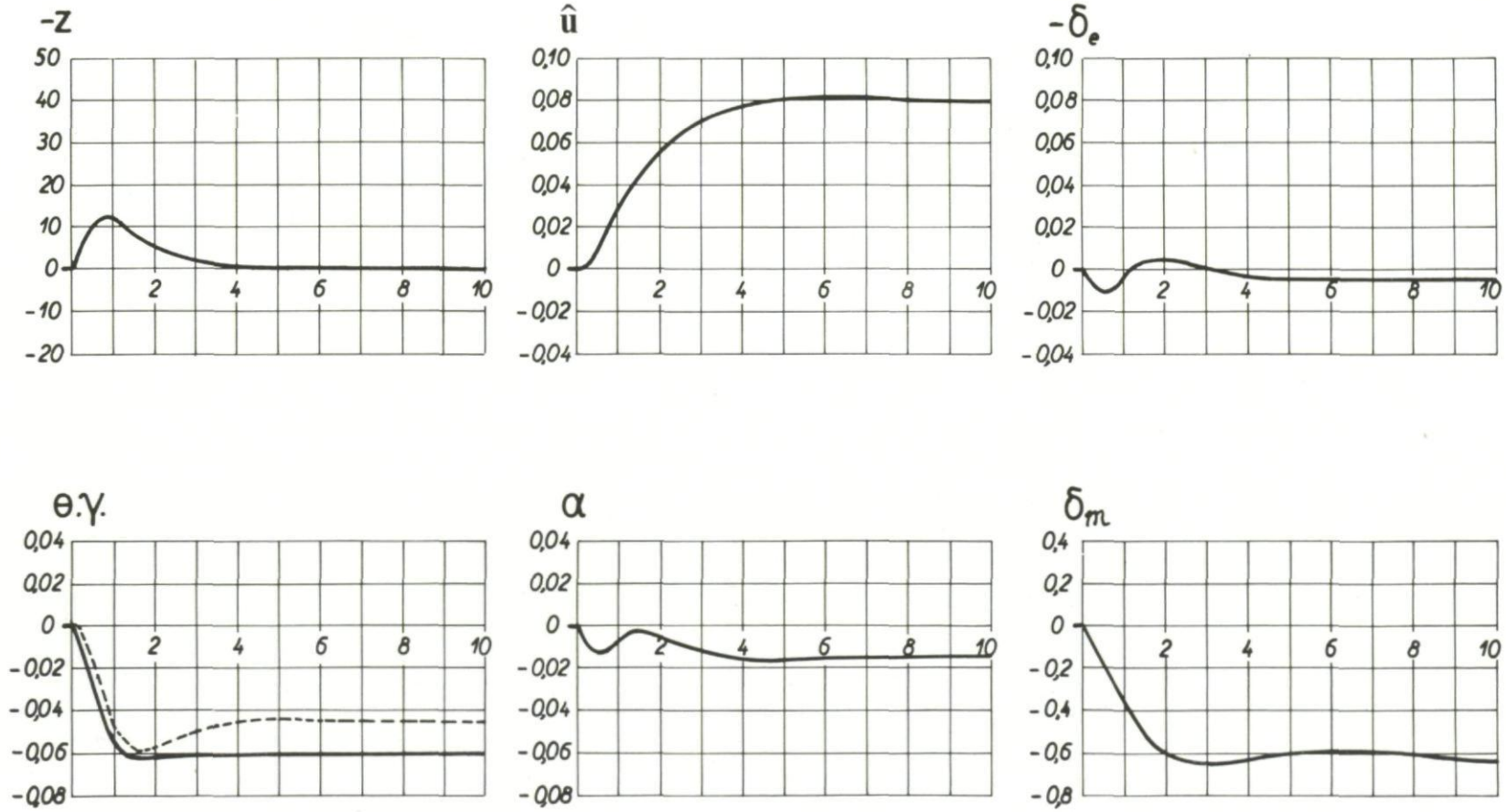

Fig.340 Response to an initial error γ, with integral control

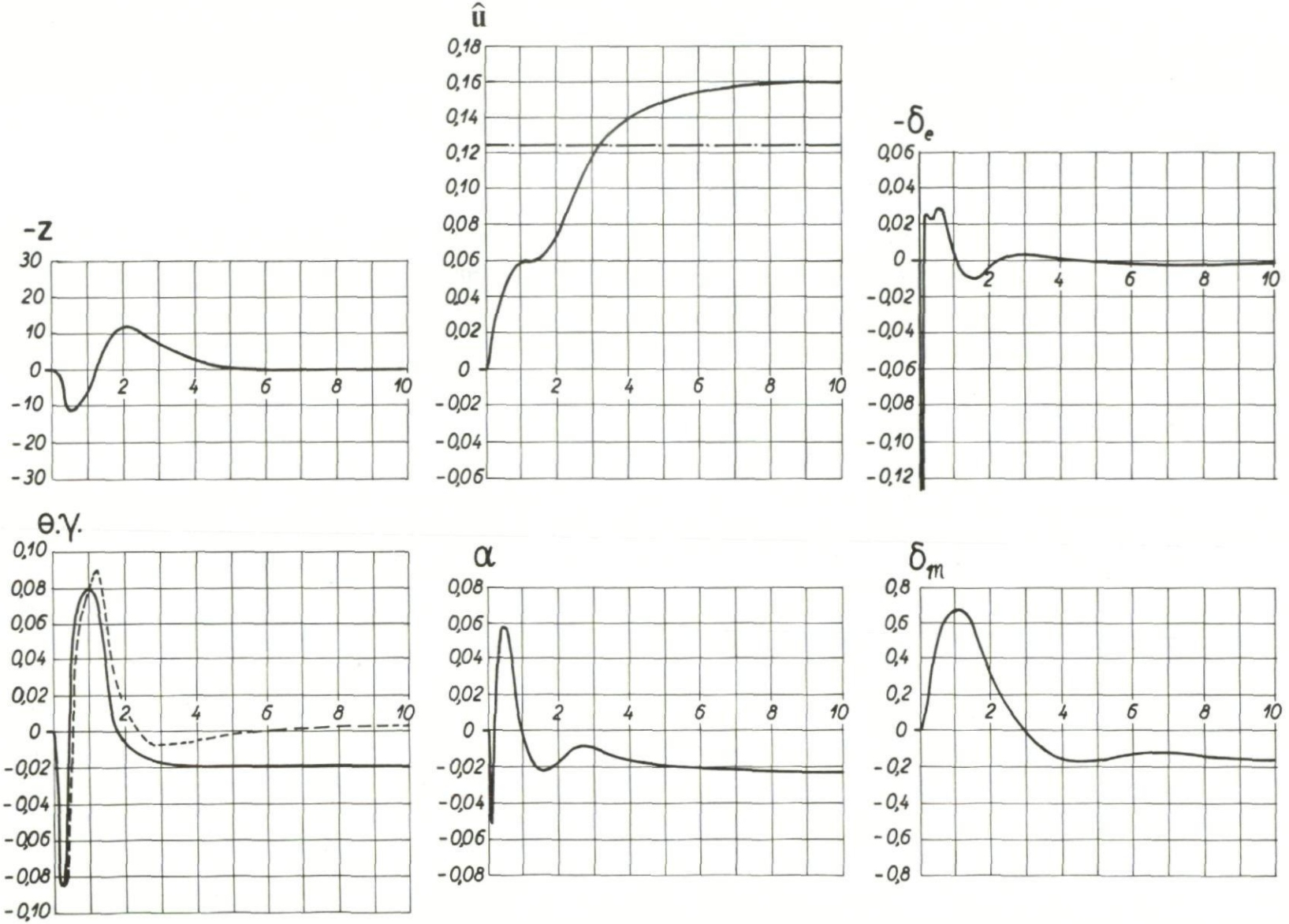

Fig.341 Response to a gust u_a, with integral control

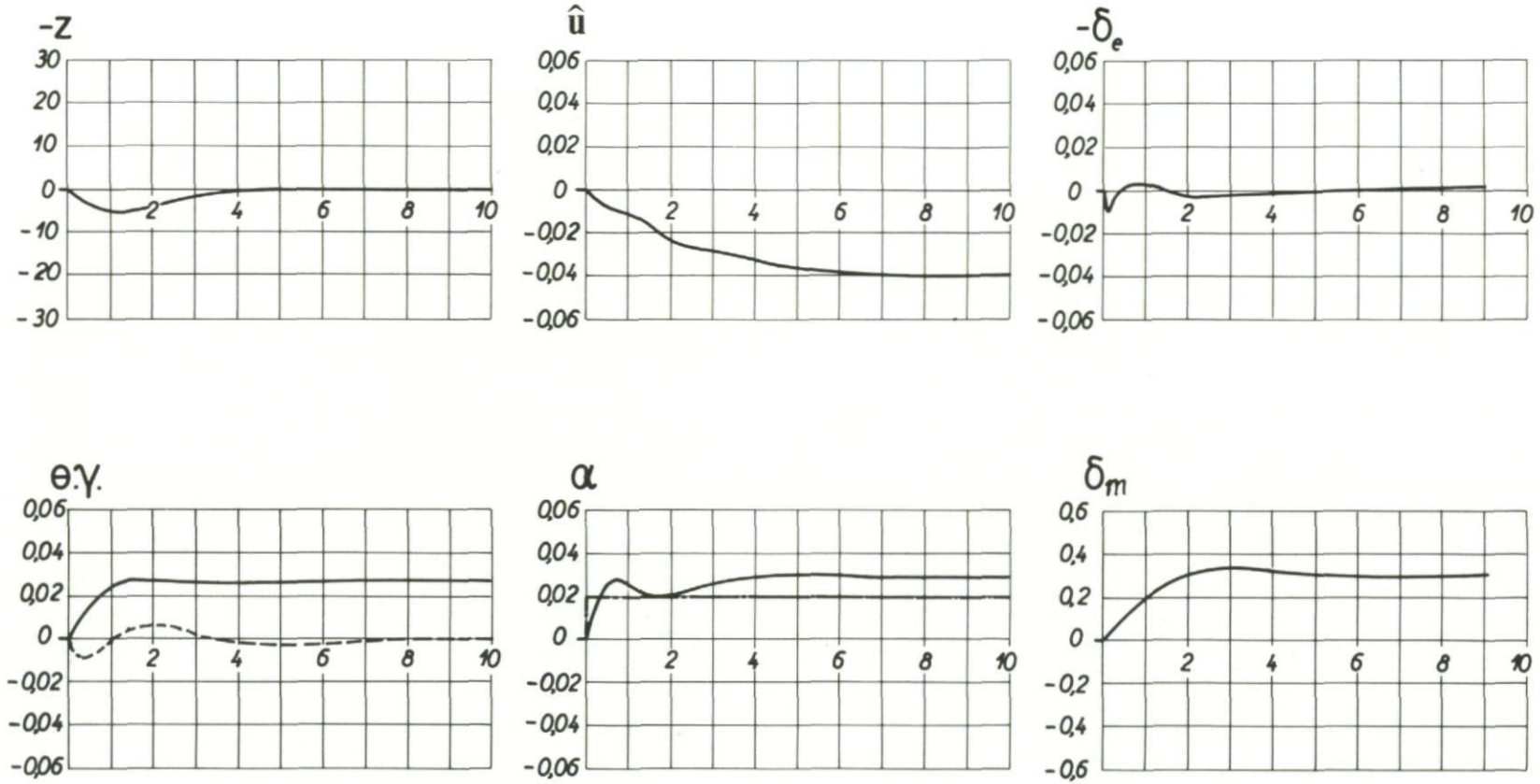

Fig.342 Response to a gust w_a, with integral control

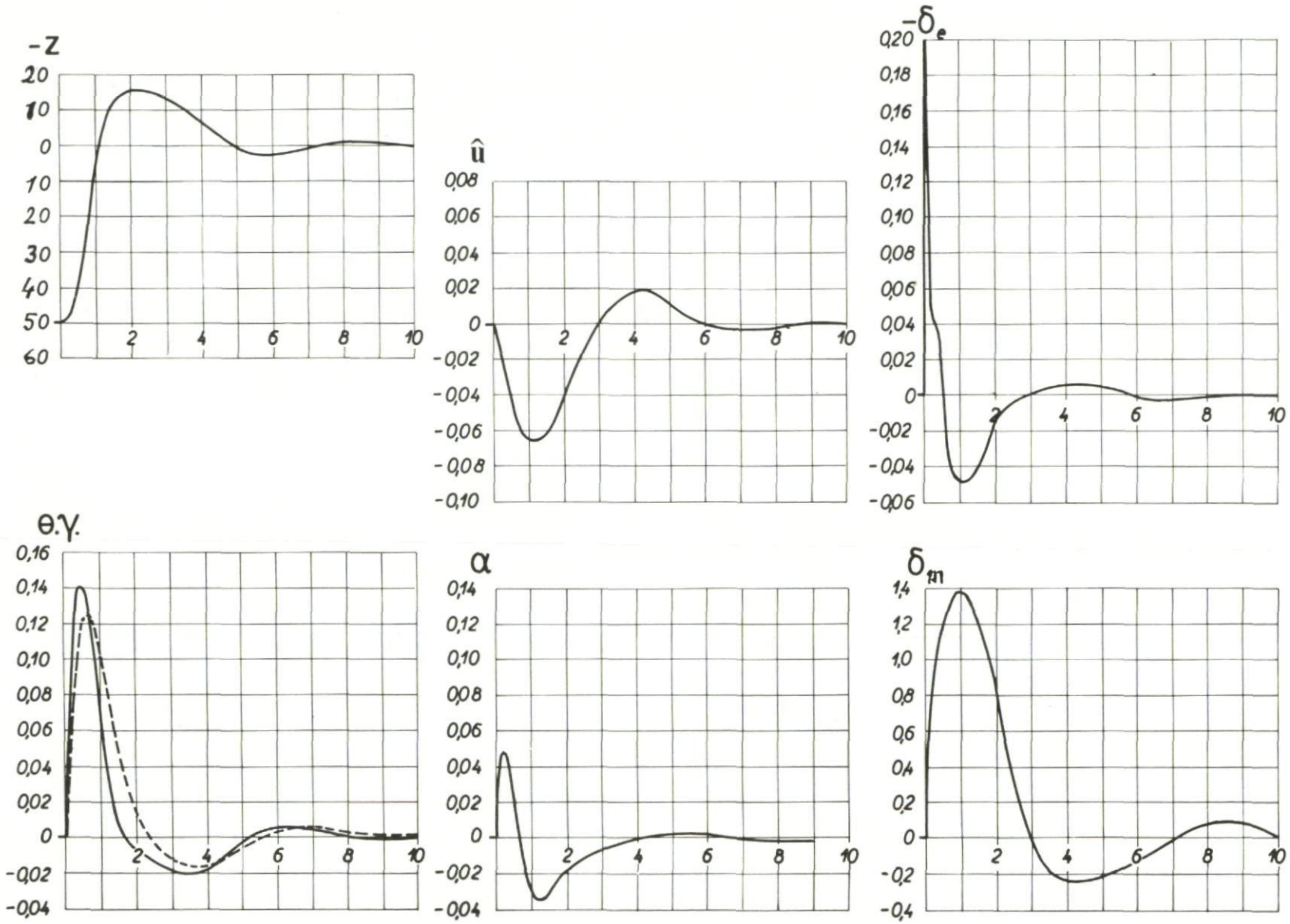

Fig.343 Response to an initial error z, with integral control

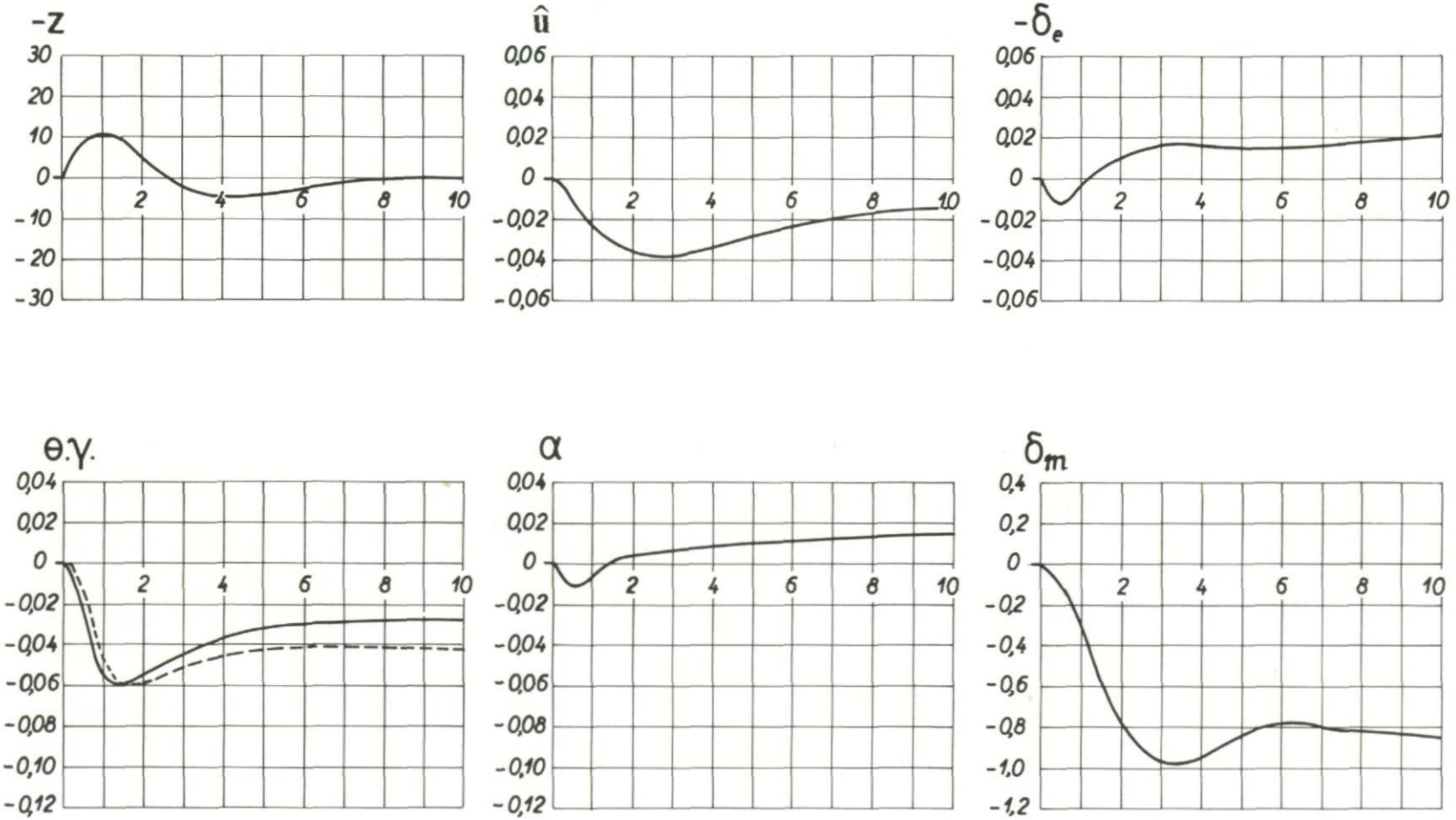

Fig.344 Response to an initial error γ, with integral control

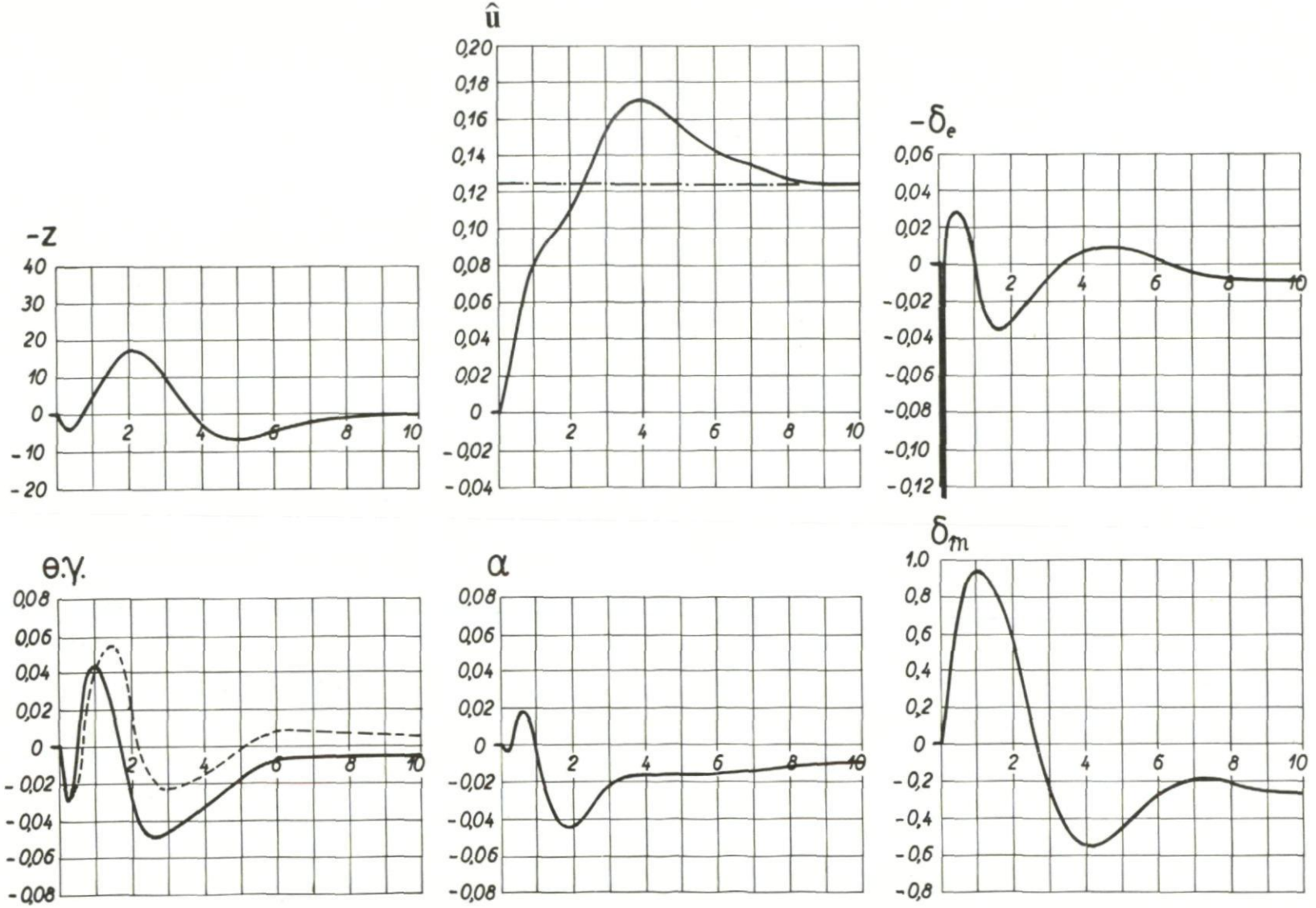

Fig.345 Response to a gust u_a, with integral control

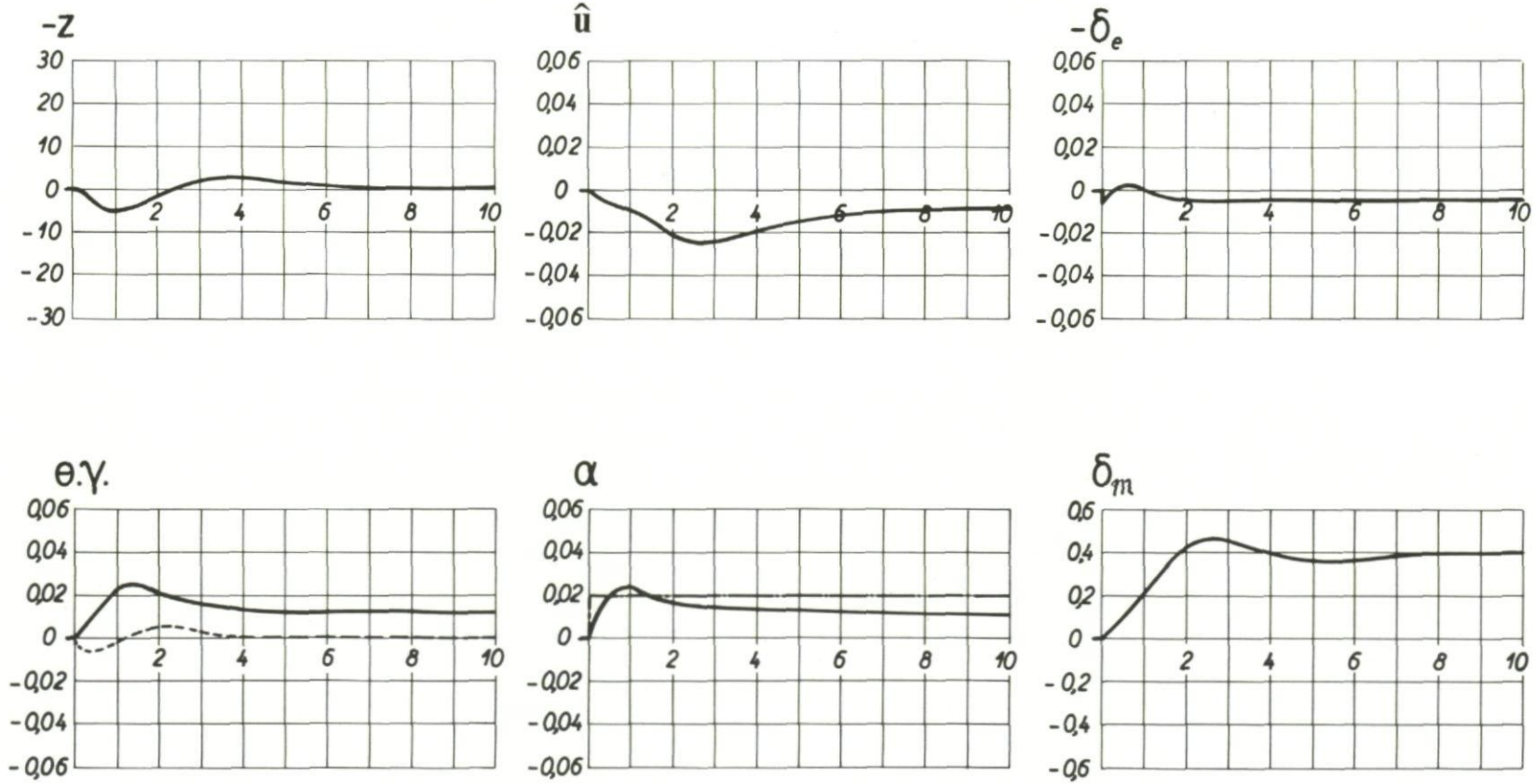

Fig.346 Response to a gust w_a, with integral control

BIBLIOGRAPHY

1. Duncan, W.J. — *The Principles of the Control and Stability of Aircraft.* Cambridge, 1952.

2. Etkin, B. — *Dynamics of Flight.* Toronto, 1959.

3. Halfman, R.L. — *Experimental Aerodynamic Derivatives of a Sinusoidally Oscillating Airfoil in Two-Dimensional Flow.* NACA T.N. 2465, November 1951.

4. Neumark, S. — *Longitudinal Stability, Speed and Height.* Aircraft Engineering, No.261, November 1950.

5. Vedrov, V.S. et alii — *The Airplane as an Object of Control.* Report No.74, Ministry of Aviation Industry (Russian), NASA, Technical Translation F.5, Oct. 1959.

6. Gait, J.S. — *Tridac. A Large Analogue Computer for Flight Simulations.* Proceedings, International Analogy Computation Meeting, Brussels, 1955.

7. Czinczenheim, J. et alii — *Le Couplage par Inertie et ses Répercussions sur les Qualités de Vol.* Docaero, May 1958.

8. Curfman, H.J., Jr. — *Theoretical and Analog Studies of the Effects of Non-Linear Stability Derivatives on the Longitudinal Motions of an Aircraft in Response to Step Control Deflections and the Influence of Proportional Automatic Control.* NACA Report 1241, 1955.

9. Foody, J.J. — *The Analogue Computer in Aircraft Design Problems Involving Non-Linearities.* Proceedings, International Analogy Computation Meeting, Brussels, 1955.

10. Neihouse, A. et alii — *Status of Spin Research for Recent Airplane Designs.* NACA R.M. L57 F 12, Aug. 1957.

11. Campbell, G. Bull, G. — *Determination of the Longitudinal Stall Dynamics of a PT-26 Airplane.* A.F. Technical Report No.6000, May 1950.

12. Campbell, G. — *Analog Computer Program on PT-26 Longitudinal Stall Responses.* Cornell Aeronautical Laboratory, FRM No.109, 20 June 1950.

13. Russell, W.R. Alford, W.L. — *Flight Investigation of a Centrally Located Rigid Force Control Stick Used with Electronic Control Systems in a Fighter Airplane.* NASA T.N. D.101, September 1959.

14. Monroe, W.R. — *Application of Electronic Simulation Techniques to the Development of Airplane Flight Control Systems.* Aeronautical Engineering Review, May 1955.

15. Mathews, C.W. — *Analog Study of the Effects of Various Types of Control Feel on the Dynamic Characteristics of a Pilot-Airplane Combination.* NACA R.M. L 55 F 01a, Aug. 1955.

16. Klemin, A. et alii — *Longitudinal Stability in Relation to the Use of an Automatic Pilot.* NACA T.N. 686, September 1938.

17. Porter, R.F. — *An Analog Computer Study of a Stability Augmentation System for F-86 E Aircraft.* Technical Note WCT 54-104, Wright Air Development Center, March 1955.

18. Sjoberg, S.A. — *A Flight Investigation of the Handling Characteristics of a Fighter Airplane Controlled Through Automatic Pilot Control Systems.* NACA R.M. L 55 F 01b, September 1955.

19. Sjoberg, S.A. — *Flying Qualities Associated With Several Types of Command Flight Control Systems.* I.A.S. Paper No. 59-134, Oct. 1959.

20. Bismut, M. Bouttes, J. — *Etude sur Simulateur des Conditions d'Approche GCA au Second Régime de Vol.* AGARD Report

21. Lina, L.S. et alii — *Flight Investigation of an Automatic Throttle Control in Landing Approaches.* NASA Memo 2-19-59 L, March 1959.

22. Porter, R.F. — *Analog Computer Study of the Automatic Flare-Out Landing of a C-54 Aircraft with an E4 Automatic Pilot.* Technical Note W.C.T.52-53, Wright Air Development Center, December 1953.

23. MacCallum, J.M. — *A Study of Automatic Flare-Out Landing Control Systems for a B-47 Aircraft.* Thesis, Resident College of The U.S.A.F. Institute of Technology, March 1955.

24. Merriam, C.W. — *Study of an Automatic Landing System for Aircraft.* Massachusetts Institute of Technology, Report No.93, May 1955.

25. Markusen, D. et alii — *Automatic Flare-Out for Landing.* Wright Air Development Center, T.Z. 55-506, March 1956.

26. Boucher, R.W. Kraft, C.C., Jr. — *Analysis of a Vane-Controlled Gust Alleviation System.* NACA T.N. 3597, April 1956.

27. Philips, W.H. — *Effect of Steady Rolling on Longitudinal and Directional Stability.* NACA T.N. 1627, June 1948.

28. Carroll, R.E. Tyler, C. — *Study of Optimum Final Approach of Aircraft.* Technical Note WCT 53-47, Wright Patterson Air Force Base, Ohio, U.S.A., July 1953.

29. Mercer, D.F. *A Quantitative Study of Instrument Approach.* Journal of the Royal Aeronautical Society, London, February 1954.

30. Tatz, A. *Final Engineering Report on Study of ILS Localizer Bends.* Report No.830, Airborne Instruments Laboratory, Mineola N.Y., Nov. 1952.

DISTRIBUTION

Copies of AGARD publications may be obtained in the various countries at the addresses given below.

On peut se procurer des exemplaires des publications de l'AGARD aux adresses suivantes.

BELGIUM BELGIQUE	Centre National d'Etudes et de Recherches Aéronautiques 11, rue d'Egmont, Bruxelles
CANADA	Director of Scientific Information Service Defense Research Board Department of National Defense 'A' Building, Ottawa, Ontario
DENMARK DANEMARK	Military Research Board Defense Staff Kastellet, Copenhagen Ø
FRANCE	O.N.E.R.A. (Direction) 25, Avenue de la Division Leclerc Châtillon-sous-Bagneux (Seine)
GERMANY ALLEMAGNE	Wissenschaftliche Gesellschaft für Luftfahrt Zentralstelle der Luftfahrtdokumentation Munchen 64, Flughafen Attn: Dr. H.J. Rautenberg
GREECE GRECE	Greek National Defense General Staff B. MEO Athens
ICELAND ISLANDE	Director of Aviation c/o Flugrad Reykjavik
ITALY ITALIE	Ufficio del Generale Ispettore del Genio Aeronautico Ministero Difesa Aeronautica Roma
LUXEMBURG LUXEMBOURG	Obtainable through Belgium
NETHERLANDS PAYS BAS	Netherlands Delegation to AGARD Michiel de Ruyterweg 10 Delft

NORWAY NORVEGE	Mr. O. Blichner Norwegian Defence Research Establishment Kjeller per Lillestrom
PORTUGAL	Col. J.A. de Almeida Viama (Delegado Nacional do 'AGARD') Direcção do Serviço de Material da F.A. Rua da Escola Politecnica, 42 Lisboa
TURKEY TURQUIE	Ministry of National Defence Ankara Attn. AGARD National Delegate
UNITED KINGDOM ROYAUME UNI	Ministry of Aviation T.I.L., Room 009A First Avenue House High Holborn London W.C.1
UNITED STATES ETATS UNIS	National Aeronautics and Space Administration (NASA) 1520 H Street, N.W. Washington 25, D.C.

Printed by Technical Editing and Reproduction Ltd
95 Great Portland St. London, W.1.